



TYPICAL FRACTURE DUE TO RUNNING AT A CRITICAL SPEED OF TORSIONAL VIBRATION.

Frontispiece.

PRACTICAL SOLUTION OF TORSIONAL VIBRATION PROBLEMS

*With Examples from Marine, Electrical, Aeronautical,
and Automobile Engineering Practice*

BY

W. KER WILSON

PH.D., M.Sc., WH.Ex., M.I.MECH.E.

SECOND EDITION

(REPRINTED)

Volume I



LONDON

CHAPMAN & HALL LTD.

11 HENRIETTA STREET W.C.2

1942

FIRST PUBLISHED 1935
SECOND EDITION (IN 2 VOLS.) 1940
REPRINTED 1942

PRINTED IN GREAT BRITAIN BY THE ABERDEEN UNIVERSITY PRESS LIMITED
ABERDEEN, SCOTLAND

BOUND BY G. & J. KITCAT LIMITED, LONDON

Flexiback Binding Patent No. 441254

PREFACE.

IN recent years investigations of the torsional vibration characteristics of shaft systems transmitting pulsating torques have become an important part of the designer's responsibility.

Indeed, satisfactory operation of high-duty transmission systems may be said to depend to a large extent on successful handling of the vibration problem.

Whilst many failures of shafting have been traced to abnormal vibration at critical speeds, satisfactory operation implies more than freedom from actual mechanical breakdown. The ideal system should exhibit no perceptible vibratory disturbance throughout the normal operating speed range, a requirement which is now an important consideration in the design of automobile transmission systems.

The rapid development of the internal combustion engine for marine propulsion is another factor which has brought the torsional vibration problem into such prominence that a definite guarantee of a smooth operating speed range is becoming a feature of many high-class marine specifications.

In electrical engineering practice, the heavy rotating masses necessary for satisfactory electrical operation of generating sets direct-coupled to internal combustion engines render this type of installation particularly susceptible to disturbing vibrations, and it is necessary to make sure that no critical or disturbing amplitude occurs near the operating speed.

In this book an attempt has been made to set down the principles and computation details of the subject in a manner suitable for everyday reference. The selection and arrangement of the subject-matter is based on several years' practical experience in carrying out torsional vibration investigations on many different types of installation; and the methods which are developed have been found reliable in practice.

It is hoped that the reader in search of specific information will be able to select data appropriate to his particular problem, and from this build up a set of standard forms suitable for rapid reference.

Acknowledgment is due to the reference works listed in the Bibliography; and to the firms whose names appear in the text for permission to reproduce diagrams of their specialities.

W. K. W.

SUNDERLAND,
October, 1934.

PREFACE TO SECOND EDITION.

A REVIEW of engineering progress during the past four or five years reveals in no small measure the tonic influence of applied vibration study with the outstanding importance of torsional vibration phenomena well established.

This period has been notable for a steady accumulation of contributions to the literature dealing with both practical and theoretical aspects of the subject, whilst at the present time there is undoubtedly an increasing tendency towards regarding vibration study as a necessary accompaniment of sound fundamental design.

The particularly insidious nature of torsional vibration is due to a capacity for destructive action without displaying the external symptoms which are usually very noticeable with other forms of vibration. In addition, torsional critical zones invariably occupy lower positions in the speed range than those corresponding to flexural modes, since the moduli of rigidity of most structural materials are less than one-half the moduli of elasticity.

Furthermore, the fatigue limits for alternating torsion are invariably about one-half the fatigue limits for alternating flexure; torsional excitations are more numerous; and, finally, whereas flexural excitations can in many cases be neutralised by simple means such as balance weights, torsional excitations usually require a change of fundamental design to bring about even partial cancellation.

In reviewing the progress made since the first edition of this book was published the following items are of special interest.

More general application of the art of tuning oscillating systems so that severe critical zones do not occur in the operating speed ranges. For example, the use of stiff connecting shafts where it is expedient to place the severe critical zones above the operating range or the use of very flexible shafts or couplings when the better solution is to place these zones below the operating range. There are indications that the trend towards higher operating speeds is exhausting the possibilities of high-frequency tuning as a method of solving torsional vibration problems, and on this account there is considerable interest in the future development of couplings employing rubber spring elements.

Considerable progress has been made in accumulating data relating to fatigue phenomena with particular reference to the influence of structural discontinuities in causing zones of high-stress concentration. The valuable work carried out at the *Institution of Automobile Engineers Research Laboratories* in this country, and at the *German Institute for Aeronautical Research*, on full-scale crankshaft elements to determine the influence of crank form and material deserves special attention.

There appears to be a general tendency to employ vibration absorbers instead of energy destroying dampers where a completely satisfactory solution cannot be obtained by tuning methods alone. Outstanding achievements in this direction are detuning flywheels and couplings, and the rotating pendulum absorber.

The rotating pendulum absorber was first used in quantity on radial aero-engines, and in a paper read at a meeting of the *Institute of Aeronautical Sciences* in 1936, Mr. Arthur Nutt, Vice-President of Engineering of the *Wright Aeronautical Corporation*, said that without question the development of the rotating pendulum absorber was one of the most valuable contributions to aircraft engine design in many years.

Since the installation of these absorbers service experience over extended periods shows an appreciable reduction in wear not only of engine parts but also of the operating mechanism of variable pitch air-screws. In the latest engines the absorbers have permitted a higher take-off speed with an actual decrease of air-screw stress due to reduction of torsional vibration. This latter point indicates that a satisfactory solution of the torsional vibration problem may also be bene-

ficial throughout the power plant. Indeed, recognition of the possibility of sympathetic response of *all* parts of an oscillating system to appropriate excitations has explained certain apparent discrepancies between practical results and theoretical predictions in cases where the theoretical treatment did not take into account the influence of all parts of the system.

Aero-Engine/Air-screw installations are particularly important examples of this aspect of the torsional vibration problem. Until quite recently it was customary to carry out a torsional vibration analysis by regarding the air-screw as a rigid flywheel having the same polar moment of inertia and then treating the simplified system as a normal multi-mass system capable of oscillating in various modes of torsional vibration, i.e. the influence of air-screw blade flexibility was neglected. It is now known, however, that this partitioning of the engine and air-screw assemblies is liable to yield gravely misleading results, and that a true solution can only be obtained by methods which take into account the characteristics of the combined engine and air-screw systems simultaneously. Unfortunately oscillating systems which contain complicated structural elements, such as air-screw blades, do not yield easily to mathematical treatment alone, although this method of attack provides a useful physical conception of the dynamic principles involved. This difficulty has been overcome by the development of suitable experimental methods, and these are described in an Appendix to Volume I of the present edition.

The introduction of flexible mountings for engines is another factor which has complicated the study of torsional vibration phenomena, especially in geared

engines where there is a particularly strong coupling between crankshaft and crankcase motions, whilst in a recent paper entitled "Strength of Marine Engine Shafting" (*N.E. Coast Instn. of Engs. & Shipbuilders*, 1939), Dr. Dorey has drawn attention to the possibility of crankshaft failure through axial or longitudinal vibration probably initiated by torsional excitations. The existence of a relationship between axial and torsional modes has not yet been definitely established, however, and is one of the items for future investigation.

Damping of torsional vibrations, especially in engine systems, has received considerable attention during the period under review, without however disclosing any better method for assessing the probable vibratory amplitudes and stresses in resonant zones than the empirical or semi-empirical formulæ commonly employed for this purpose. This work has served to emphasise the complex nature of engine damping, and has drawn attention to its non-linear character which is undoubtedly a powerful check on the growth of vibratory amplitudes. The rapid increase of hysteresis damping at stresses in the neighbourhood of the fatigue limit of the material, for example, probably accounts for absence of trouble in many an otherwise risky adventure in crankshaft design.

The assessment of torsional vibration stresses in resonance remains, therefore, a matter for establishing reliable empirical formulæ based on test results. This has naturally led to the development of accurate instruments for measuring torsional vibration frequencies and amplitudes. Apparatus is now available for all classes of installation, including high-speed automobile and aero-engine systems.

In preparing this edition an attempt has been made to bring the text and illustrations thoroughly up-to-date. This has necessitated re-writing a considerable part of the original text and the introduction of several new chapters. In addition to the inclusion of a large amount of new practical design data and a more comprehensive treatment of high-speed engine systems, the following important changes will be found :—

More comprehensive treatment of flexible couplings, including the use of rubber as a structural material with special reference to rubber-in-shear couplings.

The addition of material relating to the choice of crank sequence and firing order of various engine aggregates, including single and multi-row radial engines with articulated connected rods, and Vee-type in-line engines.

Considerable additions to the subject-matter relating to geared systems, including the treatment of geared engines supported on flexible mountings.

The material relating to vibration measuring instruments has been brought up-to-date and includes the latest types of electrical measuring instruments and a full discussion of instrument theory and calibration.

The subject-matter relating to engine damping has been completely revised.

Comprehensive treatment of the properties of materials used in transmission systems, including a study of fatigue phenomena with special reference to the influence of discontinuities in causing stress concentrations.

The material relating to damping devices has been brought up-to-date and includes a separate chapter dealing with the rotating pendulum vibration absorber.

The inclusion of a simple practical treatment of air-screw blade vibration and its influence on the vibration characteristics of aircraft power plants.

The Bibliography has been expanded considerably, and a list of British Patents relating to torsional vibration has been added in Volume II.

In conclusion the author desires once again to make acknowledgment to the reference works listed in the Bibliography and to the Firms whose names appear in the text. In addition, grateful thanks are due to many readers for helpful criticism and encouragement and to those of the author's colleagues who cheerfully undertook the task of checking portions of the manuscript. Special acknowledgment is due to Mr. R. Clink for his careful checking of proofs and for many valuable suggestions.

W. K. W.

LONDON,
June, 1940.

CONTENTS.

VOLUME I.

CHAPTER 1.

	PAGE
TORSIONAL VIBRATION	I
Stress, Strain, and Elasticity—Elastic Vibrations—Strain Energy, Resilience, and Kinetic Energy—Simple Harmonic Motion—Displacement, Velocity, and Acceleration—Periodic Time and Frequency—Free or Natural Vibrations of One-Mass Systems—Frequency Calculations—Damping Forces—Correction for Inertia of Shafting—Maximum Torque and Stress—Special One-Mass Systems—Two-Mass Systems—Position of Node—Special Two-Mass Systems—Three-Mass Systems—Principal Modes of Vibration—Positions of Nodes—Relative Vibratory Amplitudes—Special Cases—Multi-Mass Systems—Equivalent Oscillating Systems—Methods of Simplifying Multi-Mass Systems, and Comparison of the Accuracy of these Methods.	

CHAPTER 2.

NATURAL FREQUENCY CALCULATIONS	52
Principal Modes of Torsional Vibration of Multi-Mass Systems—Frequency Tabulations—Frequency Tabulations for One- and Two-Node Modes of Vibration—Calculation of Specific Vibration Stresses—Normal Elastic Curves—Practical Methods of Carrying out Frequency Tabulations—Characteristics of Direct-Coupled Electrical Generating Sets—Tuning the Oscillating System—Approximate Values of Natural Frequencies—Typical Example—Direct-Coupled Marine Installations—Practical Methods of Tuning Marine Installations—Typical Normal Elastic Curves—Characteristics of Marine Installations—Influence of the Flywheel on Torsional Vibration of Direct-Coupled Marine Installations—Automobile Transmission Systems—Aero-Engine/Air-screw Systems—Radial and In-Line Engines—Frequency Tabulation for Aero-Engine/Air-screw System.	

CHAPTER 3.

EQUIVALENT OSCILLATING SYSTEMS	109
Equivalent Masses—Crankshaft and Running Gear of Reciprocating Engines—Variation of Polar Moment of Inertia of Reciprocating Masses—Engine Driven Auxiliaries—Approximate Values of the Total Polar Moment of Inertia of Crankshaft and Running Gear of Reciprocating Engines—Polar Moment of Inertia of Marine	

Propellers and of Air-screws—Polar Moment of Inertia of Flywheels—Experimental Determination of Polar Moments of Inertia—Correction for Inertia of Shafting—Polar Moments of Inertia of Standard Solids—Equivalent Elasticities—Method of Obtaining Equivalent Length of Solid and Hollow Shafting—Tapered Shafting—Circular Shafts of Varying Diameter—Allowance for Fillets—Shaft Couplings—Cast Iron and Bronze Shafts—Values of the Elastic Moduli—Torsional Rigidity and Strength of Shafts of Non-Circular Cross-Section—Crankshaft Stiffness—Equivalent Lengths of Crankshafts of Various Designs—Automobile and Aero-Engine Crankshaft Elements—Experimental Determination of Crankshaft Stiffness—Elastically Connected Masses.

CHAPTER 4.

FLEXIBLE COUPLINGS 213

Flywheels and Couplings with Flexible Spokes—Uniformly Stressed Spokes—Resilience of Flexible Couplings—Torsional and Flexural Resilience—Comparison of Specific Resilience of Various Spring Elements—Strength of Flexible Couplings—Physical Properties of Materials of Flexible Couplings—Worked Examples—Flexible Couplings Employing Helical Springs—M.A.N. Sleeve Spring Coupling—Bibby Flexible Coupling—Rubber-in-Shear Couplings—Physical and Mechanical Properties of Structural Rubber—Ageing of Rubber—Hardness of Rubber—Effect of Temperature on Rubber—Damping Properties of Rubber—Creep and its Influence on the Permissible Working Stresses—Design of Rubber-in-Shear Couplings.

CHAPTER 5.

GEARED SYSTEMS 287

Equivalent Systems—Two-Shaft Systems—Special Cases—Tabulation Method Applied to Geared Systems—Three-Shaft Systems—Special Cases—The Nodal Drive—Multi-Shaft Systems—Special Cases—Tabulation Method for Multi-Shaft Systems—Geared Aero-Engine/Air-screw Systems—Gear Ratio—Spur, Concentric, and Epicyclic Gears—Approximate Formulae for Geared Radial Aero-Engines—Geared In-Line Aero-Engines—Gear Flexibility—Air-screw Blade Flexibility—Frame Vibration—Flexible Mountings—Effect of Flexible Mountings on Natural Frequencies of Geared Engine Installations—Special Geared Drives—Rigidly Coupled Systems—Engine Accessory Drives—Camshaft Drives—Engine Governors—Automobile Transmission Systems.

CHAPTER 6.

DETERMINATION OF STRESSES DUE TO TORSIONAL VIBRATION AT NON-RESONANT SPEEDS 410

Torque Variation—Critical Speeds—Forced Vibration—Equilibrium Amplitude—Equilibrium Stress—Dynamic Magnifier with Constant Excitation—Dynamic Magnifier with Inertia Excitation

—Two-Mass Systems—Multi-Mass Systems—Multi-Cylinder Reciprocating Engines—Harmonic Analysis of Applied Torque—Gas Pressure—Correction for Deadweight and Inertia of Reciprocating and Revolving Parts—Connecting Rod Inertia Couple—Typical Values of Harmonic Components of Tangential Effort of 2-Stroke and 4-Stroke Cycle Oil and Petrol Engines, and of Steam Engines—Articulated Connecting Rods—Resultant Harmonic Torque Energy of Multi-Cylinder Engines—Phase and Vector Diagrams—Influence of Firing Order—Engines with Two or More Cylinders Operating on Each Crankpin—Radial Engines, Single and Multi Row—Choice of Crank Sequence and Firing Order in Multi-Cylinder In-Line Engines—4-Stroke and 2-Stroke Cycle Types, Single and Double Acting—Inertia Balance and Torsional Vibration Characteristics of Multi-Cylinder In-Line Engines—Vee Engines—Inertia Balance and Torsional Vibration Characteristics of Vee Engines—Choice of Crank Sequence and Firing Order in Vee Engines—Choice of Vee Angle—Geared Engines—Phasing of Duplicated Geared Engines—Determination of Non-Excitable Modes of Vibration in Geared Systems—Marine Propeller Torque Variation—Phasing of Engine and Propeller Torques—Aero-Engine/Air-screw Systems—Engine Direct-Coupled to a Hydraulic Dynamometer—Typical Examples of Equilibrium Amplitude and Stress Calculations—Harmonic Components of Tangential Effort Curve with Variable Load and Speed—Marine, Aero-Engine, and Automobile Systems—Stress Diagrams—Forced Vibration Amplitudes—Coefficient of Speed Fluctuation—Two-, Three-, and Multi-Mass Systems—Tabulation Method of Determining Forced Vibration Amplitudes—Forced Vibration Torque and Stress.

APPENDIX TO VOLUME I.

EFFECTIVE INERTIA METHOD OF TORSIONAL VIBRATION ANALYSIS (with Special Reference to Aero-Engine/Air-screw Systems)	670
Simple Two-Mass System—Basic and Elastically Connected Portions of the Original System—Tuning Curve for Basic System—Effective Inertia Curve for Elastically Connected Portion—Resultant Tuning Curve for Complete System—Three-Mass Systems—Simple Branched Systems—Multi-Mass Systems—Typical Tuning Curves for Multi-Mass Systems—Relationship between Tuning and Effective Inertia Curves—Heavy Shaft Systems—Aero-Engine/Air-screw Systems—Air-screw Blade Vibration—Fixed Root, Rocking Hub, and Symmetrical Modes of Air-screw Blade Vibration—Influence of Rotation on Air-screw Blade Vibration—Non-Effective Harmonic Orders—Experimental Determination of the Effective Inertia Curve of an Air-screw—Summary of Vibration Characteristics of Aero-Engine/Air-screw Systems.	
BIBLIOGRAPHY	708
NAME INDEX	715
SUBJECT INDEX	717

LIST OF WORKED EXAMPLES.

I. FREQUENCY CALCULATIONS.

(a) DIRECT-COUPLED SYSTEMS.	PAGE
<i>One-mass systems</i>	15
Effect of mass of shaft	16
Maximum torque and stress	17
Shaft fixed at both ends	21
Shafts of non-circular cross-section, comparative calculations .	175
Shafts of various cross-sections and materials, comparative calculations .	182
Strain energy	18
<i>Two-mass systems</i>	26
<i>Three-mass systems</i>	35, 211
Relative amplitudes and positions of nodes	37
<i>Multi-mass systems, closely coupled type</i>	45
Position of nodes	48, 49
Reduction to equivalent two- and three-mass systems	46, 49
Relative amplitudes	47
Tabulation method	57
<i>(Note.—The above examples apply in cases where the major masses are closely coupled, e.g. oil-engine generator sets, direct-coupled aero-engine air-screw systems, etc.)</i>	
<i>Multi-mass systems, with flexible transmission shafts</i>	40
Position of nodes	43
Reduction to equivalent two- and three-mass systems	40
Relative amplitudes	42
Tabulation method	64
<i>(Note.—The above examples apply in cases where the major masses are flexibly connected, e.g. marine engines with long propeller shafts, geared aero-engine air-screw installations, automobile transmission systems, etc.)</i>	
<i>Typical systems.</i>	
<i>Aero-engine air-screw systems.</i>	
Air-screw blades, influence of rotation	703
Direct-coupled, in-line engine	102
Effect of altering mass and elasticity	103
Tabulation method	107
Direct-coupled radial engine	97
Reduction to one-mass system	98
Heavy-shaft system, effective inertia method	689

LIST OF WORKED EXAMPLES

xix

<i>Typical systems.</i>	PAGE
Automobile transmission system	91
Marine oil engine system, tabulation method	64
Effect of altering mass and elasticity	82, 85
Oil-engine/generator sets, tabulation method	57
Effect of altering mass and elasticity	80
 (b) GEARED SYSTEMS.	
<i>Two-shaft system</i>	
Tabulation method	292
Tabulation method	295
<i>Three-shaft system, with duplicated masses</i>	302
<i>Four-shaft system</i>	
Effective inertia method	307
Tabulation method	680
Tabulation method	310
With flexible couplings	308
<i>Aero-engines/air-screw systems.</i>	
In-line engine, simple spur gear	345
Influence of air-screw blade flexibility	356
Influence of flexible mountings	362
Radial engine, concentric gear	338
Concentric gear and flexible mountings	372
Epicyclic gear and flexible mountings	380
Approximate method	395
Marine geared turbine and reciprocating engine installation	315

2. EQUIVALENT OSCILLATING SYSTEMS.

(a) POLAR MOMENTS OF INERTIA.	
Conic frustum	154
Crankshaft and running gear	130
<i>Crankweb</i>	
Balanced type	156
Graphical method	157
Experimental methods of obtaining	115
Experimental methods of obtaining	147
<i>Marine propeller.</i>	
Approximate method	142
Entrained water allowance	135
Equivalent disc method	134
Graphical integration method	137
(b) TORSIONAL RIGIDITIES.	
Complex shaft	165
<i>Crankshafts</i>	
Automobile, solid and hollow	188
Automobile, solid and hollow	201
Elastically connected mass	211
Non-circular shafts	175
Effect of altering material	182

3. FLEXIBLE COUPLINGS.

(Calculation of Resilience, Stress, and Torsional Rigidity.)

Coupling with flexible spokes	238
Helical springs	246
Design of springs	249
Plate springs	261
Sleeve springs (M.A.N. type)	255
" Bibby " springs	268
Flywheel with flexible spokes	15, 237

4. STRESS CALCULATIONS—AT NON-RESONANT SPEEDS.

	PAGE
Comparative balancing calculations, in-line engines	507
Dynamic magnifier, inertia excitation	422
FORCED VIBRATION AMPLITUDES.	
<i>Analytical method.</i>	
Two-mass system, torque at one mass	630
Torque at both masses	634
Torque at node	642
Three-mass system	645
Principle of dynamic vibration absorber	650
Multi-mass system	658
<i>Tabulation method.</i>	
Two-mass system, torque at one mass	627
Torque at both masses	635
Torque at node	639
Three-mass system	645
Multi-mass system	656
Geared engines, influence of phasing of duplicated prime movers	583
<i>Impulse frequency.</i>	
Counter-rotating air-screws	599
Hydraulic dynamometer	601
Marine propeller	593
<i>Marine oil engines.</i>	
One-node mode	612
Two-node mode	617
Influence of variation of M.I.P. with speed	619
Influence of propeller torque variation	616
<i>(Note.—The above examples apply in cases where the major masses are flexibly connected, e.g. marine engines with long propeller shafts, geared aero-engines/air-screw systems, automobile transmission systems, etc.)</i>	
<i>Marine steam engines</i>	
Influence of variation of M.I.P. with speed	620
Influence of propeller phasing	623
Influence of propeller phasing	624
<i>Oil-engine/generator sets</i>	608
<i>(Note.—The above example applies in cases where the major masses are closely coupled, e.g. oil-engine/generator sets, direct-coupled aero-engine/air-screw systems, etc.)</i>	
Resultant forced vibration torque and stress due to several harmonics	662
Resultant harmonic components, one-cylinder	438
Six-cylinders	479
<i>Speed fluctuation, coefficient of.</i>	
Marine oil engine	666
Two-mass system	633, 635
Three-mass system	648
<i>Vee-engines.</i> Influence of Vee-angle on torsional vibration	569, 570, 571
With different firing orders in the two banks	579

TORSIONAL VIBRATION.

Introduction.—Since no material is perfectly rigid, the effect of applying an external force or load to a body is to produce a change of size or of shape or of both. These changes are termed *strains*. The internal equal and opposite reactions which are the result of the external force or load, and which resist deformation, are termed *stresses*.

That property of matter which enables it to resist deformation is termed *elasticity*, and in a perfectly elastic material the strain disappears after removal of the stress, i.e. the body then returns to its original configuration. Whilst no material is perfectly elastic, metals are almost perfectly elastic within certain limits of loading.

Within those limits the strain is proportional to the stress producing it. Beyond those limits the deformation is partly elastic or temporary, and partly plastic or permanent.

The point beyond which stress and strain cease to be proportional is commonly called the *elastic limit* of the material, although the modern tendency is to term it the *limit of proportionality*, since the metal still possesses some elasticity after this limit is passed.

The laws governing the elastic deformation of a shaft when an externally applied twisting moment or couple is transmitted from one end to the other are well known, and are contained in the following expression:—

$$\frac{M}{I_p} = \frac{2 \cdot f_s}{d} = \frac{G \cdot \theta}{L}, \quad \dots \quad (1)$$

where M = the external couple in lbs.-ins.,
 I_p = the polar moment of inertia of the cross-section
of the shaft in inches⁴ units

$$s = \frac{\pi}{32} \cdot d^4,$$

d = the diameter of the shaft in inches,

f_s = the shear stress in lbs. per sq. in.,

G = the modulus of rigidity in lbs. per sq. in.

= 12,000,000 for steel,

θ = angular deflection or twist of shaft in radians,

L = length of shaft in inches.

This expression shows that the strain or angular deflection is directly proportional to the stress, provided the limit of proportionality is not exceeded.

Elastic Vibrations.—When a shaft, fixed at one end, is twisted by applying an external couple at the free end, the work done against the internal elastic forces which resist deformation is termed *strain energy*, and in common with other elastic bodies the shaft possesses the property of restoring this energy when the couple is removed.

This property is termed *resilience*.

In a perfectly elastic material the whole of the strain energy is restored when the load is removed, but in the case of a shaft twisted by an external couple a proportion of the work done is absorbed in overcoming internal molecular friction, and appears as heat in the material strained.

A similar amount of energy is absorbed by frictional resistances when the shaft returns to its original configuration after the load is removed.

Within the limit of proportionality, however, only a very small proportion of the strain energy is absorbed in this way, the greater proportion being stored in the shaft. This stored energy is termed *potential energy* of strain or *resilience*, and very nearly the whole of it is restored when the load on the shaft is removed.

Beyond the limit of proportionality a progressively greater proportion of the strain energy is expended in overcoming the internal friction of the material to produce permanent deformation.

Fig. 1 shows a simple torsional pendulum, consisting of a length of shafting fixed at one end and carrying a heavy disc at the free end.

If the disc is disturbed from its position of equilibrium by the application of an external couple, strain energy is imparted to the shaft, and this energy is available for expenditure when the load is removed, assuming that the material is not stressed beyond the limit of proportionality.

The lower portion of Fig. 1 shows the disc and shaft diagrammatically. In this diagram $+a$ represents the circum-

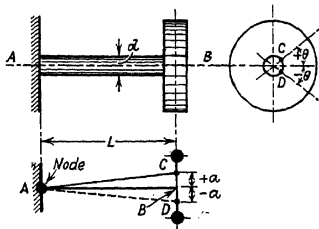


FIG. 1.—One-mass system.

ferential distance an imaginary point on the surface of the shaft at end B moves when the external couple is applied.

The corresponding angular deflection in radians is $\theta = \frac{2 \cdot a}{d}$, and since Equation (1) shows that the deflection at any other position along the shaft is directly proportional to the distance from the fixed end, the elastic deflection curve AD is a straight line of constant slope. The stress induced in the shaft which is proportional to θ/L (Equation 1) is the same at all positions between A and B.

When the external couple is removed the shaft commences to untwist. During this process a small proportion of the potential energy of strain is absorbed by frictional resistances, the greater proportion being expended in imparting motion to

the disc. This energy of motion is termed *kinetic energy*. The kinetic energy imparted to the disc attains a maximum value when the whole of the available potential energy is absorbed, i.e. when the shaft is completely untwisted and the system has regained its original configuration. At this instant the kinetic energy of the disc is equal to the potential energy of strain diminished by the small amount of energy absorbed by frictional resistances. The disc therefore continues to move beyond the original unstrained position of the system until a strain nearly equal to the original strain, but in the opposite direction, is induced in the shaft. At this instant the potential energy of strain is once more equal to the maximum kinetic energy acquired by the disc diminished by a small amount of energy absorbed in frictional resistances, and the disc comes to rest.

It is evident that in passing from one extreme position towards the other the disc gradually acquires kinetic energy until it reaches the original position of equilibrium, now the central position of its movement, and thereafter gradually loses kinetic energy. If the energy dissipated in doing work against friction during the motion of the disc is neglected, the kinetic energy of the disc at the instant it reaches the central position must be equal to the potential energy of strain at each extreme position of its movement. At any intermediate position the sum of the kinetic and potential energies must be constant, and this constant quantity of energy is termed the *energy of the vibration*.

In this example the energy of the vibration is equal to the strain energy imparted to the system by the initial displacement of the disc.

If none of this energy is absorbed in doing work against friction, the vibratory motion of the disc would continue indefinitely, the motion being shown diagrammatically in Fig. 1 by the lines AC and AD, with maximum displacements of $+a$ and $-a$ at the free end of the shaft, or, in circular measure, $+\theta$ and $-\theta$, where $\theta = \frac{2a}{d}$.

In practice, however, there is always a gradual dissipation

of energy by work done against internal and external resistances which oppose the vibration. In consequence the system gradually loses its energy of vibration, until finally the whole has been absorbed and the disc comes to rest at its original position of equilibrium.

Vibration may therefore be regarded as the process whereby an elastic system dissipates the potential energy of strain imparted to it when its equilibrium is disturbed.

The process can easily be verified experimentally by attaching a fairly heavy disc to one end of a fairly long piece of wire. If one end of the wire is held rigidly, with the disc suspended below, and the latter is given a twist and then released, it will vibrate through gradually decreasing angles until finally it comes to rest at its original position of equilibrium.

Simple Harmonic Motion.—This is the simplest type of periodic motion.

In Fig. 2a, O is a fixed point, and OC is a radius rotating with uniform angular velocity round O. AB is any diameter of the circular path described by C, and CQ is the perpendicular from C to AB for any instantaneous position of the radius OC. As the point C rotates round O with uniform angular velocity the point Q vibrates along the diameter AB about the centre O with *simple harmonic motion*. A single vibration is completed when the point C has moved once round the circle, i.e. when the motion of Q is the same as it was at the commencement of the cycle. Thus, if the cycle is assumed to commence at point D in the circular path of C or at point O in the path of Q, and the rotation of C is assumed to be counter-clockwise, then the initial movement of Q is upwards towards B. At B point Q comes to rest, its motion along AB is reversed, and it travels downwards from B to A. At A it comes to rest again, its motion is once more reversed, and it travels upwards towards O.

When it reaches O it has the same motion as at the commencement of the cycle, i.e. upwards towards B, and the cycle is therefore completed.

The time required to complete one cycle is termed the *periodic time* of the vibration, and the reciprocal of the periodic

time is termed the *frequency* of the vibration, since it is the number of complete cycles which are executed in unit time.

Let P = periodic time in seconds,

F = frequency of vibration in cycles per second,

ω = the uniform angular velocity of point C (usually termed the *phase velocity* of the vibration) in radians per second.

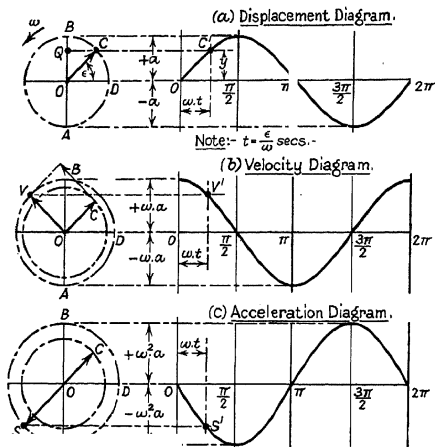


FIG. 2.—Simple harmonic motion.

Then, since each cycle is completed in one revolution of C , i.e. when the angular movement of OC is $2 \cdot \pi$ radians,

$$P = \frac{2 \cdot \pi}{\omega} = \frac{6 \cdot 2832}{\omega} \text{ secs.},$$

$$\begin{aligned} \text{or } F = \frac{I}{P} &= \frac{\omega}{2 \cdot \pi} = 0.159 I \cdot \omega \text{ vibs./sec.} \\ &= 9.55 \cdot \omega \text{ vibs./min.} \end{aligned}$$

From the geometry of Fig. 2a,

$$y = a \sin \omega \cdot t, \quad (2)$$

where $y = OQ$ = the displacement of Q from the centre of vibration O ,

$a = OC$ = the radius of the circle described by C ,

$\epsilon = \omega \cdot t$ = the angular displacement of C from the initial position D ,

t = the time in seconds, assumed to be measured from the instant C is at D .

The motion of Q can be shown conveniently by the ordinates of a displacement diagram on a time base (Fig. 2a). The maximum displacements of Q from the centre of vibration O are $+a$ and $-a$, and a is termed the *amplitude* of the vibration. The curve of displacement is a true sine curve when the point is executing simple harmonic vibrations.

In Fig. 2a the radius $OC = a$ may be regarded as the displacement vector; the displacement diagram being obtained by projecting the successive instantaneous positions of C on to the corresponding ordinates in the displacement diagram.

The velocity of Q is greatest at the instant Q passes through O in either direction, being then equal to the uniform velocity of C , viz. $\omega \cdot a$. At A and B , Q is at rest.

At any intermediate position, therefore, the velocity of Q is equal to the velocity of C resolved along AB , and from the geometry of Fig. 2b,

$$v = \omega \cdot a \cos \omega \cdot t, \quad (3)$$

where v = the velocity of Q along AB .

In Fig. 2b, $OV = \omega \cdot a$ may be regarded as the velocity vector for vibration of Q along AB , and the velocity diagram is obtained by projecting the successive instantaneous positions of V on to the corresponding ordinates in the velocity diagram.

The velocity vector is a quarter of a cycle, or $\pi/2$ radians ahead of the displacement vector.

The acceleration of Q along AB can be obtained from the acceleration of C, since the latter is merely the acceleration of a point moving in a circle with uniform angular velocity, viz. $\omega^2 \cdot a$, acting always along the radius OC towards O.

The acceleration of Q along AB is then the acceleration of C resolved along AB, and from the geometry of Fig. 2c,

$$S = -\omega^2 \cdot a \sin \omega \cdot t, \quad . \quad . \quad . \quad (4)$$

where S = the acceleration of Q along AB, which is seen to be proportional to the displacement of Q from the centre of vibration O.

The negative sign indicates that this acceleration is always directed towards the centre of vibration O.

In Fig. 2c, OS = $\omega^2 \cdot a$ may be regarded as the acceleration vector for vibration of Q along AB, and the acceleration diagram is obtained by projecting the successive instantaneous positions of S on to the corresponding ordinates in the acceleration diagram.

Since force = mass \times acceleration, equation (4) shows that the force under which a mass will execute simple harmonic vibrations must vary proportionally to the displacement from the centre of vibration, and must always be directed towards the centre of vibration.

The acceleration at any instant is

$$S = -\omega^2 \cdot a \sin \omega \cdot t \quad . \quad . \quad . \quad (4)$$

and the corresponding displacement is

$$y = a \sin \omega \cdot t \quad . \quad . \quad . \quad (2)$$

Hence, $S = -\omega^2 \cdot y$,

but $\omega = \frac{2 \cdot \pi}{P} = 2 \cdot \pi \cdot F$,

i.e. $S = \frac{4 \cdot \pi^2}{P^2} \cdot y = 4 \cdot \pi^2 \cdot F^2 \cdot y$,

or periodic time, $P = 2 \cdot \pi \sqrt{\frac{y}{S}}$ secs.

$$\begin{aligned}
 \text{Frequency of vibration, } F &= \frac{1}{2 \cdot \pi} \sqrt{\frac{S}{y}} \text{ vibs./sec.} \\
 &= \frac{1}{2 \cdot \pi} \sqrt{\frac{\text{acceleration}}{\text{displacement}}} \quad \cdot \quad \cdot \quad (5)
 \end{aligned}$$

Since the acceleration is directly proportional to the displacement, the frequency is independent of the amplitude of the vibration, and depends only on the strength of the restoring force, i.e. the restoring force per unit displacement.

The *phase* of a vibration is the fraction of a cycle which has elapsed since the vibrating point last passed through its middle position in the positive direction. Thus the phase of a vibration measures the particular point of the cycle, where the vibrating body happens to be, at some chosen instant. In Fig. 2*a* the angle $\epsilon = \omega \cdot t$ is termed the phase angle. Two vibrations are said to be in phase when they are at corresponding points of their cycles at the same instant. ω is termed the *phase velocity*, since it is the rate of change of the phase angle.

Free or Natural Torsional Vibration.—Equation (1) shows that when the disc in Fig. 1 is given an angular displacement a restoring moment is induced in the shaft which is proportional to the displacement, and which tends to return the disc to the equilibrium position. This establishes the important fact that when the disc is released it will execute rotary vibrations of the simple harmonic type until it is brought to rest by frictional resistances.

Since these vibrations are executed without any external exciting force acting on the system, and since the frictional resisting forces are usually very small, the motion is termed *free* or *natural torsional vibration*.

The expressions for angular displacement, angular velocity, and angular acceleration are the same as those already determined for linear simple harmonic motion.

In Fig. 3 the displacement diagram corresponds to the displacement diagram shown in Fig. 2 at (*a*), and represents linear displacements of the weight *W* along the circumference of a circle of radius *R*.

The linear amplitude is $\pm \alpha$ and the corresponding angular amplitude is $\pm a = \pm \alpha/R$ radians.

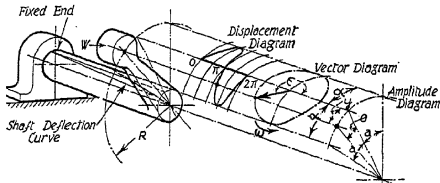


FIG. 3.—Relationship between linear and angular motion.

From Equation (2) the linear displacement of W along the circumference at radius R is

$$y = \alpha \sin \omega . t .$$

Hence the corresponding angular displacement is

$$\theta = \frac{\alpha}{R} \sin \omega . t = a \sin \omega . t .$$

Similarly, the angular velocity is

$$\Omega = \omega . a \cos \omega . t$$

and the angular acceleration is

$$\psi = -\omega^2 . a \sin \omega . t ,$$

$$\text{i.e.} \quad \theta = a \sin \omega . t , \quad . \quad . \quad . \quad . \quad (2a)$$

$$\Omega = \omega . a \cos \omega . t , \quad . \quad . \quad . \quad . \quad (3a)$$

$$\psi = -\omega^2 . a \sin \omega . t , \quad . \quad . \quad . \quad . \quad (4a)$$

where

θ = angular displacement of the disc from the equilibrium or mean position in *radians*,

a = amplitude of vibration of disc in *radians*,

Ω = angular velocity of disc in *radians/second*,

ψ = angular acceleration of disc in *radians/second²*,

t = time in seconds,

ω = phase velocity of the vibration in *radians/second*.

It is important to distinguish between Ω , the angular velocity of the disc at any instant, and $\omega = 2 \cdot \pi \cdot F$, the constant angular velocity from which the vibration is derived, the latter is termed the *phase velocity* of the vibration.

The frequency of natural torsional vibration of the disc is determined as follows :—

At either extremity of the motion of the disc the potential energy of strain and the resisting moment due to elastic forces have their maximum values,

i.e. maximum restoring torque exerted by the elastic forces, from Equation (1),

$$M_e = \frac{I_p \cdot G \cdot a}{L}.$$

The torque required to produce the acceleration $\omega^2 \cdot a$ at the position of maximum displacement of Q is

$$\begin{aligned} *M_m &= \text{moment of inertia} \times \text{angular acceleration} \\ &= J \cdot \omega^2 \cdot a. \end{aligned}$$

This result can be deduced from a consideration of the linear motion of the weight W shown in Fig. 3.

The linear acceleration of W along the circumference of a circle of radius R is

$$S = -\omega^2 \cdot a \sin \omega \cdot t. \quad . \quad . \quad (4)$$

Assuming that the masses of the connecting arm and of the shaft are negligible, and that the mass of the bob-weight is concentrated at its centre of gravity, which is at radius R from the axis of oscillation, the tangential force due to vibration of W is

$$\text{Force} = \text{mass} \times \text{linear acceleration},$$

$$\text{i.e.} \quad P = -\frac{W}{g} \cdot \omega^2 \cdot a \sin \omega \cdot t.$$

* Throughout this work moments of inertia of oscillating masses are expressed in lbs.-ins. sec.² or lbs.-ft. sec.² units. i.e. $J = \frac{WK^2}{g}$, where WK^2 is defined as the "flywheel effect" of the mass, not its moment of inertia.

Hence the torque on the shaft due to this force is

$$M = P \cdot R = -\frac{W}{g} \cdot R \cdot \omega^2 \cdot x \sin \omega \cdot t,$$

but $x = a \cdot R$,

$$\text{i.e. } M = -\frac{W}{g} \cdot R^2 \cdot \omega^2 \cdot a \sin \omega \cdot t.$$

Now $\left\{\frac{W}{g} \cdot R^2\right\}$ is the polar moment of inertia of a mass $\frac{W}{g}$ concentrated at radius R .

$$\text{Let } J = \frac{W}{g} \cdot R^2,$$

$$\text{then } M = -J \cdot \omega^2 \cdot a \sin \omega \cdot t,$$

or torque = moment of inertia \times angular acceleration.

At the position of maximum displacement,

$$M_m = J \cdot \omega^2 \cdot a.$$

Since there is no external exciting torque acting on the system and the frictional resistances are assumed to be negligible,

$$M_e = M_m,$$

$$\text{i.e. } \frac{I_p \cdot G \cdot a}{L} = J \cdot \omega^2 \cdot a,$$

$$\text{or } \omega^2 = (2 \cdot \pi \cdot F)^2 = \frac{I_p \cdot G \cdot a}{L \cdot J \cdot a}.$$

$$\text{Hence, } F = \frac{1}{2 \cdot \pi} \sqrt{\frac{I_p \cdot G}{J \cdot L}} \quad \dots \quad (6)$$

where F = natural frequency of torsional vibration
in vibrations per second,
 I_p = polar moment of inertia of cross-section
of shaft in inches⁴ units

$$= \frac{\pi}{32} \cdot d^4, \text{ for a solid circular shaft,}$$

d = diameter of shaft in inches,

G = modulus of rigidity in lbs. per sq. inch

= 12,000,000 for steel,

J = moment of inertia of disc

$$= \frac{W \cdot K^2}{g},$$

W = weight of disc in lbs.,

K = radius of gyration of disc in inches,

g = 386 ins./sec.²,

L = length of shaft in inches.

From Equation (1) it is seen that the quantity $\left(\frac{I_p \cdot G}{L}\right)$ in Equation (6) is the torque per radian of twist.

This quantity is termed the *torsional rigidity* of the system.

Let $C = \frac{I_p \cdot G}{L}$ = torsional rigidity of the system in lbs.-ins. per radian.*

Then $F = \frac{1}{2 \cdot \pi} \sqrt{\frac{C}{J}}$ vibs./sec.

$$= 9.55 \sqrt{\frac{C}{J}} \text{ vibs./min.} \quad \dots \quad (7)$$

Equation (7) can also be derived directly from Equation (5) as follows:—

$$= \frac{1}{2 \cdot \pi} \sqrt{\frac{\text{acceleration}}{\text{displacement}}} \quad \dots \quad (5)$$

Now $\text{acceleration} = \frac{\text{restoring torque}}{\text{moment of inertia}}$

and $\frac{\text{acceleration}}{\text{displacement}} = \frac{\text{restoring torque per radian}}{\text{moment of inertia}}$

$$= \frac{C}{J}$$

Hence, $F = \frac{1}{2 \cdot \pi} \sqrt{\frac{C}{J}}$ vibs./sec., as before.

Equation (6) shows that the frequency is independent of the amplitude of vibration, and that an increase of the moment of inertia of the disc, or of the length of the shaft, or a reduction

* Note.— $\theta_0 = \frac{M}{C}$,

where θ_0 = angular twist produced by torque M applied statically.

in the diameter of the shaft, will reduce the natural frequency of the system. Thus, a heavy disc carried by a long slender shaft will execute natural vibrations of much lower frequency than a comparatively light disc carried by a short stiff shaft. This can be verified experimentally by suspending a disc by means of a fairly long length of wire. As the length of the wire is shortened the natural frequency of the disc increases, and *vice versa*.

Equation (7) is based on the assumptions that the connecting shaft has no mass, and that there are no exciting or resisting forces acting on the system.

The frictional resistances which oppose vibration are termed *damping forces*, and are usually assumed to be proportional to the velocity, since this assumption appears to be reasonably correct for practical purposes. The effect of a damping force proportional to the velocity and a restoring force proportional to the displacement is to reduce both the natural frequency of the vibration and the amplitudes of successive cycles.

In practice, since the amplitudes and therefore the velocities of natural torsional vibrations are small, the effect on the frequency of vibration of a damping force proportional to the velocity is unimportant (see Chapter 7).

Correction for Mass of Shaft.—If the mass of the shaft is not negligible, but is small compared with that of the disc, the amplitude of vibration at any section of the shaft between A and B (Fig. 1) is proportional to the distance from the fixed end A.

Let this distance be l , and let J_s be the moment of inertia of the shaft, V its angular velocity at the free end, and v its angular velocity at distance l from the fixed end.

Then
$$v = \frac{V \cdot l}{L}.$$

The kinetic energy of an element of length δl , distant l from the fixed end, is

$$\frac{J_s \cdot \delta l \cdot v^2}{2 \cdot L} = \frac{J_s \cdot V^2 \cdot l^2 \cdot \delta l}{2 \cdot L^3}$$

and the total kinetic energy of the shaft is

$$\frac{J_s \cdot V^2}{2 \cdot L^3} \int_0^L l^2 \cdot \delta l = \frac{1}{3} \cdot \frac{1}{2} \cdot J_s \cdot V^2,$$

i.e. the moment of inertia of the shaft is dynamically equivalent to one-third of the same amount at the free end of the shaft, and may be taken into account if necessary by adding one-third of J_s to the moment of inertia of the disc.

In cases where the mass of the shaft is not negligible the system must be treated as a heavy shaft system. The solution for a two-mass heavy shaft system is given in Chapter 8, Equation (402), Vol. II.

EXAMPLE I.—Calculate the natural frequency of torsional vibration of the system shown in Fig. 1, assuming the following dimensions :—

Weight of disc	= 16,500 lbs.
Diameter of disc	= 204 ins.
Length of shaft	= 830 ins.
Diameter of shaft	= 16 ins.

Also calculate the maximum torque, the maximum stress, and the strain energy of the vibration, assuming that a point on the surface of the shaft at the centre line of the disc vibrates with an amplitude of $\pm \frac{1}{4}$ inch.

(i) *Natural Frequency of Torsional Vibration.*

$$F = 9.55 \sqrt{\frac{C}{J}} \text{ vibs./min.}, \quad (7)$$

$$C = \frac{G \cdot I_p}{L} \text{ lbs.-ins. per radian,}$$

where

G = modulus of rigidity = 12,000,000 lbs. per sq. in. for steel,

I_p = polar moment of inertia of cross-section of shaft

$$= \frac{\pi \cdot d^4}{32}; \quad d = \text{dia. of shaft} = 16 \text{ ins.}$$

$$= \frac{3.1416 \times 16^4}{32} = 6434 \text{ ins.}^4,$$

L = length of shaft = 830 ins.,

$$\text{i.e. } C = \frac{12000000 \times 6434}{830} = 93,020,000 \text{ lbs.-ins.}$$

per radian,

J = moment of inertia of disc

$$= \frac{W \cdot K^2}{g},$$

W = weight of disc = 16,500 lbs.,

K^2 = (radius of gyration of disc)²

= $\frac{D^2}{8}$ for a solid circular disc, where D is the diameter

$$= \frac{204^2}{8} = 5202 \text{ ins.}^2,$$

g = 386 ins. per sec. per sec.,

$$\text{i.e. } J = \frac{16500 \times 5202}{386} = 222,400 \text{ lbs.-ins. sec.}^2.$$

$$\text{Hence, finally, } F = 9.55 \sqrt{\frac{93020000}{222400}} = 195.3 \text{ vibs./min.}$$

Effect of Mass of Shaft.—The mass of the shaft may be taken into account by adding one-third of the moment of inertia of the shaft to the moment of inertia of the disc.

$$\begin{aligned} \text{Weight of shaft} &= \frac{0.283 \cdot \pi \cdot d^2 \cdot L}{4} \\ &= 0.283 \times 0.7854 \times 16^2 \times 830 \\ &= 47,250 \text{ lbs.} \end{aligned}$$

$$K^2 \text{ of shaft} = \frac{d^2}{8} = \frac{256}{8} = 32 \text{ ins.}^2,$$

$$\begin{aligned} \text{i.e. moment of inertia of shaft} = J_s &= \frac{W \cdot K^2}{g} = \frac{47250 \times 32}{386} \\ &= 3920 \text{ lbs.-ins. sec.}^2. \end{aligned}$$

Hence, the equivalent moment of inertia of the disc is

$$\begin{aligned} J_e &= J + \frac{J_s}{3} = 222,400 + \frac{3920}{3} \\ &= 223,707 \text{ lbs.-ins. sec.}^2, \end{aligned}$$

and the natural frequency of torsional vibration becomes

$$= 9.55 \sqrt{\frac{93020000}{223707}} = 194.8 \text{ vibs./min.}$$

This is a difference of only $\frac{1}{4}$ per cent. As a general rule the mass of the shaft can be neglected if the product of the length of the shaft in feet multiplied by the frequency in vibrations per second does not exceed 1000. In the present example this product is only 225, a frequency of 867 vibs./min. being required to make the product 1000. The moment of inertia of the disc corresponding to a frequency of 867 vibs./min. is 11,280 lbs.-ins. sec.², whilst the correction for the mass of the shaft lowers this frequency to 820 vibs./min., a difference of 5 per cent. The value obtained by applying the method given in Chapter 8 is 823 vibs./min.

(ii) *Maximum Torque.*

The amplitude of vibration at surface of shaft, radius 8 ins., is $\pm \frac{1}{4}$ in.

$$\begin{aligned} \text{i.e.} \quad \text{angular amplitude} &= \pm 0.25/8 \\ &= \pm 0.03125 \text{ radian.} \end{aligned}$$

$$\begin{aligned} \text{Now} \quad M &= \pm \frac{G \cdot a \cdot I_p}{L} \quad \dots \quad (1) \\ &= \pm \frac{12000000 \times 0.03125 \times 6434}{830} \\ &= \pm 2,910,000 \text{ lbs.-ins.} \end{aligned}$$

Alternatively torque = moment of inertia \times accn.

$$M = \pm J \cdot \omega^2 \cdot a,$$

where

ω = phase velocity of vibration

$$= \frac{2 \cdot \pi \cdot F}{60} \text{ radians per sec.}$$

$$= \frac{2 \times 3.1416 \times 195}{60}$$

$$= 20.5 \text{ radians per sec.,}$$

$$\begin{aligned} \text{i.e.} \quad M &= \pm 222,400 \times 20.5^2 \times 0.03125 \\ &= \pm 2,930,000 \text{ lbs.-ins.} \end{aligned}$$

(iii) *Maximum Stress.*

$$\begin{aligned} f_s &= \pm \frac{M \cdot d}{2 \cdot I_p} \quad \dots \quad (1) \\ &= \pm \frac{2910000 \times 16}{2 \times 6434} = \pm 3620 \text{ lbs.-ins.}^2. \end{aligned}$$

(iv) *Strain Energy.*

This is equal to the maximum potential energy of strain at either extreme position of the movement of the disc,

$$\begin{aligned} \text{i.e. strain energy} &= \frac{1}{2} \cdot M \cdot a = \frac{1}{2} \times 2910000 \times 0.03125 \\ &= 45,500 \text{ ins.-lbs.} \end{aligned}$$

Alternatively, it is equal to the maximum kinetic energy of the disc at the mean position of the vibration, viz. :—

$$\begin{aligned} \text{strain energy} &= \frac{1}{2} \cdot J \cdot (\omega \cdot a)^2 \\ &= \frac{1}{2} \times 222400 \times 20.5^2 \times 0.03125^2 \\ &= 45,500 \text{ ins.-lbs.} \end{aligned}$$

Note that the strain energy is directly proportional to the square of the amplitude and to the square of the frequency.

Special One-Mass Systems.—The following special arrangements are occasionally found in practice, and can be handled by the elementary relationship :—

$$F = 9.55\sqrt{C/J} \text{ vibs./min.,}$$

where F = natural frequency in vibs./min.,

C = restoring torque per radian deflection,

J = moment of inertia of oscillating system about axis of oscillation.

It is important to take care that the correct units are used throughout the calculations. If C is expressed in lbs.-ins. per radian, J must be expressed in lbs.-ins. sec.²; if C is expressed in lbs.-ft. per radian, J must be expressed in lbs.-ft. sec.².

Also, when lbs., in., and sec. units are employed the value of the gravitational constant g is 386 ins. per sec.², i.e. $J = W \cdot K^2/386$ lbs.-ins. sec.² When lbs., ft., and sec. units are employed $g = 32.2$ ft./sec.², i.e. $J = W \cdot K^2/32.2$ lbs.-ft. sec.².

In Fig. 4(a) the system consists of a shaft fixed at each end, with a disc of moment of inertia J attached at a point where the torsional rigidity of the right-hand and left-hand portions of the shaft are C_2 and C_1 respectively. The two-node frequency of a geared radial aero-engine can be estimated from a system of this type.

Since $C_1 =$ torque per radian for left-hand portion of shaft,
 $C_2 =$ torque per radian for right-hand portion of shaft.
 Total restoring torque for one radian deflection of mass
 $= (C_1 + C_2).$

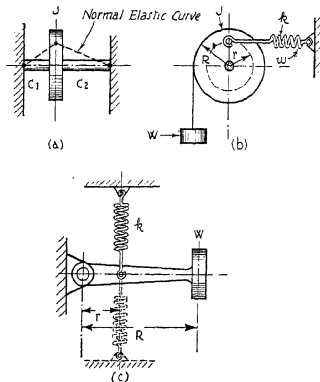


FIG. 4.—Special one-mass systems.

Hence, $F = 9.55\sqrt{\frac{C_1 + C_2}{J}}$ vibs./min. (8)

Also, if $F_1 =$ frequency of J on $C_1 = 9.55\sqrt{\frac{C_1}{J}},$
 $F_2 =$ frequency of J on $C_2 = 9.55\sqrt{\frac{C_2}{J}},$
 then $F^2 = (F_1^2 + F_2^2).$ (9)

Fig. 4(b) shows a system consisting of a disc of moment of inertia J , mounted freely, for example, on ball bearings. A weight W is attached to the disc at radius R by a flexible cord, and the motion of the disc is controlled by a spring of inch rate k acting at radius r .

In this case $k =$ load to extend spring 1 inch,

i.e. for a small circumferential deflection α , the spring force is $k \cdot \alpha$, and the torque due to the spring force is $k \cdot \alpha \cdot r$.

The corresponding angular deflection is α/r .

Hence, $C =$ restoring torque per radian displacement

$$= k \cdot \alpha \cdot r \cdot \frac{r}{\alpha} = k \cdot r^2.$$

The moment of inertia of the weight W about the axis of oscillation of the disc is $W \cdot R^2/g$,

i.e. effective moment of inertia of system $= J + W \cdot R^2/g$.

$$\text{Hence, } = 9.55 \sqrt{\frac{k \cdot r^2}{J + W \cdot R^2/g}} \text{ vibs./min.} \quad (10)$$

If the mass of the spring is not negligible, an approximate correction is to add one-third of the moment of inertia of the spring about the axis of oscillation to the effective moment of inertia of the system,

i.e. effective moment of inertia of system

$$= J + \frac{WR^2}{g} + \frac{1}{3} \frac{w \cdot r^2}{g}$$

where $w =$ weight of spring.

Fig. 4(c) shows a system consisting of a light lever hinged at one end and carrying a heavy weight W at the other end. The motion of the weight is controlled by a spring of inch rate k attached to the lever at radius r .

In this case, restoring torque for a linear displacement α at radius r is $k \cdot \alpha \cdot r$,

i.e. $C =$ restoring torque per radian $= k \cdot r^2$.

Moment of inertia of weight W about axis of oscillation $= W \cdot R^2/g$.

$$\text{Hence, } F = 9.55 \sqrt{\frac{k r^2}{W \cdot R^2/g}} = 9.55 \cdot \frac{r}{R} \sqrt{\frac{k \cdot g}{W}}. \quad (11)$$

Note that the actual values of r and R are not required, provided the ratio r/R is known, and that the frequency

increases as the point of attachment of the spring is moved towards the weight.

If a second spring is attached to the lever as indicated by the dotted lines in Fig. 4(c), and if the initial tensions of the two springs are adjusted so that there is always some tension in the springs even when the lever is at either extremity of its motion, the restoring force for a linear displacement α is $2k \cdot \alpha$.

The frequency equation is then

$$F = 9.55 \cdot \frac{r}{R} \sqrt{\quad} \quad \text{vibs./min.} \quad \dots \quad (12)$$

If the masses of the lever and springs are not negligible, an approximate correction is to add the moment of inertia of the lever plus one-third the moment of inertia of the springs about the axis of oscillation to the moment of inertia of the weight, W , about the axis of oscillation.

EXAMPLE 2.—Obtain an expression for the natural frequency of torsional vibration of the system shown in Fig. 4(a) in terms of the total shaft stiffness between the fixed ends and the ratio of the stiffnesses of the portions of shaft on either side of the flywheel.

Let C = total shaft stiffness,
 R = ratio of stiffnesses = C_2/C_1 .

If a torque T is applied at one end of a shaft of torsional rigidity (i.e. stiffness), C , the resulting twist is

$\theta = T/C$ radians,
 or $\theta_1 = T/C_1$, and $\theta_2 = T/C_2$,
 but $\theta = (\theta_1 + \theta_2)$.

Hence, $1/C = (1/C_1 + 1/C_2)$, or $C = \frac{C_1 \cdot C_2}{C_1 + C_2}$,

and since $C_2 = R \cdot C_1$,

$$C = \frac{R \cdot C_1}{(1 + R)}, \text{ i.e. } C_1 = \frac{(1 + R)C}{R}$$

From Equation (8), $F = 9.55 \sqrt{\frac{C_1 + C_2}{J}} = 9.55 \sqrt{\frac{C_1(1 + R)}{J}}$,

or, by inserting the above value for C_1 in terms of C , and rearranging,

$$F = 9.55(1 + R)\sqrt{\frac{C}{R \cdot J}} \text{ vibs./min.}$$

If the flywheel is placed at the middle of a plain shaft, i.e. if $C_1 = C_2$ or $R = 1$, the frequency equation becomes

$$F = 19.1\sqrt{C/J} \text{ vibs./min.}$$

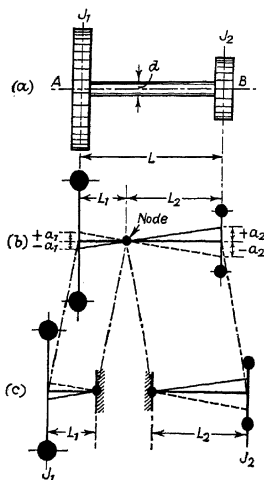


FIG. 5.—Two-mass system.

This is the lowest frequency which can be obtained by altering the position of the flywheel in Fig. 4(a), and is twice the frequency of the system shown in Fig. 1, where the flywheel is fixed to the free end of a shaft which is secured against rotation at the other end.

If the flywheel in Fig. 4(a) is moved in either direction from the mean position the frequency increases, as shown by the above equation.

Two-Mass Systems.—Fig. 5 shows a simple two-mass system consisting of a length of shafting with a heavy disc at each end.

In this case, if the shaft is supported in frictionless bearings which permit rotary motion and the discs are given small angular twists in opposite directions and then released, the system will be put into a state of torsional vibration.

At any instant when the disc at end A is moving in a clockwise direction, the disc at B is moving in a counter-clockwise direction so that the node or point where there is no vibratory disturbance is situated somewhere between the two discs.

The system can therefore be reduced to two simple one-mass systems, as shown at (c) in Fig. 5.

In the case of a shaft transmitting power, provided the applied and resisting torques are perfectly uniform, and the attached masses have a constant moment of inertia about the axis of rotation, the only effect of the elasticity of the shaft is to cause the end from which power is taken to lag behind the end at which power is applied. Under these conditions there is nothing to excite vibration once the shaft has taken up the initial torsional deflection corresponding to the torque transmitted, and as soon as any initial vibrations caused by setting the system in motion have been damped out the motion becomes uniform.

It does not, however, require a very high degree of torque variation, either at the driving end or at the driven end of the shaft to set up and sustain torsional vibration, particularly at speeds where the frequency of the periodic torque variations coincides with the natural frequency of torsional vibration of the system. These vibrations are quite independent of the steady rotation of the shaft, and for practical purposes the shaft may be assumed to be at rest and the system to be oscillating about the node.

Referring to Fig. 5, let

J_1 = moment of inertia of disc at end A.

J_2 = moment of inertia of disc at end B.

L = length of shaft.

d = diameter of shaft.

L_1 = distance from end A to node.

L_2 = distance from end B to node.

Then, natural frequency of one-mass system to left of node, from Equation (6),

$$F_1 = \frac{1}{2 \cdot \pi} \sqrt{\frac{I_p \cdot G}{J_1 \cdot L_1}} \quad \cdot \quad \cdot \quad \cdot \quad (13)$$

Natural frequency of one-mass system to right of node, from Equation (6),

$$F_2 = \frac{1}{2 \cdot \pi} \sqrt{\frac{I_p \cdot G}{J_2 \cdot L_2}} \quad \dots \quad (14)$$

The natural frequency of the whole system is therefore

$$F = F_1 = F_2.$$

Hence,
$$\frac{1}{2 \cdot \pi} \sqrt{\frac{I_p \cdot G}{J_1 \cdot L_1}} = \frac{1}{2 \cdot \pi} \sqrt{\frac{I_p \cdot G}{J_2 \cdot L_2}},$$

and since π , I_p , and G are constants,

$$\frac{L_1}{L_2} = \frac{J_2}{J_1}, \quad \dots \quad (15)$$

i.e. the node divides the length of the shaft L inversely as the moments of inertia of the discs.

Also
$$L = (L_1 + L_2) = L_1 \left[1 + \frac{J_1}{J_2} \right]$$

or
$$L_1 = \left[\frac{J_2 \cdot L}{J_1 + J_2} \right].$$

Hence, finally, from Equation (13),

$$\begin{aligned} F &= \frac{1}{2 \cdot \pi} \sqrt{\frac{I_p \cdot G (J_1 + J_2)}{J_1 \cdot J_2 \cdot L}} \\ &= \frac{1}{2 \cdot \pi} \sqrt{\frac{C (J_1 + J_2)}{J_1 \cdot J_2}} \text{ vibs./sec.} \\ &= 9.55 \sqrt{\frac{C (J_1 + J_2)}{J_1 \cdot J_2}} \text{ vibs./min.,} \quad \dots \quad (16) \end{aligned}$$

where $C = G \cdot I_p =$ torsional rigidity of shaft.

It should be noted that if the moment of inertia of one of the discs is very large compared with that of the other disc, the node is situated very close to the larger disc, and when the moment of inertia of the larger disc can be considered as infinite compared with that of the other disc, the node is situated at the larger disc. The system shown in Fig. 5 then reduces to the simple one-mass system shown in Fig. 1.

A practical example of a system of this type is a light radial aeroplane engine direct-coupled to a very heavy airscrew.

When the moments of inertia of the two discs are identical, the node is situated mid-way between them, and the frequency equation reduces to

$$F = 9.55 \sqrt{\frac{2 \cdot C}{J}} \text{ vibs./min.} \quad (17)$$

where J is the polar moment of inertia of each disc.

Comparing this with Equation (7), it is seen that the effect of replacing the single heavy disc shown in Fig. 1 by two equal discs, each having the same moment of inertia as the single disc, one situated at each end of the shaft, is to increase the natural frequency of the system to

$$F = \sqrt{2} \cdot F'$$

where F' = natural frequency of system with single heavy disc,

F = natural frequency of system with two equal discs.

If the total moment of inertia remains unaltered, i.e. if the moment of inertia of each of the two end discs is one-half the moment of inertia of the single disc shown in Fig. 1, the natural frequency of the system is doubled, assuming that the shaft stiffness is unaltered.

To obtain the same frequency, the moment of inertia of each of the two end discs in Fig. 5 must be twice the moment of inertia of the single disc shown in Fig. 1, with the same shaft stiffness.

Alternatively, the shaft stiffness must be halved if the moment of inertia of each end disc in Fig. 5 is the same as the moment of inertia of the single disc shown in Fig. 1.

Correction for Mass of Shaft.—The mass of the shaft may be taken into account in the case of the system shown in Fig. 5 by adding one-third of the moment of inertia of the length L_1 between the node and end A to the moment of inertia of the disc at end A; and one-third of the moment of inertia of the length L_2 between the node and end B to the moment of inertia of the disc at end B.

EXAMPLE 3.—Calculate the natural frequency of torsional vibration of the system shown in Fig. 5, assuming the following dimensions :—

Moment of inertia of disc at A, $J_1 = 22,400$ lbs.-ins. sec.².

Moment of inertia of disc at B, $J_2 = 728$ lbs.-ins. sec.².

Length of shaft $L = 45$ ins.

Diameter of shaft $d = 7\frac{1}{4}$ ins.

(i) Assuming that the moment of inertia of the disc at end A is infinitely large compared with that of the disc at end B.

From Equation (7),

$$F = 9.55 \sqrt{\frac{C}{J_2}}$$

where $C = G \cdot I_p$ lbs.-ins. per radian,

$G = 12,000,000$ lbs. per sq. in.,

$I_p =$ polar moment of inertia of cross-section of shaft

$$= \frac{\pi \cdot d^4}{32} = \frac{3.1416 \times 7.25^4}{32}$$

$$= 271 \text{ ins.}^4,$$

i.e. $C = \frac{12000000 \times 271}{45} = 72,300,000$ lbs.-ins. per radian.

Hence, $F = 9.55 \sqrt{\frac{72300000}{728}}$
 $= 3010$ vibs./min.

(ii) Assuming a two-mass system.

From Equation (16),

$$\begin{aligned} F &= 9.55 \sqrt{\frac{C(J_1 + J_2)}{J_1 \cdot J_2}} \\ &= 9.55 \sqrt{\frac{72300000(22400 + 728)}{22400 \times 728}} \\ &= 3060 \text{ vibs./min.} \end{aligned}$$

The error involved in the assumption of a one-mass system is therefore only about $1\frac{1}{2}$ per cent. in this example.

Special Two-Mass Systems.—The following special two-mass systems are occasionally found in practice and can be handled by the torque summation method.

Fig. 6(a) shows a two-mass system consisting of a shaft fixed at one end and carrying two masses of moments of inertia J_1 and J_2 . The torsional rigidity of the portion of shaft between the fixed end and J_2 is C_2 , whilst between masses J_2 and J_1 it is C_1 .

The frequency equation is obtained as follows :—

$$\text{Torque to left of mass } J_1 = M_1 = 0,$$

$$\text{Angle of twist at mass } J_1 = a_1,$$

$$\text{Torque to right of mass } J_1 = M_2,$$

$$\text{where } M_2 = M_1 + \text{torque to accelerate mass } J_1 \\ = 0 + J_1 \omega^2 \cdot a_1,$$

$$\text{and } \omega = \text{phase velocity of the vibrations in radians per second}$$

$$= 2 \cdot \pi \cdot F,$$

$$F = \text{frequency of vibrations in vibs./sec.}$$

From Equation (1),

$$\text{Angle of twist between } J_1 \text{ and } J_2 = M_2/C_1 = \frac{J_1 \cdot \omega^2 \cdot a_1}{C_1}.$$

$$\text{Hence, angle of twist at mass } J_2 = a_2 = a_1 - \frac{J_1 \cdot \omega^2 \cdot a_1}{C_1}.$$

Torque to right of mass J_2

$$= M_3 = M_2 + \text{torque to accelerate mass } J_2$$

$$= J_1 \cdot \omega^2 \cdot a_1 + J_2 \cdot \omega^2 \left(a_1 - \frac{J_1 \cdot \omega^2 \cdot a_1}{C_1} \right).$$

Angle of twist between mass J_2 and fixed end

$$= \frac{J_1 \cdot \omega^2 \cdot a_1}{C_2} + \frac{J_2 \cdot \omega^2}{C_2} \left(a_1 - \frac{J_1 \cdot \omega^2 \cdot a_1}{C_1} \right).$$

Hence, angle of twist at fixed end = a_3 where

$$a_3 = a_1 - \frac{J_1 \cdot \omega^2 \cdot a_1}{C_1} - \frac{J_1 \cdot \omega^2 \cdot a_1}{C_2} - \frac{J_2 \cdot \omega^2}{C_2} \left(a_1 - \frac{J_1 \cdot \omega^2 \cdot a_1}{C_1} \right),$$

but twist at fixed end = 0, i.e. $a_3 = 0$; i.e. equating the above expression for a_3 to zero, dividing throughout by a_1 , and rearranging terms, the following frequency equation is obtained:—

$$1 - \omega^2 \left\{ \frac{J_1}{C_1} + \frac{J_1}{C_2} + \frac{J_2}{C_2} \right\} + \frac{J_1 \cdot J_2 \cdot \omega^4}{C_1 \cdot C_2} = 0. \quad (18)$$

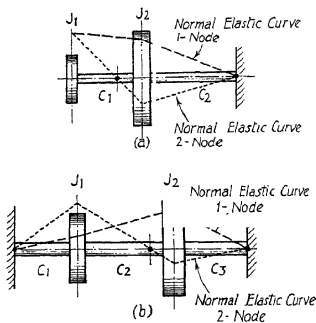


FIG. 6.—Special two-mass systems.

This equation has two roots, indicating two possible modes of vibration. Note that if $J_1 = 0$, the above expression reduces to

$$1 - \omega^2 \cdot J_2 / C_2 = 0, \quad \text{or} \quad \omega^2 = C_2 / J_2.$$

Similarly, if $J_2 = 0$, the above expression reduces to

$$1 - \omega^2 \cdot J_1 \left(\frac{C_1 + C_2}{C_1 \cdot C_2} \right) = 0, \quad \text{or} \quad \omega^2 = \frac{1}{J_1} \left(\frac{C_1 C_2}{C_1 + C_2} \right).$$

The last two expressions are the frequency equations for a simple torsional pendulum.

Also, if $J_1 = J_2 = J$, and $C_1 = C_2 = C$, Equation (18) becomes

$$1 - \frac{3J \cdot \omega^2}{C} + \frac{J^2 \cdot \omega^4}{C^2} = 0,$$

and the roots of this equation are

$$\omega^2 = 0.382 \cdot C/J \quad \text{or} \quad 2.618 \cdot C/J.$$

Fig. 6(b) shows a two-mass system in which a shaft is fixed at both ends and two masses of moments of inertia, J_1 and J_2 , are attached at positions which divide the shaft into three portions of torsional rigidities, C_1 , C_2 , and C_3 .

The frequency equation is obtained as follows:—

Torque to left of mass $J_1 = -M_o$, where $-M_o$ is the fixing couple at the left-hand end of the shaft.

Angle of twist at mass $J_1 = \frac{M_o}{C_1}$ (since angle of twist at fixed end is zero).

Torque to right of mass $J_1 = -M_o + \frac{J_1 \cdot \omega^2 \cdot M_o}{C_1}$.

Angle of twist between masses J_1 and J_2

$$= -\frac{M_o}{C_2} + \frac{J_1 \cdot \omega^2 \cdot M_o}{C_1 \cdot C_2}.$$

Angle of twist at mass $J_2 = \frac{M_o}{C_1} + \frac{M_o}{C_2} - \frac{J_1 \cdot \omega^2 \cdot M_o}{C_1 \cdot C_2}$.

Torque to right of mass J_2

$$= -M_o + \frac{J_1 \cdot \omega^2 \cdot M_o}{C_1} + J_2 \cdot \omega^2 \left\{ \frac{M_o}{C_1} + \frac{M_o}{C_2} - \frac{J_1 \cdot \omega^2 \cdot M_o}{C_1 \cdot C_2} \right\}.$$

Angle of twist between mass J_2 and right-hand end of shaft

$$= -\frac{M_o}{C_3} + \frac{J_1 \cdot \omega^2 \cdot M_o}{C_1 \cdot C_3} + \frac{J_2 \cdot \omega^2 \left\{ \frac{M_o}{C_1} + \frac{M_o}{C_2} - \frac{J_1 \cdot \omega^2 \cdot M_o}{C_1 \cdot C_2} \right\}}{C_3}.$$

Angle of twist at right-hand end of shaft

$$= \frac{M_o}{C_1} + \frac{M_o}{C_2} - \frac{J_1 \cdot \omega^2 \cdot M_o}{C_1 \cdot C_2} + \frac{M_o}{C_3} - \frac{J_1 \cdot \omega^2 \cdot M_o}{C_1 \cdot C_3} - \frac{J_2 \cdot \omega^2 \left\{ \frac{M_o}{C_1} + \frac{M_o}{C_2} - \frac{J_1 \cdot \omega^2 \cdot M_o}{C_1 \cdot C_2} \right\}}{C_3}.$$

But angle of twist at end of shaft is zero, hence the frequency equation is obtained by equating the above expression

to zero. Dividing through by the common factor M_o , and rearranging terms, the frequency equation becomes

$$\left\{ \frac{I}{C_1} + \frac{I}{C_2} + \frac{I}{C_3} \right\} - \omega^2 \left[\frac{J_2}{C_2} \left(\frac{I}{C_1} + \frac{I}{C_2} \right) + \frac{J_2}{C_1} \left(\frac{I}{C_2} + \frac{I}{C_3} \right) \right] + \frac{J_1 \cdot J_2 \cdot \omega^4}{C_1 \cdot C_2 \cdot C_3} = 0 \quad (18a)$$

This equation has two roots, indicating that there are two possible modes of vibration.

Note that if $J_1 = 0$, and $\frac{I}{C_1} + \frac{I}{C_2} = \frac{I}{C}$ (where C is the torsional rigidity of the portion of shaft between the left-hand end and mass J_2), then the frequency equation reduces to

$$\left\{ \frac{I}{C} + \frac{I}{C_3} \right\} - \omega^2 \left\{ \frac{J_2}{C \cdot C_3} \right\} = 0,$$

or
$$\omega^2 = \frac{C + C_3}{J_2},$$

which is the same form as Equation (8).

Also, if $C_1 = C_2 = C_3 = C$, and $J_1 = J_2 = J$, the frequency equation becomes

$$3 - \frac{4J \cdot \omega^2}{C} + \frac{J^2 \cdot \omega^4}{C^3} = 0.$$

The roots of this equation are

$$\omega^2 = \frac{C}{J} \quad \text{or} \quad \frac{3C}{J}.$$

The foregoing methods can be applied to systems having more than two masses, but the resulting frequency equations are very cumbersome, and their solution is tedious. It is preferable to deal with multi-mass systems by the tabulation method described later.

Three-Mass Systems.—Fig. 7 shows a simple three-mass system consisting of three heavy discs of moments of inertia J_1 , J_2 , and J_3 , connected together by two lengths of elastic shafting of torsional rigidity C_1 and C_2 .

The mass of the shafts is assumed to be negligible compared with that of the discs.

Let ω = phase velocity of the vibrations in radians per second
 $= 2 \cdot \pi \cdot F$,
 F = frequency of vibration in vibs./sec.,
 a_1 = maximum amplitude of vibration at mass J_1 in radians.

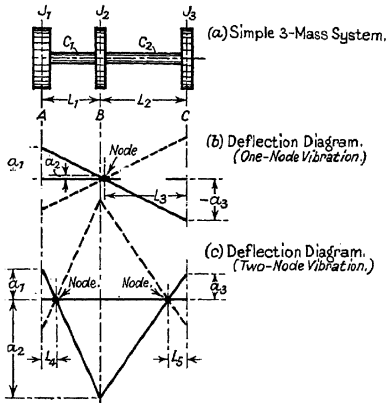


FIG. 7.—Three-mass system.

For equilibrium at the instant when the system is at the position of maximum displacement the elastic resisting torques due to twisting the shafts must exactly balance the torques due to the movements of the masses, since when a system is performing free torsional vibrations no external torques are required to keep it in motion,

i.e. torque to left of mass $J_1 = M_1 = 0$,
 angle of twist at mass $J_1 = a_1$,
 torque to right of mass $J_1 = M_2$,

where $M_2 = M_1 +$ maximum torque to accelerate mass J_1
 $= 0 + J_1 \cdot \omega^2 \cdot a_1$.

From Equation (1),

$$\text{Angle of twist between } J_1 \text{ and } J_2 = \frac{M_2}{C_1} = \frac{J_1 \cdot \omega^2 \cdot a_1}{C_1}$$

Hence, angle of twist at mass $J_2 = a_1 - \frac{J_1 \cdot \omega^2 \cdot a_1}{C_1} = a_2$.

Torque to right of mass $J_2 = M_3$,

$$\begin{aligned} \text{where } M_3 &= M_2 + \text{maximum torque to accelerate mass } J_2 \\ &= J_1 \cdot \omega^2 \cdot a_1 + J_2 \cdot \omega^2 \left[a_1 - \frac{J_1 \cdot \omega^2 \cdot a_1}{C_1} \right] \\ &= \omega^2 (J_1 \cdot a_1 + J_2 \cdot a_1) - \frac{\omega^4 \cdot J_1 \cdot J_2 \cdot a_1}{C_1} \end{aligned}$$

Angle of twist at mass J_3 ,

$$\begin{aligned} a_3 &= a_1 - \frac{J_1 \cdot \omega^2 \cdot a_1}{C_1} - \left[\frac{\omega^2 (J_1 \cdot a_1 + J_2 \cdot a_1) - \frac{\omega^4 \cdot J_1 \cdot J_2 \cdot a_1}{C_1}}{C_2} \right] \\ &= a_1 - \omega^2 \left[\frac{J_1 \cdot a_1}{C_1} + \frac{J_1 \cdot a_1}{C_2} + \frac{J_2 \cdot a_1}{C_2} \right] + \frac{\omega^4 \cdot J_1 \cdot J_2 \cdot a_1}{C_1 \cdot C_2} \end{aligned}$$

Torque to right of mass $J_3 = M_4$,

where

$$\begin{aligned} M_4 &= M_3 + \text{maximum torque to accelerate mass } J_3 \\ &= \omega^2 (J_1 \cdot a_1 + J_2 \cdot a_1) - \frac{\omega^4 \cdot J_1 \cdot J_2 \cdot a_1}{C_1} + J_3 \cdot \omega^2 \cdot a_1 \\ &\quad - \omega^4 \left[\frac{J_1 \cdot J_3 \cdot a_1}{C_1} + \frac{J_1 \cdot J_3 \cdot a_1}{C_2} + \frac{J_2 \cdot J_3 \cdot a_1}{C_2} \right] \\ &\quad + \frac{\omega^6 \cdot J_1 \cdot J_2 \cdot J_3 \cdot a_1}{C_1 \cdot C_2} \end{aligned}$$

and, since there are no external torques acting on the system,
 $M_4 = 0$,

$$\begin{aligned} \text{i.e. } \omega^2 \cdot a_1 (J_1 + J_2 + J_3) \\ - \omega^4 \cdot a_1 \left[\frac{J_1 \cdot J_2}{C_1} + \frac{J_1 \cdot J_3}{C_1} + \frac{J_1 \cdot J_3}{C_2} + \frac{J_2 \cdot J_3}{C_2} \right] \\ + \frac{\omega^6 \cdot a_1 \cdot J_1 \cdot J_2 \cdot J_3}{C_1 \cdot C_2} = 0. \end{aligned}$$

Divide through by $\omega^2 \cdot a_1$,

$$(J_1 + J_2 + J_3) - \omega^2 \left[\frac{J_1 \cdot J_2}{C_1} + \frac{J_1 \cdot J_3}{C_1} + \frac{J_1 \cdot J_3}{C_2} + \frac{J_2 \cdot J_3}{C_2} \right] + \frac{\omega^4 \cdot J_1 \cdot J_2 \cdot J_3}{C_1 \cdot C_2} = 0, \quad (19)$$

where $C_1 = \frac{G \cdot I_p}{L_1}$ and $C_2 = \frac{G \cdot I_p}{L_2}$,
 G = modulus of rigidity,
 I_p = polar moment of inertia of cross-section of shaft = $\frac{\pi \cdot d^4}{32}$,
 d = diameter of shaft,
 L_1 and L_2 = lengths of shaft between masses.

It should be noted that if any one of the masses is assumed to have zero moment of inertia, Equation (19) reduces to the expression already determined for a two-mass system, Equation (16).

Thus, if

$$J_1 = 0, \quad \omega^2 = \frac{C_2(J_2 + J_3)}{J_2 \cdot J_3},$$

$$\text{if } J_3 = 0, \quad \omega^2 = \frac{C_1(J_1 + J_2)}{J_1 \cdot J_2},$$

$$\text{if } J_2 = 0, \quad \omega^2 = \frac{C_1 C_2 (J_1 + J_3)}{(C_1 + C_2) J_1 \cdot J_3} = \frac{C(J_1 + J_3)}{J_1 \cdot J_3},$$

where $\frac{C_1}{(C_1 + C_2)} = C$, the torsional rigidity of the whole of the shafting between masses J_1 and J_3 .

Equation (19) has two real roots, so that there are two principal modes of vibration of a simple three-mass system.

The first or fundamental mode of vibration occurs when one of the end masses moves in one direction whilst the other two masses move in the opposite direction, i.e. there is a node somewhere between one of the end masses and the other two masses. The fundamental mode of vibration may therefore be defined as vibration with one node.

The second mode of vibration occurs when the two end masses move in one direction whilst the centre mass moves in the opposite direction, i.e. there are two nodes, one between each end mass and the centre mass. This second mode of vibration may therefore be defined as vibration with two nodes.

The positions of the nodal points can be determined from the expression for the angles of twist at the masses.

Thus

$$\frac{a_2}{a_1} = 1 - \frac{J_1 \cdot \omega^2}{C_1} \quad \dots \quad (20)$$

and
$$\frac{a_3}{a_1} = 1 - \omega^2 \left[\frac{J_1}{C_1} + \frac{J_1}{C_2} + \frac{J_2}{C_2} \right] + \frac{\omega^4 \cdot J_1 \cdot J_2}{C_1 \cdot C_2} \quad \dots \quad (21)$$

Since the mass of the shafting was assumed to be negligible, the deflection curve consists of straight lines, as shown in Fig. 7, so that the positions of the nodes can be obtained by assuming unit amplitude at mass J_1 and setting down the values of a_2 and a_3 given by Equations (20) and (21) at masses J_2 and J_3 respectively. The nodes are situated at the points where the deflection curve crosses the axis of the shaft.

A special case arises when the three discs have equal moments of inertia, and the torsional rigidities of the two sections of shafting are also equal.

In this case the frequency equation reduces to

$$\omega^2 = \frac{C}{J} \quad \text{or} \quad \frac{3 \cdot C}{J},$$

where $J = J_1 = J_2 = J_3$, and $C = C_1 = C_2$,

i.e. for the fundamental or one-node frequency

$$F = \frac{60 \cdot \omega}{2 \cdot \pi} = 9 \cdot 55 \sqrt{\frac{C}{J}} \text{ vibs./min.}$$

This is the same as Equation (7), indicating that the node is situated at mass J_2 .

For the two-node vibration

$$F = 9 \cdot 55 \quad \text{vibs./min.,}$$

i.e. the two-node frequency is $\sqrt{3}$ times the one-node frequency in this case.

The amplitudes of vibration, assuming unit amplitude at mass J_1 , are

$$\text{At mass } J_2, \quad a_2 = 1 - \frac{J \cdot C}{C \cdot J} = 0, \text{ i.e. the node is at mass } J_2 \text{ for the one-node frequency,}$$

$$\text{or} \quad a_2 = 1 - \frac{3 \cdot J \cdot C}{C \cdot J} = -2 \text{ for the two-node frequency.}$$

$$\text{At mass } J_3, \quad a_3 = 1 - \frac{3 \cdot J \cdot C}{C \cdot J} + \frac{J^2 \cdot C^2}{C^2 \cdot J^2} \\ = -1 \text{ for the one-node frequency,}$$

$$\text{or} \quad a_3 = 1 - \frac{1 \cdot J \cdot C}{C \cdot J} + \frac{9 \cdot J^2 \cdot C^2}{C^2 \cdot J^2} \\ = 1 \text{ for the two-node frequency.}$$

EXAMPLE 4.—Calculate the natural frequencies of torsional vibration of a system consisting of three flywheels A, B, and C (Fig. 7), weighing 2000 lbs., 1000 lbs., and 1500 lbs. respectively. The radius of gyration of each flywheel is 20 ins., and the shaft connecting A to B is 3 ins. diameter and 20 ins. long, whilst the shaft connecting B to C is 3 ins. diameter and 30 ins. long.

Also calculate the relative amplitudes of vibration at each flywheel for the two principal modes of vibration. In this example

$$J_1 = \frac{W \cdot K^2}{g} = \frac{2000 \times 20^2}{386} = 2073 \text{ lbs.-ins. sec.}^2,$$

$$J_2 = \frac{1000 \times 20^2}{386} = 1036 \text{ lbs.-ins. sec.}^2,$$

$$J_3 = \frac{1500 \times 20^2}{386} = 1554 \text{ lbs.-ins. sec.}^2,$$

$$C_1 = G \cdot I_x$$

where

$G = 12,000,000$ lbs. per sq. in. for steel,

$$I_p = \frac{\pi \cdot d^4}{32} = \frac{3 \cdot 1416 \times 3^4}{32} = 7.95 \text{ ins.}^4,$$

$L =$ length of shaft in inches,

$$\text{i.e. } C_1 = \frac{12000000 \times 7.95}{20} = 4,770,000 \text{ lbs.-ins. per radian,}$$

$$C_2 = \frac{12000000 \times 7.95}{30} = 3,180,000 \text{ lbs.-ins. per radian.}$$

The natural frequencies are obtained from Equation (19),

$$(J_1 + J_2 + J_3) - \omega^2 \left[\frac{J_1 \cdot J_2}{C_1} + \frac{J_1 \cdot J_3}{C_1} + \frac{J_1 \cdot J_3}{C_2} + \frac{J_2 \cdot J_3}{C_2} \right] + \frac{\omega^4 \cdot J_1 \cdot J_2 \cdot J_3}{C_1 \cdot C_2} = 0, \quad (19)$$

$$\text{i.e. } (2073 + 1036 + 1554)$$

$$- \omega^2 \left[\frac{2073 \times 1036}{4770000} + \frac{2073 \times 1554}{4770000} + \frac{2073 \times 1554}{3180000} + \frac{1036 \times 1554}{3180000} \right] + \frac{\omega^4 \times 2073 \times 1036 \times 1554}{4770000 \times 3180000} = 0,$$

$$\text{or } 4663 - 2.6471 \times \omega^2 + 0.00022 \times \omega^4 = 0.$$

Now, the roots of the expression

$$a \cdot m^2 + b \cdot m + c = 0$$

are

$$m = \frac{-b \pm \sqrt{b^2 - 4 \cdot a \cdot c}}{2 \cdot a},$$

and in this case $m = \omega^2$.

$$\text{Hence, } \omega^2 = \frac{2.6471 \pm \sqrt{2.6471^2 - 4 \times 4663 \times 0.00022}}{2 \times 0.00022}$$

$$= \frac{2.6471 \pm 99.10}{0.00044}$$

$$\omega = 46.4 \text{ or } 99.5 \text{ radians per sec.,}$$

$$F = \frac{60 \times \omega}{2 \times \pi} = 443 \text{ or } 947 \text{ vibs./min.}$$

Relative Amplitudes.

At mass J_2 (Equation 20),

$$\frac{a_2}{a_1} = 1 - \frac{J_1 \cdot \omega^2}{C_1}, \quad . \quad . \quad . \quad (20)$$

i.e. for one-node vibration,

$$\frac{a_2}{a_1} = 1 - \frac{2073 \times 2140}{4770000} = 0.070;$$

for two-node vibration,

$$\frac{a_2}{a_1} = 1 - \frac{2073 \times 9910}{4770000} = -3.307.$$

At mass J_3 (Equation 21),

$$\frac{a_3}{a_1} = 1 - \omega^2 \left[\frac{J_1}{C_1} + \frac{J_1}{C_2} + \frac{J_2}{C_2} \right] + \frac{\omega^4 \cdot J_1 \cdot J_2}{C_1 \cdot C_2}, \quad . \quad (21)$$

i.e. for one-node vibration,

$$\begin{aligned} \frac{a_3}{a_1} = 1 - 2140 \left[\frac{2073}{4770000} + \frac{2073}{3180000} + \frac{1036}{3180000} \right] \\ + \frac{4580000 \times 2073 \times 1036}{4770000 \times 3180000} = -1.372; \end{aligned}$$

for two-node vibration,

$$\begin{aligned} \frac{a_3}{a_1} = 1 - 9910 \left[\frac{2073}{4770000} + \frac{2073}{3180000} + \frac{1036}{3180000} \right] \\ + \frac{8210000 \times 2073 \times 1036}{4770000 \times 3180000} = 0.91. \end{aligned}$$

The deflection curves are shown in Fig. 7 for both one- and two-node modes of vibration.

The positions of the nodes can be obtained from the relative amplitudes as follows :-

(i) *For the One-node Mode of Vibration* (Fig. 7b).

The node is between mass B and mass C.

Let L_2 = length of shaft between B and C.

L_3 = distance of node from C, and assume that

$$a_1 = 1.$$

$$\begin{aligned} \text{Then } L_3 &= L_2 \left[\frac{a_3}{a_2 - a_3} \right] = \frac{30 \times 1.372}{0.070 + 1.372} \\ &= 28.54 \text{ ins.} \end{aligned}$$

(ii) *For the Two-node Mode of Vibration* (Fig. 7c).

Let L_1 = length of shaft between A and B,

L_4 = distance of one of the nodes from A, and assume that $a_1 = 1$.

$$\text{Then } L_4 = L_1 \left[\frac{a_1}{a_1 - a_2} \right] = \frac{20 \times 1}{1 + 3.307} = 4.64 \text{ ins.}$$

Let L_5 = distance of the other node from C.

$$\text{Then } L_5 = L_2 \left[\frac{a_3}{a_2 - a_3} \right] = \frac{30 \times 0.91}{3.307 + 0.91} = 6.53 \text{ ins.}$$

✓ **Multi-Mass Systems.**—The method just described can be extended to systems having four or more masses, but the frequency equations which are obtained are very cumbersome, and their solution is extremely tedious.

The tabulation method of dealing with multi-mass systems described in the next chapter is therefore a better practical way of carrying out the frequency calculations, and moreover is a convenient method for obtaining the relative amplitudes of vibration at the various masses.

In certain cases, especially where the masses form a symmetrical arrangement, a good approximation to the fundamental or one-node frequency of torsional vibration of multi-mass systems can be obtained by reducing the actual system to an equivalent two- or three-mass system.

Fig. 8 shows a seven-mass system treated in this way, the actual system being shown at (a), and the approximately equivalent three- and two-mass systems at (b) and (c) respectively. This arrangement is typical of marine installations, where the closely grouped engine masses J_1, J_2, J_3, J_4, J_5 , and J_6 are separated from the propeller mass J_7 by a long length of intermediate shafting.

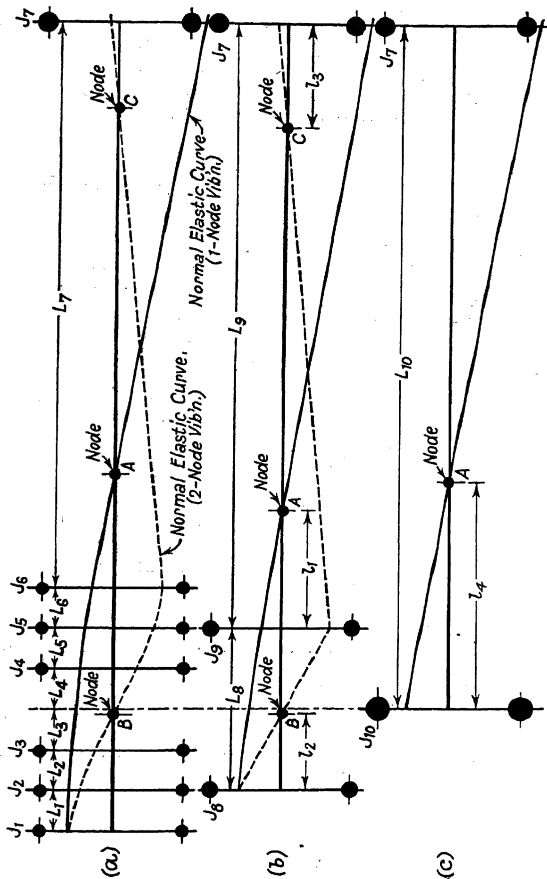


FIG. 8.—Seven-mass system.

EXAMPLE 5.—In Fig. 8a, let

$$\begin{aligned} J_1 = J_3 = J_4 = J_6 &= 44,000 \text{ lbs.-ins. sec.}^2, \\ J_2 = J_5 &= 22,000 \text{ lbs.-ins. sec.}^2, \\ J_7 &= 53,000 \text{ lbs.-ins. sec.}^2, \\ L_1 = L_2 = L_5 = L_6 &= 40 \text{ ins.}, \\ L_3 = L_4 &= 45 \text{ ins.}, \\ L_7 &= 7200 \text{ ins.}, \\ \text{diameter of shaft} = d &= 16\frac{3}{4} \text{ ins. throughout.} \end{aligned}$$

Then, Equivalent Three-Mass System (Fig. 8b),

$$\begin{aligned} J_8 = J_9 = (J_1 + J_2 + J_3) &= (J_4 + J_5 + J_6) \\ &= 110,000 \text{ lbs.-ins. sec.}^2, \\ J_7 &= 53,000 \text{ lbs.-ins. sec.}^2, \\ L_8 = (L_2 + L_3 + L_4 + L_5) &= 170 \text{ ins.}, \\ L_9 = (L_6 + L_7) &= 7240 \text{ ins.} \end{aligned}$$

Equivalent Two-Mass System (Fig. 8c),

$$\begin{aligned} J_{10} = (J_8 + J_9) &= 220,000 \text{ lbs.-ins. sec.}^2, \\ J_7 &= 53,000 \text{ lbs.-ins. sec.}^2, \\ L_{10} = (L_9 + \frac{1}{2} \cdot L_8) &= 7325 \text{ ins.} \end{aligned}$$

Natural Frequencies of Torsional Vibration.

(i) Two-Mass System (Fig. 8c).

In this case, from Equation (16),

$$F = 9.55 \sqrt{\frac{C_{10}(J_{10} + J_7)}{J_{10} \cdot J_7}} \text{ vibs./min.},$$

where

$$C_{10} = \frac{G \cdot I_p}{L_{10}},$$

I_p = polar moment of inertia of cross-section of shaft

$$= \frac{\pi \cdot d^4}{32} = \frac{3.1416 \times 16^4}{32} = 7750 \text{ ins.}^4,$$

$$\text{i.e. } C_{10} = \frac{12000000 \times 7750}{7325} = 12,700,000 \text{ lbs.-ins. per radian.}$$

Hence,

$$\begin{aligned} F &= 9.55 \sqrt{\frac{12700000(220000 + 53000)}{220000 \times 53000}} \\ &= 165 \text{ vibs./min.} \end{aligned}$$

Position of Node (Fig. 8c).

From Equation (15),

$$l_4 = \frac{J_7 \cdot L_{10}}{(J_7 + J_{10})} = \frac{53000 \times 7325}{(53000 + 220000)} \\ = 1420 \text{ ins.}$$

Also, if amplitude at $J_{10} = 1$, the amplitude at J_7 is

$$a_7 = \frac{1 \times (L_{10} - l_4)}{l_4} = \frac{1 \times (7325 - 1420)}{1420} \\ = -4.15.$$

(ii) *Three-Mass System* (Fig. 8b).

In this case, from Equation (19),

$$(J_8 + J_9 + J_7) - \omega^2 \left[\frac{J_8 \cdot J_9}{C_8} + \frac{J_8 \cdot J_7}{C_8} + \frac{J_8 \cdot J_7}{C_9} + \frac{J_9 \cdot J_7}{C_9} \right] \\ + \frac{\omega^4 \cdot J_8 \cdot J_9 \cdot J_7}{C_8 \cdot C_9} = 0,$$

where $C_8 = \frac{G \cdot I_p}{L_8} = \frac{12000000 \times 7750}{170} = 547,500,000 \text{ lbs.-ins. per radian.}$

$$C_9 = \frac{G \cdot I_p}{L_9} = \frac{12000000 \times 7750}{7240} = 12,850,000 \text{ lbs.-ins. per radian.}$$

Hence,

$$(110000 + 110000 + 53000) - \omega^2 \left[\frac{110000 \times 110000}{547500000} \right] \\ + \frac{110000 \times 53000}{547500000} + \frac{110000 \times 53000}{12850000} + \frac{110000 \times 53000}{12850000} \\ + \frac{\omega^4 \times 110000 \times 110000 \times 53000}{547500000 \times 12850000} = 0,$$

i.e. $273000 - 940 \times \omega^2 + 0.0912 \times \omega^4 = 0,$

$$\omega^2 = \frac{940 \pm \sqrt{940^2 - 4 \times 0.0912 \times 273000}}{2 \times 0.0912}$$

$$= 300 \text{ or } 10000,$$

$$\omega = 17.32 \text{ or } 100 \text{ radians per sec.,}$$

$$F = \frac{60 \times \omega}{2 \times \pi} = 165.5 \text{ or } 955 \text{ vibs./min.}$$

Relative Amplitudes and Positions of Nodes (Fig. 8b).

Let

a_8 = amplitude at J_8 ,

a_9 = amplitude at J_9 ,

a_7 = amplitude at J_7 .

Then from Equation (20),

$$\frac{a_9}{a_8} = 1 - \frac{J_8 \cdot \omega^2}{C_8}.$$

For one-node vibrations : $\omega^2 = 300$,

$$\frac{a_9}{a_8} = 1 - \frac{110000 \times 300}{547500000} = 0.9395.$$

For two-node vibrations : $\omega^2 = 10,000$,

$$\frac{a_9}{a_8} = 1 - \frac{110000 \times 10000}{547500000} = -1.01.$$

From Equation (21),

$$\frac{a_7}{a_8} = 1 - \omega^2 \left(\frac{J_8}{C_8} + \frac{J_8}{C_9} + \frac{J_9}{C_9} \right) + \frac{\omega^4 \cdot J_8 \cdot J_9}{C_8 \cdot C_9}.$$

For one-node vibrations : $\omega^2 = 300$,

$$\begin{aligned} \frac{a_7}{a_8} &= 1 - 300 \left[\frac{110000}{547500000} + \frac{110000}{12850000} + \frac{110000}{12850000} \right] \\ &\quad + \frac{300^2 \times 110000 \times 110000}{547500000 \times 12850000} \\ &= 1 - (300 \times 0.0173) + (300^2 \times 0.00000172) \\ &= -4.035. \end{aligned}$$

For two-node vibrations : $\omega^2 = 10000$,

$$\begin{aligned} \frac{a_7}{a_8} &= 1 - 10000 \times 0.0173 + 10000^2 \times 0.00000172 \\ &= 0. \end{aligned}$$

This value of $\frac{a_7}{a_8}$ indicates that there is a node at mass J_7 which is not correct. The actual value of $\frac{a_7}{a_8}$ obtained by the

tabulation method described in the next chapter is 0.021. The degree of accuracy necessary for obtaining the true value of this ratio when using the three-mass method cannot be obtained with the ordinary slide rule or four-figure logarithms.

Positions of Nodes (Fig. 8b).

Assuming that $a_8 = 1$, then

$$\begin{aligned} a_9 &= 0.9395 \text{ for one-node vibrations} \\ &= -1.01 \text{ for two-node vibrations,} \\ a_7 &= -4.035 \text{ for one-node vibrations.} \end{aligned}$$

For one-node vibrations, node at A in Fig. 8b,

$$l_1 = \frac{L_9 \times a_9}{(a_9 - a_7)} = \frac{7240 \times 0.9395}{(0.9395 + 4.035)} = 1365 \text{ ins.}$$

For two-node vibrations, nodes at B and C in Fig. 8b,

$$l_2 = \frac{L_8 \times a_8}{(a_8 - a_9)} = \frac{170 \times 1}{(1 + 1.01)} = 84.5 \text{ ins.}$$

l_3 cannot be obtained accurately by the three-mass method using the ordinary slide rule or four-figure logarithms.

SUMMARY.

Method.	Natural Frequency (Vibs./Min.).	
	One-Node.	Two-Node.
Two-mass .	165.0	—
Three-mass .	165.5	955
Tabulation .	165.5	1041

The above summary shows that in this case both the two-mass and the three-mass methods give close approximations to the value of the fundamental or one-node frequency of torsional vibration.

The two-node frequency cannot be calculated by the two-mass method; but an approximate value can be obtained by

using the three-mass method, the error in the present example being nearly 10 per cent.

In multi-mass systems there are as many principal modes of vibration as there are spaces between the masses, i.e. in the example shown in Fig. 8a there are seven masses, and therefore six principal modes of vibration. The natural

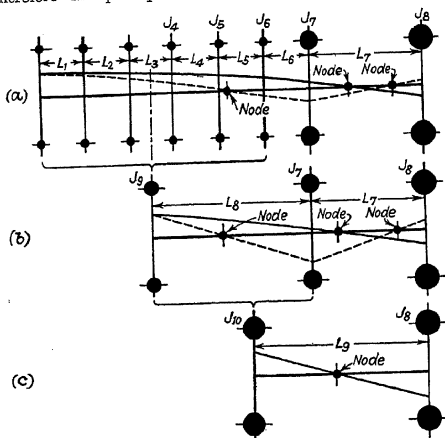


FIG. 9.—Multi-mass system.

frequencies corresponding to vibrations with three and more nodes cannot be calculated by the three-mass method.

The arrangement shown in Fig. 9 is similar to that shown in Fig. 8, except that there are eight masses instead of seven. This arrangement is typical of a marine installation having six closely grouped cylinder masses J_1 to J_6 ; a heavy flywheel J_7 , immediately after the last cylinder mass J_6 ; and the propeller mass J_8 .

The equivalent two-mass and three-mass systems are obtained as already described, care being taken to allow for the difference in the moments of inertia of J_9 and J_7 in determining the equivalent length L_9 for the two-mass system.

Thus, in Fig. 9b—three-mass system,

$$J_9 = (J_1 + J_2 + J_3 + J_4 + J_5 + J_6),$$

$$L_9 = (\frac{1}{2}L_3 + L_4 + L_5 + L_6).$$

In Fig. 9c—two-mass system,

$$J_{10} = (J_9 + J_7),$$

$$L_9 = L_7 + \frac{L_9 \cdot J_9}{(J_9 + J_7)}.$$

The approximate values of the one- and two-node natural frequencies of torsional vibration; the relative amplitudes of vibration at the various masses; and the positions of the nodes are then determined from the equivalent two- and three-mass systems exactly as already described.

The arrangement shown in Fig. 10 differs from that shown in Fig. 8, since there is only a short length of shafting between masses J_6 and J_7 .

This arrangement is typical of multi-cylinder oil engines direct-coupled to electrical generators where the flywheel effect necessary for satisfactory electrical operation is either incorporated in the rotating parts of the dynamo itself or where an auxiliary flywheel is so rigidly connected to the dynamo armature that the two can be regarded as one large mass.

EXAMPLE 6.—In Fig. 10a, let

$$J_1 = J_2 = J_3 = J_4 = J_5 = J_6 = 165 \text{ lbs.-ins. sec.}^2, \quad J_7 = 475$$

$$J_7 = 23,500 \text{ lbs.-ins. sec.}^2,$$

$$L_1 = L_2 = L_3 = L_4 = L_5 = 27 \text{ ins.},$$

$$L_6 = 32 \text{ ins.},$$

diameter of shaft $d = 8\frac{1}{4}$ ins. throughout.

(i) *Equivalent Three-Mass System* (Fig. 10b).

$$J_8 = J_9 = (J_1 + J_2 + J_3) = (J_4 + J_5 + J_6) = (165 + 165 + 165) = 495 \text{ lbs.-ins. sec.}^2,$$

$$J_7 = 23,500 \text{ lbs.-ins. sec.}^2,$$

$$L_7 = (L_2 + L_3 + L_4) = (27 + 27 + 27) = 81 \text{ ins.},$$

$$L_8 = (L_5 + L_6) = (27 + 32) = 59 \text{ ins.}$$

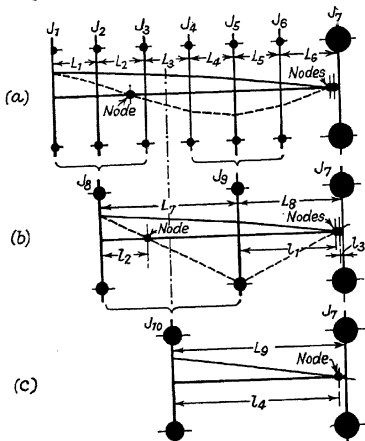


FIG. 10.—Multi-mass system (close-coupled).

Also
$$C_T = \frac{G \cdot I_p}{L_7},$$

where $G = 12000000 \text{ lbs. per sq. in.},$

$$I_p = \frac{\pi \cdot d^4}{32} = \frac{3 \cdot 1416 \times 8 \cdot 25^4}{32} = 455 \text{ ins.}^4$$

$$\text{i.e. } C_7 = \frac{12000000 \times 455}{81} = 67400000 \text{ lbs.-ins. per radian,}$$

$$C_8 = \frac{G \cdot I_p}{L_8} = \frac{12000000 \times 455}{59} = 92500000 \text{ lbs.-ins. per radian.}$$

Then, from equation (19),

$$(J_8 + J_9 + J_7) - \omega^2 \left[\frac{J_8 \cdot J_9}{C_7} + \frac{J_8 \cdot J_7}{C_7} + \frac{J_8 \cdot J_7}{C_8} + \frac{J_9 \cdot J_7}{C_8} \right] - \frac{\omega^4 \cdot J_8 \cdot J_9 \cdot J_7}{C_7 \cdot C_8} = 0.$$

$$(495 + 495 + 23500) - \omega^2 \left[\frac{495 \times 495}{67400000} + \frac{495 \times 23500}{67400000} + \frac{495 \times 23500}{92500000} + \frac{495 \times 23500}{92500000} \right] + \frac{\omega^4 \times 495 \times 495 \times 23500}{67400000 \times 92500000} = 0,$$

$$\text{or } 24490 - 0.4275 \times \omega^2 + 0.000000924 \times \omega^4 = 0,$$

$$\omega^2 = \frac{0.4275 \pm \sqrt{0.1830 - 0.0905}}{0.000001848}$$

$$= 67000 \text{ or } 396000,$$

$$\omega = 258.5 \text{ or } 629 \text{ radians/sec.},$$

$$F = \frac{60 \cdot \omega}{2 \cdot \pi} = 2470 \text{ or } 6000 \text{ vibs./min.}$$

Relative Amplitudes.

From Equation (20),

$$\frac{a_9}{a_8} = 1 - \frac{J_8 \cdot \omega^2}{C_7},$$

i.e. for one-node vibrations,

$$\frac{a_9}{a_8} = 1 - \frac{495 \times 67000}{67400000} = 1 - 0.490 = 0.510;$$

for two-node vibrations,

$$\frac{a_9}{a_8} = 1 - \frac{495 \times 396000}{67400000} = 1 - 2.910 = -1.910.$$

From Equation (21),

$$\frac{a_7}{a_8} = 1 - \omega^2 \left[\frac{J_8}{C_7} + \frac{J_8}{C_8} + \frac{J_9}{C_8} \right] + \frac{\omega^4 \cdot J_8 \cdot J_9}{C_7 \cdot C_8}.$$

For one-node vibrations,

$$\begin{aligned} \frac{a_7}{a_8} &= 1 - 66800 \left[\frac{495}{67400000} + \frac{495}{92500000} + \frac{495}{92500000} \right] \\ &\quad + \frac{66800^2 \times 495 \times 495}{67400000 \times 92500000} \\ &= 1 - (66800 \times 0.00001805) + \frac{66800^2}{25450000000} \\ &= 1 - 1.2050 + 0.1750 = -0.0300. \end{aligned}$$

For two-node vibrations,

$$\begin{aligned} \frac{a_7}{a_8} &= 1 - 396000 \times 0.00001805 + \frac{396000^2}{25450000000} \\ &= 1 - 7.15 + 6.15 = 0. \end{aligned}$$

The actual value of $\frac{a_7}{a_8}$ is 0.0096 (obtained by the tabulation method described in the next chapter), but the accuracy necessary for obtaining the true value of this ratio cannot be obtained with the three-mass method when using the ordinary slide rule or four-figure logarithms.

Positions of Nodes (Fig. 10b).

Assume that $a_8 = 1$, then for one-node vibrations,

$$l_1 = \frac{L_8 \times a_9}{(a_9 - a_7)} = \frac{59 \times 0.510}{(0.510 + 0.0300)} = 55.5 \text{ ins.}$$

For two-node vibrations,

$$l_2 = \frac{L_7 \times a_8}{(a_8 - a_9)} = \frac{81 \times 1}{(1 + 1.91)} = 27.8 \text{ ins.}$$

l_3 cannot be obtained accurately by the three-mass method, using the ordinary slide rule or four-figure logarithms.

(ii) *Equivalent Two-Mass System* (Fig. 10c).

$$J_{10} = (J_8 + J_9) = (495 + 495) = 990 \text{ lbs.-ins. sec.}^2,$$

$$J_7 = 23500 \text{ lbs.-ins. sec.}^2,$$

$$L_9 = (L_8 + \frac{1}{2}L_7) = (59 + 40.5) = 99.5 \text{ ins.},$$

$$\text{and } C_9 = \frac{G \cdot I_p}{L_9} = \frac{12000000 \times 455}{99.5} \\ = 54850000 \text{ lbs.-ins. per radian.}$$

Then from Equation (16),

$$F = 9.55 \sqrt{\frac{C_9(J_{10} + J_7)}{J_{10} \cdot J_7}} \\ = 9.55 \sqrt{\frac{54850000 (990 + 23500)}{990 \times 23500}} \\ = 2290 \text{ vibs./min.}$$

Position of Node (Fig. 10c).

$$l_4 = \frac{J_7 \cdot L_9}{(J_7 + J_{10})} = \frac{23500 \times 99.5}{(23500 + 990)} \\ = 95.5 \text{ ins.,}$$

and if amplitude at mass $J_{10} = 1$,

$$\text{amplitude at mass } J_7 = 1 \times \frac{(L_9 - l_4)}{l_4} = 1 \times \frac{(99.5 - 95.5)}{95.5} \\ = 0.042.$$

SUMMARY.

Method.	Natural Frequency (Vibs./Min.).	
	One-Node.	Two-Node.
Two-mass .	2290	—
Three-mass .	2470	6000
Tabulation .	2520	7325

This summary shows that in this example the approximate values of the one- and two-node natural frequencies of torsional vibration determined by the two- and three-mass methods are

not so close to the actual values as in the case of the arrangement shown in Fig. 8.

In systems of this type, where there are several equally spaced minor masses direct-coupled to one large major mass, a closer approximation to the fundamental or one-node frequency can be obtained by means of the following correcting factor :—

$$\text{Let } F_1 = F/K,$$

where F = one-node frequency calculated by the two-mass method,

F_1 = corrected one-node frequency,

K = correcting factor which depends on the number of minor masses as follows :—

Number of Minor Masses.	1.	2.	3.	4.	5.	6.	∞ .
K	1.00	0.93	0.92	0.91	0.91	0.91	0.90

In the present example

$$F = 2290 \text{ vibs./min.}$$

The number of minor masses is 6, hence $K = 0.91$,

$$\text{i.e. } F_1 = \frac{2290}{0.91} = 2520 \text{ vibs./min.}$$

(see also Table 6).

The corrected value therefore agrees with the value obtained by the tabulation method.

In general, if the transmission shaft between a multi-cylinder engine and the driven machine is very much more flexible than the engine crankshaft, the crankshaft masses can be replaced by a single mass equal in magnitude to the sum of the crankshaft masses and located at the centre of the engine as shown in Fig. 8c. The fundamental or one-node natural frequency of torsional vibration can then be calculated from Equation (16) without much error.

The transmission system of a marine installation where the propeller is separated from the engine by a long length of intermediate shafting is an example of an arrangement of this type.

When the stiffness of the transmission shaft is increased so that it is comparable with the stiffness of the crankshaft, as in the case of multi-cylinder engines direct-coupled to electrical generators (Fig. 10), the error introduced by reducing the system to a simple two-mass arrangement is considerable.

This error can be minimised by introducing a correcting factor, the value of which depends on the number of engine cylinders and the relative stiffness of the crankshaft and the transmission shaft.

The value of the natural frequency of torsional vibration with two nodes cannot be obtained by the two-mass method, but an approximate value can be obtained by the three-mass method.

Since, however, the stiffness of the engine crankshaft, and the disposition of the crankshaft masses have considerable influence on the value of the two-node natural frequency, it is necessary to consider the whole of the crankshaft masses acting at their respective points in order to obtain a more exact solution.

The tabulation method described in the next chapter is a convenient way of carrying out the more exact calculation.

This method enables the natural frequencies of torsional vibration with one, two, or more nodes to be obtained for any given system, as well as the relative amplitudes of vibration at the different masses and the specific vibration stresses at different points in the shaft system.

The calculations can be carried out on a 10-inch slide rule with sufficient accuracy, and by adopting a standard form for the tabulation the work becomes automatic, which is an advantage from the point of view of drawing office routine.

Incidentally the data contained in the frequency tabulation is also required for the determination of vibration amplitudes and stresses.

CHAPTER 2.

NATURAL FREQUENCY CALCULATIONS.

It has already been shown that a shaft carrying a series of masses may have several modes of free vibration, which are usually distinguished by degree numbers, i.e. vibration with one node is referred to as of the first degree; vibration with two nodes as of the second degree, and so on.

In general, when there are several attached masses there are as many principal modes of vibration as there are spaces between the masses.

The number of free vibrations per minute increases progressively with the number of nodes, and in practice only the first two principal modes of vibration are usually investigated since the serious critical speeds associated with vibrations with three and more nodes are well above the operating speed range of the engine in all normal installations.

Fig. 11 shows the normal elastic curves corresponding to the four principal modes of torsional vibration of a typical five-mass system. Since there is only one mass on the right-hand side of the node nearest to the right-hand end of the equivalent system, the natural frequencies are inversely proportional to the square roots of the nodal distances L_1 , L_2 , L_3 , and L_4 .

Frequency Tabulation.—This method is based upon the work of Gumbel and others, and depends upon the following theoretical considerations.

Referring to Fig. 12, consider a length of plain circular shafting AB, free at the ends A and B, and with a line $m-n$ on the surface parallel to the axis when the shaft is unstrained.

When executing simple harmonic torsional vibrations, the shape of the line $m-n$ at the instant of rest at the extreme positions of vibration is shown by the dotted line m_1-n

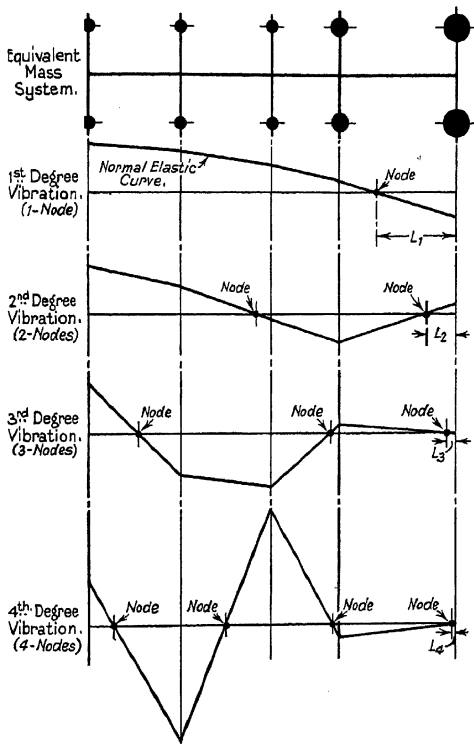


FIG. 11.—Principal modes of torsional vibration.

Consider a small section of the line m_1-n_1 of length dL , and let the angle of twist in length dL be $d\theta$ radians.

Then the *circumferential* movement of one end of line of length dL with respect to the other end is

$$da = R \cdot d\theta,$$

and the shear strain at surface is $\frac{R \cdot d\theta}{dL}$,

$$\text{or} \quad \frac{da}{dL} = R \cdot \frac{d\theta}{dL}.$$

Hence, shear stress, $f = \frac{da \cdot G}{dL}$.

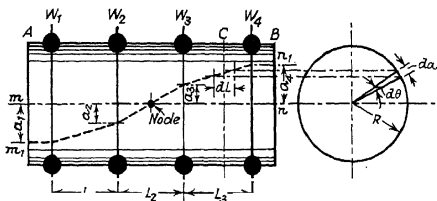


FIG. 12.—Torsional vibration.

But from Equation 1,

$$\frac{M}{I_p} = \frac{f}{R},$$

$$\text{or} \quad M = \frac{I_p}{R} \times G \times \frac{da}{dL}, \quad \dots \quad (22)$$

where M = torque and I_p = polar moment of inertia of cross-section of shaft.

Now consider a weight W lbs. on the surface of the shaft, radius R , executing simple harmonic torsional vibrations of linear amplitude a , and frequency $F = \frac{\omega}{2 \cdot \pi}$, where ω is the phase velocity of the vibration in radians per second. Then,

maximum linear acceleration of W at the extreme positions of the oscillations $= \omega^2 \times a$, ft./sec.²,

i.e. force on $W = \frac{W}{g} \times \omega^2 \times a$ lbs.

and torque on shaft $M = \frac{W}{g} \times \omega^2 \times a \times R$ lbs.-ft.
 $= \frac{I_p}{R} \times G \times \frac{da}{dL}$.

Now, assume that the shaft is reduced to an equivalent length of uniform diameter divided into sections, and that the weights of the shaft and its attachments are concentrated at these sections. If the weights are W_1, W_2, W_3 , etc., and are assumed to act at a common radius R , then

Maximum torque to right of W_1 due to oscillation of $W_1 = \frac{W_1}{g} \times \omega^2 \times a_1 \times R$,

Maximum torque to right of W_2 due to oscillation of $W_2 = \frac{W_2}{g} \times \omega^2 \times a_2 \times R$,

Maximum torque to right of W_1 and W_2 due to oscillation of W_1 and $W_2 = \frac{\omega^2 \cdot R}{g} \Sigma(W_1 \cdot a_1 + W_2 \cdot a_2)$.

For the whole length of the shaft, the torque to the right of the last weight, i.e. at B , due to the oscillation of all the masses is

$$M_A^B = \frac{\omega^2 \cdot R}{g} \sum_A^B W \cdot a. \quad (23)$$

Since the natural frequency of torsional oscillation corresponds to a condition of equilibrium between the elastic forces available from the deflection of the shaft, and the forces generated by the oscillating masses, the torques at the ends of the shaft, i.e. at A and at B , must be zero.

It has already been shown that

$$M = \frac{I_p \cdot G}{R} \times \frac{da}{dL}, \quad \dots \quad (22)$$

or slope $= \frac{da}{dL} = \frac{M \times R}{I_p \times G}$,

at surface of shaft, i.e. the torque is zero when the slope is zero.

At the end of the shaft

$$\frac{da}{dL} = \frac{\omega^2 \cdot R^2}{I_p \cdot G \cdot g} \sum_A W \cdot a \quad . \quad . \quad . \quad (24)$$

There are two unknowns in this equation, a and ω . Since a appears on both sides of the equation, its absolute value is immaterial, and may be assumed of any convenient magnitude.

ω must be chosen by trial and error, so that there is zero torque at the end of the shaft,

i.e. so that
$$\frac{\omega^2 \cdot R^2}{I_p \cdot G \cdot g} \sum_A W \cdot a = 0 \quad . \quad . \quad . \quad (25)$$

When this condition is fulfilled, the selected value of ω corresponds to one of the natural frequencies of torsional vibration and the frequency is

$$F = \frac{60 \times \omega}{2 \times \pi} \text{ vibs. per min.} \quad . \quad . \quad . \quad (26)$$

In the foregoing equations $\frac{WR^2}{g}$ is the moment of inertia of the masses about the axis of the shaft assumed concentrated at each section of the shaft.

If
$$J = \frac{WR^2}{g}$$

then slope at any section C is

$$\frac{da}{dL} = \frac{\omega^2}{I_p \cdot G} \sum^v J \cdot a \quad . \quad . \quad . \quad (27)$$

and for zero slope, and hence zero torque at the end of the shaft

$$\frac{\omega^2}{I_p \cdot G} \sum^v J \cdot a = 0 \quad . \quad . \quad . \quad (28)$$

The trial and error process of determining the natural frequencies of torsional vibration is best carried out by tabulation.

In Equation (27) a is the amplitude at the surface of the shaft, i.e. it is a linear amplitude.

Now $\theta = \text{angular amplitude} = a/R,$
 or $a = R \cdot \theta,$

i.e. Equation (27) can be written

$$\frac{da}{dL} = \frac{R}{I_p \cdot G} \sum_A^C J \cdot \omega^2 \cdot \theta.$$

From Equation (22)

$$M = \text{torque} = \frac{I_p \cdot G}{R} \cdot \frac{da}{dL}.$$

Hence, $M = \sum_A^B J \cdot \omega^2 \cdot \theta,$

and for zero torque at the end of the shaft,

$$\sum_A^B J \cdot \omega^2 \cdot \theta = 0. \quad . \quad . \quad . \quad (29)$$

This is the form which is used in the frequency tables.

Tables 1 to 4 are typical examples of the tabulation method applied to two different types of installation.

Tables 1 and 2 are the one- and two-node frequency calculations for the seven-mass system shown in Fig. 10. This arrangement is equivalent to a six-cylinder oil engine direct-coupled to an electrical generator in which the actual masses have been reduced to seven exact masses connected by sections of weightless shafting. The moments of inertia of the seven exact masses and the elasticities of the connecting shaft sections have been obtained by the methods to be explained in Chapter 3 so as to reproduce the dynamic and elastic properties of the actual system as closely as possible.

The following dimensions were assumed in building up Tables 1 and 2:—

Dimensions of engine: 6 cylinders, 4-stroke cycle, single-acting, 13½-in. bore × 18-in. stroke, 310 r.p.m., direct-coupled to a 275 kw. direct-current generator. The equivalent system is shown in Fig. 13.

Tables 1 and 2 are built up as follows: all calculations being made on an ordinary 10-inch slide-rule, using lbs., ins., seconds, units throughout.

TABLE 1.

FREQUENCY TABULATION: ONE-NODE VIBRATIONS.

2520 Vibs./Min.; $\omega = 264$ Radians/Sec.; $\omega^2 = 69,750$ Radians²/Sec.².

A	B	C	D	E	F	G	H	I	J	K
Mass.	Diameter of Shaft.	Equiv. Length of Shaft of Same Mat. as Shaft.	Moment of Inertia.	Torque per Unit Deflection.	Deflection in Plane of Mass.	Torque in Plane of Mass.	Total Torque.	Shaft Stiffness.	Change in Deflection.	Stress for 1 Degree Deflection at Mass No. r.
	d Ins.									
No. 1 cyl.	8 $\frac{1}{2}$	27	165	1.15 \times 10 ³	1.0000	1.1500 \times 10 ³	1.1500 \times 10 ³	20.2 \times 10 ³	0.0570	\pm 1820
No. 2 cyl.	8 $\frac{1}{2}$	27	165	1.15 \times 10 ³	0.9430	1.0850 \times 10 ³	2.2350 \times 10 ³	20.2 \times 10 ³	0.1105	\pm 3540
No. 3 cyl.	8 $\frac{1}{2}$	27	165	1.15 \times 10 ³	0.8325	0.9575 \times 10 ³	3.1925 \times 10 ³	20.2 \times 10 ³	0.1580	\pm 5040
No. 4 cyl.	8 $\frac{1}{2}$	27	165	1.15 \times 10 ³	0.6745	0.7750 \times 10 ³	3.9675 \times 10 ³	20.2 \times 10 ³	0.1965	\pm 6290
No. 5 cyl.	8 $\frac{1}{2}$	27	165	1.15 \times 10 ³	0.4780	0.5500 \times 10 ³	4.5175 \times 10 ³	20.2 \times 10 ³	0.2240	\pm 7150
No. 6 cyl.	8 $\frac{1}{2}$	32	165	1.15 \times 10 ³	0.2540	0.2920 \times 10 ³	4.8095 \times 10 ³	17.0 \times 10 ³	0.2833	\pm 7600
Generator	—	—	23,500	164.00 \times 10 ³	-0.0293	-4.8095 \times 10 ³	0	—	—	—

TABLE 2.

FREQUENCY TABULATION: TWO-NODE VIBRATIONS.

F = 7325 Vibs./Min.; $\omega = 767$ Radians/Sec.; $\omega^2 = 589,000$ Radians²/Sec.².

A	B	C	D	E	F	G	H	I	J	K
No. 1 cyl.	8 $\frac{1}{2}$	27	165	9.725 \times 10 ³	1.0000	9.725 \times 10 ³	9.725 \times 10 ³	20.2 \times 10 ³	0.4810	\pm 15350
No. 2 cyl.	8 $\frac{1}{2}$	27	165	9.725 \times 10 ³	0.5190	5.050 \times 10 ³	14.775 \times 10 ³	20.2 \times 10 ³	0.7310	\pm 23350
No. 3 cyl.	8 $\frac{1}{2}$	27	165	9.725 \times 10 ³	-0.2120	-2.060 \times 10 ³	12.715 \times 10 ³	20.2 \times 10 ³	0.6290	\pm 20100
No. 4 cyl.	8 $\frac{1}{2}$	27	165	9.725 \times 10 ³	-0.8410	-8.175 \times 10 ³	4.540 \times 10 ³	20.2 \times 10 ³	0.2250	\pm 7190
No. 5 cyl.	8 $\frac{1}{2}$	27	165	9.725 \times 10 ³	-1.0660	-10.350 \times 10 ³	-5.810 \times 10 ³	20.2 \times 10 ³	-0.2880	\pm 9175
No. 6 cyl.	8 $\frac{1}{2}$	32	165	9.725 \times 10 ³	-0.7780	-7.570 \times 10 ³	-13.380 \times 10 ³	17.0 \times 10 ³	-0.7876	\pm 21100
Generator	—	—	23,500	1385.000 \times 10 ³	0.0036	13.380 \times 10 ³	0	—	—	—

Column A.—This column gives a description of the various masses of the equivalent system (see Fig. 13).

Column B.—This column contains the diameters of the sections of shafting between the masses. In cases where the diameter of the shafting is not uniform throughout the system, it is usual to replace the actual lengths of shafting between each pair of masses by an equivalent length of shafting of some standard diameter such as the diameter of the crankshaft journals, as explained in Chapter 3.

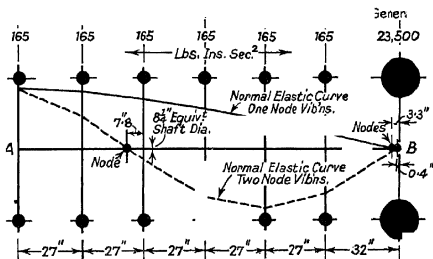


FIG. 13.—Equivalent system—direct-coupled generator.

Column C.—This column contains the equivalent lengths of the different sections of the shaft system, i.e. the lengths of standard diameter shafting having the same torsional rigidity as the corresponding lengths in the actual system (see Chapter 3).

Column D.—This column contains the moments of inertia of the various masses in lbs.-ins. sec.² units, calculated by the methods explained in Chapter 3.

Column E.—This column contains the products of the moments of inertia of the respective masses, and the square of the phase velocity of the vibration in radians/sec., i.e. the torque per unit deflection at each mass,

i.e.

$$M = J \cdot \omega^2 \cdot \theta \text{ lbs.-ins.} \\ = J \cdot \omega^2, \text{ when } \theta = 1 \text{ radian,}$$

or

$$(\text{column E}) = (\text{column D} \times \omega^2),$$

where ω = phase velocity of the vibration in radians/sec.

$$= \frac{2 \cdot \pi \cdot F}{60},$$

F = natural frequency in vibs./min.

The value of ω is assumed in the first instance until by trial and error a value is found which makes the last torque summation in column H zero. This value corresponds to one of the possible modes of free torsional vibration.

The final tables only need be recorded, i.e. Table 1 is the final table for the one-node frequency, and Table 2 that for the two-node frequency.

Column F.—This column contains the deflection at each mass starting with an assumed deflection of one radian at No. 1 mass, i.e. at the forward or free end of the crankshaft.

The deflections at other masses are obtained as the calculation proceeds by subtracting the change in deflection tabulated in column J from the corresponding value in column F, as follows :—

Deflection at No. 1 cyl. . . . = 1.0000 (line 1, col. F).

Change in defn. between cyls. 1 & 2 = 0.0570 (line 1, col. J).

Deflection at No. 2 cyl. . . . = 0.9430

This value is entered in line 2, column F.

Deflection at No. 2 cyl. . . . = 0.9430 (line 2, col. F).

Change in defn. between cyls. 2 & 3 = 0.1105 (line 2, col. J).

Deflection at No. 3 cyl. . . . = 0.8325

This value is entered in line 3, column F, and so on.

Column G.—This column contains the torques due to the oscillation of each mass, i.e. the products of columns E and F,

i.e. $M = J \cdot \omega^2 \cdot \theta$, lbs.-ins.

or (column G) = (column E) \times (column F).

Column H.—This column contains the total torque up to the next following mass, i.e. the algebraic sums of the torques tabulated in column G,

$$\begin{aligned} \text{i.e. (line 2, col. H)} &= (\text{line 1, col. H}) + (\text{line 2, col. G}) \\ &= 1.1500 \times 10^7 + 1.0850 \times 10^7 \\ &= 2.2350 \times 10^7. \end{aligned}$$

$$\begin{aligned} (\text{line 3, col. H}) &= (\text{line 2, col. H}) + (\text{line 3, col. G}) \\ &= 2.2350 \times 10^7 + 0.9575 \times 10^7 \\ &= 3.1925 \times 10^7, \text{ and so on.} \end{aligned}$$

The final value of the total torque is zero when the selected value of the angular velocity ω corresponds to one of the natural frequencies of torsional vibration.

Column I.—This column contains the torsional rigidities of the respective sections of the shaft system, calculated as follows:—

$$\begin{aligned} \text{Since} \quad & \frac{M}{I_n} = \frac{G \cdot \theta}{L}, \\ \text{or} \quad & M = \frac{G \cdot \theta \cdot I_p}{L} \end{aligned}$$

the torsional rigidity, i.e. the torque per unit deflection, is

$$C = \frac{G \cdot I_p}{L},$$

where G = modulus of rigidity in lbs. per sq. in.,
 I_p = polar moment of inertia of the cross-section of the shaft, in ins.⁴ units

$$= \frac{\pi \cdot d^4}{32},$$

d = equivalent diameter of shaft in inches (column B),

L = equivalent length of shaft in inches (column C).

In the present example,

$G = 12,000,000$ lbs. per sq. in., for mild steel,

$d = 8\frac{1}{2}$ ins. throughout,

$I_p = 455$ ins.⁴.

$$\text{Hence, } C = \frac{12000000 \times 455}{L} = \frac{546 \times 10^7}{L},$$

i.e. between cyls. 1 and 2, where $L = 27$ ins.,

$$C = \frac{546 \times 10^7}{27} = 20.2 \times 10^7 \text{ lbs.-ins./radian.}$$

This value is entered in line 1, column I.

Column J.—This column contains the change in deflection up to the next following mass, and is obtained by dividing the values in column H by the corresponding values in column I,

$$\begin{aligned} \text{i.e. } \quad \frac{d\theta}{dL} &= \frac{J \cdot \omega^2}{G \cdot I_p}, \\ \text{or } \quad d\theta &= \frac{J \cdot \omega^2 \cdot dL}{G \cdot I_p} = \frac{J}{C} \\ &= \frac{\text{column H}}{\text{column I}}. \end{aligned}$$

EXAMPLE.—

$$\begin{aligned} \text{Total torque between cyls. 1 and 2} \\ &= 1.1500 \times 10^7 \text{ (line 1, col. H).} \end{aligned}$$

$$\begin{aligned} \text{Torsional rigidity between cyls. 1 and 2} \\ &= 20.2 \times 10^7 \text{ (line 1, col. I).} \end{aligned}$$

$$\begin{aligned} \text{Change in deflection between cyls. 1 \& 2} &= \frac{1.1500 \times 10^7}{20.2 \times 10^7} \\ &= 0.0570 \text{ radian.} \end{aligned}$$

This value is entered in line 1, column J.

Column K.—This column contains the stress at each section of the shaft system for one-degree deflection at No. 1 cylinder, i.e. at end A in Fig. 13. Column K is completed after the natural frequency has been determined and the final values have been inserted in the frequency table.

The values contained in this column show the relative magnitudes of the vibration stresses at various sections of the shaft system, the diagrammatic representation of this specific stress variation being illustrated by Fig. 14.

The maximum vibration stresses occur at the nodes where

the slope of the normal elastic deflection curve is a maximum, and for the system shown in Fig. 13 the maximum values are ± 7600 and $\pm 23,350$ lbs. per sq. in. per one-degree amplitude at No. 1 cylinder for the one-node and two-node modes of vibration respectively, based on a shaft diameter of $8\frac{1}{4}$ ins.

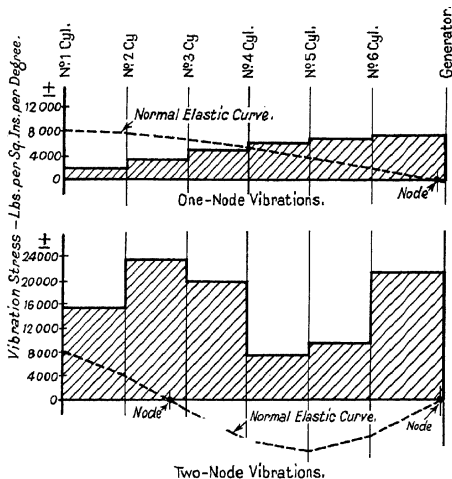


FIG. 14.—Vibration stresses per 1° deflection at No. 1 cylinder—direct-coupled generator.

The values in column K are obtained as follows :—

Since
$$\frac{M}{I_p} = \frac{2f}{a} \quad (\text{Eqn. 1}),$$

hence,
$$f = \frac{M \cdot a}{2 \cdot I_p} \text{ lbs. per sq. in.,}$$

where M = torque in lbs.-ins.,
 d = diameter of shaft in inches,
 I_p = polar moment of inertia of shaft cross-section
 in ins.⁴ units

$$I_p = \frac{\pi \cdot d^4}{32}$$

i.e. $f = \frac{16 \cdot M}{\pi \cdot d^3}$

The total torque acting in any given section of the shaft system is tabulated in column H in lbs.-ins. per radian deflection at No. 1 cylinder, and since 1 radian = 57.3 degrees, the total torque per 1-degree amplitude is

$$M = \pm \frac{(\text{values in column H})}{57.3}$$

or $f = \pm \frac{16 \times (\text{column H})}{57.3 \times \pi \times d_1^3}$
 $= \pm \frac{(\text{column H})}{11.25 \times d_1^3}$

In this equation d_1 is the *actual* diameter of the shaft at the respective sections of the shaft system, which may differ materially from the equivalent diameter used in setting down the equivalent system shown in Fig. 13.

Marine Installation.—Tables 3 and 4 contain the one-node and two-node frequency calculations for the marine installation shown in Fig. 15.

The engine dimensions are: 6 cylinders, 620 mm. bore \times 1300 mm. stroke, rated at 2750 B.H.P. and 138 r.p.m.

These tables are similar to Tables 1 and 2, except that the units are tons, feet, and seconds instead of lbs., ins., and seconds. It is generally preferable to work with the larger units in the case of large installations in order to obtain figures which are easily handled.

The following points should be noted in connection with Tables 3 and 4:—

Column B.—Enter shaft diameters in *feet*.

Column C.—Enter equivalent lengths of shaft in *feet*.

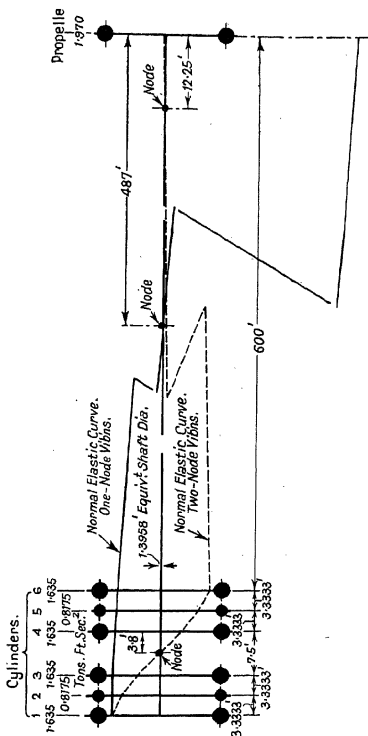


FIG. 15.—Equivalent system—marine installation.

Column D.—Enter moments of inertia of masses in *tons-ft. sec.²*.

Column I.—The torsional rigidity *C* must be expressed in *tons-ft. per radian*,

$$\text{i.e.} \quad C = \frac{G \cdot I_p}{L} \text{ tons-ft. per radian,}$$

where G = modulus of rigidity in *tons per sq. ft.*,
 I_p = polar moment of inertia of the cross-section
of the shaft in *feet⁴* units

$$= \frac{\pi \cdot d^4}{32},$$

d = equivalent diameter of shaft in *feet* (column
B),

L = equivalent length of shaft in *feet* (column **C**).

In the present Example

$G = 772,000$ tons per sq. ft., for mild steel,

$d = 1.3958$ ft. throughout,

$I_p = 0.373$ ft.⁴.

$$\text{Hence,} \quad C = \frac{772000 \times 0.373}{L} = \frac{288000}{L}.$$

Between cylinders 1 and 2, where $L = 3.3333$ ft.,

$$C = \frac{288000}{3.3333} = 86,500 \text{ tons-ft. per radian.}$$

This value is entered in line 1, column I.

Column K.—Since the total torques in column H are expressed in *tons-feet*, the expression for the stress per degree is

$$f = \frac{(\text{values in column H}) \times 2240 \times 12 \times 16}{\pi \times 57.3 \times d_1^3 \times 1728}$$

$$= \frac{1.38 \times (\text{column H})}{d_1^3} \text{ lbs. per sq. in.,}$$

where d_1 = *actual* diameter of the shaft in *feet*.

Fig. 16 shows the relative magnitudes of the vibration stresses at various sections of the shaft system, plotted from

TABLE 3.

FREQUENCY TABULATION: ONE-NODE VIBRATIONS.

 $F = 165.5$ Vibs./Min.; $\omega = 17.32$ Radians/Sec.; $\omega^2 = 300$ Radians²/Sec.².

A	B	C	D	E	F	G	H	I	J	K
Mass.	Diameter of Shaft.	Equivalent Length of Shaft of Diameter d .	Moment of Inertia.	Torque per Unit Deflection.	Deflection in Plane of Mass.	Torque in Plane of Mass.	Total Torque.	Shaft Stiffness.	Change in Deflection.	Stress for 1 Degree Deflection at Mass No. 1.
	d Feet.	L Feet.	J Tons-Ft. Sec. ²	$\frac{J \cdot \omega^2}{\text{Tons-Ft.}} / \text{Radian.}$	θ Radians.	$J \cdot \omega^2 \cdot \theta$ Tons-Ft.	$\sum J \cdot \omega^2 \cdot \theta$ Tons-Ft.	$C = G \cdot J_p / L$ Tons-Ft./Rad.	Col. H/Col. I Radians.	$1.98 \times \text{Col. H/Col. I}$ Lbs./Sq. In.
No. 1 cyl.	1.3958	3.3333	1.6350	490	1.0000	490	490	86,500	0.0057	± 676
No. 2 cyl.	1.3958	3.3333	0.8175	245	0.9943	244	734	86,500	0.0085	± 1010
No. 3 cyl.	1.3958	7.5000	1.6350	490	0.9858	484	1218	38,400	0.0317	± 1680
No. 4 cyl.	1.3958	3.3333	1.6350	490	0.9541	468	1686	86,500	0.0195	± 2325
No. 5 cyl.	1.3958	3.3333	0.8175	245	0.9346	229	1915	86,500	0.0222	± 2645
No. 6 cyl.	1.3958	600.0000	1.6350	490	0.9124	447	2362	480	4.9200	± 2650
Propeller	—	—	1.9700	591	-4.0076	-2362	0	—	—	—

TABLE 4.

FREQUENCY TABULATION: TWO-NODE VIBRATIONS.

 $F = 1041$ Vibs./Min.; $\omega = 109.1$ Radians/Sec.; $\omega^2 = 11,910$ Radians²/Sec.².

A	B	C	D	E	F	G	H	I	J	K
No. 1 cyl.	1.3958	3.3333	1.6350	19,480	1.0000	19,480	19,480	86,500	0.2252	± 9880
No. 2 cyl.	1.3958	3.3333	0.8175	9,740	0.7743	7540	27020	86,500	0.3122	± 13720
No. 3 cyl.	1.3958	7.5000	1.6350	19,480	0.4626	9010	35030	38,400	0.9390	± 18270
No. 4 cyl.	1.3958	3.3333	1.6350	19,480	-0.4764	-9270	26760	86,500	0.3090	± 13550
No. 5 cyl.	1.3958	3.3333	0.8175	9,740	-0.7854	-7650	19110	86,500	0.2210	± 9700
No. 6 cyl.	1.3958	600.0000	1.6350	19,480	-1.0064	-19603	-493	480	-1.0274	± 250
Propeller	—	—	1.9700	23,480	0.0210	493	0	—	—	—

the values contained in column K of the frequency tables. The maximum vibration stresses occur at the nodes, where the slope of the normal elastic curve is greatest. For the system shown in Fig. 15 the greatest vibration stress occurs in the intermediate shaft for one-node vibrations, and in the crankshaft for two-node vibrations. The values in column K of Table 3 are therefore based on the intermediate shaft diameter

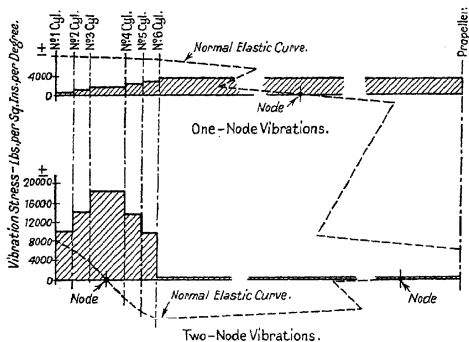


FIG. 16.—Vibration stresses per 1° deflection at No. 1 cylinder—marine installation.

of 12 ins., whilst the values in column K of Table 4 are based on the crankshaft diameter of $16\frac{3}{4}$ ins.

The actual value of the stress per degree at a particular point in the shaft system is

$$f_1 = f \left(\frac{d}{d_1} \right)^3,$$

where d = diameter used for calculating the stress values, f , given in column K of the frequency table and plotted in Fig. 16,

d_1 = actual diameter at the point under consideration.

In this example, therefore, the stresses in the 16.75-in. diameter crankshaft for the one-node mode of vibration are $(12/16.75)^3 = 0.37$ of the values given for the crankshaft sections in column K of Table 3. Hence the maximum specific stress in the crankshaft due to one-node vibration is

$$\pm (2645 \times 0.37) = \pm 980 \text{ lbs. per sq. in. per } 1^\circ,$$

which is small compared with the specific stress in the intermediate shaft, namely, ± 3260 lbs. per sq. in. per 1° .

In the case of two-node vibrations the specific stress in the intermediate shaft is $(16.75/12)^3 = 2.7$ times the value given in column K of Table 4, i.e. $\pm (250 \times 2.7) = \pm 675$ lbs. per sq. in. per 1° , compared with a specific stress of $\pm 18,270$ lbs. per sq. in. per 1° in the crankshaft.

The two-node stress in the intermediate shaft is therefore negligible compared with that in the crankshaft, even when allowance is made for the reduced size of the intermediate shaft.

General Remarks—In building up the frequency tables, it should be noted that columns A, B, C, D, E and I can be completed at the start, the remaining columns being filled in as the calculation proceeds.

The labour involved in the trial and error process can be minimised by plotting the last torque summations in column H of the frequency tables in the form of a curve on a base of assumed frequencies, as shown in Fig. 17. The points where this curve crosses the axis are the required natural frequencies of torsional vibration. Fig. 17 shows the curve completed to just beyond the two-node frequency, but in practice it is unnecessary to draw the complete diagram. One or two spots above and below each frequency value are sufficient to establish the correct values of the natural frequencies and enable the final frequency table to be completed.

The shape of the curve shown in Fig. 17 is a useful guide in carrying out the frequency calculations.

For one-node vibrations, if the residual torque in column H of the frequency tables is positive, the assumed frequency is too low; if this torque is negative the assumed frequency is too high.

For two-node vibrations, a positive residual torque indicates that the assumed frequency is too high, whilst a negative value indicates that the assumed frequency is too low.

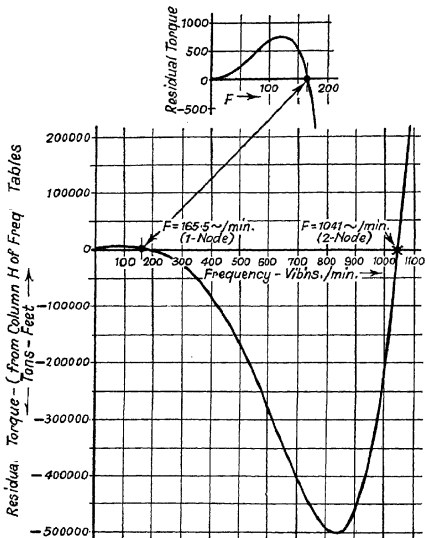


FIG. 17.—Curve showing variation of residual torque with frequency of vibration:

A knowledge of the torsional vibration characteristics of an individual type of engine is also a very useful aid in reducing the labour of building up the frequency tables, since the natural frequency of the installation can usually be surmised beforehand.

Another useful method of searching for the frequency of a given system by the tabulation method is to assume a value for the frequency, and complete the frequency table down to the last mass. Then adjust the moment of inertia of the last mass so that the final torque summation in column H is zero. This process is repeated for two or three different frequencies, the values obtained being plotted to give a graph showing the relationship between frequency and moment of inertia of the last mass. The required frequency, i.e. the frequency corresponding to the actual value of the moment of inertia of the last mass, is then read from the graph.

Normal Elastic Curve.—The values tabulated in column F of the frequency tables represent the torsional deflections at the respective masses for unit deflection at No. 1 mass when the system is executing free torsional vibrations of the corresponding normal mode, i.e. they are the relative amplitudes of vibration at various points in the system.

If these values are plotted as shown in Figs. 13 and 15, a curve of specific deflections is obtained, and this will be referred to as the *normal elastic curve* for the various modes of free vibration. The normal elastic curve is also called the *swinging form* of the vibration.

Since the masses have been assumed concentrated at definite points in the system, connected by weightless lengths of shaft, the normal elastic curve consists of a series of straight lines. The points where the curve crosses the shaft axis are the nodes.

Fig. 18 shows the normal elastic curves corresponding to four typical engine aggregates, viz. two types of direct-coupled generator, Fig. 18 *a* and *b*; and two types of marine installation, Fig. 18 *c* and *d*.

Direct-Coupled Generating Sets.—The one- and two-node normal elastic curves for two typical direct-coupled generator arrangements are shown at *a* and *b* in Fig. 18. In arrangement *a* the generator mass is separated from the flywheel mass so that an intermediate bearing can be introduced between the flywheel and the dynamo.

For fundamental or first degree vibrations, the node is

situated in the shaft section between the flywheel and the dynamo, whilst one of the nodes of the second degree vibrations is also situated at this point.

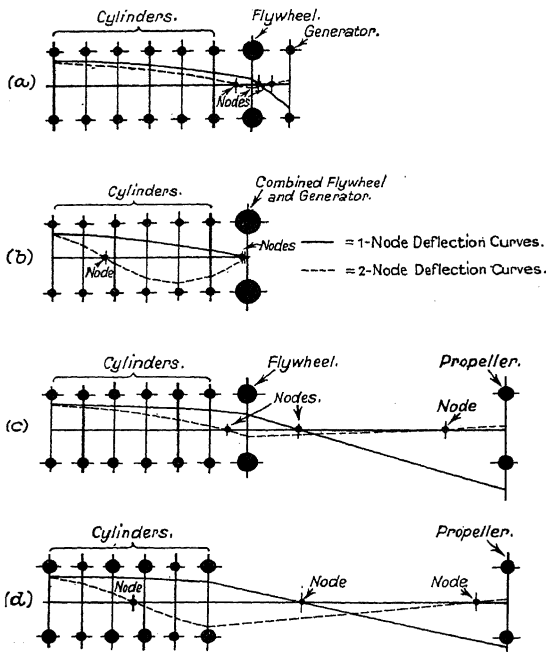


FIG. 18.—Types of normal elastic curves.

In the arrangement shown at *b* (Fig. 18) the bearing between the flywheel and the generator has been eliminated, so that the flywheel and generator masses can be regarded as a single large mass in setting down the equivalent system, i.e. the system

reduces to one having only a single major mass. An alternative method of altering arrangement *a* would be to place the generator between the engine and the flywheel.

The node for first degree vibrations and one of the nodes for second degree vibrations are situated very close to the major mass.

Arrangement *b* is preferable to arrangement *a* for the following reasons :—

- (i) The fundamental frequency is higher for arrangement *b* due to the closer grouping of the masses, and the ratio between the one- and two-node frequencies is also greater for arrangement *b*.

It is an advantage to have as high a value as possible for the natural frequency, with the object of placing all serious critical speeds above the normal operating speed.

- (ii) A comparison of the normal elastic curves for one-node vibrations shows that the slope at the node is very much greater in arrangement *a*. This implies a greater vibration stress in the section of shafting between the flywheel and the dynamo, and many failures of dynamo shafts at this point, due to running the engine in the neighbourhood of a serious critical speed, are on record.

- (iii) The ratio between the first and second degree vibrations is greater for arrangement *b*, e.g. in the case of a six-cylinder standard Diesel engine direct-coupled to a 275 kw. generator, the one- and two-node frequencies for arrangement *a* were 1450 vibs./min. and 1830 vibs./min. respectively, whilst the corresponding values for arrangement *b* were 2520 and 7325 vibs./min. respectively.

The very high two-node frequency associated with arrangement *b* ensures that only critical speeds corresponding to very high order harmonic components of the engine torque curve will be present in the operating speed range, so that critical speeds of the two-node

frequency can be neglected, as explained in Chapters 6 and 7.

In arrangement *a*, however, the two-node frequency is not very far above the one-node frequency, so that it is possible for two-node criticals of appreciable magnitude to occur within the operating speed range.

- (iv) Since the nodes are situated very close to the combined generator and flywheel mass in arrangement *b*, the actual magnitude of this mass does not appreciably affect the values of the natural frequencies. This is especially important in the case of engines direct-coupled to alternators, where a very large flywheel effect is required to ensure satisfactory parallel operation.

In general, therefore, the oscillating system of a direct-coupled generator should be designed to have as high a value for the one-node frequency of torsional vibration as possible, by grouping the cylinders as closely together as possible so as to obtain maximum stiffness in the shaft connections, and by making the crankshaft masses as light as possible. The arrangement shown at *b* in Fig. 18 should be adopted so as to obtain a favourable shape for the normal elastic curve and the highest possible value for the two-node natural frequency.

No difficulty should then be experienced in placing all serious one-node criticals above the normal operating speed; whilst for engines having up to six cylinders two-node criticals can be neglected. For engines having more than six cylinders it is advisable to investigate two-node as well as one-node vibrations.

The flywheel effect necessary for satisfactory operation of electrical generators is very much greater than that required for marine installations, but in the case of alternators running in parallel it is generally possible to incorporate the whole of the required flywheel effect in the revolving mass of the alternator itself. In the case of direct-current machines where an auxiliary flywheel is usually required, this flywheel should be placed as close to the generator as possible, and the coupling be

made so rigid that the generator and flywheel masses may be regarded as one.

This requirement can be met by avoiding the use of an intermediate bearing between the flywheel and generator, and by making the connecting shaft of generous dimensions. The omission of an intermediate bearing makes it a little more difficult to check the alignment of the engine and generator, but this difficulty can be overcome by testing with a special lining-up mandril before adding the weight of the flywheel.

An intermediate bearing is sometimes desirable in engines with few cylinders to help in supporting the weight of the relatively heavy flywheels necessary for satisfactory electrical operation. In such cases, however, the natural frequencies of torsional vibration are so high, due to the small number of cylinders, that no critical speed of practical importance occurs near the operating speed.

Methods of calculating the dimensions of flywheels for A.C. and D.C. generators are given in Chapter 12.

The following table contains approximate values of the natural frequencies of first degree or one-node torsional vibrations for direct-coupled generating sets of the four-stroke cycle, single-acting type arrangement as shown at *b* in Fig. 18 :—

TABLE 5.

No. of Cylinders.	10-in. Bore. 15-in. Stroke.	20-in. Bore. 30-in. Stroke.	30-in. Bore. 45-in. Stroke.
3	4200	2100	1400
4	3600	1800	1200
5	3200	1600	1100
6	2900	1500	1000
7	2700	1400	900
8	2600	1300	850
Vibs./Min.			

A preliminary approximate calculation of the one-node frequency can be made by reducing the system to a simple

two-mass system, as shown in Fig. 10, using Equation (16), viz. :—

$$F = 9.55 \sqrt{\frac{C(J_1 + J_2)}{J_1 \cdot J_2}} \text{ vibs./min.},$$

where

$$C = \frac{G \cdot I_p}{L} \text{ lbs.-ins. per radian,}$$

$$G = \text{modulus of rigidity} \\ = 12,000,000 \text{ lbs. per sq. in. for mild steel,}$$

$$I_p = \frac{\pi \cdot d^4}{32},$$

d = equivalent diameter of shaft in inches,

L = equivalent length of shaft from combined flywheel and generator mass to centre of cylinder group, in inches,

J_1 = total moment of inertia of crankshaft masses in lbs.-ins. sec.² units

$$= n \cdot J,$$

J = moment of inertia of crankshaft masses per cylinder,

n = number of cylinders,

J_2 = moment of inertia of combined generator and flywheel mass in lbs.-ins. sec.² units.

A closer approximation is obtained by applying the following correcting factors :—

TABLE 6.

Number of Cylinders.	1.	2.	3.	4.	5.	6.	Inf.
K	1.00	0.93	0.92	0.91	0.91	0.91	0.90

i.e. corrected frequency $F_1 = \frac{F}{K}$ vibs./min.

See also Chapter 1.

The difficulty of placing all serious criticals above the operating speed increases with the number of cylinders, particularly in the case of four-stroke cycle, single-acting engines, where half-order as well as whole order harmonic components

of the engine torque curve must be avoided; although it should usually be possible to avoid having any serious major harmonic below the running speed in the case of four-stroke cycle, single-acting engines with six or less cylinders.

For a given size of cylinder, any increase in the number of cylinders not only lowers the natural frequency slightly, but also increases the number and range of critical speeds in the vicinity of the running speed. The congestion of one-node criticals is also liable to be augmented in the case of an engine having a large number of cylinders by the appearance of two-node criticals capable of causing vibrations of disturbing amplitude, and in all such cases it is necessary to investigate two-node as well as one-node vibrations.

In investigating the torsional vibration characteristics of a range of engines of given cylinder dimensions, therefore, the principal dimensions, bore, stroke, shaft diameter, and revolutions per minute should be selected to eliminate disturbing criticals in the engine having the largest number of cylinders.

Where a preliminary examination shows that some alteration of natural frequency is desirable, the following relationships, deduced from the shape of the normal elastic curve and Equation (16), should be kept in mind:—

- (a) Since the nodes are very close to the combined flywheel and generator mass in Fig. 18*b*, an alteration in the moment of inertia of the flywheel will not appreciably alter the natural frequencies.
- (b) Assuming that the masses are already as closely grouped as possible, and that the cylinder masses are as light as possible, the only effective means of raising the natural frequency is by increasing the size of the crankshaft.

The crankshaft stiffness is best increased by enlarging the journals, or by widening the webs, because this provides increased stiffness without an appreciable increase of the polar moment of inertia of the rotating masses.

The amount of stiffening which can be obtained in this way and its effect on the natural frequency of

the system are matters which can only be determined by trial. If, however, only the crankshaft journals are increased in diameter the one-node frequency is approximately proportional to the square of the journal diameter within reasonable limits.

The increase in stiffness due to alterations of crankpin diameter is generally offset by the increased weight and polar moment of inertia of the crankpin and rotating part of the connecting rod. For this reason it is possible for an increase of crankpin diameter to lower the natural frequency in extreme cases. In general, it is inadvisable to increase the crankpin diameter with the object of increasing the natural frequency, unless it is possible to retain the original weight of the crankpin and the rotating part of the connecting rod, for example, by reducing the length of the pin and increasing the size of the hole bored through it.

- (c) In cases where the frequency cannot be altered sufficiently to remove a troublesome critical away from the operating speed, the amplitude of disturbing minor criticals can often be reduced to negligible proportions by changing the firing order, as explained in Chapters 6 and 10.

Alternatively, the same result can sometimes be achieved by altering the positions of the major masses, e.g. by placing the auxiliary flywheel at the opposite end of the crankshaft to the generator; by distributing part of the required flywheel effect in the form of counterweights attached to the crankwebs; by placing a generator at each end of the crankshaft; or by placing the generator in the centre of the engine. These methods, however, are unorthodox, and in the majority of cases a well-designed normal arrangement of engine and generator will yield a perfectly satisfactory solution to the torsional vibration problem.

- (d) In similar engines, i.e. in engines having the same stroke/bore ratio and of similar design, the natural frequencies

are inversely proportional to the bores of the cylinders and inversely proportional to the square roots of the numbers of cylinders.

Incidentally, if two similar engines having the same number of cylinders are running under equivalent conditions, i.e. piston speeds equal and indicator cards identical, the natural frequencies are directly proportional to the revolutions per minute. Hence, if the disposition of criticals is satisfactory for one engine it will also be satisfactory for the other.

In a given engine the natural frequency is approximately inversely proportional to the stroke, other dimensions remaining unaltered, i.e. the critical speeds occur at constant piston speeds.

For example, if an engine has a stroke of 3.75 ins. and a critical speed at 3500 r.p.m., the effect of reducing the stroke to 3.5 ins. is to raise the critical speed to about 3750 r.p.m., the piston speed being 2187 ft. per minute in each case.

If the mean effective pressure is unaltered therefore, this implies that alterations in engine stroke do not alter the positions occupied by the critical speeds on the power curve. Thus if a critical occurs at full power with the original stroke it will occur at full power when the stroke is altered provided the mean effective pressure remains unaltered. This conclusion should, however, be used with caution.

It should also be noted that if two engines are geometrically similar but of different sizes the natural frequencies are inversely proportional to their lengths. Also, if each throw of a crankshaft is fitted with balance weights which completely balance the rotating parts and only one-half of the reciprocating parts, then the polar moment of inertia of each crank mass is doubled and the natural frequency is reduced to $1/\sqrt{2}$ or 0.707 of the frequency with an unbalanced shaft.

EXAMPLE 7.—The one-node natural frequency of a six-cylinder engine, $13\frac{1}{2}$ -in. bore \times 18-in. stroke, direct-coupled to a dynamo is 2520 vibs./min. The crankshaft journal diameter is $8\frac{1}{4}$ ins. Estimate the probable natural frequencies, (i) when the crankshaft journal diameter is increased to 9 ins.; (ii) when the stroke is altered to $20\frac{1}{4}$ ins.

(i) Since frequency is directly proportional to the square of the crankshaft journal diameter,

$$\begin{aligned} \text{Estimated frequency with 9-in. shaft} &= 2520 \times \left[\frac{9}{8\frac{1}{4}} \right]^2 \\ &= 3000 \text{ vibs./min.} \end{aligned}$$

(ii) Since frequency is inversely proportional to stroke,

$$\begin{aligned} \text{Estimated frequency with } 20\frac{1}{4}\text{-in. stroke} &= 2520 \times \left[\frac{18}{20\frac{1}{4}} \right] \\ &= 2240 \text{ vibs./min.} \end{aligned}$$

EXAMPLE 8.—The one-node frequency of a six-cylinder engine, $13\frac{1}{2}$ -in. bore \times $20\frac{1}{4}$ -in. stroke, direct-coupled to a dynamo is 2240 vibs./min. Estimate the probable natural frequency of a similar engine having eight cylinders, 15-in. bore.

Since frequency is inversely proportional to bore,

$$\begin{aligned} \text{Estimated frequency of 15-in. bore, six-cylinder engine} &= 2240 \times \left[\frac{13\frac{1}{2}}{15} \right] \\ &= 2015 \text{ vibs./min.} \end{aligned}$$

Since frequency is inversely proportional to the square root of the number of cylinders,

$$\begin{aligned} \text{Estimated frequency of 15-in. bore, eight-cylinder engine} &= 2015 \times \sqrt{\frac{6}{8}} \\ &= 1745 \text{ vibs./min.} \end{aligned}$$

Marine Installations.—The one- and two-node normal elastic curves for two typical marine installations are shown at *c* and *d* in Fig. 18.

In both these arrangements the node for one-node vibrations is situated in the intermediate shafting between the engine and the propeller, and the shape of the normal elastic curves shows that the cylinder masses vibrate with approximately equal amplitudes whilst the amplitude of vibration at the propeller is much larger. In normal marine installations, therefore, a very close approximation to the one-node frequency can be obtained by reducing the system to a simple two-mass system, as shown in Figs. 8 and 9, and using Equation (16), viz.,

$$F = 9.55 \sqrt{\frac{C(J_1 + J_2)}{J_1 J_2}} \text{ vibs./min.}$$

In dealing with marine installations, it is usually preferable to work with foot, ton, second units,

i.e. $C = \frac{G \cdot I_p}{L}$ tons-ft. per radian,

$G =$ modulus of rigidity in tons per sq. ft.
 $= 772,000$ tons per sq. ft. for mild steel,

$I_p = \frac{\pi \cdot d^4}{32}$

$d =$ equivalent diameter of shaft in feet,

$L =$ equivalent length of shaft from propeller to centre of cylinder group in feet,

$J_1 =$ total moment of inertia of crankshaft and flywheel masses in tons-ft. sec.²,

$J_2 =$ moment of inertia of propeller in tons-ft. sec.².

In this case no correcting factor is required.

An examination of the one-node normal elastic curve and Equation (16) shows that—

- (a) The one-node frequency of marine installations is not appreciably altered by alterations in the moment of inertia of the flywheel, since the flywheel mass is not a very large proportion of the total engine masses.
- (b) The one-node frequency is also not appreciably altered by alterations of crankshaft stiffness, since the crankshaft is considerably more rigid than the intermediate shafting between the engine and the propeller.

- (c) The one-node frequency can be altered appreciably by altering the diameter of the intermediate shafting; being directly proportional to the square of the intermediate shaft diameter.
- (d) Any alteration in the moment of inertia of the propeller will also appreciably alter the one-node frequency.
- (e) The one-node frequency is inversely proportional to the square root of the length of the intermediate shafting if all other dimensions remain unaltered.

EXAMPLE 9.—The one-node frequency of a marine installation having 160 ft. of 12-in. diameter intermediate shafting is 165.5 vibs./min. Estimate: (i) The one-node frequency when the length of intermediate shafting is reduced to 50 ft. (ii) The diameter of 50 ft. of intermediate shafting for a frequency of 400 vibs./min.

- (i) Since the one-node frequency is inversely proportional to the square root of the length of the intermediate shafting,

$$\begin{aligned} \text{Estimated one-node frequency with} &= 165.5 \sqrt{\frac{160}{50}} \\ \text{50 feet of shafting, 12-in. diameter} &= 296 \text{ vibs./min.} \end{aligned}$$

- (ii) Since the one-node frequency is directly proportional to the square of the diameter of the intermediate shafting,

$$F_1 = F \times \left[\frac{d_1}{d} \right]^2,$$

where F_1 = one-node frequency corresponding to dia. d_1 ,
 F = one-node frequency corresponding to dia. d .

In this example $F = 296$ vibs./min. when $d = 12$ ins.

Hence, for $F_1 = 400$ vibs./min.,

$$400 = 296 \left[\frac{d_1}{12} \right]^2,$$

i.e. $d_1 = 13.9$ ins.

So far as one-node frequencies are concerned, there is not much difference between arrangements *c* and *d* in Fig. 18,

since the normal elastic curves for one-node vibrations are similar in shape, and the magnitude of the flywheel mass does not appreciably influence the value of the one-node frequency.

The one-node frequency of marine installations varies from 150 to 200 vibs./min. when the engine is installed amidships ; and from 300 to 400 vibs./min. when the engine is installed aft.

The problem of avoiding serious one-node criticals in a normal marine installation is not usually very difficult. There is usually only one serious critical speed to be considered, and this is generally well below the operating speed range in amidships installations, and well above it in after-end installations. Any adjustment of natural frequency which may be necessary can be made by an appropriate alteration of intermediate shaft diameter (see also Chapter 10).

In marine practice it is usually the two-node frequency which is the crux of the torsional vibration problem, mainly because critical speeds of the second degree (two-node) are more numerous than those of the first degree (one-node), and because the vibration stresses in the engine crankshaft at certain of the two-node critical speeds can be very severe.

Fig. 18 shows that the normal elastic curves for two-node vibrations differ according to the characteristics of the crankshaft masses. At *c* (Fig. 18) there is a heavy flywheel at the after-end of the engine and one of the nodes of the two-node mode of vibration is situated between the flywheel and the aftermost cylinder. The other node is situated close to the propeller. The amplitude of vibration is different for each cylinder, and is very small at the propeller.

At *d* (Fig. 18) there is no separate flywheel, the required flywheel effect being distributed along the crankshaft in the form of counterweights attached to the crankwebs.

In this case the crankshaft node has been shifted to a position very close to the centre of the cylinder group, whilst the other node has been moved closer to the propeller.

The shape of the normal elastic curve is very nearly symmetrical for the cylinder group, i.e. the crankshaft node divides the crankshaft into two parts ; the amplitudes of vibration at the cylinders situated on one side of the node being nearly

equal in magnitude but of opposite sign to those of corresponding cylinders on the other side of the node. This is an advantage, since it will be shown later that it implies almost complete cancellation of the major and some of the minor two-node criticals. The amplitude of vibration at the propeller is very small.

As a general rule the flywheel effect incorporated in marine installations should be the minimum necessary for satisfactory starting and manoeuvring, so as to provide as high a value as possible for the two-node frequency. The actual flywheel effect to be adopted in any specific installation should be adjusted to keep all important critical speeds clear of the normal running speed.

The size of flywheel necessary for satisfactory starting and manoeuvring of a marine oil engine installation may be determined by the method given in Chapter 12.

Approximate methods of calculating the two-node frequencies can be deduced from the shapes of the normal elastic curves.

(i) *Engine with Flywheel* (Fig. 18c).

If the moment of inertia of the flywheel is large compared with that of the crankshaft masses, the node will be situated close to the flywheel, i.e. the shape of the two-node normal elastic curve for the cylinder group in arrangement *c* is similar to that of the one-node curve in arrangement *b*. The two-node frequency for arrangement *c* can therefore be estimated by the method employed for estimating the one-node frequency of arrangement *b*, viz.,

$$F = 9.55 \sqrt{\frac{C(J_1 + J_2)}{J_1 \cdot J_2}} \text{ vibs./min.,}$$

where

$$C = \frac{G \cdot I_p}{L}$$

$$G = 772,000 \text{ tons per sq. ft. for mild steel,}$$

$$I_p = \frac{\pi \cdot d^4}{32} \text{ ft.}^4,$$

$$d = \text{equivalent diameter of shaft in feet,}$$

L = equivalent length of shaft from flywheel to centre of cylinder group in feet,

J_1 = total moment of inertia of crankshaft masses in tons-ft. sec.²,

J_2 = moment of inertia of flywheel in tons-ft. sec.².

The frequency calculated by the above expression should be corrected by means of the correcting factors already given (Table 6).

(ii) *Engine without Flywheel* (Fig. 18*d*).

In this case the two-node frequency can be estimated by assuming that the node is situated at the centre of the cylinder group and applying Equation (7), viz.,

$$F = 9.55 \sqrt{\frac{C}{J}} \text{ vibs./min.},$$

where $C = \frac{G \cdot I_p}{L},$

$G = 772,000$ tons per sq. ft. for mild steel,

$$I_p = \frac{\pi \cdot d^4}{32}$$

d = equivalent diameter of shaft in feet,

L = equivalent length of shaft from node to centre of cylinders on left-hand side of node,

J = total moment of inertia of crankshaft masses on left-hand side of node, in tons-ft. sec.².

The calculated frequency should be corrected by means of the correcting factor corresponding to the number of cylinders on the left-hand side of the node.

EXAMPLE 9*a*.—Estimate the two-node frequency for the marine installation shown in Fig. 15.

In this case $I_p = \frac{\pi \times 1.3958^4}{32} = 0.373 \text{ ft.}^4,$

$$L = \left[\frac{7.5}{2} + 3.3333 \right] = 7.0833 \text{ ft.},$$

$$\text{i.e.} \quad C = \frac{772000 \times 0.373}{7.0833} = 40,700 \text{ tons-ft. per radian,}$$

$$J = (1.635 + 0.8175 + 1.635) \\ = 4.0875 \text{ tons-ft. sec.}^2.$$

$$\text{Hence,} \quad F = 9.55 \sqrt{\frac{C}{J}} \\ = 998 \text{ vibs./min.}$$

Since there are three cylinders on the left-hand side of the node, the correcting factor is 0.92,

$$\text{i.e.} \quad \text{Corrected frequency} = 998/0.92 \\ = 1085 \text{ vibs./min.}$$

This is 4 per cent. higher than the value obtained by the tabulation method, and is a much closer estimate than that obtained by the more elaborate three-mass approximation.

The estimated value would have been closer to the true value if the three masses on the left-hand side of the node had been of equal magnitude.

Since the margin between the normal operating speed and one of the two-node criticals is often very small, it is necessary to calculate the value of the two-node frequency as accurately as possible, and the tabulation method should always be employed for the final calculations.

An inspection of the normal elastic curves in Fig. 18, *c* and *d*, and the foregoing approximate expressions for two-node frequency, reveals the following characteristics of marine installations:—

- (a) Since the amplitude of vibration at the propeller is small, and the rigidity of the crankshaft is very large compared with that of the intermediate shafting, alterations in the moment of inertia of the propeller or in the diameter of the intermediate shafting do not appreciably alter the two-node frequency.
- (b) The two-node frequency is appreciably altered by alterations in the diameter of the crankshaft or in the disposition of the crankshaft masses.

- (c) Within reasonable limits the two-node frequency of marine installations is directly proportional to the square of the crankshaft journal diameter.
- (d) In similar engines the two-node natural frequencies are inversely proportional to the bores of the cylinders.

The two-node frequency of marine installations usually varies from 500 to 1500 vibs./min., according to the dimensions and number of cylinders, and the disposition of the major masses. An average value for installations of moderate power is 1000 vibs./min.

The two-node frequency for a given engine does not vary appreciably with the position of the engine in the ship, since the influence of the intermediate shafting is very slight; whilst the increase of frequency as the number of cylinders is reduced is not as much as might be anticipated due to the relatively heavier flywheels which are required to ensure satisfactory starting and manœuvring in engines having a small number of cylinders.

In general, the arrangement shown in Fig. 18*d* is preferable because—

- (i) There is an appreciable increase in the value of the two-node frequency compared with arrangement *c*, and this generally enables all serious two-node criticals to be placed above the normal operating speed ranges.
- (ii) The symmetrical shape of the normal elastic curve implies that the major and certain of the minor critical speeds are eliminated. This considerably lessens the congestion of criticals in the lower speed range.

The shape of normal elastic curve shown in Fig. 18*d* is obtained when the engine masses are uniformly or symmetrically distributed along the crankshaft. This implies that the flywheel effect necessary to ensure satisfactory starting and manœuvring must be secured by a system of counterweights attached to the crankwebs. In multi-cylinder engines this method of incorporating flywheel effect has the additional

advantage of improving the internal balance of the engine by providing partial primary balance of the individual cylinders.

In the case of opposed-piston marine engines having four or more cylinders, the revolving and reciprocating parts of the engine are sufficient to provide all the flywheel effect necessary for satisfactory running without an auxiliary flywheel or crankshaft counterweights.

The symmetrical two-node normal elastic curve shown in Fig. 18*d* is also obtained when an auxiliary flywheel is placed at the forward end of the crankshaft.

The diameter of the intermediate shafting and the moment of inertia of the flywheel, whether concentrated at one point or distributed along the crankshaft, provide means for adjusting the values of the one- and two-node frequencies respectively, i.e. an alteration in the diameter of the intermediate shafting alters the one-node frequency without appreciably affecting the two-node frequency; whilst an alteration in the moment of inertia of the flywheel alters the two-node frequency without appreciably affecting the one-node frequency.

The procedure recommended for dealing with marine installations is therefore to determine from previous experience the probable value of the two-node frequency. The two-node frequency tabulation can then be completed down to the flywheel, leaving only the last two lines to be filled in by adjusting the moment of inertia of the flywheel to the value which makes the last torque summation in column H, zero.

In installations of the type shown in Fig. 18*d*, i.e. where the flywheel effect is obtained by counterweights on the crankwebs, a light turning wheel is still necessary at the after-end of the engine, so that small adjustments can be made by altering the moment of inertia of this wheel.

The one-node tabulation can then be taken in hand. This is a less sensitive calculation, and if necessary small adjustments can be made by altering the diameter of the intermediate shafting without seriously affecting the value already determined for the two-node frequency.

Automobile Transmission Systems.—Fig. 19 shows a typical automobile transmission system in which the major

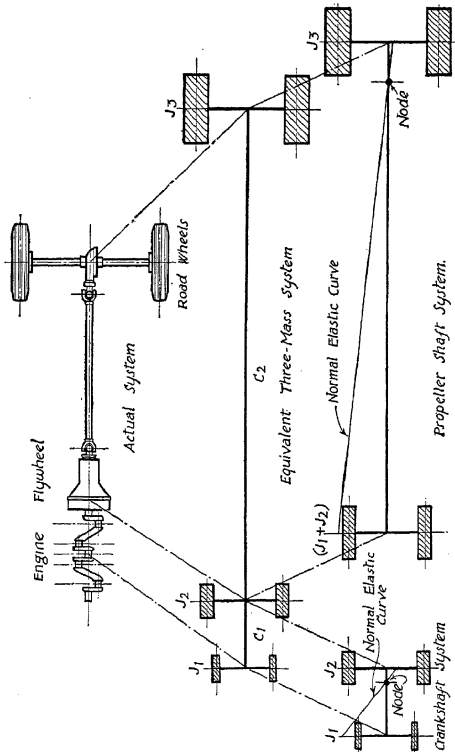


FIG. 19.—Automobile transmission system.

masses are the engine crankshaft with its attached rotating and reciprocating masses, the engine flywheel, and the road-wheels.

An approximate calculation of the natural frequencies of this system can be made by replacing the actual system by the equivalent three-mass system shown in Fig. 19. In this equivalent system J_1 is the total moment of inertia of the crank masses about the axis of rotation, J_2 is the moment of inertia of the flywheel and its attachments, and J_3 is the moment of inertia of the road-wheels reduced to crankshaft speed by the methods described in connection with geared drives in Chapter 5. C_1 is the torsional rigidity of the crankshaft, i.e. the torque required to twist this portion of the system through 1 radian, and C_2 is the combined torsional rigidity of the propeller and axle shafts.

Since the road-wheels cannot oscillate without causing a corresponding oscillation of the chassis, the value of J_3 is not strictly that of the moment of inertia of the road-wheels only. Actually, the correct assessment of road-wheel inertia is very complex. It involves questions of tyre and road-spring flexibility, the influence of tyre inflation pressure, and the coefficient of friction between the wheels and the ground. Fortunately, however, the road-wheels have a negligible effect on the value of the natural frequency of the crankshaft system, and it is therefore not necessary to assess their inertia with any great degree of accuracy.

The natural frequencies of the three-mass system shown in Fig. 19 can be calculated by Equation (19), viz. :—

$$(J_1 + J_2 + J_3) - \omega^2 \left(\frac{J_1 \cdot J_2}{C_1} + \frac{J_1 \cdot J_3}{C_1} + \frac{J_2 \cdot J_3}{C_2} \right) + \omega^4 \cdot \frac{J_1 \cdot J_2 \cdot J_3}{C_1 \cdot C_2} = 0.$$

As a general rule the value of C_1 is very much larger than C_2 , so that a further simplification can be used for preliminary estimates of the natural frequencies of the system, i.e. the actual system can be assumed to be composed of two simple

two-mass systems, the crankshaft system and the propeller shaft system, as shown in the bottom diagram in Fig. 19.

The natural frequencies of these systems are found by applying Equation (16).

For Engine Crankshaft System,

$$F = 9.55 \sqrt{\frac{C_1(J_1 + J_2)}{J_1 \cdot J_2}} \text{ vibs./min.} \quad (30)$$

The node is situated in the crankshaft, usually close to the flywheel.

For Propeller Shaft System,

$$F = 9.55 \sqrt{\frac{C_2(J_1 + J_2 + J_3)}{(J_1 + J_2)J_3}} \text{ vibs./min.} \quad (31)$$

The node is situated in the axle shafts, as a general rule.

EXAMPLE 10.—The following values may be taken as fairly representative of light car practice:—

$J_1 = 0.5 \text{ lb.-in. sec.}^2$; $J_2 = 2.5 \text{ lbs.-ins. sec.}^2$; $J_3 = 50 \text{ lbs.-ins. sec.}^2$;
 $C_1 = 1,200,000 \text{ lbs.-ins. per radian}$; $C_2 = 4000 \text{ lbs.-ins. per radian}$.

For the three-mass system shown in Fig. 19 the frequency equation becomes

$$0.015625 \omega^4 - 45026 \omega^2 + 63600000 = 0,$$

whence $\omega^2 = 2880256 \text{ or } 1408,$

or $F = 16200 \text{ or } 358 \text{ vibs./min.}$

For the separate systems shown at the bottom of Fig. 19,

(i) Crankshaft system from Equation (30)—

$$F = 9.55 \sqrt{\frac{1200000(0.5 + 2.5)}{0.5 \times 2.5}},$$

i.e. $F = 16,200 \text{ vibs./min.}$, which agrees with the value obtained from the three-mass system.

(ii) Propeller shaft system from Equation (31)—

$$F = 9.55 \sqrt{\frac{4000(0.5 + 2.5 + 50)}{(0.5 + 2.5)50}},$$

i.e. $F = 358$ vibs./min., which also agrees with the value obtained from the three-mass system.

Since the moment of inertia of the road-wheels, J_3 , cannot be calculated with any great degree of accuracy, it is interesting to notice that large changes in this quantity do not produce much change in the value of the natural frequency of the propeller-shaft system. For example, if, in the above example, the value of J_3 is reduced to 25 lbs.-ins. sec.², the frequency becomes 368 vibs./min., i.e. an increase of only 3 per cent. for a 50 per cent. reduction in the moment of inertia of the road-wheels.

Conversely, when J_3 becomes very large, Equation (31) reduces to

$$F = 9.55\sqrt{\frac{C_2}{(J_1 + J_2)'}}$$

i.e. the frequency of the propeller-shaft system when the inertia of the road-wheels is increased towards infinity becomes

$$F = 9.55\sqrt{\frac{4000}{0.5 + 2.5}} = 348 \text{ vibs./min.}$$

This is only 3 per cent. reduction in frequency for an infinite increase in the moment of inertia of the road-wheels.

The important practical significance of the foregoing results is that in any system where the torsional rigidity of one section is very much larger than that of another, close agreement with the actual frequencies is obtained by treating each part of the system separately. This confirms that in an automobile transmission system the general practice of neglecting the influence of all parts to the rear of the flywheel in calculating crankshaft frequencies is unlikely to cause serious error. It also indicates that alterations in the characteristics of the propeller shaft part of the system are not likely to effect the frequencies of the crankshaft system appreciably.

In the case of the propeller-shaft system, since the moment of inertia of the road-wheels is very large compared with that of the flywheel and clutch, large errors in estimating road-wheel inertia do not make any appreciable difference to the value

obtained for the natural frequency of the propeller-shaft system.

It should also be noted that large alterations in the inertia of the flywheel, J_2 , do not produce correspondingly large changes in the value of the crankshaft frequency. For example, if, in the foregoing example, J_2 is reduced to 1.25 lbs.-ins. sec.², the frequency becomes 17,500 vibs./min., an increase of only 8 per cent. in frequency for a 50 per cent. reduction of flywheel inertia.

Conversely, if the moment of inertia of the flywheel is very large, Equation (30) becomes

$$F = 9.55 \sqrt{\frac{C_1}{J_1}} \text{ vibs./min.}$$

Thus, in the foregoing example for very large values of flywheel inertia, the frequency of the crankshaft system becomes 14,800 vibs./min., a reduction of only 8 per cent. in frequency for an infinite increase of the moment of inertia of the flywheel.

The principal characteristics of a typical automobile transmission system are therefore—

- (i) A low-frequency vibration which is below the frequency of engine impulses for all normal operating conditions. In a four-cylinder four-stroke engine, for example, the dominating impulse frequency is two impulses per revolution, so that the synchronous condition arises at an engine speed of not more than about 200 r.p.m. In six- and eight-cylinder engines, where the dominating impulse frequencies are three and four per revolution respectively, the conditions are even more favourable, because the critical speeds will then occur at not more than 130 r.p.m. for the six-cylinder engine and 100 r.p.m. for the eight-cylinder engine.

These engine speeds are sufficiently far below the normal operating speed range to render a more detailed investigation of this mode of vibration unnecessary.

This low-frequency vibration is the one-node mode of vibration for the system as a whole, the node being

situated in the propeller shaft or rear axles. Large alterations in the moment of inertia of the road-wheels, or in the torsional rigidity of the crankshaft, do not appreciably alter this frequency, but alterations in the moments of inertia of the flywheel or engine, or alterations in the torsional rigidity of the propeller and axle shafts have an important influence.

- (ii) A high-frequency vibration which can be calculated with sufficient accuracy by neglecting all parts of the oscillating system to the rear of the flywheel. This vibration is a two-node mode of vibration for the system as a whole, with one node situated in the crankshaft near the flywheel, and the other in the propeller or axle shaft. Alterations in the moment of inertia of the flywheel or in all parts to the rear of the flywheel do not produce any appreciable change in the natural frequency of this mode of vibration, but alterations in the moment of inertia of the crankshaft masses, or in the torsional rigidity of the crankshaft, have an important influence. For example, a reduction in the number of main bearings and the consequent reduction in the length of the crankshaft produces an appreciable increase of the natural frequency.

The calculation of this mode of vibration and the evaluation of the corresponding torsional vibration stresses is the crux of the torsional vibration problem of automobile engine crankshafts.

The procedure recommended, therefore, for calculating the natural frequency of the crankshaft system of an automobile engine is to obtain the equivalent oscillating system for the crankshaft masses and flywheel, by the methods described in Chapter 3, neglecting all masses to the rear of the flywheel. The tabulation method is then applied to this system to obtain the value of the natural frequency, the normal elastic curve, and the specific vibration torques acting in each section of the crankshaft.

The main characteristics revealed by applying the tabulation

method to an automobile crankshaft system are similar to those already described for direct-coupled generator sets, and the same remarks apply to both types of installation. As a general rule the higher modes of vibration of an automobile crankshaft system are not of practical interest, because only high order criticals of small amplitude occur within the running range in the case of these higher modes.

Typical values for the natural frequencies of the fundamental mode of crankshaft vibration of automobile engines are 17,000 to 24,000 vibs./min. for four-cylinder engines; 12,000 to 17,000 vibs./min. for six-cylinder engines; and 9000 to 13,000 vibs./min. for eight-cylinder engines.

Aero Engine Crankshaft and Air-screw Systems.—

From the point of view of torsional vibration aero engines can be divided into two main classes, namely, radial and in-line engines.

The simplest type of radial engine is the single-row arrangement in which the cylinders are all in one transverse plane, the lines of stroke being equally spaced round a single crankpin, as shown in Fig. 20.

The simplest type of in-line engine is the single-bank type, in which the cylinders occupy different transverse planes and there is a crankpin in each line of stroke, as shown in Fig. 21.

Radial engines are not, however, confined to the single-row type. Two-row, and three-row radials have been developed for the higher power outputs. In multi-row radials there is a crankpin to each row. For the purpose of calculating natural frequencies, therefore, a multi-row radial engine can be regarded as an in-line engine with as many cranks as there are rows of cylinders, the moment of inertia at each crank being the sum of the moments of inertia of the reciprocating and revolving masses of all the cylinders, connecting rods, etc., in each row.

Similarly, in-line engines are not confined to a single bank of cylinders; engines with two-, three-, and four-banks of cylinders in "Horizontally Opposed," "V," "Fan," "X," and "H" formations having been developed for the higher powers. For the purpose of calculating natural frequencies, the effect of adding banks of cylinders to an in-line engine is merely to

increase the moment of inertia of the oscillating mass at each crankpin.

There is thus a tendency for the two classes to merge, although the majority of present-day radial engines are of the single-row or two-row types, and the majority of present-day in-line engines are of the single-bank or two-bank (V-formation) types.

The air-screw is driven either directly from the engine crankshaft or through reduction gearing, but the present discussion will be limited to ungeared engines. Geared aero engines are dealt with in Chapter 5.

Radial Engines.—Fig. 20 shows a typical ungeared single-row radial engine/air-screw combination.

The equivalent system is shown at the bottom of the diagram and consists of two major masses, the moment of inertia of the air-screw being very much larger than that of the engine rotating and reciprocating parts.*

The natural frequency of this system is given by Equation (16), viz.,

$$F = 9.55 \sqrt{\frac{C(J_p + J_e)}{J_p \cdot J_e}} \text{ vibs./min.},$$

where C = torsional rigidity of shaft between engine and air-screw in lbs.-ins. per radian,

J_p = moment of inertia of air-screw in lbs.-ins. sec.²,

J_e = moment of inertia of engine in lbs.-ins. sec.².

The moment of inertia of the air-screw is large compared with the moment of inertia of the engine masses, so that alterations in the moment of inertia of the air-screw do not appreciably change the natural frequency of the system.

Hence, a first approximation to the natural frequency is obtained by neglecting J_e in the numerator of the foregoing equation,

i.e.
$$F = 9.55 \sqrt{C/J_e} \text{ vibs./min.}$$

* It is shown in the Appendix to Volume I that air-screw blade flexibility can have an important influence on the torsional vibration characteristics of aero-engine/air-screw combinations. In this chapter, however, the air-screw blades are regarded as rigid.

An alteration in the torsional rigidity of the connecting shaft, C , or in the moment of inertia of the engine masses, J_e , however, can produce a considerable change of natural frequency.

The shape of the normal elastic curve is shown in the bottom diagram of Fig. 20. Due to the large air-screw inertia the node is very close to the air-screw and, as already explained, it is usually sufficiently accurate to assume that the installation reduces to a one-mass system with the engine masses swinging about a node at the air-screw.

EXAMPLE II.—In the system shown in Fig. 20, $J_p = 50$ lbs.-ins. sec.²; $J_e = 5$ lbs.-ins. sec.²; and $C = 4,000,000$ lbs.-ins. per radian. Calculate the natural frequency of vibration and the effect of the following alterations on the characteristics of the oscillating system :—

- (i) Increasing J_p to 100 lbs.-ins. sec.².
- (ii) Reducing J_p to 25 lbs.-ins. sec.².

VOL. I.—7

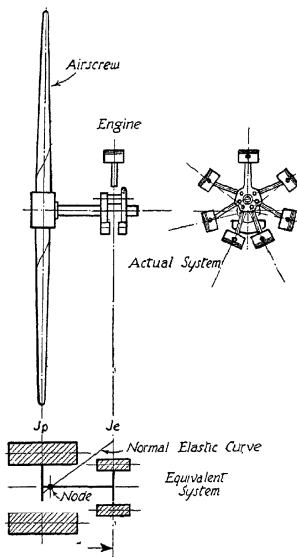


FIG. 20.—Radial aero-engine/air-screw system.

the effect of the following alterations on the characteristics of the oscillating system :—

- (iii) Increasing J_e to 6 lbs.-ins. sec.².
 (iv) Reducing C to 3,000,000 lbs.-ins. per radian.

The natural frequency of the system is obtained from the equation

$$F = 9.55 \sqrt{\frac{C(J_p + J_e)}{J_p \cdot J_e}}$$

i.e. $F = 9.55 \sqrt{\frac{4000000(50 + 5)}{50 \times 5}} = 8950$ vibs./min.

- (i) If $J_p = 100$, $F = 8750$ vibs./min.
 (ii) If $J_p = 25$, $F = 9350$ vibs./min.
 (iii) If $J_e = 6$, $F = 8250$ vibs./min.
 (iv) If $C = 3,000,000$, $F = 7750$ vibs./min.

The foregoing calculations show that the effect of doubling the moment of inertia of the air-screw is to reduce the natural frequency by only 2.3 per cent., whilst the effect of halving the moment of inertia of the air-screw is to increase the natural frequency by only 4.5 per cent.

This result is important from the practical point of view because it implies that an appreciable error in estimating the moment of inertia of the air-screw does not make any appreciable difference in the frequency calculation.

The calculations also show that an increase of 20 per cent. in the moment of inertia of the engine masses causes an 8 per cent. reduction of natural frequency; whilst a reduction of 25 per cent. in the torsional rigidity of the connecting shaft causes a 13.5 per cent. reduction of natural frequency.

In general, therefore, changes in air-screw inertia, within practical limitations, do not appreciably alter the natural frequency of the oscillating systems of these engines, and the only effective methods of changing the frequency are either to alter the inertia of the engine masses or the stiffness of the shafts connecting the engine to the air-screw.

If the system is treated as a simple one-mass system swinging about a node at the air-screw, the following results are obtained :—

$$F = 9.55 \sqrt{C/J_e} \text{ vibs./min.}$$

When $C = 4,000,000$ and $J_e = 5$,

$$F = 9.55 \sqrt{4000000/5} = 8550 \text{ vibs./min.}$$

When $C = 4,000,000$ and $J_e = 6$, $F = 7800$ vibs./min.

When $C = 3,000,000$ and $J_e = 5$, $F = 7400$ vibs./min.

These values are only from 2.5 to 5 per cent. less than the values obtained by using the two-mass method.

The oscillating systems of multi-row radial engines are preferably dealt with by similar methods to those employed for in-line engines.

In-Line Engines.—Fig. 21 shows a typical single-bank in-line engine air-screw combination.

The equivalent system is shown at the bottom of the diagram and consists of a series of comparatively small flywheels, representing the moments of inertia of the engine masses, connected to one large flywheel representing the moment of inertia of the air-screw. The moment of inertia of the air-screw is large compared with that of the engine masses, and the torsional rigidity of the air-screw shaft is usually smaller than the torsional rigidity of the crankshaft sections between each line of parts.

The general characteristics of the system shown in Fig. 21 are similar to those of the direct-coupled generating sets already discussed in this chapter.

The fundamental or one-node frequency can be calculated with a good degree of accuracy by means of the simple two-mass system shown at the bottom of Fig. 21, where

J = total moment of inertia of engine masses

$$= N \cdot J_e \text{ lbs.-ins. sec.}^2,$$

N = number of cylinders,

J_e = moment of inertia of one line of parts,

J_p = moment of inertia of air-screw, in lbs.-ins. sec.²,

C = torsional rigidity of equivalent shaft between air-screw and combined engine masses, assuming the engine masses are concentrated at the middle of the engine aggregate, in lbs.-ins. per radian.

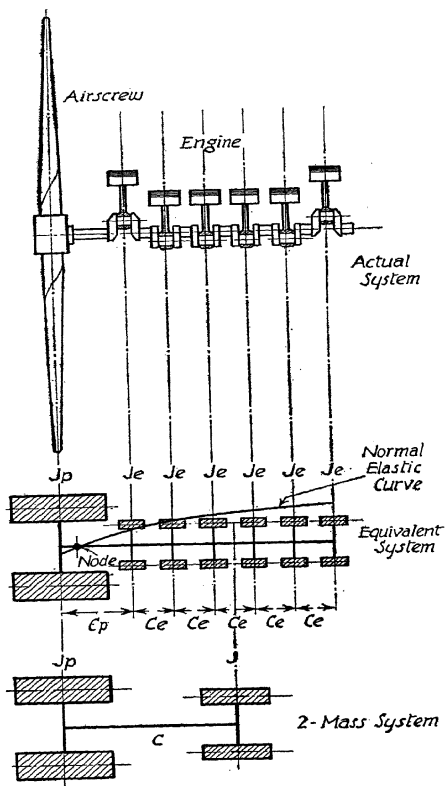


FIG. 21.—In-line aero-engine/air-screw system.

The value of C is obtained as follows :—

$$\frac{1}{C} = \frac{1}{C_p} + \frac{(N-1)}{2 \cdot C_e},$$

i.e.
$$C = \frac{2 \cdot C_p \cdot C_e}{2 \cdot C_e + (N-1)C_p} \quad \dots \quad (32)$$

Hence, the fundamental or one-node frequency of the system is given by the usual equation for a two-mass system, viz.,

$$F = \frac{9.55}{K} \sqrt{\frac{C(J_p + J)}{J_p \cdot J}} \text{ vibs./min.}, \quad \dots \quad (33)$$

where K is a correcting factor which depends on the number of cylinders as shown in Table 6.

Also, if $C_p/C_e = A$, and $J_p/J_e = B$,

$$\text{then } C = \frac{2 \cdot A \cdot C_e^2}{2 \cdot C_e + (N-1)A \cdot C_e} = \frac{2 \cdot A \cdot C_e}{2 + A(N-1)},$$

and the frequency equation becomes

$$F = \frac{9.55}{K} \sqrt{\frac{2 \cdot A(B+N)}{[2 + A(N-1)]N} \cdot \frac{C_e}{J_e}} \quad \dots \quad (34)$$

For a four-cylinder engine $K = 0.91$ and $N = 4$.

$$\text{Hence, } F = 10.5 \sqrt{\frac{A(B+4)}{2 \cdot B(2+3 \cdot A)} \cdot \frac{C_e}{J_e}} \text{ vibs./min.} \quad \dots \quad (35)$$

For a six-cylinder engine $K = 0.91$ and $N = 6$.

$$\text{Hence, } F = 10.5 \sqrt{\frac{A(B+6)}{3 \cdot B(2+5A)} \cdot \frac{C_e}{J_e}} \text{ vibs./min.} \quad \dots \quad (36)$$

As a general rule J_p is very large compared with J_e , so that the ratio J_p/J_e is also very large. This implies that N in the numerator of Equation (34) is practically negligible compared with B .

Hence Equation (34) reduces to

$$= \frac{9.55}{K} \sqrt{\frac{2 \cdot A}{N[2 + A(N-1)]} \cdot \frac{C_e}{J_e}} \quad \dots \quad (37)$$

i.e. when the air-screw moment of inertia is very large compared with the moment of inertia of one line of cylinder masses, large changes in air-screw inertia do not have any appreciable influence on the value of the fundamental frequency of the system. The frequency is, however, altered appreciably by changes of shaft stiffness, or changes in the moment of inertia of the cylinder masses.

For a four-cylinder engine, Equation (37) becomes

$$= 10.5 \sqrt{\frac{A}{2(2 + 3 \cdot A)}} \cdot \frac{C_e}{J_e} \quad (38)$$

For a six-cylinder engine, Equation (37) becomes

$$F = 10.5 \sqrt{\frac{A}{3(2 + 5 \cdot A)}} \cdot \frac{C_e}{J_e} \quad (39)$$

EXAMPLE 12.—Calculate the fundamental or one-node frequency of torsional vibration of the system shown in Fig. 22.

This is a six-cylinder aero-engine/air-screw combination, where

$$N = 6, \quad J_e = 0.15 \text{ lb.-in. sec.}^2; \quad J_p = 25.0 \text{ lbs.-ins. sec.}^2$$

$$C_e = 2,800,000 \text{ lbs.-ins./radian};$$

$$C_p = 2,020,000 \text{ lbs.-ins./radian}.$$

$$\text{Hence,} \quad A = C_p/C_e = 0.72; \quad B = J_p/J_e = 167.$$

From Equation (36),

$$\begin{aligned} &= 10.5 \sqrt{\frac{0.72(167 + 6)}{3 \times 167(2 + 5 \times 0.72)}} \cdot \frac{2800000}{0.15} \\ &= 9570 \text{ vibs./min.} \end{aligned}$$

Alternative solution, using Equation (39),

$$\begin{aligned} F &= 10.5 \sqrt{\frac{0.72}{3(2 + 5 \times 0.72)}} \cdot \frac{2800000}{0.15} \\ &= 9400 \text{ vibs./min., which is about 2 per cent.} \\ &\quad \text{less than the more accurate value.} \end{aligned}$$

EXAMPLE 13.—Calculate the fundamental frequency of the system shown in Fig. 22 when the following alterations are made:—

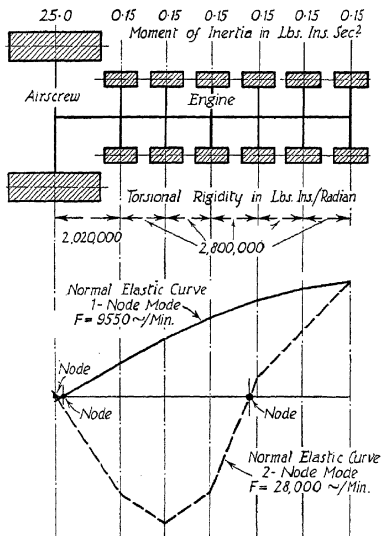


FIG. 22.—Equivalent system: six-cylinders in-line aero-engine/air-screw system.

- Moment of inertia of air-screw increased to 50 lbs.-ins. sec.².
- Moment of inertia of each line of engine masses increased to 0.30 lb.-in. sec.².
- Torsional rigidity of air-screw shaft increased to 4,040,000 lbs.-ins./radian.

In each case the remaining characteristics of the system are unaltered—

(a) When $J_p = 50$ lbs.-ins. sec.²; $B = J_p/J_e = 50/0.15 = 334$.
Hence, from Equation (36),

$$F = 10.5 \sqrt{\frac{0.72(334 + 6)}{3 \times 334(2 + 5 \times 0.72)}} \cdot \frac{2800000}{0.15}$$

$$= 9430 \text{ vibs./min.}$$

(b) When $J_e = 0.30$ lb.-in. sec.²; $B = J_p/J_e = 25/0.30 = 83.4$.
Hence, from Equation (36),

$$F = 10.5 \sqrt{\frac{0.72(83.4 + 6)}{3 \times 83.4(2 + 5 \times 0.72)}} \cdot \frac{2800000}{0.30}$$

$$= 6870 \text{ vibs./min.}$$

(c) When $C_p = 4,040,000$,

$$A = C_p/C_e = \frac{4040000}{2800000} = 1.44.$$

Hence, from Equation (36),

$$F = 10.5 \sqrt{\frac{1.44(167 + 6)}{3 \times 167(2 + 5 \times 1.44)}} \cdot \frac{2800000}{0.15}$$

$$= 10,550 \text{ vibs./min.}$$

The foregoing calculations show that doubling the inertia of the air-screw only reduces the frequency by about 2.5 per cent., whereas doubling the inertia of the engine masses reduces the frequency by 28 per cent., whilst increasing the stiffness of the air-screw shaft increases the frequency by 10 per cent.

As a general rule the most effective method of altering the fundamental or one-node frequency of systems of this type is either to alter the moment of inertia of the masses furthest from the node, i.e. furthest from the air-screw, or to alter the stiffness of that section of the shaft nearest to the node, i.e. the air-screw shaft. Alterations to masses near the node or to shafts remote from the node do not make much alteration in natural frequency. These are the basic rules to be observed when frequency alterations are under consideration.

There are other possible modes of vibration of the system shown in Fig. 22 although it is usually the fundamental or one-node mode which is the crux of the vibration problem in installations of this type.

The two-node mode of vibration can be evaluated approximately by the method described in Chapter 1 in connection with the system shown in Fig. 10, i.e. the actual system is reduced to an approximately equivalent three-mass system from which both one-node and two-node frequencies can be calculated, using Equation (19). The value obtained for two-node frequency is, however, very approximate and should only be used as a means of judging whether there is likely to be any troublesome two-node critical speeds in the operating range of the installation. If an accurate value of the two-node frequency is required the tabulation method should be employed.

Normally, there are no troublesome two-node criticals in the operating range of an in-line aero-engine/air-screw system, because only high-order harmonics are present in the operating range and these are comparatively feeble in intensity. Two-node frequencies should therefore be of interest only in abnormal cases, when the engine is very large or has a high normal operating speed, or when there is a very flexible shaft or coupling between the engine and the air-screw. In the latter case, however, the two-node frequency with a very flexible air-screw shaft will have approximately the same value as the one-node frequency with a comparatively rigid air-screw shaft.

In cases where both one-node and two-node vibrations have to be considered it should be noted that the most effective method of changing the two-node frequency is to alter the moments of inertia of the masses remote from the nodal points, or, alternatively, alter the torsional rigidities of the sections of shafting in the vicinity of the nodal points.

Alterations in the moments of inertia of masses near to the nodal points or in the torsional rigidities of shaft sections remote from the nodal points do not alter the frequency perceptibly.

Furthermore, an inspection of the normal elastic curve

for the system shown in Fig. 22 shows that the one-node frequency can be altered without appreciably altering the two-node frequency by altering the moment of inertia of the crank masses in the vicinity of the right-hand or crankshaft node in the diagram at the bottom of Fig. 22. Alterations in the moment of inertia of the mass at the left-hand nodes, i.e. the air-screw, do not appreciably alter either one-node or two-node frequencies.

When the approximate values of the one-node and two-node frequencies have been determined by approximate methods, the more accurate values should be calculated by the tabulation method, especially if it is required to evaluate the vibration stresses at critical speeds, because the frequency table contains data which is necessary for the evaluation of stresses.

A typical frequency table for a six-cylinder in-line aero-engine/air-screw system is given in Table 7. This table is based on the system shown in Fig. 22, and its construction is similar to that described in connection with Tables 1 and 2.

The stress for $\pm 1^\circ$ deflection at the free end of the crankshaft, column J in Table 7, is obtained by dividing the torque summations in column F by the modulus Z of the shaft section at which this torque acts

$$\begin{aligned} \text{where } Z &= \frac{\pi \cdot D^3}{16} \text{ ins.}^3 \text{ for solid circular shafts} \\ &= \frac{\pi(D^4 - d^4)}{16 \cdot D} \text{ ins.}^3 \text{ for hollow shafts,} \end{aligned}$$

D = outside diameter of shaft in inches,

d = inside diameter of shaft in inches.

The smallest value of Z in each section should be used. In the case of crank elements this is usually the crankpin section. The specific stresses given in column J of Table 7 are nominal stresses, i.e. no allowance should be made for stress concentrations at fillets, splines, key-ways, etc. This is because the damping factors which will be used for calculating vibration stresses have been deduced from nominal specific

stresses. The concentration factors are applied to the vibration stresses themselves.

The natural frequencies of the fundamental or one-node

TABLE 7.

FREQUENCY TABULATION: AERO-ENGINE SYSTEM.

(i) One-Node Mode: $F = 5550$ Vibs./Min.; $\omega^2 = 1,000,000$.									
A	B	C	D	E	F	G	H	I	J
Mass.	Moment of Inertia.	Torque per Unit Deflection.	Defn. in Plane of Mass.	Torque in Plane of Mass.	Total Torque.	Shaft Stiffness.	Change in Defn.	Modulus of Section of Shaft.	Stress for \pm Degree Deflection at Mass No. 1.
	$\frac{J}{\text{Lbs.-Ins.}^2}$	$\frac{J \cdot \omega^2}{\text{Lbs.-Ins./Radian}}$	θ Radian.	$J \cdot \omega^2 \cdot \theta$ Lbs.-Ins.	$\Sigma J \cdot \omega^2 \cdot \theta$ Lbs.-Ins.	$\frac{C}{\text{Lbs.-Ins./Radian}}$	$\frac{EJ \cdot \omega^2 \cdot \theta}{C}$ Radian.	Z Ins. ³	f_s Lbs./Ins. ²
No. 1 cyl.	0.15	150,000	1.0000	150,000	150,000	2,800,000	0.0555	1.5	$\pm 1,745$
No. 2 cyl.	0.15	150,000	0.9465	142,000	292,000	2,800,000	0.1042	1.5	3,400
No. 3 cyl.	0.15	150,000	0.8423	126,300	418,300	2,800,000	0.1495	1.5	4,860
No. 4 cyl.	0.15	150,000	0.6928	104,000	522,300	2,800,000	0.1865	1.5	6,070
No. 5 cyl.	0.15	150,000	0.5053	76,000	598,300	2,800,000	0.2140	1.5	6,950
No. 6 cyl.	0.15	150,000	0.2923	43,000	642,300	2,020,000	0.3180	2.0	5,570
Air-screw	25.00	25,000,000	-0.0257	-642,200	0	—	—	—	—
(ii) Two-Node Mode: $F = 28,000$ Vibs./Min.; $\omega^2 = 8,380,000$.									
No. 1 cyl.	0.15	1,288,000	1.0000	1,288,000	1,288,000	2,800,000	0.4600	1.5	$\pm 15,000$
No. 2 cyl.	0.15	1,288,000	0.5400	695,000	1,983,000	2,800,000	0.7080	1.5	23,000
No. 3 cyl.	0.15	1,288,000	-0.1680	-216,500	1,766,500	2,800,000	0.6300	1.5	20,500
No. 4 cyl.	0.15	1,288,000	-0.7980	-1,025,000	741,500	2,800,000	0.2645	1.5	8,620
No. 5 cyl.	0.15	1,288,000	-1.0625	-1,370,000	625,500	2,800,000	-0.2245	1.5	7,300
No. 6 cyl.	0.15	1,288,000	-0.8380	-1,080,000	1,708,500	2,020,000	-0.8460	2.0	14,850
Air-screw	25.00	214,500,000	0.0060	1,708,500	0	—	—	—	—

mode of torsional vibration of aero-engine/air-screw combinations varies from about 18,000 vibs./min. for small ungeared four-cylinders in-line engines to about 4500 vibs./min. for large six-cylinders in-line geared engines with two or more

banks of cylinders. Average values for single-bank four-cylinders in-line engines are 12,000 to 14,000 vibs./min., and for single-bank six-cylinders in-line engines from 10,000 to 12,000 vibs./min. The two-node frequency of these engines is generally about three times the one-node frequency.

The natural frequencies of the fundamental mode of vibration of radial engines varies from about 8000 for small ungeared single-row engines to 3000 vibs./min. for large two- and three-row geared engines, average values being 4000 to 6000 vibs./min.

CHAPTER 3.

EQUIVALENT OSCILLATING SYSTEMS.

THE oscillating systems of actual installations are usually much more complex than the ideal systems discussed in the preceding chapters.

To facilitate calculation it is necessary, therefore, to replace the complex system by a simpler system, consisting of a series of exact masses connected by sections of weightless shafting, which retains as closely as possible the dynamic and elastic characteristics of the original arrangement.

The accuracy with which the simplified system reproduces the vibrational characteristics of the original system depends, to some extent, upon experience and judgment, so that the results of torsiongraph investigations are a valuable aid in determining the allowances which should be made for each individual type of installation (see Chapter 8).

In the case of vibrations of the second degree, or two-node vibrations, of a multi-cylinder engine direct-coupled to a marine propeller, for example, where the clear speed range between two consecutive critical speeds is sometimes restricted to ten revolutions per minute of the prime mover, an error in converting the actual into the equivalent system can easily result in one or other of these criticals occurring so close to the running speed that an alteration to the system after it has been put into service is necessary for satisfactory operation.

Figs. 23 and 24 show the actual and equivalent systems for a typical direct-coupled marine installation, and a typical direct-coupled electrical generating set, respectively.

In Fig. 23 the actual system is reduced to an equivalent system consisting of eight exact masses connected by sections of shafting of uniform diameter.

In Fig. 24 the equivalent system consists of eight exact masses, since the armature of the dynamo is so rigidly connected

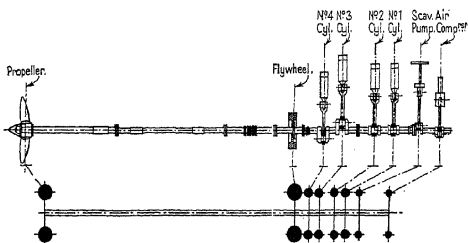


FIG. 23.—Equivalent system—marine installation.

to the flywheel that the two can be regarded as one mass without much error.

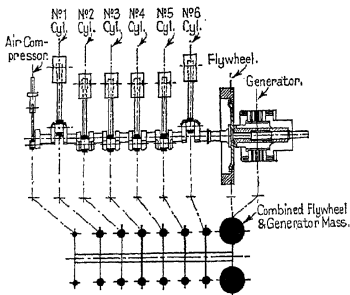


FIG. 24.—Equivalent system—direct-coupled generator.

The problem of converting a complex system into a simpler one can be divided into two main parts, viz. : I. Determination

(ii) *Crankpins* (Fig. 25).

For *Solid Crankpins*,

$$W = \frac{\pi}{4} \cdot D_2^2 \cdot B \cdot S \text{ lbs.},$$

$$K^2 = \frac{D_2^2}{8} + R^2 \text{ ins.}^2,$$

where D_2 = diameter of crankpin in inches,
 B = length of crankpin in inches,
 R = distance of centre of gravity of crankpin from
 axis of rotation, in inches,

$$\text{i.e. } W \cdot K^2 = \frac{\pi}{4} \cdot D_2^2 \cdot B \cdot S \left[\frac{D_2^2}{8} + R^2 \right] \text{ lbs.-ins.}^2,$$

$$\text{and } J = \frac{\pi}{4 \cdot g} \cdot D_2^2 \cdot B \cdot S \left[\frac{D_2^2}{8} + R^2 \right] \text{ lbs.-ins. sec.}^2. \quad (45)$$

For steel $S = 0.283$,

$$\text{i.e. } J = \frac{D_2^2 \cdot B}{1735} \left[\frac{D_2^2}{8} + R^2 \right] \text{ lbs.-ins. sec.}^2. \quad (46)$$

The foregoing expressions also apply to any solid cylindrical mass of uniform diameter, whose centre of gravity is situated at a distance R from the axis of rotation, e.g. eccentric pulleys.

For *Hollow Crankpins*,

$$W = \frac{\pi}{4} (D_2^2 - d_2^2) \cdot B \cdot S \text{ lbs.},$$

$$K^2 = \left[\frac{(D_2^2 + d_2^2)}{8} + R^2 \right] \text{ ins.}^2,$$

where d_2 = Diameter of hole through crankpin in inches,

$$\text{i.e. } W \cdot K^2 = \frac{\pi}{4} \cdot B \cdot S (D_2^2 - d_2^2) \left\{ \left[\frac{D_2^2 + d_2^2}{8} \right] + R^2 \right\} \text{ lbs.-ins.}^2,$$

$$\text{and } J = \frac{\pi}{4 \cdot g} \cdot B \cdot S (D_2^2 - d_2^2) \left\{ \left[\frac{D_2^2 + d_2^2}{8} \right] + R^2 \right\} \text{ lbs.-ins. sec.}^2. \quad (47)$$

For steel $S = 0.283$,

$$\text{i.e. } J = \frac{B}{1735} (D_2^2 - d_2^2) \left\{ \left[\frac{D_2^2 + d_2^2}{8} + R^2 \right] \right. \\ \left. \text{lbs.-ins. sec.}^2. \quad (48) \right.$$

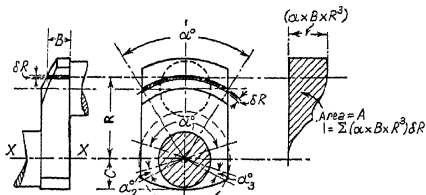


FIG. 26.—Moment of inertia of crankweb.

The foregoing expressions also apply to any hollow cylindrical mass of uniform cross-section, whose centre of gravity is situated at a distance R from the axis of rotation, e.g. eccentric sheaves.

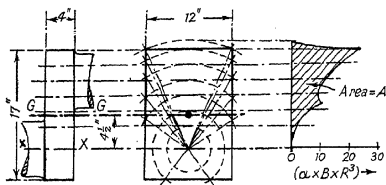


FIG. 27.—Moment of inertia of crankweb.

(iii) *Crankwebs* (Figs. 26 and 27).

Referring to Fig. 26, consider a small piece of the web of width B feet, and thickness δR feet, at radius R feet, subtending an angle α degrees at the centre of rotation.

The moment of inertia of this piece relative to the axis of rotation XX is

$$J = \frac{2 \cdot \pi \cdot R \cdot B \cdot \alpha^\circ \cdot S \cdot R^3 \cdot \delta R}{360 \cdot g} \text{ lbs.-ft. sec.}^2,$$

where S = specific weight of material in lbs. per cu. foot,
 $g = 32.2$ ft. per sec.².

Then, for the whole crankweb,

$$J = \frac{2 \cdot \pi \cdot S}{360 \cdot g} \Sigma(\alpha^\circ \cdot B \cdot R^3) \delta R \text{ lbs.-ft. sec.}^2.$$

The quantity $\Sigma(\alpha^\circ \cdot B \cdot R^3) \delta R$ is the area A under the curve shown at the right-hand side of Fig. 26.

This curve is obtained by plotting values of $(\alpha^\circ \cdot B \cdot R^3)$ at different radii. Note that α° is 360° for all values of R less than C in Fig. 26; also that when the radius R cuts the web boundary in more than two places, as at α_1 , α_2 , and α_3 in Fig. 26, $\alpha^\circ = (\alpha_1^\circ + \alpha_2^\circ + \alpha_3^\circ)$.

Let A = area under curve by planimeter in sq. ins.,
 x = horizontal scale, i.e. 1 in. = x units of
 $(\alpha^\circ \cdot B \cdot R^3)$; R and B being measured in feet,
 and α in degrees,
 y = vertical scale, i.e. 1 in. = y ft.

Then the area scale is $z = x \cdot y$,

i.e. 1 sq. in. = $x \cdot y$ units of $(\alpha^\circ \cdot B \cdot R^3) \delta R$.

Hence, finally, moment of inertia of crankweb,

$$J = \frac{2 \cdot \pi \cdot S \cdot A \cdot x \cdot y}{360 \cdot g} \text{ lbs.-ft. sec.}^2. \quad (49)$$

For steel $S = 490$ lbs. per cu. foot,

$$i.e. \quad J = \frac{A \cdot x \cdot y}{3.77} \text{ lbs.-ft. sec.}^2. \quad (50)$$

EXAMPLE 14.—Obtain the moment of inertia of the crankweb shown in Fig. 27 by the method just described, and check the result by direct calculation.

By the Graphical Method.

The values of $(\alpha^\circ \cdot B \cdot R^3)$ at different radii are given in the following table:—

TABLE 8.

Inches.	Feet.	R ³ Feet ³ .	B Feet.	Degrees.	α° . B . R ³ .
-	0.042	0.0001	0.333	360	0.012
1½	0.125	0.0019	0.333	360	0.228
2½	0.208	0.0090	0.333	360	1.080
3½	0.292	0.0250	0.333	360	3.000
4½	0.375	0.0527	0.333	304	5.340
5½	0.458	0.0961	0.333	272	8.710
6½	0.542	0.1592	0.333	166	8.810
7½	0.625	0.2441	0.333	107	8.700
8½	0.708	0.3549	0.333	90	10.650
9½	0.792	0.4968	0.333	79	13.100
10½	0.875	0.6699	0.333	70	15.600
11½	0.958	0.8792	0.333	63	18.400
12½	1.042	1.1314	0.333	58	21.850

These values were plotted using a horizontal scale of 1 in. = 5 units of (α° . B . R³), i.e. $x = 5$; and a vertical scale of 1 in. = 1/6th ft., i.e. $y = 0.1666$ ft.

The area, measured by planimeter, was found to be 12.75 sq. ins.

$$\begin{aligned} \text{Hence, } J &= \frac{A \cdot x \cdot y}{3.77} = \frac{12.75 \times 5 \times 0.1666}{3.77} \\ &= 2.82 \text{ lbs.-ft. sec.}^2. \end{aligned}$$

By Direct Calculation.

$$\begin{aligned} \text{Weight of web } W &= 4 \text{ ins.} \times 17 \text{ ins.} \times 12 \text{ ins.} \times 0.283 \\ &= 231 \text{ lbs.,} \\ K^2 &= \frac{1}{12}(17^2 + 12^2) + 4.5^2 \\ &= 56.35 \text{ ins.}^2 \\ &= 0.391 \text{ ft.}^2. \end{aligned}$$

$$\text{Hence, } W \cdot K^2 = 231 \times 0.391 = 90.5 \text{ lbs.-ft.}^2,$$

$$\text{and } J = \frac{W \cdot K^2}{g} = \frac{90.5}{32.2} = 2.81 \text{ lbs.-ft. sec.}^2.$$

This value agrees with that obtained by the graphical method.

(iv) *Crankshaft Balance Weights.*

These can be treated as forming part of the crankwebs to which they are attached.

(v) *Revolving Part of Running Gear.*

The revolving parts of the crankshaft have already been dealt with in the crankshaft calculations. There remains the revolving part of each connecting rod which may be assumed to be equivalent to three-fifths to two-thirds of the total weight of the connecting rod, concentrated at crankpin radius.

This figure can be determined experimentally by suspending the rod horizontally with the big end resting on the table of a weighing machine. The weight registered is that of the revolving part of the rod, i.e. that portion of the total weight below the centre of gravity. The reciprocating weight can be determined in a similar manner, the rod being suspended horizontally as before, but with the small end resting on the weighing machine table. The result may be checked by adding together the revolving and reciprocating weights. The sum should be equal to the total weight of the rod.

This method is not strictly accurate for connecting rods of normal design, since it neglects the effect of the oscillatory motion of the rod, but it is quite accurate enough for practical purposes (see Chapter 6).

Let W = total weight of connecting rod in lbs.,

$$\text{then revolving weight} = \frac{3}{5} \cdot W,$$

$$\text{and moment of inertia } J = \frac{3}{5} \cdot \frac{W \cdot R^2}{g} \text{ lbs.-ft. sec.}^2, \quad (51)$$

$$\text{where } \begin{array}{l} g = 32.2 \text{ ft. per sec.}^2, \\ R = \text{crank radius in feet.} \end{array}$$

In the case of reciprocating steam engines, the revolving part of the valve driving gear must also be taken into account. The moment of inertia of the eccentrics and eccentric sheaves can be calculated by the methods already given for solid and

hollow crankpins, whilst the revolving part of the eccentric rod may be assumed to be that portion of the rod which lies below the centre of gravity.

(vi) *Reciprocating Part of Running Gear.*

The reciprocating parts follow the crank movements at mid-stroke, but remain practically stationary whilst the crank is turning over top and bottom dead centres, i.e. the influence of the reciprocating parts on small rotational vibrations is a maximum when the crank is at the position corresponding to mid-stroke, and disappears when the crank is on top or bottom dead centres.

It is common practice to allow for this variation of the inertia of the reciprocating parts throughout the stroke by including only one-half of the weight of the reciprocating parts with the weight of the revolving part of the connecting rod to give an equivalent rotating mass concentrated at the crankpin.

The average value of the moment of inertia of the reciprocating parts may, however, be determined as follows:—

- Let v = linear velocity of the reciprocating parts at any instant when the crank angle is α degrees, measured from top dead centre,
 ω = angular velocity of the crankpin, assumed constant,
 R = crank radius,
 L = length of connecting rod,
 n = the ratio L/R .

Then an approximate expression for v at the crank angle α is

$$v = \omega \cdot R \left(\sin \alpha + \frac{R}{2 \cdot L} \cdot \sin 2\alpha \right).$$

Hence, the kinetic energy of the reciprocating parts at crank angle α , assuming that their weight is W , is

$$K_e = \frac{W \cdot \omega^2 \cdot R^2}{2 \cdot g} \left(\sin \alpha + \frac{R}{2 \cdot L} \cdot \sin 2\alpha \right)^2.$$

$$\text{Now} \quad K_e = \frac{J \cdot \omega^2}{2} \quad \text{or} \quad J = \frac{2 \cdot K_e}{\omega^2}.$$

$$\text{Hence,} \quad J = \frac{W \cdot R^2}{g} \left(\sin \alpha + \frac{R}{2 \cdot L} \cdot \sin 2\alpha \right)^2. \quad (52)$$

If the obliquity of the connecting rod is neglected, this expression reduces to

$$J = \frac{W \cdot R^2}{g} \cdot (\sin \alpha)^2 = \frac{W \cdot R^2}{2 \cdot g} (1 - \cos 2\alpha). \quad (53)$$

In the above expression the first term, viz. $\frac{W \cdot R^2}{2 \cdot g}$, is independent of the crank angle α , and represents the average value of the inertia of the reciprocating parts for one revolution. The second term, viz. $\frac{(W \cdot R^2 \cdot \cos 2\alpha)}{2 \cdot g}$, may be regarded as excess inertia of the second degree. The complete expression gives the instantaneous value of the inertia of the reciprocating parts corresponding to any crank angle α , and indicates that this value is zero at dead centres, and a maximum when the piston is at mid-stroke.

A more exact expression for the instantaneous value of the inertia of the reciprocating parts at any crank angle α is obtained by writing the equation for kinetic energy in the form of an expansion in terms of multiples of cosines of α , thus :

$$K_e = \frac{W \cdot \omega^2 \cdot R^2}{2 \cdot g} (A_0 + A_1 \cdot \cos \alpha + A_2 \cdot \cos 2\alpha, \\ + A_3 \cdot \cos 3\alpha + A_4 \cdot \cos 4\alpha + \dots), \\ \text{i.e. } J = \frac{W \cdot R^2}{g} (A_0 + A_1 \cdot \cos \alpha + A_2 \cdot \cos 2\alpha \\ + A_3 \cdot \cos 3\alpha + A_4 \cdot \cos 4\alpha + \dots). \quad (54)$$

The coefficients A_0, A_1, A_2, A_3 , etc., vary with the ratio $n = L/R$ as follows (see "Balancing of Engines, Steam, Gas and Petrol," by Archibald Sharp, page 126) :—

TABLE 9.

$A_0 =$	$\frac{1}{2}$	$+$	$\frac{1}{8 \cdot n^2}$	$+$	$\frac{1}{16 \cdot n^4}$	$+$
$A_1 =$	$\frac{1}{2 \cdot n}$	$+$	$\frac{1}{8 \cdot n^3}$	$+$	$\frac{15}{256 \cdot n^5}$	$+$
$A_2 =$	$-\frac{1}{2}$			$-\frac{1}{32 \cdot n^4}$		$-$
$A_3 =$	$-\frac{1}{2 \cdot n}$	$-$	$\frac{3}{16 \cdot n^3}$	$-$	$\frac{27}{256 \cdot n^5}$	$-$
$A_4 =$		$-\frac{1}{8 \cdot n^2}$		$-\frac{1}{16 \cdot n^4}$		$-$
$A_5 =$			$\frac{1}{16 \cdot n^3}$		$+\frac{15}{256 \cdot n^5}$	$+$
$A_6 =$				$\frac{1}{32 \cdot n^4}$		$+$
$A_7 =$					$-\frac{3}{256 \cdot n^5}$	$-$

The values of these coefficients for several different connecting rod/crank ratios are given in Table 10.

Table 10 may be checked by noting that when the crank is on dead centres, i.e. when $\alpha = 0$, the velocity and the kinetic energy of the reciprocating parts are both zero, or, in other words, the sum of the coefficients in Table 10 must always be zero, whatever the value of the connecting rod/crank ratio n .

It should also be noted that the values given in Table 10 confirm the approximate expression previously developed, and show that a very close approximation to the instantaneous value of the inertia of the reciprocating parts at any crank angle α may be obtained by using the simple expression

$$J = \frac{W \cdot R^2}{2 \cdot g} \cdot (1 - \cos 2\alpha) \text{ lbs.-ft. sec.}^2, \quad (53)$$

where W = weight of reciprocating parts of one cylinder in lbs.,

R = crank radius in feet,

$g = 32.2$ ft. per sec.²,

α = crank angle measured from top dead centre.

TABLE 10.
COEFFICIENTS FOR KINETIC ENERGY AND MOMENT OF INERTIA OF
RECIPROCATING PARTS.

Coefficients.	r = Length of Connecting Rod/Crank Radius.				
	4.	5.	6.	7.	8.
A ₀	0.5080	0.5051	0.5035	0.5026	0.5019
A ₁	0.1270	0.1010	0.0839	0.0718	0.0627
A ₂	-0.5001	-0.5001	-0.5000	-0.5000	-0.5000
A ₃	-0.1280	-0.1016	-0.0842	-0.0720	-0.0628
A ₄	-0.0081	-0.0051	-0.0035	-0.0026	-0.0019
A ₅	0.0010	0.0005	0.0003	0.0002	0.0001
A ₆	0.0001	0.0001	0.0000	0.0000	0.0000

The total moment of inertia of the reciprocating parts for single-cylinder and multi-cylinder oil engines, neglecting the obliquity of the connecting rod, can be calculated from the simple expression

$$J = \frac{W \cdot R^2}{2 \cdot g} \cdot (1 - \cos 2\alpha). \quad (53)$$

For Single-Cylinder Engines,

$$J = 0, \text{ when } \alpha = 0 \text{ and } 180^\circ$$

$$\frac{W \cdot R^2}{g}, \text{ when } \alpha = 90 \text{ and } 270^\circ,$$

i.e. the moment of inertia varies from 0 to $\frac{W \cdot R^2}{g}$ twice in every revolution, the mean value being $\frac{W \cdot R^2}{2 \cdot g}$

This mean value is equivalent to assuming one-half of the weight of the reciprocating parts to be concentrated at crankpin radius.

For Two-Cylinder Engines.

Two Cranks at 180°.

$$J_1 = \frac{W \cdot R^2}{2 \cdot g} \cdot (1 - \cos 2\alpha) \text{ for No. 1 cylinder,}$$

$$J_2 = \frac{W \cdot R^2}{2 \cdot g} \cdot [1 - \cos 2(\alpha + 180)] = \frac{W \cdot R^2}{2 \cdot g} \cdot (1 - \cos 2\alpha) \text{ for No 2 cylinder,}$$

$$\begin{aligned}
 J &= (J_1 + J_2) = \frac{W \cdot R^2}{g} \cdot (1 - \cos 2\alpha) \text{ for the two cylinders} \\
 &= 0, \text{ when } \alpha = 0 \text{ and } 180^\circ \\
 &= \frac{2 \cdot W \cdot R^2}{g}, \text{ when } \alpha = 90 \text{ and } 270^\circ,
 \end{aligned}$$

i.e. the total moment of inertia varies from 0 to $\frac{2 \cdot W \cdot R^2}{g}$ twice in every revolution, the mean value being $\frac{W \cdot R^2}{g}$

This mean value is equivalent to assuming one-half of the weight of the reciprocating parts of each cylinder to be concentrated at crankpin radius.

Two Cranks at 90°.

$$\begin{aligned}
 J_1 &= \frac{W \cdot R^2}{2 \cdot g} \cdot (1 - \cos 2\alpha) \text{ for No. 1 cylinder,} \\
 J_2 &= \frac{W \cdot R^2}{2 \cdot g} \cdot [1 - \cos 2(\alpha + 90)] = \frac{W \cdot R^2}{2 \cdot g} \cdot (1 + \cos 2\alpha) \\
 &\quad \text{for No. 2 cylinder,} \\
 J &= (J_1 + J_2) = \frac{W \cdot R^2}{g} \text{ for the two cylinders,}
 \end{aligned}$$

i.e. the total moment of inertia is constant throughout a revolution, and is equivalent to assuming one-half the weight of the reciprocating parts to be concentrated at crankpin radius.

For Three-Cylinder Engines.

Three Cranks at 120°.

$$\begin{aligned}
 J_1 &= \frac{W \cdot R^2}{2 \cdot g} \cdot (1 - \cos 2\alpha) \text{ for No. 1 cylinder,} \\
 J_2 &= \frac{W \cdot R^2}{2 \cdot g} \cdot [1 - \cos 2(\alpha + 60)] = \frac{W \cdot R^2}{2 \cdot g} \\
 &\quad \cdot [1 + \frac{1}{2}(\cos 2\alpha + \sqrt{3} \cdot \sin 2\alpha)], \\
 J_3 &= \frac{W \cdot R^2}{2 \cdot g} \cdot [1 - \cos 2(\alpha + 120)] = \frac{W \cdot R^2}{2 \cdot g} \\
 &\quad \cdot [1 + \frac{1}{2}(\cos 2\alpha - \sqrt{3} \cdot \sin 2\alpha)], \\
 J &= (J_1 + J_2 + J_3) = \frac{3 \cdot W \cdot R^2}{2 \cdot g} \text{ for the three cylinders,}
 \end{aligned}$$

i.e. the total moment of inertia is constant throughout a revolution, and is equivalent to assuming one-half of the weight of the reciprocating parts of each cylinder to be concentrated at crankpin radius.

For Four-Cylinder Engines.

Crank in Pairs at 180°.

By the foregoing method,

$$\begin{aligned} J &= (J_1 + J_2 + J_3 + J_4) = \frac{2 \cdot W \cdot R^2}{g} \cdot (1 - \cos 2\alpha) \\ &= 0, \text{ when } \alpha = 0 \text{ and } 180^\circ \\ &= \frac{4 \cdot W \cdot R^2}{g}, \text{ when } \alpha = 90 \text{ and } 270^\circ, \end{aligned}$$

i.e. the total moment of inertia varies from 0 to $\frac{4 \cdot W \cdot R^2}{g}$ twice in every revolution, the mean value being $\frac{2 \cdot W \cdot R^2}{g}$.

This mean value is equivalent to assuming one-half of the weight of the reciprocating parts to be concentrated at crankpin radius.

Crank Equally Spaced at 90°.

$$\text{In this case } J = (J_1 + J_2 + J_3 + J_4) = \frac{2 \cdot W \cdot R^2}{g},$$

i.e. the total moment of inertia is constant throughout a revolution, and is equivalent to assuming one-half of the weight of the reciprocating parts of each cylinder to be concentrated at crankpin radius.

In general, the total moment of inertia of the reciprocating parts of multi-cylinder engines having more than two cylinders with equally spaced cranks is constant throughout a revolution, and is equivalent to assuming one-half of the weight of the reciprocating parts of each cylinder to be concentrated at crankpin radius, neglecting the obliquity of the connecting rod.

The effect of the obliquity of the connecting rod can be taken into account by using the factors given in Table 10.

The total moment of inertia of the reciprocating masses then consists of a constant term, calculated by using the appropriate value of the factor A_0 from Table 10, and one or more

harmonically varying terms, calculated by using the appropriate values of the factors A_1, A_2 , etc., from Table 10.

In single-cylinder engines harmonically varying terms of all orders are present, but Table 10 shows that the first, second, and third orders (factors A_1, A_2 , and A_3) are predominant.

In multi-cylinder engines with equally spaced cranks, the only harmonically varying terms which are present are those whose order numbers are integral multiples of the number of equally spaced cranks, and the magnitude of any such order is its magnitude for one cylinder multiplied by the number of cylinders.

EXAMPLES.—

Two Cylinders with Cranks Equally Spaced at 180°.

$$J = \frac{2 \cdot W \cdot R^2}{g} \cdot (A_0 + A_2 \cos 2\alpha + A_4 \cos 4\alpha).$$

Three Cylinders with Cranks Equally Spaced at 120°.

$$J = \frac{3 \cdot W \cdot R^2}{g} \cdot (A_0 + A_3 \cos 3\alpha + A_6 \cos 6\alpha).$$

Four Cylinders with Cranks in Pairs at 180° (Four-Cycle Engine).

$$J = \frac{4 \cdot W \cdot R^2}{g} \cdot (A_0 + A_2 \cos 2\alpha + A_4 \cos 4\alpha).$$

Four Cylinders with Cranks Equally Spaced at 90°.

$$J = \frac{4 \cdot W \cdot R^2}{g} \cdot (A_0 + A_4 \cos 4\alpha).$$

Six Cylinders with Cranks in Pairs at 120° (Four-Cycle Engine).

$$J = \frac{6 \cdot W \cdot R^2}{g} \cdot (A_0 + A_3 \cos 3\alpha + A_6 \cos 6\alpha).$$

Six Cylinders with Cranks Equally Spaced at 60°.

$$J = \frac{6 \cdot W \cdot R^2}{g} \cdot (A_0 + A_6 \cos 6\alpha).$$

Eight Cylinders with Cranks in Pairs at 90° (Four-Cycle Engine).

$$J = \frac{8 \cdot W \cdot R^2}{g} \cdot (A_0 + A_4 \cos 4a + A_8 \cos 8\alpha).$$

Eight Cylinders with Cranks Equally Spaced at 45°.

$$J = \frac{8 \cdot W \cdot R^2}{g} \cdot (A_0 + A_8 \cos 8\alpha).$$

Effect of Variation of the Moment of Inertia of the Reciprocating Masses.

The variation of the moment of inertia of the reciprocating masses during each revolution causes a periodic variation of the natural frequency of torsional vibration. This is analogous to the variation of the natural frequency of a railway bridge as a locomotive moves from one end to the other.

This variation of natural frequency prevents the amplitude of vibration from building up to the value which would be obtained with a constant moment of inertia and constant natural frequency, and increases the speed range over which resonant effects are experienced. The influence of the variation of the moment of inertia of the reciprocating parts on the magnitude of the damping factor which determines the amplitude of torsional vibration of four-stroke cycle engines is fully discussed in a paper by V. J. Kjaer, reprinted in *Motorship*, August, 1930, page 233.*

The variation of natural frequency is larger in engines where the reciprocating parts are larger in proportion to the revolving parts, e.g. fast-running engines with solid forged crankshafts as compared with engines having built-up shafts; whilst the resultant effect in multi-cylinder engines depends also upon the shape of the normal elastic curve and the crank sequence.

In the case of one-node vibrations of marine installations, for example, where the amplitudes of vibration are very nearly

* See also M. Mancy: "Oscillations de torsion des arbres," *Mécanique*, No. 273, July-August, 1937. M. Scheuermeyer: "Einfluss der Zündfolge auf die Dreh-schwingungen Reihenmotoren," *Werft Reederei Hafen*, 1st March, 1933, page 69.

the same for all cylinders, the moment of inertia of the reciprocating masses for the engine as a whole is very nearly constant throughout a revolution, and is equivalent to one-half of the total reciprocating weight concentrated at crankpin radius.

In the case of two-node vibrations of marine installations and one-node vibrations of direct-coupled generators, however, where the amplitudes of vibration are not the same at all cylinders, the variation of natural frequency might be appreciable, e.g. in a six-cylinder, four-stroke cycle engine with cranks arranged in pairs at 120° direct-coupled to an electrical generator, the mean frequency was 760 vibrations per minute, whilst the variation of frequency was 754 to 766 vibrations per minute, i.e. a variation of nearly ± 1 per cent.

In the case of crankshaft vibration of automobile engines, and one-node vibration of direct-coupled Diesel-generator sets and aero-engine/air-screw combinations, the shape of the normal elastic curve is such that the amplitudes of vibration are not the same at all cylinders. Moreover, the heavy masses, i.e. the flywheel and clutch of an automobile engine, the combined flywheel and generator of a Diesel-generating set, and the air-screw of an aero-engine/air-screw combination are situated near the nodal point. These heavy masses, therefore, do not vibrate with any appreciable amplitude, so that the frequency of the system is mainly determined by the moment of inertia of the crank masses. In such cases the influence of the reciprocating parts, especially if they form an appreciable proportion of the total oscillating mass of each cylinder, in causing a cyclic variation of natural frequency might be appreciable. For example, Dr. Geiger has calculated that for an eight-cylinder engine of this type the apparent damping due to imperfect resonance represented about 20 per cent. of the total damping, notwithstanding the small cyclic irregularity of this engine.

The variation of natural frequency throughout a revolution can be obtained by calculating the moment of inertia of the reciprocating parts of one cylinder for a number of different positions of the crankshaft. It is then necessary to make a separate frequency tabulation for each crankshaft position,

taking care to insert the appropriate values of the moments of inertia of the reciprocating parts in column D of the frequency table.

In practical calculations, however, it is sufficient to make the usual assumption that the reciprocating parts can be taken into account by including one-half of their weight with the weight of the revolving part of the connecting rod, all acting at crankpin radius. The effect of any variation of frequency which might be present can then be taken into account by adjusting the damping factor employed for determining the amplitude of vibration at the critical speed so that the calculated amplitude agrees with the observed value.

The subject of apparent damping will, however, be discussed in more detail in Chapter 7.

The external vibration of the engine frame which accompanies torsional vibration of the shaft system is also due to the varying moment of inertia of the reciprocating parts, and would not be present if the parts in torsional vibration consisted entirely of rotating masses with the centres of gravity all situated on the axis of rotation. Due, however, to the reciprocating parts, a vertical force F , and a rocking moment M , are imposed on the engine frame.

If, for example, the shaft is given a vibratory motion, ($x = b \sin \omega . t$), the maximum values of F and M are as follows:—

$$\begin{aligned} F &= -\frac{W}{g} . b . R . \omega^2 \text{ lbs.} \\ &= -0.00034 . W . b . R . N^2 \text{ lbs.,} \end{aligned} \quad (55)$$

$$\begin{aligned} M &= -\frac{W}{g} . b . R^2 . \omega^2 . \text{ lbs.-ft.,} \\ &= -0.00034 . W . b . R^2 . N^2 \text{ lbs.-ft.,} \end{aligned} \quad (56)$$

where

W = weight of reciprocating parts in lbs.,

b = maximum amplitude of vibration in radians,

R = crank radius in feet,

ω = phase velocity of vibration in radians per sec.

$$= \frac{2 . \pi . N}{60},$$

N = revolutions per min.,

g = 32.2 ft. per sec.².

The unbalanced force F is felt as a reaction at the main bearings, and is responsible for vertical vibration of the engine frame and knocking at pistons and driving gear. It is possible for this unbalanced force to cause a derangement of the piston driving gear in serious cases.

The rocking moment M is responsible for transverse vibration of the engine frame.

In multi-cylinder engines, the average force during a revolution is one-half the values given by the foregoing expressions, multiplied by the number of cylinders.

Reciprocating Parts.—The reciprocating parts of each cylinder of an oil engine consist of,

One-third to two-fifths total weight of connecting rod.

„ piston head.

„ piston skirt (if fitted).

„ piston rod.

„ crosshead (if fitted).

„ set of piston cooling gear, including water or oil in piston and rod.

Let W = total weight of reciprocating parts for one cylinder in lbs.,

R = crank radius in feet,

$g = 32.2$ ft. per sec.².

Then effective moment of inertia of reciprocating parts is

$$J = \frac{W \cdot R^2}{2 \cdot g} \text{ lbs.-ft. sec.}^2 \text{ per cylinder.} \quad (57)$$

In the case of steam reciprocating engines, it is also necessary to take account of the reciprocating part of the valve gear. This can be done by the methods just described for dealing with the cylinder masses, and as a rule the effective moment of inertia of the reciprocating parts of the valve gear is combined with that of the nearest working cylinder.

(vii) *Engine-Driven Auxiliaries.*—Crank-driven auxiliaries, such as air-compressors and scavenge pumps, can be treated as an additional set of running gear, and the total moment of inertia calculated by the methods already described for the main cylinder running gear.

In the case of lever-driven auxiliaries—

Let W = weight of reciprocating parts of auxiliary in lbs.,

L = total stroke of auxiliary in feet.

Then effective moment of inertia of auxiliary is

$$J = \frac{W \cdot L^2}{8 \cdot g} \text{ lbs.-ft. sec.}^2. \quad . \quad . \quad (58)$$

This value is added to the moment of inertia of the cylinder from which the auxiliary is driven.

Total Moment of Inertia of Crankshaft and Running Gear of Reciprocating Engines.—This is determined by summing up the moments of inertia of the crankshaft and the revolving and reciprocating parts of the running gear. The value per cylinder is then obtained by dividing this total by the number of cylinders.

In the case of reciprocating steam engines, however, where the moment of inertia is not the same for all cylinders, each cylinder must be dealt with separately.

Crank-driven auxiliaries are treated separately, whilst the moment of inertia of lever-driven auxiliaries is added to the moment of inertia of the cylinder from which the auxiliary is driven.

These calculations should be tabulated as in Table II.

The following expression may be used for determining the approximate total moment of inertia of the crankshaft and running gear of oil engines, in cases where working drawings are not available:—

$$J = K \cdot D^2 \cdot S^3 \text{ lbs.-ft. sec.}^2 \text{ per cylinder, } . \quad . \quad (59)$$

where D = diameter of cylinder in feet,

S = stroke in feet.

The value of K depends on the type of engine, approximate values being as follows:—

$K = 3.5$ to 7.0 for medium speed trunk-piston engines, such as are employed for direct-coupled electrical generating sets. The lower value is for engines without

crankshaft balance weights, whilst the higher value applies when crankshaft balance weights are fitted.

$K = 5.0$ to 10.0 for large crosshead engines, such as are employed for marine propulsion. The lower figure is for engines without crankshaft balance weights, and the higher figure for engines with crankshaft balance weights.

$K = 3.5$ for short-stroke opposed-piston engines, and 2.75 for long-stroke opposed-piston engines. In this case S is the total combined stroke of the upper and lower pistons, and the stroke bore ratio is 3 and 4 for short and long-stroke engines respectively.

TABLE 11.

MOMENT OF INERTIA OF CRANKSHAFT AND RUNNING GEAR OF A SIX-CYLINDER FOUR-STROKE CYCLE OIL ENGINE, $13\frac{1}{2}$ -INCH BORE \times 18-INCH STROKE.

Item.	No. of.	Weight of One, Lbs.	Total Weight, Lbs.	K^2 , Ft. ² .	W. K^2 , Lbs.-Ft. ² .	J, Lbs.-Ft. Sec. ² .
Journals .	7	144	1008	0.0595	60	1.865
Crankpins .	6	114	684	0.6220	425	13.150
Crankwebs .	12	210	2520	0.3000	766	23.800
Revolving part of connecting rod . .	6	192	1152	0.5625	648	20.100
Recip. part 2	6	225	1350	0.5625	760	23.600

Total moment of inertia = 82.515,

i.e. moment of inertia per cyl. = $\frac{82.515}{6} = 13.75$ lbs.-ft. sec.².

In the case of automobile and aero engines it is more convenient to express the moment of inertia in lbs.-ins. sec.² units,

i.e.
$$J = \frac{D^2 \cdot S^3}{h} \text{ lbs.-ins. sec.}^2 \quad . \quad . \quad . \quad (60)$$

- where J = moment of inertia of revolving and reciprocating parts of one cylinder line,
 D = bore of cylinder in inches,
 S = stroke in inches,
 k = 5000 for automobile engines with crankshaft balance weights,
 = 10,000 for automobile engines without crankshaft balance weights; and for in-line aero engines with crankshaft balance weights,
 = 20,000 for in-line aero engines without crankshaft balance weights; and for radial aero engines.

The values of J obtained by using these factors are approximate and should be used for general guidance only. In the case of in-line engines with more than one bank of cylinders the value of J obtained from Equation (60), using the above values of k , should be multiplied by the number of banks to obtain the approximate moment of inertia of each crank line.

In the case of radial engines the value of J obtained by inserting the above value of k in Equation (60) should be multiplied by the number of cylinders in each row to obtain the approximate moment of inertia at each crank throw.

(b) **Moment of Inertia of a Marine Propeller or Air-screw.**—The propeller is first reduced to an equivalent disc as follows (see Figs. 28 and 29).

Describe a radius x and determine the total cross-sectional area of the blades at this radius. This total area divided by $(2 \cdot \pi \cdot x)$ is the thickness of the equivalent disc at radius x .

The complete equivalent disc is obtained by repeating this process at different radii.

The boss and that part of the propeller shaft contained in the boss may be treated as a solid of revolution,

$$\text{i.e. moment of inertia of boss} = \frac{\pi \cdot D^2 \cdot L \cdot S}{4 \cdot g} \cdot \frac{D^2}{8} \text{ lbs.-ins. sec.}^2, \quad (61)$$

where D = diameter of boss in ins.,

L = length of boss in ins.,

S = specific weight of material in lbs. per cu. in.,

g = 386 ins. per sec.².

For bronze $S = 0.315$ lb. per cu. in.,

i.e. $J = \frac{D^4 \cdot L}{12500}$ lbs.-ins. sec.². (62)

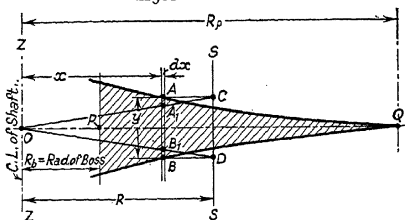


FIG. 28.—Equivalent disc.

The moment of inertia of the propeller blades is obtained from the equivalent disc as follows:—

In Fig. 28 the full lines show the outline of the equivalent disc for the propeller blades. SS is a line drawn parallel to the

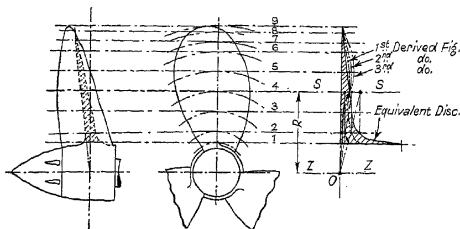


FIG. 29.—Moment of inertia of propeller blade.

axis ZZ at any desired radius (a position midway between the points P and Q is convenient).

Let the distance of SS from ZZ be R, and rule any line AB parallel to the axis ZZ, cutting the outline of the equivalent disc at A and B.

Project A and B on to SS at C and D. Join C and D to any convenient point O on the axis ZZ, cutting AB at A₁ and B₁.

Then A₁ and B₁ are points on the "first derived figure."

Repeat this process for different positions of the line AB, thus obtaining the outline of the first derived figure.

Treat the first derived figure as though it were the original figure, and so obtain the "second derived figure."

Finally, use the second derived figure to obtain the "third derived figure" in a similar manner.

Let A = area of original figure in sq. ins.,

A₁ = area of first derived figure in sq. ins.,

A₂ = area of second derived figure in sq. ins.,

A₃ = area of third derived figure in sq. ins.,

S = weight of 1 cu. in. of the material.

Then

$$A = \int_{R_b}^{R_p} y \cdot dx; \quad A_1 = \frac{1}{R} \int_{R_b}^{R_p} x \cdot y \cdot dx;$$

$$A_2 = \frac{1}{R^2} \int_{R_b}^{R_p} x^2 \cdot y \cdot dx; \quad A_3 = \frac{1}{R^3} \int_{R_b}^{R_p} x^3 \cdot y \cdot dx,$$

where R_b = radius of boss; R_p = extreme radius of blades,
i.e. weight of blades,

$$W = 2 \cdot \pi \cdot S \cdot \int_{R_b}^{R_p} x \cdot y \cdot dx \text{ lbs.},$$

$$\text{or} \quad W = 2 \cdot \pi \cdot S \cdot R \cdot A_1 \text{ lbs.} \quad . \quad . \quad . \quad (63)$$

Moment of inertia of blades about axis ZZ,

$$J = \frac{2 \cdot \pi \cdot S}{g} \cdot \int_{R_b}^{R_p} x^3 \cdot y \cdot dx \text{ lbs.-ins. sec.}^2,$$

$$\text{i.e.} \quad J = \frac{2 \cdot \pi \cdot S}{g} \cdot R^3 \cdot A_3 \text{ lbs.-ins. sec.}^2, \quad . \quad . \quad . \quad (64)$$

where $g = 386 \text{ ins. per sec.}^2$.

$$\text{Also} \quad J = \frac{W \cdot K^2}{g}$$

$$\text{i.e. radius of gyration} \quad K = R \sqrt{\frac{A_3}{A_1}} \text{ ins.} \quad . \quad . \quad . \quad (65)$$

If the equivalent disc is not drawn full size, care must be taken to allow for the vertical and horizontal scales in calculating the values of A_1 and A_3 .

EXAMPLE 15.—Fig. 29 shows one blade of a three-bladed propeller, 14 ft. 6 ins. diameter.

The equivalent disc for one blade of this propeller is also shown in Fig. 29; the horizontal scale having been made five times full size, and all thicknesses having been measured from a vertical line to reduce the work entailed in drawing the derived figures.

The thicknesses of the equivalent disc are tabulated below :—

TABLE 12.

Section.	Cross-Sectional Area of One Blade in Sq. Ins.	Radius in Ins.	Thickness of Equivalent Disc in Ins.
1	442.3	18	3.907
2	180.7	24	1.200
3	166.6	36	0.738
4	138.6	48	0.460
5	98.6	60	0.262
6	51.3	72	0.114
7	31.5	78	0.064
8	12.8	84	0.024
9	0	87	0

The equivalent disc was drawn to the following scales :—

Vertical scale (radii) : half full size (1 in. = 2 ins.).

Horizontal scale (thickness) : five times full size

(1 in. = 1/5 in.).

Hence, area scale is 1 sq. in. = $2 \times 1/5 = 2/5$ sq. in.

The areas of the first and third derived figures for one blade of this propeller, measured by planimeter on the drawing, were 60.0 and 56.9 sq. ins. respectively.

Hence, $A_1 = 2 \times 60 = 24$ sq. ins.,

i.e. assuming $S = 0.315$ lb. per cu. in. for bronze,
 $R = 48$ ins. (see Fig. 29),
 $W = 2 \times 3.1416 \times 0.315 \times \quad \times 24$
 $= 2280$ lbs. per blade.

Also

$$A_s = \frac{2 \times 56.9}{5} = 22.8 \text{ sq. ins.},$$

i.e. $J = \frac{2 \times 3.1416 \times 0.315 \times 48^3 \times 22.8}{386}$
 $= 12,900$ lbs.-ins. sec.² per blade
 $= \frac{12900}{2240 \times 12} = 0.48$ ton-ft. sec.² per blade.

Boss.—The boss and that portion of the propeller shaft contained in it is equivalent to a solid cylinder 33 ins. diameter and 33 ins. long.

Hence, $J = \frac{D^4 \cdot L}{12500} = \frac{33^4 \times 33}{12500}$
 $= 3130$ lbs.-ins. sec.²
 $= 0.116$ ton-ft. sec.².

Total moment of inertia of propeller :—

$$\begin{aligned} \text{Blades} &= 3 \times 0.48 = 1.440 \\ \text{Boss} &= 0.116 \end{aligned}$$

$$\text{Total} = 1.556 \text{ tons-ft. sec.}^2.$$

The effective moment of inertia of the propeller is greater than the foregoing calculated values due to the effect of the entrained water. According to Frahm, the allowance for entrained water varies from 20 to 30 per cent., with an average of 25 per cent. for propellers of normal design, i.e. the calculated moment of inertia should be increased by 25 per cent. before using it for calculating natural frequencies and vibration stresses. In the above example, therefore, the effective moment of inertia is

$$J = 1.556 \times 1.25 = 1.945 \text{ tons-ft. sec.}^2$$

The exact value of the allowance for entrained water cannot very well be calculated mathematically, since it depends on the

design of the propeller and the characteristics of the ship's hull. Previous experience with similar installations is the best guide as to whether an allowance of 25 per cent. will be satisfactory or not. In this connection it should be noted that the moment of inertia of the propeller mainly influences the value of the one-node frequency of marine installations, and has relatively small influence on the value of the two-node frequency, where the amplitude of vibration at the propeller is small.

It should also be noted that the effective moment of inertia of the propeller varies with the loading of the vessel, so that there is usually some difference between the one-node frequency

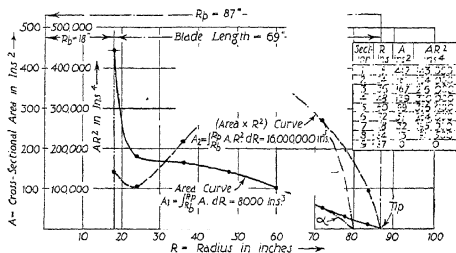


FIG. 30.—Polar moment of inertia of air-screw or propeller blade.

of vibration when the vessel is fully loaded and the propeller is fully immersed, and when the vessel is in ballast and the tips of the propeller blades are projecting above the water.

An alternative method of obtaining the polar moment of inertia of a marine propeller or air-screw blade is shown in Fig. 30.

This method is probably more accurate than the equivalent disc method just described, because it does not depend upon the accuracy of a somewhat laborious graphical construction. In the alternative method the cross-sectional areas of the blade A , at different radii R , are calculated and entered in the table shown in Fig. 30. In this table the first column contains

the number of the section ; the second column contains the radii R , at which the various sections are situated measured from the axis of rotation, in inches ; the third column contains the cross-sectional areas A , of the various sections, in square inches ; and the last column contains the products $(A \cdot R^2)$, in inches⁴, i.e. the product of cross-sectional area and radius squared at each section.

Fig. 30 is drawn for the example already worked out by the equivalent disc method, i.e. the values of the cross-sectional areas and radii are taken from Table 12.

Two curves are plotted from the values given in the table in Fig. 30, namely, a curve showing the variation of cross-sectional area with radius, and a curve showing the variation of the product $(A \cdot R^2)$ with radius.

The weight of the blade is obtained from the first curve, as follows :—

$$\begin{aligned} \text{Total volume of blade} &= \int_{R_0}^{R_p} A \cdot dR \text{ cubic inches.} \\ &= \text{area under full line curve in Fig. 30} \\ &= A_1. \end{aligned}$$

$$\text{Weight of blade, } W = S \cdot A_1,$$

where S = weight of 1 cu. in. of the material in lbs.

The area under the curve is obtained by planimeter and care must be taken in determining the area scale.

If the area is measured by planimeter in square inches and r in. on the horizontal scale represents x ins. radius, whilst r in. on the vertical scale represents y sq. ins. of cross-sectional area, then the area scale is

$$1 \text{ sq. in.} = x \cdot y \text{ ins.}^3.$$

In Fig. 30, for example, assuming that the vertical scale is r in. = 100 sq. ins. of cross-sectional area, and the horizontal scale is r in. = 10 ins. radius, then the area scale is r sq. in. = $100 \times 10 = 1000$ ins.³.

The area under the full line curve in Fig. 30 measured by planimeter is 8 sq. ins.

Hence, $A_1 = 8 \times 1000 = 8000 \text{ ins.}^3$.

The material is bronze, i.e. $S = 0.315 \text{ lb. per cu. in.}$

The weight of the blade is therefore

$$W = S \cdot A_1 = 0.315 \times 8000 = 2520 \text{ lbs.}$$

This value is about 10 per cent. greater than the value obtained by the equivalent disc method.

The polar moment of inertia of the blade is obtained from the second curve in Fig. 30 as follows:—

Polar moment of inertia = J

$$\begin{aligned} &= \frac{S}{g} \int_{R_1}^{R_2} A \cdot R^2 \cdot dR \text{ lbs.-ins. sec.}^2 \\ &= \frac{S}{g} (\text{area under dotted line curve in Fig. 30}) \\ &= \frac{S}{g} \cdot A_2, \end{aligned}$$

where S = weight of 1 cu. in. of the material in lbs.,
 $g = 386 \text{ ins./sec.}^2$.

The area scale is 1 sq. in. = $x \cdot z$,

where 1 in. on the horizontal scale represents x ins. radius, and
 1 in. on the vertical scale represents z units of the product
 (AR^2).

In Fig. 30, for example, assuming that the vertical scale is
 1 in. = 100,000 ins.⁴ of the product (AR^2), and the horizontal
 scale is 1 in. = 10 ins. radius, then the area scale is

$$1 \text{ sq. in.} = 100,000 \times 10 = 1,000,000 \text{ ins.}^5.$$

The area under the dotted line curve in Fig. 30, measured
 by planimeter, is 16 ins.².

Hence, $A_2 = 16 \times 1,000,000 = 16,000,000 \text{ ins.}^5$.

The polar moment of inertia of the blade is therefore

$$\begin{aligned} J &= \frac{S}{g} \cdot A_2 = \frac{0.315}{386} \times 16,000,000 \\ &= 13,050 \text{ lbs.-ins. sec.}^2. \end{aligned}$$

This is only 1 per cent. greater than the value obtained by the equivalent disc method, indicating that the difference in the weight calculated by the two methods is due to a difference in estimating the weight at the root end of the blade.

The radius of gyration K is easily obtained, as follows :—

$$K = \sqrt{\frac{J \cdot g}{W}} = \sqrt{\frac{A_2}{A_1}} \text{ inches.}$$

In the present example, $A_2 = 16,000,000$ and $A_1 = 8000$.

$$\text{Hence, } K = \sqrt{\frac{16000000}{8000}} = 44.7 \text{ ins.}$$

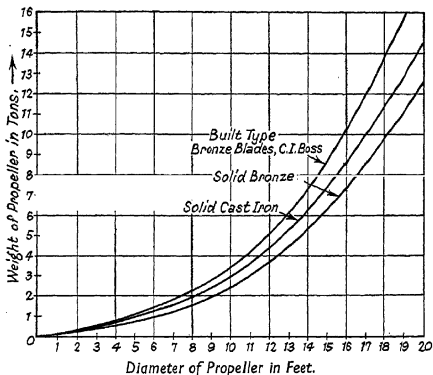


FIG. 31.—Weight of four-bladed marine propellers, including C.I. tail cap.

The method just described can be used equally successfully for determining the weight and polar moment of inertia of the blade when a piece is cut off the tip. This is useful in the case of air-screw blades where it is common practice to manufacture different diameter air-screws from one standard blade by cutting the desired amount off the tips.

For example, if the tip radius of the propeller blade of Fig. 30 is reduced from 87 ins. to 80 ins., the weight and polar moment of inertia of the shortened blade is obtained by stopping the graphical integrations at 80 ins. radius. The curves will, of course, require rounding off before calculating their areas, as shown by the chain dotted lines α and δ , to allow for the rounding off at the tip of the shortened blade.

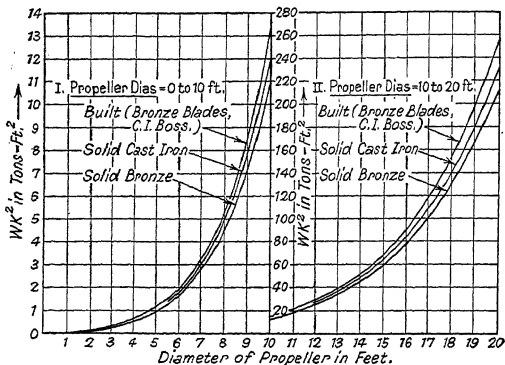


FIG. 32.— WK^2 of four-bladed marine propellers.

(Moment of inertia of propeller = $\frac{WK^2}{g} + 25$ per cent. to 30 per cent. allowance for entrained water.)

As already explained the calculated moment of inertia of a marine propeller must be increased by about 25 per cent. to allow for entrained water, but this correction is not applied to air-screws.

Figs. 31 and 32 contain the weights and WK^2 values for four-bladed marine propellers, and may be used for estimating purposes.

Figs. 33 and 34 contain the weights and WK^2 values of metal and wooden air-screws. The values include the hubs,

although as a general rule the effect of the hub on the polar moment of inertia of an air-screw is negligible.

The curves are based on good average values for two-bladed metal air-screws in the smaller diameters and for three-bladed

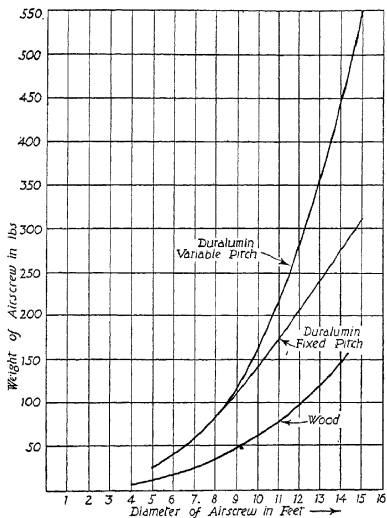


FIG. 33.—Weight of air-screws, including hub.

metal air-screws in the larger sizes. In the case of wooden air-screws the values are for two-bladed designs throughout.

The curves for four-bladed wooden air-screws lie between the curves for metal and for two-bladed wooden air-screws.

In using these curves it should be borne in mind that considerable variation in the polar moment of inertia of

air-screws of the same diameter and number of blades, but of different designs, is possible. Nevertheless, the values obtained from these curves will enable fairly accurate estimates of torsional vibration frequencies to be made, because quite a large variation in air-screw inertia does not make much difference to the frequency calculation in normal engine-air-screw installations.

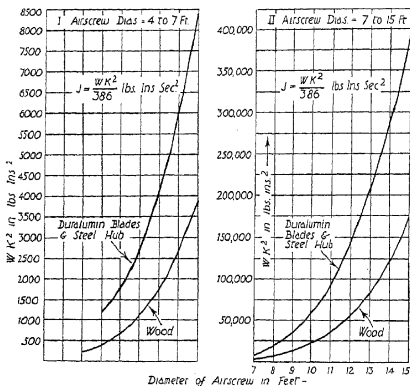


FIG. 34.— WK^2 of air-screws.

It should, however, be kept in mind that air-screw blade flexibility can have an important influence, especially in the case of high duty metal air-screws where blade scantlings are kept as small as possible to minimise weight (see the Appendix to Vol. I).

EXAMPLE 16.—Estimate the weight and effective moment of inertia of a solid bronze propeller, 16 ft. 0 in. diameter.

From Fig. 31, weight = 7.35 tons. This weight includes the boss and a cast-iron tail cap, but does not include that portion of the propeller shaft contained in the boss.

From Fig. 32, $WK^2 = 77$ tons-ft.²,

$$\begin{aligned} \text{i.e.} \quad J &= 1.25(WK^2/g) = \frac{1.25 \times 77}{32.2} \\ &= 2.99 \text{ tons-ft. sec.}^2. \end{aligned}$$

This value includes the propeller boss and a cast-iron tail cap, but does not include that portion of the propeller shaft contained in the boss.

Small Marine Propellers.—The weight and polar moment of inertia of small solid bronze three-bladed marine propellers may be estimated from the following formulæ, in the absence of specific data:—

$$\text{Weight} = W = D^3/400 \text{ lbs.} \quad . \quad . \quad . \quad (66)$$

Radius of gyration = $K = 0.27D$ ins.,

$$\text{i.e.} \quad WK^2 = D^5/5500 \text{ lbs.-ins.}^4 \text{ (excluding entrained water)} \quad . \quad . \quad . \quad (67)$$

where $D =$ diameter of propeller in inches.

(c) **Moment of Inertia of Flywheel.**—If the flywheel is simple in form, e.g. a plain disc and rim, the moment of inertia may be obtained as follows:—

$$\text{Rim.}— \quad J_r = \frac{W_r(D^2 + d^2)}{g} \text{ lbs.-ft. sec.}^2, \quad . \quad . \quad . \quad (68)$$

where

$W_r =$ weight of rim in lbs.,

$g = 32.2$ ft. sec.²,

$D =$ external diameter of rim in feet,

$d =$ internal diameter of rim in feet.

$$\text{Disc.}— \quad J_d = \frac{W_d(D_1^2 + d_1^2)}{g} \text{ lbs.-ft. sec.}^2, \quad . \quad . \quad . \quad (69)$$

where

$D_1 =$ external diameter of disc in feet,

$d_1 =$ internal diameter of disc in feet,

i.e. moment of inertia of flywheel = $J = (J_r + J_d)$.

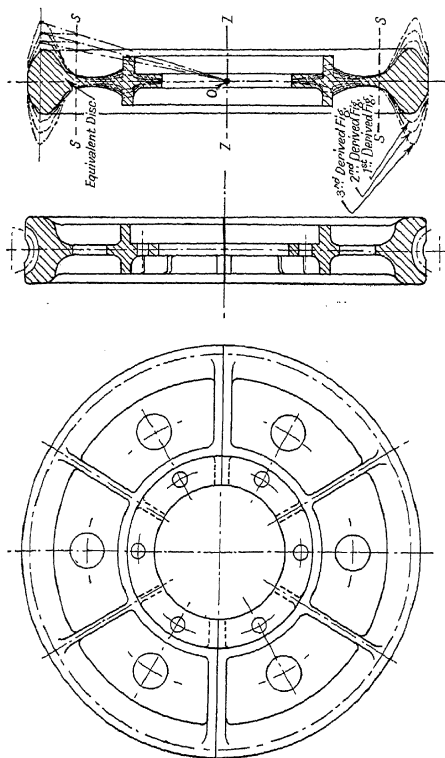


FIG. 35.—Moment of inertia of flywheel.

If the flywheel is more complicated in form, e.g. a wheel with arms, or a turning wheel of light, ribbed construction, the equivalent disc method already described should be used (Fig. 28).

Fig. 35 shows the equivalent disc and derived figures for a typical combined flywheel and turning wheel of light ribbed construction.

An experimental determination of the specific gravity of the material of cast-iron flywheels indicated that the average specific weight was only 0.25 lb. per cubic inch compared with the value generally employed, namely 0.26. The experimental value of the radius of gyration was about 4 per cent. less than the calculated value, indicating that the more open-grained

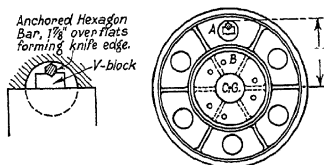


Fig. 36.—Experimental determination of moment of inertia.

material was in the flywheel rim. If, therefore, a specific weight of 0.26 is used for calculating the weight and polar moment of inertia of a heavy flywheel, the variation of density of material may be taken into account by reducing the calculated weight by 4 per cent., and by reducing the calculated polar moment of inertia by 12 per cent., to obtain the probable actual values.

These corrections may be important in systems where close tuning is necessary.

Experimental Determination of Moment of Inertia of Rotating Bodies.—The calculated value of the moment of inertia may be checked by experiment, using the compound pendulum theory.

Fig. 36 shows the arrangement. The flywheel is suspended

from a knife edge and the natural frequency of oscillation determined, taking care to avoid having too large an angle of swing. The knife edge in Fig. 36 consists of a short length of hexagon bar supported in V-blocks. Care must be taken to ensure that the support is rigid.

Let T = periodic time in seconds, i.e. the time for one complete oscillation,

K = radius of gyration of wheel about the centre of gravity (C.G.) in feet,

R = distance of C.G. of wheel from point of suspension in feet,

$$g = 32.2 \text{ ft. per sec.}^2.$$

$$\text{Then } T = 2 \cdot \pi \cdot \sqrt{\frac{K^2 + R^2}{g \cdot R}} \text{ secs.},$$

$$\text{or } K^2 = \frac{T^2 \cdot g \cdot R}{39.5} - R^2 = [0.815(T^2 \cdot R) - R^2] \text{ ft.}^2. \quad (70)$$

$$\text{Hence, } J = \frac{W}{g} \cdot K^2 \text{ lbs.-ft. sec.}^2,$$

where W = weight of flywheel in lbs.

Another simple method of determining the moment of inertia experimentally is shown in Fig. 37.

In this case the rotating body is suspended by two light wires so as to be free to oscillate in the horizontal plane.

Referring to Fig. 37,

Let W = weight of body in lbs.,

L = length of suspension wires in feet,

R = radial distance of each suspension wire from the axis of oscillation in feet.

$$\text{Then restoring force } F = W \cdot \sin \alpha = \frac{W \cdot R \cdot \theta}{L},$$

$$\text{restoring couple } M = W \cdot R^2 \cdot \theta$$

restoring couple per unit displacement

$$C = \frac{M}{\theta} = \frac{W \cdot R^2}{L}.$$

Now $T = 2 \cdot \pi \sqrt{\frac{J}{C}}$,

where T = periodic time in seconds,
 J = moment of inertia of body about axis of oscillation in lbs.-ft. sec.²,

i.e. $T = 2 \cdot \pi \sqrt{\frac{J \cdot L}{W \cdot R^2}}$

Hence, $J = \frac{W \cdot R^2 \cdot T^2}{4 \cdot \pi^2 \cdot L} = \frac{W \cdot R^2 \cdot T^2}{39 \cdot 5 \cdot L}$ lbs.-ft. sec.². . (71)

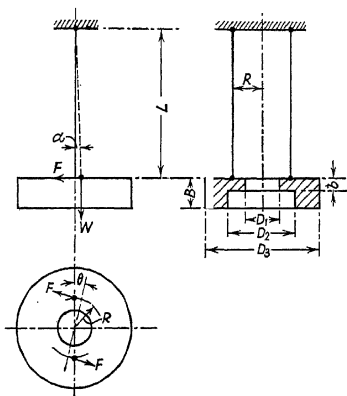


FIG. 37.—Experimental determination of moment of inertia of flywheel.

It should be noted that the above expression is independent of the number of suspension wires, so that three wires may be used for supporting heavy bodies. Care must be taken to keep the amplitude of the oscillations small.

EXAMPLE 17.—(A) A motor-car wheel, fitted with a 27-in. \times 4.4-in. tyre, was suspended on a knife edge, as shown in Fig. 36.

The distance from the point of suspension to the axis of the wheel was 8.688 ins., the weight of the wheel was 33 lbs., and the number of complete oscillations per minute was 42. Calculate the moment of inertia of the wheel.

In this case, $W = 33$ lbs.,

$$R = \frac{8.688}{12} = 0.724 \text{ ft.},$$

$$T = \frac{60}{42} = 1.429 \text{ secs.}$$

Hence,

$$\begin{aligned} K^2 &= 0.815(T^2 \cdot R) - R^2 \\ &= (0.815 \times 1.429^2 \times 0.724) - 0.724^2 \\ &= 0.681 \text{ ft.}^2, \end{aligned}$$

or

$$\begin{aligned} J &= \frac{W}{g} \cdot K^2 = \frac{33 \times 0.681}{32.2} \\ &= 0.698 \text{ lb.-ft. sec.}^2. \end{aligned}$$

- (B) The same wheel was suspended by means of two wires, as shown in Fig. 37. The length of each wire was 5.5 ft. and the radial distance of each wire from the axis of oscillation was 7.68 ins. The time for fifty complete oscillations was 170 secs. Calculate the moment of inertia of the wheel.

In this case $W = 33$ lbs.,

$$L = 5.5 \text{ ft.},$$

$$R = \frac{7.68}{12} = 0.64 \text{ ft.},$$

$$T = \frac{170}{50} = 3.4 \text{ secs.}$$

Hence,

$$\begin{aligned} J &= \frac{W \cdot R^2 \cdot T^2}{39.5 L} = \frac{33 \times 0.64^2 \times 3.4^2}{39.5 \times 5.5} \\ &= 0.718 \text{ lb.-ft. sec.}^2. \end{aligned}$$

This is within 3 per cent. of the value previously obtained.

(d) **Correction for Mass of Shafting.**—It was shown in Chapter 1 that as a general rule the mass of the shaft can be neglected if the product of the length of the shaft in feet, multiplied by the frequency in vibrations per second, does not exceed 1000.

In the case of systems consisting of two masses, A and B,

separated by a length of shafting, the mass of the shaft can be taken into account as follows. Estimate the position of the node by the methods already given. Add one-third of the moment of inertia of the length of shaft between the node and mass A to the moment of inertia of mass A ; and add one-third of the moment of inertia of the length of shaft between the node and mass B to the moment of inertia of mass B.

If there is more than one mass at one end of the system, the appropriate proportion of the moment of inertia of the connecting shaft should be equally divided amongst these masses.

When the inertia of the shaft cannot be neglected, e.g. very long shafts with light end masses, the methods given in Chapter 8 should be used [see Eqn. (402)].

(e) **General.**—Table 13 contains expressions for calculating the weights and radii of gyration of a number of standard solids.

Since most engineering structures are composed of standard forms, this table and the following rules will be found useful for estimating moments of inertia.

Rule 1.—The moment of inertia of a body with respect to any axis is the sum of the moments of inertia of any constituent parts into which we may conceive it divided,

$$\text{i.e.} \quad J = \Sigma(J_1 + J_2 + \text{etc.}). \quad (72)$$

Rule 2.—The moment of inertia of any body about any axis is equal to its moment of inertia about a parallel axis through the centre of gravity, plus the moment of inertia which the body would have about the given axis if all collected at its centre of gravity,

$$\text{i.e.} \quad J_{xx} = \left(J_{GG} + \frac{W}{g} \cdot R^2 \right), \quad (73)$$

where J_{xx} = moment of inertia about given axis xx ,
 J_{GG} = moment of inertia about a parallel axis through the centre of gravity,
 W = total weight of body,
 R = distance of the centre of gravity from the given axis xx .

TABLE 13.
MOMENTS OF INERTIA OF SOLIDS.

$$J_{xx} = \frac{W}{g} K_{xx}^2$$

J_{xx} = Moment of Inertia about Axis xx , in Lbs. Ft. Sec.²
 W = Weight of Body, in Lbs. K = Radius of Gyration, in Feet.
 S = Specific Weight of Material in Lbs./Ft.³ $g = 32.2$ Ft./Sec.²
 All Linear Dimensions to be measured in Feet.

Weight, in Lbs.

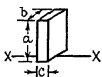
Radius of Gyration, in Feet.

Parallelepiped.

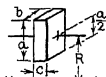
$$W = S(a \cdot b \cdot c)$$



$$K_{xx}^2 = \frac{a^2 + b^2}{12}$$



$$K_{xx}^2 = \frac{4a^2 + b^2}{12}$$

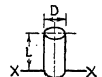


$$K_{xx}^2 = \frac{a^2 + b^2}{12} + R^2$$

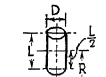
$$W = \frac{\pi}{4} D^2 L S$$



$$K_{xx}^2 = \frac{L^2}{12} + \frac{D^2}{16}$$



$$K_{xx}^2 = \frac{L^2}{3} + \frac{D^2}{16}$$



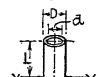
$$K_{xx}^2 = \frac{L^2}{12} + \frac{D^2}{16} + R^2$$

Hollow Cylinder.

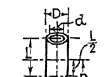
$$W = \frac{\pi}{4} (D^2 - d^2) L S$$



$$K_{xx}^2 = \frac{L^2}{12} + \frac{(D^2 + d^2)}{16}$$



$$K_{xx}^2 = \frac{L^2}{3} + \frac{(D^2 + d^2)}{16}$$

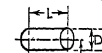


$$K_{xx}^2 = \frac{L^2}{12} + \frac{(D^2 + d^2)}{16} + R^2$$

$$W = \frac{\pi}{4} D^2 L S$$



$$K_{xx}^2 = \frac{D^2}{8}$$



$$K_{xx}^2 = \frac{D^2}{8} + R^2$$

Hollow Cylinder.

$$W = \frac{\pi}{4} (D^2 - d^2) L S$$



$$K_{xx}^2 = \frac{(D^2 + d^2)}{8}$$



$$K_{xx}^2 = \frac{(D^2 + d^2)}{8} + R^2$$

TABLE 13. (continued.)


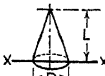

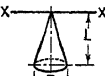
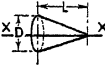
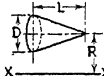
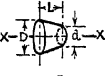
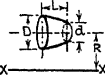
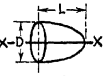
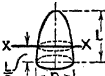

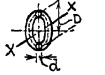

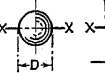
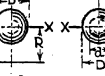

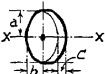
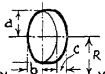
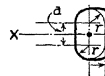
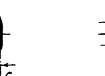
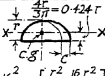
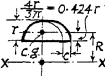
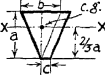
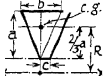
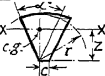
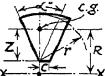

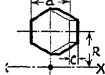
Weight, in Lbs	Radius of Gyration, in Feet.		
<u>Cone.</u> $W = \frac{\pi}{12} D^2 L S.$			
	$K_{xx}^2 = \frac{3}{80} (L^2 + D^2)$	$K_{xx}^2 = \frac{(8L^2 + 3D^2)}{80}$	$K_{xx}^2 = \frac{3}{80} (L^2 + D^2) + R^2$
<u>Cone.</u> $W = \frac{\pi}{12} D^2 L S.$			
	$K_{xx}^2 = \frac{(48L^2 + 3D^2)}{80}$	$K_{xx}^2 = \frac{3D^2}{40}$	$K_{xx}^2 = \frac{3}{40} D^2 + R^2$
<u>Frustum of Cone</u> $W = \frac{\pi}{12} L S (D^2 + D \cdot d + d^2)$			
	$K_{xx}^2 = \frac{3}{40} \left(\frac{D^5 - d^5}{D^3 - d^3} \right)$	$K_{xx}^2 = \frac{3}{40} \left(\frac{D^5 - d^5}{D^3 - d^3} \right) + R^2$	
<u>Paraboloid.</u> $W = \frac{\pi}{8} D^2 L S.$			
	$K_{xx}^2 = \frac{D^2}{12}$	$K_{xx}^2 = \frac{D^2}{24} + \frac{L^2}{16}$	
<u>Torus.</u> $W = \frac{\pi^2}{4} D \cdot d^2 S.$			
	$K_{xx}^2 = \frac{D^2}{4} + \frac{3d^2}{16}$	$K_{xx}^2 = \frac{D^2}{8} + \frac{5}{32} d^2$	$K_{xx}^2 = \frac{D^2}{4} + \frac{3d^2}{16} + R^2$
<u>Sphere.</u> $W = \frac{\pi}{6} D^3 S$ (Solid) $W = \frac{\pi}{6} (D^3 - d^3) S$ (Hollow)			
	$K_{xx} = \frac{D}{\sqrt{10}}$	$K_{xx}^2 = \frac{D^2}{10} + R^2$	$K_{xx}^2 = \frac{1}{10} \left(\frac{D^5 - d^5}{D^3 - d^3} \right)$ $K_{xx}^2 = \frac{1}{10} \left(\frac{D^5 - d^5}{D^3 - d^3} \right) + R^2$

TABLE 13 (continued.)

Weight, in Lbs.	Radius of Gyration, in Feet.		
Elliptical Lamina $W = \pi \cdot a \cdot b \cdot c \cdot S$			$K_{XX}^2 = \frac{a^2 + b^2}{4}$
Lamina with Semi-Circular Ends $W = (\pi r + 2a) \cdot c \cdot S$			$K_{XX}^2 = \frac{2a(12r^2 + a^2) + 3\pi r(2r^2 + a^2)}{12(\pi r + 2a)}$
Semi-Circular Lamina $W = \frac{1}{2} \pi \cdot r^2 \cdot c \cdot S$			$K_{XX}^2 = \frac{r^2}{2} + R^2$
Triangular Lamina $W = \frac{1}{2} a \cdot b \cdot c \cdot S$			$K_{XX}^2 = \frac{a^2}{18} + \frac{b^2}{24}$
Segment of Circular Lamina $Z = \frac{240r \sin \frac{1}{2}\alpha}{\pi \alpha}$ $W = \frac{\pi r^2 \alpha \cdot c \cdot S}{360}$			$K_{XX}^2 = \frac{r^2}{2} - Z^2$
Hexagonal Lamina $W = 0.866 a^2 \cdot c \cdot S$			$K_{XX}^2 = \frac{5}{36} a^2$

NOTE: If all linear dimensions are in inch units and weight is in lbs; then the moment of inertia is :- $J_{XX} = \frac{W}{386} \cdot K_{XX}^2$ Lbs. ins. sec²

The following Table of Specific Weights of materials gives average values for each class of material :—

TABLE 14.
SPECIFIC WEIGHTS OF MATERIALS.

	<i>Lbs. per Cubic Inch.</i>
Aluminium	0.097
Brass	0.300
Bronze and gunmetal	0.315
Copper	0.320
Duralumin	0.102
Iron	0.260
Lead	0.412
Magnesium alloy (elektron)	0.065
Monel metal	0.323
Steel	0.283
Tungsten alloy (heavy alloy)	0.600
Rubber	0.040

AIR-SCREW BLADE MATERIALS.

Birch	0.023
Compressed and impregnated wood	0.050
Mahogany	0.032
Micarta	0.049
Oak	0.029
Walnut	0.023

Notes.—The specific weight of wood is subject to a wide variation for varying moisture content.

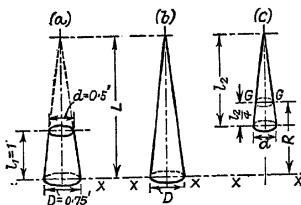


FIG. 38.—Moment of inertia of frustum of cone.

Tungsten alloy is a material recently introduced as the result of investigations carried out at the General Electric

Company's Research Laboratories, Wembley. This material has approximately the same physical properties as mild steel and is readily machinable with ordinary tools. The material has just over twice the specific weight of steel and has been used successfully for balancing internal combustion engines where space limitations prohibited the use of ordinary steels. Its tensile strength is 40 tons per sq. in., yield-point 36 tons per sq. in., Young's modulus 32,000,000 lbs. per sq. in., Brinell hardness 250 to 290.

The specific weight of rubber given in the above table is an average value for material used in the manufacture of transmission couplings.

EXAMPLE 18.—Estimate the moment of inertia of the conic frustum shown in Fig. 38 about the axis xx . The material is cast iron.

The moment of inertia of the frustum shown at (a), Fig. 38, is the difference between the moment of inertia of the large cone shown at (b), about axis xx , and that of the small cone shown at (c) about axis xx .

Moment of Inertia of Large Cone.

$$\begin{aligned} \text{Total height, } L &= \frac{h_1 \cdot D}{(D - d)} = \frac{1 \times 0.75}{(0.75 - 0.5)} \\ &= 3 \text{ ft.} \end{aligned}$$

Hence, from Table 13,

$$\begin{aligned} \text{Weight } W &= \frac{\pi \cdot D^2 \cdot L \cdot S}{12}, \text{ where } S = 450 \text{ lbs. per cu. ft.} \\ &\quad \text{for cast iron} \\ &= \frac{3.1416 \times 0.75^2 \times 3 \times 450}{12} \\ &= 199 \text{ lbs.,} \end{aligned}$$

$$\begin{aligned} K_{xx}^2 &= \frac{(8 \cdot L^3 + 3 \cdot D^2)}{80} = \frac{8 \times 3^3 + 3 \times 0.75^2}{80} \\ &= 0.921 \text{ ft.}^2. \end{aligned}$$

$$\text{Hence, } J_{xx} = \frac{199 \times 0.921}{32.2} = 5.68 \text{ lbs.-ft. sec.}^2.$$

Moment of Inertia of Small Cone.

$$\begin{aligned}\text{Weight} &= \frac{3 \cdot 1416 \times 0.5^2 \times 2 \times 450}{12} \\ &= 59 \text{ lbs.},\end{aligned}$$

$$K_{xx}^2 = \frac{3}{80} (L^2 + D^2) + R^2,$$

where R = distance of centre of gravity from axis xx

$$= \left(l_1 + \frac{l_2}{4} \right) = 1 + \frac{2}{4} = 1.5 \text{ ft.},$$

$$\begin{aligned}\text{i.e.} \quad K_{xx}^2 &= \frac{3(2^2 + 0.5^2)}{80} + 1.5^2 \\ &= 2.409 \text{ ft.}^2.\end{aligned}$$

$$\text{Hence, } J_{xx} = \frac{59 \times 2.409}{32.2} = 4.4 \text{ lbs.-ft. sec.}^2.$$

Moment of Inertia of Frustum.

$$J_{xx} = (5.68 - 4.4) = 1.28 \text{ lbs.-ft. sec.}^2.$$

The expression for the weight of a frustum is

$$\begin{aligned}W &= \frac{\pi \cdot L \cdot S}{12} (D^2 + D \cdot d + \\ &\quad 3 \cdot 1416 \times \frac{1 \times 450}{12} (0.75^2 + 0.75 \times 0.5 + 0.5^2) \\ &= 139 \text{ lbs.}\end{aligned}$$

$$\text{Also } K_{xx} = \frac{L^3}{10} \left[\frac{D^2 + 3 \cdot D \cdot d + 6 \cdot d^2}{D^2 + D \cdot d + d^2} \right] + \frac{3}{80} \left[\frac{D^5 - d^5}{D^3 - d^3} \right],$$

$$\begin{aligned}\text{i.e. } K_{xx} &= \frac{1}{10} \left[\frac{0.75^2 + 3 \times 0.75 \times 0.5 + 6 \times 0.5^2}{0.75^2 + 0.75 \times 0.5 + 0.5^2} \right] \\ &\quad + \frac{3}{80} \left[\frac{0.75^5 - 0.5^5}{0.75^3 - 0.5^3} \right] \\ &= 0.295 \text{ ft.}^2.\end{aligned}$$

$$\text{Hence, } J = \frac{W \cdot K^2}{g} = \frac{139 \times 0.295}{32.2} = 1.275 \text{ lbs.-ft. sec.}^2.$$

This agrees with the value previously calculated.

EXAMPLE 19.—Fig. 39 shows two designs of steel crankweb for an engine with a crank-throw of 2 ins. Calculate the weight and moment of inertia about the axis of rotation XX in each case.

Case I. Oval Web.

From Table 13 the weight and radius of gyration of an elliptical lamina are

$$W = \pi \cdot a \cdot b \cdot c \cdot S, \text{ and } K_{xx}^2 = \frac{a^2 + b^2}{4} + R^2.$$

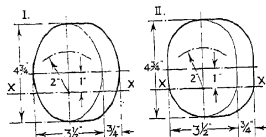


FIG. 39.—Moment of inertia of crankwebs.

In this example $a = 2.375$ ins. ; $b = 1.75$ ins. ; $c = 0.75$ ins.,
 $S = 0.283$ lb. per cu. in. for steel,
 $R =$ distance from axis of rotation to centre
of gravity of ellipse = 1 in.

Hence, $W = 3.1416 \times 2.375 \times 1.75 \times 0.75 \times 0.283$
 $= 2.77$ lbs.

Also $K_{xx}^2 = \frac{2.375^2 + 1.75^2}{4} + 1^2$
 $= 3.18$ ins.²,

i.e. $J = W \cdot K^2/386 = \frac{2.77 \times 3.18}{386} = 0.0228$ lb.-in. sec.².

Case II. Semi-Circular Ends.

From Table 13 the weight and radius of gyration of a lamina with semi-circular ends are

$$W = (\pi \cdot r + 2 \cdot a)r \cdot c \cdot S,$$

$$K_{xx}^2 = \frac{2 \cdot a(12r^2 + a^2) + 3 \cdot \pi \cdot r(2r^2 + a^2)}{12(\pi r + 2a)} + R^2.$$

In this example

$$r = 1.75 \text{ ins.}; \quad a = (4.75 - 3.5) = 1.25 \text{ ins.}, \\ c = 0.75 \text{ in.}; \quad S = 0.283 \text{ lb. per cu. in. for steel.}$$

Hence,

$$W = (3.1416 \times 1.75 + 2 \times 1.25)1.75 \times 0.75 \times 0.283 \\ = 2.97 \text{ lbs., i.e. 7.5 per cent. heavier than Case I.}$$

Also K_{xx}^2

$$= \frac{2 \times 1.25(12 \times 1.75^2 + 1.25^2) + 3 \times 3.1416 \times 1.75(2 \times 1.75^2 + 1.25^2)}{12(3.1416 \times 1.75 + 2 \times 1.25)} \\ + 1^2 = 3.32 \text{ ins.}^2,$$

$$\text{i.e. } J = W \cdot K^2/386 = \frac{2.97 \times 3.32}{386} = 0.0255 \text{ lb.-in. sec.}^2, \text{ or} \\ 12 \text{ per cent. greater than Case I.}$$

EXAMPLE 20.—Fig. 40 shows a crankweb for an automobile engine crankshaft with an integral balance weight.

Calculate the weight and moment of inertia about the axis of rotation XX.

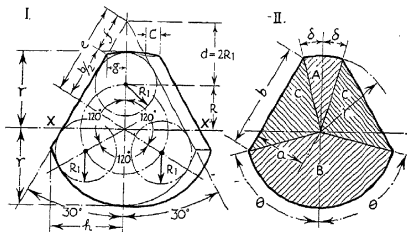


FIG. 40.—Balanced crankwebs.

The following dimensions are given :—

$$R = \text{crank-throw} = 2 \text{ ins.}; \quad r = 3.25 \text{ ins.}; \\ R_1 = 1.25 \text{ ins.}; \quad c = 0.5 \text{ in.}$$

From the geometry of the web, referring to the left-hand diagram in Fig. 40,

$$d = R_1 / \sin 30^\circ = 2 \cdot R_1 = 2 \times 1.25 = 2.5 \text{ ins.},$$

$$a = (d + R) \sin 30^\circ = (d + R)/2 = (2.5 + 2)/2 = 2.25 \text{ ins.},$$

$$b = 2\sqrt{r^2 - a^2} = 2\sqrt{3.25^2 - 2.25^2} = 4.69 \text{ ins.},$$

$$e = (d + R) \cos 30^\circ = 0.866(d + R) = 3.897 \text{ ins.},$$

$$f = \left(e - \frac{b}{2}\right) = 3.897 - 2.345 = 1.552 \text{ ins.},$$

$$g = f \cdot \sin 30^\circ = f/2 = 0.776 \text{ in.},$$

$$h = (e + 0.5b) \sin 30^\circ = \left(\frac{e + 0.5b}{2}\right) = \left(\frac{3.897 + 2.345}{2}\right) = 3.121 \text{ ins.}$$

$$\begin{aligned} \text{Also} \quad \sin \delta &= g/r = 0.776/3.25 = 0.238, \\ \delta &= 13.75^\circ, \\ \sin \theta &= h/r = 3.121/3.25 = 0.960, \\ \theta &= 74^\circ. \end{aligned}$$

The web can be divided into two circular segments and two triangles, as shown in the right-hand diagram in Fig. 40.

Segment A.

$$r = 3.25 \text{ ins. and } \alpha = 2 \cdot \delta = 2 \times 13.75 = 27.5^\circ.$$

Then from Table 13,

$$\text{Weight} = W = \frac{\pi \cdot r^2 \cdot \alpha^\circ \cdot C \cdot S}{360}, \text{ where } S = 0.283 \text{ lb. per cu. in. for steel,}$$

$$= 3.1416 \times 3.25^2 \times 27.5 \times 0.5 \times 0.283/360 = 0.358 \text{ lb.}$$

$$K_{xx} = r^2/2 = 3.25^2/2 = 5.28 \text{ ins.}^2.$$

Hence, moment of inertia of segment about polar axis $XX = J$,

$$J = WK^2/386 = 0.358 \times 5.28/386 = 0.0049 \text{ lb.-in. sec.}^2.$$

Segment B.

$$r = 3.25 \text{ ins.}, \alpha = 2 \cdot \theta = 2 \times 74 = 148^\circ.$$

$$\text{Weight} = W = 3.1416 \times 3.25^2 \times 148 \times 0.5 \times 0.283/360 = 1.93 \text{ lbs.}$$

$$K_{xx}^2 = 3.25^2/2 = 5.28 \text{ ins.}^2.$$

$$\text{Hence, } J = WK^2/386 = 1.93 \times 5.28/386 = 0.0264 \text{ lb.-in. sec.}^2.$$

Triangle C $a = 2.25 \text{ ins.}; b = 4.69 \text{ ins.}$

Then, from Table 13,

$$\begin{aligned}\text{Weight} = W &= 0.5 \cdot a \cdot b \cdot c \cdot S \\ &= 0.5 \times 2.25 \times 4.69 \times 0.5 \times 0.283 \\ &= 0.745 \text{ lb.}\end{aligned}$$

$$K_{xx}^2 = a^2/2 + b^2/24 = \frac{2.25^2}{2} + \frac{4.69^2}{24} = 3.445 \text{ ins.}^2.$$

The moment of inertia about polar axis XX is, therefore,

$$J = WK^2/386 = 0.745 \times 3.445/386 = 0.0066 \text{ lb.-in. sec.}^2.$$

The total moment of inertia of the crankweb about polar axis XX is obtained by adding together the values for the separate pieces, thus:—

Part.	Weight W.	Moment of Inertia J.
1-Segment A . .	0.358 lb.	0.0049 lb.-in. sec. ²
1-Segment B . .	1.930	0.0264
2-Triangles C . .	1.490	0.0132
Total for web . .	3.778 lbs.	0.0445 lb.-in. sec. ²

II. EQUIVALENT ELASTICITIES.

(a) **Elasticity of Shafting.**—When the shafting is not of uniform diameter throughout its length, the stiffness of each section requires separate consideration. It is convenient to replace the actual shaft by a shaft of uniform diameter D , the torsional rigidities of the sections of the equivalent shaft between the various masses being maintained the same as in the original system by an appropriate adjustment of the lengths.

The length of the equivalent shaft is determined as follows :

From Equation (1),

$$\frac{M}{I_p} = \frac{G \cdot \theta}{L},$$

where $I_p = \frac{\pi \cdot D^4}{32}$ for a solid shaft of diameter D .

Hence, torsional rigidity

$$C = \frac{M}{\theta} = \frac{G \cdot I_p}{L} = \frac{\pi \cdot D^4 \cdot G}{32 \cdot L}, \quad \dots \quad (74)$$

i.e. the torsional rigidity is directly proportional to the fourth power of the shaft diameter, and inversely proportional to the shaft length.

- Let L_1 = actual length of shaft,
 D_1 = actual diameter of shaft,
 L = equivalent length of shaft,
 D = equivalent diameter of shaft.

Then, for both sections of shaft to have the same torsional rigidity,

$$\frac{\pi \cdot D_1^4 \cdot G}{32 \cdot L_1} = \frac{\pi \cdot D^4 \cdot G}{32 \cdot L},$$

or equivalent length $L = L_1 \left(\frac{D_1^4}{D^4} \right)$ for solid shafts. . . (75)

In a similar manner it can be shown that for a hollow shaft of actual diameters D_1 and d_1 , and actual length L_1 , the length L of an equivalent solid shaft of diameter D is

$$\text{Equivalent length } L = L_1 \left[\frac{D^4}{D_1^4 - d_1^4} \right]. \quad \dots \quad (76)$$

If there are several shafts and/or flexible couplings in series the overall torsional rigidity of the complete assembly is obtained as follows:—

- Let C = overall torsional rigidity,
 C_a, C_b, C_c , etc. = torsional rigidities of the individual elements,
 L = equivalent length of the complete assembly,
 L_a, L_b, L_c , etc. = equivalent lengths of the individual elements.

Then $L = (L_a + L_b + L_c + \text{etc.} \dots)$,

but $L = U/C$; $L_a = U/C_a$; $L_b = U/C_b$; $L_c = U/C_c$; etc.,
 where U is a constant.

$$\text{Hence, } \frac{1}{C} = \left(\frac{1}{C_a} + \frac{1}{C_b} + \frac{1}{C_c} + \text{etc.} \dots \right). \quad \dots \quad (77)$$

Tapered Shafting.—For small vertex angles the equivalent length of the frustum of a circular cone is

$$L = \frac{L_1 D^4}{3(D_1 - D_2)} \left[\frac{1}{D_2^3} - \frac{1}{D_1^3} \right], \quad (78)$$

where D = diameter of equivalent uniform circular shaft of length L ,

L_1 = axial length of the frustum,

D_1 = diameter of large end of frustum,

D_2 = diameter of small end of frustum.

Equation (78) can be written

$$L = \frac{L_1 \cdot D^4 (K^3 + K + 1)}{3 \cdot D_2^4 \cdot K^3}, \quad (79)$$

where $K = D_1/D_2$.

When $K = 1$, i.e. when the shaft is of uniform diameter, Equation (79) reduces to Equation (75), which is correct.

For values of K up to and including 1.2 the error in assuming that the tapered shaft is equivalent to a parallel shaft of the same length and of diameter $(D_1 + D_2)/2$ is less than 3 per cent.

Hollow Tapered Shaft.—In the case of a shaft having a tapered bore the following method can be employed:—

Let L = equivalent length of the actual hollow shaft,

L_o = equivalent length of a solid shaft having the same dimensions as the outside dimensions of the actual shaft,

L_i = equivalent length of a solid shaft having the same dimensions as the bore of the actual shaft,

C, C_o, C_i = torsional rigidities corresponding to L, L_o and L_i respectively.

Then $C = \pi \cdot D^4 \cdot G / (32 \cdot L)$; $C_o = \pi \cdot D^4 \cdot G / (32 \cdot L_o)$;

$$C_i = \pi \cdot D^4 \cdot G / (32 \cdot L_i),$$

where D = diameter of equivalent solid parallel shaft.

Hence, $L = L_o \cdot L_i / (L_i - L_o)$ (80)

Equation (80) can be used for all normal types of hollow shaft. In the case of a hollow cylindrical parallel shaft,

outside diameter D_1 , inside diameter d_1 and length L_1 , for example :—

From Equation (75),

$$L_o = L_1 \cdot D^4/D_1^4; \quad L_i = L_1 \cdot D^4/d_1^4.$$

Hence, $L = L_o \cdot L_i/(L_i - L_o) = L_1 \cdot D^4/(D_1^4 - d_1^4)$,

which agrees with Equation (76).

Circular Shaft of Varying Diameter.—The effective

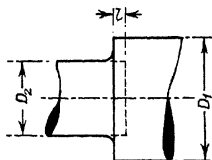


FIG. 41.—Fillet allowance.

length of a section of shafting which joins another section of larger diameter is greater than the actual length owing to local deformation at the juncture.

The smaller shaft, in effect, buries itself in the larger one, as shown in Fig. 41. The length of the smaller shaft is therefore virtually increased by

the amount l , and the length of the larger shaft decreased by the same amount.

The allowance l depends on the ratio of the shaft diameters, and may be obtained from the factors in Table 15.

TABLE 15.
EFFECTIVE LENGTHS OF SHAFTS OF VARYING DIAMETER.

Ratio:	Ratio: $\frac{l}{D_1}$
1.00	0
1.25	0.055
1.50	0.085
2.00	0.100
3.00	0.107
Infinity	0.125

Shaft Couplings.—In the case of solid forged couplings the factors already given for shafts of varying diameter may be used.

In normal designs the thickness of the couplings is about one-quarter of the shaft diameter. Hence, if a factor of 0.125 is used, the following general rule for dealing with solid forged couplings is obtained.

Assume that the shaft extends into the coupling a distance equal to one-half the thickness of the flange, and that the remainder of the flange thickness has a diameter equal to the pitch circle diameter of the coupling bolts.

In the case of keyed couplings, assume that the torsional rigidity is that of the shaft for one-half the length of the coupling, and that of the collar for the remainder.

In the case of a splined or serrated shaft, such as the air-screw shaft of an aero engine, assume that the shaft extends into the attached member a distance equal to one-third the length of the splines or serrations and that the effective outside diameter of the splined or serrated portion is equal to the pitch circle diameter of the splines or serrations.

Backlash in splined or serrated shafts tends to reduce the torsional rigidity of the connection by an amount which is not constant but which varies with the torque transmitted.

In other words, the effect of backlash is to make the connection non-linear, a subject which is discussed in Chapter 10.

In the case of members that are shrunk on to the shaft, assume that the shaft enters the attached member for a length equal to one-quarter to one-half the diameter of the shaft, the smaller value applying to tightly shrunk-on members.

In the case of a continuous sleeve or liner which is shrunk on to the shaft over a considerable length, assume that the effective outside diameter of the shaft in way of the sleeve is increased by the thickness of the sleeve, i.e. the effective radius is the radius of the shaft plus half the sleeve thickness. The stiffening effect of sleeves depends on the tightness of the fit, the length of the sleeve in relation to the shaft diameter, and the material of the sleeve.

The above rule applies to cases where the sleeve is long, is made of the same material as the shaft, and is tightly shrunk on.

When the sleeve is short it is made of more elastic material than the shaft, and a moderate fit is used, e.g. a bronze liner pressed on to a shaft, the stiffening effect is usually negligible.

As a general rule the stiffening effect of short collars or thrust rings having an axial length less than one-quarter the diameter of the shaft is also negligible.

Cast-Iron or Bronze Shafts.—When the actual shaft is made of cast iron or bronze, the equivalent length of steel shaft is given by

$$L = L_1 \left[\frac{D^4 \cdot G}{D_1^4 \cdot G_1} \right], \quad (8r)$$

where L = equivalent length of solid steel shafting,
 D = diameter of equivalent shaft,
 G = modulus of rigidity of steel,
 L_1 = actual length of cast-iron or bronze shaft,
 D_1 = actual diameter of cast-iron or bronze shaft,
 G_1 = modulus of rigidity of cast iron or bronze.

Table 16 gives the values of the moduli of rigidity for various materials:—

TABLE 16.
ELASTIC CONSTANTS.

Material.	Modulus of Elasticity, E.	Modulus of Rigidity, G.
Aluminium	10,000,000 lbs./in. ²	3,800,000 lbs./in. ²
Bronze (phosphor, manganese, and aluminium)	15,000,000	6,000,000
Cast iron	17,000,000	7,000,000
Duralumin	10,500,000	3,800,000
Gunmetal and brass	14,000,000	5,000,000
Magnesium alloy (elektron)	6,500,000	2,600,000
Monel metal	25,000,000	9,000,000
Steel	30,000,000	12,000,000
Steel (spring wire)	30,000,000	11,500,000
Steel (stainless)	28,000,000	11,800,000
Tungsten alloy (heavy metal)	32,000,000	—
Wrought iron	28,000,000	11,000,000
Rubber	500	100
Compressed and impregnated wood	3,850,000	320,000
Wood	1,500,000	80,000
Micarta	1,300,000	400,000

The values given in the above table are average values for each material. In the case of metals the variation is not great, but in the case of non-metallic materials there might

be an appreciable variation between different samples of each class.

The values given for rubber are the average values for the grade of material used in transmission couplings, but the actual value in any given case can be adjusted over a considerable range by varying the specification of the rubber.

$$\text{Note.}—G = \frac{E}{2(1 + \sigma)}, \text{ where } \sigma = \text{Poisson's Ratio}$$

$$= \frac{1}{3} \text{ to } \frac{1}{4} \text{ for most metals.}$$

EXAMPLE 21.—Calculate the length of a solid steel shaft, 8 ins. diameter, which has the same torsional rigidity as the composite shaft shown in Fig. 42.

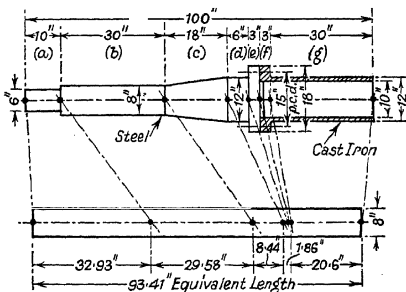


FIG. 42.—Equivalent length of complex shaft.

Section (a).—10 ins. of 6-in. diameter shaft.

The allowance for local deformation at the juncture of the 6-in. and 8-in. diameter shafts ($D_1/D_2 = 8/6 = 1.33$) is $0.07 \cdot D_2$ by interpolation from Table 15.

$$\text{Hence, Equivalent length} = (10 + 0.07 \times 6) \left[\frac{8^4}{6^4} \right],$$

$$L_a = 32.93 \text{ ins. of 8-in. diameter.}$$

Section (b).—30 ins. of 8-in. diameter shaft.

The actual length is reduced by the allowance made on section (a) for local deformation at the juncture of the 6-in. and 8-in. shafts,

$$\begin{aligned} \text{i.e.} \quad \text{Equivalent length} &= (30 - 0.07 \times 6), \\ L_b &= 29.58 \text{ ins. of 8-in. diameter.} \end{aligned}$$

Section (c).—18 ins. tapered 8-in. to 12-in. diameter.

$$\begin{aligned} \text{Equivalent length} &= \frac{L_1 \cdot D^4}{3(D_1 - D_2)} \left[\frac{1}{D_2^3} - \frac{1}{D_1^3} \right], \\ \text{i.e.} \quad L_c &= \frac{18 \times 8^4}{3(12 - 8)} \left[\frac{1}{8^3} - \frac{1}{12^3} \right] \\ &= 8.44 \text{ ins. of 8-in. diameter.} \end{aligned}$$

Section (d).—6 ins. of 12-in. diameter shaft.

The effective length of this section is the actual length plus one-half the thickness of the coupling flange,

$$\begin{aligned} \text{i.e.} \quad \text{Equivalent length} &= (6 + 1.5) \left[\frac{8^4}{12^4} \right], \\ L_d &= 1.48 \text{ in. of 8-in. diameter.} \end{aligned}$$

Section (e).—3-in. thick coupling, bolts on 15-in. P.C.D.

$$\begin{aligned} \text{Equivalent length} &= \frac{3 \left[\frac{8^4}{15^4} \right]}{2}, \\ \text{i.e.} \quad L_e &= 0.12 \text{ in. of 8-in. diameter.} \end{aligned}$$

Section (f).—3-in. thick hollow coupling, bolts on 15-in. P.C.D.

In this case the material is cast iron.

$$\text{Hence, Equivalent length} = \frac{3 \left[\frac{8^4}{15^4 - 10^4} \right] \left[\frac{12000000}{7000000} \right]}{2} \quad \begin{matrix} \text{Cast iron} \\ \text{G.C.} \end{matrix}$$

$$\text{i.e.} \quad L_f = 0.26 \text{ in. of 8-in. diameter.}$$

Section (g).—30 ins. of hollow cast-iron shaft.

$$\begin{aligned} \text{Equivalent length} &= \left[30 + \frac{3}{2} \right] \left[\frac{8^4}{12^4 - 10^4} \right] \left[\frac{12000000}{7000000} \right], \\ \text{i.e.} \quad L_g &= 20.60 \text{ ins. of 8-in. diameter.} \end{aligned}$$

Total Equivalent Length,

$$L = (L_a + L_b + L_c + L_d + L_e + L_f + L_g) \\ = 93.41 \text{ ins. of 8-in. diameter solid circular shaft (see Fig. 42).}$$

In practice the small refinements introduced into the foregoing calculation do not appreciably influence the value of the natural frequency.

For example, if the couplings and the local deformation at the juncture of the 6-in. and 8-in. sections are neglected in Fig. 42, and if the tapered portion is assumed to have a uniform diameter equal to its mean diameter, the calculation of the equivalent shaft is shortened as follows:—

Six-inch Section:

$$\text{Equivalent length} = 10 \times \frac{8^4}{6^4} = 31.6 \text{ ins.}$$

Eight-inch Section:

$$\text{Equivalent length} = 30.0 \text{ ins.}$$

Tapered Section (mean diameter = 10 ins.):

$$\text{Equivalent length} = 18 \times \frac{8^4}{10^4} = 7.4 \text{ ins.}$$

Twelve-inch Section:

$$\text{Equivalent length} = 6 \times \frac{8^4}{12^4} = 1.2 \text{ ins.}$$

Hollow Cast-Iron Section:

$$\text{Equivalent length} = 30 \left[\frac{8^4}{12^4 - 10^4} \right] \left[\frac{12000000}{7000000} \right] \\ = 19.6 \text{ ins.}$$

Hence, *Total equivalent length* = 89.8 ins.

This is 4 per cent. less than the more accurately calculated value, and since the frequency of torsional vibration is inversely proportional to the square root of the length, the probable error in the frequency calculation would be 2 per cent. high when using the approximate value for the equivalent length.

Torsional Rigidity of Shafts of Non-Circular Cross-Section.—Table 17 contains expressions for calculating the equivalent lengths of shafts of non-circular cross-section.

The classical work of Saint Venant on the torsion of prisms showed that in bars having symmetrical but non-circular cross-sections plane transverse sections do not remain plane when the bar is twisted, but become curved or warped. This warping brings about a different distribution of shear stress and shear strain from what would occur if transverse sections remained plane after twisting. As a general rule the greatest intensity of shear stress in a bar of symmetrical but non-circular cross-section occurs at a point on the perimeter of the cross-section *nearest* to the shaft axis or centroid of the cross-section. Thus in the case of an elliptical cross-section the maximum shear stress occurs on the boundary of the ellipse at the extremity of the minor axis. If the plane section had remained plane after twisting, the maximum shear stress would have occurred at the point situated at the greatest distance from the axis of twist, i.e. at the extremity of the major axis, and the shear stress would have been a minimum at the extremity of the minor axis.

Similarly, in the case of a rectangular bar the maximum shear stress occurs on the boundary of the rectangle at the middle of the longer side. The shear stress at the corners of the rectangle is zero.

These examples show that the simple theory used for solving torsion problems relating to circular bars, viz. that within the elastic limit shear stress and shear strain are proportional to the distance from the centre of the bar, cannot be applied in the case of shafts of non-circular cross-section.

The subject has been investigated both analytically and experimentally (see Bibliography). An account of Saint Venant's analytical work is given in Todhunter and Pearson's "History of the Elasticity and Strength of Materials," Vol. II, Part I, Chapter X, Cambridge University Press, whilst the elegant experimental work of A. A. Griffith and G. I. Taylor, using the soap film analogy suggested by Prandtl, is described in their paper, "The Use of Soap Films in Solving Torsion Problems," *Proceedings, Institute of Mechanical Engineers*, 1917, p. 755. A good summary of the subject is contained in Seely's "Advanced Mechanics of Materials," Chapter IX, Chapman & Hall (London).

The expressions contained in Table 17 have been mainly deduced from Saint Venant's empirical formulæ and from the results of Griffith and Taylor's soap film experiments. The following general conclusions should be noted:—

- (1) The soap film experiments showed that at external corners, such as the corners of a rectangular or triangular bar, the shear stress due to twisting is zero; whilst at internal corners, such as the corners of key-ways and the roots of splines and serrations, the shear stress due to twisting is very high. In general, the stress at any point on the boundary of a section where the section is convex outward is less than if the boundary of the section were straight, and at a sharp external corner the stress is zero. The stress at any point on the boundary of a section where the section is concave is greater than if the boundary of the section were straight, and at sharp internal corners the stress is theoretically infinite, assuming that stress remains proportional to strain. In practice, however, since all materials are more or less ductile, the stress at sharp internal corners remains finite because of local yielding of the material, which brings about a redistribution of stress in the neighbourhood of the highly stressed region. The extent of this mitigating influence depends upon the ductility of the material and the shape of the corner. *The simple precautionary measure of providing the largest possible radius in all corners should always be taken.*

The foregoing points can be verified by referring to some of the examples in Table 17. Thus the stress at the corner of a key-way is considerably greater than the stress at the centre of the key-flat when there is a small radius at the corner of the key-way, but becomes nearly equal to the stress at the centre of the key-flat when the corner radius is increased.

- (2) The soap film experiments showed that a long thin rectangular torsion member is not so stiff as a member

TABLE 17.

TORSIONAL RIGIDITY OF SHAFTS.

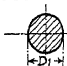


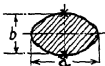
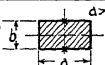
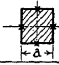
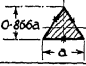
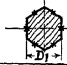
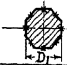
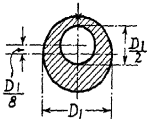
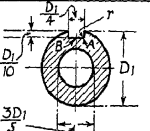
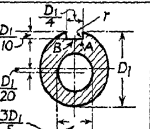
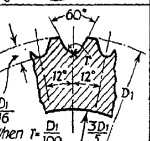
Cross-Section of Shaft	Equivalent Length of Circular Bar of Diameter D	Maximum Shear Stress	Area of Section
	$L = L_1 D^4 \left[\frac{1}{D_1^4} \right]$	$f = \frac{5.1 M}{D_1^3}$ At Periphery	$\frac{\pi}{4} D_1^2$
	$L = L_1 D^4 \left[\frac{1}{D_1^4 - d_1^4} \right]$	$f = \frac{5.1 D_1 M}{(D_1^4 - d_1^4)}$ At Periphery	$\frac{\pi}{4} (D_1^2 - d_1^2)$
	$L = L_1 D^4 \left[\frac{1.5}{(D_1 + d_1)(D_1 - d_1)} \right]$	$f = \frac{7.6 M}{(D_1 + d_1)(D_1 - d_1)^2}$	$\frac{\pi}{4} (D_1^2 - d_1^2)$
	$L = L_1 D^4 \left[\frac{(a^2 + b^2)}{2a^3 b^3} \right]$	$f = \frac{5.1 M}{ab^2}$ at X	$\frac{\pi}{4} a.b.$
	$L = L_1 D^4 \left[\frac{(a^2 + b^2)}{3.1a^3 b^3} \right]$	$f = \left[\frac{15a + 9b}{5a^2 b^2} \right] M$ at X	$a.b.$
	$L = L_1 D^4 \left[\frac{1}{1.43a^4} \right]$	$f = \frac{4.8 M}{a^3}$ at X	a^2
	$L = L_1 D^4 \left[\frac{4.53}{a^4} \right]$	$f = \frac{20 M}{a^3}$ at X	$0.433a^2$
	$L = L_1 D^4 \left[\frac{1}{1.18 D_1^4} \right]$	$f = \frac{5.3 M}{D_1^3}$ at X	$0.866 D_1^2$
	$L = L_1 D^4 \left[\frac{1}{1.10 D_1^4} \right]$	$f = \frac{5.4 M}{D_1^3}$ at X	$0.765 D_1^2$

TABLE 17 (continued).

Cross-Section of Shaft	Equivalent Length of Circular Bar of Diameter D	Maximum Shear Stress																												
	$L = L_1 D^4 \left[\frac{1.16}{D_1^4} \right]$	$f = \frac{8.1M}{D_1^3}$ at X																												
	$L = L_1 D^4 \left[\frac{K}{D_1^4} \right]$ <table border="1" data-bbox="450 630 574 742"> <thead> <tr> <th>r</th> <th>K</th> </tr> </thead> <tbody> <tr> <td>$D_1/100$</td> <td>1.28</td> </tr> <tr> <td>$D_1/50$</td> <td>1.27</td> </tr> <tr> <td>$D_1/25$</td> <td>1.26</td> </tr> <tr> <td>$D_1/15$</td> <td>1.24</td> </tr> </tbody> </table>	r	K	$D_1/100$	1.28	$D_1/50$	1.27	$D_1/25$	1.26	$D_1/15$	1.24	$f = \frac{K_1 M}{D_1^3}$ <table border="1" data-bbox="642 630 818 742"> <thead> <tr> <th>r</th> <th colspan="2">K_1</th> </tr> <tr> <th></th> <th>at A</th> <th>at B</th> </tr> </thead> <tbody> <tr> <td>$D_1/100$</td> <td>31.5</td> <td>13.4</td> </tr> <tr> <td>$D_1/50$</td> <td>19.7</td> <td>13.0</td> </tr> <tr> <td>$D_1/25$</td> <td>13.5</td> <td>12.6</td> </tr> <tr> <td>$D_1/15$</td> <td>11.0</td> <td>11.7</td> </tr> </tbody> </table>	r	K_1			at A	at B	$D_1/100$	31.5	13.4	$D_1/50$	19.7	13.0	$D_1/25$	13.5	12.6	$D_1/15$	11.0	11.7
r	K																													
$D_1/100$	1.28																													
$D_1/50$	1.27																													
$D_1/25$	1.26																													
$D_1/15$	1.24																													
r	K_1																													
	at A	at B																												
$D_1/100$	31.5	13.4																												
$D_1/50$	19.7	13.0																												
$D_1/25$	13.5	12.6																												
$D_1/15$	11.0	11.7																												
	$L = L_1 D^4 \left[\frac{K}{D_1^4} \right]$ <table border="1" data-bbox="450 816 574 927"> <thead> <tr> <th>r</th> <th>K</th> </tr> </thead> <tbody> <tr> <td>$D_1/100$</td> <td>1.29</td> </tr> <tr> <td>$D_1/50$</td> <td>1.29</td> </tr> <tr> <td>$D_1/25$</td> <td>1.28</td> </tr> <tr> <td>$D_1/15$</td> <td>1.26</td> </tr> </tbody> </table>	r	K	$D_1/100$	1.29	$D_1/50$	1.29	$D_1/25$	1.28	$D_1/15$	1.26	$f = \frac{K_1 M}{D_1^3}$ <table border="1" data-bbox="642 816 818 927"> <thead> <tr> <th>r</th> <th colspan="2">K_1</th> </tr> <tr> <th></th> <th>at A</th> <th>at B</th> </tr> </thead> <tbody> <tr> <td>$D_1/100$</td> <td>13.0</td> <td>8.7</td> </tr> <tr> <td>$D_1/50$</td> <td>9.7</td> <td>8.6</td> </tr> <tr> <td>$D_1/25$</td> <td>8.6</td> <td>8.5</td> </tr> <tr> <td>$D_1/15$</td> <td>8.3</td> <td>8.4</td> </tr> </tbody> </table>	r	K_1			at A	at B	$D_1/100$	13.0	8.7	$D_1/50$	9.7	8.6	$D_1/25$	8.6	8.5	$D_1/15$	8.3	8.4
r	K																													
$D_1/100$	1.29																													
$D_1/50$	1.29																													
$D_1/25$	1.28																													
$D_1/15$	1.26																													
r	K_1																													
	at A	at B																												
$D_1/100$	13.0	8.7																												
$D_1/50$	9.7	8.6																												
$D_1/25$	8.6	8.5																												
$D_1/15$	8.3	8.4																												
	$L = L_1 D^4 \left[\frac{K}{D_1^4} \right]$ <table border="1" data-bbox="450 1001 574 1113"> <thead> <tr> <th>r</th> <th>K</th> </tr> </thead> <tbody> <tr> <td>$D_1/100$</td> <td>1.86</td> </tr> <tr> <td>$D_1/75$</td> <td>1.79</td> </tr> <tr> <td>$D_1/50$</td> <td>1.72</td> </tr> <tr> <td>$D_1/40$</td> <td>1.64</td> </tr> </tbody> </table>	r	K	$D_1/100$	1.86	$D_1/75$	1.79	$D_1/50$	1.72	$D_1/40$	1.64	$f = \frac{K_1 M}{D_1^3}$ <table border="1" data-bbox="663 1001 792 1113"> <thead> <tr> <th>r</th> <th>K_1</th> </tr> </thead> <tbody> <tr> <td>$D_1/100$</td> <td>20.0</td> </tr> <tr> <td>$D_1/75$</td> <td>15.5</td> </tr> <tr> <td>$D_1/50$</td> <td>14.6</td> </tr> <tr> <td>$D_1/40$</td> <td>13.8</td> </tr> </tbody> </table> at X	r	K_1	$D_1/100$	20.0	$D_1/75$	15.5	$D_1/50$	14.6	$D_1/40$	13.8								
r	K																													
$D_1/100$	1.86																													
$D_1/75$	1.79																													
$D_1/50$	1.72																													
$D_1/40$	1.64																													
r	K_1																													
$D_1/100$	20.0																													
$D_1/75$	15.5																													
$D_1/50$	14.6																													
$D_1/40$	13.8																													

L = Length of solid circular shaft of diameter D Having the same torsional rigidity as length L_1 of the actual shaft.

M = Twisting moment transmitted by shaft.

having a square section of the same cross-sectional area.

For example, from Table 17, the equivalent length of a rectangular section when $a = 2b$ is

$$L = L_1 \cdot D^4 / (4.96b^4),$$

whereas the equivalent length of a square section of the same cross-sectional area, when the length of each side is a_1 , is

$$L = L_1 \cdot D^4 / (1.43a_1^4),$$

where, for equal cross-sectional areas, $a_1^2 = 2b^2$,

$$\text{i.e. } L = L_1 \cdot D^4 / (5.72b^4).$$

Hence the torsional rigidity of the square section is about 15 per cent. greater than that of a rectangular section of equal area in which the longer side is twice the shorter side.

The torsional stiffness of a long thin rectangular member is nearly the same whether the member is in the form of a simple rectangular bar or is rolled up into a U-, C-, S-, or L-shaped member, provided the width of the member remains constant and the length of the median line is unaltered.

This explains the considerable reduction of strength and stiffness when a narrow longitudinal slit is cut in a cylindrical tube, i.e. the slit converts the tube into a member having a narrow rectangular cross-section of length $\pi(D_1 + d_1)/2$ and thickness $(D_1 - d_1)/2$.

Thus, if the width b of the rectangle is small compared with the length a , the terms containing b in the numerators of the expressions for the equivalent length and shear stress of a rectangular section given in Table 17 are negligible. Hence these expressions reduce to

$$L = L_1 \cdot D^4 \left\{ \frac{1}{3.1 \cdot a \cdot b^3} \right\} \quad \text{and} \quad f = \frac{3 \cdot M}{a \cdot b^2}$$

In the case of a slit tube the length of the equivalent rectangle is $a = \pi(D_1 + d_1)/2$, and its width is $b = (D_1 - d_1)/2$.

Inserting these values in the foregoing expressions for L and f ,

$$L = L_1 \cdot D^4 \left(\frac{1.64}{(D_1 + d_1)(D_1 - d_1)^3} \right) \quad \text{and} \quad f = \frac{7.6M}{(D_1 + d_1)(D_1 - d_1)^2}$$

which are in good agreement with the values given for a slit tube in Table 17.

The soap film experiments also showed that the stiffness of any section is reduced appreciably by any discontinuity, such as a key-way, even if the discontinuity does not reduce the area of the section appreciably.

Conversely, any addition to the area of a particular section increases its stiffness, provided the configuration of the original area remains unaltered. Thus, in the examples given in Table 17 the equivalent length of a tube of external diameter D_1 , internal diameter $0.6D_1$, and length L_1 , is

$$L = 1.15 L_1 \cdot D^4/D_1^4,$$

whereas the equivalent length of the same section when a single key-way, $D_1/4$ wide and $D_1/10$ deep, is cut in it is

$$L = 1.28 L_1 \cdot D^4/D_1^4,$$

when the radius in the corner of the key-way is $r = D_1/100$.

- (3) In the case of severe discontinuities, such as key-ways and serrations, it should be noted that the values given in Table 17 for the maximum shear stresses at points of high stress concentration are theoretical values. Due to local yielding these theoretical values are not realised in practice in the case of vibratory loading, a point which is discussed more fully in Chapter 7.

General Expressions for the Torsional Rigidity of Non-Circular Shafts in Torsion.

- (a) *Solid Symmetrical Sections.*—Saint Venant found that the torsional rigidity of any solid symmetrical section is nearly the same as that of an elliptical section having the same area and the same polar moment of inertia as the actual section.
- (b) *Thin Tubular Sections.*—The following expressions give approximate values for the maximum shear

stress and equivalent length of thin tubular sections having a uniform wall thickness. (See Seely, "Advanced Mechanics of Materials," pp. 176 and 177):—

$$f = M/(2 \cdot A \cdot t), \quad \dots \quad (82)$$

$$L = P \cdot L_1 \cdot D^4/(40 \cdot 8 \cdot A^3 \cdot t), \quad \dots \quad (83)$$

where f = maximum shear stress in lbs. per sq. in.;

M = torque in lbs.-ins.,

A = area enclosed by mean periphery of section, in sq. ins.,

t = wall thickness in inches,

P = length of mean periphery in inches,

L = equivalent length of solid circular shaft of diameter D ,

L_1 = actual length of tubular section.

For example, consider the case of a hollow cylindrical section, outside diameter D_1 and inside diameter $d_1 = k \cdot D_1$,

$$A = \frac{\pi}{4} \cdot \left(\frac{D_1 + d_1}{2} \right)^2 = \pi \cdot D_1^2(1 + k)^2/16,$$

$$t = (D_1 - d_1)/2 = D_1(1 - k)/2,$$

$$P = \pi(D_1 + d_1)/2 = \pi \cdot D_1(1 + k)/2.$$

Hence,

$$f = \frac{5 \cdot 1 \cdot M}{D_1^3(1 + k)^2(1 - k)},$$

and

$$L = \frac{2 \cdot L_1 \cdot D^4}{D_1^4(1 + k)^3(1 - k)}.$$

Also, from the expressions given in Table 17 for a hollow circular section,

$$f = 5 \cdot 1 \cdot D_1 \cdot M/(D_1^4 - d_1^4) = 5 \cdot 1 \cdot M/D_1^3(1 - k^4),$$

$$\text{and } L = L_1 \cdot D^4/(D_1^4 - d_1^4) = L_1 \cdot D^4/D_1^4(1 - k^4).$$

The error in the approximate expression for different values of k is shown in the following table:—

Value of k .	Stress f .		Equivalent Length.	
	Exact.	Approximate.	Exact.	Approximate.
0.80	8.64 M/D_1^3	7.87 M/D_1^3	1.72 $L_1 \cdot D^4/D_1^4$	1.69 $L_1 \cdot D^4/D_1^4$
0.85	10.65	9.95	2.10	2.09
0.90	14.80	14.10	2.92	2.91
0.95	27.20	26.80	5.41	5.40
0.975	52.30	52.30	10.40	10.25

In the case of elliptical tubes the values of A and P can be computed from the following expressions:—

$$A = \frac{\pi}{4} a \cdot b = \text{area enclosed by mean periphery,}$$

$$= \pi \sqrt{\frac{a^2 + b^2}{2}} = \text{length of mean periphery,}$$

where a = mean length of major axis,
 b = mean length of minor axis.

The empirical expression given in Table 17 for the shear stress due to twisting a bar of rectangular cross-section yields values which are within 4 per cent. of the exact values. The expression for the equivalent length of rectangular bars yields values which are within 7 per cent. of the exact values when the ratio a/b lies between 1 and 2, and within 5 per cent. when this ratio is greater than 2.

EXAMPLE 22.—A torsional pendulum consisting of a flywheel of moment of inertia 0.357 lb.-in. sec.² is rigidly attached to the free end of a 1-in. diameter solid steel bar 12 ins. long. The other end of the bar is firmly clamped as shown in Fig. 1.

Calculate.

- I. The natural frequency of torsional vibration of the system.
- II. The maximum torque which can be imposed on the bar if the shear stress must not exceed 10,000 lbs.

per sq. in. Also the angle of twist at the flywheel when this torque is applied statically at the same point.

- III. The required lengths of shaft, assuming that the solid circular bar is replaced by bars having the various cross-sections shown in Table 17; that a shear stress of 10,000 lbs. per sq. in. must not be exceeded when the alternative bars carry the same torque as the solid circular bar; and that the natural frequency must be the same as for the solid circular bar.

I. *Natural Frequency of System.*

From Equation (7),

$$\begin{aligned} F &= 9.55\sqrt{C/J} \text{ vibs./min.}, \\ \text{where } C &= G \cdot I_p/L \text{ lbs.-ins. per radian} \\ &= \frac{D^4 \cdot G}{10.2 \cdot L} = \frac{1^4 \times 12000000}{10.2 \times 12} \\ &= 98,000 \text{ lbs.-ins. per radian,} \\ J &= 0.357 \text{ lb.-in. sec.}^2. \end{aligned}$$

$$\text{Hence, } F = 9.55\sqrt{\frac{98000}{0.357}} = 5000 \text{ vibs./min.}$$

II. *Maximum Torque.*—From Table 17, for a solid circular section,

$$\begin{aligned} f &= 5.1 M/D^3, \\ \text{where } f &= 10,000 \text{ lbs. per sq. in., } D = 1 \text{ in.} \\ \text{Hence, } M &= 10,000 \times 1^3/5.1 = 1960 \text{ lbs.-ins.} \end{aligned}$$

Angle of Twist at Flywheel.

From Equation (1)

$$\theta = \frac{M \cdot L}{G \cdot I_p},$$

$$\begin{aligned} \text{but } C &= G \cdot I_p/L, \\ \text{i.e. } \theta &= M/C, \\ \text{where } M &= 1960 \text{ lbs.-ins.,} \\ \text{and } C &= 98,000 \text{ lbs.-ins. per radian.} \\ \text{Hence, } \theta &= 1960/98,000 = 0.02 \text{ radian or } 1.15^\circ. \end{aligned}$$

IIIa. *Hollow Circular Section* (assuming $d_1 = 0.6 D_1$).

In all the following examples the appropriate expressions for shear stress and equivalent length are taken from Table 17.

Shear Stress.

$$f = 5.1 D_1 \cdot M / (D_1^4 - d_1^4) \\ = 5.85 M / D_1^3, \text{ when } d_1 = 0.6 \cdot D_1,$$

i.e. $D_1^3 = 5.85 \times 1960 / 10,000$, when $M = 1960$ lbs.-ins.
and $f = 10,000$ lbs. per sq. in.,

$$D_1 = 1.05 \text{ ins.}, \text{ and } d_1 = 0.63 \text{ in.}$$

Length of shaft.

$$L = L_1 \cdot D^4 / (D_1^4 - d_1^4).$$

If the frequency is to remain the same as for a solid circular bar 1 in. diameter and 12 ins. long, the actual length L_1 of the hollow bar must be equivalent to 12 ins. of 1 in. diameter solid circular bar, i.e. $L/D^4 = 12$, a value which holds for all the following examples.

In this case,

$$L_1 = 0.87 D_1^4 \cdot L / D^4, \text{ where } D_1 = 1.05 \text{ ins.}, \\ \text{i.e. } L_1 = 0.87 \times 1.05^4 \times 12 = 12.6 \text{ ins.}$$

IIIb. *Hollow Shaft with Longitudinal Slit*

(assuming $d_1 = 0.6 \cdot D_1$).

Shear Stress.

$$f = \frac{7.6 \cdot M}{(D_1 + d_1)(D_1 - d_1)^3} \\ = 29.7 \cdot M / D_1^3, \text{ when } d_1 = 0.6 \cdot D_1,$$

$$\text{i.e. } D_1^3 = 29.7 \times 1960 / 10,000 = 5.82, \\ \text{or } D_1 = 1.8 \text{ ins.}, \text{ and } d_1 = 1.08 \text{ ins.}$$

Length of Shaft.

$$L = \frac{1.5 L_1 \cdot D^4}{(D_1 + d_1)(D_1 - d_1)^3} \\ \text{or } L_1 = \frac{(D_1 + d_1)(D_1 - d_1)^3 \cdot L}{1.5 \cdot D^4} \\ = 0.068 \cdot D_1^4 \cdot L / D^4, \text{ when } d_1 = 0.6 \cdot D_1,$$

where $D_1 = 1.8$ ins, and $L/D^4 = 12$.

Hence, $L_1 = 0.068 \text{ in.} \times 1.8^4 \times 12 = 8.6 \text{ ins.}$

IIIc. *Ellipse* (assuming $a = 2b$).

Shear Stress.

$$f = 5.1 \cdot M / (a \cdot b^2) = 2.55 \cdot M / b^3, \text{ when } a = 2b,$$

i.e. $b^3 = 2.55 \times 1960 / 10,000 = 0.5,$
 or $b = 0.794 \text{ in.}, \text{ and } a = 2b = 1.588 \text{ ins.}$

Length of Shaft.

$$L = \frac{L_1 \cdot D^4 (a^2 + b^2)}{2 \cdot a^3 \cdot b^3},$$

or $L_1 = 3.2 \cdot b^4 \cdot L / D^4, \text{ when } a = 2b$
 $= 3.2 \times 0.794^4 \times 12 = 15.2 \text{ ins.}$

IIId. *Rectangle* (assuming $a = 2b$).

Shear Stress.

$$f = (15 \cdot a + 9 \cdot b) \cdot M / (5 \cdot a^2 \cdot b^2)$$

$$= 1.95 \cdot M / b^3, \text{ when } a = 2b,$$

or $b^3 = 1.95 \times 1960 / 10,000 = 0.382,$
 whence $b = 0.725 \text{ in.}, \text{ and } a = 2b = 1.45 \text{ ins.}$

Length of Shaft.

$$L = L_1 \cdot D^4 (a^2 + b^2) / (3.1 \cdot a^3 \cdot b^3)$$

$$= L_1 \cdot D^4 / (4.96 \cdot b^4),$$

i.e. $L_1 = 4.96 \times 0.725^4 \times 12 = 16.4 \text{ ins.}$

IIIe. *Square.*

Shear Stress.

$$f = 4.8 \cdot M / a^3,$$

or $a^3 = 4.8 \times 1960 / 10,000 = 0.94,$
 whence $a = 0.98 \text{ in.}$

Length of Shaft.

$$L = L_1 \cdot D^4 / (1.43 \cdot a^4),$$

i.e. $L_1 = 1.43 \cdot a^4 \cdot L / D^4$
 $= 1.43 \times 0.98^4 \times 12$
 $= 15.8 \text{ ins.}$

III*f*. *Equilateral Triangle.**Shear Stress.*

$$f = 20 \cdot M/a^3,$$

i.e. $a^3 = 20 \times 1960/10,000 = 3.92,$
 or $a = 1.575$ ins.

Length of Shaft.

$$L = 4.53 \cdot L_1 \cdot D^4/a^4,$$

or $L_1 = 1.57^4 \times 12/4.53 = 16.3$ ins.

III*g*. *Hexagon.**Shear Stress.*

$$f = 5.3 \cdot M/D_1^3,$$

or $D_1^3 = 5.3 \times 1960/10,000 = 1.04,$
 i.e. $D_1 = 1.014$ ins.

Length of Shaft.

$$L = L_1 \cdot D^4/(1.18 \cdot D_1^4),$$

i.e. $L_1 = 1.18 \cdot D_1^4 \cdot L/D^4$
 $= 1.18 \times 1.014^4 \times 12 = 14.9$ ins.

III*h*. *Octagon.**Shear Stress.*

$$f = 5.4 \cdot M/D_1^3,$$

or $D_1^3 = 5.4 \times 1960/10,000 = 1.06,$
 $D_1 = 1.02$ ins.

Length of Shaft.

$$L = L_1 \cdot D^4/(1.1 \cdot D_1^4),$$

i.e. $L_1 = 1.1 \cdot D_1^4 \cdot L/D^4 = 1.1 \times 1.02^4 \times 12 = 14.3$ ins.

Torsional Resilience.—The work done by a torque M in twisting a bar through an angle θ is

$$W = M \cdot \theta/2,$$

but, from Equation (1),

$$M/I_p = 2 \cdot f/d = G \cdot \theta/L,$$

or $M = 2 \cdot f \cdot I_p/d,$ and $\theta = 2 \cdot f \cdot L/G \cdot d,$
 i.e. $W = 2 \cdot I_p \cdot f^2 \cdot L/G \cdot d^2$ ins.-lbs., . . . (84)

where W = total resilience in ins.-lbs.,
 I_p = polar moment of inertia of cross-section of shaft
in ins.⁴ units,
 f = maximum shear stress in lbs. per sq. in.,
 L = length of bar in inches,
 G = modulus of rigidity in lbs. per sq. in.,
 d = diameter of bar in inches.

For a hollow circular bar, outside diameter d and inside diameter k , d ,

$I_p = \pi \cdot d^4(1 - k^4)/32$, and $V = \pi \cdot d^2(1 - k^2)L/4$,
where V = volume of bar in cubic inches.
Hence, $W_s = \text{resilience per unit volume}$
 $= f^2(1 + k^2)/(4 \cdot G)$ ins.-lbs. per cu. in. . . (85)

In the case of a very thin tube k is very nearly unity, so that Equation (85) reduces to

$$W_s = f^2/2 \cdot G \text{ for a very thin tube. . . . (86)}$$

In the case of a solid shaft k is zero, so that Equation (85) reduces to

$$W_s = f^2/4G, \text{ for a solid circular shaft. . . (87)}$$

As already explained the foregoing expressions cannot be applied to non-circular sections because plane transverse sections do not remain plane after twisting.

The specific resiliences of non-circular bars can be computed, however, from the following expression :—

$$W_s = M \cdot \theta/2V,$$

where θ = total angular deflection of bar in radians due to torque M lbs.-ins.

V = total volume of bar in cubic inches.

In this example $M = 1960$ lbs.-ins., $\theta = 0.02$ radian.

Hence, $W_s = 1960 \times 0.02/2V = 19.6/V$ ins.-lbs. per cubic inch.

The values of W_s are given in the last column of Table 18. Equations (86) and (87) show that for a given maximum stress and a given weight of material a very thin circular

tube stores twice as much energy as a solid circular bar, and it will be found that any other solid section is even less efficient than the solid circular section. The examples given in Table 18 show that the resilience per unit volume approaches that of a solid circular bar the nearer the cross-section of the bar is to a circular cross-section, e.g. a square section is more efficient than a triangular section, and a hexagonal or octagonal section is more efficient than a square section.

TABLE 18.
RESILIENCE OF TORSION BARS.

Section.	Length of Bar. Ins. L ₁ .	Volume of Bar. Cu. Ins.	Weight of Bar. Lbs.	Resilience per Unit Volume. Ins.-Lbs. per Cu. In.
Solid circular . . .	12.0	9.42	2.67	2.08
Hollow circular . . .	12.6	6.96	1.97	2.82
Hollow circular with longitudinal slit . . .	8.6	14.00	3.97	1.40
Solid elliptical . . .	15.2	15.00	4.25	1.31
Solid rectangular . . .	16.4	17.25	4.87	1.14
Solid square . . .	15.8	15.20	4.30	1.29
Solid equilateral triangular	16.3	17.50	4.95	1.12
Solid hexagonal . . .	14.9	13.20	3.74	1.48
Solid octagonal . . .	14.3	11.30	3.21	1.73

The presence of discontinuities, such as key-ways, serrations, etc., also has a considerable influence on the specific resilience of the bar, because the maximum stress to which the bar can be subjected with safety is determined by the high local stresses which occur in the region of the discontinuity. The average stress is, therefore, considerably lower in most cases than the average stress in a bar of corresponding cross-section but without any discontinuity. It should be noted, however, that the effect of a discontinuity on the permissible maximum stress, and therefore on the specific resilience of a bar, depends on the material of which the bar is made as well as on its cross-section and type of discontinuity. As a general rule, the specific resilience of two bars of identical form, containing a discontinuity such as a key-way, but of different

materials, will not be in direct proportion to the stress-carrying capacity of the two materials, because there will be a more favourable redistribution of stress in the neighbourhood of the discontinuity in the case of the more ductile material, due to local yielding at the highly stressed zones. Also, in the case of two identical bars made of the same material, the specific resilience will be greater for the bar which has the larger radii at the discontinuity, e.g. in the corners of a key-way or at the roots of serrations.

EXAMPLE 23.—Calculate the natural frequencies of the system described in Example 22, when all the bars are 12 ins. long and are made of the following materials: steel, cast iron, aluminium, bronze, magnesium alloy, and wood.

From Equation (7),

$$F = 9.55\sqrt{C/J},$$

where

$$C = G \cdot I_p/L,$$

i.e.

$$F = 9.55\sqrt{\frac{G \cdot I_p}{J \cdot L}}.$$

If only the length L and the modulus of rigidity G are altered this expression can be written

In Example 22 it was shown that the frequency of the system with steel bars having the various cross-sections described in Table 18 was 5000 vibs./min.

Table 16 shows that the modulus of rigidity of steel is 12,000,000.

Hence, $F_1 = K\sqrt{G_1/L_1}$ vibs./min.,

where F_1 = the natural frequency of the system when the modulus of rigidity of the material is G_1 , and the length of the bar is L_1 .

Similarly, $F_2 = K\sqrt{G_2/L_2}$,

i.e. $F_2 = F_1\sqrt{\frac{G_2 \cdot L_1}{G_1 \cdot L_2}}$

In this case, $G_1 = 12,000,000$,
 $L_1 =$ length of bar from column 2 of Table 18,
 $L_2 = 12$ ins.,
 $G_2 =$ modulus of rigidity from Table 16,
 $F_1 = 5000$ vibs./min.,

$$\text{i.e.} \quad F_2 = 5000 \sqrt{\frac{L_1 \cdot G_2}{12000000 \times 12}} = \frac{1}{2.4} \sqrt{L_1 \cdot G_2}$$

The values of F_2 can be computed from the above expression by the appropriate values of G_2 and L_1 from Tables 16 and 18 respectively. The results are given in Table 19.

TABLE 19.
 NATURAL FREQUENCIES OF TORSIONAL PENDULUM.

Section.	Material.					
	Steel.	Cast Iron.	Aluminium.	Bronze.	Magnesium.	Wood.
	vibs./min.	vibs./min.	vibs./min.	vibs./min.	vibs./min.	vibs./min.
Solid circular . . .	5000	3810	2810	3530	2320	407
Hollow circular . .	5120	3900	2880	3620	2370	417
Hollow circular with longl. slit*	4120	3140	2310	2900	1910	335
Solid elliptical . .	5610	4270	3150	3960	2600	457
Solid rectangular .	5840	4450	3280	4120	2710	475
Solid square . . .	5720	4350	3210	4040	2650	465
Solid triangular . .	5810	4430	3270	4100	2700	473
Solid hexagonal . .	5560	4240	3130	3930	2580	453
Solid octagonal . .	5440	4150	3060	3840	2520	442

The considerable reduction of torsional stiffness and the consequent reduction of natural frequency due to cutting a longitudinal slit in a hollow circular shaft should be noted. In the particular example given above the dimensions of the slit tube were increased to maintain the same maximum fibre stress under a given torque as for the plain tube. If the dimensions had not been increased the reduction of stiffness due to slitting the tube longitudinally is given by the expressions in Table 17.

For a plain cylindrical tube,

$$L = L_1 D^4 / (D_1^4 - d_1^4) \\ = 1.15 L_1 \cdot D^4 / D_1^4, \text{ when } d_1 = 0.6 D_1.$$

For a slit tube, $L = L_1 \cdot D^4 \left\{ \frac{1.5}{(D_1 + d_1)(D_1 - d_1)^3} \right\}$
 $= 14.65 L_1 \cdot D^4 / D_1^4, \text{ when } d_1 = 0.6 D_1,$

i.e. the torsional rigidity of the slit tube is nearly 1/10th that of the plain tube, when $d_1 = 0.6 D_1$.

(b) **Crankshaft Stiffness.**—The reduction of the actual length L in Fig. 25 of each crankshaft element between main bearing centres to an equivalent length of plain shafting L_e of diameter D of the same torsional rigidity may be carried out as follows :—

Referring to Fig. 25,

Let $C = G \cdot I_p = \frac{\pi}{32} \cdot G \cdot D^4 =$ Torsional rigidity of unit length of the equivalent shaft,

$C_1 = \frac{\pi}{32} \cdot G(D_1^4 - d_1^4) =$ Torsional rigidity of unit length of the crankshaft journals,

$C_2 = \frac{\pi}{32} \cdot G(D_2^4 - d_2^4) =$ Torsional rigidity of unit length of the crankpin,

$C_3 = E \cdot I = \frac{T \cdot W^3 \cdot E}{12} =$ Flexural rigidity of one crankweb.

Then, assuming that the deflection of the crankshaft element is mainly due to twisting of the crankpin and journals, and bending of the crankwebs, and that the bearing clearance is sufficient to permit free displacement of the journals :

(i) *Journals.*

Let $L_1 =$ length of equivalent shaft having the same torsional rigidity as each journal,

$A =$ length of journal.

Then $\frac{L_1}{C} = \frac{A}{C_1}$ or $L_1 = \frac{A \cdot C}{C_1},$

i.e.
$$L_1 = \frac{A \cdot D^4}{(D_1^4 - d_1^4)} \text{ for hollow journals}$$

$$- \frac{A \cdot D^4}{D_1^4} \text{ for solid journals.}$$

(ii) *Crankpins.*

Let L_2 = length of equivalent shaft having the same torsional rigidity as each crankpin,
 B = length of each crankpin.

Then
$$\frac{L_2}{C} = \frac{B}{C_2} \quad \text{or} \quad L_2 = \frac{C \cdot B}{C_2},$$

i.e.
$$L_2 = \frac{B \cdot D^4}{(D_2^4 - d_2^4)} \text{ for hollow crankpins}$$

$$- \frac{B \cdot D^4}{D_2^4} \text{ for solid crankpins.}$$

(iii) *Crankwebs.*

Let L_3 = length of equivalent shaft corresponding to two crankwebs.

Fig. 43 shows the deflection of a crankweb due to a couple M .

Let Y = radius of curvature of web,
 θ = difference in inclination of web at journal and crankpin, i.e. the angular deflection of the next following journal due to flexure of the crankweb.

Then from the theory of beams

$$M/I = E/Y,$$

or
$$Y = E \cdot I/M = C_3/M,$$

where $C_3 = E \cdot I = T \cdot W^3 \cdot E/12$ = flexural rigidity of the crankweb.

Also, from Fig. 43

$$\theta = R/Y = M \cdot R/C_3 = 12 \cdot M \cdot R/(T \cdot W^3 \cdot E),$$

or, for two crankwebs
$$\theta = \frac{24 \cdot M \cdot R}{T \cdot W^3 \cdot E}.$$

Hence,
$$\frac{M \cdot L_3}{C} = \frac{24 \cdot M \cdot R}{T \cdot W^3 \cdot E}$$

i.e.
$$L_3 = \frac{24 \cdot R}{T \cdot W^3 \cdot E} \times \frac{\pi \cdot G \cdot D^4}{32}$$

$$= \frac{2 \cdot 356 \cdot R \cdot G \cdot D^4}{T \cdot W^3 \cdot E}$$

Assuming that $E = 30,000,000$ lbs. per sq. in. and

$G = 12,000,000$ lbs. per sq. in. for steel,

$$L_3 = \frac{0 \cdot 942 \cdot R \cdot D^4}{T \cdot W^3} \quad \text{for two steel crankwebs.}$$

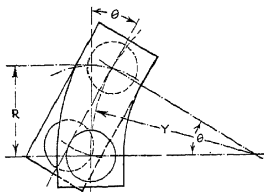


FIG. 43.—Flexure of crankweb.

(iv) *Total Equivalent Length of One Crankshaft Element.*

$$L_s = (L_1 + L_2 + L_3)$$

$$= \left[\frac{A \cdot D^4}{D_1^4} + \frac{B D^4}{D_2^4} + \frac{0 \cdot 942 \cdot R \cdot D^4}{T \cdot W^3} \right], \quad (88)$$

for solid journals and crankpins.

In applying the foregoing method, it should be noted that—

- (i) Local deformation at the juncture of journal and crankpin and web increases the effective length of the journal or crankpin.
- (ii) The effective lever arm of the couple acting on the crankwebs is less than the crank radius R , due to the attachment of the crankpin and journal.
- (iii) The effect of restraint at the bearings is to increase the stiffness of the crankshaft.

For normal running clearances of $4/1000$ to $8/1000$ of an inch, the increase of torsional rigidity compared with that of a free shaft is 5 to 10 per cent.

Exact mathematical treatment is not possible, since the elastic characteristics of the shaft in the neighbourhood of critical speeds depend, amongst other things, upon the bearing clearances which are variable and are, therefore, not even taken into account accurately in direct measurements of crankshaft stiffness.

In the case of one-node torsional vibrations of marine installations, where the length of the crankshaft is a small proportion of the total length of shafting in the system, the equivalent length of the crankshaft can be assumed to be the same as the actual length without making any appreciable difference in the value of the natural frequency. In normal installations of this type, the error in the value of the natural frequency corresponding to an error of 10 per cent. in the equivalent length of the crankshaft would be less than half per cent.

In the case of two-node vibrations of marine installations, and one-node vibrations of close-coupled electrical generating sets, however, the elastic properties of the system are mainly determined by the torsional rigidity of the crankshaft.

Since the natural frequency is approximately inversely proportional to the square root of the shaft length, an error of 10 per cent. in calculating the equivalent length of the crankshaft corresponds to an error of about 5 per cent. in the value of the natural frequency.

The equivalent length of the crankshaft should therefore be determined as carefully as possible, and the following simple empirical formula, originated by Major B. C. Carter, has proved to be satisfactory for this purpose. (See "An Empirical Formula for Crankshaft Stiffness in Torsion," by B. C. Carter, D.I.C., M.I.Mech.E., *Engineering*, 13th July, 1928, p. 36.)

Carter's empirical formula for the equivalent length of a crankshaft in bearing may be stated thus :—

exure.

$$L_e = D^4 \left[\left\{ \frac{A + 0.8 T}{D_1^4 - d_1^4} \right\} + \left\{ \frac{0.75 B}{D_2^4 - d_2^4} \right\} + \frac{1.5 R}{T \cdot W^3} \right], \quad (89)$$

for hollow journals and crankpin,

$$= D^4 \left[\left\{ \frac{A + 0.8 T}{D_1^4} \right\} + \left\{ \frac{0.75 B}{D_2^4} \right\} + \frac{1.5 R}{T \cdot W^3} \right], \quad (90)$$

for solid journals and crankpin.

The symbols correspond to those shown in Fig. 25.

This formula, which is similar in form to Equation (88), is based on actual observations, on a number of small shafts of different designs representing marine, aircraft, and motor-car practice. Assuming the test results to be exact, the range of error for all the results was ± 12 per cent., corresponding to a range of error in the frequency calculation of ± 6 per cent.

The Carter formula was used for calculating the equivalent lengths of the crankshafts of the engines of T. S. M. V. Polyphemus, tested by the Marine Oil-Engine Trials Committee. (See Appendix to "Marine Oil-Engine Trials," Sixth Report, *Proc. Inst. of Mech. Engineers*, 1931, Vol. 121, pp. 268 and 286.) These engines are each six-cylinder, four-stroke cycle, single-acting type, 620 mm. bore, 1300 mm. stroke, rated at 2750 B.H.P., and 138 r.p.m., with a crankshaft diameter of $16\frac{3}{4}$ ins. The error between the calculated frequencies and the torsigraph frequencies was $+ 2$ per cent. for the one-node frequency observed during the shop trials with the engine coupled to a dynamometer; and $+ 0.6$ per cent. for the two-node frequency observed during the sea trials.

A similar closeness of agreement between the calculated and observed values of the two-node frequencies of a large number of opposed-piston engine installations (where the crankshaft is of the type shown at D in Fig. 44, and spherical bearings are employed) has been obtained by the author, using the Carter formula for the equivalent length of the crankshaft.

EXAMPLE 24.—Calculate the equivalent length of the crankshaft element shown in Fig. 25, assuming the following dimensions, the diameter of the equivalent shaft to be the same as the diameter of the journals:—

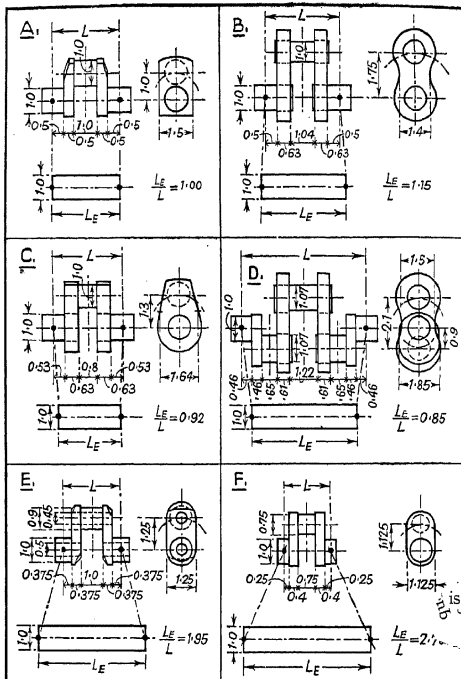


FIG. 44.—Torsional stiffness of crankshaft elements.
(Unit = diameter of shaft.)

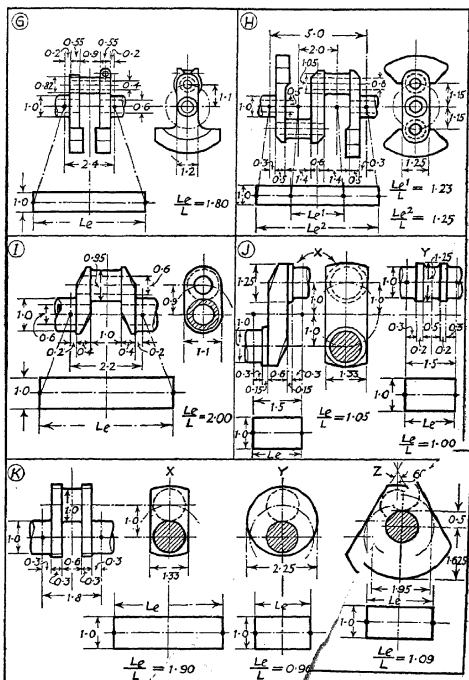


FIG. 44 (continued)

test experience with a great variety of crankshaft forms has shown that the Carter formula is exceedingly reliable for computing the overall stiffness of a crank element comprising journals, webs, and crankpin, there is no reliable experience to show that it enables the stiffness of the individual members of the crank element to be correctly assessed. From an investigation of the stiffnesses of the individual members of a shaft element of the type shown at D in Fig. 44, the author found that the Carter formula did, in fact, over-estimate the stiffness of the crankpins and under-estimate the stiffness of the webs, although the overall stiffness of the crank element was in good agreement with the experimental results.

As a result of this investigation, however, the following alternative semi-empirical expression was developed, and this gave a better indication of the distribution of stiffness in the crank element for the particular case investigated.

$$L_e = D^4 \left[\left\{ \frac{A + 0.4D_1}{D_1^4 - d_2^4} \right\} + \left\{ \frac{B + 0.4D_2}{D_2^4 - d_2^4} \right\} + \left\{ \frac{R - 0.2(D_1 + D_2)}{T \cdot W^3} \right\} \right] \quad (91)$$

In this expression the symbols have the same meanings as in Equation (89).

The form of Equation (91) is similar to that of Equation (88), the only differences being the inclusion of fillet allowances on journals and crankpin, and the adoption of an effective crank arm equal to the distance between the centres of gravity of the inner semi-circular, cross-sectional areas of the crankpin and journal.

In all the examples shown in Fig. 44, Equation (91) gives values for the ratio L_e/L which agree with the values obtained from Equation (89) within ± 10 per cent., and in the majority of cases the agreement is within ± 5 per cent. Exceptions are examples I and K, probably due to the relatively short crankthrow in example I and to the thin web in example K.

Where there is a large discrepancy between the equivalent length obtained by using Equation (89) and that obtained by using Equation (91), and where there is no experimental experience to indicate which value is nearer the true value, an average of the two calculated values will probably give reasonably accurate results.

Crankshaft stiffness can also be determined by strain energy methods, taking into account strain energy due to bending, torsion, and shear.

According to this method the effective stiffness of the crankshaft is not a constant quantity but depends on the relative values of the forces applied to the shaft. The stiffness cannot therefore be finally determined until the form of the elastic curve is known, and on this account the stiffness in one-node vibration differs from the stiffness in two-node vibration. The strain energy method is chiefly of interest in the case of crankshafts containing elements of the types shown at D and H in Fig. 44, i.e. where there is no journal bearing between adjacent crankpins and consequently where flexural displacements are liable to be more pronounced.

Although the strain energy method gives a form of crankshaft deflection which agrees more closely with experimental observations of shaft deflections under statically applied torques, there is little difference in the frequencies calculated by this method and by using the simple formulæ for crankshaft stiffness, Equations (89) and (91).

Furthermore, torsigraph observations show that in general the recorded frequencies, even for shafts containing elements of the types shown at D and H in Fig. 44, are in good agreement with the frequencies calculated by using Equations (89) and (91) for crankshaft stiffness.

It would therefore appear that the very much more involved calculations which must be made to determine crankshaft stiffness by the strain energy method are not a necessary part of practical frequency calculations.

Automobile Engine Crankshaft Elements.—Fig. 45 contains some typical crankshaft elements, the appropriate expression for calculating the equivalent length of the element being stated in each case. In all cases the formulæ have been derived from Equation (89).

The element shown at A in Fig. 45 represents each cylinder section of an in-line engine where there is a journal bearing at each side of the crankthrow.

The crankpin and journal may be either solid or hollow,
VOL. I.—13

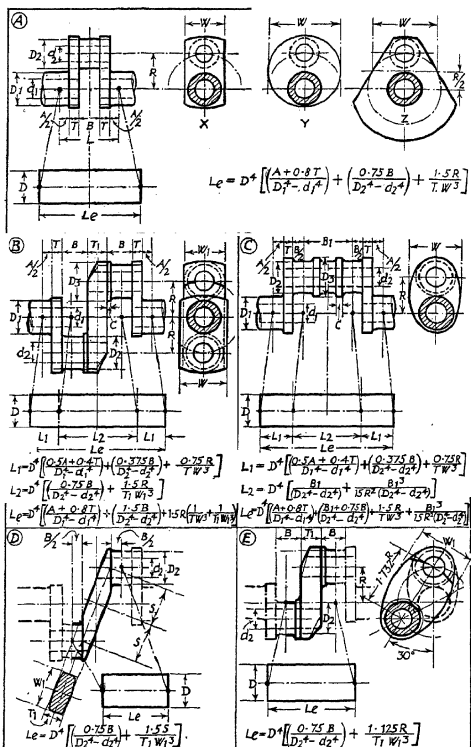


FIG. 45.—Torsional stiffness of crankshaft elements.

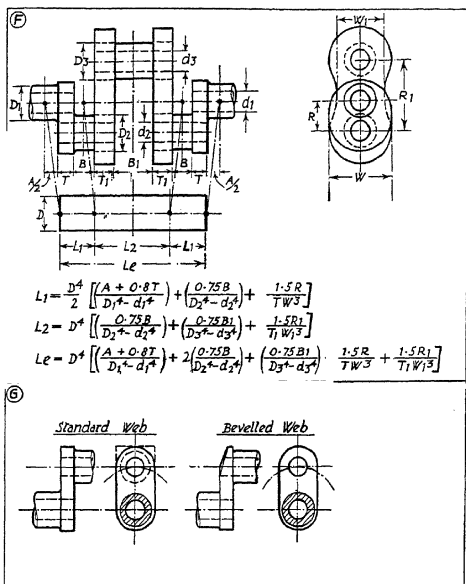


FIG. 45 (continued).

and three types of crankweb are shown in the diagram. Type X is the usual rectangular form and calls for no special comments. Type Y is a circular form, the effective width W being the diameter of the circle. This type of web is sometimes used as a journal bearing, usually with a roller bearing mounted on its periphery, in which case, of course, W must be large enough to provide a web which is concentric with the axis

of rotation. Type Z is a balanced form in which the web is extended beyond the journal to counterbalance the rotating masses. This type of web is used on four-, six-, and eight-cylinder in-line automobile engines, and its effective width W is measured at a distance $R/2$ from the axis of rotation.

In applying the formula for the equivalent length, allowance should be made for variations of journal length A , and of crankpin length B for different cylinders of the same engine. Also, if the crankpins and journals are solid, d_1 and d_2 are zero.

The element shown at B in Fig. 45 is found in three-bearing, four-cylinder in-line and in five-bearing, eight-cylinder in-line automobile engines. It is also found in two-row radial aero engines and in the Fullagar type of opposed-piston oil engine.

If the crankpins and journals are solid, then d_1 and d_2 in the expressions for equivalent length are zero. In these expressions no allowance has been made for the circular facings at the junction of the crankpins with the centre web. In the majority of examples this allowance is covered by the normal allowance for deformation at the junction of a crankpin with a web, but in exceptional cases the facings can be treated as enlarged portions of the crankpins, using the method already given for dealing with shafts of varying diameter.

For instance, the value of L_e/L given for example J in Fig. 44 is obtained from the expression for L_2 from example B of Fig. 45, as follows:—

$$L_2 = D^4 \left\{ \left(\frac{0.75B}{D_2^4 - d_2^4} \right) + \frac{1.5R}{T_1 \cdot W_1^3} \right\},$$

and from example J in Fig. 44,

$$D = 1.0; D_2 = 1.0; d_2 = 0; B = 0.6; R = 1.0;$$

$$T_1 = 0.6; W_1 = 1.33; \text{ and } L = 1.5.$$

$$\text{ce, } L_2 = (0.75 \times 0.6) + 1.5 / (0.6 \times 1.33^3)$$

$$= 0.45 + 1.06 = 1.51,$$

$$L_2/L = 1.51/1.5 = 1.01.$$

If circular facings are taken into account, the effective length of the crankpin is modified as follows:—

$$L_e = D^4$$

Diameter of circular facings = $D_3 = 1.25$, from example J
of Fig. 44,

Length of circular facings = $C = 0.15$,

i.e. $D_3/D_2 = 1.25$, and from Table 15 the appropriate allowance l/D_2 for local deformation at the junction of the crankpin and the facing is 0.055,

or $l = 0.055, D_2 = 0.055$, since $D_2 = 1.0$.

Also, the effective length of the remaining portion of the facing reduced to crankpin diameter D_2 is

$$l_1 = (C - l)D_2^4/D_3^4 = (0.15 - 0.055)/1.25^4 = 0.039.$$

Thus the modified length of the crankpin is

$$B_1 = B + l + l_1 = 0.6 + 0.055 + 0.039 = 0.694$$

and the modified equivalent length is

$$L_2 = (0.75 \times 0.694) + 1.06 = 0.52 + 1.06 = 1.58,$$

or $L_2/L = 1.58/1.5 = 1.053.$

Thus the effect of making allowance for the circular facings is to increase the equivalent length of the element by about 5 per cent.

It should be noticed that if the length C of the circular facing is less than the allowance l determined from Table 15, then the modified length of the crankpin when the circular facings are taken into account should be assumed to be

$$B_1 = (B + C).$$

The equivalent length of the element shown at J in Fig. 44 can also be determined by Equation (91) as follows:—

$$L_2 = D^4 \left[\frac{B + 0.4D_2}{D_2^4 - d_2^4} + \frac{0.5(2R - 0.4D_2)}{T_1 \cdot W_1^3} \right].$$

Where $B = 0.6$; $D = 1.0$; $D_2 = 1.0$; $d_2 = 0$; $R = 1.0$;
 $T_1 = 0.6$; $W_1 = 1.33$.

Hence, $L_2 = (0.6 + 0.4) + 0.5(2 - 0.4)/(0.6 \times 1.33^3)$
 $= 1.0 + 0.57 = 1.57,$

and since $L = 1.5$; $L_2/L = 1.05,$

In this case, therefore, the collars cannot be neglected in calculating the equivalent length of the element. It should be noted, however, that if the length of the collar is less than the allowance l , determined from Table 15, then the effective length of the crankpin is B_1 , i.e. the effect of the collar is negligible.

The element shown at D in Fig. 45 is similar to that shown at B, except that the centre crankweb is inclined and the effective length of the crankarm S is measured along the inclined centre line of the web.

The element shown at E in Fig. 45 is found in four-bearing, six-cylinder in-line engine crankshafts. In this case the effective length of the lever arm is $0.866R$, where R is the crankthrow. Also the torque acting at right angles to this lever arm is 0.866 times the torque acting at right angles to the crank arm. Hence the effective length of each half of the centre web in terms of the torque acting at right angles to the crankarm is $0.75R$, i.e. the allowance for flexure of the centre web in example E of Fig. 45 is 0.75 of the allowance for flexure of the centre web in example B.

The element shown at F in Fig. 45 is found in opposed-piston engines of the type having three crankthrows to each cylinder, such as the Junkers and Doxford engines.

The stiffness of a crankshaft element depends to some extent upon the shape of the web (see *Engineering*, 1st Nov., 1929, p. 549), and this is particularly the case when the crankpins are hollow. If the crankweb shown at the left-hand side at G in Fig. 45 is regarded as a standard of comparison, then the effect of bevelling the web as shown at the right-hand side at G in Fig. 45 is to reduce the stiffness of the crank element by from 7 to 14 per cent., say an average reduction of 10 per cent.

A small bevel or radius which is confined to the very edge of the web, however, does not affect the stiffness to any appreciable extent. The effect of making the web square cornered, as shown by the dotted lines at G in Fig. 45, is to increase the stiffness of the element by about 1 per cent.

These considerations should be borne in mind when means for altering the stiffness of a crankshaft are being considered.

It should be remembered, however, that stiffness obtained by adding material to the web, especially if the material is added near the crankpin, does not necessarily imply an increased natural frequency, because the polar moment of inertia of the web is also increased and this tends to lower the frequency. It is for this reason that an increase in journal diameter is more likely to raise the frequency than an increase in crankpin diameter.

EXAMPLE 25.—Fig. 46 shows a two-bearing, four-cylinder engine crankshaft. Obtain an expression for the overall equivalent length.

The overall equivalent length of this crankshaft is obtained from the expressions for the equivalent lengths of crankshaft elements given in Fig. 45, as follows:—

$$\Sigma L_e = \text{overall equivalent length} = (2L_1 + 2L_2 + L_3),$$

where $2L_1 = L_e$ from example A of Fig. 45.

Inserting the symbols from Fig. 46 in the expression for L_e in Fig. 45, example A, the following expression is obtained for $2L_1$:—

$$2L_1 = (A + 0.8T) + (0.75B \cdot D^4/D_1^4) + 1.5R \cdot D^4/(T \cdot W^3).$$

Also, $2 \cdot L_2 = 2 \cdot L_2$ from example B in Fig. 45,
 i.e. $2 \cdot L_2 = (1.5B \cdot D^4/D_1^4) + 3 \cdot R \cdot D^4/(T_1 \cdot W_1^3),$
 and $L_3 = L_3$ from example C of Fig. 45,
 i.e. $L_3 = B_1 \cdot D^4/D_1^4 + B_1^3 \cdot D^4/(15 \cdot R^2 \cdot D_1^4).$

Hence the overall equivalent length of this crankshaft is

$$\Sigma L_e = (A + 0.8T) + D^4[(2.25B/D_1^4) + 1.5R\{1/(T \cdot W^3) + 2/(T_1 \cdot W_1^3)\}] + (B_1/D_1^4) + B_1^3/(15 \cdot R^2 \cdot D_1^4).$$

This expression neglects the effect of the enlarged portion of the centre crankpins, but this can be taken into account separately by the method just discussed.

EXAMPLE 26.—In the case of the crankshaft element shown at A in Fig. 44, determine the values of the ratio L_e/L ,
 (a) when a hole 0.5 diameter is bored through the crankpin

and journals, and (b) when the hole through the crankpin is displaced radially outwards from the centre of the crankpin by an amount 0.125.

(a) From Equation (89),

$$L_e = D^4 \left[\frac{\{A + 0.8T\}}{\{D_1^4 - d_1^4\}} + \frac{\{0.75 \cdot B\}}{\{D_2^4 - d_2^4\}} + \frac{1.5R}{T \cdot W^3} \right].$$

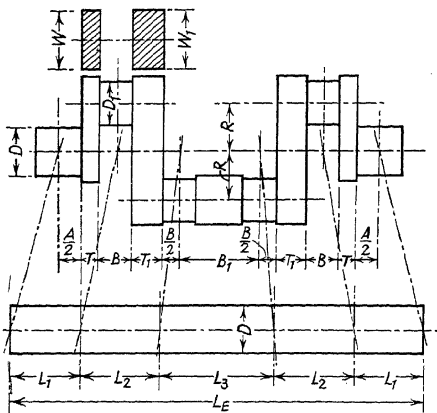


FIG. 46.—Two-bearing, four-cylinder, four-S.C., S.A. engine crankshaft.

In this case $D = 1$; $D_1 = 1$; $D_2 = 1$; $d_1 = 0.5$; $d_2 = 0.5$; $B = 1$; $R = 1$; $T = 0.5$; and $W = 1.5$.

Hence,

$$\begin{aligned} L_e &= \left\{ \frac{1.0 + 0.8 \times 0.5}{1^4 - 0.5^4} \right\} + \left\{ \frac{0.75 \times 1.0}{1^4 - 0.5^4} \right\} + \left\{ \frac{1.5 \times 1.0}{0.5 \times 1.5^3} \right\} \\ &= (1.49 + 0.8 + 0.89) \\ &= 3.18, \end{aligned}$$

and since $L = 3.0$, $L_e/L = 1.06$.

(b) From Table 17 the equivalent length of a hollow shaft with a concentric hole is

$$L = L_1 D^4 / (D_1^4 - d_1^4), \text{ where } L_1, D_1, \text{ and } d_1 \text{ are the actual dimensions of the shaft, and } D \text{ is the diameter of the equivalent shaft}$$

$$= 1.067 L_1 D^4 / D_1^4, \text{ when } d_1 = 0.5 D_1.$$

Also from Table 17 the equivalent length of a hollow shaft with an eccentric hole of diameter $d_1 = 0.5 D_1$ and $0.125 D_1$ eccentricity is

$$L = 1.16 L_1 \cdot D^4 / D_1^4,$$

i.e. the equivalent length of the shaft with the eccentric hole is about 9 per cent. greater than that of the shaft with the concentric hole.

Hence the allowance for the crankpin in the equivalent length of the crank element must be increased by this amount when the hole is bored eccentrically, i.e. the modified equivalent length is

$$L_e = 1.49 + (0.8 \times 1.16 / 1.067) + 0.89$$

$$= 1.49 + 0.87 + 0.89 = 3.25,$$

and $L_e/L = 1.08.$

The effect of boring the holes through the crankpin and journals is, therefore, to increase the equivalent length by about 6 per cent. when the crankpin hole is concentric and about 8 per cent. when it is eccentric, compared with the equivalent length for solid crankpin and journals.

In practice eccentrically disposed crankpin holes are used to facilitate machining and the insertion of oil-sealing plugs in shafts which have comparatively short crankthrows, and also to strengthen the web section at its junction with the crankpin. An eccentric crankpin hole also has the advantage of providing a larger reduction in the centrifugal loading on the bearings, and in the moment of inertia of these parts.

The following values for L_e are obtained by using Equation (91) instead of Equation (89):—

For Solid Journals and Crankpin.

$$L_e = (1.0 + 0.4) + (1.0 + 0.4) + (1 - 0.4)/(0.5 \times 1.5^3) \\ = 1.4 + 1.4 + 0.36 = 3.16,$$

and $L_e/L = 3.16/3.0 = 1.05.$

For Hollow Journals and Crankpin.

$$L_e = 1.4/0.9375 + 1.4/0.9375 + 0.36 = 1.49 + 1.49 + 0.36 \\ = 3.34,$$

and $L_e/L = 3.34/3.0 = 1.11.$

For Hollow Journals and Crankpin, with Eccentric Hole in Crankpin.

$$L_e = 1.49 + (1.49 \times 1.16/1.067) + 0.36 = 1.49 + 1.62 + 0.36 \\ = 3.47,$$

and $L_e/L = 3.47/3.0 = 1.16.$

Hence the comparative values of L_e given by Equation (9r) show that the effect of boring holes through the crankpin and journals is to increase the equivalent length by about 6 per cent., which is the same percentage reduction of stiffness as was obtained by using Equation (8g). The effect of boring the crankpin hole eccentrically, however, is to increase the equivalent length of the undrilled shaft by about 11 per cent., which is a greater reduction of stiffness than that indicated when Equation (8g) is used.

As already mentioned, if there is no previous experience to indicate which value is likely to be nearer the true value, an average of the two values should be used.

Experimental Determination of Crankshaft Stiffness.—There is considerable evidence that experimental methods in which the crankshaft is mounted in its bearings and subjected to a statically applied torque give reliable values of crankshaft stiffness for use in frequency calculations.

In a paper read before the Liverpool Engineering Society and published in the *Transactions* of the Society, Vol. LV, pp. 122 to 127, Mr. K. O. Keller describes the results of a torsion test carried out on a large opposed-piston marine oil engine crankshaft of the type shown at D in Fig. 44. This shaft was 42 ft. long, with 17-in. diameter journals and 18-in.

diameter crankpins, and the test was carried out by anchoring the coupling at one end of the shaft by means of a plate lever, and by applying a torque to the other end of the shaft by means of a similar lever and dead weights. The measured overall deflection of this shaft under a torque of 280,000 lbs.-ft. was 0.015 radian, corresponding to an overall torsional rigidity of 18,600,000 lbs.-ft. per radian. The equivalent length of 17-in. diameter plain shafting is therefore about 36 ft., corresponding to a ratio $L_e/L = 0.85$, which agrees with the value given for example D in Fig. 44.

The frequencies calculated from this value for crankshaft stiffness were subsequently found to agree with the frequencies recorded by torsigraph measurements.

In the case of small engines Dr. Geiger has stated that carefully carried out static torsion experiments on crankshafts give results which can be used in frequency calculations with the assurance that the calculated frequencies will be in good agreement with torsigraphic measurements.

The crankshaft should be mounted in its bearings, and Dr. Geiger states that bearing clearance has no apparent influence on the running stiffness of the shaft, since the torsigraph shows the same natural frequency whether this is measured at a very strong critical speed where shaft distortion due to bearing clearance might be expected to be greatest, or at a very weak critical speed where comparatively small distortions due to bearing clearance might be expected.

This experience is also characteristic of many hundreds of torsigraphic observations made by the author, both on large marine engine systems and on small high-speed engines.

Fig. 47 shows two lever arrangements for applying a pure torque to a shaft.

The arrangement shown at (A) is the simpler system and consists of two rigid bars connected to one another and to the torque lever on the shaft by suitable links or cables. The load W is applied at the middle of the shorter bar and produces a clockwise torque of magnitude $M = WR$, where R is the length of each arm of the torque lever, which is rigidly secured to one end of the shaft under test. The other end of the bar under

test must be secured against rotation by a torque reaction lever or other suitable means. In this arrangement there is a small initial torque due to the weight of unbalanced parts which can, if desired, be eliminated by suitable counter-weights.

The arrangement, shown at (B) in Fig. 47, consists of two sets of arrangement (A), and has the advantage of enabling either clockwise or counter-clockwise torques to be applied to the shaft under test merely by rolling the weight W along the loading bar. When the weight is at the centre of the loading bar there is no torque on the shaft. When the weight is rolled a distance X to the right-hand side of the centre of the loading bar a clockwise torque of magnitude $M = W \cdot R \cdot X/L$ is applied to the shaft, where the symbols have the meanings indicated in Fig. 47. When the load is moved a distance X to the left-hand side of the centre of the loading bar a counter-clockwise torque of the same magnitude is applied to the shaft. It is interesting to note that although the sum of the reactions at the two supporting brackets is, of course, equal to the load W , these reactions are equal only when the load is at the centre of the loading bar. For all other positions of the load they are unequal, and if the load could be applied at a distance L from the centre of the loading bar the reaction on one supporting bracket would be equal to the load W , and would be zero at the other supporting bracket, i.e. the system virtually reduces to the system shown at (A) in Fig. 47.

The arrangement shown at (B) in Fig. 47 provides a very convenient method of plotting torque-deflection diagrams under increasing and decreasing torques, for example, when studying hysteresis effects, the changes of torque being obtained merely by rolling the weight along the loading bar. It should be noticed, however, that the lever or other means provided for taking the torque reaction on the shaft under test must be arranged to take care of both clockwise and counter-clockwise torques if it is intended to roll the weight over the full length of the loading bar. A simple method of locking the weight carriage in any desired position should be provided (see also Fig. 148).

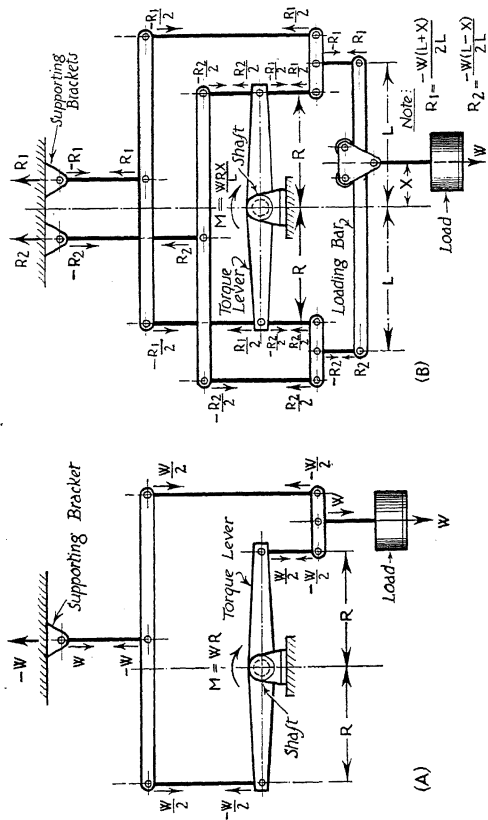


FIG. 47.—Lever systems for static torsion tests.

The total torsional deflection between one end of a crank-shaft and the other when a torque corresponding to the full load of the engine is applied at one end of the shaft varies from about 0.5° for medium and low-speed shafts, where the working stress is low, to about 1.0° for the more highly stressed shafts of high-speed automobile and aero engines. These deflections are measurable with quite simple measuring equipment, such as a micrometer or clock gauge.

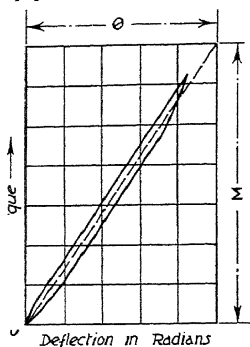


FIG. 48.—Torque-deflection diagram.

A simple and reliable method of measuring the twist in the shaft is to provide two comparatively light measuring levers, one at each end of the shaft. These levers should be independent of the main torque loading and reaction levers to avoid errors due to lever distortion, and should be of sufficient length to show a measurable deflection on the clock gauge at low values of torque loading. Clock gauge readings should be taken from each of the measuring levers. The true twist of the shaft between

the points where the measuring levers are attached is obtained from the difference of the two clock gauge readings, as follows:—

Let r = radius at which clock gauge readings are taken,

c = clock gauge reading at free end of shaft,

c_1 = clock gauge reading at anchored end of shaft.

Then θ = twist in shaft = $(c - c_1)/r$ radians

$$= 57.3 (c - c_1)/r \text{ degrees.}$$

By providing two measuring levers in this way any error due to slipping of the anchorage lever is eliminated.

A typical torque-deflection diagram is shown in Fig. 48.

This diagram was obtained by applying a pure torque to a crankshaft, the torque being applied statically with the shaft in its bearings. The torque was gradually increased from zero to a maximum and then gradually reduced back to zero again, with the result that a definite hysteresis loop was formed.

The hysteresis effect is due to a number of different causes, for example, localised elastic deformation at lever attachments and at couplings; bending deflections of keys, splines, and serrations, and gear-wheel teeth; backlash in gears, splines, serrations, and key-ways, all contribute to the formation of a hysteresis loop. Fortunately, however, the distortion due to these causes is usually confined to short portions of the curve at each end of the torque range, and between these distorted portions the load-deflection diagram consists of two parallel lines of constant slope. The slope of these two lines is the true measure of the torsional rigidity of the shaft, and the dotted line in Fig. 48 represents the torque-deflection diagram which would be obtained if all localised distortions could be eliminated.

The torsional rigidity of the shaft is easily computed from the slope of the dotted line, as follows:—

Let M = torque at any selected point on the dotted line in Fig. 48, in lbs.-ins.,

θ = the angular deflection in radians corresponding to torque M , measured on the dotted line in Fig. 48.

Then C = torsional rigidity of the shaft in lbs.-ins. per radian
 $= M/\theta$.

Mass Elastically Connected to the Main System.—

In Fig. 49 a mass J is connected to the main system at X by a shaft of torsional rigidity C .

This elastically connected mass may be replaced by an equivalent rigidly connected mass J_e , the magnitude of J_e being determined as follows:—

Let J = moment of inertia of the elastically connected mass in lbs.-ins. sec.²,

J_e = moment of inertia of equivalent rigidly connected mass in lbs.-ins. sec.²,

C = torsional rigidity of the connecting shaft XY in lbs.-ins. per radian,

ω = phase velocity of the forced vibration of the whole system, including J

$$= \frac{2 \cdot \pi \cdot F}{60} \text{ radians per sec.,}$$

F = frequency of forced vibration of the whole system in vibs. per min.,

ω_c = phase velocity of the natural vibration of the elastically connected system XY

$$= \frac{2 \cdot \pi \cdot F_c}{60} \text{ radians per sec.,}$$

F_c = frequency of natural vibration of the elastically connected system XY in vibs. per min.,

θ_y = amplitude of vibration of J in radians,

θ_x = amplitude of vibration at X in radians.

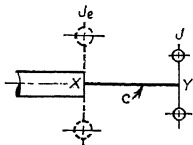


FIG. 49.—Elastically connected mass.

Then torque at X due to vibration of J with a phase velocity ω and an amplitude θ_y is

$$M_1 = J \cdot \omega^2 \cdot \theta_y \text{ lbs.-ins.}$$

Torque at X due to vibration of J_e with the same phase velocity and an amplitude θ_x is

$$M_2 = J_e \cdot \omega^2 \cdot \theta_x \text{ lbs.-ins.}$$

Hence, for J_e to have the same effect as J on the torsional vibration characteristics of the whole system,

$$M_1 = M_2,$$

i.e.
$$J_e = \frac{J \cdot \theta_y}{\theta_x}.$$

If C is infinite, i.e. if J is rigidly connected to the system,

$$\theta_y = \theta_x.$$

But it will be shown later that for any finite value of C (see Equation (234)),

$$\theta_y = \frac{\theta_x}{1 - \left[\frac{\omega}{\omega_c}\right]^2}.$$

Hence,

$$J_e = \frac{J}{1 - \left[\frac{\omega}{\omega_c}\right]^2}.$$

Now

$$\omega_c^2 = \frac{C}{J},$$

$$\text{i.e. } J_e = \frac{J}{1 - \frac{J\omega^2}{C}} = \frac{J}{1 - \frac{4\pi^2 \cdot F^2 \cdot J}{3600 C}} = \frac{J}{1 - \frac{F^2 \cdot J}{91.2 C}} \quad (92)$$

If $C/J = \omega^2$, i.e. if the natural frequency of the elastically connected system is equal to the frequency of the forced vibration, the value of J_e is infinite.

EXAMPLE 27.—Calculate the natural frequencies of torsional vibration of the system shown in Fig. 7, using the values given in Example 4, by the method just described.

From Example 4,

$$J_1 = 2073 \text{ lbs.-ins. sec.}^2,$$

$$J_2 = 1036 \text{ lbs.-ins. sec.}^2,$$

$$C_1 = 4,770,000 \text{ lbs.-ins. per radian,}$$

$$C_2 = 3,180,000 \text{ lbs.-ins. per radian,}$$

$$F = \text{natural frequency in vibs. per min.}$$

The three-mass system shown in Fig. 7 can be reduced to an equivalent two-mass system by finding the equivalent value of J_3 at J_2 ,

$$\begin{aligned} \text{i.e. } J_e &= \frac{J_3}{1 - \frac{F^2 \cdot J_3}{91.2 C_2}} = \frac{1544}{1 - \frac{1544 \times F^2}{91.2 \times 3180000}} \\ &= \frac{1544 \times 188000}{188000 - F^2}. \end{aligned}$$

The system then reduces to a simple two-mass system consisting of J_1 and $(J_e + J_2)$ connected by a shaft of torsional rigidity C_1 ,

$$\begin{aligned} \text{i.e. } F &= 9.55 \sqrt{\frac{C_1(J_1 + J_e + J_2)}{J_1(J_e + J_2)}} \\ &= 9.55 \sqrt{\frac{4770000 \left[2073 + 1036 + \frac{1544 \times 188000}{188000 - F^2} \right]}{2073 \left[1036 + \frac{1544 \times 188000}{188000 - F^2} \right]}} \end{aligned}$$

Whence, $F^4 - 1100000 F^2 + 17750000000 = 0$,

and $F = 443$ and 950 vibs. per min.

These values agree with the values of the one-node and two-node frequencies calculated by the three-mass method.

CHAPTER 4.

FLEXIBLE COUPLINGS.

FIGURE 50 shows a flexible coupling in which the torque is transmitted through flexible spokes.

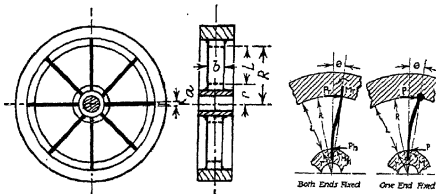


FIG. 50.—Elastically connected flywheel rim.

- Let a = thickness of each spoke, in inches,
 b = width of each spoke, in inches,
 f = bending stress in each spoke, in lbs. per sq. in.,
 i = slope of deflection curve of each spoke,
 n = number of spokes,
 r = radius to point of fixation of spoke in hub, in inches,
 y = deflection of one end of spoke relative to the other end, in inches,
 C = torsional rigidity of n spokes, i.e. of the whole coupling, in lbs.-ins. per radian,
 E = modulus of elasticity in lbs. per sq. in.,
 I = moment of inertia of cross-section of each spoke about its neutral axis, in ins.⁴ units = $a^3 \cdot b/12$,
 for rectangular spokes,

- L = bending length of each spoke, in inches = $(R - r)$,
 M = fixing couples at ends of each spoke, in lbs.-ins.,
 P = end reaction of each spoke, in lbs.,
 R = radius to point of fixation of spoke in rim, in inches,
 T = torque transmitted by coupling, i.e. by n spokes, in lbs.-ins.,
 Z = modulus of section of each spoke, in ins.³ units =
 $a^2 \cdot b/6$ for rectangular spokes,
 θ = angular deflection of rim relative to hub, in radians.

1. *Spokes Fixed at Both Ends.*—The spoke loading diagram is shown in Fig. 50.

$$\text{For force balance, } P_r + P_h = 0,$$

where P_r is the reaction at the rim and P_h is the reaction at the hub,

$$\text{or } P_h = -P_r,$$

i.e. the reactions are equal in magnitude but opposite in direction, say $\pm P$.

$$\text{For couple balance, } P \cdot L + M_r + M_h = 0.$$

Assuming that torque is transmitted from the rim to the hub,

$$\text{Input torque (at rim) } = T_r = P \cdot R + M_r = P(L + r) + M_r \text{ per spoke.}$$

$$\text{Output torque (at hub) } = T_h = -P \cdot r + M_h,$$

$$\text{but } M_h = -(P \cdot L + M_r).$$

$$\text{Hence, } T_h = -(P \cdot R + M_r),$$

i.e. the output torque is equal in magnitude but opposite in direction to the input torque.

It is convenient to regard the spoke loading as made up of two systems, viz. :—

- (i) A load P at the rim and a corresponding fixing couple $-P \cdot L$, and shearing force $-P$, at the hub, i.e. each spoke is loaded as a cantilever.

The deflection is therefore $y_1 = P \cdot L^3/(3 \cdot E \cdot I)$,
 and the slope at the rim is $i_1 = P \cdot L^2/(2 \cdot E \cdot I)$.

- (ii) A fixing couple M_r at the rim and an equal and opposite fixing couple $-M_r$ at the hub. These couples impose a constant bending moment on each spoke.

The deflection is therefore $y_2 = M_r \cdot L^2 / (2 \cdot E \cdot I)$,
and the slope at the rim is $i_2 = M_r \cdot L / (E \cdot I)$.

The total deflection of the rim relative to the hub is therefore

$$y = y_1 + y_2 = L^2(2 \cdot P \cdot L + 3 \cdot M_r) / (6 \cdot E \cdot I),$$

and the slope at the rim is

$$i = y/R = L^2(2 \cdot P \cdot L + 3 \cdot M_r) / (6 \cdot E \cdot I \cdot R),$$

but the slope at the rim is also given by $i = i_1 + i_2$,

i.e.
$$i = L(3 \cdot P \cdot L + 6 \cdot M_r) / (6 \cdot E \cdot I).$$

Since these two expressions for the slope must be equal,

$$M_r = P \cdot L(2 \cdot L - 3R) / (6 \cdot R - 3 \cdot L),$$

and the transmitted torque for n spokes, i.e. for the whole coupling, is

$$\begin{aligned} T &= n(P \cdot R + M_r) \\ &= n \cdot P(6 \cdot R^2 - 6 \cdot R \cdot L + 2L^2) / (6 \cdot R - 3 \cdot L). \end{aligned} \quad (93)$$

The deflection is
$$y = \frac{P \cdot L^3 \cdot R}{6 \cdot E \cdot I(2 \cdot R - L)}$$

and the corresponding angular deflection is

$$\theta = y/R = \frac{P \cdot L^3}{6 \cdot E \cdot I(2 \cdot R - L)}. \quad (94)$$

The torsional rigidity of n spokes, i.e. for the whole coupling, is therefore

$$C = T/\theta = 4 \cdot n \cdot E \cdot I(3 \cdot R^2 - 3 \cdot R \cdot L + L^2) / L^3. \quad (95)$$

The maximum bending stress in each spoke occurs at the hub and is given by the following expression:—

$$f_{\max} = \frac{T \cdot L(3R - L)}{n \cdot Z(6 \cdot R^2 - 6 \cdot R \cdot L + 2 \cdot L^2)}. \quad (96)$$

2. *Spokes Insecurely Fixed.*—In practice it is possible that, due to insecure fixation of the spokes, particularly at the hub, the fixing couples at each end of the spoke are nearly equal.

The following expressions apply when this occurs, i.e. when $M_r = M_h = M$:—

$$\begin{aligned} \text{Since} \quad & P \cdot L + M_r + M_h = 0, \\ \text{hence,} \quad & M_r = M_h = -P \cdot L/2, \end{aligned}$$

i.e. deflection of rim relative to hub $= y = P \cdot L^3/(12 \cdot E \cdot I)$,
or angular deflection $= \theta = y/R = P \cdot L^3/(12 \cdot E \cdot I \cdot R)$. (97)

The transmitted torque for n spokes is

$$T = n(P \cdot R - P \cdot L/2) = n \cdot P(R + r)/2 \quad (98)$$

and the corresponding torsional rigidity is

$$C = T/\theta = 6 \cdot n \cdot E \cdot I \cdot R(R + r)/L^3. \quad (99)$$

The maximum bending stress in each spoke occurs at the points of fixation in the rim and hub, and is given by the following expression :—

$$f_{\max} = \frac{T(R - r)}{n \cdot Z(R + r)} = \frac{T \cdot L}{n \cdot Z(2 \cdot R - L)}. \quad (100)$$

3. *Spokes Fixed in Hub and Free in Rim.*—The loading diagram is shown in Fig. 50.

In this case $M_r = 0$ and $M_h = M = -P \cdot L$.

The input torque is

$$T_r = P \cdot R \text{ per spoke,}$$

and the output torque per spoke is

$$T_h = -P \cdot r + M = -P \cdot r - P \cdot L = -P \cdot R,$$

i.e. the total torque transmitted by n spokes, i.e. by the whole coupling, is

$$T = n \cdot P \cdot R.$$

The deflection of the rim relative to the hub is

$$y = P \cdot L^3/(3 \cdot E \cdot I),$$

and the corresponding angular deflection is

$$\theta = y/R = P \cdot L^3/(3 \cdot E \cdot I \cdot R). \quad (101)$$

The torsional rigidity of n spokes, i.e. of the whole coupling, is therefore

$$C = T/\theta = 3 \cdot E \cdot I \cdot R^2 \cdot n/L^3, \quad (102)$$

and the maximum bending stress in each spoke occurs at the hub and is given by the following expression :—

$$f_{\max} = T \cdot L/(n \cdot R \cdot Z). \quad (103)$$

Uniformly Stressed Spokes.—Since the primary purpose of a flexible coupling is to introduce the greatest amount of flexibility into a system, i.e. to provide the greatest possible deflection under a given load for a given expenditure of material, the volumetric efficiency of the coupling is well represented by its resilience or the energy stored per unit weight.

For maximum volumetric efficiency the spring elements should represent as large a proportion of the total weight of the coupling as possible, and each spring element should be as uniformly stressed as possible so that the physical properties of the material are used to full advantage. For example, it has been shown that in the case of torsion bars a hollow cylindrical section possesses the greatest resilience per unit weight because it is subjected to very nearly uniform shear stress. A solid cylindrical torsion bar is only half as good, whilst any other section is less than half as good.

The volumetric efficiency of couplings of the type shown in Fig. 50 can therefore be increased by shaping the spokes so that they are uniformly stressed. This can be done very simply when the spokes are fixed at the hub only, and Fig. 51 shows three methods of improving the efficiency of flexible spokes.

In Diagram I, Fig. 51, the thickness of the spoke a tapers uniformly towards the hinged end, i.e. towards the rim, whilst the width of the spoke b remains constant. In Diagram II the thickness remains constant, and the width tapers gradually towards the rim.

Spoke of Constant Width and Tapering Thickness (Diagram I, Fig. 51).—The deflection of the tip under a load P is given by the following expression :—

$$y = \frac{12 \cdot P \cdot L^3 \cdot K^3}{E \cdot a^3 \cdot b(K-1)^3} \left(\log_e K - \frac{(3K-1)(K-1)}{2 \cdot K^2} \right), \quad (104)$$

where $P = T/(R \cdot n)$,

and $K =$ ratio of thickness at hub to thickness at rim.

For uniform stress the thickness of the spoke should be proportional to the square root of the bending moment, which gives the parabolic shape shown dotted in Diagram I of Fig. 51.

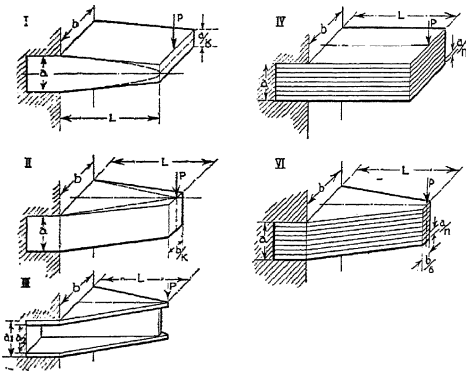


FIG. 51.—Flexible spokes.

In a truly uniformly stressed spoke of constant width and variable thickness the tip deflection is

$$y = 8 \cdot P \cdot L^3 / (E \cdot a^3 \cdot b),$$

and the corresponding angular deflection of the rim relative to the hub is

$$\theta = 8 \cdot P \cdot L^3 / (E \cdot a^3 \cdot b \cdot R). \quad (105)$$

The torque transmitted by n spokes for this deflection is

$$T = P \cdot R \cdot n.$$

Hence the torsional rigidity of the coupling is

$$C = T/\theta = E \cdot a^3 \cdot b \cdot R^2 \cdot n / (8 \cdot L^3). \quad (106)$$

The maximum bending stress occurs at the hub and is given by

$$f_{\max} = T \cdot L / (n \cdot R \cdot Z) = 6 \cdot T \cdot L / (a^2 \cdot b \cdot R \cdot n). \quad (107)$$

The equivalent length L_e of plain cylindrical shafting of diameter D , which has the same flexibility as the coupling, can be obtained as follows:—

The torsional rigidity of a length L_e of plain cylindrical shafting of diameter D is

$$C = \pi \cdot D^4 \cdot G / (32 \cdot L_e) = E \cdot a^3 \cdot b \cdot R^2 \cdot n / (8 \cdot L^3).$$

Hence,
$$L_e = \frac{D^4 \cdot G \cdot L^3}{1 \cdot 28 E \cdot a^3 \cdot b \cdot R^2 \cdot n} \quad (108)$$

Table 16 shows that for nearly all metals the ratio E/G is about 2.5, so that the above expression for L_e can be written

$$L_e = \frac{D^4 \cdot L^3}{3 \cdot 2 a^3 \cdot b \cdot R^2 \cdot n} \quad (109)$$

Spoke of Constant Thickness and Tapering Width (Diagram II, Fig. 51).—The deflection of the tip under a load P is given by the following expression:—

$$y = \frac{12 \cdot P \cdot L^3 \cdot K}{E \cdot a^3 \cdot b (K-1)^2} \left(\frac{\log_e K}{(K-1)} - \frac{(3-K)}{2} \right) \quad (110)$$

For uniform stress the width of the spoke should be proportional to the bending moment, which gives the triangular shape shown dotted in Diagram II of Fig. 51.

In the case of a truly uniformly stressed spoke of constant thickness and variable width, the tip deflection is

$$y = 6 \cdot P \cdot L^3 / (E \cdot a^3 \cdot b),$$

i.e. the angular deflection of the rim relative to the hub is

$$\theta = 6 \cdot P \cdot L^3 / (E \cdot a^3 \cdot b \cdot R). \quad (111)$$

Hence the expressions for torsional rigidity and maximum stress are as follows:—

$$C = E \cdot a^3 \cdot b \cdot R^2 \cdot n / (6 \cdot L^3), \quad (112)$$

$$f_{\max} = 6 \cdot T \cdot L / (a^2 \cdot b \cdot R \cdot n). \quad (107)$$

The expression for the equivalent length of cylindrical shafting is in this case

$$L_e = \frac{D^4 \cdot L^3}{4 \cdot 25 a^3 \cdot b \cdot R^2 \cdot n} \quad \cdot \quad \cdot \quad \cdot \quad (113)$$

A good practical approximation to a uniformly stressed cantilever of constant width and varying thickness is obtained by making the tip thickness one-third the root thickness ($K = 3$ in Diagram I of Fig. 51), and an equally good approximation for the case where the thickness is constant and the width varies is obtained when the width at the tip is one-sixth the width at the root ($K = 6$ in Diagram II of Fig. 51).

These approximations have the advantage of providing sufficient material at the tip of the spoke to take care of shear loading and in all actual examples it is important to check the shear stress in sections near the tip.

It is possible to increase the flexibility of the spoke still further by varying both width and thickness, but the gain in flexibility over the simple approximations given above is hardly sufficient to compensate for the increased manufacturing difficulties.

Expressions for torsional rigidity, equivalent length, and maximum bending stress for different types of spoke are given in Fig. 52. These expressions have been derived by the foregoing methods.

Resilience of Flexible Couplings.—The resilience of a coupling may be defined as the capacity of the coupling for storing energy or, in other words, it is the amount of energy which is restored when the load is removed from the coupling. In general, for strains within the elastic limit of the material, the resilience is one-half the product of the force or torque and the linear or angular displacement which it produces.

In the case of direct tension or compression, for example,

$$W = \text{resilience} = \text{load} \times \text{deflection}/2 = P \cdot \delta/2,$$

$$\text{but } E = \text{modulus of elasticity} = \text{stress/strain} = \frac{P \cdot L}{A \cdot \delta},$$

assuming uniform distribution of stress,

Sketch	Torsional Rigidity Lbs. Ins./Radian	Max. Bending Stress Lbs./Ins. ²
	$C = \frac{n \cdot a^3 \cdot b \cdot E (3R^2 - 3RL + L^2)}{3 \cdot L^3}$	$f = \frac{6 \cdot T \cdot L (3R - L)}{n \cdot a^2 \cdot b (6R^2 - 6RL + 2L^2)}$ <p style="text-align: center;">At Hub</p> $W = \frac{f^2 \cdot V \cdot n (3 - 3K + K^2)}{6 \cdot E (3 - K)^2}$
	<i>Insecurely Fixed Spokes</i>	
	$C = \frac{n \cdot a^3 \cdot b \cdot E \cdot R (2R - L)}{2 \cdot L^3}$	$f = \frac{6 \cdot T \cdot L}{n \cdot a^2 \cdot b (2R - L)}$ <p style="text-align: center;">At Hub and Rim</p> $W = \frac{f^2 \cdot V \cdot n (2 - K)}{36 \cdot E}$
	$C = \frac{n \cdot a^3 \cdot b \cdot E \cdot R^2}{4 \cdot L^3}$	$f = \frac{6 \cdot T \cdot L}{n \cdot a^2 \cdot b \cdot R}$ <p style="text-align: center;">At Hub</p> $W = \frac{f^2 \cdot V \cdot n}{18 \cdot E}$
	$C = \frac{n \cdot a^3 \cdot b \cdot E \cdot R^2}{8 \cdot 5 \cdot L^3}$	$f = \frac{6 \cdot 75 \cdot T \cdot L}{n \cdot a^2 \cdot b \cdot R}$ <p style="text-align: center;">At L/2</p> $W = \frac{f^2 \cdot V \cdot n}{7 \cdot 1 \cdot E}$
	$C = \frac{n \cdot a^3 \cdot b \cdot E \cdot R^2}{5 \cdot 35 \cdot L^3}$	$f = \frac{6 \cdot T \cdot L}{n \cdot a^2 \cdot b \cdot R}$ <p style="text-align: center;">At Hub</p> $W = \frac{f^2 \cdot V \cdot n}{7 \cdot 8 \cdot E}$

Symbols

C = Torsional Rigidity of Coupling, (n Spokes), in Lbs. Ins./Radian
 L_e = Equivalent Length in Inches of Cylindrical Shaft of Dia. D .
 f = Maximum Bending Stress in each Spoke, in Lbs./Ins.²
 n = Number of Spokes in Coupling.
 T = Total Torque Transmitted by Coupling, (n Spokes), in Lbs. Ins.
 W = Strain Energy for n Spokes, in In. Lbs.
 V = Volume of One Spoke in Cu. Ins.
 K = L/R .

FIG. 52.—Flexible spokes.

where L = length of specimen; A = cross-sectional area of specimen, i.e.

$$W = \frac{1}{3} \cdot \frac{f^2 \cdot V}{E}, \quad \dots \quad (114)$$

where V = volume of specimen = $A \cdot L$,
 f = stress = P/A .

Hence, if f is the stress at the elastic limit, then Equation (114) represents the greatest strain energy which can be stored in the specimen without permanent distortion. If the stress distribution is not uniform the equation is of the same form as (114), but the numerical factor is less than one-half when f is the maximum stress anywhere in the specimen.

Torsional Resilience.—When a specimen is subjected to a uniformly distributed shear stress within the elastic limit the stored strain energy, or shearing resilience, is given by the following expression:—

$$W = \frac{1}{3} \cdot \frac{f^2 \cdot V}{G}, \quad \dots \quad (115)$$

where W = shearing resilience in in.-lbs.,
 f = shear stress in lbs. per sq. in.,
 V = volume of specimen in cubic inches,
 G = modulus of rigidity in lbs. per sq. in.

This expression is similar to Equation (114), and represents the greatest strain energy which can be stored in the specimen without permanent distortion.

If the shear stress distribution is not uniform the equation is of the same form as (115), but the numerical factor is less than one-half if f is the maximum shear stress anywhere in the specimen.

In the case of a hollow cylindrical shaft subjected to torsional strain within the elastic limit, the shear stress is directly proportional to the radius, and the maximum shear stress occurs in the outermost fibres, i.e. at the outer radius R_1 .

Let f_s = maximum shear stress in lbs. per sq. in., i.e. the stress at the outer radius R_1
 R_1 = outer radius of shaft in inches,
 R_2 = inner radius of shaft in inches,
 $K = R_2/R_1$,
 V = Volume of hollow shaft = $\pi \cdot L(R_1^2 - R_2^2)$, in cubic inches.

Then the shearing resilience of any tubular element at radius r , and of thickness dr , and length L is

$$dW = \frac{2 \cdot \pi \cdot r \cdot L \cdot f^2}{2 \cdot G} \cdot dr,$$

where f = shear stress at radius $r = f_s \cdot r/R_1$.

$$\begin{aligned} \text{Hence, } W &= \frac{\pi \cdot L \cdot f_s^2}{R_1^2 \cdot G} \int_{R_2}^{R_1} r^3 \cdot dr = \frac{\pi \cdot L \cdot f_s^2}{4 \cdot G \cdot R_1^2} (R_1^4 - R_2^4) \\ &= \frac{\pi \cdot L \cdot f_s^2}{4 \cdot R_1^2 \cdot G} \cdot (R_1^2 - R_2^2)(R_1^2 + R_2^2) \\ &= \frac{f_s^2 \cdot (1 + K^2) \cdot V}{4 \cdot G} \dots \dots \dots \quad (116) \end{aligned}$$

This expression approaches the value $W = \frac{1}{2} \frac{f_s^2 \cdot V}{G}$ as K approaches unity, i.e. when R_2 is very nearly equal to R_1 .

Thus in the case of very thin tubes the strain energy stored is very nearly equal to the maximum theoretically possible (Eqn. 115). This is because for very thin tubes there is practically uniform distribution of shear stress.

Equation (116) becomes $W = f_s^2 \cdot V/4 \cdot G$ when $K = 0$ or $R_2 = 0$, i.e. for a solid cylindrical shaft. Thus the capacity of a solid cylindrical shaft for storing shear strain energy is only about one-half that of a very thin tube containing the same volume of material subjected to the same maximum shear stress.

Flexural Resilience.—The resilience of a beam can be found from the following well-known expression for flexural resilience, when the bending moment diagram is known :—

$$W = \frac{1}{2} \int \frac{M^2}{E \cdot I} \cdot dx, \quad \dots \dots \dots (117)$$

where M = bending moment,
 E = modulus of elasticity,
 I = moment of inertia of cross-section of beam
 $= a^3 \cdot b / 12$,
 a = depth of beam,
 b = width of beam.

In a simple cantilever of length L and constant rectangular section, i.e. depth a and width b , carrying a tip load P ,
 Bending moment at distance x from tip = $M = P \cdot x$.

$$\text{Hence, } W = \frac{6 \cdot P^2}{a^3 \cdot b \cdot E} \int_0^L x^2 \cdot dx \text{ (from Eqn. 117),}$$

$$\text{i.e. } W = \frac{2 \cdot P^2 \cdot L^3}{a^3 \cdot b \cdot E}$$

but f_b = maximum fibre stress = M/Z ,

where $M = P \cdot L$ = the maximum bending moment,

and Z = modulus of section = $a^2 \cdot b/6$,

$$\text{i.e. } P = f_b \cdot Z/L = f_b \cdot a^2 \cdot b/(6 \cdot L).$$

Hence,

$$W = \frac{f_b^2 \cdot a \cdot b \cdot L}{18 \cdot E}, \text{ and since } a \cdot b \cdot L = \text{volume of beam} = V,$$

$$W = \frac{f_b^2 \cdot V}{18 \cdot E} \quad \dots \quad (118)$$

If the section of the beam varies throughout its length so that the maximum fibre stress is constant at all sections the expression for strain energy is altered as follows:—

Let I_0 = moment of inertia of section at fixed end of cantilever
 $= a^3 \cdot b/12$.

Then, assuming that the cross-section varies in width, constant skin stress is obtained when the width is directly proportional to the bending moment,

$$\text{i.e. } I = a^3 \cdot b \cdot x/(12 \cdot L).$$

The expression for resilience becomes, therefore,

$$W = \frac{6 \cdot P^2 \cdot L}{a^3 \cdot b \cdot E} \int_0^L x \cdot dx = \frac{3 \cdot P^2 \cdot L^3}{a^3 \cdot b \cdot E},$$

or, substituting the value $P = f_b \cdot a^2 \cdot b / (6 \cdot L)$,

$$W = \frac{f_b^2 \cdot a \cdot b \cdot L}{12 \cdot E},$$

but volume of beam = $V = a \cdot b \cdot L / 2$ (since the plan form of the beam is a triangle).

Hence,
$$W = \frac{1}{6} \cdot \frac{f_b^2 \cdot V}{E}. \quad \dots \quad (119)$$

It can be shown that Equation (119) applies to any rectangular beam in which the skin stress is constant, and that for any other solid section the numerical factor is less than one-sixth, i.e. the resilience per unit volume is less for a given maximum fibre stress. For example, in the case of a round section the value of the numerical factor is one-eighth.

It should be noted that the total resilience of a spoke of type III in Fig. 52, i.e. where approximately uniform skin stress is obtained by varying depth of the beam, is about 25 per cent. greater than that of a spoke of type IV where the width of the beam varies, assuming the same root section in each case. This is because the volume of material in the spoke is about 25 per cent. greater for Type III.

Diagram III in Fig. 51 shows a cantilever consisting of two flanges separated by a thin web in which the stress due to flexure is approximately constant throughout the material. In the following discussion the web will be neglected and it will be assumed that the flanges do not buckle.

In this case, $I = (a_1^3 - a_2^3) b \cdot x / (12 \cdot L)$, assuming that the plan form of the beam is triangular, as for a rectangular beam with constant skin stress, where x is the distance measured from the tip,

and
$$W = \frac{6 \cdot L}{(a_1^3 - a_2^3) b \cdot E} \int P^2 \cdot x \cdot dx$$

$$\frac{3 \cdot P^2 \cdot L^3}{(a_1^3 - a_2^3) b \cdot E},$$

$$\text{but } P = f_b \cdot Z_f L = \frac{f_b(a_1^3 - a_2^3)b}{6 \cdot a_1 \cdot L},$$

$$\text{i.e. } W = \frac{f_b^2 \cdot (a_1^3 - a_2^3)b \cdot L}{12 \cdot E \cdot a_1^2} = \frac{f_b^2 \cdot a_1 \cdot b \cdot L(1 - K_1^3)}{12 \cdot E},$$

also, volume = $V = (a_1 - a_2) \cdot b \cdot L/2 = a_1(1 - K_1) \cdot b \cdot L/2$,
 where $K_1 = a_2/a_1$,

$$\text{i.e. } W = f_b^2 \cdot V(1 + K_1 + K_1^2)/(6 \cdot E). \quad (120)$$

The following table shows the variation of strain energy per unit volume with K_1 :—

$K_1 = a_2/a_1$	W.
0	$f_b^2/(6 \cdot 00 E)$
$\frac{1}{2}$	$f_b^2/(4 \cdot 57 E)$
$\frac{1}{3}$	$f_b^2/(3 \cdot 43 E)$
$\frac{1}{4}$	$f_b^2/(2 \cdot 60 E)$
1	$f_b^2/(2 \cdot 00 E)$

The value $K_1 = 0$ corresponds to a solid rectangular beam, i.e. the expression for resilience agrees with Equation (119).

The value $K_1 = 1$ is approached when the flanges are made very thin compared with the total depth of the beam. For this condition the expression for resilience approaches that for uniformly stressed material (see Equation 114).

In the case of spring elements of flexible couplings it is not practicable to employ members of the type shown in Diagram III of Fig. 51, and even if this could be done it is doubtful whether the numerical factor in the expression for resilience would be very much greater than that for a beam with uniform skin stress, viz. one-sixth, bearing in mind that effective means would be required to prevent buckling of the thin flanges.

Fig. 52 summarises the formulæ for spoked couplings and contains expressions for calculating the torsional rigidity, equivalent length, and resilience of the complete coupling, and the maximum bending stress in each spoke.

In designing couplings of this type, the spokes should be stressed to the maximum permissible value to obtain maximum resilience. The length of the spokes will usually be fixed by

consideration of the maximum permissible diameter of the coupling and the size of the hub, and the maximum torque to be transmitted by the coupling will be known. In this connection it should be noted that it is usually safe to make the coupling as strong or a little stronger than the shaft on which it is mounted, because the torque passing through the coupling even under conditions of torsional resonance is the same as that passing through the shaft except in abnormal cases.

Since the stress in the spokes for a given torque is inversely proportional to $a^2 \cdot b$, whilst the volume is proportional to $a \cdot b$, the product $f_s^2 \cdot V$ increases as the depth of the spoke a decreases.

It is an advantage, therefore, to make the spokes as wide as the space available and other structural requirements permit. A good starting-point is to assume that the width is one-half the length of the spoke.

The spokes may be separate members, as shown in Fig. 51, or they may be formed integral with the hub, as shown at IV in Fig. 53. The former method enables the spring members to be made of high tensile spring steel, whilst the latter method overcomes the difficulty of ensuring complete fixation of the roots of the spokes.

The number of spokes is limited by the diameter of the hub, and so a further advantage of making them separate members is that in cases where the number of spokes required to give the maximum permissible bending stress under the applied torque exceeds the number of slots which can be economically cut in the periphery of the hub, several thinner spokes can be accommodated in each slot, as shown at IV and V in Fig. 51. This laminated construction provides a certain amount of inter-leaf damping which may be useful in certain applications.

In the case of spokes formed integral with the hub, or with a ring which in turn is splined or keyed to the hub, care must be taken to avoid excessive stress concentration at the roots of the spokes by providing a generous radius between each pair of spokes as shown at IV in Fig. 53.

This radius should not be less than the thickness of the

spoke at its root, in which case the pitching of the spokes round the periphery of the hub is approximately $\pi \cdot a$, i.e.

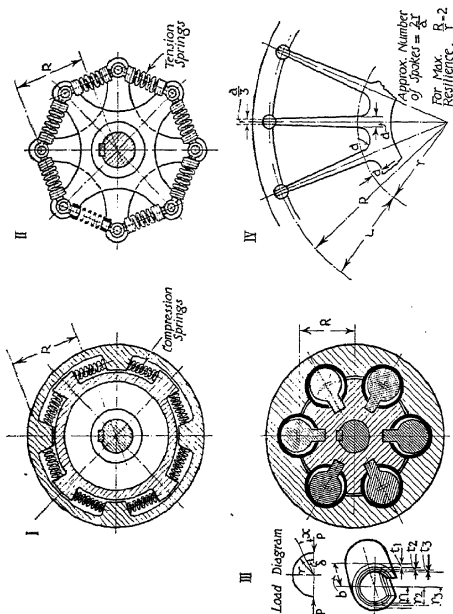


Fig. 53.—Spring couplings.

the number of spokes which can be accommodated round the periphery of a hub of radius r is $(2 \cdot r/a)$.

This avoids any serious concentration of stress at the roots of the spokes. If it is necessary to provide a greater number

of spokes than is given by the above rule care must be taken to allow for this concentration of stress. For example, if the root radius is made one-quarter the root thickness, then the stress concentration factor will be about 2 for spring steel.

In general, for maximum resilience the volume of active material, i.e. the volume of the spring elements, must be as large a proportion of the total volume as possible; the spring elements should be as uniformly stressed as possible; and the material should be stressed to the maximum permissible limit.

These considerations imply that the width/thickness ratio of the spokes should be large, taking into account structural limitations, and that a sufficient number of spokes should be provided to ensure that the material is stressed to the maximum permissible limit under the given loading conditions.

There are so many variables in the design of a coupling of this type that it is impossible to generalise further than this, and in practice the best compromise is usually obtained by successive trial for a particular application.

Table 20 compares the resilience per unit volume for different types of spring elements, assuming 100 per cent. for uniformly stressed material.

Uniform tension or compression members are impractical for use in spring couplings, unless made of rubber, because they are far too rigid.

The most efficient torsional spring element is a hollow torsion bar made of high-tensile steel, and elements of this type are commonly employed in practice, for example as quill shafts in geared drives. It is not always possible, however, to accommodate the required length of torsion bar in the space available.

An advantage of hollow or solid torsion bars is that a considerable amount of flexibility can be introduced into an oscillating system without any appreciable increase of inertia, whereas the moment of inertia of the housings of flexible couplings might alter the inertia characteristics of the system considerably. In some cases, and where doubt exists, it is advisable to investigate this point.

The solid cylindrical torsion bar is only about half as efficient as a very thin hollow torsion bar. It is commonly found in engineering practice in the form of thin quill shafts made of high-tensile steel for use in geared drives, and even more generally in the form of helical springs.

TABLE 20.
RESILIENCE PER UNIT VOLUME.

Type of Spring.	Resilience per Unit Volume.	Per Cent.
Uniformly stressed bar in tension or compression	$f^2/(2 \cdot E)$	100
Limiting value for a very thin hollow cylindrical torsion bar	$f_s^2/(2 \cdot G)$	100
Limiting value for flexural member with very thin flanges of rectangular cross-section	$f_b^2/(2 \cdot E)$	100
Solid cylindrical torsion bar	$f_s^2/(4 \cdot G)$	50
Flexural members with uniform skin stress everywhere, and rectangular cross-section	$f_b^2/(6 \cdot E)$	33
Flexural members similar to Type III in Fig. 52	$f_b^2/(7 \cdot 1 \cdot E)$	28
Flexural members similar to Type IV in Fig. 52	$f_b^2/(7 \cdot 8 \cdot E)$	26
Simple cantilever of uniform rectangular section (Type II in Fig. 52)	$f_b^2/(18 \cdot E)$	11
Flexural members similar to Type I in Fig. 52, spokes securely fixed	$f_b^2/(18 \cdot E)$ to $f_b^2/(24 \cdot E)$	11 to 8
Flexural members similar to Type I in Fig. 52, spokes insecurely fixed	$f_b^2/(18 \cdot E)$ to $f_b^2/(36 \cdot E)$	11 to 5.5

Note.—Table 20 does not take account of differences between G and E and between f_s and f_b for different materials. The percentages given in the table do not, therefore, give a direct comparison between flexural and torsional members. This matter is discussed later in connection with Tables 21 and 22.

Flexural members with very thin flanges in relation to their depth are not practicable because of the difficulty of connecting the flanges together so that buckling is prevented, and also because their bulk occupies space which can be filled more effectively by other forms of spring element.

In the case of flexural spring members, therefore, Table 20 shows that the greatest efficiency is obtained in practice when

these are designed to have a uniform skin stress everywhere. It is interesting to note, however, that the efficiency of such an element is only one-third that of a truly uniformly stressed element, but that it is about three times as efficient as the elements shown at I and II in Fig. 52.

In the case of flexible couplings employing flexible spokes, therefore, care should be taken to shape these so that the skin stress is as nearly as possible uniform throughout the spoke, in which case the torsional rigidity of the coupling is given by the following simple expression :—

$$\text{Resilience of coupling} = W = \frac{f_s^2 \cdot V \cdot n}{6 \cdot E}, \quad (121)$$

but

$$W = T \cdot \theta / 2,$$

i.e.

$$\theta = \frac{f_s^2 \cdot V \cdot n}{3 \cdot E \cdot T},$$

and

$$C = T / \theta = \frac{3 \cdot E \cdot T^2}{V \cdot f_s^2 \cdot n} \quad (122)$$

where C = torsional rigidity in lbs.-ins./radian,

E = modulus of elasticity in lbs. per sq. in.,

T = torque transmitted by coupling in lbs.-ins.,

V = volume of *one* spoke in cu. ins.,

f_s = skin stress in lbs. per sq. in. (uniform throughout the spoke),

n = number of spokes.

So far only the form of the spring elements has been considered, and nothing has been said about the relative merits of different materials.

Table 21 contains the properties of some typical materials. The working stresses quoted in this table are about one-half the fatigue limits for the respective materials, which provides a sufficient factor of safety if the parts are free from severe stress raisers, such as sharp corners or other discontinuities.

The following expression for the maximum permissible shear stress when repeated torsional stresses are superimposed on various mean stresses is given by Dr. S. F. Dorey in his paper, "Some Factors Influencing the Sizes of Crankshafts

for Double-Acting Diesel Engines" (*Trans. N.E. Coast Instn. of Engineers and Shipbuilders*, 1931). It is based on the experimental work of Dr. G. A. Hankins, and gives safe values for all ductile steels, and for values of x up to 0.4 for high tensile steels:—

$$f_s = f_t(1.85 + 1.2 \cdot x + 0.35 \cdot x^2) \quad \dots \quad (123)$$

where f_s = maximum permissible shear stress for ratio x ,

$\pm f_t$ = fatigue limit for completely reversed torsional stress,
= ultimate tensile stress/4 approximately for most steels,

x = minimum shear stress/maximum shear stress.

When $x = 1$, the range of stress is zero, and $f_s = 3.4 \cdot f_t$, which is the ultimate shear stress.

When $x = 0$, the minimum stress is zero, and $f_s = 1.85 \cdot f_t$, which is practically equal to the endurance range.

When $x = -1$, i.e. completely reversed stress, $f_s = f_t$, and the endurance range is again $2 \cdot f_t$.

The above expression shows, therefore, that if the permissible shear stress is $\pm f_s$, it is immaterial whether it is applied as a completely reversed stress or is superimposed on a steady mean stress up to a value f_s .

For example, if the maximum permissible stress in reversed torsion is $\pm 15,000$ lbs. per sq. in., there is no risk in superimposing this on a steady stress of 15,000 lbs. per sq. in., so that the shaft is subjected to zero minimum stress and 30,000 lbs. per sq. in. maximum stress. In both cases the range of stress is 30,000 lbs. per sq. in.

In the case of repeated bending stresses at various mean stresses the same remarks apply, namely, that if the permissible bending stress is $\pm f_b$, there is no risk in superimposing this on a mean steady stress up to a value f_b .

In the case of couplings subjected to periodic torque fluctuations the stress on the spring elements may be regarded as composed of a cyclic variation of stress superimposed on a steady mean stress and, provided this steady mean stress

does not exceed one-half the endurance range of the material, the spring elements of couplings transmitting periodically fluctuating torques can be safely designed from a consideration of the fluctuating part of the load only, using the working stresses given in Table 21.

Since the principal duty of flexible couplings in drives subjected to torsional vibration is to assist in absorbing the fluctuating torque loading, the specific resiliences in Table 22

TABLE 21.
PROPERTIES OF MATERIALS.

Material.	E lbs./in. ² .	G lbs./in. ² .	Permissible Working Stress.	
			f_s , lbs./in. ² .	f_t , lbs./in. ² .
30 tons/in. ² mild steel .	30,000,000	12,000,000	± 16,000	± 8,000
60 tons/in. ² alloy steel .	30,000,000	11,800,000	± 30,000	± 15,000
90 tons/in. ² spring steel .	30,000,000	11,500,000	± 50,000	± 25,000
Stainless steel (high tensile)	30,000,000	12,000,000	± 30,000	± 15,000
Stainless steel (low tensile)	30,000,000	12,000,000	± 20,000	± 10,000
Stainless steel (Austenitic).	28,000,000	11,800,000	± 20,000	± 10,000
"K" monel metal .	26,000,000	9,500,000	± 19,000	± 9,000
Bronze	15,000,000	6,000,000	± 10,000	± 5,000
Duralumin	10,000,000	3,800,000	± 9,000	± 4,500
Rubber (average values) .	500	100	± 75	± 75
	Bending moduli	Torsion moduli	Reversed bending.	Reversed torsion.

are based on the permissible working stresses and elastic moduli in Table 21. This gives the maximum specific resiliences for each stress cycle, and for the different types of spring element commonly used in practice.

Incidentally this specific resilience is the energy of the vibration per unit volume, or weight, of the spring elements when the maximum cyclic stress attains the values given in Table 21.

Table 22 shows that the greatest specific resilience is obtained with rubber in shear, although it is interesting to notice that the resilience of rubber in shear per unit volume

is very nearly the same as that of spring steel in shear per unit volume. It should be mentioned, however, that the safe working load of ≈ 75 lbs. per sq. in. depends on the strength of the bonding between the rubber and its supports.

TABLE 22.
RESILIENCE PER UNIT VOLUME AND WEIGHT.
(Inch-lbs.).

Description.		Mild Steel.	Alloy Steel.	Spring Steel.	Bronze.	Duralumin.	Rubber.
Hollow cylindrical torsion bars (e.g. quill shafts).	per cu. in.	2.7	9.5	27.0	2.1	2.7	—
	per lb.	9.5	33.5	95.0	7.0	27.0	—
Solid cylindrical torsion bars (e.g. quill shafts and helical springs).	per cu. in.	1.3	4.8	13.5	1.0	1.4	—
	per lb.	4.6	16.8	47.5	3.5	13.5	—
Flexural members with uniform skin stress everywhere, and rectangular cross-section (e.g. flexible spokes).	per cu. in.	1.4	5.0	14.0	1.1	1.4	—
	per lb.	5.0	17.7	49.5	3.7	13.5	—
Simple cantilever of uniform rectangular section (e.g. flexible spokes).	per cu. in.	0.5	1.7	4.7	0.4	0.5	—
	per lb.	1.8	6.0	16.6	1.3	4.5	—
Rubber in shear.	per cu. in.	—	—	—	—	—	28
	per lb.	—	—	—	—	—	560
Rubber in tension or compression.	per cu. in.	—	—	—	—	—	6
	per lb.	—	—	—	—	—	112

Spring steel possesses a higher specific resilience than any other metal, owing to its capacity for withstanding very much higher working stresses under both reversed bending and reversed torsion loads. Thus, on either a volume or a weight

basis the specific resilience of spring steel is about ten times that of mild steel and about thirteen times that of bronze.

In the case of duralumin the specific resilience of spring steel is from 6 to 10 times that of this light alloy on a volume basis, but only from 2 to 3.5 times on a weight basis.

Table 22 also shows that the most efficient form of spring element is a hollow cylindrical torsion bar; and that the specific resiliences of a solid cylindrical torsion bar and a flexural member of rectangular cross-section with uniform *skin* stress everywhere are very nearly the same, when the materials are required to withstand vibratory loads.

It is therefore immaterial whether torsion or flexural members are used as the spring elements of flexible couplings as far as specific resilience is concerned. The form of the coupling is, however, an important factor in deciding the type of spring. For example, the space available for installing the coupling may indicate a form of coupling in which a much greater volume of spring material can be accommodated in torsion than in bending, and in such a case torsion members would naturally be employed.

EXAMPLE 28.—A flywheel rim is attached to a shaft by eight alloy steel spokes of uniform rectangular cross-section, each spoke being 8 ins. wide. The inner radius of the fly-wheel rim is 30 ins., and the outer radius of the boss is 10 ins.

Calculate :

- (i) The thickness of each spoke, assuming that the spokes are securely built-in at each end; that the maximum bending stress in the spokes must not exceed $\pm 30,000$ lbs. per sq. in.; and that the torque transmitted from the flywheel rim to the flywheel shaft is $\pm 600,000$ lbs.-ins.
- (ii) The moment of inertia of the equivalent rigidly connected flywheel, assuming that the moment of inertia of the elastically connected flywheel rim is J .

Since the spokes are securely built in at each end and are of uniform rectangular cross-section they are of type I in Fig. 52.

(i) The maximum bending stress in each spoke is therefore

$$f = \frac{6 \cdot T \cdot L(3R - L)}{n \cdot a^2 \cdot b \cdot (6 \cdot R^2 - 6 \cdot R \cdot L + 2 \cdot L^2)} = \pm 30,000 \text{ lbs./sq. ins.,}$$

where T = applied torque = $\pm 600,000$ lbs.-ins.,

L = length of spoke = (30 ins. - 10 ins.) = 20 ins.,

R = radius to inside of rim = 30 ins.,

n = number of spokes = 8,

a = thickness of spokes in inches,

b = width of spokes in inches = 8 ins.

Hence,

$$a^2 = \frac{6 \times 600000 \times 20(3 \times 30 - 20)}{30000 \times 8 \times 8(6 \times 30^2 - 6 \times 30 \times 20 + 2 \times 20^2)},$$

i.e. $a = 1$ in.

(ii) The equivalent torsional rigidity of the spokes is

$$C = \frac{n \cdot a^2 \cdot b \cdot E(3 \cdot R^2 - 3 \cdot R \cdot L + L^2)}{3 \cdot L^3},$$

(see example I, Fig. 52),

$$\text{i.e. } C = \frac{8 \times 1^2 \times 8 \times 30000000(3 \times 30^2 - 3 \times 30 \times 20 + 20^2)}{3 \times 20^3}$$

$$= 104,000,000 \text{ lbs. ins./radian.}$$

Hence, from Equation (92),

$$J_s = \frac{J}{1 - \frac{F^2 \cdot J}{91 \cdot 2 \cdot C}}$$

$$= \frac{J}{1 - \frac{F^2 \cdot J}{950000000}} \text{ lbs.-ins. sec.}^2.$$

(Note.—Total resilience of spokes

$$= W = \frac{f^2 \cdot V \cdot n(3 - 3 \cdot K + K^2)}{6 \cdot E(3 - K)^2},$$

where $K = L/R = 20/30$,

V = volume of each spoke = $20 \times 8 \times 1 = 160$ cu. ins.

$$\text{Hence, } W = \frac{30000^2 \times 160 \times 8}{22 \cdot 6 \times 30000000} = 1 \cdot 33 \times 1280 = 1700 \text{ in.-lbs.,}$$

i.e. resilience = 1.33 in.-lbs. per cu. in. or 1700 in.-lbs. total.)

EXAMPLE 29.—Assuming that the generator mass in Table 1 is replaced by a flywheel rim connected to the shaft by eight alloy steel spokes of the dimensions given in the preceding example, calculate the moment of inertia of the flexibly-connected rim so that the one-node frequency is unaltered.

From the preceding example the moment of inertia of the equivalent rigidly connected mass is

$$J_e = \frac{J}{1 - \frac{F^2 \cdot J}{950000000}}$$

This must be equal to the moment of inertia of the generator mass in Table 1 if the one-node frequency is to remain unaltered, i.e. for a frequency of 2520 vibs./min.,

$$J_e = 23,500 \text{ lbs.-ins. sec.}^2.$$

$$\text{Hence, } 23500 = \frac{J}{1 - \frac{2520^2 J}{950000000}}$$

$$\text{or } J = 1,405 \text{ lbs.-ins. sec.}^2.$$

Note that the value of the two-node frequency with this flexibly connected flywheel rim is different from the value given in Table 2.

The amended value can be obtained by making a new frequency tabulation, using a value of 1405 lbs.-ins. sec.² for the moment of inertia of the generator mass, and a value,

$$C_e = \frac{C_1 \cdot C_2}{C_1 + C_2} \quad \text{for the stiffness of the section of shafting between no. 6 cylinder and the generator,}$$

where C_1 = actual stiffness of shafting between no. 6 cylinder and the generator

$$= 17.0 \times 10^7 \text{ lbs.-ins./radian (from column 1 of Table 1),}$$

C_2 = torsional stiffness of the flexible spokes

$$= 10.4 \times 10^7 \text{ lbs.-ins./radian,}$$

$$\text{i.e. } C_e = \left(\frac{17 \times 10.4}{17 + 10.4} \right) \times 10^7 = 6.45 \times 10^7 \text{ lbs.-ins./radian.}$$

EXAMPLE 30.—Calculate the torsional rigidity of a flexible coupling, assuming that the coupling is to be as flexible as possible, taking into account the following limitations in design:—

- (a) Coupling to be of the type which employs flexible spokes as the spring elements.
- (b) The flexible spokes to be integral with the hub.
- (c) The coupling and the mild steel shafts which it connects to be capable of transmitting a fluctuating torque of $\pm 10,000$ lbs.-ins., superimposed on a mean transmission torque of 5,000 lbs.-ins.
- (d) The outside diameter of the coupling not to exceed 12 ins.
- (e) The width of each spoke to be one-half the length of the spoke, and the shafts on which the coupling is mounted to be hollow, the inner diameter being one-half the outside diameter.

Diameter of Mild Steel Shafts.—From Table 21 the safe stress for mild steel in reversed torsion is ± 8000 lbs. per sq. in., assuming that the shafts are free from stress raisers. Since, however, in the present instance the keys or splines used for securing the two halves of the coupling to the shafts must be taken into account as stress raisers, a stress concentration factor of 2 will be assumed. The working stress is therefore ± 4000 lbs. per sq. in.

The following expression shows the general relationship between torque and shaft diameter:—

$$T = \pi \cdot D^3(1 - K^4) \cdot f_s / 16, \quad \dots \quad (124)$$

where $T =$ transmitted torque = $\pm 10,000$ lbs.-ins.,

$D =$ outside diameter of shaft in inches,

$d =$ inside diameter of shaft in inches,

$K = d/D = 1/2$ in this example,

$f_s =$ working stress = $\pm 4,000$ lbs. per sq. in.

Hence, $D^3 = 16 \cdot T / [\pi(1 - K^4)f_s]$.

For a solid shaft, $K = 0$, i.e. $D^3 = 16T / (\pi \cdot f_s) = 5 \cdot 1T / f_s$.

When $K = 1/2$, $D^3 = 5 \cdot 44T / f_s = 5 \cdot 44 \times 10,000 / 4000$,

or $D = 2 \cdot 38$ ins.

The shafts on which the coupling is mounted should therefore be about 2.4 ins. outside diameter \times 1.2 ins. bore.

The stress due to the mean transmission torque has been neglected because it has already been shown that a fluctuating stress of $\pm f_s$ can be safely superimposed on a steady stress of the same magnitude. In this example the steady stress is well below the fluctuating stress, viz. 2000 lbs. per sq. in. steady stress and ± 4000 lbs. per sq. in. fluctuating stress.

Dimensions of Spokes.—It will be assumed that the spokes are designed as cantilevers of rectangular cross-section, fixed at the hub and free at the rim, with uniform skin stress throughout, because this type gives the maximum specific resilience obtainable with any practicable form of spoke. It will also be assumed that the necessary variation of cross-section to give uniform skin stress is obtained by varying the thickness of the spoke and keeping the width constant, because this method gives a somewhat greater volume of spring material and therefore a somewhat greater total resilience than other methods of obtaining uniform skin stress.

The spokes are therefore of Type III in Fig. 52 for which the resilience per unit volume, from Table 20, is $f_b^2/(7.1E)$,

i.e. total resilience of coupling

$$= W = f_b^2 \cdot V \cdot n/(7.1E) \text{ (Type III, Fig. 52).}$$

For spring steel spokes, the permissible working stress in reversed bending, assuming that the radius at the root of each spoke is sufficient to avoid any severe stress concentration, is $\pm 50,000$ lbs. per sq. in., from Table 21.

$$\begin{aligned} \text{Hence, } W &= 50,000^2 \cdot V \cdot n/(7.1 \times 30,000,000) \\ &= 11.7V \cdot n \text{ ins.-lbs.} \end{aligned}$$

(*Note.*—This value is somewhat less than the value given in Table 22 because the skin stress in spokes of Type III in Fig. 52 is not exactly uniform throughout the beam.)

Let a = thickness of each spoke at root, in inches,
 b = width of each spoke, in inches,
 L = effective length of each spoke in inches = $(R - r)$,

- R = effective radius of spoke at rim in inches,
 r = effective radius of spoke at hub, in inches,
 $K = r/R$, i.e. $r = K \cdot R$,
 V = volume of material in each spoke, in cubic inches,
 n = number of spokes in coupling,
 $V_n = V \cdot n$ = total volume of material in spring elements
of coupling, in cubic inches.

Then, for a spoke of Type III in Fig. 52,

$$V = 2 \cdot a \cdot b \cdot L/3 = 2 \cdot a \cdot b(R - r)/3,$$

i.e. $V_n = 2 \cdot a \cdot b \cdot n(R - r)/3.$

It has already been mentioned that the radius at the roots of the spokes, when these are integral with the hub, must be sufficient to prevent concentration of stress at these points. The radius at the roots of the spokes should therefore be equal to the width of the spokes at that point, as shown at IV in Fig. 53.

This implies that the pitch of the spokes round the periphery of the hub at the effective radius r should be about $\pi \cdot a$ so that the maximum number of spokes which can be accommodated is

$$n = 2 \cdot r/a.$$

Hence, $V_n = 4 \cdot b \cdot r(R - r)/3 = 4 \cdot b \cdot R^2(K - K^2)/3.$

The volume of material in n spokes, and therefore the resilience of the whole coupling, is a maximum when $K = 1/2$,

i.e. $R = 2r$
and $V_{n \text{ max}} = b \cdot R^2/3$ cubic inches.

Since the maximum outside diameter of the coupling is limited to 12 ins., it will be assumed that the effective radius of the spokes at the rim of the coupling is $R = 5$ ins., which should allow ample margin for accommodating the tips of the spokes as shown at IV in Fig. 53.

Hence, the dimensions of the spokes are as follows:—

$$R = 5 \text{ ins.}; \quad r = R/2 = 2.5 \text{ ins.}; \quad L = (R - r) = 2.5 \text{ ins.};$$

and $n = 2 \cdot r/a = 5/a.$

The maximum stress in the spokes, from Example III, Fig. 52, is

$$f = 6.75 T \cdot L / (n \cdot a^2 \cdot b \cdot R),$$

where T = transmitted torque = $\pm 10,000$ lbs.-ins.,

L = length of spoke = 2.5 ins.,

n = number of spokes = 5/ a ,

a = thickness of spokes at root,

b = width of spokes at root = $L/2$ (specified) = 1.25 ins.,

R = effective radius of spokes at rim = 5 ins.,

f = permissible working stress = $\pm 50,000$ lbs. per sq. in. for spring steel spokes in reversed bending.

Hence,
$$50000 = \frac{6.75 \times 10000 \times 2.5}{5 \times 1.25 \times 5 \times a^2}$$

or
$$a = 0.108 \text{ in.},$$

and
$$n = 5/a = 46.$$

The spring elements of the coupling are therefore 46 spring steel spokes, 0.108 in. thick \times 1.25 ins. wide at the roots; 2.5 ins. long; 5 ins. effective radius at tip, and 2.5 ins. effective radius at hub.

Referring to Diagram IV in Fig. 53, the diameter of the hub at the bottom of the root radii of the spokes is

$$(5 - 2a) = 4.78 \text{ ins.}$$

The outside diameter of the mild steel shafts on which the coupling is mounted is 2.4 ins., so that there is ample margin for fixing the spoked member on its shaft.

Torsional Rigidity of Coupling.—The total volume of material in the coupling springs is

$$V \cdot n = 2 \cdot a \cdot b \cdot L \cdot n/3 = 2 \times 0.108 \times 1.25 \times 2.5 \times 46/3 \\ = 10.35 \text{ cu. ins.}$$

Hence, total resilience = $W = 11.7V \cdot n = 11.7 \times 10.35 = 121.0$ ins.-lbs.

Now strain energy = $W = T \cdot \theta/2,$

and torsional rigidity = $C = T/\theta.$

$$\text{Hence,} \quad W = \frac{T^2}{2C} \text{ or } C = \frac{T^2}{2W}, \quad \dots \quad (125)$$

where T = transmitted torque = 10,000 lbs.-ins.,
 W = total resilience = 121.0 ins.-lbs.,

$$\text{i.e.} \quad C = \frac{10000 \times 10000}{2 \times 121.0} = 413,000 \text{ lbs.-ins./radian.}$$

This value can be checked by means of the expression from example III of Fig. 52, viz.,

$$\begin{aligned} C &= n \cdot a^3 \cdot b \cdot E \cdot R^2 / (8.5 L^3) \\ &= \frac{46 \times 0.108^3 \times 1.25 \times 30000000 \times 5^2}{8.5 \times 2.5^3} \\ &= 410,000 \text{ lbs.-ins./radian.} \end{aligned}$$

The equivalent length of 2.4 ins. diameter solid shaft, i.e. of shaft the same diameter as the shafts on which the coupling is mounted, is given by the expression from example III of Fig. 52 as follows:—

$$\begin{aligned} L_e &= \frac{L^3 \cdot D^4}{3 \cdot n \cdot a^3 \cdot b \cdot R^2} = 3 \times \frac{2.5^3 \times 2.4^4}{46 \times 0.108^3 \times 1.25 \times 5^2} \\ &= 95 \text{ ins. of 2.4 ins. diameter solid bar.} \end{aligned}$$

It is of interest to note that an alloy steel torsion bar 1.5 ins. in diameter and 1.4 ins. long would transmit the same torque and have the same flexibility as the above coupling, assuming that this bar was free from discontinuities, so that the working stress of $\pm 15,000$ lbs. per sq. in. in reversed torsion given in Table 21 could be permitted. The weight of the torsion bar is about 7 lbs. compared with about 3 lbs. for the more highly stressed spring steel spokes of the flexible coupling. The total weight of the torsion bar assembly would, of course, be somewhat greater than 7 lbs., due to the provision of the necessary attachments to the input and output shafts, whilst the total weight of the flexible coupling would be considerably greater than that of the spokes alone. A detailed investigation would probably reveal that the total weight of the flexible coupling was at least twice that of the

torsion bar and its attachments. The principal objection to the torsion bar is the axial space required to accommodate it, whilst an advantage of the flexible coupling is that supplementary damping means can be provided more easily than in the case of a torsion bar, if this is required.

A further check on the torsional rigidity of the above flexible coupling is obtained by applying the general expression [Eqn. (122)] for the torsional rigidity of a coupling containing flexural spring elements carrying a uniform skin stress, viz.,

$$C = 3 \cdot E \cdot T^2 / (V \cdot n \cdot f_0^2), \quad \dots \quad (122)$$

i.e. in this example,

$$C = \frac{3 \times 3000000 \times 10000^2}{10 \cdot 35 \times 50000^2} = 348,000 \text{ lbs.-ins./radian.}$$

This is about 15 per cent. less than the value previously calculated, the discrepancy being due to slight lack of uniformity of skin stress in the shape of spoke chosen.

Flexible Couplings Employing Helical Springs.—

Diagrams I and II in Fig. 53 show two types of flexible coupling in which helical springs are the flexible elements. Diagram I is an arrangement employing compression springs, whilst Diagram II employs tension springs. The arrangement employing compression springs is often used as a spring drive in geared systems, the teeth of the gearwheel being cut on the periphery of the outer member. It is also used as a damped and tuned vibration absorber, the damping means being either solid friction, in which case suitable frictional surfaces are introduced between the outer and the inner members, or hydraulic friction, in which case the spring pockets are made fluid tight and are filled with oil which is forced through small openings between the pockets, when relative motion occurs between the inner and outer members, due to vibration (see Figs. 176 and 201).

In the arrangement employing tension springs, special care must be taken to permit absolutely free rotation of the end connections of the springs on their anchoring pins when relative motion occurs between the input and output sides of

the coupling. If this is not done there is serious danger of breaking the end coils of the springs.

The type of end connection shown at II in Fig. 53 is probably the most satisfactory. Two or three coils are wound tightly at each end of the spring and a screw thread is cut on the shank of the end connections. This thread is the same size and pitch as the closed end coils of the spring and is machined so that it is a tight fit when screwed into the spring. Care must be taken to remove all sharp corners. The inch rate of the spring can be controlled to a slight extent by the amount the end connections are screwed into the spring, and this is sometimes a useful method of correcting slight differences in rate between one spring and another. It should be noted, however, that whilst it is an easy matter to screw the end connections into the spring, it is not so easy to unscrew them, due to automatic tightening of the coils on the shank.

Compression springs are probably to be preferred, since it is difficult to provide really satisfactory end connections for tension springs without sacrificing a good deal of the space which would otherwise be occupied by the spring members.

In designing the springs it is necessary to make sure that there is sufficient initial tension to avoid completely unloading the springs on one side of each arm when the coupling is transmitting the designed maximum steady torque plus the maximum fluctuating torque.

The same remark applies to the initial compression of the springs in the arrangement shown at I in Fig. 53.

The strength and flexibility of couplings employing helical springs in tension or compression can be calculated as follows :—

Let T = total torque transmitted by coupling for a deflection α

$$= P \cdot n \cdot R, \text{ lbs.-ins.},$$

P = load acting along axis of each spring in lbs.,

k = inch rate of each spring, i.e. the load per unit deflection of spring, in lbs. per in.

$$= P/\alpha,$$

n = number of springs,

α = linear deflection of each spring in inches,

R = radius from axis of rotation of shaft to pitch circle radius of springs (see Fig. 53),

θ = angular deflection between input and output sides of coupling in radians.

Then $\theta = \alpha/R$, and $C =$ torsional rigidity of coupling $= T/\theta$,
i.e. $C = P \cdot n \cdot R^2/\alpha = k \cdot n \cdot R^2$ lbs.-ins. per radian. (126)

The maximum fluctuating stress in the spring can be calculated from the following expression :—

$$f_s = \frac{2.55 \cdot P \cdot D}{d^3} \text{ lbs. per sq. in.} \quad (127)$$

where $\pm P =$ maximum fluctuating load on each spring in lbs.
 $= T/(n \cdot R)$,

$D =$ mean coil diameter of spring in inches,

$d =$ diameter of spring wire in inches.

To this must be added the steady stress due to the initial tension or compression which is necessary to ensure that the springs are never completely unloaded under the most severe vibratory movements which the coupling handles. This implies that the initial load in each spring must be at least equal to the fluctuating load plus the steady mean load.

In determining the safe load on the coupling under completely reversed torsion it is necessary to take into account any discontinuities which can act as stress raisers. For example, the above expression for the maximum stress is torsional stress only, and does not take into account the effect of the ratio of wire size to mean coil diameter in introducing additional stresses which increase as this ratio diminishes.

This effect can be taken into account by multiplying the stress given by Equation (127) by the following factor :—

$$Y = \frac{(U + 1.5)}{U}, \quad (128)$$

where

$$U = D/d.$$

This expression agrees very well with the formula developed by Mr. A. M. Wahl, and shows that when $D/d = 5$ there is a 30 per cent. increase in stress. The mean coil diameter

should, if possible, be not less than eight times the diameter of the wire.

The inch rate of the spring can be calculated from the following expression :—

$$k = P/\alpha = \frac{G \cdot d^4}{8 \cdot D^3 \cdot N} \text{ lbs. per inch.}, \quad (129)$$

where G = modulus of rigidity (see Table 21),
 N = number of free coils = (total number of coils
 - 2), unless screwed end attachments are
 used.

EXAMPLE 31.—Calculate the torsional rigidity of a flexible coupling of the type shown at I in Fig. 53, assuming the following conditions :—

- (a) The pitch circle diameter of the springs to be 10 ins.
 (b) The coupling to transmit a fluctuating torque of $\pm 10,000$ lbs.-ins., superimposed on a mean transmission torque of 5000 lbs.-ins.

Spring Loads.—The total load on n springs is made up as follows :—

$$\begin{aligned} P_1 &= \text{load due to fluctuating torque} = \pm 10,000/5 \\ &= \pm 2000 \text{ lbs.}, \\ P_2 &= \text{load due to mean transmission torque} = 5000/5 \\ &= 1000 \text{ lbs.}, \end{aligned}$$

where the + sign indicates compression.

To avoid completely unloading one of the springs of each pair the initial load on the springs must be at least equal to $(P_1 + P_2)$,

$$\text{i.e.} \quad P_3 = (2000 + 1000) = 3000 \text{ lbs.}$$

Thus the initial compression in each spring to avoid unloading one of each pair completely must be $3000/n$ lbs.

The maximum total load on any spring is therefore

$$P = 2P_3/n = 2 \times 3000/n = + 6000/n, \text{ to zero.}$$

(Actually the initial compression of the springs should provide a small margin over the actual minimum required to avoid

complete unloading. It will be assumed therefore that the maximum load on any spring varies from $+6100/n$ to $+100/n$ for reversible drives.

Note that the loads are $6100/n$ to $2100/n$ per spring for the leading springs and $2100/n$ to $100/n$ per spring for the trailing springs in the case of non-reversible drives.)

Spring Dimensions.—Assuming that the springs are made of 90 tons per sq. in. spring steel and that the mean coil diameter D is four times the wire diameter d , the stress is given by Equation (127),

$$\begin{aligned} \text{i.e.} \quad f_s &= 2.55 \cdot P \cdot D/d^3, \\ \text{where} \quad f_s &= \text{permissible working stress,} \\ P &= \text{maximum load on each spring} \\ &= 6100/n, \\ D &= \text{mean coil diameter} = 4 \cdot d, \\ d &= \text{wire diameter.} \end{aligned}$$

Assuming that there are no stress raisers, the maximum permissible shear stress is given by Equation (123),

$$\text{i.e.} \quad f_s = f_t(1.85 + 1.2x + 0.35x^2).$$

Note.—In this case it is not permissible to design the spring from a consideration of the fluctuating load only, because the steady load (i.e. the sum of the initial plus mean transmission load) is greater than one-half the range of the fluctuating load

$$\begin{aligned} \text{where } f_t &= \text{fatigue limit for completely reversed torsion} \\ &= \pm 90/4 \\ &= \pm 22.5 \text{ tons per sq. in. for 90 tons per sq. in.} \\ &\quad \text{spring steel,} \\ x &= \text{minimum stress/maximum stress} = 100/6100 = \frac{1}{61}. \end{aligned}$$

$$\text{Hence, } f_s = 22.5 (1.85 + 1.2/61 + 0.35/3721) = 42 \text{ tons per sq. in.}$$

The appropriate allowance for secondary stress effects is given by Equation (128), viz.,

$$Y = (U \div 1.5) / U,$$

where $U = D/d = 4.$

$$\text{Hence, } Y = (4 \div 1.5) / 4 = 1.375.$$

Thus the maximum permissible equivalent static stress is $42 \times 1.375 = 30.5$ tons per sq. in.

A safe working stress of 60,000 lbs. per sq. in. will therefore be assumed, and since in a reversible drive the load on each spring varies from $6100/n$ to $100n$, the corresponding stress variation is from 60,000 to 980 lbs. per sq. in.

The number of springs which can be accommodated depends on the length of the circumference of the pitch circle

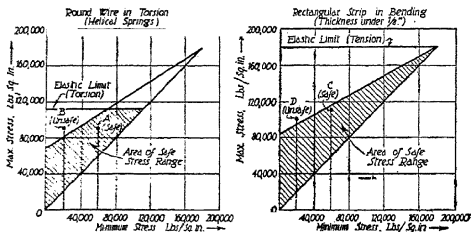


FIG. 54.—Safe stress ranges for carbon steel springs.
(Barnes-Gibson-Faymond, U.S.A.)

round which the springs are spaced. It is necessary to make one or two trial calculations before the best compromise is obtained, since there are an indefinite number of spring combinations which can be utilised. As the springs are arranged in pairs there must be an even number.

The permissible stress ranges in steel springs subjected to fluctuating loads are given in a paper by F. P. Zimmerli, entitled, "Permissible Stress Range for Small Helical Springs" (*Engineering Research Bulletin*, No. 26, July, 1934, University of Michigan). Fig. 54 shows representative diagrams for carbon steel springs in torsion and in bending.

The abscissæ and ordinates of these diagrams represent

the minimum and maximum stresses in the spring respectively, and it is essential that any point plotted from given values of minimum and maximum stress should lie within the shaded areas for satisfactory spring life. Thus, in Fig. 54, point A, representing a minimum stress of 60,000 and a maximum stress of 90,000 lbs. per sq. in. is a safe design; whilst point B, representing a minimum stress of 20,000 and the same maximum stress of 90,000 lbs. per sq. in. is an unsafe design.

Similarly, point C on the diagram for steel strip springs subjected to bending is safe, whilst point D is unsafe.

In the present example the springs are subjected to a minimum stress of 980 and a maximum stress of 60,000 lbs. per sq. in. in torsion. Fig. 54 shows that these are safe values.

In the present example it will be assumed that there are 8 springs and that the width of the abutments on the pitch line is about 1 in. The length on the pitch line which is available for accommodating each spring is therefore

$$\text{Circumference of 10 ins. diameter pitch circle} = 31.416 \text{ ins.}$$

$$\text{Space occupied by 8 abutments, each 1 in. wide on pitch line} = 8 \times 1 = 8 \text{ ins.}$$

$$\text{Length on pitch line per spring} = (31.416 - 8)/8 = 2.92 \text{ ins.,}$$

i.e. it will be assumed that each spring is 2.75 ins. long when it is in position in the coupling and when the coupling is not transmitting torque.

The maximum compressive load P on each spring is therefore

$$P = 6100/n = 6100/8 = 763 \text{ lbs.,}$$

and, from Equation (127),

$$60,000 = 2.55 \times 763 \times 4 \times d/d^3 = 7780/d^2,$$

$$\text{or } d^2 = 0.13,$$

$$d = 0.36 \text{ in.,}$$

$$D = 4 \cdot d = 4 \times 0.36 = 1.44 \text{ ins.}$$

Assuming a solid length of 2.25 ins. for each spring, i.e. allowing 0.5 in. for compression of each spring under the

transmitted torques, the maximum permissible number of coils is $2.25 \cdot 0.36 = 6.25$, say 6.

The number of free coils in each spring is therefore

$$N = (6 - 2) = 4 \text{ free coils.}$$

The inch rate is given by Equation (129), viz.,

$$k = \frac{G \cdot d^4}{8 \cdot D^3 \cdot N} = \frac{11500000 \times 0.36^4}{8 \times 1.44^3 \times 4} \\ = 2020 \text{ lbs. per in.}$$

The dimensions of each spring are therefore as follows :—

- d = diameter of wire = 0.36 in.,
 D = mean coil diameter = 1.44 ins.,
 N = number of free coils = 4 (i.e. total number of coils = 6),
 k = inch rate = 2020 lbs. per inch,
 P = safe load = 763 lbs. per spring.

Initial load = $3100/n = 3100/8 = 388$ lbs. per spring.

Initial compression = $388/2020 = 0.192$ in.

Free length = $(2.75 + 0.19) = 2.94$ ins.

Maximum load = $6100/n = 6100/8 = 763$ lbs. per spring.

Total compression = $763/2020 = 0.38$ in.

Minimum compressed length = $(2.94 - 0.38) = 2.56$ ins.

Solid length = $6 \times 0.36 = 2.16$ ins.

Since the solid length is less than the minimum compressed length the spring is suitable for the specified duty.

Torsional Rigidity of Coupling.—This is given by Equation (126), viz.,

$$C = k \cdot n \cdot R^2 \text{ lbs.-ins. per radian,}$$

where k = inch rate per spring = 2020 lbs. per inch,

n = number of springs in coupling = 8,

R = pitch circle radius of springs = 5 ins.,

i.e. $C = 2020 \times 8 \times 25 = 404,000$ lbs.-ins. per radian.

Check by Resilience Method.

The total resilience of the spring elements of the coupling is

$$W = f_s^2 \cdot V / (4 \cdot G) \text{ (see Table 20),}$$

where f_s = maximum stress due to *fluctuating* portion of the torque transmitted by the coupling.

The load per spring due to the fluctuating part of the torque is

$$P = \pm 10,000/(8 \times 5) = \pm 250 \text{ lbs.}$$

The stress in the spring due to the maximum load of 763 lbs. is 60,000 lbs. per sq. in.

Hence the stress due to the fluctuating part of the torque is

$$f_s = \pm 60,000 \times 250/763 = \pm 19,650 \text{ lbs. per sq. in.}$$

V = volume of active material in the springs

$$= \frac{\pi \cdot d^2}{4} \cdot \pi \cdot N \cdot D \cdot n = 2.47 \times 0.36^2 \times 4 \times 1.44 \times 8 \\ = 14.75 \text{ cu. ins.}$$

$$\text{Hence, } W = \frac{19650^2 \times 14.75}{4 \times 11500000} = 123.5 \text{ in.-lbs.}$$

Also, from Equation (125),

$$C = T^2/(2 \cdot W),$$

where T = fluctuating portion of transmitted torque

$$= \pm 10,000 \text{ lbs.-ins.,}$$

$$\text{i.e. } C = 10,000^2/(2 \times 123.5) = 404,000 \text{ lbs.-ins. per radian,}$$

which agrees with the value previously obtained.

This torsional rigidity is practically the same as that of the spoked coupling of Example 30.

If allowance is made for the necessary inactive end coils of each of the helical springs, the total weight of spring material in the present coupling is about 6 lbs. compared with only 3 lbs. for the spoked coupling. The weight of a coupling employing helical springs of the type shown at I in Fig. 53 is therefore, in general, greater than that of a spoked coupling having the same total flexibility, despite the fact that the resilience per unit volume and weight of solid cylindrical torsion members is practically the same as that of flexural members with uniform skin stress everywhere, as shown in Table 22.

This is because the stress in the helical springs of couplings of Type I, Fig. 53, is considerably below the maximum permissible stress due to the necessity for providing sufficient

initial compression in all the springs to avoid completely unloading one spring of each pair when the coupling is transmitting fluctuating torques. If no initial compression were provided only one-half the total number of springs would be effective, so that the resilience of the active material and the torsional rigidity of the coupling as a whole would be halved. Moreover, a coupling of this type without initial compression of the spring members is an impracticable arrangement.

M.A.N. Sleeve Spring Coupling.—The coupling shown at III in Fig. 53 was developed by the M.A.N. works for use in damping torsional vibrations. This coupling consists of a number of packets of sleeve springs, one of which is shown in detail in Fig. 53.

Each packet contains a number of neatly fitting steel sleeves, with a slot cut through the whole assembly so that the spring element comprises a number of C-springs in parallel. Maximum resilience is obtained by grading the thickness of the sleeves so that the stress is nearly constant at all points. A cylindrical member is accommodated within the innermost sleeve, and this member is provided with a tongue piece which is keyed into the hub and serves to prevent rotation of the spring packets as a whole, and also to limit the deflection of the springs, thus preventing over-stressing.

The cylindrical centre piece introduces a certain amount of non-linearity because the spring packet gradually contacts this member as the applied load increases. There is also an appreciable amount of damping due to inter-sleeve friction.

The torsional rigidity of a coupling of this type can be calculated as follows:—

Referring to the loading diagram for one sleeve shown at III in Fig. 53,

- let T = torque transmitted by coupling, in lbs.-ins.,
 N = number of spring packets,
 R = pitch circle radius of spring packets, in inches,
 P = tangential load on each spring packet = $T/(N \cdot R)$,
in lbs.,
 r = mean radius of any one sleeve, in inches,

- E = modulus of elasticity of material of sleeves, in lbs./sq. in.,
 I = moment of inertia of cross-section of one sleeve
 $= b \cdot t^3/12$, in ins.⁴ unit,
 b = length of sleeve, in inches,
 t = thickness of sleeve, in inches,
 y = tangential deflection at pitch circle of spring packets, in inches.

Then

$$\text{resilience of any one sleeve} = W = \frac{1}{2 \cdot E \cdot I} \int M_x^2 \cdot dx. \quad (117)$$

In this case $M_x = P \cdot r \cdot \sin \delta$,

$$\text{i.e.} \quad W = \frac{1}{2 \cdot E \cdot I} \int_0^{\pi} P^2 \cdot r^2 \cdot \sin^2 \delta \cdot dx,$$

but $x = r \cdot \delta$ or $\delta = x/r$.

$$\begin{aligned} \text{Hence,} \quad W &= \frac{P^2 \cdot r^2}{2 \cdot E \cdot I} \int_0^{\pi} \sin^2 x/r \cdot dx \\ &= \pi \cdot P^2 \cdot r^3 / (4 \cdot E \cdot I) \\ &= 3 \cdot \pi \cdot P^2 \cdot r^3 / (E \cdot b \cdot t^3). \quad (130) \end{aligned}$$

The strain energy is also given by the following expression :—

$$W = P \cdot y/2.$$

$$\text{Hence,} \quad y = 2W/P = 6 \cdot \pi \cdot P \cdot r^3 / (E \cdot b \cdot t^3). \quad (131)$$

If there are n sleeves in each spring packet, y is the common deflection at the pitch circle radius of all sleeves.

Let P_1, P_2, P_3 , etc., = the tangential load carried by the various sleeves of each pack, for example, load P_1 is the load carried by the outermost sleeve.

K_1, K_2, K_3 , etc., = the corresponding values of y/P ,
 i.e. $K_1 = y/P_1 = 6 \cdot \pi \cdot r^3 / (E \cdot b \cdot t^3)$.

Then P = total load on pack

$$\begin{aligned} &= (P_1 + P_2 + P_3 + \dots + P_n) \text{ lbs.} \\ &= y(1/K_1 + 1/K_2 + 1/K_3 + \dots + 1/K_n), \end{aligned}$$

whence $y = P / (1/K_1 + 1/K_2 + 1/K_3 + \dots + 1/K_n)$.

The angular deflection of the input side of the coupling relative to the output side is

$$\theta = y/R,$$

i.e. $C = \text{torsional rigidity of coupling} = T/\theta = T \cdot R/y$.

Stress in Spring Sleeves.

Let f_1, f_2, \dots, f_n , etc., = bending stresses in the various sleeves of each pack.

$$\text{Then} \quad f_n = 6 \cdot P_n \cdot r_n / (b \cdot t_n^2). \quad \dots \quad (132)$$

Since the tangential deflection at the pitch line for the whole spring pack is also the tangential deflection for each sleeve of the pack, the following relationship is obtained from Equation (131):—

$$\begin{aligned} E \cdot b \cdot y/6 \cdot \pi &= P_1 \cdot r_1^3/t_1^3 = P_2 \cdot r_2^3/t_2^3 \\ &= P_3 \cdot r_3^3/t_3^3 = \dots = P_n \cdot r_n^3/t_n^3. \end{aligned}$$

Also, since for maximum resilience the same stress must occur in each sleeve, the following relationship is obtained from Equation (132):—

$$\begin{aligned} b \cdot f/6 &= P_1 \cdot r_1/t_1^2 = P_2 \cdot r_2/t_2^2 \\ &= P_3 \cdot r_3/t_3^2 = \dots = P_n \cdot r_n/t_n^2. \end{aligned}$$

Combining these results,

$$t_2/t_1 = r_2^2/r_1^2 \text{ or } t_n/t_{(n-1)} = r_n^2/r_{(n-1)}^2, \quad \dots \quad (133)$$

$$\text{and} \quad P_2/P_1 = r_2^3/r_1^3 \text{ or } P_n/P_{(n-1)} = r_n^3/r_{(n-1)}^3, \quad \dots \quad (134)$$

i.e. the thicknesses of consecutive sleeves are proportional to the squares of the mean radii of the sleeves, and the tangential loads at the pitch lines of consecutive sleeves are proportional to the cube of the mean radii of the sleeves.

The selection of the best combination of sleeves is largely a matter for trial and error, but this process is facilitated by making the following simplifying assumptions for the first attempt.

It has already been shown that $t_2/t_1 = r_2^2/r_1^2$, and, since the sleeves fit snugly inside one another,

$$r_2 = r_1 - (t_1 + t_2)/2,$$

$$\text{i.e.} \quad t_2 = t_1 \left(\frac{r_1 - 0.5(t_1 + t_2)}{r_1} \right)^2.$$

If it is assumed that $t_2 = t_1$, and that higher powers of t can be neglected, the above expression reduces to

$$\begin{aligned} t_2 &= t_1(1 - 2 \cdot t_1/r_1), \\ \text{and } t_3 &= t_2(1 - 2 \cdot t_2/r_2), \\ t_n &= t_{n-1}(1 - 2 \cdot t_{n-1}/r_{n-1}). \end{aligned} \quad (135)$$

Also, for correct fitting of sleeves,

$$\begin{aligned} r_2 &= r_1 - 0.5(t_1 + t_2), \\ r_3 &= r_2 - 0.5(t_2 + t_3), \\ r_n &= r_{n-1} - 0.5(t_{n-1} + t_n), \end{aligned} \quad (136)$$

where r_1 and t_1 are the mean radius and thickness of the outermost sleeve.

Example 32 shows the application of the above methods to the design of a sleeve spring coupling.

EXAMPLE 32.—Calculate the torsional rigidity and load-carrying capacity of a spring sleeve coupling to fulfil the following specification :—

Pitch circle of spring packs	= $3\frac{1}{2}$ ins. radius,
Bore of housing of spring packs	= 2.75 ins.,
Number of sleeves per pack	= 6,
Number of packs	= 6,
Width of sleeves	= 2.0 ins.,
Thickness of outermost sleeve	= 0.100 in.

Since the bore of the housing for each pack is 2.75 ins. and the outermost sleeve is 0.100 in. thick, the mean radius of the outermost sleeve is (1.375 ins. - 0.050 in.) = 1.325 ins.,

i.e. $r_1 = 1.325$ ins.; and $t_1 = 0.100$ in.

The approximate dimensions of the remaining sleeves can be determined by applying Equations (135) and (136), as shown in the following tabulation :—

For example,

$$\begin{aligned} t_2 &= t_1(1 - 2 \cdot t_1/r_1) = 0.100(1 - 2 \times 0.100/1.325) \\ &= 0.085 \text{ in.,} \end{aligned}$$

$$\begin{aligned} \text{and } r_2 &= r_1 - 0.5(t_1 + t_2) = 1.325 - 0.5(0.100 + 0.085) \\ &= 1.233 \text{ ins.} \end{aligned}$$

The value of t_2 obtained by this method differs from the true value as follows:—

true value of $t_2 = t_1 \cdot r_2^2/r_1^2 = 0.100(1.233/1.325)^2 = 0.087$ in.,
or, in general, $t_n = t_{n-1}(r_n/r_{n-1})^2$.

The correct dimensions of the various sleeves can therefore be quickly determined from the approximate dimensions in columns 2 and 3 of the following table by applying the above equation. The correct dimensions are given in columns 4 and 5 of the table:—

Sleeve No.	Approximate Dimensions.		Corrected Dimensions.		Permissible Load on Sleeve.	Deflection Constants.
	r .	t .	r .	t .	P_n .	$1/K_n$.
1	1.325 ins.	0.100 in.	1.325 ins.	0.100 in.	214 lbs.	1370
2	1.233	0.085	1.232	0.087	174	1120
3	1.154	0.073	1.151	0.076	142	910
4	1.086	0.064	1.080	0.067	118	760
5	1.026	0.056	1.017	0.059	97	620
6	0.973	0.050	0.961	0.053	83	530
					$P=8281$ lbs.	$1/K=5310$

A consideration of the action of these sleeve springs shows that the stress in any fibre is always uni-directional, even when the applied torque on the coupling reverses. The greatest stress range occurs, therefore, in couplings fitted to reversible drives, in which case the minimum stress is zero. The safe stress range for rectangular strip in bending is given in Fig. 54, and for zero minimum stress the permissible maximum stress is 85,000 lbs. per sq. in.

The sixth column of the above table shows the maximum permissible load on each sleeve and is obtained from Equation (132), using a working stress of 85,000 lbs. per sq. in.

Thus, for the outermost sleeve, where $r = 1.325$ ins., $t = 0.100$ in., and $b = 2.0$ ins.,

$$P = b \cdot t^2 \cdot f / (6 \cdot r), \text{ from Equation (132),}$$

$$\text{i.e. } P_1 = 2.0 \times 0.100^2 \times 85,000 / (6 \times 1.325) = 214 \text{ lbs.}$$

The total maximum working load for all sleeves in one pack is the sum of the values in column 6 of the foregoing table, namely, 828 lbs.,

$$\text{i.e. } T = \text{maximum working torque for coupling} = 828 \times 6 \times 3.5 \\ \text{(6 packs each containing 6 sleeves at 3.5 ins. radius)} = 17,300 \text{ lbs.-ins.}$$

Column 7 of the foregoing table gives the values of $1/K$ for the various sleeves. As already shown, the common tangential deflection at the pitch circle of the spring packs is

$$y = P/(1/K) = 828/5310 = 0.156 \text{ in.},$$

and the torsional rigidity of the whole coupling is

$$C = T \cdot R/y, \text{ where } R \text{ is the pitch radius of the spring packs,} \\ = 17,300 \times 3.5/0.156 = 390,000 \text{ lbs.-ins. per radian.}$$

The angular deflection between the input and output shafts when the coupling is transmitting a torque of 17,300 lbs.-ins. is therefore

$$\theta = 17,300/390,000 = 0.0444 \text{ radian} \\ = 2.54^\circ.$$

The deflection limiting central piece should therefore be designed to permit a deflection of $\pm 2.5^\circ$ so that a torque of 17,300 lbs.-ins. can be accommodated in either direction and to ensure that the maximum stress range in the spring elements does not exceed the permissible value of 85,000 lbs. per sq. in.

Thus the maximum capacity of this coupling is $\pm 17,300$ lbs.-ins., and this can be made up of a fluctuating torque superimposed on a steady transmitted torque, provided the maximum value of the combined torque does not exceed the limit set by the stop piece. For example, a fluctuating torque of ± 8650 lbs.-ins. could be superimposed on a steady torque of 8650 lbs.-ins., in which case the maximum combined torque would be 17,300 lbs.-ins., whilst the minimum combined torque would be zero.

The deflection limiting members should be hardened on the surfaces which contact the ends of the spring sleeves, and

the sleeves themselves should be a neat sliding fit within one another (diametral clearance 0.002 in. to 0.004 in.).

The spring packs should be fitted into their bores with an initial deflection of about 0.008 in., i.e. the bores of the spring pack housing should be about 0.008 in. less in diameter than the free outside diameter of the outermost sleeve of the spring pack assembly.

This initial deflection provides sufficient pre-loading to eliminate back-lash, which is desirable when the coupling has to transmit torque in either direction.

The sleeve spring coupling of Example 32 has approximately the same load carrying capacity and the same torsional rigidity as the spoked coupling of Example 30, and the helical spring coupling of Example 31, i.e. the capacity of the couplings in Examples 30 and 31 is a fluctuating torque of $\pm 10,000$ lbs.-ins. superimposed on a steady torque of 5000 lbs.-ins. In this example, although the maximum fluctuating torque which could be superimposed on a steady torque of 5000 lbs.-ins. is $\pm 12,300$ lbs.-ins. it would be advisable to restrict the fluctuating portion to a value somewhere in the region of $\pm 10,000$ lbs.-ins. to avoid continuous hammering on the central stop piece and leave a reasonable margin for occasional overloads.

The weight of the spring material in the sleeve spring coupling is, however, 13 lbs., compared with 3 lbs. for the spoked coupling and 6 lbs. for the helical spring coupling. The sleeve spring coupling is therefore, in general, heavier than a coupling employing helical springs of the type shown at I in Fig. 53. This is mainly due to the somewhat large proportion of unstressed spring material which must be provided to take the spring reactions in the hub member (see Diagram III of Fig. 53).

Spring Plate Couplings.—Fig. 55 shows a flexible coupling in which the torque is transmitted through a number of spring steel plates accommodated in slots cut in the coupling flanges.

The torsional rigidity of this coupling is determined as follows:—

- Let R = pitch radius of flexible plates, in inches,
 n = number of plates,
 L = effective span of one plate, considered as a beam fixed at the ends, in inches,
 y = deflection of one end of the plate relative to the other end, in inches,
 P = reaction at each end of plate for a deflection y , in lbs.,
 I = moment of inertia of cross-section of one plate, about neutral axis, in inches⁴ units,
 E = modulus of elasticity, in lbs. per sq. in.

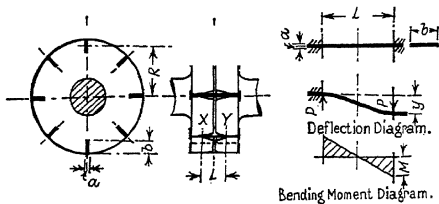


FIG. 55.—Flexible coupling.

Then, applying the equations already given for the spokes of a flexibly connected flywheel rim,

$$P = \frac{12E \cdot I \cdot y}{L^3} \quad \text{or} \quad y = \frac{P \cdot L^3}{12E \cdot I}$$

$$M_b = \frac{6E \cdot I \cdot y}{L^2} = \frac{12E \cdot I \cdot x \cdot y}{L^3}$$

$$\delta = \frac{y}{L^2} \left[3x^2 - \frac{2x^3}{L} \right]$$

The angular deflection is therefore

$$\theta = \frac{y}{R} = \frac{P \cdot L^3}{12E \cdot I \cdot R} \text{ radians.}$$

The total torque transmitted for a deflection y is

$$T = P \cdot R \cdot n \text{ lbs.-ins.}$$

Hence, the torsional rigidity of the coupling is

$$C = \frac{T}{\theta} = \frac{12P \cdot R \cdot n \cdot E \cdot I \cdot R}{P \cdot L^3} = \frac{12E \cdot I \cdot n \cdot R^2}{L^3}. \quad (137)$$

For steel plates of rectangular cross-section

$$E = 30,000,000 \text{ lbs. per sq. in.},$$

$$I = \frac{a^3 \cdot b}{12}$$

$$\text{Hence, } C = \frac{30000000 a^3 \cdot b \cdot n \cdot R^2}{L^3} \text{ lbs.-ins./radian.} \quad (138)$$

The equivalent length of shaft of diameter D is obtained as follows:—

Let L_e = equivalent length of shaft of diameter D . Then torsional rigidity of equivalent shaft is

$$C = \frac{T}{\theta} = \frac{G \cdot I_p}{L_e} = \frac{\pi \cdot D^4 \cdot G}{32L_e},$$

and, assuming $G = 12,000,000$ lbs. per sq. in. for steel,

$$C = \frac{1177000 D^4}{L_e},$$

$$\text{i.e. } \frac{1177000 D^4}{L_e} = \frac{30000000 a^3 \cdot b \cdot n \cdot R^2}{L^3}.$$

$$\text{Whence, } L_e = \frac{D^4 \cdot L^3}{25.5 a^3 \cdot b \cdot n \cdot R^2} \text{ ins.} \quad (139)$$

Stress in Plates.—The maximum bending stress is the same as already determined for the spokes of a flexibly connected flywheel rim, viz.,

$$f_{\max} = \frac{P \cdot L}{2 \cdot Z},$$

i.e. for rectangular steel plates

$$f_{\max} = \frac{3P \cdot L}{a^2 b} \text{ lbs. per sq. in.}$$

In the present case the torque transmitted by the coupling is

$$T = P \cdot R \cdot n, \quad \text{i.e. } P = \frac{T}{R \cdot n}.$$

Hence, $f_{\max} = \frac{3 \cdot T \cdot L}{a^2 \cdot b \cdot R \cdot n}$ lbs. per sq. in. . . . (140)

The maximum stress should not exceed the values given in Table 21.

Instead of providing separate slots for each plate, several plates can be assembled in each pair of slots. This laminated construction provides a certain amount of inter-plate damping which might be useful in some cases.

EXAMPLE 33.—Calculate the dimensions of a flexible coupling for a $2\frac{1}{2}$ -in. diameter shaft, assuming that there are forty-eight spring steel plates of rectangular cross-section, $\frac{3}{4}$ -in. wide.

The pitch radius of the plates is 4 ins., and the stress in the plates must not exceed 50,000 lbs. per sq. in. when the shear stress in the shaft is 6000 lbs. per sq. in. The effective span is 2 ins.

Also calculate the length of $2\frac{1}{2}$ -in. diameter shaft having the same torsional rigidity as the coupling.

The torque transmitted by a $2\frac{1}{2}$ -in. diameter steel shaft for a maximum shear stress of 6000 lbs. per sq. in. is

$$\begin{aligned} M &= \frac{\pi}{16} \cdot D^3 \cdot f = \frac{3 \cdot 1416 \times 2 \cdot 5^3 \times 6000}{16} \\ &= 18,400 \text{ lbs.-ins.} \end{aligned}$$

The stress in the plates is

$$f_{\max} = \frac{3 \cdot M \cdot L}{a^2 \cdot b \cdot n \cdot R},$$

where $L = 2$ ins.; $b = 0.75$ in.; $n = 48$ $R = 4$ ins.;
and $f_{\max} = 50,000$ lbs. per sq. in.,

$$\text{i.e. } 50000 = \frac{3 \times 18400 \times 2}{a^2 \times 0.75 \times 48 \times 4}.$$

Whence, $a = 0.124$ in.

Equivalent length of $2\frac{1}{2}$ -in. diameter shaft is

$$L_e = \frac{D^4 \cdot L^3}{25.5 a^3 \cdot b \cdot n \cdot R^2} = \frac{2.5^4 \times 2^3}{25.5 \times 0.124^3 \times 0.75 \times 48 \times 4^2} \\ = 11.15 \text{ ins.}$$

Referring to Fig. 55, it will be seen that over the length of the effective span L the sides of the grooves in the coupling flanges are flared away from the plates to permit free deflection. In practice, the shape of the sides is such that when the coupling is transmitting the maximum permissible torque the plates are in contact with the sides of the grooves. The effective span of the plates is thus very small when overloads occur, thus preventing over-stressing the material. Incidentally, the alteration in the effective span when the torque becomes excessive produces a corresponding alteration of the torsional rigidity of the coupling. This alters the torsional vibration characteristics of the system, and enables critical speeds to be passed through safely.

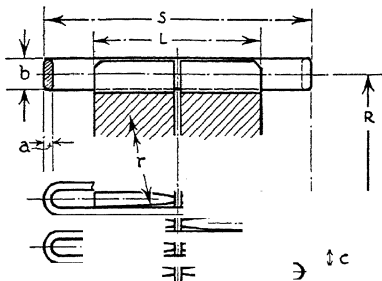
Bibby Flexible Coupling.—This coupling is described in Chapter 10, and is illustrated in Figs. 169, 170 and 171.

A fundamental and very important difference between the Bibby coupling and other couplings of the type shown in Fig. 55 is that the spring elements of the Bibby coupling consist of a series of plate springs or rungs which are connected together in grid formation as shown in Fig. 56.

This construction not only overcomes the very real difficulty of anchoring the ends of the plates in the construction shown in Fig. 55, but also provides considerably greater resilience and freedom to allow for mis-alignment of the input and output shafts.

Furthermore, the grid formation ensures that the rungs bear only on one side of the grooves for a given direction of torque loading. This avoids any tendency for the rungs to become locked in the grooves, which sometimes occurs with plain bars of the type shown in Fig. 55.

In one rather striking instance where a Bibby coupling had been operated for a long time with an abnormal amount of radial mis-alignment, and without lubrication, each rung



Normal Proportions: $S=36a$; $L=24a$; $b=4a$; $c=\pi a$;
 $n = \text{Number of Rungs} = \frac{2B}{a}$

FIG. 56.—Bibby spring coupling.

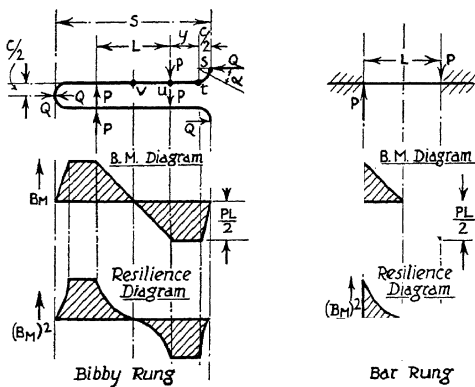


FIG. 57.—Resilience diagram.

had worn *on one side only* to about one-half its normal thickness before fracture occurred.

The forces acting on one element of the grid spring are shown in the left-hand diagrams of Fig. 57.

- Let P = tooth reactions, in lbs.,
 T = torque transmitted by coupling, in lbs.-ins.,
 R = pitch circle radius of rungs, in ins.,
 a = thickness of rung, in inches,
 b = width of rung, in inches,
 c = pitch of rungs, in inches,
 L = length over teeth, in inches,
 S = overall length of rungs, in inches,
 Q = end reactions on each rung, in lbs.,
 n = number of rungs,
 E = modulus of elasticity, in lbs. per sq. in.,
 f_b = maximum bending stress in rung, in lbs. per sq. in.,
 I = moment of inertia of cross-section of rung in ins.⁴
 $= b \cdot a^3/12$,
 M = bending moment on rung, in lbs.-ins.,
 W = resilience, in ins.-lbs.,
 r = radius of sides of teeth,
 C = torsional rigidity of coupling, in lbs.-ins./radian.

Then, referring to the top left-hand diagram in Fig. 57,

for equilibrium of each rung, $P \cdot L = Q \cdot c$,

$$\text{or } Q = P \cdot L/c.$$

It should be noted that there is no unbalanced force on each rung, and that the couple due to the tooth reactions P is balanced by the couple due to the end reactions Q . Furthermore, the end reactions Q of one rung are absorbed by the equal and opposite end reactions of the adjacent rung, so that there is no unbalanced *external* end reaction.

The maximum bending moment acting on each rung is

$$M = Q \cdot c/2 = P \cdot L/2.$$

Hence, the maximum bending stress in the rung is

$$f_b = M/Z, \quad \text{where } Z = b \cdot a^2/6,$$

for a rectangular cross-section,

i.e.
$$f_b = 3 \cdot P \cdot L / (b \cdot a^2).$$

Also, if T = torque transmitted by the coupling = $P \cdot R \cdot n$,

then,
$$f_b = \frac{3 \cdot T \cdot L}{R \cdot n \cdot b \cdot a^2} \quad \dots \quad (140a)$$

which is the same as the expression for the stress in the spring elements of the coupling shown in Fig. 55.

Equation (140a) gives the maximum bending stress which would occur in the rungs when transmitting a torque T , assuming that this torque is not sufficient to cause the rungs to contact the sides of the teeth, i.e. assuming that the distance between the tooth reactions L is not altered when the coupling is transmitting a torque T .

In practice, the maximum bending stress which can occur in the rungs is limited by the radius of the sides of the teeth, because, as the transmitted torque increases, the rungs come gradually into contact with the sides of the teeth until, finally, the reactions P occur close to the points of the teeth and the rungs are bent to the radius of curvature of the teeth.

If the radius of curvature of the teeth is r , the maximum possible bending stress in the rungs is therefore

$$f_b' = E \cdot a / (2 \cdot r) \quad \dots \quad (141)$$

Resilience of Coupling.—The shear and tensile resilience is small and will be neglected in the following treatment.

Consider one-half of a rung, $s-t-u-v$ in Fig. 57.

Bending in Portion s-t.—

$$W_1 = \frac{1}{2 \cdot E \cdot I} \int M_x^2 \cdot dx,$$

but
$$M_x = \frac{Q \cdot c}{2} \cdot \sin \alpha,$$

and
$$M = \text{maximum bending moment acting on rung} \\ = Q \cdot c/2.$$

$$\text{Hence, } W_1 = \frac{M^2}{2 \cdot E \cdot I} \int_0^{\pi \cdot c/4} \sin^2 \cdot \alpha \cdot dx.$$

$$\text{Also, } x = c \cdot \alpha/2, \text{ or } \alpha = 2x/c,$$

where x is the length of arc subtending angle α ,

$$\begin{aligned} \text{i.e. } W_1 &= \frac{M^2}{2 \cdot E \cdot I} \int_0^{\pi \cdot c/4} \sin^2 \frac{2x}{c} \cdot dx \\ &= \frac{M^2}{E \cdot I} \left(\frac{\pi \cdot c}{16} \right). \end{aligned}$$

Bending in Portion t-u.—Since in this case the bending moment is constant and equal to the maximum bending moment in the rung, viz. $M = Q \cdot c/2 = P \cdot L/2$,

$$W_2 = \frac{M^2}{2 \cdot E \cdot I} \int_0^y dx,$$

$$\text{i.e. } W_2 = \frac{M^2}{E \cdot I} \left(\frac{y}{2} \right),$$

$$\text{but } y = S/2 - L/2 - c/2 = (S - L - c)/2.$$

$$\text{Hence, } W_2 = \frac{M^2}{E \cdot I} \left(\frac{S - L - c}{4} \right).$$

Bending in Portion u-v.—Bending moment varies from zero to the maximum bending moment in the rung, viz. M ,

$$\text{i.e. } M_x = P \cdot x.$$

$$\begin{aligned} \text{Hence, } W_3 &= \frac{I}{2 \cdot E \cdot I} \int_0^{L/2} P^2 \cdot x^2 \cdot dx \\ &= \frac{P^2 \cdot L^3}{48 \cdot E \cdot I}, \end{aligned}$$

but $M = \text{maximum bending moment on rung} = P \cdot L/2$,

$$\text{i.e. } W_3 = \frac{M^2}{E \cdot I} \left(\frac{L}{12} \right).$$

Total Resilience.

$$\begin{aligned} \text{Resilience per half-rung} &= (W_1 + W_2 + W_3) \\ &= \frac{M^2}{E \cdot I} \left(\frac{\pi \cdot c}{16} + \frac{S - L - c}{4} + \frac{L}{12} \right). \end{aligned}$$

Hence, total resilience of n rungs,

$$W = \frac{M^2}{E \cdot I} \left(\frac{12S - 8L - 2 \cdot 57c}{48} \right) \cdot 2 \cdot n,$$

and since c is small compared with S and L the expression for total resilience of the coupling is

$$W = \frac{M^2}{6 \cdot E \cdot I} (3 \cdot S - 2 \cdot L) \cdot n. \quad (142)$$

**Torsional Rigidity of Coupling.*

From Equation (125), $C = T^2/(2W)$.

Now, $T =$ torque transmitted by coupling $= P \cdot R \cdot n$,

$M =$ maximum bending moment on each rung $= P \cdot L/2$.

Hence, $C =$ torsional rigidity of coupling

$$= \frac{12 \cdot n \cdot E \cdot I \cdot R^2}{L^2(3S - 2L)}, \text{ lbs.-ins./radian.} \quad (143)$$

The usual proportions of the rungs are given in Fig. 56, viz.,

$$S = 36a; \quad L = 24a; \quad b = 4a; \quad c = \pi \cdot a$$

[*Note:* c is the minimum pitch for forming the bends at the ends of the rungs. The height of the teeth can be reduced to $0.75 \cdot b$ where weight must be minimised.]

$$n \Rightarrow \text{maximum number of rungs permissible} = 2 \cdot R/a.$$

With these proportions Equation (143) reduces to

$$C = R^2 \cdot E/4320. \quad (144)$$

Also, with these proportions the expression for the maximum stress in each rung, Equation (140), reduces to

$$f_b = 9 \cdot T/(R^2 \cdot a). \quad (145)$$

Finally, since

$$T = C\theta,$$

$\theta =$ amplitude of angular deflection across coupling

$= T/C$ radian

$= 57.3T/C$ degrees,

* This treatment neglects back-lash between the rungs and grooves. A method of allowing for back-lash is given in Chapter 10.

where T and C are obtained from Equations (140) and (143) respectively.

The permissible working stress in the spring steel rungs of couplings of this type is $\pm 50,000$ lbs. per sq. in. for couplings which are used as resilient members only, and $\pm 25,000$ lbs. per sq. in. for couplings which may have to work under resonant conditions, for example, when they are used in the construction of torsional vibration detuning flywheels. The lower value of the permissible working stress allows for stress concentration at the bends at the ends of the rungs when the springs are subjected to reversed bending loads.

EXAMPLE 34.—Calculate the principal dimensions of a coupling of the type shown in Fig. 56, assuming that the transmitted torque is $\pm 10,000$ lbs.-ins., and the required torsional rigidity is 400,000 lbs.-ins. per radian. The rung proportions given in Fig. 56 may be used.

Torsional Rigidity.—From Equation (144),

$$\begin{aligned} C &= R^3 \cdot E/4320, \\ \text{i.e. } R^3 &= 400,000 \times 4320/30,000,000 \\ &= 57.5, \\ \text{or } R &= 3.86 \text{ ins.} \end{aligned}$$

Stress in each Rung.—Assuming that the coupling is not intended to run continuously under resonant conditions, a working stress of $\pm 50,000$ lbs. per sq. in. may be used.

From Equation (145)

$$\begin{aligned} f_b &= 9 \cdot T/(R^2 \cdot a). \\ \text{Hence, } a &= 9 \times 10,000/(50,000 \times 14.9) = 0.12 \text{ in.} \end{aligned}$$

The principal dimensions of the coupling are therefore

$$\begin{aligned} a &= \text{thickness of rung} = 0.12 \text{ in.} \\ b &= \text{width of rung} = 4 \cdot a = 0.48 \text{ in.} \\ S &= \text{overall length of rung} = 36 \cdot a = 4.32 \text{ ins.} \\ L &= \text{overall length of teeth} = 24 \cdot a = 2.88 \text{ ins.} \\ R &= \text{pitch circle radius of rungs} = 3.86 \text{ ins.} \\ n &= \text{number of rungs} = 2 \cdot R/a = 64. \end{aligned}$$

The total weight of the spring elements in the coupling is 4.5 lbs., which is very nearly the same weight as the spring elements of the much larger diameter spoked coupling of Example 30, and is much less than the weights of the helical spring and sleeve spring couplings of Examples 31 and 32. Since these alternative couplings have about the same torsional rigidity and are designed with a similar factor of safety it appears that the Bibby coupling is the most efficient of the types investigated.

It is of interest to compare the relative capacity for storing energy of the Bibby coupling with the coupling shown in Fig. 55.

The torsional rigidity of a coupling of the type shown in Fig. 55 having the same rung dimensions as the above Bibby coupling is given by Equation (137),

$$\begin{aligned} \text{i.e. } C &= 12 \cdot E \cdot I \cdot R^2 \cdot n/L^3 \\ &= 12 \times 30,000,000 \times 0.000069 \times 14.9 \times 64/23.8 \\ &= 1,000,000 \text{ lbs.-ins. per radian.} \end{aligned}$$

Thus the torsional rigidity of the coupling shown in Fig. 55 is two and a half times that of the Bibby coupling, in other words, the energy storing capacity, or resilience, of the Bibby coupling is two and a half times that of the coupling shown in Fig. 55. This is also illustrated by the comparative resilience diagrams in Fig. 57.

The weight of a coupling of the type shown in Fig. 55 will not be appreciably less than that of the Bibby coupling, because the active material in the overhanging ends of the Bibby rungs is replaced by the inactive material required to anchor the rungs in couplings of the type shown in Fig. 55.

It should also be noticed that the difficulty of anchoring the rungs, which is a real disadvantage in couplings of the type shown in Fig. 55, is completely overcome in the Bibby design.

Furthermore, by increasing the ratio S/L , the above comparison of resilience becomes even more favourable to the Bibby coupling.

In cases where the coupling is required to operate continuously in resonance the working stress should not exceed

$\pm 25,000$ lbs. per sq. in., as already mentioned. Where the space available for accommodating the coupling is such that the proportions of the rung given in Fig. 56 are unsuitable, Equations (140) and (143) can be used to determine the characteristics of a coupling having more suitably proportioned rungs.

Rubber-in-Shear Couplings.—In many cases the simplest and most effective solution of a torsional vibration problem is to tune the system so that no important resonant zone occurs within the operating speed range. Tuning is carried out by adjusting the inertia or the elastic characteristics of the oscillating system, so that the frequency is either raised to such a value that only high-order criticals of feeble intensity occur within the operating range, or so that the frequency is lowered to such a value that the operating range lies in the wide gap between two low-order resonant zones. In many cases a solution by increasing the natural frequency to a sufficiently high value is undesirable, because it entails a disproportionate increase in the scantlings of crankshafts and transmission shafts, which in turn means a large increase in overall weight of the power plant, a point of fundamental importance in transport and aeronautical applications.

Moreover, the trend towards higher operating speeds is tending to make such a solution increasingly difficult, in other words, speed increases are tending to do more than offset possible frequency increases.

There remains the possibility of a solution by lowering the frequency, and this implies either an increase in the polar moments of inertia of the oscillating members or an increase in the flexibilities of the elastic connections.

An increase in the polar moments of inertia is obviously undesirable, since it not only implies an appreciable increase in overall weight but also might introduce difficulties due to the introduction of critical zones, corresponding to higher modes of vibration, into the operating speed range. Provided sufficiently compact flexible elements are available, however, the alternative method, i.e. an increase in the flexibility of the elastic connections, can be successfully utilised. This method

avoids weight increases, and the flexible element can generally be introduced in such a manner that troublesome critical zones, due to other modes of vibration, are avoided.

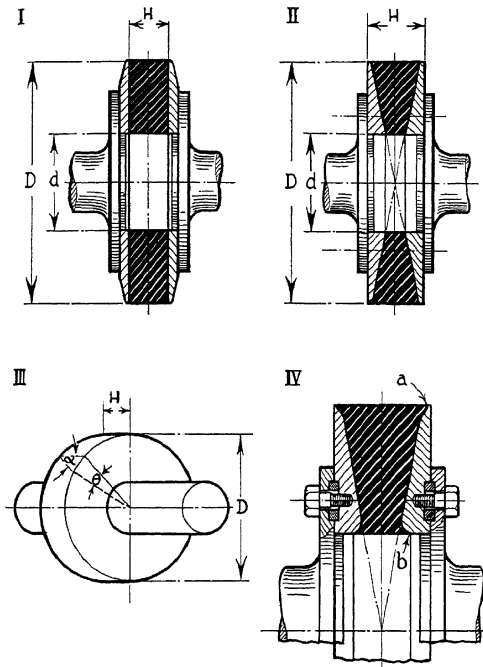


FIG. 58.—Rubber-in-shear couplings.

Various types of flexible couplings employing metallic spring elements have already been described, all of which have been successfully used in practice.

Their range of flexibility is somewhat limited, however, since they tend to become unduly heavy and bulky when large increases in the flexibility of the elastic connections is required.

An alternative type of flexible coupling, which can be built in a very compact form, is the rubber-in-shear type shown in Fig. 58. In its simplest form a rubber-in-shear coupling consists of a flat steel plate on the input side of which is bonded a disc of rubber. The other face of the rubber disc is bonded to a similar steel plate on the output side of the coupling.

The use of rubber as a structural material is a comparatively recent engineering development following the introduction of reliable bonding processes, so that the following notes relating to its physical and mechanical properties are of interest.

Pure rubber is almost never used for structural purposes. Structural rubber is invariably an "alloyed" material, i.e. the rubber is compounded with various other ingredients. When subjected to a temperature of 150° C. the physical properties of rubber compounds containing sulphur and certain other ingredients become stabilised. This process, which is probably the most important in rubber technology, is known as vulcanisation. During the vulcanising process the compound is usually confined within a metal mould and subjected to a pressure of several hundreds of pounds per square inch.

Rubber is practically incompressible, having a bulk modulus of 300,000 to 400,000 lbs. per sq. in., and will not deflect if fully confined. It is a non-conductor of electricity and a poor conductor of heat. It is not easily injured by castor or other vegetable oils, but mineral oils and solvents such as naphtha readily attack it. Flexible glyptal lacquer or plasticised shellac form a useful protective coating against oil drips.

Ageing of Rubber.—Rubber and its compounds are subject to a natural ageing effect which tends to stiffen the material, to reduce its elasticity, and render it brittle. Ageing of rubber is caused in two ways, by the continuation of the vulcanising process during use and by oxidation.

Anti-oxidants are available which stop the continuation of vulcanisation and restrain oxidation. Preservatives have little effect on the hardness of rubber compounds, although those of a resinous nature might have a slightly softening influence. Permanent hardening with age is a very slow process, and as a general rule aged vulcanised rubbers regain most of their initial softness when heated, for example, when boiled in water for a few minutes.

A point to be kept in mind when designing rubber components is that thin sections exposed to the air should be avoided since such sections are more easily destroyed by oxidation. In the case of thick sections it is only a small depth of rubber at the exposed surface that is affected.

The commencement of actual ageing can be considerably delayed by stopping the vulcanising process short of the optimum cure time. This leaves a percentage of free sulphur which must be absorbed before the optimum is reached and reversion can take place.

In some quarters this is considered to be the ideal state of vulcanisation with a view to securing good ageing properties. It should be borne in mind, however, that certain applications require the use of rubber compounds containing as small an amount of free sulphur as possible to avoid corrosion of parts in contact with the rubber, for example, rubber-lined stern tubes of ships.

Automobile experience indicates that rubber components can be expected to give from eight to nine years useful life. Other authorities state that a durability of from five to fifteen years can be expected, depending on the exact quality and the particular application. A reasonable estimate for design purposes is at least four years, with a possible maximum of eight years under favourable conditions.

Effect of Temperature on Rubber Compounds.—Since structural rubber compounds are obtained from substances manufactured at a temperature of 160° C. it is evident that the durability of the finished product cannot be guaranteed for steady temperatures exceeding 80° to 100° C. The rubber becomes softer under increasing temperature, the deformation

under a given load increases, and the hysteresis loss decreases. It is therefore important to protect rubber against rising temperature, and care should be taken in design to shape the components so that they are favourable for heat dissipation. It should be kept in mind that rubber is a poor conductor of heat and that whilst this is of advantage for heat insulation applications it hinders the flow of heat generated under excessive stress cycles and can be a source of serious temperature rise.

Safe practical temperature ranges for rubber compounds lie between -18° C. and $+50^{\circ}$ C. In exceptional circumstances steady temperatures as high as 80° C. can be tolerated with certain compounds, but this value should not be regarded as a figure to be used generally. The effect of low temperature is to harden the rubber and render it brittle. For example, at -75° C. rubber becomes so brittle that it breaks under a sharply applied blow.

This brittleness disappears again, however, when the temperature is restored to normal. Special rubber compounds are available which can be used at temperatures as low as -25° C. which is still, however, not as low as the minimum temperature attainable at high altitudes in the case of aeronautical applications, e.g. -45° C. at 30,000 ft., and -57° C. at 35,000 ft. and above.

In the case of rubber compounds used as flexible couplings or for engine mounting systems, however, the vibratory nature of the loadings can be assumed to cause sufficient internal heating to maintain the temperature of the rubber at a tolerable value even at high altitudes.

Hardness of Rubber.—Experiment has indicated that with strict manufacturing control the qualities of rubber generally used for flexible couplings and engine mountings give practically the same elastic properties for a given shape and hardness. The hardness of rubber compounds is measured by a standard instrument known as the Shore Durometer and the degree of hardness is expressed on a simple numerical scale, for example, "Shore Hardness 35," and so on. The Shore Durometer consists of a spring-loaded flat-tipped tapering needle 1.5 mm. in diameter tapered to 0.75 mm. With this instrument hard

qualities give high hardness readings and vice-versa. The softest grade of rubber registers about 30 and the hardest about 90, the latter representing hard vulcanite. The usual range for structural rubber suitable for flexible couplings is from 35 to 70 Shore. The Shore Durometer is a simple instrument, but considerable skill is required to ensure that consistent readings are obtained. In this respect the instrument compares with the caliper rather than the micrometer, and for this reason it is considered good practice to retain one particular instrument for final checking of products and to make one particular person responsible for carrying out the tests.

Hardness increases with the proportion of mineral fillers, and for high grade mixings carbon black pigments are extensively used for this purpose.

Hardness also increases with increasing sulphur content and with an advance in vulcanisation. High proportions of sulphur, e.g. 20 to 30 per cent., produce a rigid hard rubber.

This facility for changing the hardness of rubber compounds over a wide range is of considerable value in cases where rubber is used for controlling the vibration frequencies of oscillating systems. This is a unique property of rubber. Thus the shear modulus of structural rubber of Shore hardness 30 is about 50 lbs. per sq. in., whereas for Shore Hardness 70 it is about 150 lbs. per sq. in., i.e. a three-fold increase. In the case of steel, on the other hand, the modulus of rigidity lies between 11,000,000 and 12,000,000 lbs. per sq. in. irrespective of the physical or other mechanical properties of the material.

The flexibility of a rubber coupling can therefore be varied over a wide range by changing the hardness of the rubber without altering the dimensions of the coupling.

It should be borne in mind, however, that it is possible for a skilled rubber technologist to produce more than one rubber mix indicating the same hardness but each having different mechanical properties. It is therefore necessary to adhere strictly to a definite rubber mix for each specific application, and to exercise strict control over every stage of the production processes.

Damping Properties of Rubber.—The damping properties of rubber depend to some extent on the compounding ingredients and their proportion. For example, pure gum has little hysteresis although there is usually sufficient to be of some practical value for damping purposes. An increase in the proportion of lamp black has a marked effect on the damping properties, and high hysteresis values are obtained by loading the rubber with pigments.

Rubber compounds having high hysteresis are best avoided for structural applications, however, because they have also a high rate of creep, i.e. they tend to settle down under load so that they do not return to their original configuration when the load is removed. This is fatal where the alignment of the parts connected by the rubber element must be maintained.

Rubber compounds having high hysteresis and low creep have not been discovered.

The work absorbed during each load alternation in the case of rubber decreases with increasing frequency of alternation and tends towards a limiting value. The damping properties are also a function of the vibratory amplitude. This implies that the vibrational characteristics of oscillating systems employing rubber as a spring element are not strictly linear. It should also be noted that damping values derived from static hysteresis experiments are not of much value. For example, conical disc couplings of the type shown at II in Fig. 58 average 16 to 18 per cent. static hysteresis loss, whereas the dynamic value is nearer 6 per cent.

It is very difficult, therefore, to make general rules relating to the damping properties of rubber because of the great differences of amplitude, frequency, and loading found in practice between one particular example and another.

As a general rule the quickest method of finding a solution in a particular case is to assume that the system obeys the laws of linearity for the purpose of the initial design and then by careful testing to determine whether any alteration is desirable. If the tests indicate that some change is required this can usually be carried out merely by changing the hardness of the rubber compound.

The damping energy ratios for a typical range of structural rubber compounds are given in the attached table. The energy loss and dynamic magnifier can be determined by the methods given in Chapter 7, as follows:—

Let ψ_s = damping energy ratio,
 δW = energy absorbed by damping per cycle,
 W = strain energy at commencement of cycle,
 θ = amplitude at commencement of cycle,
 $\delta\theta$ = reduction of amplitude per cycle,
 M = dynamic magnifier,
 λ = logarithmic decrement per cycle.

Then, from Equation (300), $\psi_s = 2 \cdot \lambda = \delta W/W$,
 and, from Equation (305), $M = 2 \cdot \pi/\psi_s$,
 $\lambda = \psi_s/2 = \delta\theta/\theta$.

For example, if $\psi_s = 0.18$,
 $\delta W = 0.18 \cdot W$,
 $\delta\theta = 0.09 \cdot \theta$,
 $M = 6.283/0.18 = 35$.

Working Stresses.—Permissible working stresses are naturally governed by the quality of the rubber and of the bonding process. The tensile strength of rubber compounds varies widely with quality, for example, from as low as 100 lbs. per sq. in. calculated on the original cross-section to as much as 4000 lbs. per sq. in. of the original cross-section.

The elongation at rupture varies from as little as 10 per cent. to as much as 800 per cent. Average values for good quality structural rubber are tensile strength 2000 to 3500 lbs. per sq. in., of original cross-section, and elongation 600 to 800 per cent.

Owing to its non-crystalline or amorphous character and low elastic moduli rubber is not subject to fatigue failure except in cases where excessive heat is generated in the material through hysteresis. This is a further point in favour of avoiding rubber compounds having high hysteresis.

With regard to bonding strength, modern brass plating processes have an ultimate tensile strength at the bonding

surface as high as 800 to 1000 lbs. per sq. in., depending on the hardness of the rubber, whilst in general applications a bonding strength of at least 200 to 400 lbs. per sq. in. of bonded area can be safely relied upon.

Brass plating methods of bonding are generally accepted as giving the best results. They can be used for bonding rubber to any material which will take the brass plating, although, so far, the greatest success has been obtained with steel and to a lesser degree with one or two of the light alloys.

The main essential so far as steel is concerned is that it must have a low carbon content, certainly not greater than 0.4 per cent., and preferably down to 0.18 per cent.

The most important characteristic from the point of view of permissible working stress is, however, the creep characters of the compound employed, and most working stress limitations hinge about this single property.

Normal working stresses in tension, torsion, or shear should be limited to from 40 to 70 lbs. per sq. in. of cross-section, whilst the strain should not be permitted to exceed about 70 to 80 per cent.

Creep tests over long periods confirm that these limitations will ensure satisfactory service. The above values of permissible stress apply to both the rubber itself and to the bonded surfaces.

In the case of rubber-in-shear flexible couplings a working shear stress of 60 to 85 lbs. per sq. in. is reasonable, whilst the coupling can be permitted to carry a compressive stress of 85 lbs. per sq. in. due to the axial thrust of a propeller or air-screw. In exceptional cases the compressive stress can be permitted to reach 130 lbs. per sq. in.

The properties of structural rubber suitable for use in flexible couplings are given in the following table. The values given in the table are from figures published by the United States Rubber Company and relate to U.S. Structural Rubber.

Whilst these values are believed to be fairly representative it should be kept in mind that considerable variations are liable to exist between the products of different manufacturers. It is to be hoped that with the increasing use of rubber for

engineering applications an effort will soon be made to produce standardised grades of rubber to definite specifications. This would enable a suitable grade of rubber to be selected with the same facility as it is possible to select definite grades of steel for specific duties.

In the meantime it is advisable to obtain design data from the individual manufacturer.

TABLE 23.
PROPERTIES OF STRUCTURAL RUBBER.

Shore Hardness.	Specific Gravity.	Ult. Tensile on Original Cross-Section. Lbs./In. ² .	Elongation. Per Cent.	Shear Modulus. Lbs./In. ² .	Average Tensile Modulus. Lbs./In. ² .	Damping Energy Ratio.
30	1.01	2000	850	48	128	0.16
40	1.06	2800	750	65	190	0.18
50	1.11	3500	700	84	240	0.39
60	1.17	3500	600	108	—	0.61
70	1.24	3000	700	166	—	0.77

Note.—Specific gravity of raw rubber = 0.925,
Bulk modulus of rubber = 300,000 to 400,000
lbs. per sq. in.

Design of Rubber-in-Shear Couplings.—The strength and torsional rigidity of the parallel disc coupling shown at I in Fig. 58 can be calculated by applying the well-known expressions for shafts subjected to torsion.

Let T = torque transmitted, in lbs.-ins.,
 D = outer diameter of rubber disc, in inches,
 d = inner diameter of rubber disc, in inches,
 f_s = surface shear stress in lbs., per sq. in.,
 H = axial length of rubber disc, in inches,
 C = torsional rigidity of coupling, in lbs.-ins./radian,
 G = shear modulus of rubber, in lbs. per sq. in.

$$\text{Then } f_s = \frac{16 \cdot T \cdot D}{\pi(D^4 - d^4)} \text{ lbs. per sq. in.,} \quad . \quad . \quad . \quad (146)$$

$$C = T/\theta = \frac{\pi(D^4 - d^4) \cdot G}{32 \cdot H} \text{ lbs.-ins./radian.} \quad . \quad (147)$$

In this type of coupling the maximum shear stress occurs at the periphery of the rubber disc and diminishes uniformly to zero at the axis of the coupling in the same manner as for shafts in torsion.

The conical disc type of coupling shown at II in Fig. 58 is more commonly employed for rubber-in-shear couplings, since it provides a uniform distribution of shear stress across the coupling, i.e. the shear stress at the periphery is the same as that at the inner radius.

In this type of coupling

$$f_s = \frac{16 \cdot K \cdot T \cdot D}{\pi(D^4 - d^4)} \text{ lbs. per sq. in.} \quad (148)$$

and
$$C = \frac{\pi(D^4 - d^4) \cdot G}{32 \cdot H \cdot K} \text{ lbs.-ins./radian} \quad (149)$$

where K has the following values :-

d/D .	K.
1.0	1.00
0.8	0.88
0.6	0.80
0.4	0.73
0.2	0.67
0.0	0.63

As already explained the shear stress should be limited to about 60 lbs. per sq. in. to avoid trouble due to creep.

It is also desirable to calculate the surface shear strain. Referring to Diagram III of Fig. 58,

let θ = angle of twist across coupling = T/C ,

α = angle of surface shear.

Then $D \cdot \theta/2 = H \cdot \alpha$,

or $\alpha = D \cdot \theta/(2 \cdot H)$ radian = shear strain. (150)

As already explained this should not exceed 70 to 80 per cent. or 40° to 45° to avoid trouble due to creep.

Diagram IV of Fig. 58 shows a method adopted in the Pendulastic type of rubber-in-shear coupling to avoid stress concentration and therefore a tendency for the bonded surface to open slightly at the outer and inner peripheries.

This is achieved by spreading the bonding areas at these points as shown at *a* and *b* in the diagram. Similar methods are employed by other manufacturers.

It is also desirable to arrange the coupling bolts or studs which connect the coupling flanges of the input and output shafts so that they do not penetrate through the bonded surface into the rubber. This avoids an interruption of the bonded areas and also the introduction of points of stress concentration.

In designing bonded rubber parts the mould and the moulding process have to be given careful consideration. An important point is to ensure that stripping and removal of the components is made easy, especially under mass production conditions, since the moulds cannot be handled by bare hands. Even with the easiest of moulds extraction requires some skill. A further point is that any undue strain on the component during the stripping process is liable to have serious effects on the bond, since bonded rubber components are not very strong at vulcanising temperatures.

Fig. 59 shows a design of rubber-in-shear flexible coupling patented by Messrs. Armstrong Siddeley Motors for air-screw drives. An inner driving member is mounted on the air-screw shaft splines, a disc of rubber being bonded to each side of the steel driving disc. The outer faces of the rubber discs are bonded to the driven plates, which in turn are bolted to the air-screw hub. The bolts pass through holes bored through the rubber and metal discs with sufficient clearance to permit the normal amount of twist under service conditions. Damping is provided by spring loaded friction washers inserted between the driving and driven sleeves.

Fig. 60 shows a marine installation comprising two Pendulastic conical disc couplings arranged one on each side of the thrust block of a Diesel engine propeller drive. In this case the engine itself is mounted on rubber and the couplings permit sufficient angular freedom to act as universal joints between the engine and the propeller.

Fig. 61 shows two designs of Metalastik rubber-in-shear couplings. The right-hand photograph shows a normal type conical disc coupling whilst the left-hand photograph shows

a coupling in which stops are provided to limit the angular movement to a predetermined amount. Limiting stops are necessary in certain arrangements to guard against excessive

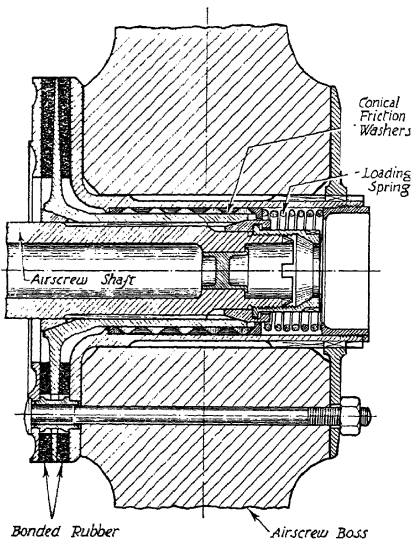


FIG. 59.—Elastic coupling for air-screw (Armstrong Siddeley Motors).

twist and load when starting up or under occasional abnormal shocks.

Fig. 61a shows a range of "Dynaflex" rubber-in-shear couplings.

The "Couploflex" type is made in two forms, namely, a simple disc arrangement which is suitable for small powers

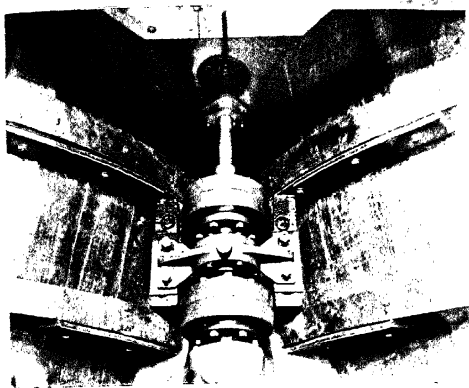


FIG. 60.—Application of "Pendulastic" rubber-in-shear couplings in a marine Diesel installation.



METALASTIK Coupling with limited angular movement. For waterpumps, dynamos, etc.



METALASTIK Coupling. "Vee" type

FIG. 61.—"Metalastik" rubber-in-shear couplings.

[To face page 282.]

and a three-plate arrangement suitable for powers of 5 h.p. upwards. Fig. 61*b* shows a recent development of the three-plate arrangement. The centre plate operates against the two outer plates so that for a given overall diameter the three-plate coupling is capable of transmitting appreciably greater powers than the simple two-plate design.

In the design shown in Fig. 61*b* a number of rubber-lined recesses are formed round the periphery of the centre plate. The bolts and distance pieces which connect the two outer plates pass through these recesses, so that in cases of abnormal overloads the distance pieces contact with the ends of the recesses, thus preventing undue strain. Additional strength can be provided by replacing the separate distance pieces by a continuous ring passing round the outside of the coupling. This not only gives additional strength but can be made to serve as a casing for protecting the rubber from oil drips.

Couplings of this type have been successfully supplied up to 21 ins. outside diameter, transmitting 20,000 lbs.-ft. torque for use on engine test installations.

The "Radiaflex" bobbin type coupling forms a very useful and flexible arrangement, but its overall dimensions are considerably greater than those of other types. Where space and weight are not of primary importance, however, the bobbin type coupling provides a comparatively inexpensive and reliable solution. It has, for example, been used successfully on radial aero-engine test bed installations.

In the "Cardaflex" coupling the special hyperbolic contour of the rubber element gives an even stress throughout the rubber. This coupling has very great torsional and conical flexibilities and is, therefore, suitable for applications where these properties are required. For example, for driving independent auxiliaries from an engine where positive alignment of the engine and the auxiliary cannot be maintained. In such cases a Cardaflex coupling is provided at each end of the auxiliary drive shaft and this enables quite appreciable relative displacements to occur without detriment. The rubber element of this type of coupling is remarkably resistant to destruction, and in one test sustained a torsional deflection of 272° with

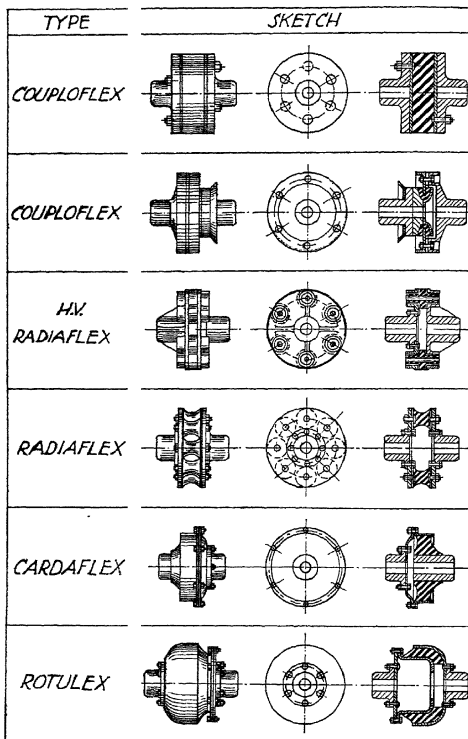


FIG. 61a.—“Dynaflex” type rubber-in-shear couplings.

REMARKS	
	Coupling for small powers 0.15 to 3.5 H.P. at 1000 R.P.M. Suitable for all speeds of rotation.
Flexibility	<u>Torsional</u> — Considerable — up to about 15° <u>Parallel Misalignment</u> — Considerable — 2mm. upwards. <u>Conical Misalignment</u> — Moderate — up to 5° angular displacement of shaft. <u>Longitudinal</u> — Comparatively small.
	Coupling for 5 H.P. upwards at 1000 R.P.M. with shafts normally aligned. Overall dimensions relatively small.
Flexibility	<u>Torsional</u> — Considerable — 5° to 8° <u>Parallel Misalignment</u> — Small, 1mm misalignment is possible. <u>Conical Misalignment</u> — Small. 5° maximum. <u>Longitudinal</u> — Very small.
	For high speeds of rotation or high powers when small overall dimensions are required. Light, capable of carrying high overloads.
Flexibility	<u>Torsional</u> — Normal — up to 5° <u>Parallel Misalignment</u> — Considerable — up to 5 m.m. <u>Conical Misalignment</u> — Normal — up to 5° <u>Longitudinal</u> — Very small.
	For all powers with speeds of rotation up to 1500 R.P.M. Recommended for high elastic qualities. May be used when overall dimensions and speeds permit, in particular for couplings the shafts of which are liable to faulty angular or linear alignment.
Flexibility	<u>Torsional</u> — Very considerable — up to 20° <u>Parallel Misalignment</u> — Considerable — up to 20 m.m. <u>Conical Misalignment</u> — Considerable — up to 15° <u>Longitudinal</u> — Normal — up to 5 m.m.
	Flexible universal joint. Replaces mechanical and sliding cardan joints. Can be combined with a centering mechanism in the case of high speeds of rotation.
Flexibility	<u>Torsional</u> — Very high — up to 90° <u>Parallel Misalignment</u> — Small — 1 to 3 m.m. <u>Conical Misalignment</u> — Very high — 30° and over. <u>Longitudinal</u> — Very high — 10 to 50 m.m.
	Flexible universal joint. Replaces mechanical joint, in particular where small overall diameters are required.
Flexibility	<u>Torsional</u> — Considerable — up to 10° <u>Parallel Misalignment</u> — About 2 m.m. <u>Conical Misalignment</u> — Up to 30° <u>Longitudinal</u> — 2 m.m. — maximum.

only slight knotting of the rubber and with no apparent damage to the bond. On releasing the load the coupling returned to its original static position and appearance.

The "Rotulex" coupling is used as a universal flexible joint and has successfully replaced mechanical universal joints

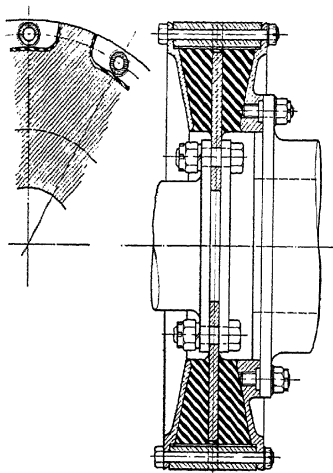


FIG. 61b.—"Dynaflex" rubber-in-shear coupling (3-plate type).

on automobile propeller shafts. The additional damping provided by the rubber is useful for resisting starting shocks, especially when the couplings are used as universal joints for shafts with a comparatively large included angle between their axes.

CHAPTER 5.

GEARED SYSTEMS.

Equivalent Systems.—A geared transmission system consists of a series of rotating masses of moments of inertia J_a, J_b , etc., attached to shafts of torsional rigidities C_a, C_b , etc., which are geared together so that the mean angular velocities of the respective shafts and masses are q_a, q_b , etc.

The determination of the torsional vibration characteristics of such a system is considerably simplified if the actual system is first replaced by a dynamically equivalent system in which all shafts and masses rotate with the same mean angular velocity, or, in other words, in which the gear ratios of the several elements of the dynamically equivalent system are all 1/1.

Assuming that the connections inside the gearbox are torsionally rigid, the following relationships exist between the properties of the original system and the properties of the dynamically equivalent system :—

(i) Let q_n = mean angular velocity of shaft n of the original system,

q = mean angular velocity of *all* shafts of the dynamically equivalent system,

N_n = r.p.m. of shaft n of original system,

N = r.p.m. of *all* shafts of equivalent system,

then $q/N = q_n/N_n$ or $q/q_n = N/N_n$.

(ii) Let M_n = the mean or the fluctuating torque in shaft n of the original system,

M = equivalent torque in corresponding shaft of equivalent system,

then $M_n \cdot q_n = M \cdot q$ or $M/M_n = q_n/q = N_n/N$.

- (iii) Let θ_n = angular amplitude of vibration of shaft n of original system,
 θ = equivalent amplitude of vibration of corresponding shaft of equivalent system,

then $\theta/q = \theta_n/q_n$ or $\theta/\theta_n = q/q_n = N/N_n$.

- (iv) Let J_n = moment of inertia of mass on shaft n of original system,
 J = equivalent moment of inertia of mass on corresponding shaft of equivalent system,

then kinetic energy of mass J_n on shaft n is

$$K_n = \frac{1}{2} \cdot J_n \cdot q_n^2.$$

Kinetic energy of mass J on corresponding shaft of equivalent system is

$$K = \frac{1}{2} \cdot J \cdot q^2,$$

and since

$$K_n = K,$$

$$J/J_n = (q_n/q)^2 = (N_n/N)^2.$$

- (v) Let $C_n = M_n/\theta_n$ = torsional rigidity of shaft n of original system,
 $C = M/\theta$ = equivalent torsional rigidity of corresponding shaft of equivalent system,

then strain energy of shaft n ,

$$P_n = \frac{1}{2} \cdot M_n \cdot \theta_n = \frac{1}{2} \cdot C_n \cdot \theta_n^2.$$

Strain energy of corresponding equivalent shaft,

$$P = \frac{1}{2} \cdot M \cdot \theta = \frac{1}{2} \cdot C \cdot \theta^2,$$

and since

$$P_n = P,$$

$$C/C_n = (\theta_n/\theta)^2 = (q_n/q)^2 = (N_n/N)^2.$$

Summary.—

$$M/M_n = N_n/N, \quad . \quad . \quad . \quad (151)$$

$$\theta/\theta_n = N/N_n, \quad . \quad . \quad . \quad (152)$$

$$J/J_n = (N_n/N)^2, \quad . \quad . \quad . \quad (153)$$

$$C/C_n = (N_n/N)^2, \quad . \quad . \quad . \quad (154)$$

where N_n = revs. per min. of shaft n of original system,

N = revs. per min. of *all* shafts of equivalent system.

Equations (151) to (154) may also be used for converting any quantities obtained by calculations based on the equivalent system into corresponding quantities for the original system.

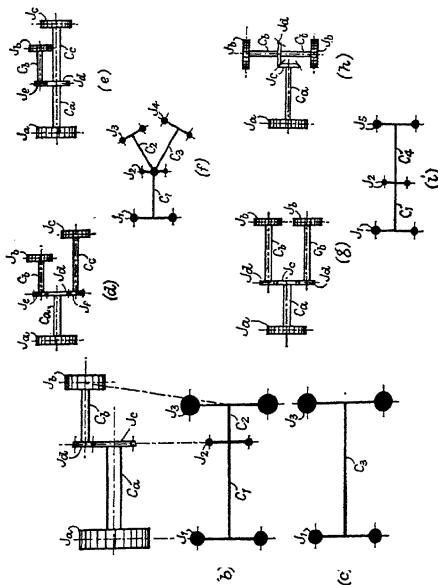


FIG. 62.—Geared systems.

Two-Shaft Systems.—Fig. 62a shows a simple geared system consisting of masses of moments of inertia J_a and J_b attached to shafts of torsional rigidities C_a and C_b ; the shafts being geared together by gears of moments of inertia J_c and J_d .

The speeds of the two shafts are N_a and N_b revs. per min. respectively.

Fig. 62*b* shows an equivalent system in which all shafts and all masses of the original system shown in Fig. 62*a* are replaced by dynamically equivalent shafts and masses all rotating with the speed of shaft a , viz. N_a revs. per min.,

$$\begin{aligned} \text{i.e.} \quad J_1 &= J_a, \\ J_2 &= [J_c + J_d(N_b/N_a)^2], \quad [\text{from Eqn. (153)}], \\ J_3 &= J_b(N_b/N_a)^2, \quad . \quad . \quad [\text{from Eqn. (153)}], \\ C_1 &= C_a, \\ C_2 &= C_b(N_b/N_a)^2. \quad . \quad . \quad [\text{from Eqn. (154)}]. \end{aligned}$$

The original system therefore reduces to the three-mass system shown in Fig. 62*b*, and the natural frequencies of torsional vibration may be calculated from Equation (19), viz.

$$(J_1 + J_2 + J_3) - w_c^2 \left[\frac{J_1 \cdot J_2}{C_1} + \frac{J_1 \cdot J_3}{C_1} + \frac{J_1 \cdot J_3}{C_2} + \frac{J_2 \cdot J_3}{C_2} \right] + \frac{w_c^4 \cdot J_1 \cdot J_2 \cdot J_3}{C_1 \cdot C_2} = 0.$$

This equation may also be written

$$(J_1 + J_2 + J_3) - w_c^2 (J_2/w_1^2 + J_3/w_1^2 + J_1/w_2^2 + J_2/w_2^2) + w_c^4 \cdot J_2/w_1^2 \cdot w_2^2 = 0, \quad (155)$$

where $w_1 = \sqrt{C_1/J_1}$ = phase velocity of natural vibration of mass J_1 on its shaft regarded as fixed at the gearbox,

$w_2 = \sqrt{C_2/J_3}$ = phase velocity of natural vibration of mass J_3 on its shaft regarded as fixed at the gearbox,

w_c = phase velocity of natural vibration of whole system

$$= \frac{2 \cdot \pi \cdot F_c}{60},$$

F_c = natural frequency of torsional vibration of whole system in vibs./min.

There are two real roots of Equation (155), indicating two possible modes of vibration. The connections inside the gear-

box are assumed to be torsionally rigid, and the moments of inertia of the shafts have been assumed to be negligible compared with those of the masses and gears.

The arrangement shown in Fig. 62*a* is typical of many practical applications of geared drives where the gearing is usually single or double-reduction. If double-reduction gearing is employed, care must be taken to use the correct speed for the first reduction wheel and second reduction pinion when obtaining the equivalent moments of inertia of these parts from Equation (153). The speed of the first reduction pinion is, of course, that of the primary shaft, and the speed of the second reduction wheel is that of the secondary shaft.

The following special cases should be noticed :—

- (i) If $J_1 = J_3 = J$ and $C_1 = C_2 = C$, i.e. $w_1 = w_2 = w$,

Equation (155) reduces to

$$(J_2 + 2J) - \frac{2 \cdot w_c^2}{w^2} (J_2 + J) + w_c^4 \cdot J_2/w^4 = 0,$$

i.e. $w_c^2 = w^2$ or $w^2(2 \cdot J + J_2)/J_2$. . . (156)

In this case there are two possible modes of vibration. The fundamental mode is a one-node mode with the node situated at the gears. The fundamental frequency is therefore equal to the natural frequency of either mass, J_1 or J_3 , on its shaft regarded as fixed at the gearbox.

- (ii) If the moments of inertia of the gears are negligible compared with those of the masses J_1 and J_3 , the system shown in Fig. 62*b* reduces to the two-mass system shown in Fig. 62*c*.

The natural frequency is therefore obtained from Equation (16), viz.,

$$w_c^2 = C_3(J_1 + J_3)/J_1 \cdot J_3,$$

but

$$C_3 = C_1 \cdot C_2/(C_1 + C_2).$$

Hence,

$$w_c^2 = \frac{C_1 \cdot C_2(J_1 + J_3)}{J_1 \cdot J_3(C_1 + C_2)}. \quad \cdot \quad \cdot \quad \cdot \quad (157)$$

Equation (157) may also be written

$$w_c^2 = \frac{w_1^2 \cdot w_2^2 (J_1 + J_3)}{(J_1 \cdot w_1^2 + J_3 \cdot w_2^2)} \quad (158)$$

Equation (158) may be obtained directly from Equation (155) by substituting $J_2 = 0$ in the latter equation.

In this case there is only one possible mode of vibration.

- (iii) If the moments of inertia of the gears are negligible, $J_1 = J_3 = J$ and $C_1 = C_2 = C$, i.e. $w_1 = w_2 = w$, in Fig. 62*b*,

Equation (158) reduces to

$$w_c^2 = w^2 = \frac{C}{J} \quad (159)$$

In this case there is only one possible mode of vibration, and the natural frequency is equal to that of either mass on its shaft assumed to be fixed at the gearbox. The node is therefore situated at the gearbox.

Equation (159) also applies in cases where $J_a = J_b$ and $C_a = C_b$ in Fig. 62*a*.

EXAMPLE 35.—Calculate the natural frequencies of the geared system shown in Fig. 62*a*, assuming the following values :

$$\begin{aligned} J_a &= 2.7 \text{ tons-ft. sec.}^2, & J_b &= 1.8 \text{ tons-ft. sec.}^2, \\ J_c &= 1.6 \text{ tons-ft. sec.}^2, & J_d &= 0.022 \text{ tons-ft. sec.}^2, \\ C_a &= 1000 \text{ tons-ft. per radian}, \\ C_b &= 600 \text{ tons-ft. per radian}. \end{aligned}$$

The normal speed of shaft *a* is 100 r.p.m., and of shaft *b* 300 r.p.m.

The original system is first reduced to the dynamically equivalent system shown in Fig. 62*b*, in which the speed of all shafts and all masses is assumed to be, say, that of shaft *a*, viz. 100 r.p.m.,

$$\begin{aligned} \text{i.e. } J_1 &= J_a = 2.7 \text{ tons-ft. sec.}^2, \\ J_2 &= J_c + J_d(N_b/N_a)^2 = 1.6 + 0.022 (300/100)^2 \\ &= 1.8 \text{ tons-ft. sec.}^2, \end{aligned}$$

$$J_3 = J_3(N_b/N_a)^2 = 1.8(300/100)^2 \\ = 16.2 \text{ tons-ft. sec.}^2,$$

$$C_1 = C_a = 1000 \text{ tons-ft. per radian,}$$

$$C_2 = C_b(N_b/N_a)^2 = 600 (300/100)^2 \\ = 5400 \text{ tons-ft. per radian.}$$

$$\text{Also } w_1^2 = C_1/J_1 = 1000/2.7 = 370 \text{ (radians/sec.)}^2, \\ w_2^2 = C_2/J_3 = 5400/16.2 = 333 \text{ (radians/sec.)}^2.$$

Hence, from Equation (155),

$$(2.7 + 1.8 + 16.2) - w^2(1.8/370 + 16.2/370 + 2.7/333 \\ + 1.8/333) + w^4 \times 1.8/(370 \times 333) = 0,$$

$$\text{i.e. } 20.7 - 0.0622 \cdot w^2 + 0.000146 \cdot w^4 = 0, \\ w = 19.1 \text{ or } 62.5 \text{ radians/sec.,}$$

$$\text{or } F = \frac{60 \cdot w}{2\pi} = 182 \text{ or } 596 \text{ vibs./min.}$$

These frequencies correspond to the one- and two-node modes of vibration respectively.

The critical speeds of torsional vibration may be determined as follows:—

Assuming that a prime-mover having an impulse frequency of six impulses per revolution is attached to shaft *a*, then the critical speeds of shaft *a* are $182/6 = 30.3$ r.p.m. for the one-node mode and $596/6 = 99.3$ r.p.m. for the two-node mode. A torsigraph applied to shaft *a* would therefore record vibrations having six complete oscillations per revolution of shaft *a* at each of these speeds. Since shaft *b* rotates at three times the speed of shaft *a*, the corresponding critical speeds of shaft *b* are $30.3 \times 3 = 91$ r.p.m. and $99.3 \times 3 = 298$ r.p.m. respectively, i.e. a torsigraph applied to shaft *b* would record vibrations having $182/91 = 596/298 = 2$ complete oscillations per revolution of shaft *b*.

If, however, the prime-mover is attached to shaft *b*, the critical speeds of shaft *b* are $182/6 = 30.3$ r.p.m. and $596/6 = 99.3$ r.p.m. respectively, i.e. a torsigraph applied to shaft *b* would record vibrations having six complete oscillations per revolution of shaft *b*. Since shaft *a* rotates at one-third the speed of shaft *b*, the corresponding critical speeds of shaft *a* are $30.3/3 = 10.1$

r.p.m. and $99\cdot3/3 = 33\cdot1$ r.p.m. respectively, i.e. a torsigraph applied to shaft *a* would record vibrations having

$$182/10\cdot1 = 596/33\cdot1 = 18$$

complete oscillations per revolution of shaft *a*.

In other words, if

n_a = order number referred to shaft *a*,

n_b = order number referred to shaft *b*,

N_a = R.P.M. of shaft *a*,

N_b = R.P.M. of shaft *b*,

ϕ = gear ratio = N_b/N_a ,

then, $n_a \cdot N_a = n_b \cdot N_b$,

i.e. $n_a = n_b \cdot \frac{N_b}{N_a} = \phi \cdot n_b$,

or, $n_b = n_a/\phi$ (159*a*)

Tabulation Method.—The natural frequencies of torsional vibration of geared systems can also be determined by the tabulation method described in Chapter 2 (see Tables 1 to 4). In the case of geared systems, the tabulation is modified as follows:—

Commencing at one of the free ends of the system, the table is completed in the usual way until the gear faces are reached. The deflection at the gear face, column F, is then multiplied by the gear ratio to obtain the corresponding value after passing through the gears; whilst the total torque up to the same point, column H, is divided by the gear ratio to obtain the corresponding value after passing through the gears. The frequency table is then completed to the end of the system in the usual way.

Tables 24 and 25 are the frequency tabulations for the one-node and two-node modes of vibration of the geared system shown in Fig. 62*a*, using the values given in Example 35.

The tables are started from mass J_a , and the gear ratio* is

* Strictly speaking, the gear ratio is positive if the shafts rotate in the same direction as in the case of epicyclic gears, and it is negative if the shafts rotate in opposite directions, as in the case of simple spur gears. This sign convention is important when dealing with systems having several branches, but not in cases where there is only one branch.

TABLE 24.

FREQUENCY TABULATION : ONE-NODE VIBRATIONS : GEARED SYSTEM.

 $F = 182 \text{ Vibs./Min.}; w = 19.1 \text{ Radians/Sec.}; w^2 = 364.5.$

A	D	E	F	G	H	I	J
Mass. (Fig. 62a.)	Moment of Inertia, J Tons-Ft. Sec. ² .	Torque per Unit Deflection, J Tons-Ft./Radian.	Deflection in Plane of Mass, θ Radians.	Torque in Plane of Mass, J Tons-Ft.	Total Torque, $\sum J_i \omega^2 \theta$ Tons-Ft.	Shaft Stiffness C Tons-Ft./Radian.	Change in Deflection, Col. H/Col. I Radians.
J_a	2.7	984.1	1.0000	984.1	984.1	1000	0.9841
J_b	1.6	583.2	0.0159	9.27	993.37	—	—
GEAR RATIO = 300/100 = 3/1.							
J_1	0.022	8.02	$0.0159 \times 3 = 0.0477$	0.38	$993.37/3 + 0.38$ $= 331.50$	600	0.5525
J_2	1.8	656.1	-0.5048	-331.5	0	—	—

TABLE 25.
 FREQUENCY TABULATION: TWO-NODE VIBRATIONS: GEARED SYSTEM.
 $F = 596 \text{ Vibs./Min.}; w = 62.4 \text{ Radians/Sec.}; \omega^2 = 3897.$

A	D	E	F	G	H	I	J
Mass. (Fig. 634.)	Moment of Inertia, Tons-Ft. Sec. ²	Torque per Unit Deflection, Tons-Ft./Radian.	Deflection in Plane of Mass, Radians.	Torque in Plane of Mass, Tons-Ft.	Total Torque, Tons-Ft.	Shaft Stiffness C Tons-Ft./Radian.	Change in Deflection, Col. H/Col. I Radians.
J_a	2.7	10522	1.0000	10522	10522	1000	10.522
J_b	1.6	6235	-9.522	-59370	-48848	—	—
GEAR RATIO = $300/100 = 3/1.$							
J_a	0.022	86	$-9.522 \times 3 = -28.566$	-2457	$-48848/3 = -16283$	600	-31.233
J_b	1.8	7015	2.667	18740	0	—	—

3/1. Fig. 63 shows the one- and two-node normal elastic curves for this system, plotted from the specific deflections in column F of the frequency tables.

This method may also be used in cases where there are several masses at each side of the gear-box.

Three-Shaft Systems.

—Fig. 62*d* shows a geared system consisting of three shafts of torsional rigidities C_a , C_b , and C_c , with attached masses of moments of inertia J_a , J_b and J_c respectively. The moments of inertia of the gears are J_d , J_e and J_f , and the speeds of the shafts are N_a , N_b and N_c .

Fig. 62*f* shows an equivalent system in which all shafts and all masses of the original system shown in Fig. 62*d* are replaced by dynamically equivalent shafts and masses all rotating with the speed of shaft a , viz. N_a revs. per min.,

$$\begin{aligned} \text{i.e. } J_1 &= J_a, \\ J_2 &= [J_d + J_e(N_b/N_a)^2 + J_f(N_c/N_a)^2], \quad [\text{from Eqn. (153)}] \\ J_3 &= J_b(N_b/N_a)^2, \quad . \quad . \quad . \quad [\text{from Eqn. (153)}] \\ J_4 &= J_c(N_c/N_a)^2, \quad . \quad . \quad . \quad [\text{from Eqn. (153)}] \\ C_1 &= C_a, \\ C_2 &= C_b(N_b/N_a)^2, \quad . \quad . \quad . \quad [\text{from Eqn. (154)}] \\ C_3 &= C_c(N_c/N_a)^2, \quad . \quad . \quad . \quad [\text{from Eqn. (154)}] \end{aligned}$$

The natural frequencies of torsional vibration of the system shown in Fig. 62*f* may be obtained from the following equation :—

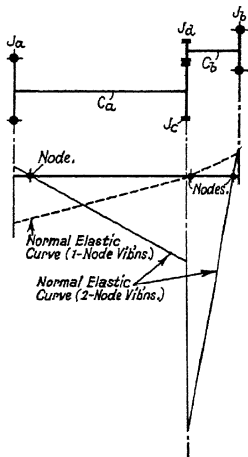


FIG. 63.—Simple geared system.

$$\begin{aligned}
 (J_1 + J_2 + J_3 + J_4) - w_c^2 \left[\frac{(J_2 + J_3 + J_4)J_1}{C_1} + \frac{(J_1 + J_2 + J_4)J_3}{C_2} \right. \\
 \left. + \frac{(J_1 + J_2 + J_3)J_4}{C_3} \right] \\
 + w_c^4 \left[\frac{J_1 \cdot J_3(J_2 + J_4)}{C_1 \cdot C_2} + \frac{J_3 \cdot J_4(J_1 + J_2)}{C_2 \cdot C_3} + \frac{J_1 \cdot J_4(J_2 + J_3)}{C_1 \cdot C_3} \right] \\
 - \frac{w_c^6 \cdot J_1 \cdot J_2 \cdot J_3 \cdot J_4}{C_1 \cdot C_2 \cdot C_3} = 0.
 \end{aligned}$$

This equation may also be written

$$\begin{aligned}
 (J_1 + J_2 + J_3 + J_4) \\
 - w_c^2 [(J_2 + J_3 + J_4)/w_1^2 + (J_1 + J_2 + J_4)/w_2^2 \\
 + (J_1 + J_2 + J_3)/w_3^2] \\
 + w_c^4 [(J_2 + J_4)/w_1^2 \cdot w_2^2 + (J_1 + J_2)/w_2^2 \cdot w_3^2 + \\
 (J_2 + J_3)/w_1^2 \cdot w_3^2] - w_c^6 \cdot J_1/(w_1^2 \cdot w_2^2 \cdot w_3^2) = 0, \quad (160)
 \end{aligned}$$

where $w_1 = \sqrt{C_1/J_1}$ = phase velocity of natural vibration of mass J_1 on its shaft regarded as fixed at the gearbox,

$w_2 = \sqrt{C_2/J_3}$ = phase velocity of natural vibration of mass J_3 on its shaft regarded as fixed at the gearbox,

$w_3 = \sqrt{C_3/J_4}$ = phase velocity of natural vibration of mass J_4 on its shaft regarded as fixed at the gearbox,

w_c = phase velocity of natural vibration of whole system

$$= 2 \cdot \pi \cdot F/60 \text{ radians per sec.},$$

F = natural frequency of torsional vibration of whole system in vibs./min.

There are three real roots of Equation (160) indicating three possible modes of vibration of the whole system.

The following special cases should be noticed :-

- (i) The arrangement shown in Fig. 62e consists of two masses J_a and J_c attached to the extremities of one shaft with a third mass J_b connected through gearing to an intermediate point in the same shaft.

In this case the equivalent system, Fig. 62*f*, is obtained as follows:—

$$\begin{aligned} J_1 &= J_a, \\ J_2 &= [J_d + J_e(N_b/N_a)^2], & . & . & \text{[from Eqn. (153)]} \\ J_3 &= J_b(N_b/N_a)^2, & . & . & \text{[from Eqn. (153)]} \\ J_4 &= J_c \text{ (since } J_a \text{ and } J_c \text{ are attached to the same shaft),} \\ C_1 &= C_a, \\ C_2 &= C_b(N_b/N_a)^2, & . & . & \text{[from Eqn. (154)]} \\ C_3 &= C_c \text{ (since } N_c = N_a). \end{aligned}$$

The natural frequencies may be determined from Equation (160), using the above equivalent values.

This arrangement is found in marine installations of the type where an exhaust steam turbine is geared into the main propelling shaft between the direct-coupled main engine and the propeller (see Figs. 174 and 175).

- (ii) If the moments of inertia of the gears are negligible compared with those of the masses J_1 , J_3 , and J_4 , i.e. if $J_2 = 0$, Equation (160) reduces to

$$\begin{aligned} (J_1 + J_3 + J_4) - w_c^2[(J_3 + J_4)/w_1^2 + (J_1 + J_4)/w_2^2 \\ + (J_1 + J_3)/w_3^2] \\ + w_c^4[J_4/(w_1^2 \cdot w_2^2) + J_1/(w_2^2 \cdot w_3^2) + J_3/(w_1^2 \cdot w_3^2)] = 0. \quad (161) \end{aligned}$$

In this case there are two possible modes of vibration.

- (iii) If $J_b = J_c$, $N_b = N_c$, and $C_b = C_c$, i.e. $w_2 = w_3$, the system shown in Fig. 62*d* reduces to that shown in Figs. 62*g* or 62*h*.

The arrangement shown in Fig. 62*g* is typical of installations where two identical prime-movers are connected by gearing to a common transmission shaft, e.g. geared oil engines for marine propulsion.

The arrangement shown in Fig. 62*h* is found in motor-car transmission systems, where J_b is the moment of inertia of each rear wheel assembly, and C_b is the torsional rigidity of each back axle shaft.

The arrangements shown in Figs. 62*g* or 62*h* may be replaced by the equivalent system shown in Fig. 62*i*, in which all shafts

and all masses are assumed to rotate with the speed of shaft a , viz. N_a rev./min.,

$$\begin{aligned} \text{i.e.} \quad J_1 &= J_a, \\ J_2 &= [J_c + 2 \cdot J_a(N_b/N_a)^2], \\ J_3 &= 2 \cdot J_b(N_b/N_a)^2 = 2J_b, \\ C_1 &= C_a, \\ C_4 &= 2 \cdot C_b(N_b/N_a)^2 = 2C_2. \end{aligned}$$

[*Note*.—In the general case where there are n geared masses instead of only two, $J_2 = [J_c + n \cdot J_a(N_b/N_a)^2]$,

$$C_4 = n \cdot C_b(N_b/N_a)^2 \quad \text{and} \quad J_3 = n \cdot J_b(N_b/N_a)^2.]$$

The system therefore reduces to a three-mass system, and the natural frequencies may be obtained from Equation (155) by substituting J_5 for J_3 and C_4 for C_2 , i.e. $w_2^2 = C_4/J_5$.

Alternatively, the natural frequencies may be obtained from Equation (160). In applying Equation (160), however, it should be noted that in the present case $J_3 = J_4$ and $w_2 = w_3$, i.e. for the arrangement shown in Figs. 62*g* or 62*h*, Equation (160) reduces to

$$\begin{aligned} (J_1 + J_2 + 2 \cdot J_3) \\ - w_c^2 [(J_2 + 2 \cdot J_3)/w_1^2 + 2(J_1 + J_2 + J_3)/w_2^2] \\ + w_c^4 [2(J_2 + J_3)/w_1^2 \cdot w_2^2 + (J_1 + J_2)/w_2^4] \\ - w_c^6 \cdot J_2/w_1^2 \cdot w_2^4 = 0. \quad \dots \quad (162) \end{aligned}$$

Equation (162) shows that there are three possible modes of vibration, whereas Equation (155) indicates only two.

The third mode, however, is merely the natural frequency of mass J_b in Figs. 62*g* or 62*h* on its shaft regarded as fixed at the gearbox, viz.,

$$w_c^2 = C_b/J_b = C_4/J_5. \quad \dots \quad (163)$$

The other two frequencies given by Equation (162) have the same values as the two frequencies given by Equation (155).

It is simpler, therefore, to obtain the values of the three possible frequencies by applying Equations (155) and (163) rather than Equation (162).

Alternatively the natural frequencies and the shapes of the normal elastic curves can be obtained by applying the tabulation method to the equivalent system shown in Fig. 62*i*.

The tabulation method is also useful when there are several masses on each shaft.

In the case of two multi-cylinder engines geared to a common propeller shaft, it is important to remember, however, that in addition to the various modes of vibration obtained by applying the tabulation method to the complete equivalent system, there are other modes corresponding to vibration of the duplicated engine systems regarded as fixed at the gearbox.

The following special characteristic of an installation consisting of two identical oil engines geared into a common propeller shaft should be noted. If the crankshafts are set in phase (an arrangement commonly adopted to provide synchronised starting and manoeuvring), and the indicator diagrams from all cylinders are identical, those critical speeds corresponding to modes of vibration where the duplicated crank masses swing against each other about nodes at the gearbox are unexcitable. In the case of four-stroke cycle internal combustion engines corresponding cylinders of each engine must fire simultaneously for *all* harmonic orders to cancel, i.e. the firing interval between corresponding cylinders must be 0° and not 360° . The phasing of geared engines is considered in greater detail in Chapter 6.

(iv) If the moment of inertia of the gears in the arrangements shown in Figs. 62*g* and 62*h* is negligible, i.e. if $J_2 = 0$, the expression for calculating the natural frequencies reduces to

$$w_0^2 = w_2^2 \quad \text{or} \quad w_1^2 \cdot w_2^2 \left[\frac{J_1 + J_5}{J_1 \cdot w_1^2 + J_5 \cdot w_2^2} \right], \quad (164)$$

where $w_2^2 = C_b/J_b = C_4/J_5 =$ phase velocity of mass J_b on its shaft regarded as fixed at the gearbox.

In this case there are two possible values for the natural frequency; the lowest or fundamental value, $F = \frac{60 \cdot w_2}{2 \cdot \pi}$, corresponding to vibration about a single node situated at the gearbox.

- (v) Referring to Fig. 62*f*, if $J_1 = J_3 = J_4$ and $C_1 = C_2 = C_3$, i.e. $w_1 = w_2 = w_3$, the expression for calculating the natural frequencies reduces to

$$w_c^2 = w_1^2 \quad \text{or} \quad w_1^2 \frac{(3 \cdot J_1 + J_2)}{1} \quad . \quad . \quad (165)$$

In this case there are two possible values of the natural frequency; the fundamental value corresponding to vibration about a single node situated at the gearbox.

If the moment of inertia of the gears is negligible, Equation (165) reduces to

$$w_c^2 = w_1^2.$$

In this case there is only one value for the natural frequency, corresponding to vibration about a single node situated at the gearbox. The natural frequency of the whole system is therefore equal to the natural frequency of any one of the masses on its shaft regarded as fixed at the gearbox.

The foregoing methods of reducing the number of possible modes of vibration of a geared system by a suitable adjustment of the moments of inertia of one or more masses or of the elasticities of one or more shafts is the principal underlying the "nodal drive" originated by Dr. J. H. Smith in collaboration with Messrs. Workman, Clark & Co., Ltd., Belfast, for simplifying the problem of dealing with torsional vibrations of marine geared turbine installations.

EXAMPLE 36.—Calculate the natural frequencies of torsional vibration of the geared system of Example 35, assuming that mass J_3 is duplicated, i.e. the system becomes similar to that shown in Fig. 62*g*.

Referring to Figs. 62*g* and 62*i*, and using the values given in Example 35,

$$J_a = 2.7 \text{ tons-ft. sec.}^2,$$

$$J_b = 1.8 \text{ tons-ft. sec.}^2,$$

$$J_c = 1.6 \text{ tons-ft. sec.}^2,$$

$$J_d = 0.022 \text{ tons-ft. sec.}^2,$$

$$C_a = 1000 \text{ tons-ft. per radian,}$$

$$C_b = 600 \text{ tons-ft. per radian,}$$

and $N_b/N_a = 300/100 = 3/1.$

Hence, in Fig. 62*i*

$$\begin{aligned} J_1 &= J_a = 2.7 \text{ tons-ft. sec.}^2, \\ J_2 &= [J_c + 2 \cdot J_d(N_b/N_a)^2] = [1.6 + 2 \times 0.022 \times 3^2] \\ &= 2.0 \text{ tons-ft. sec.}^2, \\ J_3 &= 2 \cdot J_b(N_b/N_a)^2 = 2 \times 1.8 \times 3^2 \\ &= 32.4 \text{ tons-ft. sec.}^2, \\ C_1 &= C_a = 1000 \text{ tons-ft. per radian,} \\ C_4 &= 2 \cdot C_b(N_b/N_a)^2 = 2 \times 600 \times 3^2 \\ &= 10,800 \text{ tons-ft. per radian.} \end{aligned}$$

From Equation (163) :

$$\begin{aligned} w_c^2 &= C_4/J_3 = 10800/32.4 = 333, \\ w_c &= 18.25 \text{ radians/sec.,} \end{aligned}$$

$$\text{i.e. } F_c = \frac{60 \cdot w_c}{2 \cdot \pi} = 9.55 \times 18.25 = 174 \text{ vibs./min.}$$

From Equation (155) :

$$(J_1 + J_2 + J_3) - w_c^2(J_2/w_1^2 + J_3/w_1^2 + J_1/w_2^2 + J_2/w_2^2) + w_c^4 \cdot J_2/w_1^2 \cdot w_2^2 = 0,$$

$$\begin{aligned} \text{where } w_1^2 &= C_1/J_1 = 1000/2.7 = 370, \\ w_2^2 &= C_4/J_3 = 10800/32.4 = 333, \end{aligned}$$

$$\text{i.e. } (2.7 + 2.0 + 32.4) + w_c^2(2.0/370 + 32.4/370 + 2.7/333 + 2.0/333) + w_c^4 \cdot 2.0/(370 \times 333) = 0.$$

$$\begin{aligned} 37.1 - 0.1070 \cdot w_c^2 + 0.0000162 \cdot w_c^4 &= 0, \\ w_c^2 &= 367 \text{ or } 6238, \\ w_c &= 19.15 \text{ or } 79.0 \text{ radians/sec.,} \\ F_c &= 9.55 w_c \\ &= 183 \text{ or } 755 \text{ vibs./min.} \end{aligned}$$

The three possible values of the natural frequency of torsional vibration of this system are therefore 174, 183, and 755 vibs./min. The lowest or fundamental frequency, viz. 174 vibs./min., corresponds to vibration about a node situated at the gearbox.

Multi-Shaft Systems.—The system shown in Fig. 64 consists of n masses connected by n shafts to a common gearbox.

Let $J_1, J_2, J_3 \dots J_n$ = the equivalent polar moments of inertia of the elastically connected masses,

$C_1, C_2, C_3 \dots C_n$ = the equivalent torsional rigidities of the connecting shafts,

$J_{(n+1)}$ = the equivalent polar moment of inertia of the combined gear mass.

[*Note*.—The expression “equivalent” means that the actual values of these quantities have been reduced to equivalent values by taking into account the gear ratios, as already explained (see also Ex. 37).]

$\omega_1, \omega_2, \omega_3 \dots \omega_n$ = phase velocities of the natural vibration of each of the elastically connected masses on its shaft considered as fixed at the gearbox,

ω = phase velocity of natural vibration of the whole system.

Then $\omega_1^2 = C_1/J_1$; $\omega_2^2 = C_2/J_2$; $\omega_3^2 = C_3/J_3 \dots \omega_n^2 = C_n/J_n$,

and it can be shown that

$$J_{(n+1)} = \frac{C_1}{\omega^2 - \omega_1^2} + \frac{C_2}{\omega^2 - \omega_2^2} + \frac{C_3}{\omega^2 - \omega_3^2} \dots + \frac{C_n}{\omega^2 - \omega_n^2}. \quad (166)$$

For example, in the case of a two shaft system,

$$J_3 = \frac{C_1}{\omega^2 - C_1/J_1} + \frac{C_2}{\omega^2 - C_2/J_2},$$

which can be written

$$(J_1 + J_2 + J_3) - \omega^2(J_1/\omega_1^2 + J_2/\omega_2^2 + J_3/\omega_1^2 + J_3/\omega_2^2) + \omega^4 \cdot J_3/\omega_1^2 \cdot \omega_2^2 = 0.$$

This is the same as Equation (155) when the slight difference in notation is taken into account.

The following special cases should be noted:—

When $\omega_1 = \omega_2 = \omega_3 = \dots = \omega_n = \Omega$,

$$(\omega^2 - \Omega^2)^n \left\{ J_{(n+1)} - \frac{(C_1 + C_2 + C_3 + \dots + C_n)}{(\omega^2 - \Omega^2)} \right\} = 0, \quad (167)$$

$$\text{i.e. } \omega^2 = \Omega^2 \text{ or } \left[\frac{(C_1 + C_2 + C_3 + \dots + C_n)}{J_{(n+1)}} + \Omega^2 \right]. \quad (168)$$

For example, in a two-shaft system, the roots of Equation (167) become

$$\omega^2 = \Omega^2 \text{ or } \Omega^2 \left[\frac{J_1 + J_2 + J_3}{J_3} \right]. \quad (169)$$

The expression for the second root of Equation (167) can be written

$$\omega^2 = \Omega^2 \cdot \left[\frac{J_1 + J_2 + J_3 + \dots + J_n + J_{(n+1)}}{J_{(n+1)}} \right]. \quad (170)$$

This expression clearly shows that when $J_{(n+1)}$ is very large compared with $(J_1 + J_2 + J_3 + \dots + J_n)$, the second root of Equation (167) is very nearly equal to the first, irrespective of the number of shafts.

In general, therefore, a system of the type shown in Fig. 64, consisting of n shafts and $(n+1)$ masses may have as many different modes of natural vibration as there are shafts, i.e. n different modes, and it is necessary to ensure that excessive torque variation does not occur through resonance between the frequency of the torque impulses and the natural frequency of any one of these modes.

If, however, the characteristics of the system are chosen so that the natural frequency of each mass on its shaft regarded as fixed at the gearbox is the same for all the masses, then the possible number of modes of natural vibration of the system

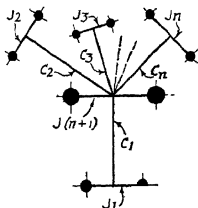


FIG. 64.—Multi-shaft system.

as a whole is reduced to two, irrespective of the number of masses. The natural frequency of one of these two modes is merely the natural frequency of each mass on its shaft regarded as fixed at the gearbox, as shown in Equation (168).

Furthermore, Equation (170) shows that if the moment of inertia of the gearbox masses is very large compared with the total moment of inertia of the elastically connected masses, then the natural frequencies of the two possible modes of vibration of the system as a whole are very nearly equal, and the

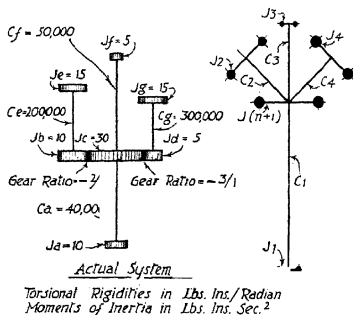


FIG. 65.—Four-shaft system.

torsional vibration characteristics of the system are not materially affected when one or more of the elastically connected masses is disconnected from the system.

It is therefore apparent that by tuning the system in this manner, either by adjusting the torsional rigidities of the several shafts, or by adjusting the moments of inertia of the several oscillating masses, or by adopting a particular gear ratio between one part of the system and another, or by combining these methods, the problem of avoiding dangerous resonant conditions may be considerably simplified.

Generally it will be found most convenient in practice to

adjust the torsional rigidities of the connecting shafts, for example, by inserting suitable flexible couplings in the shafts. Preferably these couplings should be constructed with a high damping capacity, for example, by incorporating springs having a non-linear load-deflection characteristic, or by incorporating a material having high internal damping capacity, such as rubber.

EXAMPLE 37.—Calculate the natural frequencies of torsional vibration of the four-shaft geared system shown in Fig. 65.

The equivalent system is obtained by replacing the side shaft masses and shafts by equivalent masses and shafts rotating at the speed of the centre shaft,

$$\begin{aligned} \text{i.e. } J_1 &= J_a = 10 \text{ lbs.-ins. sec.}^2, \\ J_2 &= J_e \cdot (2^2) = 4 \times 15 = 60 \text{ lbs.-ins. sec.}^2, \\ J_3 &= J_f = 5 \text{ lbs.-ins. sec.}^2, \\ J_4 &= J_g \cdot (3^2) = 9 \times 15 = 135 \text{ lbs.-ins. sec.}^2, \\ J_{(n+1)} &= J_c + (2^2) \cdot J_b + (3^2) \cdot J_d = 30 + (4 \times 10) \\ &\quad + (9 \times 5) = 115 \text{ lbs.-ins. sec.}^2, \\ C_1 &= C_a = 40,000 \text{ lbs.-ins./radian}, \\ C_2 &= C_e \cdot (2^2) = 4 \times 200,000 = 800,000 \text{ lbs.-ins./radian}, \\ C_3 &= C_f = 50,000 \text{ lbs.-ins./radian}, \\ C_4 &= C_g \cdot (3^2) = 9 \times 300,000 = 2,700,000 \\ &\quad \text{lbs.-ins./radian}. \end{aligned}$$

$$\begin{aligned} \text{Hence, } \omega_1^2 &= C_1/J_1 = 40,000/10 = 4000, \\ \omega_2^2 &= C_2/J_2 = 800,000/60 = 13,333, \\ \omega_3^2 &= C_3/J_3 = 50,000/5 = 10,000, \\ \omega_4^2 &= C_4/J_4 = 2,700,000/135 = 20,000. \end{aligned}$$

The frequency equation is obtained by inserting the above values in Equation (166),

$$\text{i.e. } 115 = \frac{40000}{\omega^2 - 4000} + \frac{800000}{\omega^2 - 13333} + \frac{50000}{\omega^2 - 10000} + \frac{2700000}{\omega^2 - 20000}.$$

Whence, by trial and error,

$$\begin{aligned} \omega^2 &= 4105, 10,080, 14,650, \text{ or } 49,700, \\ \text{or } \omega &= 64.1, 100.4, 121.0, \text{ or } 222.7 \text{ radians/sec.}, \\ \text{and } F &= 9.55\omega = 612, 960, 1156, \text{ or } 2127 \text{ vibs./min.} \end{aligned}$$

EXAMPLE 38.—Calculate the necessary torsional rigidities of the flexible couplings which must be inserted in three of the shafts of the system shown in Fig. 65 so that the natural frequencies of each mass on its shaft regarded as fixed at the gearbox are equal. Calculate also the natural frequencies of this modified system.

Since the alteration is to be made by inserting flexible couplings in three of the four shafts of the system shown in Fig. 65, it is necessary to choose as basis the shaft and mass giving the lowest frequency when the shaft is regarded as fixed at the gearbox. From Example 37 it is seen that mass J_a on shaft C_a has the lowest frequency when the shaft is regarded as fixed at the gearbox,

i.e. from Example 37, $\omega_1^2 = \Omega^2 = 4000$.

Let C_e' = modified value of C_e ,
 C_f' = modified value of C_f ,
 C_g' = modified value of C_g .

Then, since all masses on their shafts regarded as fixed at the gearbox must have the same natural frequency, i.e. the same value of ω^2 ,

Shaft C_e : $C_e'/J_e = C_e'/15 = 4000$,

i.e. $C_e' = 60,000$ lbs.-ins. per radian.

Also, $1/C_e' = 1/C_e + 1/C_e''$, [from Eqn. (77)],

i.e. $1/60,000 = 1/200,000 + 1/C_e''$.

Hence, $C_e'' = 85,700$ lbs.-ins. per radian,

where C_e'' = required torsional rigidity of flexible coupling in shaft C_e .

Shaft C_f : $C_f'/5 = 4000$, or $C_f' = 20,000$ lbs.-ins. per radian.

Also, $1/C_f' = 1/C_f + 1/C_f''$,

i.e. $1/20,000 = 1/50,000 + 1/C_f''$,

whence $C_f'' = 33,400$ lbs.-ins. per radian,

where C_f'' = required torsional rigidity of flexible coupling in shaft C_f .

Shaft C_g : $C_g'/15 = 4000$, or $C_g' = 60,000$ lbs.-ins. per radian.

Also, $1/C_g' = 1/C_g + 1/C_g''$,
 i.e. $1/60,000 = 1/300,000 + 1/C_g''$,
 whence $C_g'' = 75,000$ lbs.-ins. per radian,
 where $C_g'' =$ required torsional rigidity of flexible coupling on shaft C_g .

Natural Frequencies of Complete System.—The various quantities in the equivalent system shown in Fig. 65, given in Example 37, are modified as follows by the above alterations:—

$C_1 = C_a = 40,000$ lbs.-ins./radian, as before, since this is the basic shaft.

$C_2 = C_g'(2^2) = 240,000$ lbs.-ins./radian.

$C_3 = C_g' = 20,000$ lbs.-ins./radian.

$C_4 = C_g'(3^2) = 540,000$ lbs.-ins./radian.

The moments of inertia of the masses are unaltered, i.e.

$J_1 = 10$; $J_2 = 60$; $J_3 = 5$; $J_4 = 135$; and $J_{(n+1)} = 115$
 lbs.-ins. sec.²,

and $\omega_1^2 = \omega_2^2 = \omega_3^2 = \omega_4^2 = \Omega^2 = 4000$.

Hence, from Equation (168),

$$\omega^2 = 4000 \text{ or } \left(\frac{40000 + 240000 + 20000 + 540000}{115} + 4000 \right)$$

$$= 4000 \text{ or } 11,300,$$

i.e. $\omega = 63.2$ or 106.3 radians/sec.,

and $F = 603$ or 1015 vibs./min.

In this case, therefore, there are only two modes of natural torsional vibration compared with four in the previous example. One of these modes is merely the vibration of each duplicated branch regarded as fixed at the gearbox. The two natural frequencies can be brought closer together by increasing the moment of inertia of the gears, as already explained.

Thus, if the equivalent moment of inertia of the gears is increased tenfold the frequencies become 603 and 688 vibs./min., a difference of only 14 per cent.

Multi-Shaft Systems : Tabulation Method.—The natural frequencies of the multi-shaft system shown in Fig. 65 can be determined by the tabulation method, as shown in the following Tables :—

TABLE 26.

FREQUENCY TABULATION : MASSES J_a AND J_c ON SHAFT C_a .F = 2127 Vibs. Min. : $\omega^2 = 49,700$.

J.	$J.\omega^2$.	θ .	$J.\omega^2.\theta$.	$\Sigma J.\omega^2.\theta$.	C.	$\Sigma J.\omega^2.\theta/C$.
10	497,000	1.00	497,000	497,000	40,000	12.42
30	1,491,000	-11.42	-17,012,000	-16,515,000	—	—

i.e. $\theta_c =$ specific amplitude at $J_c = -11.42$,
 $T_1 =$ resultant specific torque due to vibration of J_a and J_c
 $= -16,515,000$.

TABLE 27.

FREQUENCY TABULATION : MASS J_f ON SHAFT C_f .

J.	$J.\omega^2$.	θ .	$J.\omega^2.\theta$.	$\Sigma J.\omega^2.\theta$.	C.	$\Sigma J.\omega^2.\theta/C$.
5	248,500	α	248,500 . α	248,500 . α	50,000	4.97 . α
—	—	-3.97 . α	—	—	—	—

i.e. $\theta_c =$ specific amplitude at $J_c = -3.97 . \alpha$,but, from Table 26, $\theta_c = -11.42$,hence, $-3.97 . \alpha = -11.42$, or $\alpha = 2.88$,

i.e. Table 27 becomes

5	248,500	2.88	715,000	715,000	50,000	14.30
—	—	-11.42	—	—	—	—

i.e. $T_2 =$ resultant specific torque due to vibration of J_f
 $= 715,000$.

TABLE 28.
FREQUENCY TABULATION: MASSES J_b AND J_c ON SHAFT C_e .

J.	$J \cdot \omega^2$.	θ .	$J \cdot \omega^2 \cdot \theta$.	$\Sigma J \cdot \omega^2 \cdot \theta$.	C.	$\Sigma J \cdot \omega^2 \cdot \theta / C$.
15	745,500	β	$745,500 \cdot \beta$	$745,500 \cdot \beta$	200,000	$3.73 \cdot \beta$
10	497,000	$-2.73 \cdot \beta$	$-1,355,000 \cdot \beta$	$-609,500 \cdot \beta$	—	—

i.e. $\theta_b =$ specific amplitude at $J_b = -2.73 \cdot \beta$.

The gear ratio between J_c and J_b is $-2/1$,

hence $\theta_b = -2 \cdot \theta_c = 2 \times 11.42 = 22.84$,

or $-2.73 \cdot \beta = 22.84$,

and $\beta = -8.36$,

i.e. Table 28 becomes

15	745,500	-8.36	-6,240,000	-6,240,000	200,000	-31.20
10	497,000	22.84	11,390,000	5,150,000	—	—

i.e. $T_3 =$ resultant specific torque due to vibration of J_b and J_c
 $= 5,150,000$.

TABLE 29.
FREQUENCY TABULATION: MASSES J_d AND J_e ON SHAFT C_e .

J.	$J \cdot \omega^2$.	θ .	$J \cdot \omega^2 \cdot \theta$.	$\Sigma J \cdot \omega^2 \cdot \theta$.	C.	$\Sigma J \cdot \omega^2 \cdot \theta / C$.
15	745,500	δ	$745,500 \cdot \delta$	$745,500 \cdot \delta$	300,000	$2.48 \cdot \delta$
5	248,500	$-1.48 \cdot \delta$	$-367,000 \cdot \delta$	$378,500 \cdot \delta$	—	—

i.e. $\theta_d =$ specific amplitude at $J_d = -1.48 \cdot \delta$.

The gear ratio between J_e and J_d is $-3/1$,

hence $\theta_d = -3 \cdot \theta_e = 3 \times 11.42 = 34.26$,

or $-1.48 \cdot \delta = 34.26$,

and $\delta = -23.10$,

i.e. Table 29 becomes

15	745,500	-23.10	-17,200,000	-17,208,000	300,000	-57.36
	244,500	34.26	8,508,000	-8,700,000	—	—

i.e. $T_4 =$ resultant specific torque due to vibration of J_d and J_g
 $= -8,700,000.$

Having selected a trial value for the frequency of the system, Tables 26 to 29 are built up as follows:—

Table 26.—This is the basic table and is compiled by selecting one of the branches of the geared system and assuming unit amplitude at the mass at the free end of this branch. In the present example shaft C_a has been chosen as the basic branch, although any other branch could have been selected. The basic table terminates at the point where the other branches join the basic branch. Any continuation of the basic branch beyond the point at which the other branches join it, as in this example, is itself to be regarded as another branch having a gear ratio of $1/x$. Table 26 gives the specific amplitude at the point where the other branches join the basic branch and also the resultant specific torque, i.e. the torque for unit deflection at the free end of the basic branch, due to vibration of all masses on the basic branch.

Table 27.—This table applies to the continuation of the basic shaft, i.e. to mass J_f on shaft C_f , and is commenced by assuming an amplitude α at the free end of the branch. The table then gives the amplitude at the point where this branch joins the basic branch in terms of α .

The absolute value of α is determined from the value obtained for the amplitude at the junction point from Table 26, taking care to allow for the gear ratio between the basic branch and the branch under consideration. In the case of Table 27 the gear ratio is $1/x$ since this branch is merely a continuation of the basic branch.

When the numerical value of α is known Table 27 is completed and gives the value of the resultant specific torque due to vibration of all masses on this branch.

Tables 28 and 29 are compiled in the same way as Table 27, by assuming amplitudes β and δ at the free ends of the respective branches and equating the corresponding amplitudes at the point where the branches join the basic branch to the known amplitude at this point, given by Table 26, taking care to allow for the gear ratios between the subsidiary branches and the basic branch. Note that since the driving and driven shafts rotate in opposite directions the gear ratios are negative.

The foregoing method of compiling the frequency tables ensures that the geometrical relationships between the various component parts of the geared system are maintained.

If the value selected for the frequency of the system is in fact the frequency of one of the modes of natural vibration of the system there will be no external torque acting on the system, and this is the criterion which must now be applied to the results given by Tables 26 to 29.

From these Tables we have—

T_1 = resultant specific torque due to vibration of all masses on the basic branch = - 16,515,000.

T_2 = resultant specific torque due to vibration of all masses on shaft $C_1 = 715,000$, and since the gear ratio between this branch and the basic branch is $1/1$, the resultant specific torque referred to the basic branch is

$$T_2' = 1 \times 715,000 = 715,000.$$

T_3 = resultant specific torque due to vibration of all masses on shaft $C_2 = 5,150,000$, and since the gear ratio between this branch and the basic branch is $-2/1$, the resultant specific torque referred to the basic branch is

$$T_3' = -2 \times 5,150,000 = -10,300,000.$$

T_4 = resultant specific torque due to vibration of all masses on shaft $C_3 = -8,700,000$, and since the gear ratio between this branch and the basic branch is $-3/1$, the resultant specific torque referred to the basic branch is

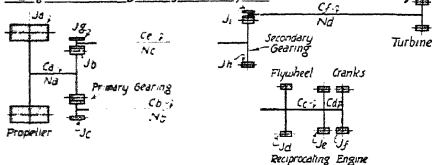
$$T_4' = 3 \times 8,700,000 = 26,100,000.$$

Hence, resultant specific torque for whole system,

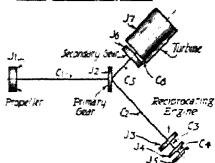
$$\begin{aligned}\Sigma T &= T_1 - T_2' - T_3' - T_4' \\ &= -16,515,000 - 715,000 - 10,300,000 + 26,100,000 \\ &= 0,\end{aligned}$$

i.e. the selected value is the natural frequency of one of the modes of vibration of the whole system.

I Diagrammatic Arrangement of Actual System



Equivalent System Referred to Propeller Shaft Speed



Approximate Equivalent System Referred to Propeller Shaft Speed

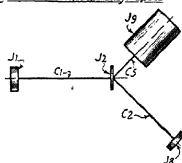


FIG. 66.—Geared marine installation.

The specific amplitudes at all masses, i.e. the amplitudes for unit amplitude at mass \$J_a\$ on the basic shaft, are given in the tables, and these enable the normal elastic curves to be plotted and the positions of the nodes to be determined. The tables also give the actual specific torques at all points in the system.

The tabulation method can be extended to deal with systems having any number of branches with any number of masses on each branch. In a great many practical cases, however,

the actual system can be reduced to a simpler equivalent system which can be treated by the shorter methods and formulæ previously described. In cases where the tabulation method is necessary, however, the arithmetical work can be reduced by applying the shorter methods to an approximately equivalent system. This will give some indication of the frequency values to be assumed in compiling the frequency tables.

The following example illustrates the application of the foregoing methods to a typical geared installation from marine engineering practice.

EXAMPLE 39.—Determine the natural frequencies of the principal modes of vibration of the system shown in Fig. 66, assuming the following data :—

Moments of Inertia of Masses.

$J_a = 810.0$ lbs.-ft. sec. ²
$J_b = 82.0$
$J_s = 3.0$
$J_d = 33.5$
$J_e = 19.5$
$J_f = 19.5$
$J_g = 0.3$
$J_h = 25.0$
$J_i = 0.03$
$J_j = 6.8$

Torsional Rigidities of Shafts.

$C_a = 455,000$ lbs.-ft. radian
$C_b = 145,000$
$C_s = 2,940,000$
$C_d = 5,725,000$
$C_e = 162,000$
$C_f = 179,500$

Speeds of Shafts.

$N_a = 110$ revs./min.
$N_b = 255$
$N_e = 530$
$N_d = 4,500$

This system consists of a steam turbine (mass J_j) and a reciprocating steam engine (masses J_d , J_e , and J_f), geared into a common propeller shaft.

The turbine is connected through double reduction gearing and the reciprocating engine through single reduction gearing. Flexible couplings are provided between the turbine and the secondary pinion; between the reciprocating engine flywheel and the engine pinion; and between the primary gearwheel and the propeller. The flexibility between the engine flywheel and the engine pinion is further increased by a quill shaft, and a quill shaft is also provided between the secondary gearwheel and the primary pinion in the turbine drive. The

torsional rigidities given above include allowances for these flexible couplings and quill shafts.

Approximate Calculation of Natural Frequencies.—The first step is to reduce the whole system to an equivalent system referred to propeller shaft speed, because this will enable the principal characteristics of the system to be judged for the purpose of reducing it to the simplest possible approximately equivalent system.

The equivalent system is determined by the methods already described, as follows :—

Diagram I in Fig. 66 shows the actual system in diagram form, whilst Diagram II shows the equivalent system referred to propeller shaft speed, N_a .

In Diagram II :

$$J_1 = J_a = 810 \text{ lbs.-ft. sec.}^2.$$

$$\begin{aligned} J_2 &= J_b + J_e(N_b/N_a)^2 + J_g(N_e/N_a)^2 \\ &= 82 + 3(255/110)^2 + 0.3(530/110)^2 \\ &= 105 \text{ lbs.-ft. sec.}^2. \end{aligned}$$

$$J_3 = J_d(N_b/N_a)^2 = 33.5(255/110)^2 = 180 \text{ lbs.-ft. sec.}^2.$$

$$J_4 = J_f = J_c(N_b/N_a)^2 = 19.5(255/110)^2 = 105 \text{ lbs.-ft. sec.}^2.$$

$$\begin{aligned} J_6 &= J_h(N_e/N_a)^2 + J_i(N_d/N_a)^2 = 25(530/110)^2 \\ &\quad + 0.03(4500/110)^2 \\ &= 630 \text{ lbs.-ft. sec.}^2. \end{aligned}$$

$$J_7 = J_j(N_d/N_a)^2 = 6.8(4500/110)^2 = 11,370 \text{ lbs.-ft. sec.}^2.$$

$$C_1 = C_a = 455,000 \text{ lbs.-ft./radian.}$$

$$\begin{aligned} C_2 &= C_b(N_b/N_a)^2 = 145,000(255/110)^2 \\ &= 780,000 \text{ lbs.-ft./radian.} \end{aligned}$$

$$\begin{aligned} C_3 &= C_e(N_b/N_a)^2 = 2,940,000(255/110)^2 \\ &= 15,800,000 \text{ lbs.-ft./radian.} \end{aligned}$$

$$\begin{aligned} C_4 &= C_d(N_b/N_a)^2 = 5,725,000(255/110)^2 \\ &= 30,800,000 \text{ lbs.-ft./radian.} \end{aligned}$$

$$\begin{aligned} C_5 &= C_g(N_e/N_a)^2 = 162,000(530/110)^2 \\ &= 3,750,000 \text{ lbs.-ft./radian.} \end{aligned}$$

$$\begin{aligned} C_6 &= C_j(N_d/N_a)^2 = 179,500(4500/110)^2 \\ &= 300,000,000 \text{ lbs.-ft./radian.} \end{aligned}$$

The flywheels representing the various masses in Diagram II of Fig. 66 are approximately to scale, and from this diagram and the above values of the equivalent moments of inertia and torsional rigidities, it is seen that the system reduces to a three branched arrangement, the junction of the three branches being at the primary gearwheel.

The propeller shaft branch consists of a single mass, the propeller, flexibly connected to the primary gearwheel.

The turbine branch consists of two masses, the turbine itself, and the secondary gear assembly, connected by a shaft of comparatively small flexibility to the main gearwheel.

The reciprocating engine branch consists of three masses, the engine crank masses and the flywheel, flexibly connected to the main gearwheel.

Since the equivalent torsional rigidity of the shaft connecting the turbine to the secondary gear assembly is very large compared with that of the shaft connecting the secondary gear assembly to the primary gearwheel, there will not be much error in regarding the turbine and the secondary gear assembly as one mass.

Similarly, since the equivalent torsional rigidities of the shafts connecting the crank masses and flywheel of the reciprocating engine are very large compared with that of the shaft connecting the flywheel to the main gearwheel, there will not be much error in regarding the two engine crank masses and the flywheel mass as one mass.

Hence the equivalent system shown at II in Fig. 66 can be replaced by the approximately equivalent system shown at III, without introducing much error.

In Diagram III of Fig. 66 :

$$\begin{array}{ll}
 J_1 = 810 \text{ lbs.-ft. sec.}^2, & C_1 = 455,000 \text{ lbs.-ft./radian,} \\
 J_2 = 105, & C_2 = 780,000, \\
 J_3 = J_3 + J_4 + J_5 & C_3 = 3,750,000. \\
 = 180 + 105 + 105 = 390, & \\
 J_6 = J_6 + J_7 = 630 + 11,370 & \\
 = 12,000. &
 \end{array}$$

The natural frequencies can now be determined by means of Equation (166),

$$\text{i.e.} \quad J_{(n-1)} = \frac{C_1}{\omega^2 - \omega_1^2} + \dots + \frac{C_n}{\omega^2 - \omega_n^2} \quad (166)$$

where, in this case,

$$\omega_1^2 = C_1 J_1 = 455,000,810 = 562,$$

$$\omega_2^2 = C_2 J_2 = 780,000,390 = 2000,$$

$$\omega_3^2 = C_3 J_3 = 3,750,000,12,000 = 312,$$

$$J_{(n-1)} = J_2 = 105.$$

Hence, the frequency equation is

$$105 = \frac{455000}{\omega^2 - 562} + \frac{780000}{\omega^2 - 2000} + \frac{3750000}{\omega^2 - 312}.$$

Inspection of Diagram III of Fig. 66 indicates that because of the very large moment of inertia of the turbine and because this inertia is connected to the primary gearwheel by a shaft which is much more rigid than the other two shafts, the frequencies of two of the principal modes of vibration of the system will probably be very nearly the same as the frequencies of the propeller and reciprocating masses on their shafts regarded as fixed at the primary gearwheel, i.e. $\omega^2 = 562$ and 2000 respectively, or $F = 226$ and 427 vibs./min. These values are a useful aid in solving the frequency equation.

The true values of the three roots of the frequency equation are

$$\omega^2 = 534, 1733, \text{ and } 48,000,$$

$$\text{i.e.} \quad \omega = 23.1, 41.6, \text{ and } 219 \text{ radians/sec.},$$

or $F = 221, 397, \text{ or } 2090$ vibs./min., corresponding to vibration with one, two, and three nodes respectively.

Tabulation Method.—This is essentially a trial and error process, although in most cases the values obtained from an

approximately equivalent system, such as that shown at III in Fig. 66, will considerably reduce the amount of labour involved in determining the final tabulations for each mode of vibration.

The following tables show the final frequency tabulation for the three-node mode of vibration of the system shown at I in Fig. 66. The value of ω^2 determined by the tabulation method is 47,500, corresponding to a three-node frequency of 2080 vibs./min., which is very nearly the same as the value determined from the approximately equivalent system shown at III in Fig. 66.

In the following tabulations the reciprocating engine branch has been taken as the basic branch:—

TABLE 30.

FREQUENCY TABULATION: RECIPROCATING ENGINE BRANCH.

$$F = 2080 \text{ Vibs./Min.}; \omega^2 = 47,500.$$

Mass.	J.	J. ω^2 .	θ .	J. $\omega^2 \theta$.	$\Sigma J. \omega^2 \theta$.	C.	$\Sigma J. \omega^2 \theta / C$.
J_f	19.5	926,000	1.0000	926,000	926,000	5,725,000	0.1618
J_e	19.5	926,000	0.8382	776,000	1,702,000	2,940,000	0.5790
J_g	33.5	1,590,000	0.2592	412,000	2,114,000	145,000	14.580
J_e	3.0	142,500	-14.3208	-2,040,750	73,250	—	—

i.e. $\theta_1 =$ specific amplitude at engine pinion = -14.3208,

$T_1 =$ specific torque at engine pinion = 73,250,

and since gear ratio = -110/255 = -1/2.32 (negative because driving and driven shafts rotate in opposite directions),

hence, $\theta_1' =$ specific amplitude at primary wheel

$$= 14.3208/2.32 = 6.175,$$

$T_1' =$ specific torque at primary wheel

$$= -73,250 \times 2.32 = -170,000.$$

TABLE 31.

FREQUENCY TABULATION: TURBINE BRANCH.

Mass.	J.	J. ω ² .	θ.	J. ω ² . θ.	ΣJ. ω ² . θ.	C.	ΣJ. ω ² . θ/C.
J ₁	6.5	323,000	α	323,000α	323,000α	179,500	1.800α
J ₂	0.03	1,425	-0.800. α	-1,140α	321,860α	—	—
<i>Secondary Gear Ratio = - 530,4500 = - 1/8.5.</i>							
J ₃	25.0	1,187,000	0.8α 8.5 = 0.094α	111,700α	-8.5 (321,860α) + 111,700α = -2,618,300α	162,000	-16.15
J ₄	0.3	14,250	16.244α	231,500α	-2,386,800α	—	—

and since gear ratio = $-110/530 = -1/4.82$ (negative because driving and driven shafts rotate in opposite directions),

θ_2' = specific amplitude at primary wheel =

$$-16.244\alpha/4.82 = -3.375\alpha,$$

i.e. $-3.375\alpha = 6.175$, from Table 30,

or $\alpha = -1.83$.

Hence, Table 31 becomes

6.5	323,000	-1.83	-591,000	-591,000	179,500	-3.295	
0.03	1,425	1.465	2,085	-588,915	—	—	
<i>Gear Ratio = - 1/8.5.</i>							
25.0	1,187,000	-0.172	-204,500	4,795,500	162,000	29.6	
0.3	14,250	-29.772	-423,500	4,372,000	—	—	

i.e. θ_2 = specific amplitude at turbine primary pinion =

$$-29.772$$

T_2 = specific torque at turbine primary pinion = 4,372,000,

and since gear ratio = $-110.530 = -1/4.82$,
 hence, $\theta_2' =$ specific amplitude at primary wheel
 $= 29.772/4.82 = 6.175$,
 $T_2' =$ specific torque at primary wheel
 $= -4,372,000 \times 4.82$
 $= -21,070,000$.

TABLE 32.

FREQUENCY TABULATION : PROPELLER BRANCH.

Mass.	J.	J. ω^2 .	δ .	J. $\omega^2 \cdot \delta$.	$\Sigma J. \omega^2 \cdot \delta$.	C.	$\Sigma J. \omega^2 \cdot \delta / C$.
J _a	810	38,500,000	δ	38,500,000 δ	38,500,000 δ	455,000 δ	84.6 δ
J _b	82	3,890,000	$-83.6 \cdot \delta$	$-325,000,000\delta$	$-286,500,000\delta$	—	—

i.e. $\theta_3 =$ specific amplitude at primary wheel = -83.6δ
 $= 6.175$, from Table 30,
 or, $\delta = -6.175/83.6 = -0.074$.

Hence, Table 32 becomes

810	38,500,000	-0.074	$-2,840,000$	$-2,840,000$	455,000	-6.249
82	3,890,000	6.175	$24,080,000$	$21,240,000$	—	—

i.e. $T_3 =$ specific torque at primary wheel = $21,240,000$.
 The resultant torque due to vibration of all the masses in the system is

$$\Sigma T = (T_1' + T_2' + T_3) = -170,000 - 21,070,000 + 21,240,000 = 0.$$

Hence the selected value $\omega^2 = 47,500$ corresponds to one of the modes of torsional vibration of the system. The specific amplitudes and torques at all points in the system are given in the above tables, the former indicating that there are three nodes, one in the shaft connecting the engine flywheel to the engine pinion, one in the shaft connecting the turbine to the secondary pinion, and one in the shaft connecting the propeller to the primary gearwheel.

Table 33 contains the final frequency tabulations for the three principal modes of torsional vibration of the system shown in Fig. 66. The locations of the nodes are shown in the diagram at the foot of each tabulation. For the one-node mode the node is located in the shaft between the secondary gearwheel and the primary turbine pinion. For the two-node mode there is one node in the shaft between the secondary gearwheel and the primary turbine pinion, and one in the shaft between the propeller and the primary gearwheel. For the three-node mode one node is in the shaft between the turbine and the secondary turbine pinion, one in the shaft between the reciprocating engine and its pinion, and one in the shaft between the propeller and the primary gearwheel.

The following general conclusion can be deduced from the shapes of the normal elastic curves in the dynamically equivalent system, i.e. the equivalent system in which the masses are assumed to have the same angular velocity. In this example the propeller shaft is chosen as the reference shaft and the normal elastic curves in the dynamically equivalent system referred to propeller shaft speed are also shown at the foot of Table 33.

One-Node Mode.—Since the specific amplitude at the propeller is considerably larger than that at any other point in the dynamically equivalent system the principal forcing and damping torques are those originated by the propeller.

Furthermore, the most effective method of altering the tuning of the one-node mode of vibration of this installation is either to alter the polar moment of inertia of the propeller or to alter the torsional rigidity of the propeller shaft. Due to the small specific amplitudes at the turbine and reciprocating engine (in the dynamically equivalent system), changes in the moment of inertia of either of these masses will produce comparatively small changes in the tuning of the one-node frequency.

Two-Node Mode.—In this case the normal elastic curves in the dynamically equivalent system indicate that the specific amplitude is considerably greater at the reciprocating engine than at any other point in the system. Hence the principal

TABLE 33.

FREQUENCY TABULATIONS: MARINE-GEARED INSTALLATION.

One-Node Mode; $F = 221$ Vibs./Min.; $\omega^2 = 533$.

Mass.	J.	J. ω^2 .	θ .	J. $\omega^2 \theta$.	$\Sigma J. \omega^2 \theta$.	C.	$\frac{\Sigma J. \omega^2 \theta}{C}$.
RECIPROCATING ENGINE BRANCH.							
J_1	19.5	10,400	1.0000	10,400	10,400	5,725,000	0.0018
J_2	19.5	10,400	0.9982	10,390	20,790	2,940,000	0.0071
J_3	33.5	17,900	0.9911	17,750	38,540	145,000	0.2660
J_4	3.0	1,600	0.7251	1,160	38,800	—	—
Gear Ratio = -1/2.32.							
$\theta_1' = -\frac{0.7251}{2.32} = -0.313$; $T' = -38,800 \times 2.32 = -90,000$.							
TURBINE BRANCH.							
J_1	6.8	3,630	17.600	64,000	64,000	179,500	0.356
J_2	0.03	16	17.244	276	64,276	—	—
Gear Ratio = -1/8.5.							
J_3	25.0	13,300	-2.025	-26,900	-573,900	162,000	-3.54
J_4	0.3	160	1.515	242	-573,658	—	—
Gear Ratio = -1/4.82.							
$\theta_2' = -\frac{1.515}{4.82} = -0.313$; $T_2' = 573,658 \times 4.82 = 2,760,000$.							
PROPELLER BRANCH.							
J_1	810	432,000	-6.150	-2,656,300	-2,656,300	455,000	-5.837
J_2	82	43,700	-0.313	-13,700	-2,670,000	—	—
$T_3 = -2,670,000$; i.e. $(T_1' + T_2' + T_3) = 0$.							

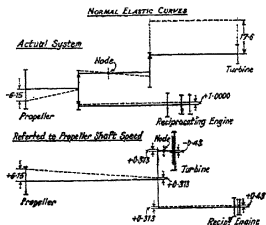


TABLE 33 (continued).

Two-Node Mode; $F = 395$ Vibs./Min.; $\omega^2 = 1710$.

Mass.	J.	J. ω^2 .	θ .	J. ω^2 . θ .	$\Sigma J.\omega^2$. θ .	C.	$\frac{\Sigma J.\omega^2.\theta}{C}$.
RECIPROCATING ENGINE BRANCH.							
J_f	19.5	33,350	1.0000	33,350	33,350	5,725,000	0.0058
J_e	19.5	33,350	0.9942	33,100	66,450	2,940,000	0.0226
J_d	33.5	57,300	0.9716	55,700	122,150	145,000	0.8420
J_c	3.0	5,130	0.1296	666	122,816	—	—
Gear Ratio = $-1/2.32$.							
$\theta_1' = -\frac{0.1296}{2.32} = -0.056$; $T_1' = -122,816 \times 2.32 = -284,200$.							
TURBINE BRANCH.							
J_j	6.8	11,620	0.507	5,916	5,916	179,500	0.033
J_i	0.03	51	0.474	24	5,940	—	—
Gear Ratio = $-1/8.5$.							
J_k	25.0	42,800	-0.056	-2,390	-52,938	162,000	-0.325
J_v	0.3	513	0.269	138	-52,800	—	—
Gear Ratio = $-1/4.82$.							
$\theta_2' = -\frac{0.269}{4.82} = -0.056$; $T_2' = 52,800 \times 4.82 = 254,220$.							
PROPELLER BRANCH.							
J_a	810	1,385,000	0.027	37,800	37,800	455,000	0.083
J_b	82	140,000	-0.056	-7,820	29,980	—	—
$T_3 = 29,980$; i.e. $(T_1' + T_2' + T_3) = 0$.							

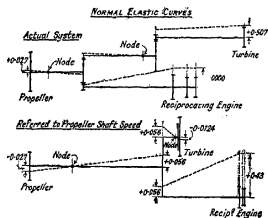
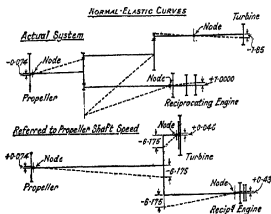


TABLE 33 (continued).

Three-Node Mode; $F = 2,080$ Vibs./Min.; $\omega^2 = 47,300$.

Mass.	J.	J. ω^2 .	θ .	J. $\omega^2 \theta$.	$\Sigma J. \omega^2 \theta$.	C.	$\frac{\Sigma J. \omega^2 \theta}{C}$.
RECIPROCATING ENGINE BRANCH.							
J_r	19.5	926,000	1.0000	926,000	926,000	5,725,000	0.1618
J_e	19.5	926,000	0.8382	776,000	1,702,000	2,940,000	0.5790
J_s	33.5	1,590,000	0.2592	412,000	2,114,000	145,000	14.580
J_e	3.0	142,500	-14.3208	-2,040,750	73,250	—	—
Gear Ratio = -1/2.32.							
$\theta_1' = \frac{14.3208}{2.32} = 6.175$; $T_1' = -73,250 \times 2.32 = -170,000$.							
TURBINE BRANCH.							
J_f	6.8	323,000	-1.830	-591,000	-591,000	179,500	-3.295
J_t	0.03	1,425	1.465	2,085	-588,915	—	—
Gear Ratio = -1/8.5.							
J_b	25.0	1,187,000	-0.172	-204,500	4,795,500	162,000	29.6
J_f	0.3	14,250	-29.772	-423,500	4,372,000	—	—
Gear Ratio = -1/4.82.							
$\theta_2' = \frac{29.772}{4.82} = 6.175$; $T_2' = -4,372,000 \times 4.82 = -21,070,000$.							
PROPELLER BRANCH.							
J_s	810	38,500,000	-0.074	-2,840,000	-2,840,000	455,000	-6.249
J_b	82	3,890,000	6.175	24,080,000	-21,240,000	—	—
$T_3 = 21,240,000$; i.e. $(T_1' + T_2' + T_3) = 0$.							



forcing and damping torques for this mode of vibration are those originated by the reciprocating engine. Due to the small specific amplitudes at the propeller and turbine these components are unlikely sources of excitation or damping. For the same reasons the most effective method of altering the tuning of the two-node mode of vibration is either to alter the polar moment of inertia of the reciprocating engine masses or to alter the torsional rigidity of the shaft connecting the engine flywheel to the engine pinion.

Three-Node Mode.—In this case the specific amplitude in the dynamically equivalent system is much greater at the primary gear masses than at any other point in the system. Hence the principal forcing and damping torques for this mode of vibration are those originated by the primary gears. Although there may be considerable damping action at the gears it is unlikely that any severe period disturbance will be originated by modern accurately cut gearing. For this reason it is unlikely that the system will be subjected to any severe resonant vibration of the three-node mode.

The most effective method of altering the tuning of the three-node mode of vibration is either to alter the polar moment of inertia of the primary gear masses, or to alter the torsional rigidity of the shaft connecting the primary turbine pinion to the primary gearwheel. Alterations in the moments of inertia of the propeller, turbine, or reciprocating masses are not likely to have much effect on the three-node vibration frequency due to the relatively small specific amplitudes at these points.

General.—A study of the normal elastic curves in the dynamically equivalent systems for this installation shows that alterations in propeller inertia will affect the tuning of the one-node mode of vibration without having much effect on the two- and three-node modes, and that propeller torque variation is the principal cause of excitation and damping of one-node vibrations.

Engine torque variation and torque variation due to errors in the construction of the gearing are not likely to have any pronounced effect in exciting one-node vibration due to the relatively small specific amplitudes at these points.

Alterations in the moment of inertia of the reciprocating engine masses will affect the tuning of the two-node mode of vibration without having much effect on the one- and three-node modes, and the principal cause of excitation and damping of two-node vibrations is that due to the reciprocating engine.

Propeller and gearing damping will be comparatively small, due to the relatively small specific amplitudes at these points.

Alterations in the moment of inertia of the turbine and secondary gearing will not have much effect on any mode of vibration, because in all cases the specific amplitudes at these points are relatively small. For the same reason, apart from the fact that the turbine exerts a sensibly constant torque, the turbine and secondary gearing are unlikely sources of excitation or damping.

Alterations in the moment of inertia of the primary gear masses alter the tuning of the three-node mode of vibration without having much effect on the one-node mode. They will also affect the two-node mode, but not to the same degree. Errors in the manufacture or erection of the primary gearing are the most effective sources of excitation of three-node vibrations, but such errors should not occur in modern gearing.

The principal source of damping of three-node vibrations is also at the primary gears, since the specific amplitude at this point is much greater than at any other part of the system.

It is also worth noting that the frequency of the propeller on the propeller shaft regarded as fixed at the gearbox is 226 vibs./min., which is only 2.5 per cent. greater than the one-node frequency given in Table 33.

Hence the characteristics of this installation, so far as one-node vibrations are concerned, can be examined with sufficient accuracy for practical purposes by regarding the propeller on its shaft as a separate system fixed at the gearbox. The amplitudes of the one-node critical speeds can then be determined from considerations of propeller excitation and damping forces acting on this separated system.

The frequency of the engine masses on the engine pinion shaft regarded as fixed at the gearbox is 427 vibs./min., which

is about 8 per cent. greater than the two-node frequency given in Table 33. Hence a good approximation to the characteristics of two-node vibration of this system will be obtained by regarding the engine on its shaft as a separate system fixed at the gearbox. The amplitudes of two-node vibration can then be determined from a consideration of engine excitation and damping forces acting on this separated system.

As already explained, if the gearing is well made there should be no serious three-node vibration.

Since the engine system consists of more than one mass there is also the possibility of higher modes of vibration than the three-node mode. These are unlikely to be the cause of serious resonant vibration, however, because their high frequency implies that only high-order disturbances of feeble magnitude will occur in the running speed range.

These conclusions have been borne out in practice.

Geared Aero-Engine/Air-screw Combinations.—The gear ratios commonly employed in aero-engine practice vary from about 0.4 to about 0.7. The simplest arrangement is a straightforward spur gear having a pinion on the crankshaft geared into a wheel on the air-screw shaft. The wheel may have either external or internal teeth, and in either case the axis of the air-screw shaft is offset from the crankshaft axis. It should be noted that the amount of offset is less when an internally toothed wheel is employed, and that with internal teeth in the air-screw gearwheel the air-screw rotates in the same direction as the crankshaft. The torque reaction on the gearbox is thus the difference between the input and output torques, whereas it is the sum of these torques when an externally toothed wheel is used on the air-screw shaft.

The principal disadvantage of internally toothed wheels, however, is the difficulty of providing adequate support for the overhung pinion on the crankshaft, and the overhung wheel on the air-screw shaft.

The most popular type of gear is one in which the axis of the air-screw shaft is concentric with the crankshaft axis, and the air-screw and crankshaft rotate in the same direction.

The former consideration provides a compact gear assembly, whilst the torque reaction on the gearbox and therefore the strain on the nose of the engine is appreciably reduced when the input and output shafts rotate in the same direction, being equal to the difference of the input and output torques instead of their sum.

Fig. 67 shows a number of types of concentric reduction gearing, each of which is used in current aero-engine practice.

The type shown at I in Fig. 67 consists of a pinion A secured to the driving end of the crankshaft and gearing into a primary gearwheel C mounted on a layshaft. This primary wheel is rigidly connected to a secondary pinion D mounted on the same layshaft, which in turn gears with the secondary gearwheel B secured to the air-screw shaft. In actual practice there may be three or four layshafts evenly spaced round the crankshaft pinion and air-screw shaft gearwheel, each taking a share of the load.

The overall gear ratio is determined as follows :—

- Let A = number of teeth in crankshaft (primary) pinion,
 B = number of teeth in air-screw shaft (secondary) gearwheel,
 C = number of teeth in layshaft (primary) gearwheel,
 D = number of teeth in layshaft (secondary) pinion.

$$\text{Then Gear ratio} = \frac{\text{air-screw shaft speed}}{\text{crankshaft speed}} = \phi = \frac{A \cdot D}{C \cdot B}. \quad (171)$$

The air-screw rotates in the same direction as the crankshaft and the dimensions of the gears are chosen so that the air-screw shaft is concentric with the crankshaft.

In determining the equivalent dynamic system it is also necessary to know the speed of the layshaft gears. This is determined as follows :—

$$\frac{\text{layshaft speed}}{\text{crankshaft speed}} = \phi_1 = A/C. \quad (172)$$

Diagram II of Fig. 67 shows an epicyclic gear consisting of a bevel gear A secured to the driving end of the crankshaft, which gears into a number (usually three) of planet wheels C,

free to rotate on arms formed integral with the air-screw shaft. The planets C also gear into a bevel gear D which is secured to the engine crankcase, and is therefore restrained from rotating.

Let A = number of teeth in bevel gear on crankshaft,
 C = number of teeth in each planet wheel,
 D = number of teeth in bevel gear which is secured to crankcase.

$$\text{Then } \phi = \text{gear ratio} = \frac{\text{air-screw shaft speed}}{\text{crankshaft speed}} = \frac{1}{1 + D/A}, \quad (173)$$

i.e. the gear ratio is independent of the number of teeth in the planets, the air-screw rotates in the same direction as the crankshaft, and the air-screw shaft is concentric with the crankshaft.

$$\text{Also } \phi_1 = \frac{\text{planet speed}}{\text{crankshaft speed}} = \phi(1/K), \quad (174)$$

$$\text{where } K = \frac{\text{teeth in each planet}}{\text{teeth in fixed bevel}} = C/D.$$

The above expression for ϕ_1 is strictly correct only when the axes of the arms are at right angles to the axis of the crankshaft.

ϕ_1 approaches the value $R(1 + 1/K)$ as the axes of the arms approach a condition where they are parallel with the crankshaft axis, i.e. as the arrangement shown at II in Fig. 67 approaches the arrangement shown at III.

The following table gives some commonly used values of D/A, and the corresponding gear ratios :—

D/A	0.500	0.750	1.000	1.250	1.500
$\phi = \text{Gear ratio}$.	0.666	0.571	0.500	0.444	0.400

Diagram III in Fig. 67 shows an epicyclic gear consisting of an annulus A with internal teeth, secured to the driving end of the crankshaft, and a cage B, secured to the air-screw shaft. Cage B carries a number of planets (usually three or four), C, which gear into the annulus A and into a sun wheel D,

which is secured to the crankcase and is therefore restrained from rotating.

Let A = number of teeth in annulus,
 C = number of teeth in each planet,
 D = number of teeth in sun wheel.

$$\text{Then } p = \text{gear ratio} = \frac{\text{air-screw shaft speed}}{\text{crankshaft speed}} = \frac{1 + 2K}{2(1 + K)}, \quad (175)$$

where $K = \frac{\text{teeth in planet}}{\text{teeth in sun}} = C/D$.

$$\text{Also } p_1 = \frac{\text{planet speed}}{\text{crankshaft speed}} = \frac{(1 + 2K)}{2K} = p(1 + 1/K). \quad (176)$$

The following table gives some commonly used values of K with the corresponding gear ratios :—

FIXED SUN.

$K = \frac{\text{teeth in planet}}{\text{teeth in sun}}$	1/2	1/3	1/4
$p = \frac{\text{speed of air-screw}}{\text{speed of engine}}$	0.666	0.625	0.600
$p_1 = \frac{\text{speed of planets}}{\text{speed of engine}}$	2.000	2.500	3.000

Diagram IV in Fig. 67 shows an epicyclic gear, similar to that shown in Diagram III, except that the annulus is secured to the crankcase and is therefore restrained from rotating, whilst the sun is secured to the driving end of the crankshaft.

Let A = number of teeth in annulus,
 C = number of teeth in each planet,
 D = number of teeth in sun.

$$\text{Then } p = \text{gear ratio} = \frac{\text{air-screw shaft speed}}{\text{crankshaft speed}} = \frac{1}{2(1 + K)}, \quad (177)$$

where $K = \frac{\text{teeth in each planet}}{\text{teeth in sun}} = C/D$.

The air-screw rotates in the same direction as the crankshaft and the air-screw shaft is concentric with the crankshaft.

$$\text{Also } \dot{\phi}_1 = \frac{\text{planet speed}}{\text{crankshaft speed}} = -1/(2K) = -\dot{\phi}(1+1/K). \quad (178)$$

The following table gives some commonly used values of K with the corresponding gear ratios:—

FIXED ANNULUS.

$K = \frac{\text{teeth in planets}}{\text{teeth in sun}}$	1/2	1/3	1/4
$\dot{\phi} = \frac{\text{speed of air-screw}}{\text{speed of engine}}$	0.333	0.375	0.400
$\dot{\phi}_1 = \frac{\text{speed of planets}}{\text{speed of engine}}$	-1.000	-1.500	-2.000

The above tables show that a simple epicyclic gear with a fixed sun (Type III in Fig. 67) is not suitable for gear ratios below 0.600, whilst with a fixed annulus (Type IV in Fig. 67) it is not suitable for gear ratios much above 0.400. This is because the planets become too small.

It should be specially noted that a simple epicyclic gear of Types III and IV cannot be used for a gear ratio of 0.500, since the ratio K would be zero, i.e. the planets would have no dimensions.

For gear ratios in the neighbourhood of 0.500, therefore, it is necessary to use either a compounded epicyclic gear of Types III and IV or else to use gears of the types shown at I and II in Fig. 67.

Equivalent System.—The equivalent system for a geared radial aero-engine/air-screw installation is shown at V in Fig. 67. In this diagram,

J_a = moment of inertia of air-screw,

J_e = moment of inertia of air-screw shaft portion of gear assembly,

J_b = moment of inertia of crankshaft portion of gear assembly,

J_m = moment of inertia of engine masses.

C_b = torsional rigidity of air-screw shaft,

C_a = torsional rigidity of crankshaft.

Also, let $N_a =$ r.p.m. of crankshaft,
 $N_b =$ r.p.m. of air-screw shaft,
 $\phi =$ gear ratio $= N_b/N_a$.

The moments of inertia of the air-screw and engine are determined by the methods already discussed and this calls for no special comment except to mention that although the air-screw blades are generally assumed to be rigid, the effect of blade flexibility can be very noticeable. This point will be discussed later.

The determination of the moment of inertia of the gears and the allocation of the appropriate amounts to the air-screw and crankshafts is straightforward in cases where a simple spur reduction gear is employed.

Where concentric gears of the types shown in Fig. 67 are used, however, the equivalent moments of inertia are determined as follows:—

Referring to Diagram I in Fig. 67—

Let $J_a =$ moment of inertia of crankshaft pinion A about its axis of rotation,

$J_b =$ moment of inertia of air-screw shaft gearwheel B about its axis of rotation,

$J_w =$ moment of inertia of each layshaft assembly, wheels C and D, about their axis of rotation,

$n =$ number of layshaft assemblies.

Since neither the crankshaft nor the air-screw shaft can execute torsional vibrations without at the same time causing corresponding vibration of the layshaft assemblies, allowance must be made for this in evaluating the equivalent moments of inertia of the gearing.

If there is a flexible connection between wheels C and D on the layshafts the system must be regarded as consisting of six masses and three shafts as shown in the small diagram at V in Fig. 67. This system is composed of the air-screw shaft J_a and the air-screw gearwheel J_b at the ends of the air-screw shaft C_b ; the layshaft gears at the ends of the layshaft; and the engine J_a and the engine pinion J_a at the ends of the crankshaft C_a .

As a general rule, however, the layshaft gears can be regarded as rigidly connected, so that the equivalent dynamic system reduces to a system composed of four masses and two shafts, as shown at V in Fig. 67, where

$$J_c = J_v; \text{ and } J_b = J_u + J_w \cdot p_1^2 \cdot n,$$

i.e. the moment of inertia of the layshaft gear assemblies is combined with the moment of inertia of the crankshaft pinion, where

$$p_1 = A/C = \text{speed of layshafts/speed of crankshaft.}$$

The natural frequencies of the system may then be determined by tabulation.

Alternatively the system may be further simplified by reducing all moments of inertia and torsional rigidities to equivalent values referred to crankshaft speed, as shown at VI in Fig. 67.

In this diagram, using the methods already discussed,

$$\begin{aligned} J_3 &= J_d \cdot p^2; \quad J_2 = J_b + J_c \cdot p^2; \quad J_1 = J_a, \\ C_2 &= C_b \cdot p^2; \quad C_1 = C_a, \end{aligned}$$

$$\text{where } p = \frac{\text{speed of air-screw shaft}}{\text{speed of crankshaft}} = N_b/N_a.$$

The natural frequencies of torsional vibration may then be determined from Equation (19), viz.,

$$\begin{aligned} (J_1 + J_2 + J_3) - \omega^2 \left(\frac{J_1 \cdot J_2}{C_1} + \frac{J_1 \cdot J_3}{C_1} \right. \\ \left. + J_1 \cdot J_3 + \frac{J_2 \cdot J_3}{C_1} \right) + \frac{\omega^4 \cdot J_1 \cdot J_2 \cdot J_3}{C_1 \cdot C_2} = 0. \end{aligned}$$

The determination of the equivalent moment of inertia of an epicyclic gear assembly differs somewhat from the foregoing treatment.

Referring to Diagram III in Fig. 67:

Since torsional vibration of either the crankshaft annulus or the air-screw shaft cage produces corresponding vibration of the planets, allowance must be made for this in determining

the equivalent moment of inertia of the gearing. The following treatment assumes no elastic deflection to take place between the various elements of the gear assembly due to transmission of torque.

Let J_u = moment of inertia of annulus member A attached to crankshaft, about its axis of rotation,

J_v = moment of inertia of cage member B attached to air-screw shaft, about its axis of rotation,

J_w = moment of inertia of each planet C about an axis through its centre of gravity, i.e. about the axis of the planet spindle,

J_x = moment of inertia of each planet about the crankshaft axis, assuming the mass of each planet to be concentrated at the centre of gravity of the planet, i.e. J_x does not include the moment of inertia of the planet about its own axis of rotation,

n = number of planets.

Then, referring to Diagram V in Fig. 67,

$$J_c = J_v + J_x \cdot n; \quad J_b = J_u + J_w \cdot \phi_1^2 \cdot n,$$

where $\phi_1 = \frac{\text{planet speed}}{\text{crankshaft speed}} = \phi(1 + 1/K) = \frac{N_b}{N_a}(1 + 1/K),$

$$K = \frac{\text{number of teeth in planet}}{\text{number of teeth in sun}}.$$

The equivalent system referred to engine speed, Diagram VI in Fig. 67, is determined as already described.

The determination of the equivalent gear inertias J_c and J_b , for the arrangements shown at II and IV in Fig. 67, differs in detail from the above treatment, as follows :—

For arrangement II :

$$J_c = J_v + n(J_x + J_w/2), \quad \text{and} \quad J_b = J_u + J_w \cdot \phi_1^2 \cdot n,$$

where, in this case,

J_a = moment of inertia of each bevel planet about the crankshaft axis, assuming the mass of each planet is concentrated at the centre of gravity of the planet,

J_g = moment of inertia of arms carrying the planets, about the crankshaft axis,

J_u = moment of inertia of bevel wheel secured to crankshaft, about its axis of rotation,

J_w = moment of inertia of each bevel planet, about the planet spindle,

$$p_1 = p(1/K) = \frac{N_b}{N_a} \left(\frac{1}{K} \right),$$

$$K = \frac{\text{number of teeth in each planet C}}{\text{number of teeth in fixed bevel D}},$$

n = number of planets.

Note.—In the above expression for J_e the term $J_w/2$ is the moment of inertia of each planet about a diametral axis through the c.g., and is included because the planets rotate once round their diametral axes for each revolution of the air-screw shaft.

For arrangement IV :

where $J_c = J_v + J_n \cdot n$; and $J_b = J_u + J_w \cdot p_1^2 \cdot n$,
 J_v = moment of inertia of cage member B attached to air-screw shaft, about its axis of rotation,

J_n = moment of inertia of each planet C about the crankshaft axis, assuming that the mass of each planet is concentrated at the centre of gravity of the planet,

J_u = moment of inertia of sun wheel D secured to crankshaft, about its axis of rotation,

J_w = moment of inertia of each planet C about an axis through its centre of gravity, i.e. about the axis of the planet spindle,

$$p_1 = -p(1 + 1/K) = -\frac{N_b}{N_a}(1 + 1/K),$$

K = teeth in planet/teeth in sun,

n = number of planets.

EXAMPLE 40.—The equivalent moments of inertia and shaft stiffnesses shown at V in Fig. 67, for a single-row radial aero-engine, air-screw installation with concentric reduction gear have the following values :—

J_d = moment of inertia of air-screw = 480 lbs.-ins. sec.².

J_c = moment of inertia of air-screw gear = 0.8 lbs.-ins. sec.².

J_b = moment of inertia of crankshaft gear = 0.8 lbs.-ins. sec.².

J_a = moment of inertia of crank masses = 6.5 lbs.-ins. sec.².

C_b = torsional rigidity of air-screw shaft = 8,000,000 lbs.-ins./radian.

C_a = torsional rigidity of crankshaft = 2,500,000 lbs.-ins./radian.

ϕ = gear ratio = $\frac{\text{air-screw speed}}{\text{crankshaft speed}} = 0.500$ (positive because the air-screw rotates in same direction as the engine).

Determine the natural frequencies of the installation.

The characteristics of the equivalent system referred to engine speed (Diagram VI in Fig. 67) are as follows :—

$J_3 = J_d \cdot \phi^2 = 480 \times 0.5^2 = 120$ lbs.-ins. sec.².

$J_2 = J_b + J_c \cdot \phi^2 = 0.8 + (0.8 \times 0.5^2) = 1.0$ lbs.-ins. sec.².

$J_1 = J_a = 6.5$ lbs.-ins. sec.².

$C_2 = C_b \cdot \phi^2 = 8,000,000 \times 0.5^2 = 2,000,000$ lbs.-ins./radian.

$C_1 = C_a = 2,500,000$ lbs.-ins./radian.

Hence, from Equation (19),

$$(J_1 + J_2 + J_3) - \omega^2 \left(\frac{J_1(J_2 + J_3)}{C_1} + \frac{J_3(J_1 + J_2)}{C_2} \right) + \frac{\omega^4 \cdot J_1 \cdot J_2 \cdot J_3}{C_1 \cdot C_2} = 0,$$

$$\text{i.e. } (6.5 + 1.0 + 120) - \omega^2 \left(\frac{6.5(1.0 + 120)}{2500000} + \frac{120(6.5 + 1.0)}{2000000} \right) + \frac{\omega^4 \times 6.5 \times 1.0 \times 120}{2500000 \times 2000000} = 0,$$

$$\text{or } 0.00039\omega^4 - 1911.5\omega^2 + 318,750,000 = 0.$$

There are two real roots to this equation, namely,

$$\omega^2 = 173,000 \text{ or } 4,725,000,$$

i.e. $\omega = 416 \text{ or } 2175 \text{ radians/sec.},$

and $F = 3970 \text{ or } 20,750 \text{ vibs./min.}$

Alternatively, by tabulation method :

TABLE 34.

One-Node Mode; Geared Radial Engine; F=3970 Vibs./Min.; $\omega^2=173,000$.

Mass.	J.	J. ω^2 .	θ .	J. $\omega^2 \theta$.	$\Sigma J. \omega^2 \theta$.	C.	$\Sigma J. \omega^2 \theta / C$.
J _a Engine	6.5	1,125,000	1.0000	1,125,000	1,125,000	2,500,000	0.4500
J _b	0.8	138,400	0.5500	76,000	1,201,000	—	—
<i>Gear ratio = 0.5</i>							
J _c J _d Air-screw	0.8 480.0	138,400 83,000,000	0.2750 -0.0300	38,000 -2,490,000	2,440,000 →0	8,000,000 —	0.3050 —

TABLE 35.

Two-Node Mode; Geared Radial Engine; F = 20,750 Vibs./Min.;

$$\omega^2 = 4,725,000.$$

J.	J. ω^2 .	θ .	J. $\omega^2 \theta$.	$\Sigma J. \omega^2 \theta$.	C.	$\Sigma J. \omega^2 \theta / C$.
6.5 Engine	30,700,000	1.0000	30,700,000	30,700,000	2,500,000	12.300
0.8	3,780,000	-11.3000	-42,700,000	-12,000,000	—	—
<i>Gear Ratio = 0.500.</i>						
0.8 480.0 Air-screw	3,780,000 2,270,000,000	-5.6500 0.0200	-21,350,000 45,400,000	-45,350,000 →0	8,000,000 —	-5.6700 —

The frequencies given by the tabulation method are seen to be in agreement with the formula frequencies. In the case of the one-node mode the node is situated close to the air-screw, and the air-screw amplitude is very small, indicating that there will be no appreciable air-screw damping or excitation.

In the case of the two-node mode one of the nodes is situated in the crankshaft near to the engine, whilst the other node is situated in the air-screw shaft very close to the air-screw. The air-screw amplitude is very small, so that there will be no appreciable air-screw damping or excitation in this case also.

Approximate Formulæ for Estimating the Natural Frequencies of Radial Aero-Engine/Air-screw Installations.—When the oscillating system is reduced to an equivalent system referred to crankshaft speed, as shown at VI in Fig. 67, it will be found that the equivalent moment of inertia of the combined gear masses is small compared with that of the engine masses, whilst the equivalent moment of inertia of the air-screw is large compared with that of the crank masses.

Hence a reasonably good approximation to the frequency of the one-node mode of torsional vibration can be obtained by neglecting the gear masses and by assuming that the node occurs at the air-screw. The system then reduces to a simple torsional pendulum consisting of the engine masses J_1 , at one end of a shaft of torsional rigidity C , where

$$C = \frac{C_1 \cdot C_2}{C_1 + C_2} \text{ in the notation of Diagram VI of Fig. 67,}$$

$$\begin{aligned} \text{i.e. } F_1 = \text{one-node frequency} &= 9.55\sqrt{C/J_1} \\ &= 9.55\sqrt{\frac{C_1}{J_1(C_1 + C_2)}} \text{ approx.} \end{aligned}$$

In Example 40,

$$\begin{aligned} J_1 &= 6.5 \text{ lbs.-ins. sec.}^2; \quad C_1 = 2,500,000 \text{ lbs.-ins./radian,} \\ &\quad C_2 = 2,000,000 \text{ lbs.-ins./radian.} \end{aligned}$$

$$\begin{aligned} \text{Hence, } F_1 &= 9.55\sqrt{\frac{2500000 \times 2000000}{6.5 \times 4500000}} \\ &= 3950 \text{ vibs./min. approx.} \end{aligned}$$

This value is only about 1/2 per cent. less than the value obtained by tabulation.

Since the moment of inertia of the air-screw is large and the moment of inertia of the gears is small compared with that of the crank masses, alterations of air-screw or of gear inertia do not appreciably alter the one-node natural frequency of torsional vibration of radial engines. The most effective method of altering this frequency is, therefore, to alter either the moment of inertia of the engine masses, or the torsional rigidity of the crankshaft or air-screw shaft.

In the case of the two-node mode of vibration of geared radial engines the nodes occur very close to the air-screw and engine masses. The system, therefore, is approximately equivalent to a single mass J_2 in Diagram VI of Fig. 67, situated at the junction of two shafts of torsional rigidities C_1 and C_2 , the other ends of these shafts being fixed.

The approximate frequency equation for this mode of vibration is therefore

$$F_2 = 9.55 \sqrt{(C_1 + C_2)/J_2}, \text{ approx.},$$

using the notation of Diagram VI of Fig. 67.

In Example 40,

$$J_2 = 1.0 \text{ lbs.-ins. sec.}^2 \text{ (equivalent inertia of gear masses referred to crankshaft speed),}$$

$$C_1 = 2,500,000 \text{ lbs.-ins./radian,}$$

$$C_2 = 2,000,000 \text{ lbs.-ins./radian.}$$

$$\text{Hence, } F_2 = 9.55 \sqrt{(2,500,000 + 2,000,000)/1.0} = 20,250 \text{ vibs./min. approx.}$$

This is only 1.5 per cent. less than the frequency obtained by tabulation.

Alterations in the moment of inertia of the air-screw or of the engine masses do not appreciably alter the two-node frequency. The most effective way of altering the two-node frequency is therefore by altering either the moment of inertia of the combined gear masses, or the torsional rigidity of either the crankshaft or the air-screw shaft.

In general, therefore, alterations in the moment of inertia of the engine masses alter the tuning of the one-node mode of torsional vibration of a geared radial engine system without appreciably affecting the two-node mode, whilst alterations in the moment of inertia of the gears alter the two-node mode without appreciably affecting the one-node mode. Alterations in the torsional rigidity of either the crankshaft or the air-screw shaft affect both modes.

Changes in air-screw inertia, within practical limits, do not appreciably affect either mode of vibration.

Normally, there are no troublesome two-node criticals in the operating range of a geared radial engine, because only high-order harmonics of the second-degree or two-node forcing torques are present in the operating range, and these are of comparatively feeble intensity. The one-node criticals are usually the crux of the torsional vibration problem of this type of installation.

The natural frequencies of geared radial aero-engine/air-screw installations vary from about 3000 to 6000 vibs./min. These values are somewhat lower than the values for corresponding direct drive engines, due to the additional flexibility imparted to the system by the gearing.

The oscillating systems of multi-row radial engines are preferably dealt with by similar methods to those employed for in-line engines.

In-Line Geared Aero-Engine/Air-Screw Combinations.—Fig. 68 shows a typical six-cylinder in-line aero-engine/air-screw installation, where

J_s = moment of inertia of crank masses per cylinder =
 moment of inertia of rotating parts plus one-half
 moment of inertia of reciprocating masses (in the
 case of engines having two or more banks of cylinders
 operating on a single crankshaft, J_s is the moment
 of inertia of the rotating parts of each crankthrow,
 plus one-half the moment of inertia of the recip-
 rocating parts of all the cylinders operating on one
 crankthrow. As a general rule the moment of

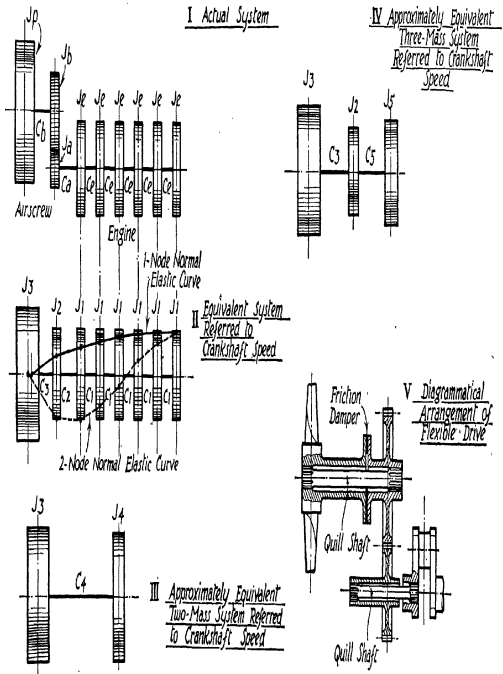


FIG. 68.—Geared in-line aero-engine.

inertia of the reciprocating parts of the master cylinder will differ somewhat from that of each of the auxiliary cylinders, i.e. the total moment of inertia of the reciprocating parts for each crankthrow is not the moment of inertia of the reciprocating parts of one cylinder multiplied by the number of cylinders operating on one crankthrow),

- J_p = moment of inertia of the air-screw,
 J_a = moment of inertia of crankshaft gear,
 J_b = moment of inertia of air-screw shaft gear,
 C_e = torsional rigidity of each section of crankshaft between adjacent cylinders,
 C_a = torsional rigidity of driving end of crankshaft,
 C_b = torsional rigidity of air-screw shaft.

The equivalent system, referred to crankshaft speed, is shown at II in Fig. 68, where

$$\begin{aligned}
 J_1 &= J_e, & C_1 &= C_e, \\
 J_2 &= J_a + \phi^2 \cdot J_b, & C_2 &= C_a, \\
 J_3 &= \phi^2 \cdot J_p, & C_3 &= \phi^2 \cdot C_b,
 \end{aligned}$$

$$\phi = \text{gear ratio} = N_b/N_a = \frac{\text{air-screw r.p.m.}}{\text{engine r.p.m.}}$$

[ϕ is positive or negative according to type of gear, as already explained].

Approximate Expressions for Calculation of One-node Torsional Vibration Frequency.—The moment of inertia of the combined gear masses referred to crankshaft speed is usually of the same order of magnitude as the moment of inertia of one set of crank masses, i.e. J_2 is usually approximately equal to J_1 , and C_2 is usually approximately equal to C_1 .

The equivalent system shown at II in Fig. 68 is therefore approximately the same as the simple two-mass system shown at III, where

$$\begin{aligned}
 J_4 &= n \cdot J_1 + J_2, \\
 \frac{I}{C_4} &= \frac{2}{C_1} + \frac{I}{C_2} + \frac{I}{C_3}.
 \end{aligned}$$

$$\text{Hence, } F_1 = \text{one-node frequency} = \frac{9.55}{k} \sqrt{\frac{C_4(J_3 + J_4)}{J_3 \cdot J_4}},$$

$k = \text{correcting factor given in Table 6}$
 $= 0.91 \text{ for } 4, 6 \text{ and } 8 \text{ crankthrows.}$

EXAMPLE 41.—The moments of inertia and shaft stiffnesses of the system shown at I in Fig. 68 have the following values :—

$$\begin{aligned} J_e &= 0.350 \text{ lbs.-ins. sec.}^2; & J_a &= 0.100 \text{ lbs.-ins. sec.}^2; \\ J_b &= 0.675 \text{ lbs.-ins. sec.}^2; & J_p &= 120.0 \text{ lbs.-ins. sec.}^2; \\ C_e &= 6,500,000 \text{ lbs.-ins./radian}; & C_a &= 7,500,000 \text{ lbs.-ins./} \\ & & & \text{radian}; \end{aligned}$$

$$C_b = 4,500,000 \text{ lbs.-ins. per radian};$$

$$p = \text{gear ratio} = \frac{\text{air-screw r.p.m.}}{\text{engine r.p.m.}} = 2/3 \text{ [since there is only one branch in this example the sign of this value is unimportant].}$$

Determine the natural frequency of the one-node mode of torsional vibration.

The characteristics of the equivalent system referred to crankshaft speed are as follows (see Diagram II, Fig. 67) :—

$$\begin{aligned} J_1 &= J_e = 0.350 \text{ lbs.-ins. sec.}^2, \\ J_2 &= J_a + p^2 \cdot J_b = 0.100 + \frac{(4 \times 0.675)}{9} \\ &= 0.400 \text{ lbs.-ins. sec.}^2, \\ J_3 &= p^2 \cdot J_p = 4 \times 120/9 = 53.3 \text{ lbs.-ins. sec.}^2, \\ C_1 &= C_e = 6,500,000 \text{ lbs.-ins./radian}, \\ C_2 &= C_a = 7,500,000 \text{ lbs.-ins./radian}, \\ C_3 &= p^2 \cdot C_b = 4 \times 4,500,000/9 = 2,000,000 \text{ lbs.-ins./radian}. \end{aligned}$$

Hence, the approximately equivalent two-mass system (Diagram III in Fig. 68) has the following characteristics :—

$$\begin{aligned} J_4 &= n \cdot J_1 + J_2 = (6 \times 0.35) + 0.4 = 2.5 \text{ lbs.-ins. sec.}^2, \\ J_3 &= 53.3 \text{ lbs.-ins. sec.}^2. \\ \frac{I}{C_4} &= \frac{2.0}{C_1} + \frac{I}{C_2} + \frac{I}{C_3} = \frac{2.0}{6500000} + \frac{I}{7500000} + \frac{I}{2000000} \\ &= \frac{I}{1063000}, \end{aligned}$$

$$\text{i.e. } C_4 = 1,063,000 \text{ lbs.-ins./radian.}$$

Hence, for a six-cylinder engine ($k = 0.91$),

$$F_1 = \frac{9.55}{0.91} \sqrt{\frac{1063000(53.3 + 2.5)}{53.3 \times 2.5}} = 7000 \text{ vibs./min.}$$

Alternative Calculation, using the Tabulation Method :

TABLE 36.

ONE-NODE MODE, GEARED SIX-CYLINDER IN-LINE ENGINE.

$$F = 6920 \text{ Vibs./Min. ; } \omega^2 = 526,000.$$

Mass.	J Lbs.-Ins. Sec. ² .	J. ω^2 Lbs.-Ins./Rad.	θ Radian.	J. $\omega^2 \cdot \theta$ Lbs.-Ins.	$\Sigma J.\omega^2 \cdot \theta$ Lbs.-Ins.	C Lbs.-Ins./Rad.	$\Sigma J.\omega^2 \cdot \theta$ Radian.
J _e	0.35	184,000	1.0000	184,000	184,000	6,500,000	0.0283
J _e	0.35	184,000	0.9717	179,000	363,000	6,500,000	0.0558
J _e	0.35	184,000	0.9159	166,500	531,500	6,500,000	0.0817
J _e	0.35	184,000	0.8342	153,500	685,000	6,500,000	0.1035
J _e	0.35	184,000	0.7287	134,000	819,000	6,500,000	0.1260
J _e	0.35	184,000	0.6027	111,000	930,000	7,500,000	0.1240
J _a	0.10	52,600	0.4787	25,200	955,200	—	—
<i>Gear Ratio = $\phi = 2/3$.</i>							
J _b	0.675	355,000	0.3191	113,500	1,546,300	4,500,000	0.3436
J _s	120.00	63,100,000	-0.0245	-1,546,300	0	—	—

(See Table 24 for method of applying the gear ratio.)

The one-node frequency by the tabulation method is therefore only about 1 per cent. lower than the frequency calculated by the approximate formula, when the appropriate correcting factor from Table 6 is applied.

Table 36 and Diagram II of Fig. 68 show that the node for the one-node mode of torsional vibration is very close to the air-screw, so that alterations in the moment of inertia of the air-screw within practicable limitations do not affect the one-node frequency to any appreciable extent. The most effective method of altering the one-node frequency is either to alter the moment of inertia of the engine masses furthest

from the node, or the torsional rigidity of the shaft sections nearest to the node.

For example, the addition of balance weights to the crankwebs of an in-line engine lowers the one-node frequency by 5 to 10 per cent., depending on the amount of counter-weighting employed.

Alterations to crankthrow dimensions within practicable limits do not, as a rule, produce much change of frequency. It will generally be found desirable to confine any alteration of crankshaft dimensions to the journals, because the effect of altering the dimensions of the crankpins is to produce an appreciable alteration in the moment of inertia of the rotating parts, which practically cancels the effect of such dimensional changes on the inter-crank stiffness.

In the case of crankshafts with rectangular webs, however, it is possible to obtain a useful alteration in inter-throw stiffness without much alteration in inertia by changing from rectangular to oval webs.

The one-node natural frequencies of geared in-line aero-engine/air-screw combinations varies from about 4500 vibs./min. in large multi-bank engines to about 14,000 vibs./min. in small single-bank four-cylinder engines.

The possibility of vibration with more than one-node should not be overlooked, although it is usually the one-node frequency which is the crux of the torsional vibration problem in installations of this type. The two-node frequency can be evaluated approximately by reducing the equivalent system to a three-mass system, as shown at IV in Fig. 68, where

$$J_5 = 6 \times 0.35 = 2.10 \text{ lbs.-ins. sec.}^2,$$

$$I/C_5 = I/C_2 + 2.5/C_1 = 1/7,500,000 + 2.5/6,500,000,$$

or $C_5 = 1,930,000 \text{ lbs.-ins./radian.}$

Then, applying Equation (19), the one-node frequency of this three-mass system is 6525 vibs./min. and the two-node frequency is 30,600 vibs./min. The correct values of these frequencies, determined by the tabulation method, are 6920 vibs./min. and 22,000 vibs./min. for the one-node and two-node modes respectively. The three-mass method gives, therefore,

a fairly good approximation to the one-node frequency, but is unreliable for two-node frequency calculations. The value obtained by the three-mass method is, however, a useful guide in starting the two-node frequency tabulations.

Assuming that the maximum operating speed in this example is 2000 r.p.m., since the 3rd order one-node critical speed occurs at $6920/3 = 2307$ crankshaft r.p.m., the one-node torsional vibration characteristics will require very careful analysis. In the case of the two-node mode of vibration only orders higher than the 10th occur in the working speed range, so that troublesome two-node vibration is unlikely in this case.

Examples do occur in practice, however, where two-node vibration cannot be disregarded, for example, in the larger sizes of power-plant, or in cases where the maximum operating speed is exceptionally high, or when the equivalent inertia of the gear assembly is large, and especially if it is separated from the air-screw by a comparatively flexible air-screw shaft.

In such cases a solution can sometimes be obtained by so tuning the system that all troublesome one-node criticals occur below the operating speed range, whilst all troublesome two-node criticals occur above the operating range.

The shapes of the respective normal elastic curves are the best guides to the tuning characteristics of a given system. For example, the normal elastic curves in Diagram II of Fig. 68 indicate that for the one-node mode of vibration alteration in air-screw inertia is unlikely to cause any noticeable change in the value of the one-node frequency because the air-screw is very close to the node. As already mentioned, the most effective place to carry out changes of this description is at the masses furthest away from the node where the vibratory amplitude is greatest. Alterations in the stiffness of the shaft sections remote from the node, on the other hand, will not make any appreciable change in frequency, whereas changes of shaft stiffness at the node will produce the greatest effect. Thus an alteration in the stiffness of the air-screw shaft C_b , or in the stiffness of the engine pinion shaft C_a , will produce the greatest change in the one-node frequency of the system shown in Fig. 68. In this connection it is of interest to mention that for a

given degree of flexibility between the air-screw and the crank mass adjacent to the gear assembly the shortest arrangement is obtained when the high-speed shaft, i.e. C_a , is made as short as possible (see Example 62).

The same general rules apply to the tuning of the two-node frequency. Thus the two-node normal elastic curve in Diagram II of Fig. 68 indicates that changes in air-screw inertia will not have much effect on the two-node frequency, since the node is practically at the air-screw. Changes in the gear inertia or in the inertia of the crank masses at either end of the crankshaft will, on the other hand, produce the greatest tuning effect because the relative vibratory amplitude at these points is large. Alternatively, effective tuning will be obtained by changing the stiffness of the air-screw shaft C_b , or that of the crankshaft section at the crankshaft node. An interesting feature is that changes in the stiffness of the pinion shaft C_a are unlikely to produce much change in the value of the two-node frequency, because the slope of the normal elastic curve between the gear assembly and the adjacent crank mass is small.

Now it has already been mentioned that changes of pinion shaft stiffness do alter the one-node frequency, so that the following useful characteristic of the system is revealed, namely :—

Changes in the stiffness of the air-screw shaft change both the one-node and the two-node frequencies, whilst changes in the pinion shaft stiffness change the one-node frequency without having much effect on the two-node frequency. This is a characteristic which might be useful in certain cases as a means for obtaining a favourable tuning of both the one and the two-node frequencies.

Diagram V of Fig. 68 shows a method of providing additional flexibility without an abnormal increase of length. The arrangement consists of a quill shaft accommodated inside the hollow air-screw and gearwheel shafts.

The driving torque is transmitted through splined or other suitable connections, and since all bending loads are carried by the outer shafts the quill has only to carry the torque loading. The body of the quill is a simple highly polished rod

free from stress-raising discontinuities, so that it can be permitted to carry a higher nominal stress than an air-screw or pinion shaft of orthodox design.

These factors enable the diameter of the quill to be made appreciably smaller than the diameter of a normal type of air-screw shaft, and since the stiffness of a shaft is proportional to the fourth power of the diameter it follows that a quill drive will be much more flexible than a normal drive of the same overall length.

If necessary a quill drive can also be provided between the crankshaft and the engine pinion, although this device is seldom used in aero-engine practice.

An interesting variation of the quill drive is also shown in Diagram V of Fig. 68, namely, the incorporation of a friction damper which is inserted between the gear and the air-screw so as to take advantage of the comparatively large relative vibratory amplitude between these two parts which results from the introduction of the quill. The friction surfaces of the damper are loaded by a suitable arrangement of springs or by the axial pull or thrust of the air-screw.

An arrangement of this type has been developed by Junkers.

Quill drives are also used for driving auxiliaries such as super-chargers, and in some designs a safety device is provided which consists of a much stronger tubular shaft surrounding the quill. The tubular shaft is in two parts, one connected to the driving member and the other to the driven member. These two parts are connected by loosely fitting dogs, the circumferential clearance being sufficient to permit all normal torsional deflections of the quill. In the event of a quill failure, however, or of abnormal vibratory motions the dogs come into action and the drive is taken through the outer tube. A protective device of this type is also useful in cases where the auxiliary shaft, in addition to its normal duty, is used for connecting a starting motor to the crankshaft, since it enables the heavy starting torques to be transmitted through the dogs instead of through the quill.

Gear Flexibility.—In the foregoing discussion it was assumed that no elastic yielding occurred in the gear assembly.

Actually, a considerable amount of yielding does take place, due to deformations at tooth contact surfaces; bending of teeth under the pitch line loads; deflections of wheel discs; and deflections of gear housings due to torque reaction from the gearing. The allowance to be made for gear flexibility varies from zero to about 30 or 40 per cent. increase in the *equivalent flexibility* between the air-screw and the first crank mass. The corresponding reduction in one-node frequency varies from zero to about 15 per cent.

The increase of 30 to 40 per cent. in flexibility of the equivalent air-screw shaft applies to simple spur gearing, and to concentric bevel gears of the type shown at II in Fig. 67 where there is appreciable flexibility in the arms carrying the bevel planet wheels. The increase in flexibility of concentric spur gears of the types shown at I, III, and IV in Fig. 67 is small because the reaction members are comparatively rigid, and the torque reaction on the reaction member is the difference between the input and output torques instead of the sum as with simple spur gears.

An important contributory factor to gear flexibility is the backlash of the gears. In an article in *The Engineer*, 23rd Aug., 1935, page 199, entitled "Torsional Vibrations with Angular Backlash," W. A. Tuplin shows that the effect of backlash increases with an increase in the ratio (angular backlash/angle of twist produced by mean torque), or with a decrease in the ratio (amplitude of vibratory torque/mean torque).

In a drive with no angular backlash each critical speed is fairly sharply tuned, whereas with angular backlash the natural frequency has not a single value but increases as the amplitude of vibration increases up to a certain limiting value which is determined by the ratio (angular backlash/angle of twist produced by mean torque). The effect of backlash is therefore to widen the range of speed over which severe vibration may be experienced and for this reason it is desirable to minimise backlash. It is also important to avoid torque reversal at the gear teeth throughout the operating speed range, and this implies a small value of the ratio (amplitude of vibratory torque/mean torque), so that for this reason also it is necessary

to minimise backlash, thereby narrowing the speed range over which severe vibration may be experienced when starting or stopping the engine, if there happens to be an unavoidable critical zone in the speed range between the idling and running ranges.

A simple approximate method for investigating the effect of backlash is given in Chapter 10.

***Air-Screw Flexibility.**—The foregoing methods of calculating the natural frequencies of torsional vibration of aero-engine/air-screw installations assume that the air-screw is rigid, i.e. that it can be replaced by a rigid flywheel having the same polar moment of inertia as the actual air-screw. It is well known that the blades of an air-screw can themselves vibrate in a great many different flexural modes and the advent of the metal air-screw, particularly the modern high duty types of large diameter and controllable pitch, has focussed attention on the necessity for dealing with air-screw blade vibration in a satisfactory manner.

It has been shown in theory and proved by experiment that the practice of regarding the air-screw as a rigid body is apt in many cases to result in quite important errors in the evaluation of the natural frequencies of torsional vibration of engine air-screw systems.

For example, Professor Lürenbaum gives an interesting example in an article entitled "Vibration of Crankshaft-Propeller Systems," *S.A.E. Journal*, December, 1936, which is shown in Fig. 69. Diagram I shows the torsional vibration resonance curves mentioned in Lürenbaum's article. These curves are plotted from torsigraph measurements in a four-cylinder in-line aero-engine. The dotted curve was obtained with the engine running on the test bench coupled to a brake propeller. In this case both the 6th and 8th order major critical speeds are clearly defined, and correspond to a frequency of about 11,000 vibs./min. The full line curve is plotted from torsigraph measurements taken with an air-screw fitted to the same engine, the only difference from the

* See Appendix to Volume I for a practical method of dealing with air-screw blade flexibility.

former condition being the substitution of the air-screw for the brake propeller. In this case there are two 6th order

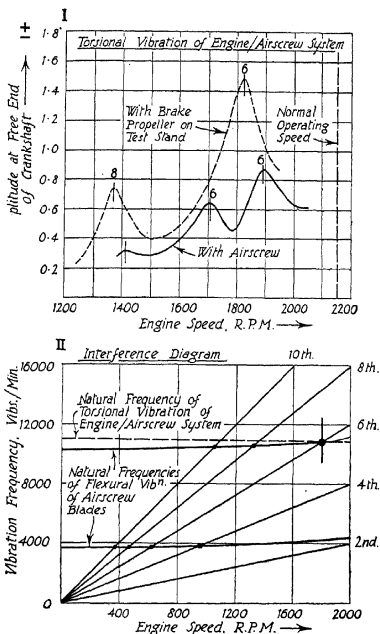


Fig. 69.—Vibration of engine/air-screw system.

critical speeds, one about 4 per cent. above and the other about 5 per cent. below the 6th order test bench critical.

Diagram II is an interference diagram for this installation. This chart shows very clearly the points at which there is coincidence between the frequencies of all exciting impulses and the natural frequencies of the various modes of vibration of the installation. The frequencies of the excitation impulses are shown by the excitation lines radiating from the origin. Thus the 2nd order excitation line is obtained by noting that the frequency of the second order impulse is 2 per revolution. Hence at, say, 2000 r.p.m. the excitation impulse frequency is $2 \times 2000 = 4000$ impulses/min.

It is customary to show only the important excitation lines on the interference chart. In the present example, since the engine is a four-cylinder in-line type the important excitations are the 2nd, 4th, 6th, etc., harmonic components of the engine torque curve.

The natural frequency of torsional vibration of the engine/air-screw system, assuming a rigid air-screw, appears as a horizontal line at the frequency 10,950 vibs./min., on the interference diagram, whilst the natural frequencies of the various modes of flexural vibration of the air-screw blades appear as slightly tilted horizontal lines. The increase in the flexural vibration frequency of the air-screw blades with r.p.m. is due to the effect of centrifugal force in increasing the flexural rigidity of the blades as the rotational speed increases. A potential danger zone exists at all points where an excitation line crosses a natural frequency line. In the present example, the interference diagram shows that there is coincidence between the 6th order harmonic of the engine torque curve, the natural frequency of torsional vibration of the engine/air-screw system, and the 2nd degree mode of flexural vibration of the air-screw blades, at a speed of about 1825 r.p.m. This is therefore a particularly severe danger zone.

The result of this condition at 1825 r.p.m. is shown at I in Fig. 69. With the brake propeller both the 6th and 8th order criticals are clearly defined at the calculated speeds, so that evidently the error in neglecting the flexibility of the blades of this propeller was negligible. In the case of the air-screw, however, the effect of blade flexibility is very pro-

nounced, the air-screw, in fact, functioning as a vibration absorber for the crankshaft system, and splitting the original resonance peak into two smaller peaks.

A conception of the effect of blade flexibility can be obtained from the diagrams shown in Fig. 70.

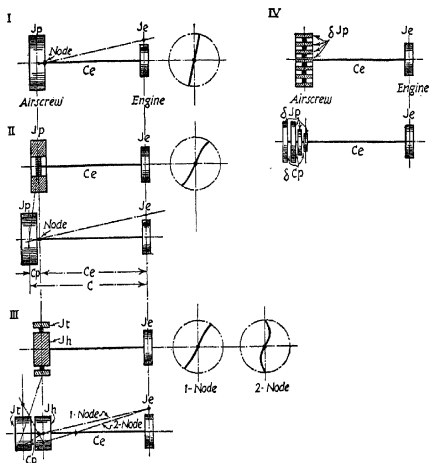


FIG. 70.—Vibration of engine/air-screw system.

Diagram I shows a simple two-mass system with rigid flywheels at each end of the shaft. Assuming that the moment of inertia of the engine masses is $J_e = 0.4$ lbs.-ins. sec.², and that of the rigid air-screw is $J_p = 5$ lbs.-ins. sec.², whilst the torsional rigidity of the shaft is $C_e = 500,000$ lbs.-ins. per radian, then the natural frequency of torsional vibration of the system is

$$\begin{aligned}
 F &= 9.55 \sqrt{\frac{C_e(J_e + J_p)}{J_e \cdot J_p}} = 9.55 \sqrt{\frac{500000(0.4 + 5.0)}{0.4 \times 5.0}} \\
 &= 11,100 \text{ vibs./min.}
 \end{aligned}$$

In Diagram II the rim of the flywheel representing the air-screw is shown connected to the shaft by flexible spokes. If it is assumed that the flexibility of the spokes is such that the natural frequency of the rim on the spokes is the same as the natural frequency of the engine masses on the shaft, then

$$\begin{aligned}
 C &= \text{combined torsional rigidity of spokes and shaft} \\
 &= C_e \cdot C_p / (C_e + C_p),
 \end{aligned}$$

where $C_e = 500,000$ lbs.-ins./radian.

Also, $C_p/J_p = C_e/J_e$,

i.e. $C_p = C_e \cdot J_p/J_e = 6,250,000$ lbs.-ins./radian.

and $C = \frac{500000 \times 6250000}{6750000} = 462,500$ lbs.-ins./radian.

$$\begin{aligned}
 \text{Hence, } F &= 9.55 \sqrt{\frac{C(J_e + J_p)}{J_e \cdot J_p}} = 9.55 \sqrt{\frac{462500 \times (0.4 + 5.0)}{0.4 \times 5.0}} \\
 &= 10,650 \text{ vibs./min.}
 \end{aligned}$$

This value is about 4 per cent. lower than the value obtained when the air-screw is assumed to be rigid.

Since the flexibility of an air-screw blade varies throughout its length and is smallest at the root, Diagram III is probably a closer approximation to the actual conditions. In this diagram a proportion of the air-screw inertia, viz. J_h , is assumed to be rigidly connected to the shaft, whilst the remainder, viz. $J_s = (J_p - J_h)$, is represented by a flywheel rim connected by flexible spokes to the hub.

As before, it will be assumed that the natural frequency of the flexibly connected rim on its spokes is the same as the natural frequency of the engine and hub masses on their shaft, i.e. that the rim system is tuned as an undamped vibration absorber for the engine/hub system.

Under these conditions the following relationship holds:—

$$\frac{C_p}{J_s} = \frac{C_e(J_e + J_h)}{J_e \cdot J_h}.$$

In the present example the following values will be assumed :—

$$J_e = 0.4; J_h = 4.0; J_t = 1.0 \text{ (i.e. } J_p = J_h + J_t = 5.0, \text{ as before).}$$

$$C_e = 500,000.$$

Hence,

$$C_p = \frac{500000 \times 1.0(0.4 + 4.0)}{0.4 \times 4.0} = 1,375,000 \text{ lbs.-ins./radian.}$$

The natural frequencies of the combined system can be calculated by means of Equation (19), i.e.

$$(J_t + J_h + J_e) - \omega^2 \left(\frac{J_t(J_h + J_e)}{C_p} + \frac{J_e(J_t + J_h)}{C_e} \right) + \frac{\omega^4 \cdot J_t \cdot J_h \cdot J_e}{C_p \cdot C_e} = 0$$

In this case the frequency equation reduces to

$$7,425,000 - 9.9\omega^2 + 0.0000032\omega^4 = 0,$$

$$\text{or } \omega^2 = \frac{9.9 \pm \sqrt{98.01 - 95.04}}{0.0000064} = 1,280,000 \text{ or } 1,815,000.$$

Hence, $F = 10,800$ or $12,850$ vibs./min.

The effect of flexibility in this case is to split the "rigid" resonance peak into two peaks, one about 16 per cent. higher than the original and the other about 3 per cent. lower than the original.

The value 10,800 is a one-node mode, the node being situated in the shaft as shown at III in Fig. 70. The normal elastic curve shows that the hub amplitude for the one-node mode is zero, but that there is an appreciable tip amplitude which is a possible source of high blade root stress at resonance. The value 12,850 vibs./min. is a two-node mode with one node in the shaft and the other node in the blades.

The normal elastic curve for the two-node mode indicates that the tip amplitude is larger than the amplitude at the engine. Hence this mode of vibration is a possible cause of blade tip failures. It should be specially noted that in cases where the flexibility of the air-screw blades is such that the blades act

as vibration absorbers for the engine shaft, very large blade tip amplitudes can be developed without correspondingly large shaft amplitudes. Thus torsionograph records from the shaft are not always a safe criterion of blade stressing, and it is now recognised that blade as well as shaft motion must be investigated.

Diagram IV in Fig. 70 shows the actual air-screw blades replaced by a series of flywheel rims connected by flexible spokes. The system then reduces to a shaft with the engine masses at one end and a series of more or less closely coupled masses at the other end representing the air-screw. This is probably a truer picture of the actual state of affairs in an engine/air-screw system, and indicates the possibility of a large number of different modes of vibration.

Indeed, the problem of calculating the coupled frequencies of an engine/air-screw system remains unsolved, although some light was thrown on the subject by Major B. C. Carter in his paper "Airscrew Blade Vibration," *Journal R.Ae.S.*, 1937.

The importance of measuring both shaft and blade movements is becoming well recognised as the only safe method of ensuring the stability of the complete installation, and methods are now available for taking vibration records from air-screw blades under running conditions, both on the test bench and in flight, as well as for taking reliable torsionograph records of shaft vibration. An excellent description of this work is given in a paper by Frank W. Caldwell entitled "Propellers for Aircraft Engines of High Power," *Gesammelte Vorträge der Hauptversammlung, 1937, der Lilienthal-Gesellschaft für Luftfahrtforschung*.

Engine Frame Vibration.—The introduction of flexible engine mounts, particularly those which make use of rubber in shear, for connecting an engine crankcase to its supporting frame, has added a further complication to the calculation of the natural frequencies of torsional vibration of the complete system. These mounts permit the whole engine aggregate, including the air-screw in the case of aero-engines, to execute torsional vibrations relative to the supporting frame or fuselage.

The natural frequency of torsional vibration of the crankcase/mount system can be calculated from the moment of inertia of the non-rotating parts of the engine aggregate and the torsional rigidity of the mounts. It is customary to regard this frequency as separate and distinct from the natural frequency of torsional vibration of the engine/air-screw system, the latter being calculated from the inertias and elasticities of the engine and air-screw rotating and reciprocating parts and their connecting shafts.

For ungeared engines there is not much error in regarding these two frequencies as separate phenomena, because the only coupling between the two is the inertia coupling which exists between the pistons and cylinders. This inertia coupling is very slight and is not of practical importance.

In the case of geared engines, however, the gearing introduces a strong reaction torque on the crankcase so that any vibratory movement of the gearing causes a corresponding vibratory movement of the crankcase, i.e. crankcase and crankshaft oscillations are strongly coupled.

This implies that the crankcase and crankshaft frequencies can no longer be regarded as separate phenomena, the general effect of the coupling being to replace the uncoupled frequencies by two new coupled frequencies. The lowest coupled frequency is lower than the lowest uncoupled frequency, and the highest coupled frequency is higher than the highest uncoupled frequency.

In an article entitled "The Torsional Critical Speeds of Geared Airplane Engines," *Journal of the Aeronautical Sciences*, October, 1937, J. P. Den Hartog and J. P. Butterfield showed that these deviations might be as much as 15 per cent. in either direction.

The following method of calculating the coupled frequencies is similar to the method already described for branched systems with several masses on each branch. It is therefore applicable to the most complicated arrangements, although the arithmetical work becomes formidable as the complexity increases. It is therefore advisable to simplify the system as much as possible before commencing the calculation.

Diagram I of Fig. 71 shows a geared system employing simple spur gears.

Let a = angular velocity of pinion,
 b = angular velocity of wheel,
 c = angular velocity of crankcase.

In accordance with the usual convention it is assumed in the first instance that all motions have the same sign, and that clockwise rotation is positive.

Then, from the velocity diagram in Fig. 71, assuming positive values from left to right,

Linear velocity of periphery of pinion = $r \cdot a$.
 Linear velocity of periphery of wheel = $R \cdot b$.
 Linear velocity of wheel centre, referred to
 centre of pinion = $(R + r) \cdot c$.

Hence, at point of contact of pinion with wheel,

$$(R + r) \cdot c - R \cdot b = r \cdot a,$$

$$\text{or } c = \frac{R \cdot b + r \cdot a}{R + r} = \frac{b - \phi \cdot a}{1 - \phi} \quad (179)$$

$$\text{where } \phi = \text{gear ratio} = \frac{\text{air-screw speed}}{\text{crankshaft speed}} = \frac{b}{a} = \frac{r}{R}.$$

The expression for ϕ is obtained by making $c = 0$ in Equation (179).

Also, since for simple harmonic motion, velocity is directly proportional to amplitude, Equation (179) expresses the geometrical relationships between the angular amplitudes, where

a = angular amplitude of pinion,
 b = angular amplitude of wheel,
 c = angular amplitude of crankcase.

From the tooth load diagram, assuming clockwise torque positive,

$$\begin{aligned} \text{Torque of engine on pinion} \\ = T_a = P \cdot r. \end{aligned}$$

Torque of air-screw on wheel

$$= T_b = P \cdot R = -T_a/p, \quad (180)$$

Torque of crankcase on gear

$$= T_c = -P(R + r) = -(T_a + T_b). \quad (181)$$

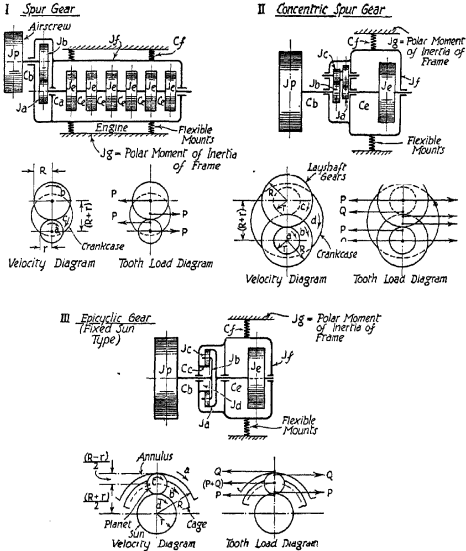


FIG. 71.—Geared aero-engines.

In the following treatment the oscillating system is divided into three branches, namely, the *crankshaft branch* terminating at the engine pinion; the *air-screw branch* terminating at

the air-screw gearwheel; and the *crankcase branch* terminating at the gearbox. The frequency tables are set down for each branch in the usual way, commencing at the free end of each branch, assuming a value for the natural frequency of the combined system.

The chosen value of the frequency constant corresponds to one of the natural frequencies of torsional vibration of the combined system when the geometrical relationship given in Equation (179) and the torque relationships of Equations (180) and (181) are fulfilled.

A convenient method of carrying out the tabulations is to regard one element of the system, for example, the flexibility of the crankcase mounts, as an adjustable variable and determine the dimensions of this element which make the chosen frequency a natural frequency of the combined system.

The following example is based on the system of Example 41, i.e. referring to Diagram I of Fig. 71.

EXAMPLE 42.—

$$J_e = 0.35 \text{ lbs.-ins. sec.}^2; \quad J_a = 0.100 \text{ lbs.-ins. sec.}^2;$$

$$J_b = 0.675 \text{ lbs.-ins. sec.}^2.$$

$$J_p = 120.0 \text{ lbs.-ins. sec.}^2; \quad J_f = 400.0 \text{ lbs.-ins. sec.}^2;$$

$$J_g = 10,000 \text{ lbs.-ins. sec.}^2.$$

$$C_e = 6,500,000 \text{ lbs.-ins./radian}; \quad C_a = 7,500,000 \text{ lbs.-ins./radian}.$$

$$C_b = 4,500,000 \text{ lbs.-ins./radian}.$$

C_f = torsional rigidity of the engine mounts.

Gear ratio = air-screw speed/crankshaft speed

$$= r/R = p = -2/3.$$

Determine the value of C_f so that one of the coupled frequencies is, say, $F = 1500$ vibs./min., and then determine the other coupled frequency.

Note.—The values of the polar moments of inertia and of the torsional rigidities are the actual values, i.e. no adjustment must be made to take into account the different speeds of rotation of the shafts.

TABLE 37.

Crankshaft Branch ; F = 1500 Vibs./Min. ; $\omega^2 = 24,700$.

Mass.	J.	J. ω^2 .	θ .	J. ω^2 . θ .	Σ J. ω^2 . θ .	C.	Σ J. ω^2 . θ /C.
J _e	0.35	8,650	1.0000	8,650	8,650	6,500,000	0.0013
J _s	0.35	8,650	0.9987	8,625	17,275	6,500,000	0.0027
J _s	0.35	8,650	0.9960	8,615	25,890	6,500,000	0.0040
J _s	0.35	8,650	0.9920	8,580	34,470	6,500,000	0.0053
J _s	0.35	8,650	0.9867	8,540	43,010	6,500,000	0.0066
J _s	0.35	8,650	0.9801	8,480	51,490	7,500,000	0.0069
J _a	0.10	2,470	0.9732	2,400	53,890	—	—
Col.	1	2	3	4	5	6	7

Whence $T_a = 53,890$ lbs.-ins., $a = 0.9732$.

Table 37 is constructed as follows. Columns 1, 2, and 6 can be filled in from the available data. The amplitude at the first mass is assumed to be unity and the table is then completed in the normal manner.

The final amplitude in column 3 is the specific amplitude at the engine pinion, i.e. a ; and the final torque summation in column 5 is the resultant specific torque of the engine on the engine pinion, i.e. T_a .

TABLE 38.

Air-screw Branch ; F = 1500 Vibs./Min. ; $\omega^2 = 24,700$.

Mass.	J.	J. ω^2 .	θ .	J. ω^2 . θ .	Σ J. ω^2 . θ .	C.	Σ J. ω^2 . θ /C.
J _s	120.000	2,965,000	α	2,965,000 . α	2,965,000 . α	4,500,000	0.66 . α
J _b	0.675	16,666	0.34 . α	5,660 . α	2,970,660 . α	—	—
Col.	1	2	3	4	5	6	7

Whence $T_b = 2,970,660 . \alpha$; and $b = 0.3400 . \alpha$,but $T_b = -T_a/b$, from Equation (180),i.e. $2,970,660 . \alpha = 53,890 \times 3/2 = 80,835$,or $\alpha = 0.0272$;

by substituting this value of α , Table 38 becomes

J_p	120,000	2,965,000	0.0272	80,680	80,680	4,500,000	0.0179
J_b	0.675	16,666	0.0093	155	80,835	—	—

i.e. $T_b = 80,835$ and $b = 0.0093$.

Table 38 is constructed as follows. Since unit amplitude has already been assumed for the amplitude at the first mass of Table 37, a value α is assumed for the amplitude of the first mass in Table 38.

Table 38 commences at the air-screw mass and is completed in the usual manner. The final amplitude in column 3 is the specific amplitude at the air-screw shaft gearwheel, i.e. it is the amplitude at this point corresponding to unit amplitude at the free end of the engine crankshaft.

The final torque summation in column 5 is the specific torque at the air-screw shaft gearwheel.

The air-screw shaft gearwheel amplitude and torque are expressed in terms of the assumed air-screw amplitude, α .

The value of α is obtained from Equation (180), using the value of T_a given by Table 37. This enables numerical values to be inserted in Table 38.

TABLE 39.

Crankcase Branch ; F = 1500 Vibs./Min. ; $\omega^2 = 24,700$.

Mass.	J.	$J \cdot \omega^2$.	θ .	$J \cdot \omega^2 \cdot \theta$.	$\Sigma J \cdot \omega^2 \cdot \theta$.	C.	$\Sigma J \cdot \omega^2 \cdot \theta / C$.
J_g	10,000	247,000,000	-0.0163	-4,034,725	-4,034,725	9,820,000	-0.4113
J_f	400	9,880,000	0.3950	3,900,000	-134,725	—	—
Col.	1	2	3	4	5	6	7

Table 39 commences with the frame (or fuselage) inertia J_g . This is given as 10,000 lbs.-ins. sec.² in the present example, but it is a quantity which is generally difficult to obtain. In the absence of a definite value, it will be sufficiently accurate

to assume in most cases that J_g is about 100 times greater than J_f . For instance, in accordance with this rule, if J_g had been assumed to be 40,000 lbs.-ins. sec.² in the present example, then the value of torsional rigidity of the crankcase mounts would have been 10,100,000 lbs.-ins. per radian, a difference of only 3 per cent. Due to the increased moment of inertia of the frame, the frame amplitude would have been reduced to ± 0.0041 radian for ± 1.0 radian at the free end of the engine crankshaft, but the frame motion is in any case very small and therefore not of much practical importance.

In constructing Table 39 the values of J_g , J_f , $J_g \cdot \omega^2$, and $J_f \cdot \omega^2$ can be entered in the table from the known data.

The final torque summation in column 5 is the torque of the crankcase on the gearing, i.e. T_e , and this can be calculated from Equation (181), using the values of T_a and T_b given by Tables 37 and 38, i.e.

$$T_e = -(T_a + T_b) = -(53,890 + 80,835) = -134,725 \text{ lbs.-ins.}$$

The final deflection in column 3 is the deflection at the crankcase, i.e. c , and this can be calculated from Equation (179), using the values of a and b given by Tables 37 and 38,

$$\begin{aligned} \text{i.e.} \quad c &= \frac{b - p \cdot a}{1 - p} = \frac{0.0093 + 0.6666 \times 0.9732}{1.6666} \\ &= 0.3950 \text{ radian.} \end{aligned}$$

This value is entered at the bottom of column 3.

The final torque in column 4 can now be calculated from the final values in columns 2 and 3, i.e. final value to be entered in column 4 = $(0.3950 \times 9,880,000) = 3,900,000$ lbs.-ins.

The value in the top line of columns 4 and 5 is obtained by subtracting the bottom value in column 4 from the bottom value in column 5, i.e. value to be entered at the top of columns 4 and 5 = $(-134,725 - 3,900,000) = -4,034,725$ lbs.-ins.

The top line of column 3 is obtained by dividing the top value of column 4 by the top value in column 2, i.e. top value in column 3 = $(-4,034,725/247,000,000) = -0.0163$ radian.

The change in deflection given in column 7 is obtained by subtracting the final from the initial deflection in column 3,

i.e. top line of column 7 = $(-0.0163 - 0.395) = -0.4113$ radian.

Finally, the torsional rigidity of the crankcase mounts, i.e. the top line of column 6, is obtained by dividing the top line of column 5 by the top line of column 7, i.e. torsional rigidity of mounts = $(4,034,725/0.4113) = 9,820,000$ lbs.-ins. per radian.

It should be noticed that Table 39 is constructed by using the arithmetical processes normally employed when building up a frequency table.

Although the various operations appear somewhat lengthy when described in detail, the actual work is carried out very rapidly once the construction of a normal frequency table is understood.

From Table 39 the torsional rigidity of the crankcase mounts for a coupled frequency of 1500 vibs./min. is 9,820,000 lbs.-ins./radian, and that the node occurs in the mounts themselves, i.e. in the connection between the crankcase and the frame.

If the crankcase on its mounts is regarded as a separate system, the uncoupled frequency is

$$F = 9.55 \sqrt{\frac{C_r(J_f + J_a)}{J_f \cdot J_a}} \text{ vibs./min.}$$

In the present example

$$\begin{aligned} F &= 9.55 \sqrt{\frac{9820000(400 + 10000)}{400 \times 10000}} \\ &= 1525 \text{ vibs./min.,} \end{aligned}$$

also the uncoupled frequency of the crankshaft/air-screw system is 6920 vibs./min., from Table 36 of Example 41.

Hence the coupled frequency which has just been calculated is the lower mode of coupled vibration, and this is about 1.5 per cent. lower than the lower uncoupled frequency.

It is interesting to note that the specific amplitude at the crankcase is large, indicating that at speeds in the neighbourhood of resonance between the engine impulse frequency and the natural frequency of the crankcase on its mounts very

large vibratory movements of the flexibly mounted crankcase are likely to occur. This is borne out in practice. For example, in the case of automobile or aero engines employing rubber-in-shear in the crankcase attachments to the frame, very large crankcase movements are experienced at low r.p.m. when passing through the crankcase/mount resonant speed unless stops are provided to limit the motion.

For this reason these attachments should have sufficient flexibility to place the frequency of the crankcase/mount system well below the lowest engine impulse frequency at idling speeds. In practice it is usual to design the mounts so that the lowest engine impulse frequency is about $\sqrt{2}$ times the crankcase/mount frequency, considering the crankcase on its mounts as a separate torsionally flexible system. Example 41 shows that when the two uncoupled frequencies are far apart there is not much error in regarding the crankcase/mount and the engine/air-screw systems as separate systems, and in any case the actual value of the coupled frequency will be somewhat lower than the uncoupled frequency, so that the actual ratio between the engine impulse frequency and the crankcase/mount frequency will be somewhat greater than $\sqrt{2}$. The resonance curve in Fig. 75 shows that when the frequency ratio is $\sqrt{2}$ the dynamic magnifier is unity, i.e. there is no dynamic magnification of the torque impulses. Hence, if the frequency ratio is somewhat greater than $\sqrt{2}$, there will be a slight additional attenuation of the torque impulses, so that the error in regarding the crankcase/mount system as a separate system is in the right direction.

In a six-cylinder in-line, 4-S.C., S.A. engine, for example, the main impulse frequency is three impulses per revolution, and Table 37 shows that so far as the crankcase/mount frequency of the system is concerned all cylinders vibrate with approximately equal amplitudes. It will be shown later that under this condition the only unbalanced harmonic components of the engine torque are those having a frequency equal to an integral multiple of one-half the number of cylinders in the case of a 4-S.C., S.A. engine, i.e. the 3rd, 6th, 9th, etc.,

components for a six-cylinder engine. Thus in the case of a six-cylinder in-line 4-S.C., S.A. engine the lowest engine impulse frequency is three impulses per revolution. If the engine is to run satisfactorily at an idling speed of 700 r.p.m., corresponding to a minimum impulse frequency of $3 \times 700 = 2100$ impulses per minute, the crankcase/mount frequency should be not more than $2100/\sqrt{2} = 1490$ vibs./min. The 6th order impulse frequency of this engine at a speed of 700 r.p.m. is $6 \times 700 = 4200$ vibs./min., which is far removed from the proposed crankcase/mount frequency.

It should also be noted that since Table 37 shows that all parts of the crankshaft branch vibrate with approximately equal amplitudes, there is practically no twist and therefore no vibration stress in the shaft, due to this mode of vibration. Also, Table 38 shows that the specific amplitudes of the air-screw branch are very small, so that there will be practically no vibratory movement of this section of the system.

In other words, the engine pinion rolls back and forth on the practically stationary air-screw gearwheel, carrying all parts of the engine crankshaft mass system and the crankcase with it but without causing any appreciable distortion of the crankshaft.

The principal vibratory stress occurs therefore in the connections between the crankcase and the frame.

The foregoing characteristics are typical of systems where the uncoupled frequency of the crankcase/mount system is considerably lower than the uncoupled frequency of the crankshaft/air-screw system. The absence of any severe vibratory stress in the crankshaft when passing through the resonant speed of the lower coupled frequency is an additional advantage of systems arranged in this way.

Higher Frequency of the Coupled System.—The method is similar in every respect to that already described.

A clue to the probable higher frequency of the coupled system can be obtained by calculating the higher uncoupled frequency, viz. that of the crankshaft/air-screw system. This frequency is given in Table 36 of Example 41, viz. $F = 6920$ vibs./min. With this value as a guide the higher coupled

frequency of the same installation was calculated by trial and error, using the tabulation method just described.

The final frequency Table is given in Table 40, from which the higher coupled frequency is seen to be $F = 7030$ vibs./min. or about 1.5 per cent. higher than the uncoupled frequency of the crankshaft/air-screw system. Table 40 shows a very convenient standard method of setting down computations of this type.

One node of the higher coupled mode of vibration is located in the air-screw shaft, close to the air-screw, and the other node is located in the connections between the crankcase and the frame.

The specific deflection of the crankcase is very small, so that the vibratory motion is almost entirely confined to the crankshaft and air-screw branches.

In general, therefore, when the natural frequency of the crankcase on its mounts is appreciably different from the natural frequency of the crankshaft/air-screw system, there is not much error in assuming that the coupled frequencies are substantially the same as the uncoupled frequencies, i.e. the crankcase/mount and the crankshaft/air-screw systems can be regarded as separate systems. In the present example, for instance, the error due to neglecting the coupling effect is only 1.5 per cent.

Concentric Spur Gear.—Diagram II of Fig. 71 shows an aero-engine/air-screw system in which the air-screw shaft is concentric with the engine crankshaft (see also Diagram I of Fig. 67).

The method just described for a simple spur gear arrangement requires some modification when other types of gear are employed. The following treatment of a concentric spur gear can be applied to systems having any number of oscillating masses on the various branches, although in Diagram II of Fig. 71 a single-row radial engine is shown merely for the purpose of minimising the arithmetical work by having only a single engine mass to deal with. It will also be assumed that the pitch radii of the layshaft pinions and wheels are the same as the pitch radii of the engine pinion and air-screw shaft gearwheel respectively, since this is the arrangement which

TABLE 40.

FREQUENCY TABULATION: HIGHER-COUPLED MODE.

 $F = 7030 \text{ Vibs./Min.}; \omega^2 = 542,500; \rho = -2/3.$

Mass.	J.	ω^2 .	θ .	J. ω^2 . θ .	ΣJ . ω^2 . θ .	C.	$\frac{\Sigma J \cdot \omega^2 \cdot \theta}{C}$		
J_e	0.35	190,000	1.0000	190,000	190,000	6,500,000	0.0292	←-CRANKSHAFT BRANCH-→	
J_e	0.35	190,000	0.9708	184,400	374,400	6,500,000	0.0576		
J_e	0.35	190,000	0.9132	173,400	547,800	6,500,000	0.0844		
J_e	0.35	190,000	0.8288	157,400	705,200	6,500,000	0.1085		
J_e	0.35	190,000	0.7203	136,900	842,100	6,500,000	0.1295		
J_e	0.35	190,000	0.5908	112,100	954,200	7,500,000	0.1272		
J_a	0.10	54,250	0.4636	25,100	979,300	—	—		
Whence $T_a = 979,300$ and $a = 0.4636$.									
J_b	120.000 0.675	65,100,000 366,000	α -13.45%	65,100,000 -4,925,000	65,100,000 60,175,000	4,500,000 —	14.45%		←-AIR-SCREW BRANCH-→
Whence $T_b = 60,175,000 = -T_a/\rho = 979,300 \times 3/2 = 1,468,900$, or, $\alpha = 0.0244$.									
J_b	120.000 0.675	65,100,000 366,000	0.0244 -0.3287	1,589,000 -120,100	1,589,000 1,468,900	4,500,000 —	0.3531		
Whence $T_b = 1,468,900$ and $b = -0.3287$.									
J_c J_f	10,000 400	5,425,000,000 217,000,000	0.0000 -0.0118	115,700 -2,563,900	115,700 -2,448,200	9,820,000 —	0.0118 —	←-CRANKCASE BRANCH-→	
Where $T_c = -(T_a + T_b) = -(979,300 + 1,468,900) = -2,448,200$									
$c = \frac{b - \rho \cdot a}{1 - \rho} = \frac{-0.3287 + \frac{0.4636 \times 2}{3}}{1 + 2/3} = -0.0118.$									
Check: $(T_a + T_b + T_c) = (979,300 + 1,468,900 - 2,448,200) = 0.$									

is most likely to be preferred in practice in cases where there is only one layshaft. If there are several layshafts it might be found advantageous from the point of view of tooth loading to increase the diameter of the engine pinion and reduce the diameter of the layshaft pinion.

Let a = angular velocity of engine pinion,
 b = angular velocity of air-screw shaft gearwheel,
 c = angular velocity of layshafts,
 d = angular velocity of crankcase,
 r = radius of engine and layshaft pinions,
 R = radius of air-screw shaft and layshaft gearwheels.

Then, from the velocity diagram, Case II, Fig. 71:

At point of contact of engine pinion and layshaft gearwheel,

$$(R + r) \cdot d - R \cdot c = r \cdot a. \quad (182)$$

At point of contact between layshaft pinion and air-screw shaft gearwheel,

$$(R + r) \cdot d - r \cdot c = R \cdot b. \quad (183)$$

Subtract (182) from (183),

$$c(R - r) = R \cdot b - r \cdot a,$$

or

$$c = \frac{R \cdot b - r \cdot a}{R - r}. \quad (184)$$

Equations (182), (183), and (184) establish the geometrical relationships which must be fulfilled by the motions of the various elements of the gearing.

$$\text{The gear ratio} = \frac{\text{air-screw speed}}{\text{engine speed}} = b/a.$$

This can be obtained from Equations (182) and (183) by assuming that d , the crankcase velocity, is zero and then solving the equations simultaneously,

i.e.

$$b/a = r^2/R^2,$$

a result which agrees with Equation (171) for the case where the number of teeth in primary and secondary pinions and in primary and secondary wheels are equal.

Equation (182) also shows that when the crankcase is stationary the ratio (layshaft speed/engine speed) = $-r/R$, which agrees with Equation (172).

Torque Relationships.—From the tooth load diagram of Case II, Fig. 71,

$$T_a = \text{torque of engine on engine pinion} = P \cdot r,$$

$$T_b = \text{torque of air-screw on air-screw shaft gearwheel} \\ = -Q \cdot R,$$

$$T_c = \text{torque of crankcase on gear} = (Q - P)(R + r),$$

$$T_p = \text{torque on gear due to inertia reaction of layshaft} \\ \text{gears} = J_c \cdot \omega^2 \cdot c.$$

$$\text{Also } T_p = (P \cdot R - Q \cdot r) = J_c \cdot \omega^2 \cdot c.$$

The foregoing geometrical and torque relationships enable the coupled frequencies to be calculated by the tabulation method already described for plain spur gearing. The following example gives the details of a typical calculation:—*

EXAMPLE 43.—This example is based on the system shown at II in Fig. 71.

* In cases where the pitch radii of the layshaft wheels and pinions are not the same as the pitch radii of the air-screw shaft gearwheel and engine pinion respectively, the following more general expressions should be used:—

Let

$$\begin{aligned} r_1 &= \text{radius of engine pinion,} \\ r_2 &= \text{radius of layshaft pinion,} \\ R_1 &= \text{radius of layshaft gearwheel,} \\ R_2 &= \text{radius of air-screw shaft gearwheel.} \end{aligned}$$

The remaining symbols are unaltered.

Then, from the geometry of the gearing $(R_1 + r_1) = (R_2 + r_2)$, and the geometrical and torque relationships become

$$(R_1 + r_1)d - R_1 \cdot c = r_1 \cdot a, \quad \dots \quad (185)$$

$$(R_1 + r_1)d - r_2 \cdot c = R_2 \cdot b, \quad \dots \quad (186)$$

$$c = \frac{R_2 \cdot b - r_1 \cdot a}{R_1 - r_2}. \quad \dots \quad (187)$$

$$p = \frac{b}{a} = \frac{r_1 \cdot r_2}{R_1 \cdot R_2},$$

$$T_a = P \cdot r_1,$$

$$T_b = -Q \cdot R_2,$$

$$T_c = (Q - P)(R_2 + r_2) = (Q - P)(R_1 + r_1),$$

$$T_p = J_c \cdot \omega^2 \cdot c = (P \cdot R_1 - Q \cdot r_2).$$

- Where J_e = moment of inertia of crank masses = 6.5 lbs.-ins. sec.²,
 J_p = moment of inertia of air-screw = 480.0 lbs.-ins. sec.²,
 J_a = moment of inertia of engine pinion = 0.25 lbs.-ins. sec.²,
 J_b = moment of inertia of air-screw shaft gearwheel = 1.5 lbs.-ins. sec.²,
 J_c = moment of inertia of layshaft gears = 2.0 lbs.-ins. sec.²,
 J_f = moment of inertia of crankcase = 300.0 lbs.-ins. sec.²,
 J_g = moment of inertia of frame = 30,000 lbs.-ins. sec.²,
 C_e = torsional rigidity of engine shaft = 2,600,000 lbs.-ins./radian,
 C_b = torsional rigidity of air-screw shaft = 8,000,000 lbs.-ins./radian,
 C_f = torsional rigidity of connections between crankcase and frame,
 r = radius of engine and layshaft pinions = 1.75 ins.
 R = radius of air-screw and layshaft gearwheels = 2.5 ins.

Note.— J_e is the total moment of inertia of the layshaft gears about the axis of rotation of the layshaft, i.e. it is equal to the moment of inertia of each layshaft assembly multiplied by the number of layshafts.

$$\begin{aligned} \phi &= \text{gear ratio} = \text{air-screw speed/crankshaft speed} \\ &= r^2/R^2 = 0.49. \end{aligned}$$

Calculate the torsional rigidity C_f of the flexible connections between the crankcase and the frame for a coupled frequency of 3020 vibs./min., i.e. $\omega^2 = 100,000$, then determine the natural frequency of the other mode of coupled vibration.

TABLE 41.

Crankshaft Branch ; $F = 3020$ Vibs./Min. ; $\omega^2 = 100,000$.

Mass.	J.	$J.\omega^2$.	θ .	$J.\omega^2.\theta$.	$\Sigma J.\omega^2.\theta$.	C.	$\Sigma J.\omega^2.\theta/C$.
J_a	6.5	650,000	1.0000	650,000	650,000	2,600,000	0.2500
J_b	0.25	25,000	0.7500	18,750	668,750	—	—

Whence $T_a = 668,750$; and $a = 0.7500$,
 but $T_a = P.r = 1.75.P$, from tooth load diagram,
 i.e. $P = 668,750/1.75 = 382,143$.

TABLE 42.

Air-screw Branch ; $F = 3020$ Vibs./Min. ; $\omega^2 = 100,000$.

Mass.	J.	$J.\omega^2$.	θ .	$J.\omega^2.\theta$.	$\Sigma J.\omega^2.\theta$.	C.	$\Sigma J.\omega^2.\theta/C$.
J_p	480.0	48,000,000	α	48,000,000 α	48,000,000 α	8,000,000	6.000 α
J_b	1.5	150,000	-5.000 α	-750,000 α	47,250,000 α	—	—

Whence $T_b = 47,250,000\alpha$; and $b = -5.000\alpha$,
 but $T_b = -Q.R = -2.5.Q$, from tooth load diagram,
 i.e. $Q = -47,250,000\alpha/2.5 = -18,900,000\alpha$. (188)
 Also $T_p =$ inertia reaction torque of layshaft gears
 $= J_e.\omega^2.c$

$= 2.0 \times 100,000 \times c = 200,000.c$,
 but $T_p = (P.R - Q.r)$ from tooth load diagram
 $= 382,143 \times 2.5 + 18,900,000\alpha \times 1.75$
 $= 955,357 + 33,075,000\alpha$,
 i.e. $200,000.c = 955,357 + 33,075,000\alpha$,
 or $c = 4.7769 + 165.375\alpha$. (189)

Again, from Equation (184),

$$c = (R.b - r.a)/(R - r)$$

$$= \frac{-2.5 \times 5.0\alpha - 1.75 \times 0.75}{2.5 - 1.75},$$

i.e. $c = -16.666\alpha - 1.75$. (190)

From Equations (189) and (190),

$$\alpha = -0.0359, \text{ and } c = -1.153.$$

When this value of α is substituted, Table 42 becomes

J_a	480.0	48,000,000	-0.0359	-1,720,000	-1,720,000	8,000,000	-0.2150
J_b	1.5	150,000	0.1791	26,900	-1,693,100	—	—

Whence $T_b = -1,693,100$; $b = 0.1791$; and $Q = 677,000$,
 $T_p = 200,000$. $c = -200,000 \times 1.153 = -230,600$.

TABLE 43.

Crankcase Branch; $F = 3020$ Vibs./Min.; $\omega^2 = 100,000$.

Mass.	J.	$J \cdot \omega^2$.	θ .	$J \cdot \omega^2 \cdot \theta$.	$\Sigma J \cdot \omega^2 \cdot \theta$.	C.	$\Sigma J \cdot \omega^2 \cdot \theta / C$.
J_r	30,000	3,000,000,000	0.0041	12,355,000	12,355,000	33,000,000	0.3741
J_f	300	30,000,000	-0.3700	-11,100,000	1,255,000	—	—
Col.	1	2	3	4	5	6	7

Where T_c = torque of crankcase on gear = last line of column 5

$$= (Q - P)(R + r) \quad (\text{from tooth load diagram})$$

$$= (677,000 - 382,143)(2.5 + 1.75) = 1,255,000,$$

and d = amplitude at crankcase = last line of column 3

$$= (R \cdot c + r \cdot a)/(R + r) \quad (\text{from Equation (182)})$$

$$= -2.5 \times 1.153 + 1.75 \times 0.75 = -0.3700.$$

Hence, C_f = torsional rigidity of the connections between crankcase and frame = 33,000,000 lbs.-ins./radian.

Note.— ΣT = resultant torque on gearbox

$$= (T_a + T_b + T_c + T_p)$$

$$= 668,750 - 1,693,100 + 1,255,000$$

$$- 230,600 = 50,$$

i.e. the resultant torque is practically zero, which is a good check on the accuracy of the foregoing treatment.

The natural frequency of the crankcase/mount system considered as a separate system is 3160 vibs./min., whilst the uncoupled frequency of the engine/air-screw system is 3910 vibs./min. Hence the frequency which has just been calculated is the lower coupled frequency and this is $4\frac{1}{2}$ per cent. lower than the lower uncoupled frequency. For this mode of coupled vibration there are two nodes, one in the air-screw shaft close to the air-screw, and the other in the elastic connections between the crankcase and the frame.

Higher Mode of Coupled Vibration.—The most direct method of determining the natural frequency of the higher mode of coupled vibration is to carry out several sets of tabulations of the type just described, but for different assumed values of the natural frequency, adjusting the torsional rigidity of the elastic connection between the crankcase and the frame in each case, so that the necessary torque and gear deflection equations are satisfied. A curve is then constructed showing the variation of frequency with torsional rigidity of the elastic connections between the crankcase and the frame. The value of the higher coupled frequency can then be read off the curve at the known value of the torsional rigidity of the elastic connections, viz. 33,000,000 lbs.-ins./radian.

The following tables give the final tabulations for the higher coupled frequency:—

TABLE 44.

Crankshaft Branch ; F = 4075 Vibs./Min. ; $\omega^2 = 182,000$.

Mass.	J.	J. ω^2 .	θ .	J. $\omega^2 \theta$.	$\Sigma J. \omega^2 \theta$.	C.	$\Sigma J. \omega^2 \theta / C$.
J_e	6.5	1,183,000	1.0000	1,183,000	1,183,000	2,600,000	0.455
J_a	0.25	45,500	0.545	24,800	1,207,800	—	—

Whence

$$T_a = 1,207,800 ; a = 0.545 ;$$

$$P = 1,207,800 / 1.75 = 690,000.$$

TABLE 45.

Air-screw Branch; $F = 4075$ Vibs./Min.; $\omega^2 = 182,000$.

Mass.	J.	J. ω^2 .	δ .	J. ω^2 . θ .	Σ J. ω^2 . θ .	C.	Σ J. ω^2 . θ /C.
J _p	480.0	87,360,000	α	87,360,000 α	87,360,000 α	8,000,000	10.92 α
J _b	1.5	273,000	-9.92 α	-2,710,000 α	84,650,000 α	—	—

Whence $T_b = 84,650,000\alpha$; $b = -9.92\alpha$;

$$Q = -84,650,000\alpha/2.5 = -33,860,000\alpha,$$

also $T_p = J_p \cdot \omega^2 \cdot c = 2.0 \times 182,000 \times c = 364,000 \cdot c$,but $T_p = (P \cdot R - Q \cdot r) = 690,000 \times 2.5$

$$+ 33,860,000\alpha \times 1.75$$

$$= 1,725,000 + 59,260,000\alpha,$$

i.e. $c = 4.74 + 162.81\alpha$,again, $c = (R \cdot b - r \cdot a)/(R - r)$

$$= \frac{-2.5 \times 9.92\alpha - 1.75 \times 0.545}{2.5 - 1.75},$$

or $c = -33.1\alpha - 1.272$,hence, $\alpha = -0.0307$, and $c = -0.256$, and Table 45 becomes

J _p	480.0	87,360,000	-0.0307	-2,682,000	-2,682,000	8,000,000	-0.3352
J _b	1.5	273,000	0.3045	83,000	-2,599,000	—	—

Whence $T_b = -2,599,000$; $b = 0.3045$;

$$Q = 2,599,000/2.5 = 1,039,500,$$

and $T_p = 364,000 \cdot c = -364,000 \times 0.256 = -93,200$.

TABLE 46.

Crankcase Branch; $F = 4075$ Vibs./Min.; $\omega^2 = 182,000$.

Mass.	J.	J. ω^2 .	δ .	J. ω^2 . θ .	Σ J. ω^2 . θ .	C.	Σ J. ω^2 . θ /C.
J _p	30,000	5,460,000,000	-0.0005	-2,545,000	-2,545,000	34,200,000	-0.0745
J _r	300	54,600,000	0.0740	4,030,000	1,485,000	—	—

$$\text{Where } T_e = (Q - P)(R + r) = (1,039,500 - 690,000)4.25 \\ = 1,485,000$$

$$\text{and } d = (R \cdot c + r \cdot a)/(R + r) = (-2.5 \times 0.256 \\ + 1.75 \times 0.545)/4.25 = 0.074.$$

$$\text{Note.}—\Sigma T = (T_a + T_b + T_c + T_d) = (1,207,800 \\ - 2,599,000 + 1,485,000 - 93,200) = 600,$$

i.e. the resultant torque is practically zero, and also the torsional rigidity of the connections between the crankcase and the frame in Table 46 is very nearly the same as the value in Table 43.

Hence the value $F = 4075$ is the natural frequency of the higher coupled mode of vibration of this system. The natural frequency of the engine/air-screw system, considered as a separate system is 3910 vibs./min., so that the higher coupled frequency is about $4\frac{1}{2}$ per cent. higher than the higher uncoupled frequency.

In this system, therefore, where the uncoupled frequency of the crankcase/mount system is comparatively close to the uncoupled frequency of the engine/air-screw system, the effect of the coupling provided by the gearing is to lower the lower uncoupled frequency by about $4\frac{1}{2}$ per cent. and to raise the higher uncoupled frequency by about $4\frac{1}{2}$ per cent. It should be noted that if plain spur gearing of the same ratio had been used instead of concentric gearing the gear reaction would have been greater, and therefore the coupling effect would have been even greater than $4\frac{1}{2}$ per cent.

Epicyclic Gear.—Diagram III of Fig. 71 shows another common type of concentric gear, i.e. an epicyclic gear. The particular arrangement shown in this diagram employs a fixed sun so that the gear is suitable for ratios of 0.600 to 0.666 as already discussed.

Thus, if the annulus is driven by the engine and the air-screw by the planet cage, the air-screw will rotate at 0.600 to 0.666 of the engine speed, depending on the tooth relationships employed. Alternatively, if the engine drives the planet cage and the air-screw is driven by the annulus, the air-screw will rotate at 1.666 to 1.5 times engine speed, but this type of gear is not usually found in aero-engine practice.

For gear ratios between 0.333 and 0.400 the annulus is fixed and the engine drives the sun and the air-screw is driven by the planet cage. In this case the air-screw rotates at 0.333 to 0.400 of the engine speed.

The following treatment is based on an epicyclic gear with fixed sun, as shown in Fig. 71, but the method is also applicable to the case where the annulus is fixed merely by making the appropriate changes in the engine and air-screw branches of the system before commencing the tabulations.

Referring to Diagram III of Fig. 71,

Let a = angular velocity of annulus,
 b = angular velocity of cage,
 c = angular velocity of planets,
 d = angular velocity of sun,
 r = radius of sun wheel,
 R = radius of annulus.

Then, from the velocity diagram, Case III of Fig. 71,

At point of contact of planets with sun,

$$\frac{(R+r)}{2} \cdot b - \frac{(R-r)}{2} \cdot c = r \cdot d. \quad (191)$$

At point of contact of planets with annulus,

$$\frac{(R+r)}{2} \cdot b + \frac{(R-r)}{2} \cdot c = R \cdot a, \quad (192)$$

i.e. $R \cdot a - r \cdot d = (R-r) \cdot c, \quad (193)$

and $R \cdot a + r \cdot d = (R+r) \cdot b. \quad (194)$

These equations express the geometrical relationships between the gear elements.

From the tooth load diagram, Case III, Fig. 71,

T_a = torque on annulus = torque of engine on gear in this case.

T_b = torque on cage = torque of air-screw on gear in this case.

T_c = torque on sun = torque of crankcase on gear in this case.

T_p = torque on gear due to inertia reaction of planets
 $= J_e \cdot \omega^2 \cdot c.$

Calculate the torsional rigidity C_f of the flexible connections between the crankcase and the frame for a coupled frequency of 4275 vibs./min., i.e. $\omega^2 = 200,000$. Then determine the natural frequency of the other mode of coupled vibration.

Note.— J_e is the total moment of inertia of the planets about their axles, i.e. it is the moment of inertia of one planet multiplied by the number of planets.

Since, in this case, the sun is fixed, the annulus is driven by the engine, and the planet cage drives the air-screw, the gear ratio p is

$$p = \frac{\text{air-screw speed}}{\text{engine speed}} = b/a.$$

Hence, from Equation (194), when $d = 0$ (sun fixed),

$$p = b/a = R/(R + r) = 6/9 = 0.6666,$$

i.e. the air-screw rotates in the same direction as the engine at 0.6666 times engine speed. This result agrees with the result given by Equation (175).

TABLE 47.

Crankshaft/Annulus Branch ; F = 4275 Vibs./Min. ; $\omega^2 = 200,000$.

Mass.	J.	J. ω^2 .	θ .	J. $\omega^2 \cdot \theta$.	$\Sigma J. \omega^2 \cdot \theta$.	C.	$\Sigma J. \omega^2 \cdot \theta / C$.
J_a	6.5	1,300,000	1.0000	1,300,000	1,300,000	2,600,000	0.5000
J_b	2.0	400,000	0.5000	200,000	1,500,000	—	—

Whence $T_a = 1,500,000$; $a = 0.5000$;

$$Q = T_a/R, \text{ from Equation (195),}$$

$$= 1,500,000/6 = 250,000.$$

TABLE 48.

Air-screw/Cage Branch ; F = 4275 ; $\omega^2 = 200,000$.

Mass.	J.	J. ω^2 .	θ .	J. $\omega^2 \cdot \theta$.	$\Sigma J. \omega^2 \cdot \theta$.	C.	$\Sigma J. \omega^2 \cdot \theta / C$.
J_p	480.0	96,000,000	α	96,000,000 α	96,000,000 α	8,000,000	12.000 α
J_b	2.5	500,000	-11.0 α	-5,500,000 α	90,500,000 α	—	—

Whence $T_b = 90,500,000\alpha$; $b = -11.0\alpha$,

$$\begin{aligned} \text{but } T_b &= -(P+Q)(R+r)/2, \text{ from Equation (196),} \\ &= -(P+250,000)(6+3)/2 \\ &= -4.5P - 1,125,000, \end{aligned}$$

$$\text{i.e. } -4.5P - 1,125,000 = 90,500,000\alpha,$$

$$\text{or } P = -250,000 - 20,111,111\alpha. \quad (199)$$

$$\begin{aligned} \text{Again, } T_p &= J_e \cdot \omega^2 \cdot c = 0.1 \times 200,000 \cdot c = 20,000 \cdot c, \\ &\text{from Equation (198),} \end{aligned}$$

$$\begin{aligned} \text{also } T_p &= (P-Q)(R-r)/2, \text{ from Equation (198),} \\ &= (P-250,000)(6-3)/2 = 1.5P - 375,000. \end{aligned}$$

$$\text{Hence } 1.5P - 375,000 = 20,000c,$$

$$\text{or } P = 250,000 + 13,333c. \quad (200)$$

From Equations (199) and (200),

$$20,111,111\alpha + 13,333c = -500,000. \quad (201)$$

$$\text{From Equation (192), } b \frac{(R+r)}{2} + c \frac{(R-r)}{2} = R \cdot a,$$

$$\text{but } a = 0.5, \text{ from Table 47,}$$

$$\text{and } b = -11.0\alpha, \text{ from Table 48,}$$

$$\text{i.e. } -11\alpha(6+3) + c(6-3) = 2 \times 6 \times 0.5$$

$$-16.5\alpha + 0.5c = 1. \quad (202)$$

From Equations (201) and (202),

$$\alpha = -0.0256; c = 1.1541; P = 265,400,$$

$$\text{also } T_p = 20,000c = 23,080.$$

Substituting this value of α , Table 48 becomes

J_p	480.0	96,000,000	-0.0256	-2,460,230	-2,460,230	8,000,000	-0.3075
J_b	2.5	500,000	0.2819	140,950	-2,319,280	—	—

$$\begin{aligned} \text{Whence } T_b &= -2,319,280; b = 0.2819, \\ T_e &= P \cdot r, \text{ from Equation (197),} \end{aligned}$$

$$\text{i.e. } T_e = 265,400 \times 3 = 796,200.$$

Also, from Equation (194),

$$R \cdot a + r \cdot d = (R + r)b,$$

i.e. $(6 \times 0.5) + (3 \times d) = (6 + 3) \times 0.2819,$
 or $d = -0.1543.$

The above values of T_c and d can now be used to construct the frequency table for the crankcase/sun branch, as follows :—

TABLE 49.

Crankcase/Sun Branch ; F = 4275 Vibs./Min. ; $\omega^2 = 200,000.$

Mass.	J.	J. ω^2 .	θ .	J. $\omega^2 \cdot \theta$.	J. $\omega^2 \cdot \theta$.	C.	J. $\omega^2 \cdot \theta/C$.
J_s	30,000	6,000,000,000	0.0016	9,583,630	9,583,630	64,700,000	0.1478
J_r	300	60,000,000	-0.1462	-8,772,000	811,630	100,000,000	0.0081
J_a	0.5	100,000	-0.1543	-15,430	796,200	—	—

$$\begin{aligned} \text{Check } \Sigma T &= (T_a + T_b + T_c + T_p) \\ &= (1,500,000 - 2,319,280 + 796,200 + 23,080) \\ &= 0. \end{aligned}$$

Table 49 shows that the torsional rigidity of the flexible connections between the crankcase and the frame is 64,700,000 lbs.-ins. per radian for a coupled frequency of 4275 vibs./min. There are two nodes, one in the air-screw/cage branch, close to the air-screw ; and the other in the crankcase/sun branch in the flexible connections between the crankcase and the frame.

Due to the relatively small moment of inertia of the planets about their axles there is not much error in neglecting this quantity in the frequency tabulations, and when this is done the arithmetical work is considerably simplified since P is then equal to Q.

Table 50 shows the frequency tabulations for the lower and higher coupled frequencies when the planetary inertia is neglected. The torsional rigidity of the flexible connections between the crankcase and the frame for a lower coupled frequency of 4275 vibs./min. is 63,800,000 lbs.-ins. per radian, which is in very close agreement with the value previously

obtained by the lengthier method which includes planetary inertia. The higher coupled mode of vibration is 4625 vibs./min., from Table 50.

TABLE 50.
COUPLED FREQUENCIES: AERO-ENGINE WITH 0.666 EPICYCLIC GEAR:
FIXED SUN.

Lower Mode of Coupled Vibration.

$$F = 4275 \text{ Vibs./Min.}; \omega^2 = 200,000.$$

Mass.	J.	J. ω^2 .	θ .	J. $\omega^2 \cdot \theta$.	$\Sigma J. \omega^2 \cdot \theta$.	C.	$\frac{\Sigma J. \omega^2 \cdot \theta}{C}$	↑ CRANKSHAFT/ANNULUS BRANCH. ↓
J _a J _a	6.5 2.0	1,300,000 400,000	1.0000 0.5000	1,300,000 200,000	1,300,000 1,500,000	2,600,000 —	0.5000 —	
Whence $T_a = 1,500,000$, and $a = 0.5000$, i.e. $P = T_a/R = 1,500,000/6 = 250,000$.								
J _b J _b	480.0 2.5	96,000,000 500,000	α -11.02x	96,000,000x -5,500,000x	96,000,000x 90,500,000x	8,000,000 —	12.02x —	↑ ← AIR-SCREW/CAVE BRANCH → ↓
Whence $T_b = 90,500,000x = -P(R+r)$, i.e. $\alpha = \frac{-250,000 \times 9}{90,500,000} = -0.0248$.								
J _b J _b	480.0 2.5	96,000,000 500,000	-0.0248 0.2742	-2,387,000 137,000	-2,387,000 -2,250,000	8,000,000 —	-0.2990 —	
Whence $T_b = -2,250,000$, and $b = 0.2742$.								
J _f J _f J _a	30,000 300 0.5	6,000,000,000 60,000,000 100,000	0.0018 -0.1637 -0.1774	10,949,740 -10,182,000 -17,740	10,949,740 767,740 750,000	63,800,000 100,000,000 —	0.1715 0.0077 —	↑ CRANKCASE/SUN BRANCH. ↓
Where $T_a = Pr = 250,000 \times 3 = 750,000$, $d = \frac{(R+r) \cdot b - R \cdot a}{r} = \frac{9 \times 0.2742 - 6 \times 0.5}{3} = -0.1774$								
Check: $\Sigma T = (T_a + T_b + T_c) = 1,500,000 - 2,250,000 + 750,000 = 0$.								

TABLE 50 (continued).

Higher Mode of Coupled Vibration.

 $F = 4625 \text{ Vibs./Min.}; \omega^2 = 235,000.$

Mass.	J.	J. ω^2 .	θ .	J. $\omega^2 \cdot \theta$.	$\Sigma J \cdot \omega^2 \cdot \theta$.	C.	$\frac{\Sigma J \cdot \omega^2 \cdot \theta}{C}$.	CRANKSHAFT/ANGULUS BRANCH.
J _e J _a	6.5 2.0	1,327,000 470,000	1.0000 0.4120	1,327,000 193,000	1,527,000 1,720,000	2,600,000 —	0.5880 —	
Whence $T_a = 1,720,000$, and $a = 0.412$, i.e. $P = T_a/R = 1,720,000/6 = 287,000.$								
J _b J _s	480.0 2.5	112,700,000 588,000	α -13.1x	112,700,000x -7,700,000x	112,700,000x 105,000,000x	8,000,000 —	14.1x —	↑ ↓
Whence $T_b = 105,000,000x = -P(R + r)$, i.e. $\alpha = \frac{-287,000 \times 9}{105,000,000} = -0.0246.$								
J _b J _s	480.0 2.5	112,700,000 588,000	-0.0246 0.3214	-2,770,000 189,000	-2,770,000 -2,581,000	8,000,000 —	-0.3450 —	↑ ↓
Whence $T_b = -2,581,000$, and $b = 0.3214.$								
J _p J _r J _d	30,000 300 0.5	7,050,000,000 70,500,000 117,500	-0.0014 0.2486 0.1402	-9,625,450 10,470,000 16,450	-9,625,450 844,550 861,000	64,000,000 100,000,000 —	-0.1500 0.0084 —	↑ ↓
Where $T_c = P.r. = 287,000 \times 3 = 861,000$, $d = \frac{(R+r)b - R.a}{r} = \frac{9 \times 0.3214 - 6 \times 0.412}{3} = 0.1402.$								
Check: $\Sigma T = (T_a + T_b + T_c) = (1,720,000 - 2,581,000 + 861,000) = 0.$								

The uncoupled frequencies are 4460 vibs./min. for the engine/air-screw system and 4450 vibs./min. for the crankcase/mount system, i.e. the lower coupled frequency is about 4 per cent. lower than the lower uncoupled frequency, and the

higher coupled frequency is about 4 per cent. higher than the higher uncoupled frequency. It is interesting to note that although the two uncoupled frequencies are practically coincident the coupled frequencies differ from the respective uncoupled frequencies by the comparatively small amount of 4 per cent. This is because the coupling due to the gearing is comparatively small, i.e. the gear ratio itself is high, 0.666, and with epicyclic gearing the air-screw rotates in the same direction as the engine crankshaft, so that the torque reaction on the gearcase is the difference between the input and output torques. A much greater difference, as much as 15 per cent. either way, between the coupled and uncoupled frequencies is experienced when the gear ratio is low and when the output shaft rotates in the opposite direction to the input shaft, so that the torque reaction on the gearcase is the sum of the input and output torques.

Approximate Method for Calculating the Coupled Frequencies of a Geared Engine/Air-Screw Installation.—The following approximate method for calculating the coupled frequencies of a geared engine/air-screw installation is based on an analysis of the torsional critical speeds of geared aeroplane engines by J. P. Den Hartog and J. P. Butterfield in *The Journal of the Aeronautical Sciences*, October, 1937. It will be found useful for a preliminary investigation of the characteristics of an installation and will considerably reduce the arithmetical work involved in applying the more accurate tabulation method just described.

The following assumptions have been made in obtaining the approximate solution :—

- (i) The moments of inertia of the gear masses have been neglected.
- (ii) The moment of inertia of the fuselage has been assumed to be infinite.
- (iii) The inertia coupling between the pistons and cylinders has been neglected.

Item (i) is the principal source of error in this approximate method, since the moments of inertia of the gear masses are

not usually negligibly small compared with the other oscillating parts. Item (ii) does not cause much error, because the moment of inertia of the fuselage is always very large compared with the moments of inertia of the other parts of the system. Item (iii) also does not cause much error, because the moment of inertia of the reciprocating parts of the engine is usually small compared with the moments of inertia of other parts of the system.

Referring to Fig. 71 :—

- Let J_s = moment of inertia of the crank masses,
 J_p = moment of inertia of the air-screw,
 J_f = moment of inertia of the crankcase,
 C_s = torsional rigidity of engine shaft,
 C_b = torsional rigidity of air-screw shaft,
 C_o = torsional rigidity of connection between the reaction element of the gearing and the crankcase,
 C_f = torsional rigidity of the connection between the crankcase and the fuselage (or frame),
 ϕ = gear ratio = air-screw speed/engine speed,
 K = coupling factor, defined by Equation (206),
 ω_s = phase velocity of engine/air-screw system, regarded as a separate system,
 ω_f = phase velocity of crankcase/mount system, regarded as a separate system,
 ω = phase velocities of the coupled modes of vibration,
 F_s = natural frequency of engine/air-screw system
 $= 9.55 \cdot \omega_s$ vibs./min.,
 F_f = natural frequency of crankcase/mount system
 $= 9.55 \cdot \omega_f$ vibs./min.,
 F = natural frequencies of coupled system = $9.55 \cdot \omega$ vibs./min.

Then, (a) *Natural Frequency of Torsional Vibration of the Engine/Air-Screw System regarded as a Separate System.*

$$s^2 = \frac{1/J}{(1/C) + (1 - \phi^2)/(C_o \cdot \phi^2)}, \quad \cdot \quad \cdot \quad (203)$$

where $J =$ "combined inertia" of engine/air-screw system

$$= \frac{\phi^2 \cdot J_e \cdot J_p}{\phi^2 \cdot J_p + J_e}$$

Since J_p is usually very large compared with J_e there is not much error in neglecting the term J_e in the denominator of the above expression for J , in which case $J = J_e$.

$C =$ "combined torsional rigidity" of engine/air-screw system

$$= \frac{\phi^2 \cdot C_e \cdot C_b}{\phi^2 \cdot C_b + C_e}$$

Note that ϕ , the gear ratio, is positive if the air-screw shaft rotates in the same direction as the engine shaft, i.e. in the case of concentric spur gears or epicyclic gears. Alternatively ϕ is negative if the air-screw shaft rotates in the opposite direction to the engine shaft, i.e. in the case of plain spur gears.

Also, if the coupling between the reaction element of the gear and the crankcase is very rigid, i.e. C_e is very large, the second term in the denominator of Equation (203) is negligible and Equation (203) becomes

$$\omega_s^2 = C/J = \frac{C_e \cdot C_b (\phi^2 \cdot J_p + J_e)}{J_e \cdot J_p (\phi^2 \cdot C_b + C_e)} \quad (204)$$

This is the usual expression for a simple two-mass geared system.

Equation (203) shows that appreciable changes in the uncoupled frequency of the engine/air-screw system can be made by changing the stiffness of the connection between the reaction element of the gearing and the crankcase.

In practice this is accomplished by inserting a spring connection between the sun wheel and the crankcase in the case of an epicyclic gear with fixed sun, or between the annulus and the crankcase in the case of an epicyclic gear with fixed annulus. In the case of spur gears the same result would be obtained by inserting a spring connection between the gear housing and the crankcase.

(b) *Natural Frequency of Torsional Vibration of the Crankcase/Mount System regarded as a Separate System.*

$$\omega_f^2 = C_f/J_f. \quad . \quad . \quad . \quad (205)$$

It is preferable to arrange the mounts so that the crankcase tends to oscillate about a longitudinal axis passing through the centre of gravity of the combined engine and air-screw masses, as shown in Fig. 72, since this avoids displacement of the centre of mass and, consequently, the introduction of impulsive forces on the supporting frame when the power plant oscillates under the action of torque impulses. When this is done J_f is defined as follows:—

$$J_f = J_o + \frac{W}{g} \cdot a^2,$$

where J_o = moment of inertia of the stationary parts about an axis passing through the centre of gravity of the combined engine and air-screw masses, parallel to the longitudinal axis of the engine crankshaft. Note that J_o does not include the moment of inertia of the air-screw or the rotating parts of the shaft system, but that it does include the moment of inertia of the reciprocating masses of the engine, assuming that these are "frozen" at mid-stroke.

The value of J_o can be determined experimentally by the method shown in Fig. 37. In applying this method it is advisable to use a tri-filar suspension instead of the bi-filar suspension shown in Fig. 37.

W = weight of the rotating parts, i.e. of all parts, including the air-screw, which are not included in J_o ,

a = distance between the axis of rotation and the parallel axis through the centre of gravity.

In the case of an eccentric gear where the axis of rotation of the air-screw differs from the axis of rotation of the crankshaft the expression for J_f becomes

$$J_r = J_c + \frac{W_1}{g} \cdot a^2 + \frac{W_2}{g} \cdot b^2 \text{ (see Diagram II of Fig. 72),}$$

where W_1 = weight of rotating parts of crankshaft,

W_2 = weight of air-screw and rotating parts of air-screw shaft.

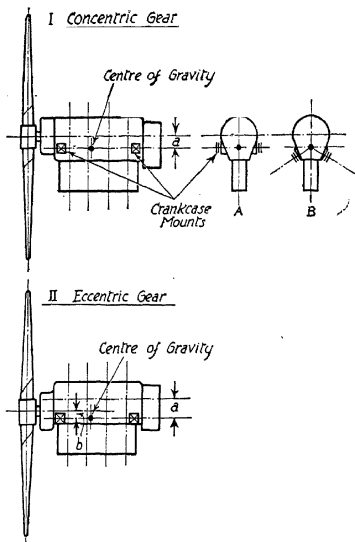


FIG. 72.—Crankcase inertia of geared engine.

If the crankcase mounts cannot be located on the horizontal plane containing the centre of gravity as shown at (A) in Diagram I of Fig. 72, they can be inclined as shown at (B),

so that the crankcase is still free to oscillate about the longitudinal axis through the centre of gravity. Arrangement (B) suffers from the disadvantage, however, that side thrusts are imposed on the engine supporting frame.

(c) *Coupling Factor.*

$$K^2 = \frac{J(1 - \phi)^2}{J_f \cdot \phi^2} \quad . \quad . \quad . \quad (206)$$

and since it has already been shown that in most practical cases $J = J_e$ there is not much error in writing Equation (206) as follows:—

$$K^2 = \frac{J_e(1 - \phi)^2}{J_f \cdot \phi^2} \quad . \quad . \quad . \quad (207)$$

Note.—(i) For a direct drive where $\phi = 1$, the coupling factor is zero.

(ii) The coupling factor is large, i.e. strong coupling, for low gear ratios (small values of ϕ).

(iii) The coupling factor is large if the crankcase inertia is small (small values of J_f).

(iv) The coupling factor is larger for simple spur gears (ϕ negative), than for concentric gears (ϕ positive).

(d) *Coupled Frequency Equation.*

$$\omega^4 - \omega_e^2 \cdot \omega^2 [1 + (\omega_f/\omega_e)^2 + K^2] + \omega_f^2 \cdot \omega_e^2 = 0. \quad (208)$$

This equation indicates that there are two coupled frequencies. It should be noted that if the crankcase inertia J_f is very small, or if the crankcase mounts are very stiff, i.e. C_f very large, then ω_f^2 approaches infinity, and Equation (208) reduces to

$$\omega^2 - \omega_e^2 = 0, \text{ or } \frac{\omega}{\omega_e} = 1 \quad . \quad . \quad . \quad (209)$$

i.e. there is only one coupled frequency, and that is the frequency of the engine/air-screw system regarded as a separate system. The coupling factor K does not influence the result.

Alternatively, if the crankcase inertia, J_f , is very large, or

if the crankcase mounts are very flexible, i.e. C_f very small, then ω_f^2 approaches zero, and Equation (208) reduces to

$$\omega^2 = \omega_s^2(1 + K^2), \text{ or } \frac{\omega}{\omega_s} = \sqrt{1 + K^2}. \quad (210)$$

In this case also there is only one coupled frequency, but this is influenced by the coupling factor K . Since, however, the moment of inertia of the crankcase J_f is generally very large compared with J in Equation (206), the coupling factor is usually comparatively small. Hence, in this case also ω does not greatly differ from ω_s , i.e. the coupled frequency is again practically the same as that of the engine/air-screw system, regarded as a separate system.

The principal significance of the above results is that if the crankcase/mount frequency is either very low or very high, i.e. approaching either zero or infinity, there is only one coupled frequency and this is practically the frequency of the engine/air-screw system, regarded as a separate system.

If, on the other hand, the crankcase/mount frequency has a finite value which, however, is either considerably higher or considerably lower than the engine/air-screw frequency, it will be found that there are two coupled frequencies, the lower of which is lower than the lower uncoupled frequency and the higher of which is higher than the higher uncoupled frequency. It can also be shown that an alteration in the crankcase/mount system, for example, by changing the torsional rigidity of the mounts, will change the crankcase/mount frequency without appreciably altering the engine/air-screw frequency. Conversely, an alteration in the characteristics of the engine/air-screw system, for example, by changing the torsional rigidity of the connection between the fixed member of an epicyclic gear and the crankcase, will change the engine/air-screw frequency without appreciably altering the crankcase/mount frequency.

Lastly, it is of interest to determine the value of the coupled frequencies when the uncoupled frequencies have the same value, i.e. when $\omega_s = \omega_f$, because this is the condition for maximum coupling effect in any given example.

For this condition Equation (208) becomes

$$\omega^4 - (2 + K^2)\omega_s^2 \cdot \omega^2 + \omega_s^4 = 0, \quad (211)$$

or
$$\omega^2 = 0.5\omega_s^2[(2 + K^2) \pm K\sqrt{4 + K^2}]. \quad (212)$$

In most practical cases K^2 is small compared with K , so that there is usually not much error in neglecting K^2 in the above expression,

i.e.
$$\omega^2 = \omega_s^2(1 \pm K), \quad (213)$$

whence $\omega/\omega_s = \sqrt{1 \pm K}$ approximately, when $\omega_s = \omega_f$. (214)

The following table shows the value of ω/ω_s for various values of K , when $\omega_s = \omega_f$:—

K.	ω/ω_s (Approximate Value).	ω/ω_s (Real Value).
0	1.0000	1.0000
0.02	1.0100 and 0.9900	1.0105 and 0.9901
0.04	1.0198 and 0.9798	1.0202 and 0.9802
0.06	1.0296 and 0.9695	1.0304 and 0.9705
0.08	1.0392 and 0.9592	1.0408 and 0.9608
0.10	1.0488 and 0.9487	1.0513 and 0.9513
0.20	1.0955 and 0.8944	1.1049 and 0.9050
0.30	1.1402 and 0.8367	1.1612 and 0.8612
0.40	1.1832 and 0.7746	1.2198 and 0.8198
0.50	1.2247 and 0.7071	1.2807 and 0.7808

* In practice the value of K rarely exceeds 0.10 for aero-engine/air-screw installations, due to the comparatively large moment of inertia of the crankcase compared with that of the engine crankshaft masses. The foregoing table shows that for values of K up to 0.10 the approximate expression given in Equation (214) can be used for the case when $\omega_s = \omega_f$, without much error.

It can be shown that, when the uncoupled frequency of the engine/air-screw system is not greatly different from the

* In extreme cases, however, K can be as much as 0.25 for radial engines, and 0.50 for high-speed in-line engines driving the air-screw through reduction gears of low ratio.

uncoupled frequency of the crankcase/mount system, any change in the characteristics of either system will have an appreciable effect on both coupled frequencies.

The foregoing considerations are of great practical importance when methods of tuning geared installations are being investigated. For example, there is not much advantage in altering the characteristics of the engine/air-screw system with the object of bringing about a more favourable disposition of the various critical speeds, corresponding to one of the coupled frequencies, if by so doing the disposition of the critical speeds corresponding to the other coupled frequency becomes less favourable. For this reason it is generally advantageous to provide the greatest possible difference between the values of the engine/air-screw frequency and the crankcase mount/frequency. When this is done changes in the characteristics of, say, the engine/air-screw system do not appreciably affect the crankcase/mount frequency.

Since it is difficult and in any case undesirable, from the point of view of transmission of vibration, to provide sufficient rigidity in the crankcase/mount system to ensure that the crankcase/mount frequency is a very large multiple of the engine/air-screw frequency, the better practical solution is to provide sufficient flexibility in the crankcase mounts to ensure the lowest possible crankcase/mount frequency which is compatible with mechanical requirements. This can be readily accomplished by means of rubber-in-shear engine mountings, which not only enable undesirable coupling effects to be avoided, but serve to prevent transmission of vibration to the surrounding structure. Care must be taken, however, to allow for the coupling effect on the engine/air-screw frequency, since, as shown by Equation (210), the coupling factor K does influence the value of the engine/air-screw frequency when a flexible engine mount is employed.

The strongest coupling effects occur when the two uncoupled frequencies are close together; when the gear ratio is small; when the crankcase inertia is small; and when the air-screw shaft rotates in the opposite direction to the engine shaft.

EXAMPLE 45.—Calculate the coupled frequencies of the installation of Example 43, using the approximate method just described.

From Example 43 (see Diagram II of Fig. 71).

$$\begin{aligned} J_e &= 6.5; J_p = 480.0; J_f = 300.0 \text{ lbs.-ins. sec.}^2, \\ C_e &= 2,600,000; C_b = 8,000,000; C_f = 33,000,000 \text{ lbs.-} \\ &\quad \text{ins./radian,} \\ \phi &= 0.49. \end{aligned}$$

(i) *Uncoupled Frequency of Engine/Air-Screw System.*

Since there is no flexible connection between the reaction element of the gearing and the crankcase in this case, the second term in the denominator of Equation (203) is zero. Hence Equation (204) can be used to determine the uncoupled frequency of the engine/air-screw system,

$$\text{i.e. } \omega_s^2 = C/J,$$

$$\begin{aligned} \text{where } C &= \frac{\phi^2 \cdot C_e \cdot C_b}{\phi^2 \cdot C_b + C_e} = \frac{0.49^2 \times 2600000 \times 8000000}{0.49^2 \times 8000000 + 2600000} \\ &= 1,104,700 \text{ lbs.-ins./radian,} \end{aligned}$$

$$\text{and } J = \frac{\phi^2 \cdot J_e \cdot J_p}{\phi^2 \cdot J_p + J_e} = \frac{0.49^2 \times 6.5 \times 480}{0.49^2 \times 480 + 6.5} = 6.153.$$

$$\text{Hence, } \omega_s^2 = 1,104,700/6.153 = 179,500.$$

The uncoupled frequency of the engine/air-screw system is therefore 4040 vibs./min., which is about 3 per cent. higher than the value obtained in Example 43. This discrepancy is due to neglecting gear inertia in the present example.

(ii) *Uncoupled Frequency of Crankcase/Mount System.*

This is obtained from Equation (205), viz.,

$$\omega_r^2 = C_f/J_f = 33,000,000/300 = 110,000,$$

i.e. the uncoupled frequency of the crankcase/mount system is $F = 3160$ vibs./min., which is the same as the value in Example 43, since 33,000,000 is the value of the torsional rigidity of the crankcase mounts determined in Example 43.

(iii) *Coupling Factor.*

$$\text{From Equation (206), } K^2 = \frac{J(1 - \phi)^2}{J_f \cdot \phi^2},$$

$$\text{i.e. in this example } K^2 = \frac{6 \cdot 153(1 - 0 \cdot 49)^2}{300 \times 0 \cdot 49^2} = 0 \cdot 0222.$$

(iv) *Coupled Frequencies.*

These are obtained from Equation (208), viz.,

$$\omega^4 - \omega_s^2 \cdot \omega^2 [1 + (\omega_f/\omega_s)^2 + K^2] + \omega_f^2 \cdot \omega_s^2 = 0,$$

i.e. in this example

$$\omega^4 - 179,500\omega^2 \left[1 + \left(\frac{110,000}{179,500} \right)^2 + 0 \cdot 0222 \right] + 110,000 \times 179,500 = 0,$$

$$\text{or } \omega^4 - 293,483\omega^2 + 19,745,000,000 = 0.$$

$$\text{Hence, } \omega^2 = 189,027 \text{ or } 104,456,$$

$$\text{and } F = 9 \cdot 55\omega = 4150 \text{ or } 3080 \text{ vibs./min.}$$

Thus the approximate method gives coupled frequencies of 4150 and 3080 vibs./min. compared with 4075 and 3020 vibs./min. given by the tabulation method of Example 43. The discrepancy is due to neglecting gear inertia in the present example.

Special Geared Drives.—Fig. 73 shows some interesting geared drives and contains one or two arrangements which are not commonly employed.

In the arrangement shown at I in Fig. 73 the gearing is placed at the forward end of the installation, with the object of providing a longer length of propeller shafting, thus increasing the flexibility of the propeller drive.

In marine installations with machinery installed aft this device does provide an appreciable degree of increased flexibility in the propeller shafting, and in cases where the increased flexibility is necessary for satisfactory tuning of the system, the increase in length of the propeller shafting is probably a more economical method than the installation of a flexible coupling between the propeller and the main gearwheel, bearing in mind that in high-powered, slow-speed installations the flexible coupling would be proportionately large and heavy.

Arrangements II and III show two methods of constructing a double-reduction gearing assembly. In arrangement II a flexible quill shaft is provided between the primary gearwheel

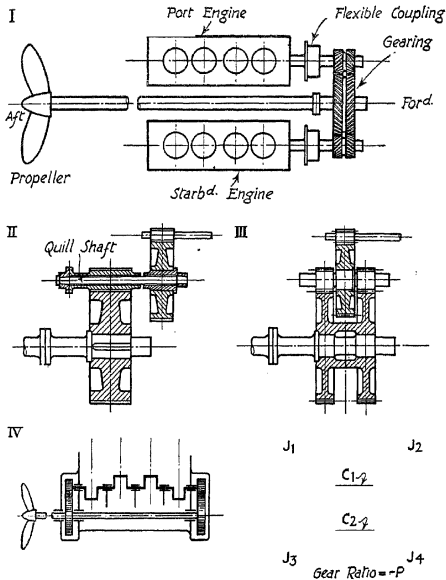


FIG. 73.—Special gearing arrangements.

and the secondary pinion, whereas, in arrangement III, the gear assembly is practically rigid. Both arrangements have been used successfully in practice. The advantages claimed

for arrangement II are that the flexibility of the quill shaft compensates to some extent for errors in gear cutting and assembly, whilst in some quarters it is considered that this arrangement gives a stiffer gearcase. The chief advantage of III is that the elimination of the flexible quill shaft removes one of the principal flexibilities in the system, and thus eliminates one possible mode of vibration. From the torsional vibration point of view, therefore, arrangement III is simpler than II, since the number of principal modes of vibration with III is one less than with II. With modern methods of gear tooth generation, troubles due to gear inaccuracies should not be experienced with arrangement III.

The arrangement shown at IV is quite unusual and has not been used to any noticeable extent in practice. Power is taken from two points in the crankshaft simultaneously, and the underlying object of this scheme is to reduce the torsional deflections which occur in the crankshaft and to give higher natural frequencies of torsional vibration. Since any deflection of the crankshaft must be accompanied by a proportionate deflection of the layshaft, the torsional rigidity of the layshaft must be added to that of each section of the crankshaft when calculating the natural frequencies of the whole system. If the gear ratio differs from unity the equivalent torsional rigidity of the layshaft should be used, as previously explained.

Diagram V of Fig. 73 shows a simple system of the type shown in Diagram IV, consisting of two masses, J_1 and J_2 , on a mainshaft of torsional rigidity C_1 . The layshaft, of torsional rigidity C_2 , is connected to each end of the main shaft by gears of ratio P , where

$$P = \text{speed of layshaft/speed of mainshaft.}$$

The polar moments of inertia of the pinions on the layshaft are J_3 and J_4 .

Then, referring all masses and elasticities to mainshaft speed,

Equivalent inertia at left-hand end of mainshaft

$$J_5 = (J_1 + J_3 \cdot P^2), \text{ from Equation (153),}$$

Equivalent inertia at right-hand end of mainshaft :

$$J_6 = (J_2 + J_4 \cdot P^2),$$

Equivalent torsional rigidity of mainshaft :

$$C_3 = (C_1 + C_2 \cdot P^2), \text{ from Equation (154),}$$

i.e. the equivalent system consists of two masses, J_5 and J_6 , on a shaft of torsional rigidity C_3 , and the natural frequency is given by Equation (16).

Hence,

$$F = 9.55 \sqrt{C_3(J_5 + J_6)/(J_5 \cdot J_6)},$$

or

$$F = 9.55 \sqrt{(C_1 + C_2 \cdot P^2) [1/(J_1 + J_3 \cdot P^2) + 1/(J_2 + J_4 \cdot P^2)]}.$$

If $J_1 = J_2 = J$, J_3 and J_4 are negligible ;

$$C_1 = C_2 = C; \text{ and } P = 1,$$

$$F = 9.55 \sqrt{4 \cdot C/J} \text{ vibs./min.}$$

The natural frequency of a simple two-mass system consisting of a mass J at each end of a shaft of torsional rigidity C is, from Equation (16),

$$F = 9.55 \sqrt{2 \cdot C/J}.$$

Hence the result of fitting the layshaft is, in this case, to increase the frequency by 40 per cent.

If P is made large a large increase of frequency is obtained with a comparatively light layshaft. If, on the other hand, P is appreciably smaller than unity, the change of frequency will not be very marked.

The foregoing discussion assumes that the gears are very accurately generated and are assembled without backlash. The assumption of no backlash is permissible so long as the mean torque transmitted exceeds the torque variation, but under no-load conditions this assumption is no longer strictly valid. The possibility of trouble with the gearing is probably the chief difficulty in applying the scheme in practice.

Another novel form of geared drive proposed by Junkers for wing mounted aero-engines also employs a layshaft located

below the crankshaft running the full length of the engine. In installations of this type the engine usually projects some distance beyond the wing so that the crankcase is subjected to twisting loads caused by transmission of torque reaction from the air-screw to the point of attachment of the engine to the wing. The consequent crankcase distortion is apt to be objectionable, especially in the case of geared engines with magnesium alloy crankcases, a material with rather low elastic moduli. In this Junkers construction this defect is overcome

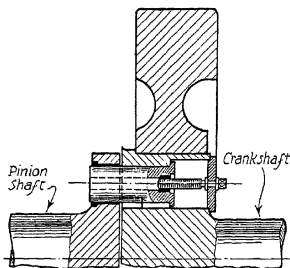


FIG. 74.—Torsionally rigid coupling.

by driving the layshaft by gearing located at the end remote from the air-screw, i.e. the end adjacent to the point of attachment of the crankcase to the wing. In this way the torque reaction is taken by the wing mounting. Incidentally the long layshaft between the gearing and the air-screw provides a substantially flexible airscrew drive which may or may not be advantageous according to the characteristics of individual installations.

Since satisfactory tuning of any given oscillating system depends on the selection of suitable values for the various inertias and elasticities it is desirable for the designer to have at his disposal means for adjusting these quantities in any desired direction. Couplings with a large range of adjustable flexibility have already been described, whilst a method of increasing the torsional rigidity of a section of shafting, in cases where an increase in the dimensions of the shaft is not possible, is shown in Diagrams IV and V of Fig. 73. In certain cases it is required to provide a coupling which permits free move-

ments in an axial direction whilst retaining the maximum degree of torsional rigidity of the connection.

Fig. 74 shows such a coupling, the design illustrated having been successfully used in geared oil engine installations for connecting the engine to its pinion. Messrs. Blohm and Voss have built many ships with geared oil engine propulsion in which couplings of this type are used between the main engines and their pinions. Presumably in these installations the use of a coupling having very small torsional flexibility enabled the designers to place all the serious critical speed zones above the operating range. An important point to be kept in mind when the coupling between the engine and the gearing is rigid, and a heavy flywheel is fitted to reduce speed fluctuations at the gears, is that the flywheel inertia is added to the inertia of the system. As explained in connection with Diagram III of Fig. 73 this provides a practically rigid gear assembly and reduces the number of degrees of freedom of the whole system to a minimum. It is essential, however, to employ gears with very accurately generated teeth and ensure that the alignment of the gearing is correct, otherwise trouble originated by gear cutting and mounting inaccuracies might be encountered.

The coupling shown in Fig. 74 consists of the flywheel hub, which is rigidly bolted to the driving end of the crankshaft, and a coupling flange formed integral with the pinion. The two parts of the coupling are connected by four very generously proportioned bolts located axially in the holes in the flywheel hub. The located screws are designed so that the main driving bolts can be withdrawn easily if it is desired to uncouple one of the engines.

Generous bearing surfaces, i.e. large diameter bolts, are necessary, not only to provide the required degree of torsional rigidity, but also to eliminate wear and to prevent "freezing" of the bolts against axial movements when the coupling is transmitting torque. This tendency of the friction between the contacting surfaces to prevent axial movement under load is one of the criticisms applied to turbine claw couplings, but Messrs. Blohm and Voss's successful experience appears to

indicate that this trouble is overcome in the design shown in Fig. 74.

It may be, however, that owing to the extreme accuracy of modern gear cutting the axial movements imposed on the bolts are very small.

Engine Accessories.—The following accessories are usually driven from the engine: camshafts, magnetos, dynamos, service pumps, and superchargers. As a general rule the moments of inertia of these accessories are so small, even when driven at a higher speed than that of the engine, and the flexibility of their drives is so large, that their influence can be disregarded so far as torsional vibration of the main system is concerned. This is especially true when the drives are taken from the driving end of the crankshaft, because the node for fundamental torsional vibration of the main system is located near this end. Incidentally, it is preferable to drive the important accessories such as camshafts and superchargers from this end of the crankshaft, because the amplitude of vibration is very small at this point.

In this connection experience with accessory drives of automobile and aero-engines indicates that trouble is likely to occur when the vibratory amplitude at the point from which the accessories are driven exceeds $\pm 0.5^\circ$.

Where the polar moment of inertia of an accessory is appreciable compared with that of the principal oscillating masses of the main system, or where the accessory drive is comparatively rigid, it is advisable to include it in the calculations. This merely requires an extension of the frequency tabulations to include the accessory, which is a simple matter when the accessory is driven from the free end of the crankshaft, but is troublesome when it is driven from the driving end of the crankshaft, because in the latter case the accessory and its drive must be regarded as a branch from the main system.

Fortunately, however, in aero-engine/air-screw systems the large moment of inertia of the air-screw implies that there is a node near the driving end of the crankshaft for both the one-node and the two-node modes of torsional vibration (see Fig.

22). Hence, in practice, the influence of any accessory driven from the driving end of the crankshaft on the main system is imperceptible.

In the case of accessories driven from the free end of the crankshaft, the only alteration in procedure is to commence the frequency tabulation for the crankshaft/air-screw system at the accessory instead of at the free end of the crankshaft. Care should be taken to allow for the gear ratio in the case of gear-driven accessories.

If the accessory is chain driven and the chain is not too long the drive should be regarded as rigid, but allowance should be made for any difference of speed between the accessory and the crankshaft in calculating the equivalent moment of inertia of the accessory.

If the accessory is belt driven the torsional rigidity of the belt drive can be estimated by the methods given in Chapter 8 for the belt drives of torsigraphic apparatus. In general, however, the torsional rigidity of even short rubber or rubber and canvas belts is so small that the influence of any accessory driven in this way is negligible.

Although the above discussion shows that in most practical cases the influence of engine-driven accessories on the characteristics of the main system is negligible, the possibility of resonance in the auxiliary drive itself must not be overlooked. The main and accessories systems are subject to the action of a very large number of periodic forces of different frequencies, which are dissipated harmlessly by imperceptible vibratory movements of the system, so long as resonant conditions do not arise. In the event of resonance occurring between the frequency of one of these periodic forces, even though it be of comparatively feeble magnitude, and a natural frequency of the system, very large vibratory disturbances are likely to occur.

The main and accessory systems are capable of executing torsional vibration in a great many different modes, and vibration of an accessory drive is liable to occur when resonance is established between a high-frequency disturbing force and one of the higher modes of natural vibration of the combined

system. In such a case the accessory drive may well appear to be the only part of the system affected, because the motion of the main system may be insignificant, i.e. the accessory system will appear to vibrate with a node at the point of attachment to the main system. Where there is any doubt about the stability of an accessory drive, therefore, the natural frequency of the accessory system, regarded as fixed at the point of attachment to the main system, should be calculated, and then the installation should be examined for possible sources of high-frequency excitation forces, for example, forces corresponding to the frequency of engagement of gearwheel teeth or torque variation in camshafts, which are likely to synchronise with the natural frequency of the accessory drive. If a resonant condition exists it is necessary to retune the accessory drive, either by altering the flexibility of the drive or by altering the mass. Alternatively, it might be possible to introduce additional damping, although this method is only desirable if the system cannot be retuned effectively.

In the case of camshafts, for example, the most effective method of avoiding excessive vibratory motion, due to the transmission of vibration from the crankshaft, is to drive the camshaft from the driving end of the crankshaft, i.e. from a point near a crankshaft node. If, on the other hand, the trouble is due to forced vibration of the camshaft, due to torque variation in the camshaft itself, causing reversals of torque and therefore hammering at the teeth of the driving gears, an effective remedy is to drive an accessory such as a dynamo from the free end of the camshaft. The torque variation in the camshaft is then superimposed on the mean torque required to drive the accessory, and if this mean torque is sufficiently large torque reversal will be eliminated.

If the trouble is due to resonant vibration in the camshaft the camshaft system can be retuned in various ways, for example, by drilling a hole half way along the shaft, commencing at the free end. This removes material from the free end of the shaft, which reduces the moment of inertia at that point, whilst at the same time the torsional rigidity at the driven end, i.e. at the virtual node of the camshaft system, is

maintained, so that the net effect is to raise the frequency of the camshaft system.

Alternatively the natural frequency of the camshaft system can be lowered by attaching a flywheel mass to the free end of the camshaft, for example, by driving an auxiliary, such as a service pump, from the free end of the camshaft.

Backlash in the camshaft driving gears can also be used as an adjustable variable for tuning the camshaft system, since Equation (438a) in Chapter 10, Volume II, indicates that the general effect of an increase of backlash is to lower the natural frequency of the system, and vice-versa.

An interesting practical example of resonance in a camshaft system is given by Mr. A. T. Gregory of the Ranger Engineering Corporation, U.S.A., in a paper entitled "Progress in the Development of In-line Air-cooled Engines" (S.A.E. Preprint 1939).

In the case discussed by Mr. Gregory the original camshaft system of a 6-cylinder, 4-stroke cycle, in-line, aero-engine had an effective polar moment of inertia of 0.0237 lbs.-ins. sec.², and a non-linear stiffness characteristic composed of a linear portion of torsional rigidity 17,100 lbs.-ins. per radian with a backlash in the driving gears and shaft splines of $2.8^\circ (\pm 1.4^\circ)$.

Torsiograph tests revealed a resonant zone at 2100 *crankshaft* r.p.m., having an amplitude of twist across the camshaft of $\pm 4.5^\circ$ with a frequency of 3 practically sinusoidal impulses per *crankshaft* revolution or 6 per *camshaft* revolution, i.e. a frequency of 6300 vib./min. excited by the fundamental torque impulse frequency of the engine. Below 2100 r.p.m. the twist amplitude varied between $\pm 2.5^\circ$ and $\pm 3.5^\circ$ down to an engine speed of 1300 r.p.m.

The backlash was reduced to $2.2^\circ (\pm 1.1^\circ)$ and this was found to be effective in removing the resonant zone outside the speed range up to 2300 r.p.m., but the twist amplitudes remained between $\pm 2.5^\circ$ and $\pm 3.5^\circ$ for speeds above 1800 *crankshaft* r.p.m.

The backlash was then restored to its original value of $2.8^\circ (\pm 1.4^\circ)$ and the effective inertia of the camshaft system was increased to 0.0518 lbs.-ins. sec.² by adding a flywheel

weighing 2.6 lbs. This change resulted in lowering the resonant zone to 885 engine r.p.m. at which speed the twist amplitude was $\pm 2.3^\circ$; whilst the amplitude was below $\pm 1^\circ$ at all speeds above 1100 engine r.p.m.

This result can be considered very satisfactory bearing in mind that experience has shown that twist amplitudes below $\pm 1^\circ$ in the operating range have no appreciable influence on engine smoothness and ensure satisfactory and safe valve gear and camshaft drive operation.

It is desirable, however, to make sure that any changes made in the camshaft system do not have an adverse influence on the vibrational characteristics of the crankshaft system, since, strictly speaking, the camshaft and crankshaft systems cannot be regarded as separate systems.

Where the engine speed is controlled by a governor, especially if a very close degree of speed regulation is required, it is desirable to drive the governor from a point near the crankshaft node where the shaft amplitude and therefore the cyclic speed variation is a minimum (see Chapter 6). Equation (421), Vol. II, shows that the cyclic speed variation is directly proportional to the vibratory amplitude so that in extreme cases it is conceivable that an engine with a very small degree of cyclic speed variation at the nodal point in the shaft where the vibratory amplitude is negligible may yet possess a very large degree of speed variation at the free end of the crankshaft where the vibratory amplitude is large. If the governor is driven from the free end of the crankshaft of such an engine, therefore, trouble will be experienced if the degree of cyclic speed variation of the shaft is greater than the degree of speed regulation which the governor is designed to maintain.

In the case of spark ignition engines variations in spark timing may result from non-uniform rotation of the timing cam caused by torsional vibration in the drive.

In Technical Note No. 651, National Advisory Committee for Aeronautics, "Effect of Spark Timing on the Knock Limitations of Engine Performance," considerable reduction of the non-knocking power range of an engine due to irregular spark timing is revealed.

Automobile Transmission Systems.—For the one-node mode of vibration the torque variation is more severe in the propeller shaft or rear axle, and is comparatively small in the engine crankshaft. The normal elastic curve is similar in shape to the one-node normal elastic curve of a marine installation shown in Fig. 18*c*, i.e. all cylinders vibrate with approximately equal amplitudes so that there is usually only one critical speed of practical importance in the running speed range. The maximum vibration stress at this critical speed occurs at the nodal point, i.e. in the propeller shaft or rear axle, and breakages due to one-node torsional vibration are therefore most likely to occur in these parts.

Due to the low value of the one-node frequency, the one-node critical speed occurs at a low number of engine revolutions in direct drive. Hence the one-node natural frequency determines the slowest speed at which the engine will operate smoothly in direct drive. The one-node frequency is lowered by thinning the propeller shaft or by increasing the moment of inertia of the flywheel.

In the case of two-node vibrations, the normal elastic curve is similar in shape to the two-node normal elastic curve of a marine installation shown in Fig. 18*c*, i.e. all cylinders do not vibrate with the same amplitude. Hence minor, as well as major, critical speeds will occur within the running speed range. The torque variation is more severe in the engine crankshaft, and is comparatively slight in the propeller shaft and rear axle. The maximum torsional vibration stress occurs at the crankshaft node, i.e. close to the flywheel, and this is the place where crankshaft breakages due to two-node vibrations are likely to occur. Even if actual breakdown does not take place, however, harsh running at engine speeds corresponding to the positions of all two-node criticals of disturbing amplitude will occur, unless the shaft system is properly designed with the object of providing smooth-running conditions over the whole speed range.

As in the case of torsional vibrations of marine installations the crux of the problem is the disposition and magnitude of the two-node critical speeds. The ideal solution is to design the transmission system so that all two-node criticals of disturbing

amplitude are situated above the highest engine speed. Much can be done in this direction by making the engine crankshaft as short and as stiff as possible, and the engine masses as light as possible. In the case of four-cylinder engines, for example, the two-node frequency is so high in relation to the frequency of the engine impulses due to the short crankshaft that two node criticals of disturbing amplitude are rare. In the case of straight-six and straight-eight engines, however, there may be some difficulty in obtaining a sufficiently high value for the two-node frequency merely by altering the dynamic and elastic properties of the system. In such cases a torsional vibration damper is fitted to the free end of the engine crankshaft (see Chapter 10).

Owing to the much greater flexibility of the propeller shaft and rear axle compared with that of the crankshaft, the one-node natural frequency and the amplitude of the predominant one-node torsional vibrations can be obtained without much error by assuming that the system is a simple two-mass system with the engine and flywheel masses at one end of the shafting and the road wheels at the other end.

Also, since the crankshaft node in the case of the two-node mode of vibration is close to the flywheel, the two-node natural frequency and the amplitudes at two-node critical speeds can be calculated without much error by assuming that the oscillating system consists only of the engine and flywheel masses, i.e. by neglecting all parts of the transmission system behind the flywheel.

In engines fitted with a hydraulic coupling between the crankshaft and the propeller shaft, e.g. the Daimler fluid flywheel transmission, the coupling effectively isolates the transmission shaft from engine torque variations by destroying the dynamic co-operation of the two parts into which it divides the whole oscillating system. It is necessary, however, to examine each of the two parts into which the system is divided for possible causes of resonant torsional vibration in each self-contained part. Since the principal stimulating source, viz. engine harmonic torque variations, is isolated from the transmission shaft by the hydraulic coupling, and since there is

usually no serious harmonic disturbing torque in the transmission system itself, the latter should operate smoothly at all speeds. The magnitude of the vibration amplitudes at critical speeds corresponding to the one-node mode of vibration of the engine-flywheel part of the system must be investigated, however. Since the node is situated close to the hydraulic coupling, these calculations are very similar to the two-node calculations for an installation not fitted with hydraulic transmission.

The only circumstance under which large vibratory amplitudes may be transmitted from one part of a system to another part through a hydraulic coupling is when the natural frequencies of the two parts of the system are identical. This condition is quite exceptional, however, and in any case is easily avoided by an appropriate alteration of mass or elasticity.

The general tendency towards higher crankshaft revolutions and improved engine mountings has undoubtedly emphasised the necessity for a thorough investigation of the torsional vibration characteristics of automobile transmission systems.

CHAPTER 6.

DETERMINATION OF STRESSES DUE TO TORSIONAL VIBRATION AT NON-RESONANT SPEEDS.

SOME degree of torque variation is required to produce and sustain torsional vibrations. In the case of a shaft transmitting power, provided the applied and resisting torques are perfectly uniform, and the attached masses have a constant moment of inertia relative to the axis of rotation, the only effect of the elasticity of the shaft is to cause the end from which power is taken to lag behind the end at which power is applied.

Under these conditions there is nothing to excite vibration, once the shaft has taken up the initial torsional deflection corresponding to the torque transmitted, and as soon as any initial transient vibrations caused by setting the system in motion have been damped out, the motion becomes uniform.

It does not require a very high degree of torque variation, however, either at the driving or at the driven end of the shaft to set up and sustain torsional vibration, particularly at speeds where the frequency of the periodic torque variations coincides with the natural frequency of torsional vibration of the system.

In the case of the internal combustion engine in particular, where the cyclic torque variation is considerable, it is possible for torsional vibrations of dangerous amplitude to occur at resonant or "critical" speeds. Hence a proper relationship between the elastic and the dynamic properties of the oscillating system and the type and speed of the prime mover must be adopted to avoid these critical speeds, i.e. the shaft system must be tuned to suit the peculiarities of the prime mover employed, and care must be taken to avoid running

the engine at "critical" speeds, where the amplitude of vibration is sufficient to cause serious additional stress in the shafting.

Forced Vibrations.—Outside the critical zone damping has very little influence on the amplitude of vibration, and is neglected in the following calculations. This gives vibration stress values at speeds outside the critical zone slightly in excess of the probable actual values, which is preferable to an under-estimation.

Consider a simple two-mass system consisting, for example, of a length of elastic shafting with the engine masses, including the flywheel at one end and the propeller mass at the other end.

The inertia of the end masses instigates an angular displacement about a mean position quite independent of the uniform rotation of the shafting, whilst the torque due to the engine mean turning effort does not affect the period of vibration but merely alters the centre of oscillation.

Let M = instantaneous torque,

J = moment of inertia of attached masses,

$|\theta|$ = instantaneous angular displacement of masses.

$$\text{Then} \quad M = \frac{J \cdot d^2|\theta|}{dt^2} \quad \dots \quad (215)$$

The propeller, moment of inertia J_p , vibrates about the axis of the shaft under the action of a periodic torque proportional at any instant to the amplitude of the elastic twist ($|\theta| = \theta_e - \theta_p$), between the engine and the propeller, where θ_e is the amplitude at the engine, and θ_p is the amplitude at the propeller.

The constant angular deflection due to the transmission of the mean driving torque is here neglected, since it does not influence torsional vibration.

The general equation connecting applied torque, angular deflection, and shear stress in a shaft for deflections within the elastic limit of the material is

$$\frac{M}{I_n} = \frac{2f_s}{d} = \frac{G \cdot |\theta|}{L}$$

where M = applied torque, I_p = polar moment of inertia of shaft,
 f_s = shear stress, d = diameter of shaft,
 $|\theta|$ = angular deflection, L = length of shaft,

$$\text{i.e.} \quad M = I_p \cdot G \cdot |\theta| \quad \dots \quad (216)$$

The following expression for propeller torque is obtained by substituting Equation (216) in Equation (215),

$$\frac{J_p \cdot d^2 \theta_p}{dt^2} = \frac{I_p \cdot G \cdot |\theta|}{L}, \quad \dots \quad (217)$$

$$\text{or} \quad \frac{d^2 \theta_p}{dt^2} = \frac{I_p \cdot G \cdot |\theta|}{J_p \cdot L} \quad \dots \quad (218)$$

The same torque acts at the same instant on the engine masses, but in the opposite sense, and, in addition, there is the torque due to the driving forces acting on the engine crankpins.

The driving forces may be assumed to consist of a constant tangential effort, acting at crank radius R , which represents the mean tangential effort of the driving forces, and a series of harmonically varying tangential efforts, $|T_1|$, $|T_2|$, $|T_3|$, \dots , $|T_n|$, all acting at crankpin radius. The general expression for the instantaneous intensities of these periodic forces can be written

$$|T| = |T_n| \cdot \sin w \cdot t, \quad \dots \quad (219)$$

where $|T_n|$ = maximum intensity of the n th order component of the tangential effort curve in lbs. (*not lbs. per sq. in.*),

w = phase velocity

$$= \frac{2 \cdot \pi \cdot N \cdot n}{60},$$

N = revolutions per minute,

n = number of complete oscillations in one revolution,

t = time.

For the engine masses, Equation (217) becomes, therefore,

$$\frac{J_e \cdot d^2\theta_e}{dt^2} = -\frac{I_p \cdot G \cdot |\theta|}{L} + |T_n| \cdot R \cdot \sin \omega \cdot t, \quad (220)$$

$$\text{i.e.} \quad \frac{d^2\theta_e}{dt^2} = \frac{I}{J_e} \left[|T_n| \cdot R \cdot \sin \omega \cdot t - \frac{I_p \cdot G \cdot |\theta|}{L} \right]. \quad (221)$$

Subtract Equation (218) from Equation (221):

$$\frac{I}{J_e} (|T_n| \cdot R \cdot \sin \omega \cdot t) = \frac{d^2(\theta_e - \theta_p)}{dt^2} + \frac{I_p \cdot G \cdot |\theta|}{L} \left[\frac{I}{J_e} + \frac{I}{J_p} \right]. \quad (222)$$

But $|\theta| = (\theta_e - \theta_p)$, and for harmonically varying oscillations the instantaneous amplitude is given by

$$|\theta| = |\theta_{\max}| \cdot \sin \omega \cdot t, \quad (223)$$

$$\text{or} \quad d^2\theta = -\omega^2 \cdot |\theta_{\max}| \cdot \sin \omega \cdot t. \quad (224)$$

Substituting Equations (223) and (224) in Equation (222), and dividing both sides by the common factor $(\sin \omega \cdot t)$, gives

$$\frac{|T_n| \cdot R}{J_e} = -\omega^2 \cdot |\theta_{\max}| + \frac{I_p \cdot G \cdot |\theta_{\max}| (J_e + J_p)}{L (J_e \cdot J_p)}. \quad (225)$$

$$\text{Hence,} \quad |\theta_{\max}| = \frac{|T_n| \cdot R}{J_e \left[\frac{I_p \cdot G (J_e + J_p)}{L (J_e \cdot J_p)} - \omega^2 \right]}. \quad (226)$$

The amplitude of this vibration becomes theoretically infinite if the denominator of Equation (226) becomes zero,

$$\text{i.e. when} \quad \omega^2 = \omega_c^2 = \frac{I_p \cdot G (J_e + J_p)}{L (J_e \cdot J_p)}. \quad (227)$$

$$\text{If} \quad N_c = \text{critical speed} = \frac{30 \cdot \omega_c}{\pi \cdot n} \text{ revs. per min.,}$$

$$\text{then} \quad N_c = \frac{9 \cdot 55}{n} \sqrt{\frac{I_p \cdot G (J_e + J_p)}{L (J_e \cdot J_p)}}. \quad (228)$$

$$\text{and} \quad F = \text{natural frequency} = n \cdot N_c = 9 \cdot 55 \sqrt{\frac{C (J_e + J_p)}{L (J_e \cdot J_p)}}, \quad (229)$$

$$\text{where} \quad C = \text{torsional rigidity of shaft} = \frac{I_p \cdot G}{L}$$

The periodic torque in the shaft reaches a maximum at the same time as the angular deflection,

$$\text{i.e.} \quad M_{\max} = \frac{I_p \cdot G \cdot |\theta_{\max}|}{L} = C \cdot |\theta_n|$$

Hence, the maximum vibration stress is

$$f_s = \frac{M_{\max}}{Z} = \frac{C \cdot |\theta_{\max}|}{Z}, \quad (230)$$

where Z = polar moment of resistance of shaft

$$= \frac{\pi \cdot d^3}{16}, \text{ for a solid shaft.}$$

If the value of w_e^2 in Equation (227) is substituted in Equation (226), the latter expression reduces to

$$|\theta_{\max}| = \frac{|T_n| \cdot R}{J_e(w_e^2 - w^2)}. \quad (231)$$

Also, if the periodic force causes very slow vibrations, i.e. if the engine is running very slowly, the limiting case, when $w = 0$, is approached. The corresponding limiting value of the torsional vibration amplitude $|\theta_0|$, which will be referred to as the *Equilibrium Amplitude*, will be as follows:—

$$|\theta_0| = \frac{|T_n| \cdot R}{J_e \cdot w_e^2}$$

or, substituting for w_e^2 from equation (227),

$$|\theta_0| = \frac{|T_n| \cdot R \cdot L \cdot J_p}{I_p \cdot G(J_e + J_p)} = \frac{|T_n| \cdot R \cdot J_p}{C(J_e + J_p)}. \quad (232)$$

The equilibrium stress is obtained as follows:—

$$\text{Equilibrium stress} = f_{s0} = \frac{C \cdot |\theta_0|}{Z} = \frac{|T_n| \cdot R \left[\frac{J_p}{J_e + J_p} \right]}{Z}. \quad (233)$$

The ratio $|\theta_{\max}|/|\theta_0|$ will be referred to as the dynamic magnifier and is obtained by dividing Equation (231) by Equation (232),

$$\begin{aligned}
 \text{i.e. Dynamic magnifier} &= \frac{|\theta_{\max}|}{|\theta_0|} = \frac{C(J_e + J_p)}{J_e \cdot J_p (\omega_c^2 - \omega^2)} \\
 &= \frac{1}{(\omega_c^2 - \omega^2)} \\
 &= \frac{1}{1 - \frac{\omega^2}{\omega_c^2}} \\
 &= \frac{1}{1 - \frac{N^2}{N_c^2}} \quad \cdot \quad \cdot \quad (234)
 \end{aligned}$$

where N = applied frequency,
 N_c = natural frequency.

Fig. 75 gives the values of the dynamic magnifiers for different frequency ratios, without damping. It should be noticed that without damping the amplitude becomes theoretically infinite when the applied frequency is equal to the natural frequency, and that the amplitude of the vibration is less than the equilibrium amplitude when the frequency ratio exceeds 1.414.

Table 51 contains the values of the dynamic magnifiers for different frequency ratios.

Fig. 75 (p. 416) and Table 51 (p. 417) are based on the assumption that the excitation torque, and therefore the values of the corresponding harmonic components, are constant over the whole of the speed range.

It will be shown later that this condition is not generally fulfilled in practice, although certain types of transmission systems have a constant excitation torque over a limited speed range. In such cases the values given in Table 51 can only be applied over this limited speed range. Outside this range it is necessary to determine the altered values of the harmonic components due to the changes in the value of the excitation torque, and then to recalculate the values of the equilibrium amplitudes or stresses before applying the dynamic magnifiers in Table 51. This task may be somewhat simplified if the magnitude of a harmonic component changes with speed

in accordance with a definite law. An important special case of this kind is when the magnitude of a harmonic component is directly proportional to the square of the speed. The har-

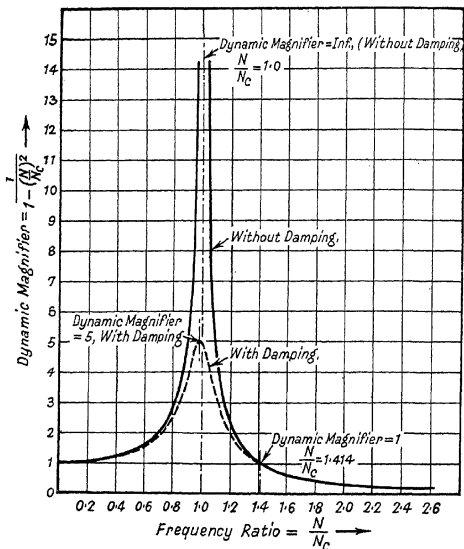


FIG. 75.—Dynamic magnifiers with constant excitation torque.

monic components of the tangential effort curve due to the inertia of the reciprocating parts of an engine vary in magnitude according to this law (see Table 54).

The values of the dynamic magnifiers when the magnitudes

TABLE 51.
DYNAMIC MAGNIFIERS (WITHOUT DAMPING).
(Excitation Torque Constant.)

N/N _c	Dync. Magnr.	N/N _c	Dync. Magnr.	N/N _c	Dync. Magnr.	N/N _c	Dync. Magnr.
0.100	1.01	0.905	5.53	1.030	16.39	1.210	2.16
0.200	1.04	0.910	5.82	1.035	14.08	1.220	2.05
0.300	1.10	0.915	6.14	1.040	12.20	1.230	1.95
0.400	1.19	0.920	6.51	1.045	10.87	1.240	1.86
0.500	1.34	0.925	6.93	1.050	9.71	1.250	1.78
0.550	1.43	0.930	7.40	1.055	8.85	1.300	1.45
0.600	1.56	0.935	7.95	1.060	8.06	1.350	1.22
0.650	1.73	0.940	8.59	1.065	7.46	1.400	1.04
0.700	1.96	0.945	9.35	1.070	6.90	1.450	0.91
0.750	2.28	0.950	10.26	1.075	6.41	1.500	0.80
0.760	2.37	0.955	11.36	1.080	6.02	1.600	0.64
0.770	2.46	0.960	12.76	1.085	5.65	1.700	0.53
0.780	2.56	0.965	14.54	1.090	5.32	1.800	0.45
0.790	2.66	0.970	16.92	1.095	5.03	1.900	0.38
0.800	2.78	0.975	20.24	1.100	4.76	2.000	0.34
0.810	2.91	0.980	25.25	1.110	4.31	2.100	0.29
0.820	3.05	0.985	33.56	1.120	3.94	2.200	0.26
0.830	3.22	0.990	50.25	1.130	3.61	2.300	0.23
0.840	3.41	0.995	100	1.140	3.34	2.400	0.21
0.850	3.60	1.000	Infty.	1.150	3.10	2.500	0.19
0.860	3.85	1.005	100	1.160	2.89	2.600	0.17
0.870	4.11	1.010	50.00	1.170	2.71	2.700	0.16
0.880	4.43	1.015	33.34	1.180	2.55	2.800	0.15
0.890	4.81	1.020	25.00	1.190	2.40	2.900	0.14
0.900	5.26	1.025	19.61	1.200	2.27	3.000	0.13

of the harmonic components are directly proportional to the square of the speed may be determined as follows:—

Let $|T_{ne}|$ = maximum value of n th order harmonic component of the tangential effort curve, when $\omega = \omega_c$. This will be referred to as the equilibrium torque,

$|T_n|$ = maximum value of n th order harmonic component at speed ω ,

then $|T_n| = |T_{nc}|(\omega/\omega_c)^2$.
 Also, if $|\theta_0| =$ equilibrium amplitude (due to application of $|T_{nc}|$),

$|\theta_{\max}| =$ maximum amplitude at speed ω .

Then, by substituting $|T_n| = |T_{nc}|(\omega/\omega_c)^2$ in Equation (231),

$$|\theta_0| = \frac{|T_{nc}| \cdot R}{J_e \cdot \omega_c^2},$$

$$|\theta_{\max}| = \frac{|T_{nc}|(\omega/\omega_c)^2 \cdot R}{J_e(\omega_c^2 - \omega^2)},$$

$$\text{i.e. dynamic magnifier} = \frac{|\theta_{\max}|/|\theta_0|}{1 - (\omega/\omega_c)^2} = \frac{(N/N_c)^2}{1 - (N/N_c)^2} \quad (235)$$

where $N =$ applied frequency,
 $N_c =$ natural frequency.

Fig. 76 shows the resonance curve for this type of excitation, and Table 52. gives a list of dynamic magnifiers for different frequency ratios when damping is neglected.

TABLE 52.

DYNAMIC MAGNIFIERS (WITHOUT DAMPING).

Excitation Torque Directly Proportional to (R.P.M.)².

N/N_c	Dync. Magnr.	N/N_c	Dync. Magnr.	N/N_c	Dync. Magnr.	N/N_c	Dync. Magnr.
0.100	0.010	0.850	2.604	0.995	99.25	1.100	5.762
0.200	0.042	0.875	3.267	1.000	Inf.	1.125	4.765
0.300	0.099	0.900	4.263	1.005	100.8	1.150	4.101
0.400	0.190	0.910	4.816	1.010	50.75	1.175	3.627
0.500	0.333	0.920	5.510	1.020	25.74	1.200	3.278
0.550	0.434	0.930	6.402	1.030	17.42	1.250	2.778
0.600	0.562	0.940	7.591	1.040	13.26	1.300	2.449
0.650	0.732	0.950	9.256	1.050	10.76	1.400	2.042
0.700	0.961	0.960	11.76	1.060	9.091	1.500	1.800
0.750	1.286	0.970	15.92	1.070	7.901	2.000	1.333
0.800	1.778	0.980	24.25	1.080	7.010	2.500	1.190
0.825	2.131	0.990	49.25	1.090	6.316	3.000	1.125

Fig. 76 shows that when the frequency ratio is $\sqrt{2}$ the dynamic magnifier is 2, i.e. the vibration amplitude or stress is twice the equilibrium amplitude or stress when the operating speed is 1.414 times the critical speed.

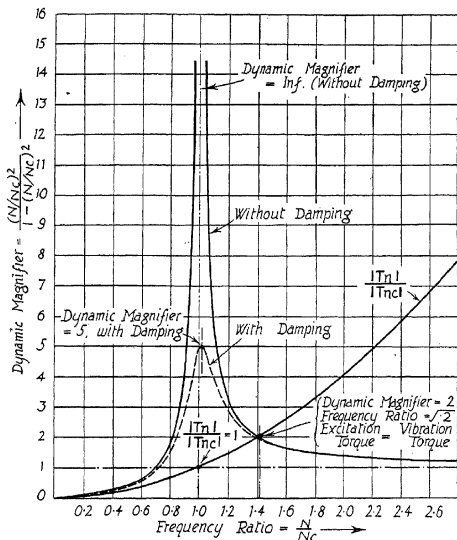


FIG. 76.—Dynamic magnifiers with excitation torque directly proportional to N^2 .

Since, however, the ratio of applied torque to equilibrium torque is also 2 for a frequency ratio of 1.414, it follows that there is no actual magnification of the applied torque at this frequency ratio. Another important characteristic of Fig. 76

is that the forced vibration torque in the connecting shaft is greater than the applied torque for all values of frequency ratio less than 1.414, whilst it is less than the applied torque for frequency ratios greater than 1.414. This is the same as for the constant applied torque resonance curve of Fig. 75.

It is also evident that the dynamic magnifier is zero when the speed is zero and that it approaches unity as the speed approaches infinity. The former condition is explained by the fact that the excitation torque becomes zero at zero speed, and the latter condition by the fact that the excitation torque and the speed both approach infinite values simultaneously.

It is important to realise that with a constant excitation torque the forced vibration amplitudes or stresses can be made very small merely by increasing the operating speed and without any alteration of critical speed, as shown in Fig. 75. When, however, the excitation torque varies directly as the square of the speed the forced vibration amplitudes or stresses cannot be made smaller than the equilibrium amplitudes or stresses by an increase of operating speed. For this latter condition the equilibrium amplitude or stress is calculated from the same equations as are used when the excitation torque is constant, i.e. Equations (232), (233), (239), (240), (241), (245), (246), (247) and (248), but the values of the harmonic components used in these equations must be the values corresponding to the excitation torque when the transmission system is running at the critical speed. It is therefore evident that the forced vibration amplitudes and stresses can only be reduced below the existing equilibrium amplitudes and stresses by lowering the critical speed, i.e. by reducing the natural frequency of the system. When this is done the equilibrium amplitudes and stresses must be recalculated, using the values of the harmonic components corresponding to the excitation torque at the new critical speed, and these new values will be less than the values corresponding to the original critical speed.

Fig. 77 illustrates the foregoing point. The full lines show the conditions with the critical speed at its original position in the speed range, namely 100 r.p.m., whilst the dotted lines show the condition when the critical speed is reduced to 66.7

r.p.m. In the following discussion it will be assumed that $|T_{nc}|$, etc., represent torques instead of tangential efforts.

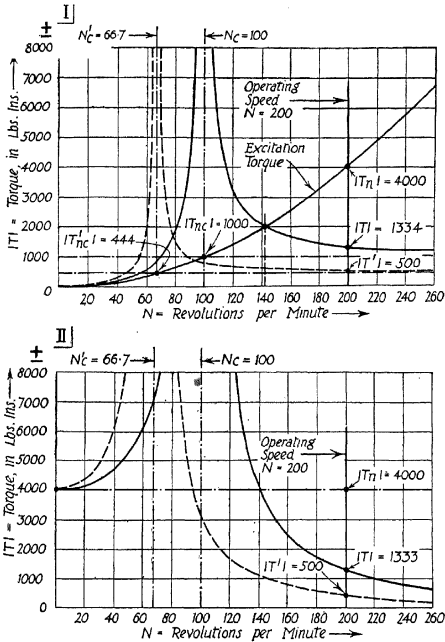


FIG. 77.—Forced vibration amplitudes.

The excitation torque curve is shown on Diagram I, the original equilibrium torque, $|T_{nc}|$, having a value of 1000

lbs.-ins. in this example. Since the forced vibration amplitudes, stresses, and torques at any speed are all proportional to one another, it follows that

$$\text{Dynamic magnifier} = |\theta_{\max}|/|\theta_0| = f_s/f_{s0} = |T|/|T_{nc}|,$$

where $|T|$ is the torque induced in the connecting shaft by the exciting torque $|T_n|$.

Hence, from Equation (235),

$$|T|/|T_{nc}| = \frac{(N/N_c)^2}{1 - (N/N_c)^2} = \text{the dynamic magnifier.}$$

Assuming an original critical speed $N_c = 100$ r.p.m., the frequency ratio at 200 r.p.m. is $N/N_c = 2$, and, from Table 52, the dynamic magnifier at 200 r.p.m. is 1.333,

$$\text{i.e. } |T| = 1.333 \times 1000 = 1333 \text{ lbs.-ins.}$$

The complete resonance curve for a critical speed of 100 r.p.m. is shown by the full lines in Diagram I of Fig. 77. Diagram II shows how the magnitude of the forced vibration torque at 200 r.p.m. could have been obtained from a curve of the type shown in Fig. 75, using the dynamic magnifiers given in Table 51. It is first necessary to determine the excitation torque at the operating speed, i.e. at 200 r.p.m. In this case the forcing torque is proportional to N^2 and has a value 1000 at the critical speed, hence,

$$\begin{aligned} |T_n| &= \text{forcing torque at 200 r.p.m.} = 1000 \times \left(\frac{200^2}{100}\right) \\ &= 4000 \text{ lbs.-ins.} \end{aligned}$$

This is the value which must be taken for the equilibrium torque when constructing the resonance curve shown by the full lines in Diagram II of Fig. 77, i.e. it is assumed that this forcing torque remains constant, whilst the frequency is varied. Then, from Table 51, the dynamic magnifier for a frequency ratio $200/100 = 2$ is 0.3333.

Hence, $|T| = 4000 \times 0.3333 = 1333$ lbs.-ins., as before.

Diagram I shows that no matter how much the operating speed is increased the forced vibration torque cannot be reduced

below the equilibrium torque, viz. 1000 lbs.-ins., so long as the critical speed remains at 100 r.p.m.

If it is desired to reduce the forced vibration torque at 200 r.p.m. to 500 lbs.-ins., the required change in frequency can be obtained as follows:—

Referring to Diagram II of Fig. 77, the dynamic magnifier, when the forced vibration torque at 200 r.p.m. is 500 lbs.-ins., is $500/4000 = 1/8$. Now for a resonance curve of the type shown in Diagram II,

$$\text{Dynamic magnifier} = \frac{1}{1 - (N/N_c')^2}$$

This gives a value $1/8$ when the frequency ratio (N/N_c') is 3.

Note.—Strictly speaking the dynamic magnifiers for all speeds on the right-hand side of the resonant speed have negative values, i.e. this flank of the resonance curve should really be plotted below the base line of the diagram. It is, however, more convenient to plot it as shown in the diagrams.

Hence, the required position of the critical speed is

$$N_c' = N/3 = 200/3 = 66.7 \text{ r.p.m.}$$

Referring now to Diagram I of Fig. 77.

The equilibrium torque at the new critical speed is

$$|T_{nc'}| = 1000(66.7/100)^2 = 444 \text{ lbs.-ins.}$$

Also, from Table 52, the dynamic magnifier for the new frequency ratio, $N/N_c' = 3$, is 1.125.

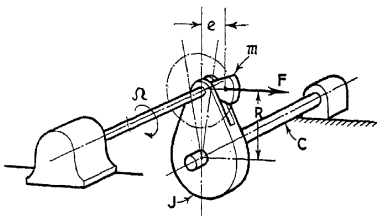
Hence the new value of the forced vibration torque at 200 r.p.m. is

$$|T'| = 444 \times 1.125 = 500 \text{ lbs.-ins., which is the desired value.}$$

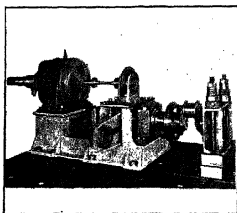
The new resonance curve is shown by the dotted lines, and it should be noted that with this new position of the critical speed it is not possible to reduce the forced vibration torque below 444 lbs.-ins., no matter how much the operating speed is increased.

Fig. 78 shows an application where the magnitude of the forcing torque is proportional to the square of the speed. The apparatus illustrated is a fatigue testing machine used by the

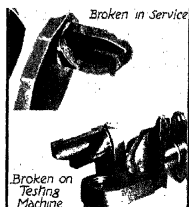
D.V.L. for investigating the strength of full-size crankshaft elements. The illustrations are reproduced from a paper by Professor Karl Lürenbaum entitled "Belastung und Tragfähigkeit von Flugmotoren Kurbelwellen," *Gesammelte Vorträge*



Diagrammatic Arrangement



Fatigue Testing Machine for Full Scale Crank Elements



Fatigue Tests on Aero-Engine Crankshafts.

FIG. 78.—Fatigue testing machine (D.V.L.).

de Hauptversammlung, 1937, der Lilienthal Gesellschaft für Luftfahrtforschung.

One end of the crank element under test is fixed to the bracket shown at the right-hand side of the illustration and a beam with movable weights is secured to the other end of the crank element. The arrangement therefore is equivalent to

the simple torsional pendulum shown in the diagrammatic arrangement in Fig. 78, the elasticity of the crank representing the spring member C, and the loaded beam representing the inertia element J.

The weights can be moved along the beam for the purpose of altering the moment of inertia of the system and by this means the vibrating system can be adjusted to the desired test frequency. The system is excited by an unbalanced rotating mass, driven by a variable speed electric motor which applies a once per revolution torque variation to the specimen.

The exciting torque is therefore given by the following expression :—

$$|T_n| = F \cdot R = m \cdot \Omega^2 \cdot e \cdot R,$$

where R = radius of application of the unbalanced force F,
 m = unbalanced mass of exciter,
 Ω = angular velocity of exciter mass,
 e = distance of c.g. of unbalanced mass from its axis of rotation.

Also, if ω_c = angular velocity of exciter corresponding to the resonant frequency of the system,

$$|T_{nc}| = \text{the equilibrium torque,}$$

then $|T_{nc}| = m \cdot \omega_c^2 \cdot e \cdot R.$

And the torque applied to the shaft at any other speed ω outside the resonant zone is obtained by multiplying $|T_{nc}|$ by the dynamic magnifiers in Table 52. The shape of the resonance curve is that shown in Fig. 76.

The amplitude at any speed ω is obtained as follows :—

$$\text{Equilibrium amplitude} = \theta_0 = |T_{nc}|/C = m \cdot \omega_c^2 \cdot e \cdot R/C,$$

but $\omega_c^2 = C/J,$

where C = torsional rigidity of shaft,
 J = polar moment of inertia of attached flywheel mass.

Hence, $\theta_0 = m \cdot e \cdot R/J,$

and $\theta_{\max}/\theta_0 = \frac{(N/N_c)^2}{1 - (N/N_c)^2},$ at non-resonant speeds.

The torque and amplitude in the resonant zone cannot, of course, be determined by the above expression since they depend largely upon the amount of damping in the system.

A typical service fracture is shown in Fig. 78 compared with a fracture produced on the testing machine. It is evident that in both cases characteristic torsional vibrational fractures have been obtained.

Summary of Formulæ for Two-Mass Systems.

(a) *Expression for Critical Speed:—*

$$N_c = \frac{9.55}{n} \sqrt{\frac{C(J_e + J_p)}{J_e \cdot J_p}}, \quad (\text{from Eqn. 229})$$

where N_c = n th order critical speed, revs. per min.,

n = number of complete oscillations per rev.,

J_e = moment of inertia of engine masses,

J_p = moment of inertia of propeller,

C = torsional rigidity of shafting

$G \cdot I_p$

G = modulus of rigidity = 12,000,000 lbs./sq. in., or
772,000 tons/sq. ft. for carbon and alloy steel shafts,

I_p = polar moment of inertia of cross-section of shaft

$$= \frac{\pi \cdot d^4}{32},$$

d = diameter of shaft,

L = length of shaft,

i.e. $C = \frac{1175000 \cdot d^4}{L}$, if d and L are in inches; C in
lbs.-ins./radian

$= \frac{75500 \cdot d^4}{L}$, if d and L are in feet; C in
tons-ft./radian.

Hence, for steel shafts,

$$N_e = \frac{10350 \cdot d^2}{n} \sqrt{\frac{(J_e + J_p)}{L \cdot J_e \cdot J_p}} \text{ r.p.m.,} \quad (236)$$

when d and L are in inches, and J_e and J_p in lbs.-ins. sec.² units,

$$= \frac{2620 \cdot d^2}{n} \sqrt{\frac{(J_e + J_p)}{L \cdot J_e \cdot J_p}} \text{ r.p.m.,} \quad (237)$$

when d and L are in feet, and J_e and J_p in tons-ft.-sec.² units.

(b) *Expression for Equilibrium Amplitude* (i.e. amplitude when $N = 0$):—

$$|\theta_0| = \frac{|T_n| \cdot R \cdot J_p}{C(J_e + J_p)}, \quad (232)$$

where $|\theta_0|$ = equilibrium amplitude in radians,*

$|T_n|$ = n th order harmonic component of tangential effort curve for whole cylinder group in lbs.,

R = crank radius = stroke/2 for single-piston engines; and (total combined stroke)/4 for opposed-piston engines.

For steel shafts,

$$|\theta_0| = \frac{|T_n| \cdot R \cdot L}{1175000 \cdot d^4} \left(\frac{J_p}{J_e + J_p} \right) \text{ radians,} \quad (238)$$

when R , L , and d are in inches, $|T_n|$ in lbs., and J_p and J_e in lbs.-ins. sec.² units,

$$= \frac{|T_n| \cdot R \cdot L}{75500 \cdot d^4} \left(\frac{J_p}{J_e + J_p} \right) \text{ radians,} \quad (239)$$

when R , L , and d are in feet, $|T_n|$ in tons, and J_p and J_e in tons-ft. sec.² units.

Note.— $|\theta_0|$ is the total deflection of one end of the shaft relative to the other end, when $N = 0$.

* *Note.*—In Equation (232) $|\theta_0|$ is the equilibrium amplitude of twist between J_e and J_p . In multi-mass system the term equilibrium amplitude usually refers to the equilibrium amplitude at the free end of the shaft.

(c) *Expression for Equilibrium Stress* :—

$$R / \underline{J_p} \quad . \quad . \quad (233)$$

where $Z =$ polar moment of resistance of shaft
 $\frac{\pi \cdot d^3}{16}$

$$\text{Hence, } f_{s0} = \frac{5 \cdot 1 \cdot |T_n| \cdot R}{d^3} \left(\frac{J_p}{J_e + J_p} \right) \text{ lbs./sq. in., } \quad (240)$$

when d and R are in inches, $|T_n|$ in lbs., and
 J_e and J_p in lbs.-ins. sec.² units,

$$= \frac{79 \cdot 3 \cdot |T_n| \cdot R}{d^3} \left(\frac{J_p}{J_e + J_p} \right) \text{ lbs./sq. in., } \quad (241)$$

when d and R are in feet, $|T_n|$ in tons, and J_e
and J_p in tons-ft. sec.² units.

(d) *Expression for Maximum Stress at N Revolutions per Minute
(Damping Neglected)* :—

$$f_s = f_{s0} \times (\text{dynamic magnifier})$$

$$= f_{s0} \times \left[1 - \frac{\bar{N}}{N_c^2} \right] \text{ lbs. per sq. in. (from Eqn. 234)}$$

The magnitudes of the dynamic magnifiers for different values of the ratio N/N_c are given in Table 51.

The foregoing expressions may be used in cases where the oscillating system can be reduced to a simple equivalent two-mass system, e.g. for the one-node mode of vibration of marine installations where the engine masses are separated from the propeller by a long length of intermediate shafting, the torsional rigidity of which is small compared with that of the engine crankshaft.

In such cases the stress values obtained by assuming an equivalent two-mass system are not greatly different from the values obtained by more elaborate methods.

In cases where the torsional rigidity of the engine crankshaft is not large compared with that of the intermediate

shafting, or where there are a number of masses connected by sections of shafting of approximately equal torsional rigidity, the foregoing simple treatment cannot be employed.

The two-node mode of vibration of marine installations, and the one-node mode of vibration of close-coupled electrical generating sets, are examples of installations where a more elaborate treatment is necessary to obtain a satisfactory solution.

Equilibrium Amplitude—Multi-Mass Systems.—It has already been mentioned that in the case of a shaft transmitting power, provided the applied and resisting torques are perfectly uniform, the only effect of the elasticity of the shafting is to cause the end from which power is being taken to lag behind the end at which power is applied.

If, however, the applied and resisting torques are suddenly removed, the shaft is put into a state of free vibration, and the curve of angular displacement can be analysed into a series of normal elastic curves, each corresponding to one of the normal modes of free vibration of which the system is capable.

The amplitude of any one of these modes of vibration under the above conditions will be referred to as the *Equilibrium Amplitude*, since it is the amplitude which is attained without any magnification due to resonance with an external pulsating couple.

The stress corresponding to the equilibrium amplitude will be referred to as the *Equilibrium Stress*.

Note.—The equilibrium amplitude and stress in a multi-mass system varies throughout the system. Unless stated otherwise, however, the terms *equilibrium amplitude* and *equilibrium stress* will be used to denote the equilibrium amplitude at the free end of the shaft and the maximum value of the equilibrium stress respectively.

The equilibrium amplitude of any normal mode can be obtained by equating the work done by the external couple when the shaft is deflected from its mean position to one extreme of its angular displacement (i.e. through the angle corresponding to the equilibrium amplitude), to the maximum potential energy of the vibration.

Consider a simple system having a mass of moment of inertia J at one end, fixed at the other end, and subjected to the action of an external couple M at some intermediate point.

Let θ = amplitude at the point where the mass is attached,

θ_1 = amplitude at the point where the couple is applied,

w_c = phase velocity

$$= \frac{2 \cdot \pi \cdot F}{60} \text{ radians per sec.},$$

F = frequency of vibration in oscillations/min.

Then work done by external couple in moving shaft through an amplitude θ_1 is

$$E_c = \frac{1}{2} \cdot M \cdot \theta_1.$$

The maximum torque due to the inertia of the attached mass is

$$M_1 = J \cdot w_c^2 \cdot \theta,$$

i.e. maximum potential energy, $E_p = \frac{1}{2} \cdot J \cdot w_c^2 \cdot \theta^2$.

For equilibrium $E_c = E_p$,

$$\text{or} \quad \frac{1}{2} \cdot M \cdot \theta_1 = \frac{1}{2} \cdot J \cdot w_c^2 \cdot \theta^2,$$

$$\text{whence} \quad \theta^2 = \frac{M \cdot \theta_1}{J \cdot w_c^2} \quad \dots \quad (242)$$

Let a = ordinate on normal elastic curve at point where the actual amplitude is θ ,

a_1 = ordinate on normal elastic curve at point where the actual amplitude is θ_1 .

$$\text{Then} \quad \frac{\theta_1}{a_1} = \frac{\theta}{a}; \quad \text{or} \quad \theta = \frac{a \cdot \theta_1}{a_1},$$

$$\text{i.e.} \quad \frac{\theta \cdot a \cdot \theta_1}{a_1} = \frac{M \cdot \theta_1}{J \cdot w_c^2}, \quad (\text{from Eqn. 242})$$

$$\text{or} \quad \theta = \frac{M \cdot a_1}{\omega_c^2 \cdot J \cdot a} \quad \dots \quad (243)$$

Now, let θ_0 = the amplitude at any selected datum point where the amplitude on the normal elastic curve is a_0 .

Then, since $\theta_0/a_0 = \theta/a$,

$$\theta_0 = \frac{M \cdot a_1 \cdot a_0}{w_c^2 \cdot J \cdot a^2} \quad \dots \quad (244)$$

where θ_0 is the equilibrium amplitude at that point in the system where the amplitude on the normal elastic curve is a_0 . It is customary to assume unit amplitude at the free end of the shaft when setting down the normal elastic curve, and when this is done the expression for the equilibrium amplitude is obtained by putting $a_0 = 1$ in Equation (244),

i.e.
$$\theta_0 = \frac{M \cdot a_1}{w_c^2 \cdot J \cdot a^2} \quad \dots \quad (245)$$

Note that in the case of a simple torsional pendulum where the mass is at the free end of the shaft, if the exciting couple is also applied at the free end of the shaft, then $a = a_1 = a_0 = 1$, Equation (245) reduces to

$$\begin{aligned} \theta_0 &= \frac{M}{w_c^2 \cdot J} \\ &= \frac{M}{C}, \text{ since } w_c^2 = C/J, \text{ for a simple torsional pendulum,} \end{aligned}$$

C = the torsional rigidity of the shaft.

In an actual installation having several attached masses, and subjected at various points to the action of several applied couples, Equation (245) becomes

$$\theta_0 = \frac{T_n \cdot A \cdot R \cdot \Sigma a}{w_c^2 \cdot \Sigma (J \cdot a^2)} \text{ radians,} \quad \dots \quad (246)$$

where θ_0 = equilibrium amplitude at free end of crankshaft,
 T_n = maximum value of n th order harmonic component of tangential effort curve for one cylinder, in lbs. per sq. in. of cylinder area,
 A = area of cylinder in sq. ins.,
 R = crank radius
 = (total combined stroke)/4, for opposed-piston engines,

Σa = vector sum of ordinates at each cylinder from normal elastic curve, assuming unit amplitude at free end of crankshaft,

w_o = phase velocity, in radians per sec.

$$= \frac{2 \cdot \pi \cdot F}{60},$$

F = natural frequency of vibration, in oscillations per minute,

$\Sigma(J \cdot a^2)$ = effective moment of inertia of system referred to free end of crankshaft, i.e. the arithmetic sum of the products of the moments of inertia of the respective masses and the squares of the ordinates at each mass from the normal elastic curve, assuming unit amplitude at the free end of the crankshaft,

D = diameter of cylinder in inches.

If R is in feet and J is in tons-ft. sec.², Equation (246) reduces to

$$\frac{1.83 \cdot D^2 \cdot R \cdot T_n \cdot \Sigma a}{F^2 \cdot \Sigma(J \cdot a^2)} \text{ degrees.} \quad (247)$$

Notes on Equation (246) :-

If Equation (246) is applied to a simple two-mass system consisting of a single cylinder engine mass J_e at one end of a shaft of torsional rigidity C , and a propeller mass J_p at the other end, the following result is obtained :-

Let θ_{e0} = equilibrium amplitude at engine,

θ_{p0} = equilibrium amplitude at propeller,

T_n = n th order harmonic component of tangential effort curve of engine.

Then $|\theta_0| = (\theta_{e0} - \theta_{p0})$ = equilibrium amplitude of twist between J_e and J_p ,

but
$$\theta_{p0} = \theta_{e0} \left(1 + \frac{J_e}{J_p} \right),$$

also
$$T_n \cdot A \cdot R \cdot \Sigma a = |T_n| \cdot R \cdot \theta_{e0}$$

and
$$\Sigma(J \cdot a^2) = J_e \left[1 + \frac{J_e}{J_p} \right].$$

Hence, Equation (246) becomes

$$\theta_{e0} = \frac{|T_n| \cdot R}{\omega_e^2 \cdot J_e \left[1 + \frac{J_e}{J_p} \right]},$$

i.e.
$$|\theta_0| = \frac{|T_n| \cdot R}{\omega_e^2 \cdot J_e} = \frac{|T_n| \cdot R \cdot J_p}{C(J_e + J_p)},$$

which agrees with Equation (232).

If R is in inches and J in lbs.-ins. sec.², Equation (246) reduces to

$$\theta_0 = \frac{4100 \cdot D^2 \cdot R \cdot T_n \cdot \Sigma a}{F^2 \cdot \Sigma (J \cdot a^2)} \text{ degrees.} \quad (248)$$

Equilibrium Stress.—The equilibrium stress is obtained from the equilibrium amplitude, in degrees, by multiplying the latter by the stress for one degree deflection at the free end of the crankshaft given in column K of the frequency table (see Tables 1, 2, 3, and 4).

Application to Multi-Cylinder Engines.—In applying the foregoing analysis to an actual installation, the principle of linear superposition plays an important part. This principle may be stated as follows:—

In any linear elastic system the motion produced by two or more sets of periodically varying forces, acting simultaneously, is equal to the sum of the motions which would be produced by the separate forces acting alone, due regard being given to the phase relations between the respective components.

Thus the motion produced by the varying torque of a single cylinder is the sum of the motions which would be produced by the separate components of the torque curve if these were assumed to be acting alone; and the motion produced by a group of cylinders is the sum of the motions produced by the separate cylinders.

In dealing with multi-cylinder installations it is necessary therefore to separate the tangential effort curve into its harmonic components and to give each of these separate consideration. In any given system certain components will predominate whilst others will be negligible.

In the case of one-node vibrations, i.e. vibrations of the first degree, of marine installations, for example, the node is so disposed relative to the engine crankshaft that all cylinders vibrate with nearly equal amplitudes. The only critical speeds of serious importance are the major criticals, i.e. those critical speeds at which the number of oscillations per revolution is equal to or is an integral multiple of the number of cylinders in the case of 2 S.C., S.A. engines where the working cycle occupies one revolution of the engine. In the case of 4 S.C.,

S.A. engines where the working cycle occupies two revolutions, the major criticals are those critical speeds at which the number of oscillations per revolution is equal to one-half the number of cylinders or is an integral multiple of one-half the number of cylinders. The minor criticals cancel.

For two-node vibrations, i.e. vibrations of the second degree, one of the nodes usually falls within the crankshaft, and where a heavy flywheel is fitted it is generally located close to the flywheel. In that case, the cylinders remote from the flywheel are more effective in producing vibration than those situated close to that point, so that only partial cancellation of the minor criticals takes place. Hence, serious second degree vibrations can occur at both major and minor criticals, depending on the elasticity of the system, the positions of the principal masses, the type of prime mover, and the firing order.

By constructing vector diagrams showing the phase relations between the impulses imparted by the several cylinders, the resultant impulse imparted by the entire group of cylinders for any particular critical is obtained. This matter is fully explained later.

Harmonic Components of Tangential Effort Curve.—

The tangential effort curve of an internal combustion engine repeats after every complete working cycle. For a four-stroke cycle, single-acting engine the interval of repetition is two revolutions, and for a two-stroke cycle, single-acting engine it is one revolution. This curve may therefore be represented by a Fourier series consisting of a constant term and a series of harmonically varying terms having 1, 2, 3, 4, etc., repetitions per cycle.

The constant term is merely the mean tangential effort, and can be determined as follows :—

- Let P_m = mean indicated pressure in lbs./sq. in.,
 L = total stroke in feet,
 A = area of cylinder in sq. ins.,
 N = revolutions per minute,
 n = number of working cycles per minute
 = $N/2$ for 4-S.C., S.A. engines

- $= N$ for 4-S.C., D.A. and 2-S.C., S.A. engines
 $= 2 \cdot N$ for 2-S.C., D.A. engines,
 T_m = mean tangential effort in lbs./sq. in.,
 R = crank radius in feet
 $= L/4$ for opposed-piston engines,
 I.H.P. = indicated horse power.

$$\text{Then I.H.P.} = \frac{P_m \cdot L \cdot A \cdot n}{33000} = \frac{2 \cdot \pi \cdot R \cdot N \cdot T_m \cdot A}{33000}$$

$$\text{i.e.} \quad T_m = \frac{P_m \cdot L \cdot n}{2 \cdot \pi \cdot R \cdot N}$$

Hence, for four-stroke cycle, single-acting engines, where $n = N/2$,

$$T_m = \frac{P_m}{2 \cdot \pi}$$

For four-stroke cycle, double-acting, and two-stroke cycle, single-acting engines, where $n = N$ and $L = 2R$,

$$\begin{aligned}
 T_m &= \frac{P_m}{\pi} \text{ for single-piston engines, where } L = 2 \cdot R, \\
 &= \frac{2 \cdot P_m}{\pi} \text{ for opposed-piston engines, where } L = 4 \cdot R.
 \end{aligned}$$

For two-stroke cycle, double-acting engines, where $n = 2 \cdot N$,

$$T_m = 2 \cdot P_m$$

The mean turning moment is given by the following expression :—

$$\text{Mean turning moment} = T_m \cdot A \cdot R \text{ lbs.-ft.}$$

It is convenient to describe the several harmonics of the tangential effort curve in terms of the number of complete impulses per revolution of the prime mover, and to refer to these as the order numbers of the harmonics.

Thus for a four-stroke cycle, single-acting engine, where the complete working cycle occupies two revolutions, there will be harmonic components of the $\frac{1}{2}$, 1, $1\frac{1}{2}$, 2, $2\frac{1}{2}$, etc., orders; whilst for a two-stroke cycle, single-acting engine, where the working cycle occupies one revolution, there are no half orders.

For example, the third order component of the tangential

effort curve repeats itself three times in each revolution irrespective of the type of prime mover, when the above notation is used.

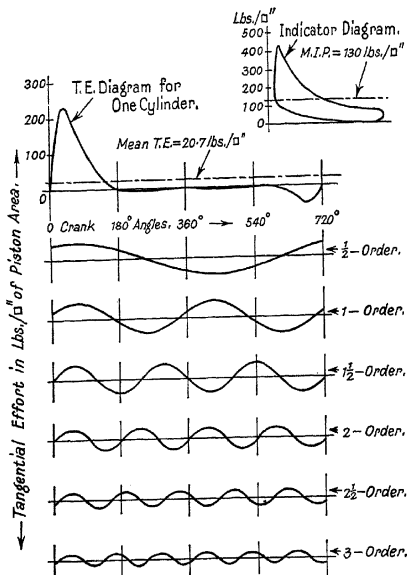


FIG. 79.—Harmonic components of tangential effort diagram for one-cylinder 4-S.C., S.A. petrol engine.

These component curves do not represent work, since there is an equal number of positive and negative areas for each working cycle; but when the ordinates are added to the

constant term, which represents the mean tangential effort, a true copy of the tangential effort curve is obtained.

Fig. 79 shows the tangential effort curve and the first six harmonic components for a 4-S.C., S.A. petrol engine.

It is sufficient for the frequency of application of any one of the harmonic components of the tangential effort curve to coincide with one of the natural frequencies of torsional oscillation of the system for resonance to occur. It has already been mentioned that the various modes of free vibration are referred to by degree numbers. Hence, a third order, second degree vibration can also be described as the third harmonic of the two-node natural frequency of the system. A vibration of this type would arise in the presence of a third order harmonic component of the tangential effort curve, and resonance would occur when the product of the order number and the number of revolutions per minute became equal to the two-node natural frequency of torsional vibration, i.e. when the engine revolutions were exactly one-third of the two-node natural frequency.

Harmonic Analysis of Tangential Effort Curve.—The Fourier series for the tangential effort curve may be written thus :—

$$\begin{aligned} T &= T_m + \Sigma(A_n \sin n \cdot \theta + B_n \cos n \cdot \theta) \\ &= T_m + \Sigma T_n \sin (n \cdot \theta + \alpha_n), \end{aligned}$$

where T_m = constant mean tangential effort,

T_n = maximum value of the n th order resultant harmonic component,

n = order number, i.e. the number of complete impulses per revolution of the prime mover,

θ = crank angle,

α_n = phase angle.

Also, it can be shown that—

$$\begin{aligned} T_n &= \sqrt{A_n^2 + B_n^2}, \\ \text{Tan } \alpha_n &= \frac{B_n}{A_n}. \end{aligned}$$

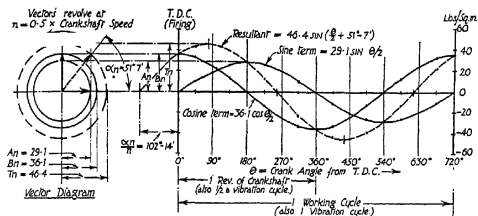
Fig. 80 gives a graphical interpretation of the above expressions where Diagram I shows the sine and cosine terms

and their resultant for the half-order harmonic component of the tangential effort curve of a four-stroke cycle single-acting engine. The data is taken from Table 53, namely:—

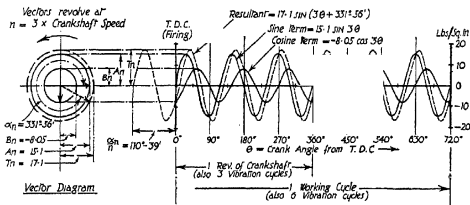
Sine term	$A_n = 29.1$ lbs. per sq. in. of piston area,
Cosine term	$B_n = 36.1$ „ „ „ „ „
Resultant	$T_n = \sqrt{A_n^2 + B_n^2} = 46.4,$
Phase angle	$\alpha_n = \tan^{-1} B_n/A_n = 51^\circ-7',$
Order number	$n = 0.5.$

The resultant is the algebraic sum of the sine and cosine terms, and variations of the amplitudes of the sine and cosine terms and of the resultant with time (or crank angle) are shown by plotting the vertical projections of the three rotating vectors on a base of crank angles. The sum of the sine and cosine vectors is obtained in the usual way by completing the parallelogram and drawing the diagonal shown dotted in the vector diagrams in Fig. 80. Since it is customary to take top dead centre (i.e. the position of the crank when the combustion stroke commences) as the origin of time for each working cycle, the vector representing the sine term must be set in phase or in counter-phase with the crank according to whether A_n is positive or negative. It will be assumed that upward projections are positive and that the vectors rotate in a counter-clockwise direction. These conventions imply that if A_n is positive the sine vector is set off to the right, whilst if A_n is negative the sine vector is set off to the left. The vector representing the cosine term must be set off at 90 degrees to the sine vector, and in accordance with the foregoing conventions the cosine vector is set off vertically upwards when B_n is positive and vertically downwards when B_n is negative. In this way the correct phasing of the resultant vector is assured.

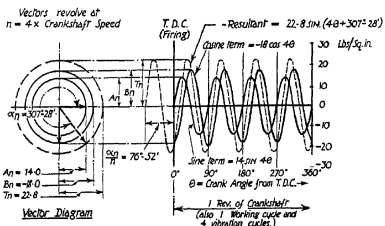
Since by definition the order number n is the number of complete vibration cycles which are completed in one revolution of the crankshaft, the rotating vectors must make n complete revolutions for each revolution of the crankshaft. Hence for each 360 degrees of crankshaft rotation the vectors



I 1/2-ORDER COMPONENT (4-STROKE CYCLE ENGINE)



II 3RD ORDER COMPONENT (4-STROKE CYCLE ENGINE)



III 4TH ORDER COMPONENT (2-STROKE CYCLE ENGINE)

FIG. 80.—Harmonic components of tangential effort diagram for one cylinder.

must rotate $360 \cdot n$ degrees, i.e. 360 degrees on the vector diagram represent $360/n$ crankshaft degrees.

In Diagram I of Fig. 80, therefore, where $n = 0.5$, each complete revolution of the vectors represent $360/0.5 = 720$ crankshaft degrees, and there is half a vibration cycle in each revolution of the crankshaft.

It should be noted that the resultant vector leads the crank by α_n/n degrees, where in Diagram I

$$\alpha_n/n = (51^\circ - 7')/0.5 = (102^\circ - 14').$$

It is also of interest to note that

$$A_n = T_n \cos \alpha_n, \quad \text{and} \quad B_n = T_n \sin \alpha_n.$$

Diagram II of Fig. 80 shows the graphical construction for the 3rd order harmonic component of a four-stroke cycle, single-acting engine. In this case also the data is taken from Table 53. Since B_n is negative the cosine vector is set off vertically downwards. The vectors rotate through $360 \cdot n = 360 \times 3 = 1080^\circ$ for each revolution of the crankshaft, i.e. there are three vibration cycles per crankshaft revolution and the resultant vector leads the crank by $\alpha_n/n = (331^\circ - 56')/3 = 110^\circ - 39'$.

Diagram III of Fig. 80 shows the graphical construction for the 4th order harmonic component of a two-stroke cycle engine. Since B_n is negative the cosine vector is set off vertically downwards. The vectors rotate through $360 \cdot n = 360 \times 4 = 1440^\circ$ for each revolution of the crankshaft, i.e. there are four vibration cycles per crankshaft revolution and the resultant vector leads the crank by α_n/n or $(307^\circ - 28')/4 = 76^\circ - 52'$.

The values of the coefficients A_n and B_n are determined by making an harmonic analysis of the tangential effort curve, either by means of a mechanical harmonic analyser, or by calculation. The values of T_n and of the phase angle α_n may then be determined from the corresponding values of A_n and B_n . (See Appendix, Vol. II, for method of carrying out an harmonic analysis.)

The effect of inertia on torque may be taken into account either by correcting the tangential effort curve for inertia effects before making the analysis, or by correcting the harmonic coefficients obtained from an analysis of the gas pressure curve alone.

The following series of tables shows the latter method applied to the tangential effort curve of a four-stroke cycle, single-acting petrol engine operating with a mean indicated pressure of 130 lbs./sq. in. (see Fig. 79).

TABLE 53.

HARMONIC COMPONENTS OF TANGENTIAL EFFORT CURVE.

(i) Gas Pressure.

Harmonic Order. n .	Sine Term. A_n . Lbs./Sq. In.	Cosine Term. B_n . Lbs./Sq. In.	Resultant. T_n . Lbs./Sq. In.	Phase Angle. α_n .
$\frac{1}{2}$	29.1	36.1	46.4	$51^\circ-7'$
1	44.5	15.6	47.3	$19^\circ-19'$
$1\frac{1}{2}$	41.8	-2.36	41.9	$356^\circ-47'$
2	30.0	-7.50	30.9	$345^\circ-58'$
$2\frac{1}{2}$	20.65	-9.30	22.7	$335^\circ-46'$
3	15.1	-8.05	17.1	$331^\circ-56'$
$3\frac{1}{2}$	10.9	-8.80	14.0	$321^\circ-6'$
4	6.9	-9.00	11.3	$307^\circ-28'$
$4\frac{1}{2}$	4.1	-8.25	9.22	$296^\circ-27'$
5	2.55	-7.60	8.02	$288^\circ-33'$
$5\frac{1}{2}$	1.55	-7.15	7.29	$282^\circ-14'$
6	1.20	-3.75	3.95	$287^\circ-43'$

Mean tang. effort	$T_m = \frac{P_m}{2 \cdot \pi} = \frac{130}{2 \cdot \pi} = 20.7 \text{ lbs./sq. in.}$
-------------------	---

Note.—The magnitude of the phase angle is determined as follows:—

- (i) If A_n is positive, and B_n is positive, α_n is in the first quadrant, i.e. between 0° and 90° .
- (ii) If A_n is negative, and B_n is positive, α_n is in the second quadrant, i.e. between 90° and 180° .

- (iii) If A_n is negative, and B_n is negative, α_n is in the third quadrant, i.e. between 180° and 270° .
- (iv) If A_n is positive, and B_n is negative, α_n is in the fourth quadrant, i.e. between 270° and 360° .

TABLE 54.*

HARMONIC COMPONENTS OF TANGENTIAL EFFORT CURVE.

(ii) Correction for Inertia of Reciprocating Parts.

Harmonic Order.		H_n .	T_n . Lbs./Sq. Ins.
1	$\sin \theta$	0.06351	8.770
2	$\sin 2\theta$	-0.50012	-69.000
3	$\sin 3\theta$	-0.19193	-26.500
4	$\sin 4\theta$	-0.01613	-2.250
5	$\sin 5\theta$	0.00258	0.356
6	$\sin 6\theta$	0.00039	0.019

Note.—There are no cosine terms, and no half orders.

$$T_n = 0.0000284 \times W \times R \times N^2 \times H_n \text{ lbs./sq. in. of piston area,}$$

* Table 57 gives the values of H_n for different values of the ratio :
 $n = (\text{length of connecting rod/crank radius}).$

The values of H_n in Tables 54 and 57 are obtained from the following expressions :—

Harmonic Order.		Expression for H_n .		
1	$\sin \theta$	$+\frac{1}{4n}$	$+\frac{1}{16n^3}$	$+\frac{15}{512n^5}$
2	$\sin 2\theta$	$-\frac{1}{2}$	$-\frac{1}{32n^4}$	$-\frac{1}{32n^6}$
3	$\sin 3\theta$	$-\frac{3}{4n}$	$-\frac{9}{32n^3}$	$-\frac{81}{512n^5}$
4	$\sin 4\theta$	$-\frac{1}{4n^2}$	$-\frac{1}{8n^4}$	$-\frac{1}{16n^6}$
5	$\sin 5\theta$	$+\frac{5}{32n^3}$	$+\frac{75}{512n^5}$	
6	$\sin 6\theta$	$+\frac{3}{32n^4}$	$+\frac{3}{32n^6}$	

- where $T_n = n$ th order inertia tangential effort,
 $W =$ weight of reciprocating parts in lbs. per sq. in. of piston area (assumed to be 0.2 in this example),
 $R =$ crank radius in inches (assumed to be 1.875 ins. in this example),
 $N =$ revolutions per minute (assumed to be 3600 in this example),
 $H_n =$ multiplier (the tabulated values are for a Conn. Rod/Crank ratio of 4).

TABLE 55.*

HARMONIC COMPONENTS OF TANGENTIAL EFFORT CURVE.

(iii) Correction for Deadweight of Reciprocating and Revolving Parts.

Harmonic Order.		Reciprocating Parts.		Revolving Parts.		Total T_n Lbs./Sq. In.
		H_n	T_n	H_n	T_n	
1	$\sin \theta$	1.00000	0.2000	1.00000	0.57	0.77
2	$\sin 2\theta$	0.12710	0.0254	None	None	0.0254
4	$\sin 4\theta$	-0.00103	-0.0002	"	"	-0.0002
6	$\sin 6\theta$	0.00010	0.0000	"	"	0.0000

* Table 57 gives the values of H_n for different (connecting rod/crank) ratios.

The values of H_n in Tables 55 and 57 are obtained from the following expressions:—

Harmonic Order.		Expression for H_n .
1	$\sin \theta$	1.000
2	$\sin 2\theta$	$+\frac{1}{2n} + \frac{1}{8n^3} + \frac{15}{256n^5} +$
4	$\sin 4\theta$	$-\frac{1}{16n^3} - \frac{3}{64n^5} -$
6	$\sin 6\theta$	$+\frac{1}{85.3n^5} +$

Note.—There are no cosine terms, and no odd orders except the first.

$T_n = W \times H_n$ lbs. per sq. in. of piston area,
 where $W =$ wt. of reciprocating or unbalanced revolving parts in lbs. per sq. in. of piston area (assumed to be 0.2 and 0.57 lbs./sq. in. in this example),
 $H_n =$ multiplier (the tabulated values are for a Conn. Rod/Crank ratio of 4).

In Table 55 the values of T_n are for a vertical engine. In cases such as an engine with inclined banks of cylinders, or with radially disposed cylinders, where the line of stroke is inclined to the vertical at an angle ϕ , as shown in Table 57, the expression for T_n becomes

For the Reciprocating Parts,

$$T_n = (W \cdot H_n) \cdot \cos \phi.$$

Thus $T_n = W \cdot H_n$ for a vertical engine where $\phi = 0$
 $= 0$ for a horizontal engine where $\phi = 90^\circ$ or 270°
 $= -W \cdot H_n$ for an inverted engine where $\phi = 180^\circ$.

For the Revolving Parts.

In the case of the revolving parts the expression for the tangential effort due to the deadweight is

$$T = W(\cos \phi \cdot \sin \theta + \sin \phi \cdot \cos \theta).$$

The correction for the deadweight of the revolving parts may therefore affect both the sine and cosine components of the gas pressure. The following table gives the corrections for some commonly used values of ϕ :—

ϕ .	A_1 .	B_1 .
	Sine Compt.	Cos Compt.
0° (vertical engine)	1.0000	0
45°	0.7071	0.7071
90° (horizontal engine)	0	1.0000
180° (inverted engine)	-1.0000	0
225°	-0.7071	-0.7071
270° (horizontal engine)	0	-1.0000

Corrections for the deadweight of the running gear only affect the 1st order components and as a general rule are small and can be neglected, especially in the case of high-speed engines.

TABLE 56.*
HARMONIC COMPONENTS OF TANGENTIAL EFFORT CURVE.
(iv) Correction for Connecting Rod Couple.

Harmonic Order.		H_n .	T_n . Lbs./Sq. In.
2	$\sin 2\theta$	-0.03124	-4.64
4	$\sin 4\theta$	0.00101	0.1515
6	$\sin 6\theta$	-0.00002	-0.0030

Note.—There are no cosine terms, and no odd orders.

$$T_n = \frac{0.0000284 \times W(a \cdot b - K^2)N^2 \cdot H_n}{R}$$

where W = total weight of connecting rod in lbs./sq. in. of piston area (assumed to be 0.36 in this example),
 a = distance of centre of gravity of rod from small end (assumed to be 1.8 ins. in this example),
 b = distance of centre of gravity of rod from big end (assumed to be 6.2 ins. in this example),

* The values of H_n in Tables 56 and 57 are obtained from the following expressions:—

Harmonic Order.		Expression for H_n .
2	$\sin 2\theta$	$-\frac{1}{2n^2} + \frac{1}{32n^6} +$
4	$\sin 4\theta$	$+\frac{1}{4n^4} + \frac{1}{8n^8} +$
6	$\sin 6\theta$	$-\frac{3}{32n^6} -$

where

$$\frac{\text{length of connecting rod}}{\text{crank radius}}$$

K = radius of gyration of rod about centre of gravity
(assumed to be 3.01 ins. in this example),

R = crank radius (assumed to be 1.875 ins. in this example),

H_n = multiplier (the tabulated values are for a Conn. Rod/Crank ratio of 4).

The above expression for T_n indicates that the correction couple for the rod would be zero if ($a \cdot b = K^2$), in which case the rod would be dynamically equivalent to a mass m_1 concentrated at the crosshead or gudgeon pin and a mass m_2 concentrated at the crankpin, such that

$$\begin{aligned}(m_1 + m_2) &= \text{the total mass of the rod,} \\ m_1 \cdot a &= m_2 \cdot b.\end{aligned}$$

This condition would be very nearly realised if the actual rod consisted of two large ends connected by a very thin bar. If, on the other hand, the rod was equivalent to a uniform bar of length L the value of ($a \cdot b - K^2$) would be $L^2/6$.

In practice the value of ($a \cdot b - K^2$) is usually very small and in some cases might even be negative, for example, in cases where the big-end keep is very heavy. In small high-speed engines the value of ($a \cdot b - K^2$) usually lies between $L^2/20$ and $L^2/30$, although it is difficult to give any truly representative value due to the large variations in the design of these components.

The exact value is easily determined experimentally in any given example. Thus the values of a and b can be obtained by weighing the rod as explained in Chapter 3. The value of K^2 , i.e. the radius of gyration squared, can be obtained by swinging the rod as a compound pendulum (see Fig. 36, and Equation 70), i.e. expressing Equation (70) in inch units,

$$K^2 = [(9.77 \cdot T^2 \cdot R) - R^2] \text{ ins.}^2,$$

where, in this case,

T = periodic time in seconds = $60/N$,

N = number of complete oscillations per minute,

R = distance from point of oscillation to centre of gravity of rod (see Fig. 36).

The value of K^2 can be checked by swinging the rod first from the small end and then from the big end. The two values should agree.

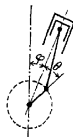
In most practical cases the correction for the connecting rod couple is very small and is neglected. It would always be possible to reduce it to zero by designing the rod so that

TABLE 57.
HARMONIC COMPONENTS OF TANGENTIAL EFFORT CURVE.
(Multipliers for Inertia, Deadweight, and Connecting Rod Couple Corrections.)

	Harmonic Order.		$n = \left(\frac{\text{Length of Connecting Rod}}{\text{Crank Radius}} \right)$.						
			3	$3\frac{1}{2}$	4	$4\frac{1}{2}$	5	$5\frac{1}{2}$	6
INERTIA CORRECTION (RECIPROCATING PARTS)	1	$\sin \theta$	+0.0857	+0.0729	+0.0635	+0.0562	+0.0506	+0.0458	+0.0420
	2	$\sin 2\theta$	-0.5004	-0.5002	-0.5001	-0.5001	-0.5001	-0.5000	-0.5000
	3	$\sin 3\theta$	-0.2611	-0.2211	-0.1920	-0.1698	-0.1523	-0.1371	-0.1263
	4	$\sin 4\theta$	-0.0304	-0.0213	-0.0161	-0.0126	-0.0102	-0.0084	-0.0070
	5	$\sin 5\theta$	+0.0064	+0.0039	+0.0026	+0.0018	+0.0013	+0.0010	+0.0007
	6	$\sin 6\theta$	+0.0013	+0.0007	+0.0004	+0.0002	+0.0002	+0.0001	+0.0001
DEADWEIGHT CORRECTION (RECIP. PARTS)	1	$\sin \theta$	+1.0000	+1.0000	+1.0000	+1.0000	+1.0000	+1.0000	+1.0000
	2	$\sin 2\theta$	+0.1674	+0.1459	+0.1271	+0.1125	+0.1010	+0.0917	+0.0839
	4	$\sin 4\theta$	-0.0024	-0.0016	-0.0010	-0.0007	-0.0005	-0.0004	-0.0003
	6	$\sin 6\theta$	+0.0001	+0.0000	+0.0000	+0.0000	+0.0000	+0.0000	+0.0000
CONN. ROD COUPLE CORRECTION	2	$\sin 2\theta$	-0.0555	-0.0408	-0.0312	-0.0247	-0.0200	-0.0165	-0.0139
	4	$\sin 4\theta$	+0.0033	+0.0017	+0.0010	+0.0006	+0.0004	+0.0003	+0.0002
	6	$\sin 6\theta$	-0.0001	-0.0001	-0.0000	-0.0000	-0.0000	-0.0000	-0.0000

Notes.—(1) There are no cosine components.

- (2) For engines with line of stroke inclined at an angle ϕ the values of the corrections for deadweight of the reciprocating parts must be multiplied by $(\cos \phi)$. The other corrections are unaltered.



$(a \cdot b - K^2) = 0$, but in most cases this would require the addition of material beyond the crankpin or the crosshead, which might introduce other difficulties, especially in aero-engine design where weight is important.

TABLE 58.
HARMONIC COMPONENTS OF TANGENTIAL EFFORT CURVE CORRECTED FOR INERTIA.

Harmonic Order.	Sine Terms.					Cosine Terms. B _n .	Resultants. T _n .	Phase Angles. α _n .
	Gas Pressure.	Inertia.	Dead-weight.	Conn. Rod Couple.	Nett Sine Term. A _n .			
$\frac{1}{2}$	29.1	—	—	—	29.1	36.1	46.4	51°-7'
1	44.5	8.77	0.77	—	54.04	15.6	56.2	16°-4'
$1\frac{1}{2}$	41.8	—	—	—	41.8	-2.36	41.9	356°-47'
2	30.0	-69.00	0.025	-4.64	-43.615	-7.50	44.0	189°-49'
$2\frac{1}{2}$	20.65	—	—	—	20.65	-9.30	22.7	335°-46'
3	15.10	-26.50	—	—	-11.40	-8.05	13.95	215°-16'
$3\frac{1}{2}$	10.9	—	—	—	10.9	-8.80	14.00	321°-6'
4	6.9	-2.25	—	0.15	4.80	-9.00	10.20	298°-6'
$4\frac{1}{2}$	4.1	—	—	—	4.10	-8.25	9.22	296°-27'
5	2.55	0.356	—	—	2.906	-7.60	8.16	290°-58'
$5\frac{1}{2}$	1.55	—	—	—	1.55	-7.15	7.29	282°-14'
6	1.20	0.091	—	-0.003	1.216	-3.75	3.94	287°-56'

Table 59 gives a summary of the maximum values of the resultant harmonic components of the tangential effort curve with and without correction for inertia. It should be noted that inertia has comparatively small influence on all orders above the 4th, its main effect being confined to the 1st, 2nd, and 3rd orders.

Table 59 is based on a mean indicated pressure of 130 lbs. per sq. in.

The values of the harmonic components for other types of engine may be determined approximately from the values for a 4-stroke cycle, single-acting engine, as follows:—

(i) *Four-Stroke Cycle, Double-Acting Engine.*

Orders 1, 3, 5, 7, etc. = 0, very nearly.

Orders $\frac{1}{2}$, $1\frac{1}{2}$, $2\frac{1}{2}$, $3\frac{1}{2}$, etc. = $\sqrt{2} \times$ values for 4-S.C., S.A. engine.

Orders 2, 4, 6, 8, etc. = $2 \times$ values for 4-S.C., S.A. engine.

TABLE 59.

RESULTANT HARMONIC COMPONENTS OF TANGENTIAL EFFORT CURVE FOR ONE-CYLINDER, 4-S.C., S.A. PETROL ENGINE.

M.I.P. = 130 Lbs./Sq. Ins.

Harmonic Order.	Values of T_n (Lbs./Sq. In.).	
	Without Inertia.	With Inertia.
$\frac{1}{2}$	± 46.4	± 46.4
1	47.3	56.2
$1\frac{1}{2}$	41.9	41.9
2	30.9	44.0
$2\frac{1}{2}$	22.7	22.7
3	17.1	13.95
$3\frac{1}{2}$	14.00	14.00
4	11.30	10.20
$4\frac{1}{2}$	9.22	9.22
5	8.02	8.16
$5\frac{1}{2}$	7.29	7.29
6	3.94	3.94

- (ii) *Two-Stroke Cycle, Single-Acting Engine.*—There are no half-order components, and the values of the remaining orders are twice the corresponding values for a 4-S.C., S.A. engine for single-piston engines; and four times the corresponding values for a 4-S.C., S.A. engine for opposed-piston engines.
- (iii) *Two-Stroke Cycle, Double-Acting Engine.*—There are no half-order components, and the values of the odd order components are very nearly zero. The values of the even order components are four times the corresponding values for a 4-S.C., S.A. engine.

The foregoing rules must be regarded as approximations only. In the case of double-acting engines, for example, the presence of the piston rod and the difference in the characteristics of the indicator diagrams from the top and bottom ends introduces orders which should not be present theoretically.

If a turning effort diagram is available, the values of the harmonic components may be determined by harmonic analysis

TABLE 60.

RESULTANT HARMONIC COMPONENTS OF TANGENTIAL EFFORT CURVE FOR ONE CYLINDER (AT FULL LOAD).

In Lbs./Sq. In. of Piston Area.

Harmonic Order.	Internal Combustion Engines.					Triple Expansion Steam Engines.		
	4-Stroke.		2-Stroke Cycle.			H.P. Cylinder.	M.P. Cylinder.	L.P. Cylinder.
	Single-Acting.	Double-Acting.	Single-Acting.		Double-Acting.			
			Single-Piston.	Opposed-Piston.				
$\frac{1}{2}$	±40	±55	—	—	—	—	—	
1	40	6	±80	±160	±12	±15	± 5	
$1\frac{1}{2}$	40	55	—	—	—	—	—	
2	35	70	70	140	140	75	25	
$2\frac{1}{2}$	30	40	—	—	—	—	—	
3	25	10	50	100	20	12	4	
$3\frac{1}{2}$	20	25	—	—	—	—	—	
4	15	30	30	60	60	9	3	
$4\frac{1}{2}$	10	15	—	—	—	—	—	
5	8	7	16	32	14	4	1·3	
$5\frac{1}{2}$	6	9	—	—	—	—	—	
6	4·5	9	9	18	18	3	1·0	
$6\frac{1}{2}$	3·5	5·2	—	—	—	—	—	
7	3·0	2·0	6	12	4	1·5	0·5	
$7\frac{1}{2}$	2·5	3·7	—	—	—	—	—	
8	2·0	4·0	4	8	8	1·0	0·3	
$8\frac{1}{2}$	1·5	2·2	—	—	—	—	—	
9	1·0	1·0	2	4	2	—	—	
$9\frac{1}{2}$	0·8	1·2	—	—	—	—	—	
10	0·7	1·4	1·4	2·8	2·8	—	—	
$10\frac{1}{2}$	0·6	0·9	—	—	—	—	—	
11	0·5	0·5	1·0	2·0	1·0	—	—	
$11\frac{1}{2}$	0·4	0·6	—	—	—	—	—	
12	0·3	0·6	0·6	1·2	1·2	—	—	

as already described. Table 60 has been compiled from published data relating to the various types of engines, and the values contained in it may be used in cases where a special harmonic analysis has not been made.

The harmonic components for the steam engines are based on the following mean indicated pressures :—

H.P. = 100 lbs. per sq. in.,

M.P. = 33 lbs. per sq. in.,

L.P. = 11 lbs. per sq. in.

The values for other mean pressures are approximately proportional to the mean indicated pressure, and are based on the average area of the top and the bottom sides of the piston.

An important difference between a multi-cylinder steam engine of the multiple expansion type and an internal combustion engine is that the phase angles, α_n , are not the same for all cylinders in the case of the steam engine.

This implies that whereas the phase angle may be neglected in the case of an internal combustion engine, it must be considered in the case of a steam engine.

This point is discussed later.

Table 61 gives the values of the sine and cosine components of the tangential effort curve for one cylinder of a 4-S.C., S.A. engine for gas pressure alone and for orders 1, 2, 3, and 4. These values are required in cases where it is necessary to correct the sine component for inertia.

TABLE 61.

SINE AND COSINE COMPONENTS OF TANGENTIAL EFFORT CURVE FOR ONE-CYLINDER, FOUR-STROKE CYCLE, SINGLE-ACTING OIL ENGINES.
(SLOW AND MEDIUM SPEED TYPES.)

Harmonic Order.	Mean Indicated Pressure in Lbs. per Sq. In.									
	0		30		60		100		130	
	Sine.	Cosine.	Sine.	Cosine.	Sine.	Cosine.	Sine.	Cosine.	Sine.	Cosine.
1	11.5	0	18.5	4.5	25.5	9.0	35.0	14.0	42.0	17.5
2	18.0	0	23.0	-1.5	28.0	-3.5	33.5	-6.5	37.0	-9.5
3	17.5	0	20.0	-1.5	22.0	-3.5	23.5	-6.5	23.5	-9.5
4	13.0	0	14.0	-1.5	14.5	-3.0	14.5	-5.5	13.5	-7.0

The approximate values for other types of engine may be determined as shown on page 448.

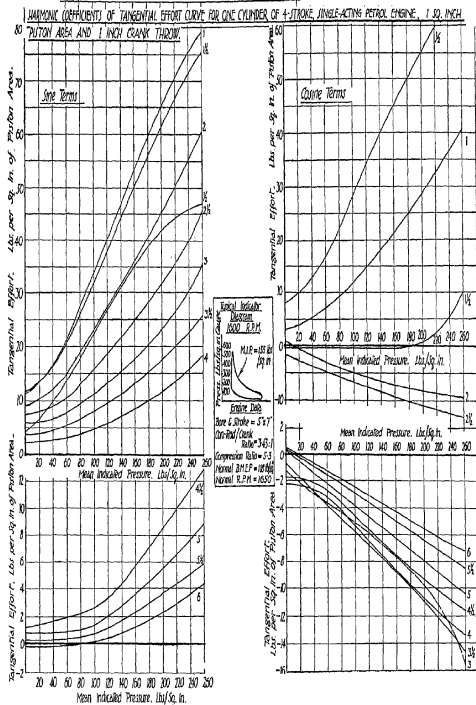


FIG. 81.—Harmonic coefficients, 4-stroke cycle, single-acting petrol engine (orders $\frac{1}{2}$ to 6).
 (Plotted from R.A.E. Report E.D.O. 136.)

Fig. 81 gives the values of the harmonic components of the tangential effort curve of a 4-S.C., S.A. petrol engine for orders $\frac{1}{2}$ to 6, and covers a range of mean indicated pressures up to 260 lbs. per sq. in., so that it includes modern high-duty engines.

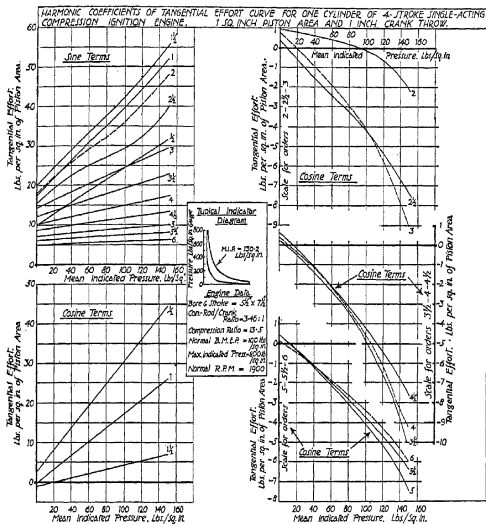


FIG. 82.—Harmonic coefficients, 4-stroke cycle, single-acting compression ignition engine. (Plotted from R.A.E. Report E.D.O. 136.)

The sine and cosine components are given separately, because in high-speed engines inertia effects have considerable influence on the 1st, 2nd, and 3rd order terms. Fig. 82 is a similar diagram for *high-speed compression ignition* oil engines. Fig. 83 contains diagrams giving the values of the resultant

harmonic components for a 4-S.C., S.A. *petrol* engine and a *high-speed compression ignition* engine for orders $6\frac{1}{2}$ to $11\frac{1}{2}$. The sine and cosine components are not given separately for these higher orders because inertia corrections are not required.

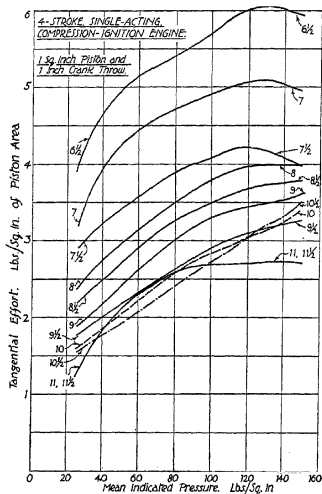


FIG. 83.—Resultant harmonic coefficients, 4-stroke cycle, single-acting compression ignition engine (order $6\frac{1}{2}$ to $11\frac{1}{2}$). (Plotted from R.A.E. Report E.D.O. 136.)

These diagrams are based on data contained in Air Ministry Report E.D.O. 136, by permission of the Controller of H.M. Stationery Office.

In the case of spark ignition (*petrol*) engines an extensive investigation carried out in the M.I.T. Automotive Engine

Laboratory under different operating conditions of throttle variation, compression ratio, spark advance, and mixture ratio showed that the ratio (component harmonic torque/mean torque) changed very little with engine conditions, and for the

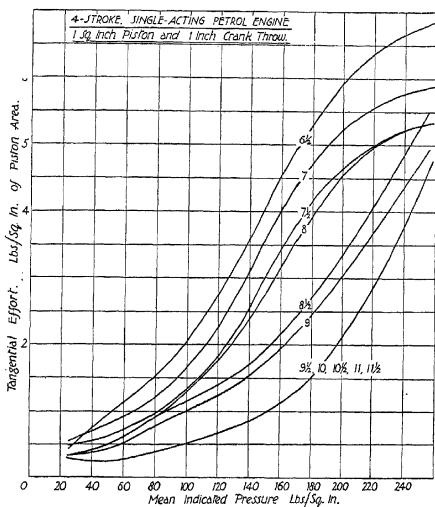


FIG. 83.—Resultant harmonic coefficients, 4-stroke, single-acting petrol engine (orders 6½ to 11½). (Plotted from R.A.E. Report E.D.O. 136.)

3rd and higher harmonic orders was well represented by the expression

$$T_n/T_m = \frac{6.3 \cdot C}{5 \cdot n^2}$$

where T_n = maximum value of the resultant n th order harmonic component of tangential effort curve in lbs. per sq. in. (The inertia correction is negligible for orders higher than the 3rd),
 T_m = mean indicated tangential effort in lbs. per sq. in.,
 C = compression ratio,
 n = harmonic order number.

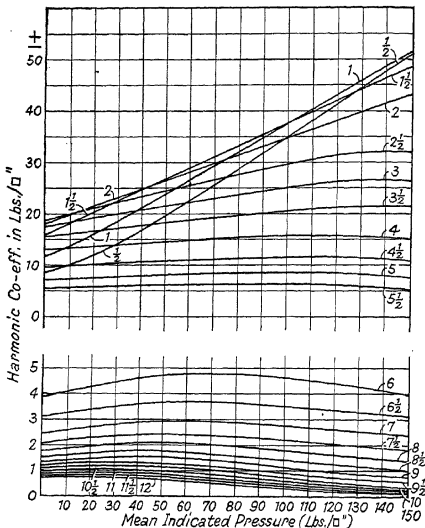


FIG. 83A.—Resultant harmonic components of tangential effort diagram for one-cylinder, 4-S.C., S.A. oil engine—slow and medium speed types.

(See "Harmonic Analysis of Engine Torque Due to Gas Pressure," by E. S. Taylor and E. W. Morris, *Journal of the*

Aeronautical Sciences, Vol. 3, February, 1936; also *S.A.E. Journal*, March, 1936, p. 82.)

Since in a 4-S.C., S.A. engine, $T_m = P_m/(2 \cdot \pi)$, the above expression can be written

$$T_n = P_m \cdot C/(5 \cdot n^2), \quad \dots \quad (249)$$

where P_m = mean indicated pressure in lbs. per sq. in.

Note that Equation (249) applies to the 3rd and higher harmonic orders only, i.e. $n = 3, 3.5, 4, 4.5$, etc.

The maximum values of the resultant harmonic components, neglecting inertia, for *large slow-speed* 4-S.C., S.A. heavy oil engines are given in Fig. 83A (Fig. 109 in Vol. II, and reproduced here for convenience of reference). The values for other types of engine may be determined approximately from the values for a 4-S.C., S.A. engine by applying the rules given earlier in this chapter.

Harmonic Components of Tangential Effort Curve with Articulated Connecting Rods.—In engines having more than one piston operating on each crankpin, for example, radial engines, or in-line engines with two or more banks of cylinders, such as V and fan-type engines, one piston is connected to the crankpin by a normal connecting rod system, and this is usually called the master connecting rod, whilst the other piston (or pistons) is connected to the same crankpin by one of the arrangements shown in Fig. 84.

- (a) When there is only one auxiliary cylinder operating on the same crankpin as the master cylinder the common crankpin is made of sufficient length to accommodate the big-end bearings of the two connecting rods side by side. In this case the crank/connecting rod mechanism is the same for both cylinders, and the methods just described can be applied to each of the two cylinders. The total torque summation for the two cylinders must be made according to the rules described later, to take into account the phase displacement caused by the inclination of the line of stroke of one piston relative to the other—arrangement (a) in Fig. 84.

- (b) When there is only one auxiliary cylinder operating on the same crankpin as the master cylinder the big-end of one connecting rod operates directly on the common crankpin, whilst the big-end of the second connecting rod operates on bearing surfaces formed on the outside of the big-end of the first connecting rod. The master connecting rod is forked to permit relative angular motion of the two connecting rods. In this case also the crank/connecting rod mechanism is the same for both cylinders, and the methods just described can be applied to each of

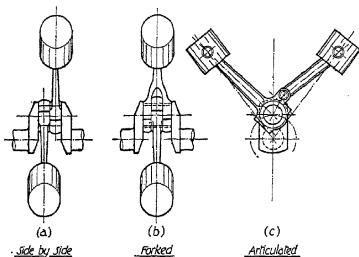


FIG. 84.—Connecting rod systems.

- the two cylinders. The total torque summation for the two cylinders must be made according to the rules described later, to take into account the phase displacement caused by the inclination of the line of stroke of one piston relative to the other, and in computing inertia effects care must be taken to allow for any differences of form and weight between the forked master connecting rod and the plain auxiliary connecting rod—arrangement (b) in Fig. 84.
- (c) When there is one or more auxiliary cylinders operating on the same crankpin the auxiliary connecting rods are articulated on the big-end of the master connecting

rod. The motions of the auxiliary pistons are generally regarded as being controlled by the motion of the master connecting rod, and the methods just described can only be applied to the master connecting rod system—arrangement (c) in Fig. 84.

The modern tendency is to dispense with articulated connecting rods when there are only two pistons operating on a common crankpin and to use the arrangements described in (a) or (b). The arrangement described in (b) is usually favoured in aero-engine practice owing to the difficulty of providing adequate big-end bearings with the side-by-side arrangement. In automobile practice, where the duty required of the power plant is not so onerous, the side-by-side arrangement tends to be favoured because the connecting rods are then all of the same design and the expense of manufacturing forked rods is avoided.

Articulated systems are used in fan, X, and radial type aero engines where there are several auxiliary cylinders operating on the same crankpin.

Accurate analysis of the torque characteristics of an articulated system is exceedingly complex, and no simple treatment is possible.

An analysis in which the effect of articulation is neglected is undoubtedly useful as a preliminary approach to the problem, but it tends to hide certain peculiarities of an articulated system which, unfortunately, present-day experience of torsional vibration phenomena in engines of this type has shown to be by no means negligible. This matter will be referred to later, and in the meantime the following method of determining the harmonic components of the tangential effort curve of an engine with articulated connecting rods will be found as simple as the complexities of the problem permit.

In the following method the magnitudes of the harmonic components for the combined tangential effort curve for the master cylinder and all articulated cylinders operating on the same crankpin are obtained. Thus each harmonic component is the total component for all cylinders operating on the common crankpin, and this eliminates all difficulties due

- R_1 = length of artic arm,
 L = length of master connecting rod,
 L_1 = length of articulated connecting rod,
 θ = crank angle, measured from top dead centre of master cylinder (firing centre),
 δ = angular spacing of cylinders, measured from master cylinder in direction of rotation of crankpin,
 α = angularity of master connecting rod,
 β = angularity of articulated connecting rod,
 ψ = angular spacing of artic pin, measured from master connecting rod.

No definite rules can be given for the proportions of an articulated mechanism. In the case of engines having several articulated cylinders, such as radial aero engines, the articulated pistons differ among themselves. For example, if R_1 , L_1 , δ , and ψ are identical for all cylinders it will be found that there is an appreciable difference between the strokes, and therefore between the compression ratios of the various cylinders.

Several methods are employed for correcting this difference to a greater or lesser extent. In some cases the angle ψ between the artic pin and the master connecting rod is varied; in other cases the length R_1 of the artic arm or the length L_1 of the articulated connecting rod is varied; or again, the variation of stroke is neglected and the compression ratio is corrected by suitable variations of clearance space. Combinations of the above methods are also found in practice. As a general rule, however, the angular spacing of the cylinders is equal.

One important special case does occur, however, and that is when the angle between the artic pin and the master connecting rod is made equal to the angular spacing of the cylinders. This case is shown applied to a five-cylinder radial engine at the left-hand side of Fig. 85, although it is more frequently found in V and fan-type engines.

When this condition is fulfilled, i.e. when $\psi = \delta$, Equations (250) and (253) become

$$S = R \cdot \cos(\delta - \theta) + R_1 \cdot \cos \alpha + L_1 \cdot \cos \beta, \quad (254)$$

$$\sin \beta = [R \cdot \sin(\delta - \theta) + R_1 \cdot \sin \alpha] / L_1. \quad (255)$$

The articulated piston displacements can be calculated with any desired degree of accuracy by means of Equations (250) to (255) and the values obtained all refer to top dead centre of the master piston as datum.

If the engine has already been built an alternative method is to measure the displacements directly, bearing in mind that if the 4th order harmonic components are required from the subsequent harmonic analysis the piston displacements must be accurate to at least four figures. If the 6th order harmonic components are required the displacements must be accurate to at least five figures. It is doubtful, however, whether much reliance can be placed on calculated values of orders higher than the 4th, because the working clearances and elastic deformations of the engine under load may be as much as 0.01 ins.

Tangential Effort Diagram for Gas Pressure.—The indicator diagram which is used for the master cylinder can also be used for the articulated cylinders. The gas pressure corresponding to a given angular displacement of the crankpin is obtained from the indicator diagram in the usual way by marking off a length along the base line of the diagram equal to the displacement of the articulated piston along its stroke for a given crankpin displacement. Care must be taken to see that the correct firing sequence of the articulated cylinders in relation to the master cylinder is used when transferring piston displacements to the indicator diagram. Since the master cylinder is used as datum, the master cylinder fires when $\theta = 0$, and the complete cycle occupies 720° for four-stroke engines and 360° for two-stroke engines.

From the geometry of an articulated mechanism the following relationship exists between the gas pressure and the corresponding tangential effort at the crankpin (see "Handbook of Aeronautics," Volume II):—

$$T/P = \sec \beta \left\{ \frac{R_1 \cdot \sin (\delta - \psi + \beta + \alpha) \cdot \cos \theta}{L \cdot \cos \alpha} - \sin (\beta + \delta - \theta) \right\} \quad (256)$$

where P = gas pressure on articulated piston in lbs. per sq. in.
at crank angle θ ,

T = corresponding tangential effort on crankpin in
lbs. per sq. in. at crank angle θ .

In the special case, when $\psi = \delta$, Equation (256) becomes

$$T/P = \sec \beta \left\{ \frac{R_1 \cdot \sin(\alpha + \beta) \cdot \cos \theta}{L \cdot \cos \alpha} - \sin(\beta + \delta - \theta) \right\} \quad (257)$$

The foregoing equations enable the displacement and tangential effort of the articulated piston to be calculated for different angular positions of the crankpin starting from the common datum, $\theta = 0$, when the master piston is on firing centre.

These values should be calculated for at least every 15° of crankpin rotation, so that at least twenty-four ordinates per revolution are available for the subsequent harmonic analysis.

If there are several articulated pistons operating on the same crankpin a separate set of calculations is required for each, since the motions of the articulated pistons differ among themselves.

The work is best carried out by tabulation, the values of the piston displacements, gas pressures, and tangential efforts being entered in adjacent columns opposite the corresponding crankpin positions. Values for all the articulated pistons should appear in the table.

Harmonic Components of Tangential Effort Diagram for Gas Pressure.—The values of T for all the articulated pistons should be summed algebraically for each crankpin position and the resultant values representing the total tangential effort exerted by all the articulated pistons on the common crankpin should be plotted on a base of crank angles. In the case of four-stroke cycle engines where the complete working cycle occupies two crankpin revolutions the base will occupy 720° , whilst for two-stroke cycle engines where the working cycle occupies only one revolution of the crankpin the base will occupy 360° . According to the notation adopted in this book the harmonic order numbers represent the number of complete impulses in

each revolution of the crankpin. Hence in the case of four-stroke cycle engines the 1st, 2nd, 3rd, 4th, etc., harmonic components obtained by analysis of the tangential effort on a 720° base are the $\frac{1}{2}$, 1, 1.5, 2, etc., orders. In the case of two-stroke cycle engines the harmonic components obtained by analysis of the 360° base diagram are also the order numbers and there are no half-orders.

The resultant tangential effort diagram for the articulated pistons should be harmonically analysed to obtain the values of the sine and cosine components as follows :—

$$T' = T_m' + \Sigma(A_n' \sin n \cdot \theta + B_n' \cos n \cdot \theta), \quad (258)$$

where T' is the resultant tangential effort exerted on the common crankpin by all the articulated pistons when the crank angle is θ .

The values of the sine and cosine components for the master cylinder can be obtained from diagrams of the type shown in Figs. 81 and 82, so that if these are added, algebraically, to the values given by Equation (258) the resultant harmonic components due to gas pressure on both master and articulated pistons are obtained,

$$\text{i.e. } Q_n = [(A_n + A_n') \sin n\theta + (B_n + B_n') \cos n \cdot \theta], \quad (259)$$

where Q_n = the n th order harmonic component of the combined tangential effort of master and all articulated pistons, in lbs. per sq. in. of the piston area of one cylinder,

A_n and B_n = the n th order sine and cosine components for the master cylinder (from diagrams such as Figs. 81 and 82),

A_n' and B_n' = the n th order sine and cosine components for the combined tangential effort of all the articulated pistons, obtained as just described,

n = the order number, i.e. the number of complete impulses per revolution of the crankpin. In the case of four-stroke cycle engines there are half as well as whole orders.

Tangential Effort Due to Inertia of Reciprocating Parts of the Articulated Cylinders.—Since engines with articulated pistons

are invariably of the high-speed type the corrections for dead-weight can be neglected. The correction for connecting rod couple is also small and is usually neglected for both master and articulated connecting rods. It is difficult to obtain for an articulated rod, although an analytical expression is given by Dr. Root in his book "Dynamics of Engine and Shaft." The remaining correction is that due to the inertia of the reciprocating parts, and this cannot be neglected.

When the crank angle is θ , let

F = inertia force due to the reciprocating parts of the articulated cylinder, in lbs. per sq. in. of piston area,

T = the tangential effort due to this inertia force, in lbs. per sq. in. of piston area,

y = the displacement of the articulated piston, in inches,

v = the velocity of the articulated piston, in ins./sec.,

u = the acceleration of the articulated piston, in ins./sec./sec.,

W = the weight of the reciprocating parts of the articulated cylinder, in lbs. per sq. in. of piston area,

R = crank radius in inches,

N = revolutions per minute,

ω = angular velocity of the crankpin in radians per second, assumed constant

$$= \pi \cdot N/30.$$

Then, since at any instant the rate of doing work on the piston must be the same as the rate of doing work on the crankpin,

$$F \cdot v = T \cdot R \cdot \omega \quad (\text{Note: } T \cdot R = \text{instantaneous torque}),$$

$$\text{or} \quad T = \frac{F \cdot v}{\omega \cdot R}$$

$$\text{but} \quad F = W \cdot u/g, \text{ where } g = 386 \text{ ins./sec./sec.},$$

$$\text{i.e.} \quad T = \frac{W \cdot v \cdot u}{\omega \cdot R \cdot g}$$

$$\text{Now} \quad v = \omega \cdot \frac{dy}{d\theta}; \text{ and } u = \omega^2 \cdot \frac{d^2y}{d\theta^2}.$$

$$\text{Hence,} \quad \frac{W \cdot \omega^2 \left(\frac{dy}{d\theta}\right) \cdot \left(\frac{d^2y}{d\theta^2}\right)}{R \cdot g} \cdot \frac{0.0000284 \cdot W \cdot N^2}{R} \cdot \left(\frac{dy}{d\theta}\right) \cdot \left(\frac{d^2y}{d\theta^2}\right)$$

$$\text{or } T_n = \frac{0.0000284 \cdot W \cdot N^2}{R} \cdot (Z_n),$$

where T_n = the n th order harmonic component of the inertia tangential effort for one articulated cylinder, in lbs. per sq. in. of piston area,

$$Z_n = \text{the value of } \left(\frac{dy}{d\theta}\right) \cdot \left(\frac{d^2y}{d\theta^2}\right) \text{ for the } n\text{th order.}$$

The values of Z_n are obtained as follows:—

The piston displacement curve is drawn on a crank angle base for each articulated cylinder, using Equations (250) to (255), and assuming that $\theta = 0$ when the master piston is at firing centre, i.e. all values for the articulated cylinders are referred to firing centre of the master cylinder as datum, since this simplifies the summation of the values for individual cylinders when obtaining the resultant harmonic component for all the pistons operating on the one crankpin.

Since the piston motion completes its cycle in one revolution of the crankpin, the piston displacement diagram is plotted on a base of 360° . The harmonic components obtained by analysis of this piston displacement curve are thus the order numbers also, i.e. there are no half order components of the tangential effort curve of a four-stroke cycle engine.

Each piston displacement curve is separately analysed to obtain the sine and cosine components of the first six orders. Orders higher than the 6th are negligible, and as already mentioned the practical reliability of the values for orders higher than the 4th is extremely doubtful, due to the distortions which occur in the mechanism under load.

Let the Fourier series for the displacement of an articulated piston be

$$y = (a_0 + a_1 \sin \theta + a_2 \sin 2\theta + a_3 \sin 3\theta + \dots + a_8 \sin 8\theta + b_1 \cos \theta + b_2 \cos 2\theta + b_3 \cos 3\theta + \dots + b_8 \cos 8\theta).$$

$$\text{Then } \frac{dy}{d\theta} = (a_1 \cos \theta + 2 \cdot a_2 \cos 2\theta + 3 \cdot a_3 \cos 3\theta + \dots + 8 \cdot a_8 \cos 8\theta - b_1 \sin \theta - 2 \cdot b_2 \sin 2\theta - 3 \cdot b_3 \sin 3\theta - \dots - 8 \cdot b_8 \sin 8\theta),$$

$$\text{and } \frac{d^2y}{d\theta^2} = (-a_1 \sin \theta - 4 \cdot a_2 \sin 2\theta - 9 \cdot a_3 \sin 3\theta - \dots - 64 \cdot a_8 \sin 8\theta \\ - b_1 \cos \theta - 4 \cdot b_2 \cos 2\theta - 9 \cdot b_3 \cos 3\theta - \dots - 64 \cdot b_8 \sin 8\theta),$$

$$\text{whence } T = \frac{0.0000284 \cdot W \cdot N^2}{R} \left(\frac{dy}{d\theta} \right) \cdot \left(\frac{d^2y}{d\theta^2} \right) \\ = \frac{0.0000284 \cdot W \cdot N^2}{R} (C_1' \sin \theta + C_2' \sin 2\theta \\ + C_3' \sin 3\theta + \dots + C_8' \sin 8\theta \\ + D_1' \cos \theta + D_2' \cos 2\theta \\ + D_3' \cos 3\theta + \dots + D_8' \cos 8\theta),$$

where the values of C_n' and D_n' are obtained by multiplying out and simplifying the two series for piston velocity and acceleration. The values of these coefficients are given in Table 62.

When there are several auxiliary pistons articulated to the same crankpin the above analysis must be carried out for each articulated cylinder separately.

The resultant sine and cosine components of any given order for all the articulated pistons operating on a common crankpin are obtained by summing algebraically the sine and cosine components for the separate cylinders.

In the case of the master cylinder there are no cosine components and the value of the sine component for any given order can be obtained from the data given in Table 57. Since the same datum has been used for both master and articulated cylinders the sine and cosine components of the inertia tangential effort for all cylinders operating on the same crankpin can be obtained by adding algebraically the sine components for the master cylinder to the corresponding sine components for the resultant effect of all the articulated cylinders.

Finally, the values of the harmonic components of the total tangential effort exerted on the crankpin by the master and all articulated cylinders are obtained by adding, algebraically, the inertia corrections to the gas pressure harmonics previously calculated.

TABLE 62.

HARMONIC COMPONENTS OF TANGENTIAL EFFORT CURVE OF AN ARTICULATED CYLINDER.

(Correction for Inertia of Reciprocating Parts.)

Sine Coefficients.	
1st order	$(a_1 \dots + 3 \cdot a_2 \cdot a_3 + 6 \cdot a_3 \cdot a_4 + 10 \cdot a_4 \cdot a_5 + \dots$ $+ b_1 \cdot b_2 + 3 \cdot b_2 \cdot b_3 + 6 \cdot b_3 \cdot b_4 + 10 \cdot b_4 \cdot b_5 + \dots)$
2nd order	$C_2' = (a_1^2/2 - b_1^2/2 + 3 \cdot a_1 \cdot a_3 + 8 \cdot a_2 \cdot a_4 + 15 \cdot a_3 \cdot a_5$ $+ 24 \cdot a_4 \cdot a_6 + \dots + 3 \cdot b_1 \cdot b_3 + 8 \cdot b_2 \cdot b_4 + 15 \cdot b_3 \cdot b_5$ $+ 24 \cdot b_4 \cdot b_6 + \dots)$
3rd order	$C_3' = (3 \cdot a_1 \cdot a_3 - 3 \cdot b_1 \cdot b_3 + 6 \cdot a_1 \cdot a_4 + 15 \cdot a_2 \cdot a_5 + 27 \cdot a_3 \cdot a_6$ $+ 42 \cdot a_4 \cdot a_7 + \dots + 6 \cdot b_1 \cdot b_4 + 15 \cdot b_2 \cdot b_5 + 27 \cdot b_3 \cdot b_6$ $+ 42 \cdot b_4 \cdot b_7 + \dots)$
4th order	$C_4' = (6 \cdot a_1 \cdot a_3 + 4 \cdot a_2^2 - 6 \cdot b_1 \cdot b_3 - 4 \cdot b_2^2 + 10 \cdot a_1 \cdot a_5$ $+ 24 \cdot a_2 \cdot a_6 + 42 \cdot a_3 \cdot a_7 + 64 \cdot a_4 \cdot a_8 + \dots + 10 \cdot b_1 \cdot b_5$ $+ 24 \cdot b_2 \cdot b_6 + 42 \cdot b_3 \cdot b_7 + 64 \cdot b_4 \cdot b_8 + \dots)$
5th order	$C_5' = (10 \cdot a_1 \cdot a_4 + 15 \cdot a_2 \cdot a_3 - 10 \cdot b_1 \cdot b_4 - 15 \cdot b_2 \cdot b_3$ $+ 15 \cdot a_1 \cdot a_6 + 35 \cdot a_2 \cdot a_7 + 60 \cdot a_3 \cdot a_8 + 90 \cdot a_4 \cdot a_9 + \dots$ $+ 15 \cdot b_1 \cdot b_6 + 35 \cdot b_2 \cdot b_7 + 60 \cdot b_3 \cdot b_8 + 90 \cdot b_4 \cdot b_9 + \dots)$
6th order	$C_6' = (15 \cdot a_1 \cdot a_3 + 24 \cdot a_2 \cdot a_4 + 13 \cdot 5 \cdot a_3^2 - 15 \cdot b_1 \cdot b_3$ $- 24 \cdot b_2 \cdot b_4 - 13 \cdot 5 \cdot b_3^2 + 21 \cdot a_1 \cdot a_7 + 48 \cdot a_2 \cdot a_8$ $+ 81 \cdot a_3 \cdot a_9 + 120 \cdot a_4 \cdot a_{10} + \dots + 21 \cdot b_1 \cdot b_7$ $+ 48 \cdot b_2 \cdot b_8 + 81 \cdot b_3 \cdot b_9 + 120 \cdot b_4 \cdot b_{10} + \dots)$
Cosine Coefficients.	
1st order	$D_1' = (a_1 \cdot b_2 + 3 \cdot a_2 \cdot b_3 + 6 \cdot a_3 \cdot b_4 + 10 \cdot a_4 \cdot b_5 + \dots$ $- b_1 \cdot a_2 - 3 \cdot b_2 \cdot a_3 - 6 \cdot b_3 \cdot a_4 - 10 \cdot b_4 \cdot a_5 + \dots)$
2nd order	$D_2' = (a_1 \cdot b_1 + 3 \cdot a_1 \cdot b_3 + 8 \cdot a_2 \cdot b_4 + 15 \cdot a_3 \cdot b_5 + 24 \cdot a_4 \cdot b_6$ $+ \dots - 3 \cdot b_1 \cdot a_3 - 8 \cdot b_2 \cdot a_4 - 15 \cdot b_3 \cdot a_5 - 24 \cdot b_4 \cdot a_6$ $\dots)$
3rd order	$D_3' = (3 \cdot a_1 \cdot b_2 + 3 \cdot a_2 \cdot b_1 + 6 \cdot a_1 \cdot b_4 + 15 \cdot a_2 \cdot b_5$ $+ 27 \cdot a_3 \cdot b_6 + 42 \cdot a_4 \cdot b_7 + \dots - 6 \cdot b_1 \cdot a_4 - 15 \cdot b_2 \cdot a_5$ $- 27 \cdot b_3 \cdot a_6 - 42 \cdot b_4 \cdot a_7 \dots)$
4th order	$D_4' = (6 \cdot a_1 \cdot b_3 + 8 \cdot a_2 \cdot b_2 + 6 \cdot a_2 \cdot b_1 + 10 \cdot a_1 \cdot b_5 + 24 \cdot a_2 \cdot b_6$ $+ 42 \cdot a_3 \cdot b_7 + 64 \cdot a_4 \cdot b_8 + \dots - 10 \cdot b_1 \cdot a_5 - 24 \cdot b_2 \cdot a_6$ $- 42 \cdot b_3 \cdot a_7 - 64 \cdot b_4 \cdot a_8 \dots)$
5th order	$D_5' = (10 \cdot a_1 \cdot b_4 + 10 \cdot b_1 \cdot a_4 + 15 \cdot a_2 \cdot b_3 + 15 \cdot a_3 \cdot b_2$ $+ 15 \cdot a_1 \cdot b_6 + 35 \cdot a_2 \cdot b_7 + 60 \cdot a_3 \cdot b_8 + 90 \cdot a_4 \cdot b_9 + \dots$ $- 15 \cdot b_1 \cdot a_3 - 35 \cdot b_2 \cdot a_4 - 60 \cdot b_3 \cdot a_5 - 90 \cdot b_4 \cdot a_6 \dots)$
6th order	$D_6' = (15 \cdot a_1 \cdot b_5 + 15 \cdot a_2 \cdot b_1 + 24 \cdot a_2 \cdot b_4 + 24 \cdot a_4 \cdot b_3$ $+ 27 \cdot a_2 \cdot b_6 + 21 \cdot a_1 \cdot b_7 + 48 \cdot a_2 \cdot b_8 + 81 \cdot a_3 \cdot b_9 + 120 \cdot a_4 \cdot b_{10}$ $+ \dots - 21 \cdot b_1 \cdot a_7 - 48 \cdot b_2 \cdot a_8 - 81 \cdot b_3 \cdot a_9 - 120 \cdot b_4 \cdot a_{10}$ $\dots)$

Thus, if Q_n = the value of the total n th order harmonic component of the tangential effort exerted by the master cylinder and all articulated cylinders, including the corrections for inertia of the reciprocating parts, in lbs. per sq. in. of the piston area of one cylinder,

A_n and B_n = the n th order sine and cosine gas pressure components for the master cylinder (obtained from diagrams such as Figs. 81 and 82),

A_n' and B_n' = the n th order sine and cosine gas pressure components for all the articulated cylinders (obtained in the manner just described),

C_n = the n th order sine inertia component for the master cylinder (obtained from the coefficients in Table 57. There are no cosine components for the master cylinder),

C_n' and D_n' = the n th order sine and cosine inertia components for all articulated cylinders (obtained in the manner just described):

$$\begin{aligned} \text{then } Q_n &= [(A_n + A_n' + C_n + C_n') \cdot \sin n \cdot \theta \\ &\quad + (B_n + B_n' + D_n') \cdot \cos n \cdot \theta] \\ &= T_n \cdot \sin (n \cdot \theta + \alpha_n), \end{aligned}$$

$$\text{where } T_n = \sqrt{(A_n + A_n' + C_n + C_n')^2 + (B_n + B_n' + D_n')^2},$$

$$\text{and } \tan \alpha_n = \frac{(B_n + B_n' + D_n')}{(A_n + A_n' + C_n + C_n')}.$$

T_n is the maximum value of the resultant n th order harmonic component of the tangential effort of all cylinders, master and articulated, operating on the common crankpin, including all inertia corrections. In a multi-crank engine it is the value for each crank.

α_n is the resultant phase angle for all the cylinders operating on the common crankpin, i.e. α_n/n is the angle by which the resultant vector, of amplitude T_n , leads the crankpin (see Fig. 80).

Table 62A gives the magnitudes of the harmonic components of the resultant torque curves for the master and all articulated

cylinders of representative 7- and 9-cylinder radial aero engines, including the inertia corrections.

These values are expressed as a percentage of the mean torque of the engine at rated power and speed, and are useful as a guide in cases where specific information is not available.

TABLE 62A.

RESULTANT HARMONIC COMPONENTS OF TORQUE CURVES OF SEVEN- AND NINE-CYLINDER SINGLE-ROW RADIAL AERO ENGINES.

Order Number.	Resultant Component as a Percentage of the Mean Engine Torque.	
	Seven Cylinders.	Nine Cylinders.
	%	%
0.5	0.0	0.0
1.0	33.0	19.0
1.5	2.0	0.0
2.0	11.0	9.0
2.5	2.9	1.2
3.0	1.2	0.4
3.5	84.0	1.8
4.0	0.0	0.0
4.5	6.6	44.0
5.0	0.9	0.0
5.5	2.0	3.4
6.0	1.3	0.0
6.5	0.0	1.2
7.0	14.0	0.4
7.5	—	0.0
8.0	—	0.6
8.5	—	0.0
9.0	—	13.0

Resultant Harmonic Torque Energy for the Entire Group of Cylinders of a Multi-Cylinder Engine—Phase and Vector Diagrams.—It has just been shown that the tangential effort diagram for a single-cylinder engine may be split up into a constant mean force which does not produce vibration, and a series of harmonically varying forces, the maximum values of which for different types of engine are given in Table 60.

The work done by the harmonic torque of the n th order by the m th cylinder is proportional to

$$W_m = \pi \cdot a_m \cdot T_n \cdot A \cdot R \cdot \dots \quad (260)$$

where a_m is the ordinate on the normal elastic curve corresponding to the m th cylinder (see "Torsional Vibration," by W. A. Tuplin, Chapman & Hall, London).

The work done by the entire group of cylinders is therefore proportional to

$$\Sigma W_m = \pi \cdot T_n \cdot A \cdot R \cdot \Sigma a_m \cdot \dots \quad (261)$$

Since there is a definite phase relationship between the torques of the various cylinders, Σa_m is the *vector* or geometric sum of the deflections on the normal elastic curve.

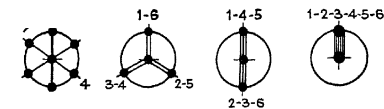
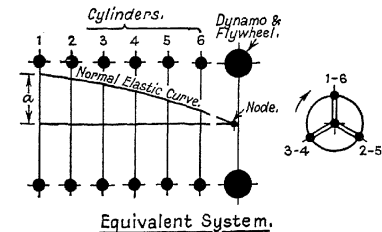
Its value is determined by means of the phase and vector diagrams shown in Figs. 86 and 87.

Phase Diagrams.—The phase diagrams in Fig. 86 are for a 6-cylinder, 4-stroke cycle, single-acting engine, with crank arrangement 1-6, 3-4, 2-5, and firing order 1-3-5-6-4-2.

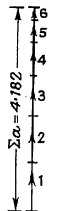
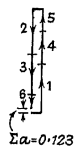
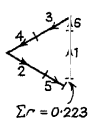
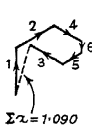
It is assumed that 360° in the phase diagrams represents one vibration, so that for a 4-stroke cycle, single-acting engine, where the working cycle occupies two revolutions, 360° in the phase diagrams represents two revolutions of the crankshaft, i.e. 360° in the shaft diagram is represented by 180° in the phase diagrams. Now, harmonic order $\frac{1}{2}$ corresponds to one complete vibration per working cycle, or per two revolutions, so that for this order the cylinders come into action in the phase diagrams at intervals equal to half the firing interval apart and in the same order as the firing order, i.e. with cranks at 120° , and firing intervals of 120° , the cylinders come into action in the phase diagram for order $\frac{1}{2}$ at intervals of 60° , and in the same order as the firing order, viz. 1-3-5-6-4-2, in Fig. 86.

For order 1 each cylinder must pass over double the phase angle to be at top dead centre that it did for order $\frac{1}{2}$, so that the phase diagram for order 1 is obtained by doubling all the angles in the phase diagram for order $\frac{1}{2}$.

Similarly, the phase diagrams for orders $1\frac{1}{2}$, 2, $2\frac{1}{2}$, etc., are obtained by multiplying the angles for order $\frac{1}{2}$ by 3, 4, 5, etc.



Phase Diagrams.



$$\text{Orders} \rightarrow \begin{array}{l} \frac{1}{2} - 3\frac{1}{2} - 6\frac{1}{2} - 9\frac{1}{2} \\ 2\frac{1}{2} - 5\frac{1}{2} - 8\frac{1}{2} - 11\frac{1}{2} \end{array} \quad \left\| \begin{array}{l} 1-4-7-10 \\ 2-5-8-11 \end{array} \right\| \quad \left\| \begin{array}{l} 1\frac{1}{2} - 4\frac{1}{2} - 7\frac{1}{2} - 10\frac{1}{2} \end{array} \right\| \quad \left\| \begin{array}{l} 3-6-9-12 \end{array} \right\|$$

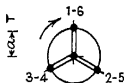
Vector Diagrams.
(1-Node Vibns.)

FIG. 86.—Phase and vector diagrams—4-S.C., S.A. 6-cylinder oil engine.

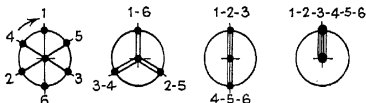
Cylinders.

Normal Elastic Curve (1-Node)

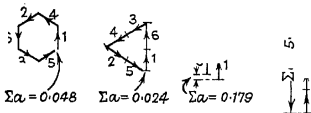
Normal Elastic Curve (2-Node)



Equivalent System.



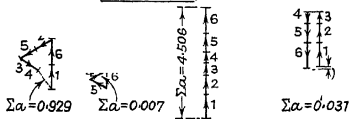
Phase Diagrams.



Orders $\rightarrow \begin{matrix} \frac{1}{2} & -3\frac{1}{2} & -6\frac{1}{2} & -9\frac{1}{2} \\ 2\frac{1}{2} & -5\frac{1}{2} & -8\frac{1}{2} & -11\frac{1}{2} \end{matrix} \parallel \begin{matrix} 1-4-7-10 \\ 2-5-8-11 \end{matrix} \parallel \begin{matrix} \frac{1}{2} & -4\frac{1}{2} & -7\frac{1}{2} & -10\frac{1}{2} \\ 3-6-9-12 \end{matrix}$

Vector Diagrams.

(1-Node Vibns.)



Vector Diagrams.

(2-Node Vibns.)

FIG. 87.—Phase and vector diagrams—4-S.C., S.A. 6-cylinder marine oil engine.

For the example shown in Fig. 86 it will be found that the phase diagrams repeat after the 3rd order, i.e. the phase diagram for order $\frac{1}{2}$ also represents orders $3\frac{1}{2}$, $6\frac{1}{2}$, $9\frac{1}{2}$, etc., and orders $2\frac{1}{2}$, $5\frac{1}{2}$, $8\frac{1}{2}$, $11\frac{1}{2}$, etc., and so on.

It should be noticed that in a 6-cylinder, 4-S.C., S.A. engine, the phase relationship for orders 3, 6, 9, 12, etc., is zero, i.e. for these orders all cylinders act simultaneously.

These orders are known as major orders, and all others as minor orders. As stated above, the phase diagrams repeat after the major orders are reached, i.e. after the 3rd order for a 6-cylinder, 4-S.C., S.A. engine, and after the 4th order for an 8-cylinder, 4-S.C., S.A. engine, since in the case of 4-stroke cycle, single-acting engines the major orders are integral multiples of half the number of cylinders for all normal crankshaft arrangements.

For 2-stroke cycle, single-acting engines, where the working cycle occupies one revolution, 360° in the phase diagrams represents one revolution of the crankshaft, i.e. there are no half orders. With equally-spaced cranks, the first order phase diagram is therefore an exact reproduction of the crank sequence diagram, and as in the case of 4-S.C., S.A. engines, the phase diagrams for the 2nd, 3rd, 4th, etc., orders are obtained from the phase diagram for order 1 by multiplying all angles by 2, 3, 4, etc.

In this case the major orders are integral multiples of the number of cylinders, i.e. 4, 8, 12, etc., for a 4-cylinder engine; 6, 12, 18, etc., for a 6-cylinder engine, etc., and the phase diagrams repeat after the major orders are reached.

In general, the phase diagrams for any crankshaft arrangement and firing order, and for any engine, may be obtained by applying the following rule: Assume that No. 1 crank is of zero angle and that the angles of all other cranks are measured from No. 1 crank.

Then the phase diagram for any particular order is obtained by multiplying the angles through which the shaft must turn from the firing of No. 1 cylinder to the firing of each of the other cylinders, by the order number of the particular component under consideration.

In the arrangement shown in Fig. 86, for example, the phase angles for the various orders are as follows:—

TABLE 63.

PHASE ANGLES—4-S.C., S.A. 6-CYLINDER ENGINE.

(Firing Order : 1-3-5-6-4-2.)

Cylinder No.	Firing Angle.	Phase Angles.					
		$\frac{1}{2}$ -Order.	1-Order.	$1\frac{1}{2}$ -Order.	2-Order.	$2\frac{1}{2}$ -Order.	3-Order.
1	0°	0°	0°	0°	0°	0°	0°
2	60°	300	600	900	1200	1500	1800
3	120	60	120	180	240	300	360
4	480	240	480	720	960	1200	1440
5	240	120	240	360	480	600	720
6	360	180	360	540	720	900	1080

This rule can also be deduced from Fig. 80 where it is shown that the resultant vector rotates at n times the speed of the crankshaft. Thus 1° of crankshaft rotation is equivalent to n degrees of vector rotation, where n is the number of complete vibration cycles in each crankshaft revolution.

If there are m cylinders firing at equal intervals the firing interval is $720/m$ degrees of crankshaft rotation for 4-stroke engines and $360/m$ degrees of crankshaft rotation for 2-stroke engines.

The corresponding angles between consecutive vectors in the phase diagrams are $720 \cdot n/m$ for 4-stroke engines and $360 \cdot n/m$ for 2-stroke engines, where n has the values 0.5, 1.0, 1.5, etc., for 4-strokes and 1, 2, 3, etc., for 2-strokes. The vectors are all in phase and can be added algebraically when $n/m = 0.5$ for 4-stroke engines and when $n/m = 1.0$ for 2-stroke engines. For all other values of n/m the vectors must be added geometrically.

Since the resultant harmonic components in Table 60 are for the combined effect of the top and bottom ends in the case

of double-acting engines, the rules already given for single-acting engines may be applied.

The same remark applies to opposed-piston engines, since the resultant harmonic components for this type of engine given in Table 60 are for the combined effect of the upper and lower pistons referred to a crank radius equal to total combined stroke divided by 4.

Vector Diagrams.—The vector diagrams for a 6-cylinder, 4-S.C., S.A. engine are shown in Fig. 86. They are constructed from the phase diagrams as follows :—

The vectors for the various cylinders are drawn parallel to the corresponding cranks in the phase diagram for the particular order being investigated. The lengths of the vectors are the lengths of the corresponding ordinates on the normal elastic curve. The values of the vector sums Σa for the different orders are stated on the vector diagrams in Fig. 86, and these are the values which are used in the expression already given for the equilibrium amplitude.

In setting down the vector diagrams, care must be taken to use the normal elastic curve corresponding to the mode of vibration being investigated. For example, the diagrams in Fig. 87 are for a 6-cylinder, 4-S.C., S.A. marine engine, where both one- and two-node vibrations have to be considered. The vector diagrams for the one-node mode of vibration are therefore obtained from the phase diagrams, using the deflections given by the normal elastic curve corresponding to the one-node mode of vibration. For the two-node vector diagrams, the normal elastic curve corresponding to the two-node mode of vibration must be used.

Where the node falls within the cylinder group, the vectors corresponding to cylinders on one side of the node must be set down in the opposite sense to the vectors for the cylinders on the other side of the node.

It is evident from the method of obtaining the vector diagrams that an alteration in the firing order, or an alteration in the shape of the normal elastic curve will modify the relative magnitudes of the vector sums. In the case of 2-stroke cycle engines an alteration of firing order implies an alteration

of crank sequence, but in the case of 4-stroke cycle engines there are usually a number of different firing orders for each crank sequence.

Since for multi-cylinder, internal combustion engines the n th order harmonic component of the tangential effort curve has the same value for all cylinders, and since the torque energy for any one cylinder is proportional to the maximum angular displacement at that cylinder, it follows that the relative magnitudes of the torque energy available at the several cylinders are proportional to the relative amplitudes of the ordinates on the normal elastic curve at the points corresponding to the positions of the respective cylinders.

For example, if the cranks of all cylinders were in phase, i.e. if they all reached firing centre together, and if they all fired simultaneously, the resultant harmonic torque energy for the whole group of cylinders would simply be proportional to the summation of the ordinates on the normal elastic curve corresponding to the positions occupied by the various cylinders. Further, if the ordinates on the normal elastic curve were all of equal amplitude, the resultant harmonic torque energy for the entire group of cylinders would be equal to the torque energy for one cylinder multiplied by the number of cylinders.

In an actual example, however, the cranks are not in phase, but are usually arranged to give equal firing intervals over the complete working cycle, i.e. for a 2-S.C., S.A. engine the cranks are spaced $360/m$ degrees apart, and for a 4-S.C., S.A. engine $720/m$ degrees apart, where m is the number of cylinders. In this case, if the ordinates on the normal elastic curve were all of equal amplitude, the rule for higher order inertia forces would apply, viz. the unbalanced torque energy orders would be integral multiples of the number of cylinders for 2-S.C., S.A. engines, and of half the number of cylinders for 4-S.C., S.A. engines; whilst the magnitude of any particular unbalanced order would be the magnitude for one cylinder multiplied by the number of cylinders. All other orders would cancel.

In practice, however, the ordinates on the normal elastic curve are not equal for all cylinders, although this condition is very nearly approached in the case of one-node vibrations of

marine installations with a long length of intermediate shafting between the cylinder group and the propeller (see one-node normal elastic curve in Fig. 87), i.e. in cases where the node is a considerable distance from the cylinder group. This explains why only major orders are usually of any practical importance in the case of one-node vibrations of marine installations. In the majority of cases, however, the ordinates on the normal elastic curve are appreciably different for the various cylinders, and due allowance must be made for this in obtaining the resultant torque energy for any particular order.

Since the greatest vibration stress in the case of two-node vibrations occurs at the crankshaft node, it is very important to determine the magnitudes of vibration stresses due to minor, as well as major, harmonics. The possibility of obtaining a favourable readjustment of the relative magnitudes of the various harmonics by altering the firing order, or the disposition of the masses, should have full consideration. In certain cases, the so-called minor harmonics can be sufficiently powerful to cause severe damage to the crankshaft.

The position of the crankshaft node is of considerable importance in determining the relative magnitudes of the vector sums. For example, if the system is so arranged that the node lies at the centre of the cylinder group, the ordinates of the normal elastic curve will be equally disposed on either side of the node. This will result in practically complete cancellation of the major harmonics, as shown in Fig. 87.

The foregoing rules are based on the following assumptions :—

- (i) That the operating conditions are identical in all the cylinders of a multi-cylinder engine, i.e. that the maximum values of the n th order harmonic components of the tangential effort curve are the same for all cylinders. This demands that erratic combustion due, for example, to uneven fuel injection in the case of compression ignition engines, or uneven ignition timing or mixture distribution in the case of petrol engines, does not arise. These faults do occur

- in practice, but, as a general rule, they are disclosed by a characteristic roughness of engine operation.
- (ii) That the resultant n th order vector for any given cylinder of a multi-cylinder engine is in phase with the crank of that cylinder, i.e. that the n th order harmonic component attains its maximum value T_n , when the crankpin has moved one-quarter of a vibration cycle from the top dead centre, or firing, position. This assumption means that the phase angle α_n in Fig. 80 is neglected and is permissible in cases where the characteristics of the tangential effort diagrams are identical for all cylinders, so that the same harmonic analysis can be used throughout.

These assumptions are very nearly true for multi-cylinder internal combustion engines where the dimensions of all the cylinders are the same and where an attempt is made to ensure the same operating conditions in all cylinders.

Fig. 88 indicates a method of constructing a curve showing the variation of the total amplitude of the half-order harmonic component for the entire group of cylinders over one crankshaft revolution, for a 6-cylinder in-line, 4-stroke cycle petrol engine. In this diagram the phase angle is taken into account and the data is from Diagram I of Fig. 80.

From Diagram I of Fig. 80 the maximum amplitude of the resultant n th order component for each cylinder is $T_n = 46.4$ lbs. per sq. in., and the phase angle is $\alpha_n = 51^\circ - 7'$. The firing order and normal elastic curve are assumed to be the same as in Fig. 86, so that the half-order phase diagram is the same as that in Fig. 86 and the cylinders come into action in the phase diagram at equal intervals of 60° and in the same order as the firing order, namely, 1-3-5-6-4-2. In accordance with usual practice the top dead centre position of No. 1 crankpin will be taken as the reference point, and the half-order phase diagram in Fig. 88 is represented by the outer circle with the cylinder numbers enclosed in circles and in the correct firing sequence with the vectors rotating counter-clockwise. Since the phase angle α_n is the angle by which

the resultant vector for each cylinder leads the crank, the resultant vectors for each cylinder must be set down $51^{\circ}-7'$ in advance of the respective crankpins in the phase and vector diagram in Fig. 88. The lengths of the vectors are made proportional to the lengths of the ordinates on the normal elastic curve at each cylinder, assuming unit amplitude at No. 1 cylinder. The variation of amplitude for each cylinder, for one revolution of the crankshaft, can then be plotted on a base representing two revolutions of

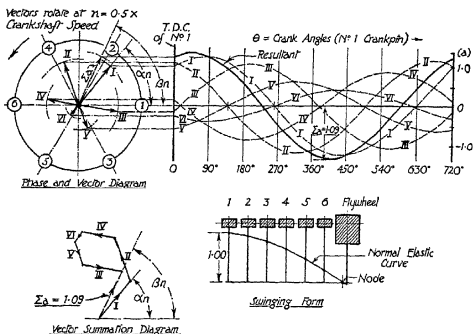


FIG. 88.—Total amplitude of the half-order harmonic component for a 6-cylinder, 4-stroke cycle engine.

No. 1 crankpin (one working cycle) by assuming that each vector rotates at n times crankshaft speed, i.e. at one-half the speed of the crankshaft, and then transferring the vertical projections of each vector to the ordinates at the appropriate crank angles. This process is clearly shown in Fig. 88, where the dotted curves indicate the variation of the half-order harmonic amplitude for each of the six cylinders. The total amplitude of the half-order component for the six cylinders can be obtained by adding the curves for the individual cylinders algebraically.

An alternative method of determining the total amplitude for the six cylinders is to draw the vector summation diagram shown at the left-hand bottom corner of Fig. 88. This summation diagram is drawn in the manner already described, and the length of the closing vector, shown dotted, is scaled to give the value of the maximum amplitude of the total half-order harmonic component for the six cylinders. The inclination of this closing vector to the horizontal is the phase angle β_n of the total vector. β_n is the angle by which the total vector leads No. 1 crankpin, so that if the closing vector in the vector summation diagram in Fig. 88 is transferred to the phase and vector diagram, the variation of amplitude of the total n th order harmonic over two revolutions of No. 1 crankpin can be plotted by assuming that this vector rotates at one-half the speed of the crankshaft and then transferring its vertical projections to the ordinates at the appropriate crank angles. The total n th order amplitudes obtained in this way will be found to agree with those obtained by summing the individual curves.

The vector summation diagram in Fig. 88 is seen to be identical in form with the vector diagram shown in Fig. 86, and in each case the value of Σa is 1.09. The only difference is that in Fig. 86 the phase angle has been neglected, whilst in Fig. 88 the total vector is shown in correct phase relationship to No. 1 crankpin. Since this phase relationship is not required for evaluating vibration amplitudes and stresses, and since the same value of Σa is obtained irrespective of the orientation of the vector diagram relative to the crankpin the phase angle will be neglected in all calculations relating to this type of engine.

In multiple-expansion, multi-cylinder steam engines, however, the dimensions of the cylinders and the operating conditions differ among the cylinders. It is therefore necessary in this case to take the phase angle into account. The method just described for a 6-cylinder, 4-stroke petrol engine (Fig. 88) can be used, bearing in mind the following modifications in the procedure :—

- (i) The resultant vector for each crank should be obtained by harmonically analysing the tangential effort diagram for the combined effect of the top and bottom

sides of the cylinder. This applies in all cases where the engine is double-acting, i.e. to all normal types of steam engine.

- (ii) The length of the resultant vector for the m th crankpin should be proportional to the length of the ordinate on the normal elastic curve a_m , multiplied by the maximum value of the n th order harmonic component T_{mn} of the tangential effort curve for the m th cylinder expressed in lbs. and not in lbs. per sq. in. of piston area.

This is necessary because cylinder dimensions and operating pressures vary among the cylinders. In all normal steam engines the strokes of the different cylinders are equal, but in the very unlikely event of a difference in stroke among the cylinders this would have to be taken into account when plotting the tangential effort diagrams.

- (iii) The resultant vector for each cylinder must lead the crank by the appropriate phase angle, determined by a harmonic analysis of the separate tangential effort diagrams for each cylinder.
- (iv) Since the working cycle is completed in one revolution of the crankshaft the curve showing the variation of the amplitude of the harmonic components need only extend over 360° of crankpin rotation, as in the case of 2-stroke cycle internal combustion engines.

The maximum amplitude of the total harmonic component for the entire cylinder group is obtained by drawing a vector summation diagram as shown in Fig. 88, the length of the closing vector being the value of $T_{mn} \cdot a_m$, where, in this case, $T_{mn} \cdot a_m$ is the maximum value of the total n th order harmonic component of the combined tangential effort for all cylinders in lbs.

The work done by the entire group of cylinders is then

$$\Sigma W_m = \pi \cdot R \Sigma T_{mn} \cdot a_m \text{ lbs.-ins. per cycle.}$$

Note.—If $a_m = 1$ for No. 1 crank, then ΣW_m is the work done per cycle per unit deflection at No. 1 crank.

As a rule the torsional vibration problem in steam engine installations is not so severe as in internal combustion engine installations. Examples of failures of steam engine transmission systems are comparatively rare, because the engines are of the double-acting type and have relatively short and rigid crankshafts, whilst the magnitudes of the disturbing harmonic components are relatively small.

Two examples will suffice, however, to show that even in the case of steam engine installations it is very desirable to investigate the torsional vibration problem. In the first example a medium speed compound steam engine was employed to drive a large fan for mine ventilation. The fan was close-coupled to the engine and shortly after installation the bolts in the coupling between the engine and the fan were broken. These breakages continued in spite of oversize replacements, and eventually the trouble was overcome by increasing the size of the driving shaft.

In the second example the failure of the tail-end shaft of a triple expansion marine steam engine was traced to resonance between the 3rd order harmonic component of the tangential effort of the engine and the one-node mode of vibration of the transmission system at the normal operating speed. The amplitude of vibration at the resonant speed was such that a movement of ± 2 ins. occurred at each crankpin three times per revolution, and the crankshaft appeared to rotate with three distinct jerks in each revolution. The trouble was entirely removed by replacing the original propeller shafting by shafting of larger diameter.

Where the characteristics of the transmission system are such that only the one-node mode of vibration requires investigation, and where there is a long flexible transmission shaft, so that the node is remote from the engine crankshaft, e.g. in marine propelling installations where the engine is amidships, the whole cylinder group vibrates with very nearly the same amplitude, i.e. the ordinates on the normal elastic curve are very nearly the same for all cylinders, as shown in Fig. 15.

In such cases an appreciably simpler method of evaluating

the work done by the entire cylinder group, when the prime mover is a multiple-expansion steam engine, is to plot a diagram showing the combined tangential effort for the entire cylinder group. If this diagram is harmonically analysed the total harmonic components for the entire cylinder group are obtained directly.

The work done by the entire cylinder group is then

$$W = \pi \cdot T \cdot R \text{ lbs.-ins. per cycle per unit amplitude at engine,}$$

where T = the maximum value of the n th order harmonic component of the combined tangential effort curve for the entire group of cylinders, in lbs.,

R = common crank radius, in inches.

Internal Combustion Engines with Two or More Pistons Operating on Each Crankpin.

Radial Engines.—Fig. 89 shows a 5-cylinder radial engine. For any given position of the common crankpin the torque due to any given cylinder will not be altered if the whole piston/connecting rod/crank assembly of that cylinder is rotated about the crankshaft axis until the line of stroke of the piston is vertical. The complete engine, in other words, can be regarded as composed of a number of superimposed single-crank engines so that from the point of view of shaft torque an equivalent in-line engine is obtained by rotating each cylinder mechanism until its line of stroke is vertical. This is a convenient method of studying shaft torque in engines of the Vee, fan, or radial type, and the equivalent in-line engine for the 5-cylinder radial is shown at the right-hand side in Fig. 89.

If equal cylinder spacing is assumed in the radial arrangement then the equivalent in-line engine is a normal 5-crank arrangement with equally spaced cranks. The phase diagrams can therefore be constructed by the methods already described for in-line engines. In the case of 4-stroke cycle engines the firing order must be 1-3-5-2-4 to provide equal firing intervals.

Since the cylinders are all in the same transverse vertical plane the vibration amplitude is identical for all cylinders, so that the only unbalanced harmonic components of the shaft torque are the 2·5, 5, 7·5, 10, etc., orders, i.e. the major orders. In general, therefore, the unbalanced torque energy orders for 4-stroke cycle radial engines with unarticulated connecting rods are all integral multiples of one-half the number of cylinders, and the magnitude of any particular unbalanced

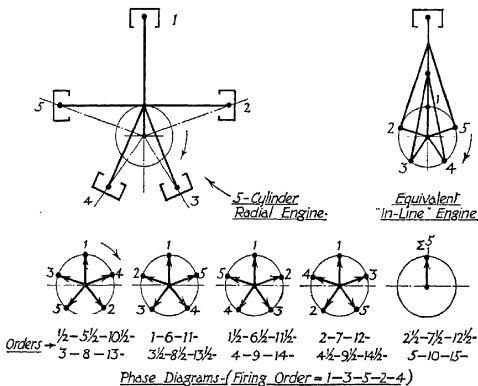


FIG. 89.—Phase diagrams—radial engine.

order is the magnitude for one cylinder multiplied by the number of cylinders. It should be noted that this rule applies only if there is an odd number of cylinders, so that the firing intervals are equal.

In 2-stroke cycle radial engines there may be either an odd or an even number of cylinders, and in both cases the only unbalanced torque energy orders are integral multiples of the number of cylinders, whilst the magnitude of any particular

unbalanced order is the magnitude for one cylinder multiplied by the number of cylinders.

Thus in a 5-cylinder radial the lowest critical speed is the 2.5th order for a 4-stroke engine and the 5th order for a 2-stroke engine and there is a clear range between these criticals and the 5th and 10th orders respectively. As a rule the fundamental critical speed of radial engines is well below the operating speed range, so that the torsional vibration problem is not usually so difficult as in in-line engines, bearing in mind that only major criticals have to be dealt with and that if the fundamental major critical is well down the speed range all higher orders are even further removed from the operating range. This is especially the case in large geared radial engines where the natural frequency is low. In small direct-driving radials, where the natural frequency is higher, difficulty is sometimes experienced in placing the fundamental critical speed sufficiently far below the operating range, and in some cases it is necessary to work with this critical above the running range.

The above discussion neglects the effect of articulation. This subject has already been dealt with at some length, and a method of evaluating the resultant harmonic components for an engine with articulated connecting rods has been described. In evaluating the harmonic components of the tangential effort due to the inertia of the reciprocating parts of a radial engine with equally spaced cylinders it will be found that the cosine terms of the articulated cylinders on one side of the master connecting rod cancel the cosine terms of the articulated cylinders on the other side of the master rod, i.e. in the 5-cylinder radial shown in Fig. 89, if the master cylinder is No. 1 then the cosine terms of cylinders 2 and 3 cancel the cosine terms of cylinders 4 and 5. The sine terms of the articulated cylinders are additive, but it is only necessary to evaluate these terms for the cylinders on one side of the master rod. Thus, in Fig. 89, if the sums of the sine terms for cylinders 2 and 3 are obtained, then the magnitudes of the inertia tangential effort components for the whole engine are double these values.

The principal effect of articulation is to introduce at once

a revolution surge into the torque diagram. This articulation surge is clearly shown in Fig. 90, which is the torque curve for a 9-cylinder, single-row radial engine.

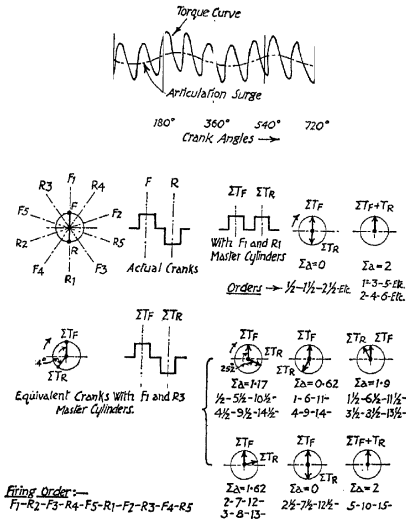


FIG. 90.—Phase diagrams—radial engines.

It is necessary, therefore, to take into account the possibility of a 1st order critical speed as well as the major criticals already mentioned, although up to the present little trouble has been experienced with 1st order criticals, because the frequency of the system has been sufficiently high to place it well above the maximum operating speed. The modern trend,

however, towards larger engines and lower gear ratios tends to lower the natural frequency of the system and so bring this 1st order critical into the operating speed range, especially in the case of 2-row radial engines with the rows staggered and with the two crankpins set at 180° . With such an arrangement the two master cylinders fire at 360° intervals, so that the 1st order harmonic due to articulation of one row adds to the corresponding harmonic of the second row.

Once the harmonic components of the tangential effort curve for all the cylinders of one row of a multi-row radial engine have been determined the harmonic components for the engine as a whole can be obtained by the methods already given for in-line engines, i.e. each crankpin of the multi-row radial can be regarded as one crankpin of an in-line engine and phase and vector diagrams can be drawn as for an in-line engine.

A 10-cylinder, 2-row radial engine is shown in Fig. 90. In this arrangement there are two rows of five cylinders operating on two crankpins spaced at 180° . For even-firing the cylinders in the two rows are staggered and the firing sequence is the same in each row, i.e. alternative cylinders in one row fire consecutively. The firing sequence is therefore $F_1-R_2-F_3-R_4-F_5-R_1-F_2-R_3-F_4-R_5$, where F designates cylinders in the front row and R those in the rear row. From considerations of secondary balance of the reciprocating masses the master cylinder in the rear row is placed at 180° to the master cylinder in the front row, i.e. the master cylinders are F_1 and R_1 in Fig. 90. As already explained, since the cylinders of each row are all in the same transverse vertical plane the vibration amplitude is identical for all cylinders, so that a 2-row radial can be regarded as a 2-crank engine in which the values of the harmonic components, acting on each crankpin, are the total values obtained by summing the individual components for all the cylinders of one row, i.e. ΣT_F and ΣT_R .

Furthermore, since the method which has been described for obtaining the total values of the harmonic components for a whole row of cylinders takes the line of stroke of the master cylinder as datum, the cranks of the equivalent in-line engine must also be in phase with the lines of stroke of the master

cylinders in each row. Thus, if F_1 and R_1 are the master cylinders in the arrangement shown in Fig. 90, the equivalent in-line arrangement is obtained by swinging crank R through 180° so that the line of stroke of master cylinder R_1 is brought into coincidence with the line of stroke of master cylinder F_1 . This crank arrangement is shown at the right-hand side of Fig. 90. For even-firing intervals the master cylinder in row R fires 360° after the master cylinder in row F , and the corresponding angle in the half-order phase diagram is therefore 180° . The remaining phase diagrams are obtained from the half-order diagram in the usual way, and these show that all half-orders are balanced but that orders 1-3-5, etc., and 2-4-6 are completely unbalanced. It has already been shown, however, that if articulation is neglected the only unbalanced orders for each row of five cylinders are the 2.5, 5, 7.5, 10, etc., orders, whilst the principal effect of articulation is to introduce a first order surge in the tangential effort diagram. Hence for the complete two-row engine the only unbalanced orders are the 5, 10, 15, etc., orders and the 1st order, due to articulation, which is twice as large as the 1st order for one row of five cylinders.

The evenness of firing will not be appreciably disturbed if some other cylinder in the rear row is chosen as the master cylinder.

For example, if cylinder R_3 (or R_4) is chosen as the master cylinder in the rear row, then the firing interval between the master cylinder F_1 in the front row and the master cylinder R_3 in the rear row is 504° or 144° , and the corresponding angle in the half-order phase diagram is 252° or 72° . The remaining phase diagrams are obtained from the half-order diagram in the usual way and these show that with this arrangement of master cylinders all orders are unbalanced, except orders $2\frac{1}{2}$, $7\frac{1}{2}$, $12\frac{1}{2}$, etc., when R_3 fires 504° after F_1 .

Since, however, the only unbalanced orders for each row of cylinders when articulation is neglected are the 2.5, 5, 7.5, 10, etc., orders, whilst the principal effect of articulation is to introduce a 1st order surge, the only unbalanced orders are the 5, 10, 15, etc., orders and the 1st order surge as in the

previous arrangement. The magnitudes of the 5, 10, 15, etc., orders are the same as in the previous arrangement of master cylinders. The magnitude of the first order is, however, reduced to less than one-third of its former value, i.e. to about 60 per cent. of the value for a single row of cylinders. In cases where the 1st order is within or near the running range of the engine, therefore, this alternative arrangement of the master cylinders might be a means of avoiding excessive vibration. It must be noted, however, that with this alternative arrangement of the master cylinders the secondary inertia force will not be completely balanced.

The alternative arrangement with R_3 firing 144° after F_1 can be investigated in the same way. It will be found, however, that although the magnitude of the 1st order is again reduced to 60 per cent. of its value for a single row of cylinders the $2\frac{1}{2}$, $7\frac{1}{2}$, $12\frac{1}{2}$, etc., orders, as well as the 5, 10, 15, etc., orders are completely unbalanced. This alternative is therefore inferior.

Double-row radial engines may also be arranged with the cylinders in axial alignment instead of being staggered. For even-firing impulses the two cranks must then be in phase instead of being spaced at 180° , and this arrangement of cranks gives unbalanced secondary inertia forces. An investigation of the unbalanced torque orders shows that the same general conclusions apply here as in the case just discussed. Thus, if the master rods operate in the two coaxial cylinders, say cylinders F_1 and R_1 , the total 1st order harmonic torque is twice the value for one row of cylinders. Furthermore, the unbalanced secondary inertia force is twice the value for one row of cylinders. If, on the other hand, cylinder F_1 is chosen as the master cylinder in the front row, whilst cylinder R_3 (or R_4) is chosen as the master cylinder in the rear row, then the 1st order harmonic component is reduced to one-third, i.e. to 60 per cent. of the value for a single row of cylinders, whilst the secondary inertia force is partially balanced.

Assuming that the vibratory amplitude is the same at all the rows of a multi-row radial aero-engine, then the following expression gives the angles of rotation of the crankshaft from

firing centre of the master cylinder in one row to firing centre of the master cylinder in another row which will cause cancellation of any chosen harmonic of the engine torque:—

(i) For 2-stroke cycle engines where the working cycle occupies $2 \cdot \pi$ radians (360°).

$$\delta = \frac{2 \cdot \pi}{n \cdot N}, \frac{2 \cdot \pi}{n} \left[\frac{1}{N} + 1 \right], \frac{2 \cdot \pi}{n} \left[\frac{1}{N} + 2 \right], \dots, \frac{2 \cdot \pi}{n} \left[\frac{1}{N} + (n - 1) \right] \dots \quad (261a)$$

(ii) For 4-stroke cycle engines where the working cycle occupies $4 \cdot \pi$ radians (720°).

$$\delta = \frac{2 \cdot \pi}{n \cdot N}, \frac{2 \cdot \pi}{n} \left[\frac{1}{N} + 1 \right], \frac{2 \cdot \pi}{n} \left[\frac{1}{N} + 2 \right], \dots, \frac{2 \cdot \pi}{n} \left[\frac{1}{N} + (2 \cdot n - 1) \right], \dots \quad (261b)$$

where, δ = angle of rotation of crankshaft from firing centre of the master cylinder of one row to firing centre of the master cylinder of another row for cancellation of the n th order harmonic,

n = harmonic order number to be cancelled,

N = number of rows of cylinders.

The above expressions merely state the phase relationships which must exist between the firing points of the several master cylinders so that the resultant n th order torque summation for the engine as a whole is zero. They are readily deduced from wave diagrams.

There are, in general, several values of δ , the number of alternatives depending on the particular value of n , any one of which will bring about cancellation of the chosen harmonic.

Having determined the values of δ , the arrangement of the engine cranks and cylinders must be examined to see if the master cylinders can be selected so that one of the required values of δ is obtained.

For example, in the 10-cylinder, two-row, 4-stroke cycle radial engine shown in Fig. 90, equation (261b) reduces to

$$\delta = \frac{\pi}{n}, \frac{3 \cdot \pi}{n}, \frac{5 \cdot \pi}{n}, \frac{7 \cdot \pi}{n}, \dots, \frac{2 \cdot \pi}{n} (2 \cdot n - \frac{1}{2}), \text{ (since } N = 2\text{)}.$$

Thus, for cancellation of the 1st order harmonic ($n = 1$),

$$\delta = \pi \text{ or } 3 \cdot \pi.$$

Now in a conventional engine of this type the angle between the cranks is π radians (180°) from considerations of engine balance. Hence with this type of crankshaft the master cylinders must be in axial alignment for a firing interval of π or $3 \cdot \pi$, i.e. for cancellation of the 1st order harmonic.

In conventional engines, however, the cylinder rows are staggered from considerations of engine cooling, so that the above condition cannot be fulfilled.

A considerable reduction of the amplitude of the resultant 1st order component is nevertheless obtained by choosing cylinders which are nearly in axial alignment as the master cylinders, i.e. cylinders F_1 and either R_3 or R_4 in Fig. 90. When this is done the magnitude of the 1st order component is about one-third of its value when F_1 and R_1 in Fig. 90 are the master cylinders, as previously explained.

An alternative arrangement is to move the crankpins into axial alignment, i.e. angle between cranks zero. The master cylinders must be spaced π radians (180°) apart to give a firing interval of π or $3 \cdot \pi$, and thus cause cancellation of the 1st order harmonic, i.e. F_1 and R_1 in Fig. 90 become the master cylinders. This is the conventional arrangement of cylinders but the crank arrangement is unconventional.

For cancellation of the 2nd order harmonic ($n = 2$),

$$\delta = \pi/2, 3 \cdot \pi/2, 5 \cdot \pi/2, \text{ or } 7 \cdot \pi/2.$$

Hence in a conventional two-row radial engine with cranks at 180° the master cylinders must be 90° or 270° apart for cancellation of the 2nd order harmonic.

This condition cannot be obtained by an engine of the type shown in Fig. 90, i.e. a two-row radial with 5-cylinders in each row, but an appreciable reduction of the resultant 2nd order harmonic is obtained by choosing cylinders which are nearly 90° , or 270° apart as master cylinders. For example, if F_1 and either R_2 or R_3 are chosen as master cylinders in Fig. 90, the magnitude of the 2nd order harmonic is reduced to about one-third of its value with the conventional arrangement where F_1 and R_1 are the master cylinders.

Cancellation of the 2nd order component is also obtained if the crankpins are moved into axial alignment, i.e. angle between cranks zero, and the master cylinders are spaced 90° apart, but in this case both cylinder spacing and crank arrangement are unconventional.

A third alternative is to place the cranks at 90° , in which case the master cylinders must be in axial alignment which is another unconventional arrangement.

Equation (261b) reveals a point of special interest in connection with the half-order components of 4-stroke cycle engines of conventional design. If the values of δ for the half-order components are calculated, i.e. putting $n = \frac{1}{2}, 1\frac{1}{2}, 2\frac{1}{2}$, etc., in Equation (261b), it will be found that one of the values of δ is $2 \cdot \pi$ in all cases. This indicates that if the firing interval between the master cylinders is $2 \cdot \pi$, then all half-order components are cancelled, a condition which is fulfilled with conventional arrangements of two-row radials where the crankpins are spaced 180° apart, the cylinder rows are staggered and the master cylinders are 180° apart with a firing interval of 360° .

The above discussion of 2-row radials assumes that the shape of the normal elastic curve is such that the amplitudes of vibration are substantially the same at each row of cylinders. If the ordinates of this curve at the cylinders differ appreciably this should be taken into account in drawing the vector diagrams, just as in the case of an in-line engine.

Multi-Cylinder In-Line Internal Combustion Engines.

—It has already been mentioned that alterations of firing order or changes in the shape of the normal elastic curve modify

the relative amplitudes of the disturbances at different resonant speeds. A speed range free from serious resonant zones is, of course, essential for safe operation, whilst disturbances which cannot be regarded as really dangerous are best avoided if their elimination does not handicap the design in other directions.

There are several important factors to be considered in addition to torsional vibration when a power transmission system is designed.

The engine should be free from serious unbalance due to the inertia forces originated by the motions of the reciprocating and rotating parts.

The sequence of firing should be such that no undue load is imposed on any bearing, and the arrangement of crankshaft should not cause a concentration of inertia loading on any one journal. The latter condition cannot always be fulfilled. For example, in a 4-stroke cycle, 6-cylinder in-line engine with the crankshaft arranged as shown in Fig. 86, so that even firing intervals are obtained and so that there is collective primary and secondary balance of inertia forces, the journal between Nos. 3 and 4 cylinders carries the major part of the combined inertia load of these two cylinders.

In such cases the bearing load can be relieved by attaching balance weights to the crankwebs and this has the further advantage of relieving the crankcase inertia loading. It must be borne in mind, however, that the addition of these balance weights increases the polar moment of inertia of the mass system and so causes an appreciable reduction of natural frequency unless this can be offset by an appropriate increase in the stiffness of the crank elements, e.g. by increasing the size of the journals or of the crankwebs.

In the case of aero engines, where any addition to the total weight of the engine must be amply justified, the amount of counterweighting added to the crankwebs should be the minimum necessary to give reasonable bearing loads, although it should be noted that a properly counterweighted aero-engine crankshaft might actually save on total engine weight by unloading the crankcase to the extent of permitting a lighter crankcase to be used.

An alternative method of reducing the inertia loading on the bearings and crankcase which can be used in medium-speed and high-speed engines fitted with steel or cast-iron connecting rod big-end housings is to replace the steel or iron big-end keeps by keeps made from forged aluminium alloy.

Where total weight is important this has the advantage of giving a reduction in overall weight and a reduction in the inertia loading on the big-end bearings, main bearings, and crankcase.

As a general rule the addition of counterweights to an in-line engine crankshaft, even if the engine is inherently balanced, has important advantages from the point of view of bearing loads and the reduction of stresses and distortions in the crankcase, and is to be recommended in all cases where it does not render the torsional vibration problem more difficult.

Another important factor to be kept in mind is that of crankshaft manufacture, because if the configuration of the crankshaft is such that good grainflow cannot be obtained in the neighbourhood of the junctions of the journals, pins, and webs, trouble may be encountered due to fatigue cracking at those points. Finally, the importance of an efficient induction system giving good mixture distribution must be kept in mind when choosing the arrangement of the crankshaft and the firing order for multi-cylinder, 4-stroke cycle petrol engines.

The theoretical number of different crank arrangements increases rapidly with the number of cylinders. In the following discussion the change of firing order which occurs automatically when the direction of rotation of the engine is reversed is not counted as a separate arrangement, because so far as torsional vibration and engine balance are concerned the two conditions of operation are identical. Thus from the torsional vibration point of view the 4-cylinder firing order 1-3-4-2 is the same as the reverse order 1-2-4-3, and the 8-cylinder firing order 1-8-2-5-6-3-4-7 is the same as the corresponding reverse order 1-7-4-3-6-5-2-8.

(Note.—It should not be inferred from this that the torsional vibration characteristics of a marine engine are the same when going astern as they are for ahead running. This is true only

if the cylinder pressures are the same for both conditions of operation. In practice the power available for astern operation is sometimes considerably smaller than full power for ahead operation, and this naturally gives a reduced speed range when running astern.)

It can be shown that the theoretical number of different crank arrangements for a 2-stroke cycle, in-line engine with m cylinders and m equally spaced cranks is

$$M = \frac{m!}{m} = (m-1)!$$

where $m! = m(m-1)(m-2)(\dots)(1)$.

Since, however, from the standpoint of torsional vibration and engine balance clockwise and counter-clockwise rotations are interchangeable, the *effective* number of different crank arrangements is

$$M = \frac{(m-1)!}{2} = 0.5(m-1)(m-2)(\dots)(1),$$

i.e. for a 5-cylinder engine of this type,

$$M = 4 \times 3 \times 2/2 = 12, \text{ effective number of different crank arrangements.}$$

These twelve arrangements are as follows, and in each case the corresponding reverse order is shown at the right-hand side:—

<i>Clockwise.</i>	<i>Counter-clockwise.</i>
1-2-3-4-5	1-5-4-3-2
1-2-3-5-4	1-4-5-3-2
1-3-2-4-5	1-5-4-2-3
1-3-2-5-4	1-4-5-2-3
1-2-4-3-5	1-5-3-4-2
1-2-4-5-3	1-3-5-4-2
1-4-2-3-5	1-5-3-2-4
1-4-2-5-3	1-3-5-2-4
1-2-5-3-4	1-4-3-5-2
1-2-5-4-3	1-3-4-5-2
1-5-2-3-4	1-4-3-2-5
1-5-2-4-3	1-3-4-2-5

The total *effective* numbers of different crank arrangements for 2-stroke cycle engines with equally spaced cranks and various numbers of cylinders are as follows:—

<i>Number of Cylinders.</i>	<i>Effective Number of Crank Arrangements.</i>
3	1
4	3
5	12
6	60
7	360
8	2,520
9	20,160
10	181,440

In 2-stroke cycle engines the firing order is the same as the crank sequence and a change of firing order can only be made by changing the crankshaft. Since the working cycle occupies one crankshaft revolution there are no half-order harmonics, and the 1st order phase diagram is a replica of the crank sequence diagram. The remaining phase diagrams are easily obtained from the 1st order diagram, as already explained.

In 4-stroke cycle engines having an odd number of cylinders the crankpins are equally spaced round the crank circle and even firing impulses are obtained by firing every other cylinder as its crankpin passes firing centres. Since the working cycle of a 4-stroke cycle engine occupies 720° this gives an even number of firing impulses when the crankpins are evenly spaced round the crank circle. Thus, in a 5-cylinder engine with crank sequence 1-5-2-3-4 there would be five impulses in 720° , i.e. 2.5 impulses per crankshaft revolution and the firing order would be 1-2-4-5-3. The only alternative firing order with this crank sequence is 1-5-2-3-4, but in this case the cylinders would fire consecutively, so that there would be a whole revolution of the crankshaft without any firing at all. This alternative firing order is therefore of no practical value.

The effective number of different firing orders in the case of 4-stroke cycle engines having an odd number of cylinders is therefore the same as the effective number of different crank arrangements as already discussed in connection with 2-stroke cycle engines.

In 4-stroke cycle in-line engines having an even number of cylinders the crankpins are arranged in pairs at equal angular intervals round the crank circle, and one half of the crankshaft

is the mirror image of the other half. This arrangement provides complete primary and secondary balance of inertia forces and couples as well as even firing intervals.

It can be shown that the theoretical number of these balanced crankshaft arrangements is as follows :—

$$M = \frac{(0.5m - 1)!}{2} = 0.5(0.5m - 1)(0.5m - 2)(\dots) \dots (1),$$

where m = total number of cylinders.

In an 8-cylinder in-line, 4-stroke cycle engine, for example, the number of balanced crankshaft arrangements is

$$M = 0.5(3 \times 2 \times 1) = 3.$$

These are (1, 8) - (2, 7) - (3, 6) - (4, 5),
 (1, 8) - (2, 7) - (4, 5) - (3, 6),
 (1, 8) - (3, 6) - (2, 7) - (4, 5),

the crankpins being spaced in pairs at equal intervals of 90° round the crankpin circle.

It can also be shown that the theoretical number of different firing orders for each balanced crankshaft arrangement is

$$M' = 2^{\binom{m}{2} - 1}.$$

Thus for an 8-cylinder, 4-stroke cycle, in-line engine with a balanced crankshaft the theoretical number of firing orders for each arrangement of balanced cranks is

$$M' = 2^3 = 8,$$

and since there are three different balanced crankshaft arrangements the total theoretical number of different firing orders for an 8-cylinder engine of this type is $(8 \times 3) = 24$.

The eight different firing orders corresponding to the third balanced crankshaft arrangement listed above are

1-3-2-4-8-6-7-5
 1-3-2-5-8-6-7-4
 1-3-7-4-8-6-2-5
 1-3-7-5-8-6-2-4
 1-6-2-4-8-3-7-5
 1-6-2-5-8-3-7-4
 1-6-7-4-8-3-2-5
 1-6-7-5-8-3-2-4

i.e. one cylinder of each pair fires as the pair of crankpins pass firing centres. Hence there are eight evenly spaced firing impulses in 720° or four impulses at 90° in each revolution of the crankshaft.

(*Note.*—As already explained there is a reverse firing order, i.e. 1-5-7-6-8-4-2-3, etc., corresponding to each of the orders listed above. These reverse orders are not considered as separate orders, however, because the balancing and torsional vibration characteristics are the same for either direction of rotation.)

The theoretical numbers of balanced crankshaft arrangements and of firing orders for engines having various numbers of cylinders are as follows :—

No. of Cyls.	No. of Balanced Crankshaft Arrangements.	No. of Firing Orders per Crankshaft Arrangement.	Total Number of Firing Orders.
6	1	4	4
8	3	8	24
10	12	16	192
12	60	32	1920

The foregoing analysis shows that the number of different firing orders multiplies enormously as the number of cylinders increases. In practice, however, many of these crankshaft arrangements are unusable for one or other of the reasons already mentioned. Nevertheless, there remains plenty of scope for exploring alternative arrangements with the object of finding the best all-round compromise between torsional vibration characteristics, engine balance, and other important design considerations.

It is impossible to go very deeply into the question of crankshaft arrangements here, so attention will be confined to a description of arrangements which are usually found in practice. These arrangements are given in Table 64 and may be found useful as a guide in starting a new design.

It has already been mentioned that a change of firing order of a 2-stroke cycle engine necessitates changing the crankshaft.

TABLE 64.

CRANKSHAFT ARRANGEMENTS FOR IN-LINE ENGINES.

FOUR-STROKE CYCLE, SINGLE-ACTING, IN-LINE ENGINES.							
Number of Cylinders	Crack Diagram	1/2-Order Phase Diagram	Order of Firing and Crank Angles	Total Unbalanced Forces and Moments of Crankshaft	Engine Balancing Forces	Balancing Factors	
						$\frac{M}{S}$	$\frac{R}{P}$
1	4		1-3-4-2 2 at 180°	2, 4, 6, etc.	None Even Orders = 0	Nil	Nil
2	4		1-3-4-2 Uneven	4, 8, 12, Etc.	2, 6, 10, Etc. 4, 8, 12, Etc. = 0	Nil	1.41 $\frac{4.00}{9}$
3	4		1-3-2-4 Uneven	4, 8, 12, Etc.	None Even Orders = 0	Nil	3.16 Nil
4	5		1-2-4-5-3 2 1/2 at 144°	2 1/2, 5, 7 1/2, Etc.	None 2 1/2, 5, 7 1/2, Etc. = 0	Nil	0.45 $\frac{4.98}{9}$
5	6		1-5-3-6-2-4 3 at 120°	3, 6, 9, Etc.	1 1/2, 4 1/2, 7 1/2, Etc. Odd and Even Orders = 0	Nil	Nil
6	7		1-3-5-7-6-4-2 3 1/2 at 102 2/3°	3 1/2, 7, 10 1/2, Etc.	None 3 1/2, 7, 10 1/2, Etc. = 0	Nil	0.25 $\frac{0.90}{9}$
7	7		1-5-2-4-6-3-7 3 1/2 at 102 2/3°	3 1/2, 7, 10 1/2, Etc.	None 3 1/2, 7, 10 1/2, Etc. = 0	Nil	Nil
8	8		1-6-2-5-8-3-7-4 4 at 90°	4, 8, 12, Etc.	None Odd and Even Orders = 0	Nil	Nil
9	8		1-5-2-6-4-8-3-7 4 at 90°	4, 8, 12, Etc.	2, 6, 10, Etc. 4, 8, 12, Etc. = 0	Nil	Nil
10	9		1-2-4-6-8-9-7-5-3 4 1/2 at 80°	4 1/2, 9, 13 1/2, Etc.	None 4 1/2, 9, 13 1/2, Etc. = 0	Nil	0.19 $\frac{0.55}{9}$
11	9		1-5-9-3-6-8-2-4-7 4 1/2 at 80°	4 1/2, 9, 13 1/2, Etc.	None 4 1/2, 9, 13 1/2, Etc. = 0	Nil	0.92 $\frac{1.13}{9}$
12	10		1-6-2-8-4-10-5-9-3-7 5 at 72°	5, 10, 15, Etc.	2 1/2, 7 1/2, 12 1/2, Etc. Odd and Even Orders = 0	Nil	Nil
13	12		1-8-3-9-2-7-12-5-10-4-11-6 6 at 60°	6, 12, 18, Etc.	None Odd and Even Orders = 0	Nil	Nil
14	12		1-7-5-11-10-12-11-10-9-8-6-3 3 at 120°	3, 6, 9, Etc.	All Orders = 0	Nil	Nil

TABLE 64 (continued).

TWO-STROKE CYCLE, SINGLE-ACTING, IN-LINE ENGINES.										
Reference Number	Number of Cylinders	Crank Diagram	1st Order phase Diagram	Order of Firing and Firing impulses per rev	Totally Unbalanced Torque Orders		Engine Balancing Factors			
					Node near end of Crankshaft	Node at centre of Crankshaft	Forces		Couplers	
							Primary	Secondary	Primary	Secondary
15	4			1-3-2-4 4 at 90°	4, 8, 12, Etc.	2, 6, 10, Etc. [4, 8, 12, Etc.=0]	Nil	Nil	1.41	$\frac{4.00}{9}$
16	4			1-3-4-2 4 at 90°	4, 8, 12, Etc.	None [Even Orders=0]	Nil	Nil	3.15	Nil
17	5			1-5-2-3-4 5 at 72°	5, 10, 15, Etc.	None [5, 10, 15, Etc.=0]	Nil	Nil	0.45	$\frac{4.98}{9}$
18	6			1-5-3-4-2-6 6 at 60°	6, 12, 18, Etc.	3, 9, 15, Etc. [6, 12, 18, Etc.=0]	Nil	Nil	Nil	$\frac{3.45}{9}$
19	6			1-4-5-2-3-6 6 at 60°	6, 12, 18, Etc.	None [6, 12, 18, Etc.=0]	Nil	Nil	Nil	$\frac{6.93}{9}$
20	6			1-4-2-6-3-5 6 at 60°	6, 12, 18, Etc.	3, 9, 15, Etc. [Even Orders=0]	Nil	Nil	3.46	Nil
21	7			1-6-3-4-5-2-7 7 at 51 2/3°	7, 14, 21, Etc.	None [7, 14, 21, Etc.=0]	Nil	Nil	0.25	$\frac{0.90}{9}$
22	7			1-6-5-3-2-7-4 7 at 51 2/3°	7, 14, 21, Etc.	None [7, 14, 21, Etc.=0]	Nil	Nil	Nil	$\frac{9.15}{9}$
23	8			1-8-2-5-6-3-4-7 8 at 45°	8, 16, 24, Etc.	None [8, 16, 24, Etc.=0]	Nil	Nil	0.13	$\frac{1.41}{9}$
24	8			1-8-2-6-4-5-3-7 8 at 45°	8, 16, 24, Etc.	4, 12, 20, Etc. [8, 16, 24, Etc.=0]	Nil	Nil	0.45	Nil
25	8			1-8-3-4-7-2-5-6 8 at 45°	8, 16, 24, Etc.	None [8, 16, 24, Etc.=0]	Nil	Nil	0.89	Nil
26	9			1-9-2-7-4-5-6-3-8 9 at 40°	9, 18, 27, Etc.	None [9, 18, 27, Etc.=0]	Nil	Nil	0.19	$\frac{0.55}{9}$
27	9			1-8-5-2-9-4-3-7-6 9 at 40°	9, 18, 27, Etc.	None [9, 18, 27, Etc.=0]	Nil	Nil	0.92	$\frac{1.13}{9}$
28	10			1-10-2-8-4-6-5-7-3-9 10 at 36°	10, 20, 30, Etc.	5, 15, 25, Etc. [10, 20, 30, Etc.=0]	Nil	Nil	Nil	$\frac{0.90}{9}$

In 4-stroke cycle engines with balanced type crankshafts and an even number of cylinders there are several alternative firing orders for each crankshaft arrangement. Hence in this type of engine it is useful to remember that the effect

orders for each case, assuming that the node is either at the end of the crankshaft or else that it is remote from the crankshaft, i.e. assuming that the shape of the normal elastic curve is as shown for the one-node mode of vibration at (b) and (d) in Fig. 18, respectively. By totally unbalanced orders is meant those orders for which the vectors are added arithmetically.

When the node is either at the end of the crankshaft or is remote from the crankshaft the totally unbalanced orders are the so-called major orders, i.e. orders $m/2$, $2m/2$, $3m/2$, etc., for 4-stroke cycle engines and orders m , $2m$, $3m$, etc., for 2-stroke cycle engines, where m is the number of cylinders, although it should be noted that this rule only applies if the firing intervals are equally spaced throughout the working cycle.

It should also be noted that if the node is so remote from the crankshaft that the amplitude of vibration is substantially the same at all cylinders, then these major orders are the only unbalanced orders since all minor orders cancel.

Column 7 of Table 64 gives the totally unbalanced harmonic orders for each case, assuming that the node is at the centre of the crankshaft, i.e. the shape of the normal elastic curve is as shown for the two-node mode of vibration at (d) in Fig. 18. In this case the so-called major orders cancel, due to the symmetrical shape of the normal elastic curve, and in a great many cases there are no totally unbalanced harmonic orders.

The expedient of so arranging the transmission system that the node is situated at the centre of the crankshaft is therefore a very useful method of minimising torsional vibration in cases where it can be applied.

This expedient has been used with complete success for eliminating all major criticals corresponding to the two-node mode of vibration of marine oil engine installations, the node being brought to the centre of the crankshaft either by reducing the size of the flywheel at the driving end of the crankshaft (or eliminating it altogether) and fitting a suitable flywheel at the free end of the crankshaft, or by eliminating the flywheel altogether and obtaining the required flywheel effect by fitting counterweights to the crankwebs.

The last four columns of Table 64 contain factors which enable the unbalanced forces and couples to be calculated for each case, as follows :—

Let W = weight of unbalanced rotating parts of one cylinder, in lbs.,

W' = weight of unbalanced reciprocating parts of one cylinder, in lbs.,

R = crank radius, in inches,

N = revolutions, per minute,

L = pitch centres of cylinders, in inches (assumed constant),

q = ratio : length of connecting rod/crank radius,

F_p = maximum unbalanced primary force for whole engine, in lbs.,

F_s = maximum unbalanced secondary force for whole engine, in lbs.,

C_p = maximum unbalanced primary couple for whole engine, in lbs.-ins.,

C_s = maximum unbalanced secondary couple for whole engine, in lbs.-ins.

Then, assuming equal cylinder pitches,

$$F_p = 0.0000284 \cdot (W + W') \cdot R \cdot N^2 \cdot K_p, \quad (262)$$

$$F_s = 0.0000284 \cdot W' \cdot R \cdot N^2 \cdot K_s, \quad (263)$$

$$C_p = 0.0000284 \cdot (W + W') \cdot R \cdot N^2 \cdot L \cdot K_p', \quad (264)$$

$$C_s = 0.0000284 \cdot W' \cdot R \cdot N^2 \cdot L \cdot K_s', \quad (265)$$

The maximum values of the primary forces and couples can be reduced by attaching balance weights to the crankwebs, and this has the further advantage of relieving the loading on the bearings and on the crankcase. In cases where counterweights are added to all crankwebs the balance weight moment about the centre of the crankshaft should not exceed

$$(W_b \cdot R) = [W + W'(1 + 1/q)] \cdot R, \quad (266)$$

where W_b = weight of balance weight per cylinder assumed concentrated at crankpin radius directly opposite the crankpin.

With balance weights of this magnitude the primary unbalance along the line of stroke is the same as the primary unbalance along a line at right angles to the line of stroke, and the maximum unbalanced primary force and couple for the whole engine become

$$F_p = 0.0000142 \cdot R \cdot N^2 \cdot K_p \cdot W'(1 - 1/q). \quad (267)$$

$$C_p = 0.0000142 \cdot R \cdot N^2 \cdot L \cdot K_p' \cdot W'(1 - 1/q). \quad (268)$$

If the balance weights are made larger than given by Equation (266) there will be overbalance along a line at right angles to the line of stroke.

It should be borne in mind, however, that the addition of balance weights to an oscillating system lowers the natural frequency of torsional vibration, and this might be undesirable if it causes an important critical speed to be brought into the running speed range. Also, the introduction of large additional weight for balancing purposes would not be permissible in aero engines unless offset by gains in other directions, such as, for example, the ability to operate the engine at higher speeds, or to reduce the weight of other parts of the engine. In any given example the size of the balance weights can be minimised by using only two balancing masses, one attached to each of the endmost crankwebs in correct phase relationship to the crankpins.

Secondary forces and couples cannot be balanced by balance weights attached to the crankwebs.

The following points should be kept in mind when comparing the balancing characteristics of engines.

A good criterion of engine balance is to determine the amplitude which the unbalanced force or couple would produce if the engine were free in space, i.e. not restrained by more or less elastic supports.

Let F = maximum amplitude of the unbalanced force, in lbs.,

M = total weight of engine, in lbs.,

$\omega = n \cdot \Omega$, where n is the number of force cycles per revolution of the crankshaft, and Ω is the angular velocity of the crankshaft,

δ = the maximum amplitude of vibration of the engine, assuming that it is free in space.

Then, since force = mass \times acceleration,

$$F = M \cdot \omega^2 \cdot \delta/g, \text{ or } \delta = F \cdot g/(M \cdot \omega^2),$$

where $g = 386 \text{ ins./sec.}^2$.

The corresponding expression for an unbalanced couple of maximum amplitude C is

$$C = \frac{J \cdot \omega^2 \cdot \theta}{J \cdot \omega^2} \text{ or } \theta = \frac{C \cdot g}{J \cdot \omega^2},$$

where J = moment of inertia of engine about an axis through the centre of gravity perpendicular to the plane in which the couple acts, in lbs.-ins.²,

θ = maximum amplitude of angular vibration.

For a primary force $n = 1$, since there is only one force cycle per revolution of the crankshaft.

Hence, $\omega = \Omega$, and $\delta = F \cdot g/(M \cdot \Omega^2)$.

For a secondary force $n = 2$, since there are two force cycles per revolution of the crankshaft.

Hence, $\omega = 2 \cdot \Omega$, and $\delta = F \cdot g/(4 \cdot M \cdot \Omega^2)$.

Thus the amplitude of the vibratory disturbance due to a secondary force or couple is one-quarter that due to a primary force or couple of the same magnitude.

It should also be noted that since the force due to unbalance is itself directly proportional to the square of the speed, the vibration amplitudes calculated by the foregoing method are independent of the r.p.m. of the engine.

This method therefore affords a convenient means for comparing the balancing characteristics of engines without reference to speed.

For example, primary force = $F = W \cdot \Omega^2 \cdot R/g$,

where W = weight of unbalanced parts, assuming them to be concentrated at crank radius R,

then $\delta = W \cdot R/M$.

For a secondary force, $F = W' \cdot \Omega^2 \cdot R / (g \cdot q)$,

where W' = weight of the reciprocating parts,

q = ratio (connecting rod length/crank radius),

then $\delta = W' \cdot R / (4 \cdot q \cdot M)$.

EXAMPLE.—Compare the balance of the following engines:—

(i) A 4-cylinder 4-stroke cycle petrol engine—

Weight of engine,	$M = 300$ lbs.,
Weight of recip. parts,	$W' = 12$ lbs. (4 sets),
Crank radius,	$R = 3$ ins.,
Conn. rod/crank,	$q = 3.5$.

(ii) A medium speed 4-cylinder, 4-stroke cycle oil engine—

Weight of engine,	$M = 40,000$ lbs.,
Weight of recip. parts,	$W' = 1,800$ lbs. (4 sets),
Crank radius,	$R = 8$ ins.,
Conn. rod/crank,	$q = 5$.

In both cases the engines have conventional 4-stroke cycle crankshafts so that secondary forces are completely unbalanced.

Then, for (i) $\delta = 12 \times 3 / (4 \times 3.5 \times 300) = 0.0085$ in.,

for (ii) $\delta = 1800 \times 8 / (4 \times 5 \times 40,000) = 0.018$ in.

Thus the second engine would vibrate through more than twice the amplitude of the first if permitted to move freely in space, and these movements would occur irrespective of the r.p.m. of the engines.

The amplitude of any vibratory disturbance caused by the action of unbalanced forces or couples depends on whether or not their frequency of application is near the natural frequency of any part of the surroundings. The modern tendency is to mount the engine on flexible supports, for example, on steel or rubber springs, which are adjusted so that the lowest frequency of application of any unbalanced force or couple is at least $\sqrt{2}$ times the natural frequency of vibration of the engine on its mounting.

The force transmitted to the surroundings when the engine is mounted on spring supports may be determined as follows:—

Let F_{nc} = the maximum value of the n th order harmonic component of the applied force when the frequency ratio is unity. This will be called the equilibrium force,

F = the transmitted force,

F_n = the maximum value of the n th order harmonic component of the applied force at the operating speed.

Then, since the magnitude of the applied force is directly proportional to the square of the speed,

$$F_{nc} = F_n(N_c/N)^2,$$

where

N_c = the n th order critical speed,

N = the operating speed,

and

$$F = F_{nc} \left\{ \frac{(N/N_c)^2}{1 - (N/N_c)^2} \right\}.$$

The values of the bracketed expression for different frequency ratios are given in Table 52.

F is the force induced in the springs by the applied force when the operating speed is N and the natural frequency of the engine on its spring mountings is N_c . Since the springs are the only connection between the engine and its surroundings the above expression also gives the value of the transmitted force. Damping in the spring mountings is neglected.

It is of interest to calculate the relative values of the transmitted force for primary and secondary applied forces of the same magnitude, assuming that the frequency of application of the primary force is 1.414 times the natural frequency of the engine on its mountings. For this condition, as already explained, there is no dynamical magnification of the primary force when it is transmitted to the surroundings.

Let N = the operating speed, for both primary and secondary forces,

N_c = the critical speed for primary forces = $N/1.414$.

Hence, frequency ratio for primary forces = 1.414, and the corresponding dynamic magnifier from Table 52 is 2, i.e. the transmitted force is twice the primary equilibrium force. Since, however, the ratio of applied force to equilibrium force is also 2 for a frequency ratio of 1.414, it follows that the transmitted force is equal to the applied force, i.e. there is no dynamical magnification.

In the case of the secondary force, since there are two force cycles per revolution of the crankshaft the critical speed is

$$N_e' = N_e/2 = N/2.828.$$

Hence the frequency ratio for secondary forces is 2.828 and the corresponding dynamic magnifier, by interpolation from Table 52, is 1.143. In this case, however, the ratio of applied force to equilibrium force is

$$F_{ne}'/F_n = (N_e'/N)^2 = (1/2.828)^2 = 1/8.$$

Hence the effective value of the dynamic magnifier is (1.143/8) or 0.143, i.e. the magnitude of the transmitted force due to secondary unbalance is one-seventh that due to primary unbalance when the primary frequency ratio is 1.414.

The ratio (secondary transmitted force/primary transmitted force) diminishes as the primary frequency ratio increases and approaches a limit of one-quarter when the frequency ratio becomes very large.

The above calculations can be considerably simplified when the operating speed is constant, by substituting the expression for equilibrium force in the expression for transmitted force. When this is done the value of the transmitted force is

$$F = F_n \left\{ \frac{1}{1 - (N/N_e)^2} \right\}.$$

The values of the bracketed expression for different frequency ratios are given in Table 51.

Thus, for a primary force, when $N_e = N/1.414$, the above expression reduces to $F = F_n$, i.e. the transmitted force is equal to the applied force, as already shown.

For a secondary force applied at the same operating speed,

$N_0 = N/2.828$, and the above expression reduces to $F = F_n/7$. Thus, as before, when the magnitude of an applied secondary force is the same as the magnitude of an applied primary force, the transmitted secondary force is only one-seventh of the transmitted primary force for a primary frequency ratio of 1.414.

Experience with engines mounted on rubber-in-shear has shown the following results:—

Frequency Ratio.	Per Cent. Insulation.	Remarks.
$N/N_0 = 4.0$	93 per cent.	excellent
3.0	88	very good
2.5	81	good
2.0	67	fair
1.5	20	poor
1.4	none	—

The satisfactory operation of high-speed, 4-stroke cycle petrol engines in motor-cars is an illustration of the effectiveness of a low-frequency engine mounting system in preventing the transmission of high-frequency forces. This type of engine has a large unbalanced secondary force, but is mounted on a flexible support.

It should be noted, however, that when the engine is so rigidly attached to its foundation that the natural frequency of the engine on its mounting is greater than the frequency of application of the primary force, the transmitted primary will always be greater than the applied primary, assuming that there is no damping. If there is a secondary force of the same magnitude as the applied primary force, the magnitude of the transmitted secondary may be either greater or smaller than that of the transmitted primary, depending on the particular relationship between the operating speed and the secondary critical speed. If the engine/mount frequency is greater than the frequency of application of the secondary forces both primary and secondary transmitted forces will be dynamically magnified. For this reason the type of crankshaft

used in 4-cylinder motor-car engines, No. 1 in Table 64, is not popular for engines which have more or less rigid foundations, and is generally replaced by a crankshaft with crankpins spaced at equal angles of 90° round the crankpin circle, No. 2 in Table 64, notwithstanding the fact that the firing impulses are then uneven.

It is of interest to compare the relative magnitudes of a force and a couple each having the same frequency of application and each producing the same degree of vibration in the structure. This can be done by equating the work done on the structure by the force and couple respectively.

For a given amplitude of vibration the work done by a force is proportional to the amplitude and is greatest when the force is applied at an anti-node. The work done, and therefore the vibratory disturbance, is theoretically zero when the force is applied at a node. For a couple the work done is a maximum when the couple is applied at a node and is proportional to the slope of the deflection curve at the node. The work done, and therefore the vibratory disturbance, is theoretically zero when the couple is applied at an anti-node.

There is not much error in assuming that the deflection curve is truly sinusoidal, in which case the greatest slope, i.e. the slope at the node, is $2 \cdot \pi \cdot a/L$.

Hence, for equal vibratory effects,

$$C(2 \cdot \pi \cdot a/L) = F \cdot a,$$

$$\text{or} \quad C = \left(\frac{L}{2 \cdot \pi} \right) \cdot F,$$

where C = couple in lbs.-ins.,

F = force in lbs.,

L = wave-length of vibratory motion imparted to structure, in inches,

a = amplitude of vibratory motion imparted to structure, in inches.

In the case of the fundamental mode of vibration of a ship's hull the wave-length of the vibratory motion of the hull is usually greater than the total length of the ship. For example,

in the case of a 400-ft. ship the wave-length for the fundamental mode of hull vibration will be about 5000 ins.

$$\text{Hence,} \quad C = \frac{5000}{6.283} = 800 \text{ . F,}$$

i.e. a very large unbalanced couple would be required to produce the same vibratory disturbance as a small unbalanced force at the same frequency of application.

An engine with an unbalanced force is best placed at a position in the structure which corresponds to a node when the structure vibrates. Thus in the case of ships where the nodes for the fundamental mode of vibration are usually located, about $\frac{1}{4}$ th to $\frac{3}{4}$ rd the length of the vessel from each end, an engine with unbalanced forces would be best placed near the stern of the ship, as in oil tank steamers with machinery aft. In the case of engines with unbalanced couples, on the other hand, the best location for the engine is at an anti-node, i.e. amidships. Hence, if the engines of a ship are placed amidships, unbalanced forces should be small; if placed aft, unbalanced couples should be small. These principles can also be applied to the mounting of an aero engine.

To sum up, therefore, the following points should be kept in mind when comparing engines from the point of view of balance :—

- (a) Provided the minimum r.p.m. for continuous operation is greater than the natural frequency of the engine on its mounting structure the vibratory effects of an unbalanced secondary force or couple will certainly be less than one-quarter the effect produced by an unbalanced primary force or couple of the same magnitude. Thus, in general, secondary unbalance is much less objectionable than primary unbalance.
- (b) A very large unbalanced couple is usually required to produce the same vibratory disturbance as a small unbalanced force of the same frequency. Thus, in general, unbalanced couples are much less objectionable than unbalanced forces.

In other words, an engine with an unbalanced couple is better than an engine with an unbalanced force, even if the magnitude of the unbalanced couple is comparatively large whilst that of the unbalanced force is comparatively small; and an engine with an unbalanced secondary force or couple is better than an engine with an unbalanced primary force or couple of the same respective magnitudes, provided care is taken in the design of the engine mount.

In this connection it is worth noting that the straight-eight, 4-stroke cycle engine of reference 9 in Table 64 has been used in practice without causing any perceptible vibratory disturbances, notwithstanding the comparatively large magnitude of the unbalanced secondary couple.

In all multi-cylinder engines there are unbalanced forces and couples of higher order than the second, but their magnitude is so small and their frequency so high that they do not normally cause any perceptible disturbances.

The following notes should be read in conjunction with Table 64. All the arrangements listed have been used successfully in practice. Throughout this table it is assumed that the cylinder pitches are equal. In some cases an improvement in engine balance can be obtained by having unequal cylinder pitches. Some notes on this subject are given by P. Cormac in an article in *Engineering*, 11th October, 1929, p. 458.

Four-Stroke Cycle, Single-Acting, In-Line Engines.

Four-Cylinder.—No. 1 is used for high- and medium-speed engines where the natural frequency of the engine on its mounting is sufficiently below the frequency of the secondary unbalanced force to avoid perceptible structural vibration from this cause. It is used in all 4-cylinder, 4-stroke cycle motor-car engines. It is unsuitable for main engines on board ship because of starting and reversing difficulties, whilst if it is used for marine auxiliary engines care must be taken to make sure that the secondary unbalanced force will not be transmitted to the hull, because the frequency of this force is too

near the natural frequency of the engine mounting or other parts of the hull structure. The latter remark also applies where the starting and reversing difficulty is overcome by fitting a clutch and reversing gear, or a reversible propeller.

No. 2 is used for direct reversing engines and also where the secondary force of No. 1 is likely to cause perceptible vibratory disturbances. There are many instances in practice where engines built with crank arrangement No. 1 caused such severe vibratory disturbances that secondary balancing equipment or special engine mountings had to be incorporated before the engines could be put into regular service.

No. 3 is of interest because the principal unbalance is a primary couple. It is not used for simple 4-cylinder aggregates because of this comparatively large unbalanced primary couple, but it is used in engine aggregates where the primary forces can be balanced for each crank separately. In such cases the engine as a whole possesses complete primary and secondary balance. For example, in the case of an 8-cylinder, 90° Vee-engine the primary forces due to each pair of pistons operating on each crankpin can be balanced by a rotating balance weight attached to the crankwebs opposite each crankpin.

The principal torsional vibration characteristics of the three arrangements are as follows:—

If the node is remote from the crankshaft, as in the case of the one-node mode of vibration of a marine propeller drive or of any transmission system in which there is great flexibility between the engine and the driven machine, the only totally unbalanced orders are the 2, 4, 6, etc., orders for arrangement No. 1, and the 4, 8, 12, etc., orders for arrangement Nos. 2 and 3. All other harmonic orders are completely balanced for arrangement No. 1, but for arrangement Nos. 2 and 3 all the half orders are more or less unbalanced, the 1.5, 5.5, 9.5, etc., and 2.5, 6.5, 10.5, etc., order vectors being large, and the 0.5, 4.5, 8.5, etc., and 3.5, 7.5, 11.5, etc., order vectors being of medium magnitude.

If the node is situated near the end of the crankshaft, as in the case of the one-node mode of vibration of an engine close-coupled to an electrical generator, the totally unbalanced

orders are the major orders, i.e. orders 2, 4, 6, etc., for No. 1 arrangement; and orders 4, 8, 12, etc., for Nos. 2 and 3 arrangements. In addition, the remaining orders in each case are more or less unbalanced. With arrangement No. 1 the half-order vectors are large and the odd order vectors are small; with arrangement No. 2 the remaining even order vectors and the half-order vectors are large, whilst the odd order vectors are small; with arrangement No. 3 the remaining even order vectors are small and the half-order and odd order vectors are large.

If the node is situated at the centre of the crankshaft, as in the case of the one-node mode of vibration of an engine with the driven unit situated at the centre of the cylinder aggregate; or with two identical driven units, one at each end of the crankshaft; or the two-node mode of vibration of a transmission system, where the driven unit is separated from the engine by a shaft or coupling of great flexibility, and where the flywheel effect is distributed along the engine in the form of crankweb balance weights or else is provided by a single flywheel at the centre of the engine, or by two flywheels, one at each end of the crankshaft, there are no totally unbalanced harmonic orders for arrangement Nos. 1 and 3, whilst orders 2, 6, 10, etc., are totally unbalanced for arrangement No. 2.

In the case of No. 1 arrangement orders 2, 4, 6, etc., and 1, 3, 5 are completely balanced, so that the only orders remaining are the half orders and even these are partially balanced. With arrangement No. 2 orders 4, 8, 12, etc., are totally balanced; the remaining even order and the half-order vectors are large, and the odd order vectors are small. With arrangement No. 3 all even orders are completely balanced, leaving only the odd and half-order vectors partially unbalanced.

It is evident, therefore, that by so arranging the system that the node is brought to the centre of the crankshaft a considerable improvement in the torsional vibration characteristics of the system can be achieved. This improvement is most pronounced for No. 1, where all except the half orders are completely cancelled. In No. 3 all except the half and odd

orders are completely cancelled, whilst in No. 2 only orders 4, 8, 12, etc., are completely cancelled; orders 2, 6, 10, etc., being totally unbalanced.

Five-Cylinder.—No. 4 is the crank arrangement usually adopted for 5-cylinder engines, because it gives the best degree of engine balance. There is only one practical firing order for 4-cycle engines of this type, namely, 1-2-4-5-3, and firing impulses occur at even intervals of 144° throughout the 720° working cycle. As already mentioned there are altogether twelve different methods of arranging the five crankpins round the crank circle, and these have already been given. Many of them are ruled out by considerations other than torsional vibration, but if for some reason or other the torsional vibration characteristics corresponding to the above generally accepted 5-cylinder crank arrangement are unsatisfactory it might be worth while exploring the remaining crank arrangements for a more favourable compromise between the various design considerations.

If the node is remote from the crankshaft the only unbalanced harmonic orders are the 2.5, 5, 7.5, etc., orders, irrespective of the particular firing order employed.

If the node is near the end of the crankshaft minor orders as well as major orders are unbalanced. With crank sequence 1-5-2-3-4 and firing order 1-2-4-5-3 (No. 4 in the table) the 0.5, 3, 5.5, etc., and the 2, 4.5, 7, etc., order vectors are large, and the 1, 3.5, 6, etc., and 1.5, 4, 6.5, etc., order vectors are small. If the crank sequence is altered to 1-2-4-5-3 with firing order 1-4-3-2-5, the 0.5, 3, 5.5, etc., and 2, 4.5, 7, etc., order vectors are small, and the remaining minor order vectors are large. In both cases the 2.5, 5, 7.5, etc., order vectors are completely unbalanced.

With crank sequence 1-2-4-5-3 the primary couple factor becomes $K_p' = 4.98$, and the secondary couple factor becomes $K_s' = 0.45/g$, i.e. the unbalanced primary couple is increased ten times compared with crank sequence 1-5-2-3-4.

With crank sequence 1-5-2-3-4 and firing order 1-2-4-5-3 there are no large vectors in the gaps between consecutive major orders.

If the node is at the centre of the crankshaft there are no totally unbalanced harmonic orders. With firing order 1-2-4-5-3 the vector sums are very nearly zero for orders 1, 3·5, 6, etc., and 1·5, 4, 6·5, etc. With firing order 1-4-3-2-5 the vector sums are very nearly zero for orders 0·5, 3, 5·5, etc., and 2, 4·5, 7, etc. In both cases orders 2·5, 5, and 7·5 are completely balanced. Thus for firing order 1-2-4-5-3 the only unbalanced orders are the 0·5, 3, 5·5, etc., and 2, 4·5, 7, etc., orders, whilst for firing order 1-4-3-2-5 the only unbalanced orders are the 1, 3·5, 6, etc., and 1·5, 4, 6·5, etc., orders.

Six-Cylinder.—No. 5 is the universally accepted crank arrangement for 6-cylinder, in-line, 4-stroke cycle engines, because it provides even firing intervals and complete primary and secondary engine balance.

As already explained there are four different firing orders corresponding to this crank arrangement, which, incidentally, is the only balanced crank arrangement for a 6-cylinder, 4-cycle engine. These four firing orders are as follows :—

1-2-3-6-5-4	(or	1-4-5-6-3-2)
1-2-4-6-5-3	(or	1-3-5-6-4-2)
1-5-3-6-2-4	(or	1-4-2-6-3-5)
1-5-4-6-2-3	(or	1-3-2-6-4-5)

Firing order 1-5-3-6-2-4 is the one usually adopted, especially for petrol engines, where it has the advantage of providing a neat and efficient induction system. Thus when two carburettors are employed this firing order fulfils the conditions that there should be no overlapping of the induction periods of the cylinders drawing from one carburettor, and the induction piping should be as short as possible.

This point is shown in Fig. 91 where the induction manifold for two different firing orders is shown.

This firing order is also popular in engines where there is no induction problem, because it ensures that no two adjacent cylinders fire consecutively.

Where the node is remote from the engine the only unbalanced harmonic orders, irrespective of the firing order, are the 3, 6, 9, etc., orders, and these orders are totally unbalanced.

If the node is situated near the end of the crankshaft,

however, minor orders as well as the 3, 6, 9, etc., major orders are unbalanced.

Alterations of firing order only affect the half-order harmonics, all other harmonics remain unaltered. With firing order 1-5-3-6-2-4 the 1·5, 4·5, 7·5, etc., order vectors are comparatively large, and the other half-order vectors are comparatively small. With firing order 1-2-4-6-5-3 the 1·5, 4·5, 7·5, etc., order vectors are comparatively small, and the other

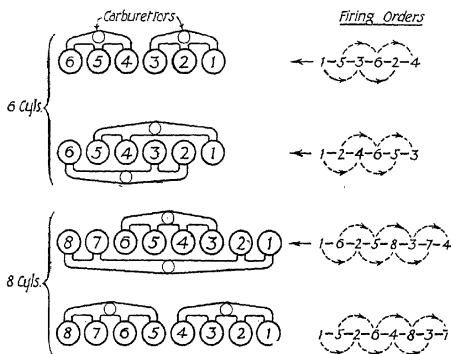


FIG. 91.—Induction manifolds of petrol engines.

half-order vectors are comparatively large. *With this firing order, therefore, there are no large vectors in the gaps between consecutive major orders.*

With firing order 1-5-4-6-2-3 the vector sums for the two groups of half orders have approximately the same magnitude.

The expedient of altering the firing order can therefore be used in cases where unsatisfactory operation is due to the presence of a large half order critical speed in the operating range. For example, if a 4·5 order was found to be trouble-

some with firing order 1-5-3-6-2-4, a cure might be provided by changing to firing order 1-2-4-6-5-3, and so on.

If the node is situated at the centre of the crankshaft the only unbalanced orders are the half orders, all others are completely cancelled. With firing order 1-5-3-6-2-4 the 1·5, 4·5, 7·5, etc., order vectors are large, and the remaining half-order vectors small.

With firing order 1-2-4-6-5-3 the 1·5, 4·5, 7·5, etc., order vectors are small, and the remaining half-order vectors large. With firing order 1-5-4-6-2-3 the vector sums for the two groups of half orders have approximately the same magnitude. The foregoing remarks show that the expedient of bringing the node to the centre of the crankshaft is a very effective means for clearing the speed range of critical zones.

If two cylinders are permitted to fire simultaneously, i.e. firing order (1, 6)-(3, 4)-(2, 5), and the node is at the centre of the crankshaft, there are no unbalanced orders. This arrangement provides three impulses every two revolutions spaced at 240° intervals, so that the torque variation would be similar to that of a 3-cylinder engine.

Seven-Cylinder.—No. 6 is the usually accepted crank sequence and firing order for a 7-cylinder engine, because it provides the best degree of engine balance. There are, however, 360 different 7-cylinder crank arrangements, one alternative being shown at No. 7 in the table.

This second arrangement, No. 7, is interesting because only the secondary couple is unbalanced. Although the magnitude of this couple is about ten times that of the secondary couple of No. 6, the elimination of the primary couple in No. 7 might make this a smoother arrangement, bearing in mind that secondary effects are less important than primary effects from the point of view of structural vibration, provided there is no possibility of resonance between the frequency of this unbalanced couple and the natural frequency of any part of the surrounding structure.

If the node is remote from the crankshaft the only unbalanced harmonic orders are the 3·5, 7, 10·5, etc., orders, irrespective of the particular firing order employed.

If the node is near the end of the crankshaft minor orders as well as major orders are unbalanced. With crank sequence 1-6-3-4-5-2-7 and firing order 1-3-5-7-6-4-2, No. 6 in the table, the 1·5, 5, 8·5, etc., and 2, 5·5, 9, etc., order vectors are very nearly zero; the 0·5, 4, 7·5, etc., and the 3, 6·5, 10, etc., order vectors are large, and the 1, 4·5, 8, etc., and 2·5, 6, 9·5, etc., order vectors are small. *With this crank sequence and firing order, therefore, there are no large vectors in the gaps between consecutive major orders.* If the crank sequence is altered to 1-5-6-2-3-7-4 with firing order 1-6-3-4-5-2-7, the 1, 4·5, 8, etc., and 2·5, 6, 9·5, etc., order vectors are very nearly zero; the 0·5, 4·0, 7·5, etc., and 3, 6·5, 10, etc., order vectors are small, and the 1·5, 5, 8·5, etc., and 2, 5·5, 9, etc., order vectors are large. In both cases the 3·5, 7, 10·5, etc., orders are completely unbalanced. It should also be noted that with crank sequence 1-5-6-2-3-7-4 the primary unbalanced couple factor becomes $K_p = 0.9$, and the secondary unbalanced couple factor becomes $K_s' = 10/q$, i.e. both primary and secondary balance is worse than for arrangement No. 6 in the table.

In arrangement No. 7 in the table the 3·5, 7, 10·5, etc., orders are also completely unbalanced; the 1, 4·5, 8, etc., and 2·5, 6, 9·5, etc., order vectors are small, the 0·5, 4, 7·5, etc., and 3, 6·5, 10, etc., order vectors are of medium magnitude, and the 1·5, 5, 8·5, etc., and 2, 5·5, 9, etc., order vectors are large.

If the node is at the centre of the crankshaft there are no totally unbalanced orders. For crank sequence 1-6-3-4-5-2-7 and firing order 1-3-5-7-6-4-2 the only important unbalanced orders are the 0·5, 4, 7·5, etc., and 3, 6·5, and 10, etc., orders, the vector sums being small or zero for all other orders. For crank sequence 1-5-6-2-3-7-4 and firing order 1-6-3-4-5-2-7 the only important unbalanced orders are the 1·5, 5, 8·5, etc., and 2, 5·5, 9, etc., orders, the vector sums being small or zero for all other orders. For crank sequence 1-6-5-3-2-7-4 and firing order 1-5-2-4-6-3-7 the only important unbalanced orders are the 1·5, 5, 8·5, etc., and 2, 5·5, 9, etc., orders, the vector sums for all other orders being small or zero.

Eight-Cylinder.—There are three balanced crankshaft arrangements for 8-cylinders, in-line, 4-stroke cycle engines,

one of which is No. 8 in the table. This is the arrangement usually adopted in practice, and consists of two 4-cylinder shafts of the type shown at No. 2 in the table, but with the crankpins arranged so that the four pins in one-half of the 8-cylinder shaft are the mirror images of the four pins in the other half. This arrangement therefore provides the good balance of No. 2 arrangement in each half of the crankshaft whereby frame loading is minimised.

There are eight different firing orders corresponding to this crank arrangement, the firing order quoted in the table being one of the orders used in motor-car practice and having the advantage that no two adjacent cylinders fire consecutively.

A list of the eight different orders has already been given as well as a list of the three different balanced crank arrangements.

From the construction of these lists it should not be difficult to write out corresponding lists of firing orders for the other two balanced crankshaft arrangements, if required.

If the node is remote from the crankshaft the only unbalanced harmonic orders are the 4, 8, 12, etc., orders, all others are completely balanced.

If the node is situated near the end of the crankshaft minor as well as major harmonic orders are unbalanced. Like the 6-cylinder balanced crankshaft arrangement alterations of firing order only affect the half-order harmonics, all other orders are unaltered. With firing orders 1-3-2-4-8-6-7-5 and 1-3-2-5-8-6-7-4 the 0.5, 4.5, 8.5, etc., and 3.5, 7.5, 11.5, etc., order vectors are comparatively large, and the remaining half-order vectors are comparatively small.

With firing orders 1-6-2-4-8-3-7-5 and 1-6-2-5-8-3-7-4 the 0.5, 4.5, 8.5, etc., and 3.5, 7.5, 11.5, etc., order vectors are comparatively small, and the remaining half-order vectors are comparatively large.

The vector sums have approximately the same magnitudes for the four groups of half orders in the case of the remaining four firing orders.

If the node is at the centre of the crankshaft the only unbalanced orders are the half orders, all others are completely

cancelled. The relationship between the half-order vectors with different firing orders is the same as already described for the case when the node is situated near the end of the crankshaft.

The expedient of bringing the node to the centre of the crankshaft is therefore a very effective method of clearing the speed range of critical speeds.

The balanced crankshaft arrangement (1, 8)-(2, 7)-(4, 5)-(3, 6) is also used in practice. The eight different firing orders corresponding to this crank arrangement are as follows:—

1-2-4-3-8-7-5-6
 1-2-4-6-8-7-5-3
 1-2-5-3-8-7-4-6
 1-2-5-6-8-7-4-3
 1-7-4-3-8-2-5-6
 1-7-4-6-8-2-5-3
 1-7-5-3-8-2-4-6
 1-7-5-6-8-2-4-3

As before, if the node is near the end of the crankshaft minor as well as major orders are unbalanced. Changes of firing order only affect the magnitudes of the half-order vectors, all others remain unaltered.

Orders 4, 8, 12, etc., are completely unbalanced, as in the case of No. 8 in the table; the 1, 5, 9, etc., and 3, 7, 11, etc., order vectors are small for this arrangement, whilst for No. 8 in the table they are nearly zero; the 2, 6, 10, etc., order vectors are nearly zero for this arrangement, whereas they are small for No. 8 in the table. The magnitudes of the half-order vectors depend on the firing order employed.

With firing orders 1-2-4-6-8-7-5-3 and 1-2-5-6-8-7-4-3 the 0·5, 4·5, 8·5, etc., and 3·5, 7·5, 11·5, etc., order vectors are comparatively large and the remaining half-order vectors are comparatively small. With firing orders 1-7-4-3-8-2-5-6 and 1-7-5-3-8-2-4-6 the 0·5, 4·5, 8·5, etc., and 3·5, 7·5, 11·5, etc., order vectors are comparatively small, and the remaining half-order vectors are comparatively large. The half-order vectors for any given harmonic order have approximately the same magnitudes for the remaining four firing orders.

Firing order 1-2-4-6-8-7-5-3 is of special interest because in

this case there are no large vectors in the gaps between consecutive major orders, a condition which cannot be obtained with crank arrangement No. 8 in the table.

If the node is at the centre of the crankshaft the only unbalanced orders are the half orders, all others are completely cancelled. The relationship between the half-order vectors with different firing orders is the same as already described for the case when the node is near the end of the crankshaft.

A disadvantage of the type of crankshaft just described is that although the engine as a whole possesses complete primary and secondary balance there is a large unbalanced primary couple in each half of the crankshaft which might be a source of vibration, especially if the crankcase is weak. In aero engines this might lead to an increase in weight due to the necessity for additional stiffness in the crankcase.

The crankshaft arrangement shown at No. 9 in the table, although not of the balanced type, has been used in practice for straight-eight engines.

It is composed of two 4-cylinder shafts of the type shown at No. 1 in the table, placed end to end. With this arrangement there is a comparatively large unbalanced secondary couple, in fact this secondary couple is the largest of any listed in the table. In spite of this, however, engines of this type have been successfully applied in practice without causing any noticeable structural vibration. A great deal depends, however, on the particular application and especially on whether there is likely to be resonance between the frequency of the couple and the natural frequency of any part of the surrounding structure.

A more serious disadvantage of No. 9 arrangement is the large centrifugal loading on the crankshaft journals between Nos. 2 and 3 and Nos. 6 and 7 cylinders. Each of these journals has to carry the combined centrifugal load of two cylinders. In arrangement No. 8 the only journal carrying the combined centrifugal loading of two cylinders is the journal between Nos. 4 and 5 cylinders, i.e. the journal at the centre of the engine, where it is possible to provide increased length if required.

Like No. 8 changes of firing order only affect the half-order harmonics, but unlike No. 8 the 2, 6, 10, etc., orders are completely unbalanced when the node is situated at the centre of the crankshaft, and for this condition the only completely balanced orders are the 4, 8, 12, etc., orders.

In general, therefore, No. 8 crank arrangement is much better than No. 9. The chief virtue of No. 9 is ease of manufacture, since the whole shaft can be forged as a flat forging and then be given only one twist to form the crankshaft.

Nine-Cylinder.—No. 10 is the usually accepted crank sequence and firing order for a 9-cylinder engine, because it provides the best degree of engine balance. There are, however, altogether 20,160 different arrangements, and one alternative which has very good balancing characteristics is shown at No. 11 in the table. There is plenty of scope for exploring 9-cylinder arrangements in cases where the standard crank sequence does not appear to be the best solution. No. 10 arrangement in the table is, however, very good from torsional vibration as well as the engine balance viewpoints. The only important harmonic orders are the 4·5, 9, 13·5, etc., orders, and even these are eliminated when the node is moved to the centre of the crankshaft. *Moreover, with this crank sequence there are no large vectors in the gaps between consecutive major criticals.*

Ten-Cylinder.—There are twelve balanced crankshaft arrangements and sixteen different firing orders corresponding to each arrangement.

The arrangement shown at No. 12 in the table is generally accepted and consists of two sets of five cranks of the type shown at No. 4 in the table, arranged in mirror formation. In this way the balance of each half of the crankshaft is as good as for the 5-crank arrangement shown at No. 4, whilst the engine as a whole has no primary or secondary unbalance.

The sixteen different firing orders, corresponding to the crank arrangement shown at No. 12 in the table, are

1-5-2-3-4-10-6-9-8-7
 1-5-2-3-7-10-6-9-8-4
 1-5-2-8-4-10-6-9-3-7
 1-5-2-8-7-10-6-9-3-4
 1-5-9-3-4-10-6-2-8-7
 1-5-9-3-7-10-6-2-8-4
 1-5-9-8-4-10-6-2-3-7
 1-5-9-8-7-10-6-2-3-4
 1-6-2-3-4-10-5-9-8-7
 1-6-2-3-7-10-5-9-8-4
 1-6-2-8-4-10-5-9-3-7
 1-6-2-8-7-10-5-9-3-4
 1-6-9-3-4-10-5-2-8-7
 1-6-9-3-7-10-5-2-8-4
 1-6-9-8-4-10-5-2-3-7
 1-6-9-8-7-10-5-2-3-4

If the node is remote from the crankshaft the only unbalanced orders are the 5, 10, 15, etc., orders, all others are completely balanced.

If the node is situated near the end of the crankshaft minor as well as major orders are unbalanced. Like a 6- and 8-cylinder balanced crankshaft arrangement alterations of firing order only affect the half-order harmonics, all other orders are unaltered.

With firing order 1-6-2-8-4-10-5-9-3-7 the only important unbalanced orders are the 5, 10, 15, etc., major orders, and the 2.5, 7.5, 12.5, etc., minor orders, all others are small. If the firing order is altered to 1-6-9-3-4-10-5-2-8-7 the important unbalanced orders are the 5, 10, 15, etc., major orders and the 1.5, 6.5, 11.5, etc., and 3.5, 8.5, 13.5, etc., minor orders, all others are small. With this alternative firing order the 2.5, etc., orders are made small at the expense of bringing the 1.5, etc., and 3.5, etc., orders into prominence.

A further improvement in the disposition of the critical speeds can be obtained by adopting a different crankshaft arrangement, viz. (1, 10)-(3, 8)-(5, 6)-(7, 4)-(9, 2) and a firing order 1-3-5-7-9-10-8-6-4-2. With this crank arrangement and firing order the only important harmonic orders are the 5, 10, 15, etc., major orders, and the 0.5, 5.5, 10.5, etc., and 4.5, 9.5, 14.5, etc., minor orders, all other orders are small. *In this case there are no large vectors in the gaps between consecutive major orders.*

This improvement, however, is obtained at the expense of a much increased unbalanced primary couple in each half of the crankshaft. The engine, as a whole, has, of course, collective primary and secondary balance, but the presence of a large unbalanced primary couple in each half of the crankshaft might cause trouble, due to frame deflection, unless balance weights are attached to the crankwebs for the purpose of minimising this unbalance, or unless a suitably stiffened crankcase is employed. In either case the additional weight would be a disadvantage in aero-engine practice.

If the node is at the centre of the crankshaft, the only unbalanced harmonic orders are the half orders, all others are zero. In No. 12 arrangement in the table with firing order 1-6-2-8-4-10-5-9-3-7 the 2·5, 7·5, 12·5, etc., orders are totally unbalanced, but for the other arrangements these orders are partially balanced. As a general rule the half-order vectors are small, and their magnitudes can be changed if desired by alterations of firing order.

If two cylinders are permitted to fire simultaneously, i.e. firing order (1, 10)-(2, 9)-(4, 7)-(5, 6)-(3, 8) in the case of No. 12 in the table, and the node is at the centre of the crankshaft, there are no unbalanced harmonic orders. This arrangement provides five impulses every two revolutions, evenly spaced at 144° intervals, so that the torque variation is similar to that of a 5-cylinder engine. With simultaneous firing therefore the engine should be free for all practical purposes from torsional vibrational disturbances for that mode of vibration corresponding to a node at the centre of the crankshaft. If other important modes of vibration exist, these must, of course, be investigated separately.

Twelve-Cylinder.—There are sixty balanced crankshaft arrangements of the type shown at No. 13 in the table, and there are thirty-two different firing orders corresponding to each crankshaft arrangement.

If the node is remote from the crankshaft the only unbalanced harmonic orders are the 6, 12, 18, etc., major orders, and these are totally unbalanced.

If the node is near the end of the crankshaft the major

orders, i.e. orders 6, 12, 18, etc., are completely unbalanced, and the only important minor orders are the half orders, all others are small. Like the 6-, 8-, and 10-cylinder balanced crankshaft arrangements changes of firing order only affect the half-order components, which implies that the relative magnitudes of the half-order vectors can be altered by changes of firing order.

If the node is at the centre of the crankshaft the only unbalanced harmonic orders are the half orders, all others are completely balanced, irrespective of firing order. Changes of firing order will alter the relative magnitudes of the half-order vectors.

In the arrangement shown at No. 14 in the table two cylinders fire simultaneously, as indicated by the half-order phase diagram. The crankshaft consists of two 6-cylinder balanced crankshafts, similar to No. 6 in the table but placed end to end, so that one is the mirror image of the other. The engine therefore possesses complete primary and secondary balance.

Firing impulses occur at equal intervals of 120° .

If the node is remote from the crankshaft the only unbalanced harmonic orders are the major orders, viz. the 3, 6, 9, etc., orders, and these orders are totally unbalanced. If the node is near the end of the crankshaft the major orders are again totally unbalanced, and in addition the half-order vectors may be of appreciable magnitude. The relative magnitudes of the half orders can be altered by changing the firing order, but such changes do not affect the remaining orders.

If the node is at the centre of the crankshaft there are no unbalanced harmonic orders. This is because cylinders which are symmetrically disposed relative to the centre of the crankshaft fire simultaneously, so that the vibratory energy imparted by a cylinder on one side of the centre of the crankshaft is neutralised by the vibratory energy imparted by the symmetrically disposed cylinder on the other side of the crankshaft centre.

There is no special advantage in this simultaneous firing arrangement when the node is not situated at the centre of the

crankshaft, but in cases where the node can be brought to this position simultaneous firing is a means of bringing about complete cancellation of all the harmonic orders.

Complete cancellation of all the harmonic orders can also be obtained with the 6-cylinder arrangement No. 5; the 8-cylinder arrangement No. 8; the 10-cylinder arrangement No. 12; and the 12-cylinder arrangement No. 13, by arranging the system so that the node occurs at the centre of the crankshaft and by firing symmetrically disposed cylinders simultaneously.

The advantage of the 12-cylinder arrangement, shown at No. 14 in the table, is that the firing intervals in each half of the crankshaft are even. The firing order in each half of the crankshaft should be chosen so that a satisfactory disposition of critical speeds is obtained for each half, considered as a separate unit.

Two-Stroke Cycle, Single-Acting, In-Line Engines.—

The task of investigating the torsional vibration characteristics of 2-stroke cycle engines is somewhat easier than in the case of the 4-stroke cycle type because 2-stroke engines have no half-order components, and, moreover, the firing order is the same as the crank sequence. The following notes should be read in conjunction with Table 64.

Four-Cylinder.—No. 15 is the crankshaft arrangement usually employed for 2-cycle engines because it gives the best degree of engine balance of any 4-crank arrangement.

No. 16 is interesting because with this arrangement secondary couples are balanced. The primary couple, however, is more than twice as great as in No. 15, and for this reason No. 16 is usually only found in engine aggregates where the primary forces are balanced for each line of parts separately, or alternatively, where special arrangements are made to eliminate the primary couple, for example, by using bob-weights or pairs of oppositely rotating primary balancing masses.

No. 16 is suitable for 4-cylinder opposed-piston engines, for example, because the primary forces can be balanced for each cylinder separately by adjusting the strokes of the two

pistons in inverse proportion to the reciprocating weights of the two sets of running gear. When this is done the engine is in complete primary and secondary balance.

The principal torsional vibration characteristics of the two arrangements are as follows:—

If the node is remote from the crankshaft the only unbalanced harmonic orders are the 4, 8, 12, etc., orders, all others are completely balanced.

If the node is near the end of the crankshaft orders 4, 8, 12, etc., are totally unbalanced in both cases, and the minor orders are also unbalanced. With firing order 1-3-2-4 the odd minor order vectors are small and the even ones are large.

With firing order 1-3-4-2, i.e. No. 16, the odd minor order vectors are large and the even ones small. *In this case there are no large vectors in the gaps between consecutive major criticals.*

If the node is at the centre of the crankshaft, the major orders, i.e. orders 4, 8, 12, etc., are completely balanced in both cases. With firing order 1-3-2-4 the even minors are completely unbalanced, but the odd minor order vectors are small. With firing order 1-3-4-2 the even minor order vectors are completely balanced, but the odd minor order vectors are large.

Firing order 1-3-4-2 with the crankshaft node at the centre of the crankshaft is used for large opposed-piston marine oil engines and by this means a speed range free from major criticals is obtained. The remaining odd order minors are suppressed by means of a detuning flywheel, to be described later.

Five-Cylinder.—No. 17 is the arrangement usually adopted in practice and this is the same crank sequence as for 4-stroke cycle engines. The firing order, however, differs from that for 4-stroke engines because in this case it must be the same as the crank sequence, viz. 1-5-2-3-4.

There are altogether twelve different crank arrangements, and these have already been listed, but, as previously explained, No. 17 in the table gives the best degree of engine balance.

If the node is remote from the crankshaft the major orders, i.e. orders 5, 10, 15, etc., are the only unbalanced harmonics.

If the node is near the end of the crankshaft minor as well

as major orders are unbalanced. With firing order 1-5-2-3-4 the 1, 6, 11, etc., and 4, 9, 14, etc., order vectors are small, and the remaining minor order vectors are large.

If the node is at the centre of the crankshaft the 5, 10, 15, etc., orders are completely balanced, and the 1, 6, 11, etc., and 4, 9, 14, etc., order vectors are small. There are no totally unbalanced orders.

An alternative arrangement not shown in the table is crank sequence and firing order 1-2-4-5-3. With this sequence the primary couple factor is increased to $K_p' = 4.98$, whilst the secondary couple factor is reduced to $K_s' = 0.45/q$. This large reduction of secondary couple makes this alternative arrangement very attractive in engines where primary forces are balanced for each cylinder separately. For this reason and also because the torsional vibration characteristics are favourable it is used in marine practice for large opposed piston oil engines, a type in which it is easy to provide primary balance for each cylinder separately.

If the node is remote from the crankshaft the only unbalanced harmonics with firing order 1-2-4-5-3 are the 5, 10, 15, etc., orders, and these are totally unbalanced.

If the node is near the end of the crankshaft the 5, 10, 15, etc., orders are still totally unbalanced, and in addition the 1, 6, 11, etc., and 4, 9, 14, etc., order vectors are large, but the remaining vectors are small.

If the node is at the centre of the crankshaft the 5, 10, 15, etc., orders are completely balanced, and the above relationship exists between the remaining vectors. In the large opposed-piston marine oil engines mentioned above the crankshaft node is located at the centre of the crankshaft, a tuning flywheel being attached to the free end of the shaft for this purpose. By this means a speed range free from major criticals has been achieved. *With this sequence there are no large vectors in the gaps between consecutive major criticals.*

In the case of solid forged shafts for small high- and medium-speed engines the two shaft arrangements just described would be forged as flat forgings with crankpins Nos. 1, 3, and 5 in line and crankpins Nos. 2 and 4 also in line but at 180° to the

first three. The correct spacing of the pins would then be obtained by twisting the journal sections through angles of 36° and 108° , i.e. two journals twisted through 36° and the other two through 108° . A crankshaft having the crank sequence and firing order 1-3-5-2-4 would be less severely strained in manufacture because each journal would only require twisting through 36° to form the complete shaft from a flat forging of the shape just described.

With crank sequence 1-3-5-2-4, however, the primary couple factor is $K_p' = 2.62$, and the secondary couple factor is $K_s' = 4.25/g$, i.e. the primary couple is more than five times that for No. 17 in the table.

If the node is remote from the crankshaft the only unbalanced harmonic orders with firing order 1-3-5-2-4 are the 5, 10, 15, etc., orders.

If the node is at the end of the crankshaft the 5, 10, 15, etc., orders are totally unbalanced, and all the remaining orders are of appreciable magnitude. If the node is near the centre of the crankshaft orders 5, 10, 15, etc., are completely balanced, but all the remaining order vectors are of appreciable magnitude. It would appear therefore that firing order 1-3-5-2-4 is inferior for both balancing and torsional vibration to No. 17 in the table, but this depends to some extent on the position occupied by the critical speeds in relation to the speed range of the engine.

Six-Cylinder.—No. 18 is the crank arrangement usually employed in practice because it gives the best degree of engine balance, the only important unbalance being a small secondary couple.

There are altogether sixty different 6-cylinder crank sequences and firing orders, and for all of these if the node is remote from the crankshaft the only unbalanced harmonic orders are the 6, 12, 18, etc., orders.

With firing order 1-5-3-4-2-6, i.e. No. 18 in the table, if the node is near the end of the crankshaft, orders 6, 12, 18, etc., are totally unbalanced; the 3, 9, 15, etc., order vectors are large, the remaining odd order vectors are small, and the remaining even order vectors are of medium magnitude.

If the node is at the centre of the crankshaft orders 3, 9, 15, etc., are totally unbalanced; orders 6, 12, 18, etc., are completely balanced, the remaining odd order vectors are small, and the remaining even order vectors are large.

No. 19 is sometimes favoured in practice because the crankthrows are arranged in pairs at 180° , whereas in No. 18 the crankthrows are arranged in two sets of three at 120° .

No. 19 also possesses complete primary balance, but the secondary couple is twice as large as in No. 18.

If the node is near the end of the crankshaft with firing order 1-4-5-2-3-6, i.e. No. 19, orders 6, 12, 18, etc., are completely unbalanced; the remaining even order vectors are large, and all odd order vectors are small.

If the node is at the centre of the crankshaft, there are no totally unbalanced orders; orders 6, 12, 18, etc., are completely balanced; the 3, 9, 15, etc., vectors are of medium magnitude, the remaining odd order vectors are small, and the remaining even order vectors are large.

The interest of No. 20 lies in the fact that secondary couples are balanced. There is, however, an unbalanced primary couple which renders this crank arrangement undesirable except in cases where the primary forces can be balanced for each crankthrow separately. For example, it is suitable for 6-cylinder opposed-piston engines, where the primary forces can be balanced by making the strokes of the pistons inversely proportional to the respective reciprocating weights.

It is also suitable for a 12-cylinder, 2-stroke cycle 90° Vee-engine where the primary force, due to the reciprocating parts of each pair of pistons acting on a common crankpin, can be balanced by counterweights attached to the crankwebs opposite the crankpin.

If the node is near the end of the crankshaft, orders 6, 12, 18, etc., are totally unbalanced; the 3, 9, 15, etc., order vectors are large, the remaining odd order vectors are of medium magnitude, and the remaining even order vectors are small.

If the node is at the centre of the crankshaft, orders 3, 9, 15, etc., are totally unbalanced; the remaining odd order vectors

are of appreciable magnitude, but all even orders are totally balanced.

Crank sequence and firing order 1-3-5-6-4-2, not shown in the table, is interesting because there are no large vectors in the gaps between consecutive major orders when the node is near the end of the crankshaft. If the node is at the centre of the crankshaft the only unbalanced orders are the odd orders, and these are small. The engine possesses complete secondary balance, but the primary unbalanced couple factor is $K_p' = 7.2$, so that this crank arrangement is unsuitable for high-speed engines unless of a type with primary forces balanced for each line of parts separately, such as opposed-piston engines with unequal strokes, or 12-cylinder 90° Vee-engines.

A 6-cylinder, 2-stroke cycle engine can also be made from the 4-stroke cycle balanced crankshaft arrangement shown at No. 5 in the table. When this is done two cylinders must fire simultaneously, i.e. the firing order for the arrangement shown at No. 5 in the table would be (1, 6)-(2, 5)-(3, 4).

There is no advantage in doing this if the node is near the end of the crankshaft, but if the node is at the centre of the crankshaft complete cancellation of all harmonics is obtained. This is because cylinders which are disposed symmetrically on either side of the node fire simultaneously, so that the vibrational energy imparted by a cylinder on one side of the crankshaft centre is neutralised by the vibrational energy imparted by the symmetrically disposed cylinder on the other side of the crankshaft centre.

By this means an engine aggregate is obtained which is for all practical purposes free from torsional vibration due to cylinder impulses and is also in complete primary and secondary balance.

It must be borne in mind, however, that this is only true for the mode of vibration which corresponds to a node at the centre of the crankshaft. If other modes exist these must, of course, be investigated.

Seven-Cylinder.—No. 21 is the arrangement usually adopted in practice for both 4-stroke cycle and 2-stroke cycle engines, since it gives the best degree of engine balance. There

are altogether 360 different crank arrangements for a 7-cylinder engine, and in each case the only unbalanced harmonic orders, when the node is remote from the crankshaft, are the 7, 14, 21, etc., orders, which are totally unbalanced.

If the node is near the end of the crankshaft, with crank sequence and firing order 1-6-3-4-5-2-7, No. 21 in the table, the 7, 14, 21, etc., orders are totally unbalanced; the 4, 11, 18, etc., vectors are large, and the remaining vectors are small.

If the node is at the centre of the crankshaft, the 7, 14, 21, etc., orders are completely balanced, and the above relationship exists between the remaining vectors.

No. 22 in the table is interesting because only the secondary couple is unbalanced, which might provide a smoother engine aggregate in certain cases, as already mentioned.

If the node is near the end of the crankshaft the 7, 14, 21, etc., orders are totally unbalanced; the 2, 9, 16, etc., and 5, 12, 19, etc., vectors are large, and the remaining vectors are small.

If the node is at the centre of the crankshaft the 7, 14, 21, etc., vectors are completely balanced and the above relationship exists between the remaining vectors.

Crank sequence 1-2-4-6-7-5-3, not shown in the table, is interesting because there are no large vectors in the gaps between consecutive major criticals.

If the node is near the end of the crankshaft the 7, 14, 21, etc., orders are totally unbalanced, the 1, 8, 15, etc., and 6, 13, 20, etc., order vectors are large, and the remaining vectors are small.

If the node is at the centre of the crankshaft the 7, 14, 21, etc., orders are completely balanced, and the above relationship exists between the remaining vectors.

With this crank sequence the secondary couple factor is only $K_s' = 0.25/g$, but the primary couple factor is $K_p' = 9.8$. Due to the large primary couple this crank arrangement would require large crankweb counterweights, especially in the case of high-speed engines. It is therefore not a desirable arrangement for aero engines where weight must be minimised.

Eight-Cylinder.—The arrangements shown at 23, 24 and 25 in the table have all been used in practice. The first arrangement has the smallest unbalanced primary couple, but there is also an unbalanced secondary couple.

The other two arrangements have larger primary couples, but the secondary couples are balanced. There are altogether 2520 different 8-cylinder crank arrangements, and in all cases when the node is remote from the crankshaft the only unbalanced harmonic orders are the 8, 16, 24, etc., orders.

With arrangement 23 in the table, if the node is near the end of the crankshaft, the 8, 16, 24, etc., orders are completely unbalanced; the 3, 11, 19, etc., 5, 13, 21, etc., and 4, 12, 20, etc., order vectors are large, and the remaining vectors are small. If the node is at the centre of the crankshaft the 8, 16, 24, etc., orders are completely balanced, and the foregoing relationship exists between the remaining vectors.

With the arrangement shown at 24 in the table, if the node is near the end of the crankshaft the 8, 16, 24, etc., vectors are completely unbalanced; the 4, 12, 20, etc., vectors are large, and the remaining vectors are small or moderate.

If the node is at the centre of the crankshaft the 8, 16, 24, etc., orders are completely balanced; the 4, 12, 20, etc., vectors are completely unbalanced, and the remaining vectors are small or moderate.

With the arrangement shown at 25 in the table, if the node is near the end of the crankshaft the 8, 16, 24, etc., vectors are completely unbalanced; the 3, 11, 19, etc., and 5, 13, 21, etc., vectors are large, and the remaining vectors are small or moderate. If the node is at the centre of the crankshaft the 8, 16, 24, etc., orders are completely balanced, and the above relationship exists between the remaining vectors.

Crank sequence and firing order 1-2-4-6-8-7-5-3 is of interest because there are no large vectors in the gaps between consecutive major orders. This arrangement is not shown in the table. If the node is near the end of the crankshaft the 8, 16, 24, etc., orders are completely unbalanced; the 1, 9, 17, etc., and 7, 15, 23, etc., order vectors are large, and the remaining vectors are small.

If the node is at the centre of the crankshaft the only unbalanced orders are the odd orders, and of these the 1, 9, 17, etc., and 7, 15, 23, etc., order vectors are large, and the remainder are small.

There is no unbalanced secondary couple with this crank sequence, but the unbalanced primary couple factor is $K_p' = 12.9$. This large unbalanced primary couple is a disadvantage, especially in high-speed engines.

An 8-cylinder, 2-stroke cycle engine can also be made from any of the 4-stroke cycle engine balanced crankshaft arrangements, for example, No. 8 in the table. When this is done two cylinders must fire simultaneously. Thus, if the arrangement shown at No. 8 in the table is adopted the firing order for the 2-stroke cycle engine would be (1, 8)-(3, 6)-(2, 7)-(4, 5).

There is no advantage in doing this, however, if the node is near the end of the crankshaft, because although the engine possesses complete primary and secondary balance, the crankshaft must be stronger to withstand the double impulses and there are only four main torque impulses per revolution instead of eight.

If, however, the node is at the centre of the crankshaft, there are no unbalanced harmonic orders, because cylinders which are disposed symmetrically on either side of the node fire simultaneously, so that the vibrational energy imparted by a cylinder on one side of the centre of the crankshaft is neutralised by the vibrational energy imparted by the symmetrically disposed cylinder on the other side of the centre of the crankshaft. This arrangement therefore provides an engine which is for all practical purposes free from torsional vibration due to cylinder impulses and is also in complete primary and secondary balance.

It must, of course, be borne in mind that this is only true for the mode of vibration which corresponds to a node at the centre of the crankshaft. If other modes of vibration exist, these must be investigated separately.

Nine-Cylinder.—Nos. 26 and 27 are the arrangements usually adopted in practice because they provide the best degree of engine balance.

There are altogether 20,160 different crank arrangements, and in all cases, if the node is remote from the crankshaft, the only unbalanced harmonic orders are the 9, 18, 27, etc., orders.

If the node is near the end of the crankshaft the 9, 18, 27, etc., orders are completely unbalanced, and all other orders are partially unbalanced. The relative magnitudes of the various orders can easily be determined by drawing the phase diagrams and evaluating the various vector summations.

If the node is at the centre of the crankshaft orders 9, 18, and 27 are completely balanced, leaving only the remaining orders partially unbalanced.

Crank sequence and firing order 1-2-4-6-8-9-7-5-3, not shown in the table, is of interest because there are no large vectors in the gaps between consecutive major orders.

With this crank sequence the secondary couple factor is $K_s' = 0.19/q$, and the primary couple factor is $K_p' = 16.2$. The large primary couple renders this crank arrangement undesirable.

Ten-Cylinder.—There are altogether 181,440 different 10-cylinder, 2-stroke crank arrangements, and in all cases the only unbalanced orders are the 10, 20, 30, etc., when the node is remote from the crankshaft.

The arrangement shown at No. 28 in the table is one which provides complete primary balance of the engine and leaves a comparatively small secondary couple unbalanced.

If the node is near the end of the crankshaft the 10, 20, 30, etc., orders are completely unbalanced, and in addition the remaining orders are partially unbalanced.

If the node is at the centre of the crankshaft the 10, 20, 30, etc., orders are completely balanced, but the 5, 15, 25, etc., orders are completely unbalanced. The remaining orders are partially unbalanced.

Crank sequence No. 28 gives large vector summations for the 5, 15, 25, etc., orders when the node is near the end or at the centre of the crankshaft. These can be considerably reduced by adopting crank sequence 1-7-8-3-4-10-5-2-9-6, not shown in the table, but at the expense of introducing an unbalanced primary couple. The primary couple factor is

$K_p' \approx 2.06$, and there is also an unbalanced secondary couple having a factor $K_s' = 0.73/q$.

A 10-cylinder, 2-stroke engine can also be made from any of the 10-cylinder 4-stroke cycle balanced crankshaft arrangements, for example No. 12, in the table. When this is done two cylinders must fire simultaneously, the firing order for a 2-stroke cycle engine with No. 12 crank arrangement being (1, 10)-(5, 6)-(2, 9)-(3, 8)-(4, 7).

There is no advantage in doing this if the node is near the end of the crankshaft, but if the node is at the centre of the shaft complete cancellation of all harmonic orders is obtained, as already explained.

Thus an engine is provided which is free for all practical purposes from torsional vibration disturbances due to engine impulses, and which, moreover, is in complete primary and secondary balance. It must be borne in mind, of course, that this is true only for the mode of vibration corresponding to a node at the centre of the crankshaft. If other important modes exist these must be investigated separately.

Two-Stroke Cycle, Double-Acting, In-Line Engines.—

When investigating the torsional vibration characteristics of double-acting engines it is convenient to combine the tangential effort diagrams for the upper and lower sides of the piston before making an harmonic analysis.

The harmonic analysis of this combined tangential effort diagram then gives the values of the sine and cosine components for one cylinder and these, in turn, can be combined with any important inertia or other corrections to obtain the resultant harmonic components for one cylinder. In other words, once the harmonic components are determined for the combined effect of the upper and lower sides of the piston of a double-acting engine, these can be employed in all subsequent calculations exactly as though the engine was of the single-acting type.

If the tangential effort diagrams for both sides of the piston of a double-acting engine were identical, the instantaneous tangential effort for each cylinder would be the sum of two identical expressions differing in phase by 180° . The odd

harmonics would therefore cancel, leaving only the even orders to be considered. In practice, however, the two expressions are not identical, due to the influence of the connecting and piston rods and the different combustion characteristics between the upper and lower sides of the piston. The odd harmonics cannot therefore be neglected in practice, although they are of much smaller magnitude than the adjacent even order harmonics (see Table 60).

Four-Cylinder.—The crank arrangements used for single-acting, 2-stroke cycle engines can also be used for double-acting engines of this type. No. 15 in the table is the arrangement usually employed, because it provides the best degree of engine balance. It should be noted that with any of the 2-stroke cycle, single-acting crankshaft arrangements shown in the table the top side of one piston of a double-acting engine fires simultaneously with the bottom side of another piston. Thus, with crankshaft arrangement No. 15, the firing order is (1T, 2B)–(3T, 4B)–(2T, 1B)–(4T, 3B), i.e. there are four impulses per revolution at equal intervals of 90° the same as for a single-acting engine.

The relative magnitudes of the vector sums for the different harmonic orders are determined in the same way as for single-acting engines, so that the remarks already made in connection with 4-cylinder, 2-stroke cycle, single-acting engines also apply here. It should be borne in mind, however, that the odd order harmonic components are relatively smaller than the adjacent even order harmonic components in the case of double-acting engines. This implies that odd order critical speeds are in general less objectionable than the even order criticals.

Thus with crank arrangement No. 16, if the node is situated at the centre of the crankshaft, the only unbalanced harmonic orders are the odd orders, and since the magnitudes of the odd order harmonic components for a double-acting engine are smaller than for a single-acting engine the torsional vibration characteristics of the double-acting type should be more favourable from this point of view. Unfortunately a disadvantage of crank arrangement No. 16 is the somewhat large

unbalanced primary couple, which could be reduced considerably by employing crankweb balance weights, and could be eliminated if reciprocating bob-weights were also employed. It should be borne in mind, however, that the addition of balance weights to the oscillating system lowers the natural frequency of torsional vibration, and this might be undesirable if it causes an important critical speed to be brought into the running speed range. The size of the balance weights can be minimised by using only two balancing masses attached to the endmost crankwebs in correct phase relationship with the crankpins.

No. 29 is a crank arrangement which avoids simultaneous firing of the top side of one piston with the bottom side of another. With this arrangement there are eight impulses per revolution evenly spaced at 45° intervals.

If the node is remote from the crankshaft the only totally unbalanced harmonics are the 8, 16, 24, etc., orders. All the remaining even order vectors are completely cancelled, and the odd order vectors are partially cancelled.

Since the odd order harmonic components are comparatively small the problem of dealing with the odd order criticals should not, in general, be serious.

If the node is near the end of the crankshaft, the 8, 16, 24, etc., orders are completely unbalanced, and the remaining even orders and the odd orders are usually small.

If the node is at the centre of the crankshaft there are no completely unbalanced orders; the 4, 12, 20, etc., orders and the 8, 16, 24, etc., orders are completely balanced, leaving only the remaining even orders and the odd orders as possible sources of torsional vibration.

A disadvantage of this crank arrangement is the presence of a somewhat large primary force and primary couple, but these can be considerably reduced by employing balance weights if this can be done without lowering the natural frequency of the system to an undesirable extent.

No. 30 in the table is another crank arrangement which provides eight firing impulses evenly spaced at 45° intervals. The torsional vibration characteristics of an engine with this

crank sequence are somewhat similar to those of an engine with No. 29 crank arrangement. The principal difference between the two arrangements is that with No. 30 the only completely balanced orders when the node is at the centre of the crankshaft are the 8, 16, 24, etc., orders. In this respect, therefore, No. 30 is inferior to No. 29. No. 30 is superior to No. 29, however, from the point of view of engine balance, because with No. 30 the unbalanced primary couple is considerably smaller, and the unbalanced secondary couple is also somewhat smaller.

An advantage of both No. 29 and No. 30 is that the 4th order torque reaction force and couple on the engine frame is completely balanced, whereas with any of the 2-stroke cycle, single-acting engine crankshaft arrangements, e.g. Nos. 15 and 16 in the table, the 4th order torque reaction force on the frame is completely unbalanced. This is important in relation to engine frame vibration.

Five-Cylinder.—Any of the 5-cylinder crank arrangements employed for single-acting engines can also be used for the double-acting type. No. 31 in the table shows the arrangement usually employed, because it provides the best degree of engine balance. The use of an odd number of cylinders for double-acting engines automatically avoids simultaneous firing of the top side of one piston with the bottom side of another piston. Thus in a 5-cylinder, double-acting engine there are ten firing impulses per revolution evenly spaced at 36° intervals.

As already explained, since the harmonic components are the resultant values for the combined effect of the top and bottom sides of each piston, the vector summations are carried out in precisely the same way as for a single-acting engine.

The remarks already made in connection with 5-cylinder, 2-stroke cycle, single-acting engines are therefore applicable to double-acting engines having the same crankshaft arrangements, bearing in mind, however, that the odd order harmonic components of the double-acting engine combined tangential effort diagram are relatively small.

Six-Cylinder.—Any of the crank arrangements normally employed for single-acting, 6-cylinder, 2-stroke cycle engines can also be used for the double-acting type. No. 18 in the

table is the crank arrangement usually employed because it provides the best degree of engine balance. With this arrangement the top side of one piston fires simultaneously with the bottom side of another piston, so that there are six impulses per revolution at even intervals of 60° . The double-acting engine firing order with this crank arrangement is (1T, 4B)-(5T, 2B)-(3T, 6B)-(4T, 1B)-(2T, 5B)-(6T, 3B).

The remarks already made in connection with 2-stroke cycle, single-acting engines also apply to double-acting engines using the same crankshaft arrangements, bearing in mind, however, that the odd order harmonic components are relatively small.

No. 32 in the table is a 6-cylinder crank arrangement with complete primary and secondary force and couple balance. This arrangement is the same as the 4-stroke cycle engine crank arrangement No. 5. In this case simultaneous firing of the top sides of two pistons occurs alternately with simultaneous firing of the bottom sides of two other pistons, so that here also there are six impulses per revolution equally spaced at intervals of 60° .

If the node is remote from the crankshaft the only unbalanced harmonic orders are the 3, 6, 9, etc., orders, and these are completely unbalanced.

It should be borne in mind, however, that the odd order harmonic components are relatively small. If the node is near the end of the crankshaft the 3, 6, 9, etc., orders are completely balanced, and the remaining orders are nearly completely balanced. If the node is at the centre of the crankshaft, all orders are completely balanced, so that for all practical purposes the engine is free from torsional vibration due to engine impulses. This remark is only true, of course, for the mode of vibration corresponding to a node at the centre of the engine, and for identical combustion characteristics in all cylinders.

No. 33 in the table is a crank arrangement which avoids simultaneous firing of the top side of one piston with the bottom side of another piston. With this arrangement there are twelve impulses per revolution evenly spaced at intervals of 30° .

If the node is remote from the crankshaft the 12, 24, 36, etc., orders are completely unbalanced, and the 3, 15, 27, etc., and 9, 21, 33, etc., orders are partially unbalanced. All other orders are completely balanced. It should be borne in mind that for the odd unbalanced orders the harmonic components are relatively small. If the node is near the end of the crankshaft the 12, 24, 36, etc., orders are completely unbalanced; the 3, 15, 27, etc., and 9, 21, 33, etc., order vectors are large, and the remaining vectors are small or moderate.

If the node is at the centre of the crankshaft the 12, 24, 36, etc., orders are completely balanced; there are no completely unbalanced orders; the 3, 15, 27, etc., and 9, 21, 33, etc., order vectors are large, and the remaining vectors are small or moderate. With this crank arrangement there are unbalanced primary and secondary couples, the primary couple being particularly undesirable. It could be considerably reduced, however, by employing crankweb balance weights, the size of which could be minimised by using only two balancing masses attached to the endmost crankwebs in correct phase relationship with the crankpins.

An advantage of this crank arrangement is that the 6th order torque reaction forces and couples acting on the engine frame are completely balanced, whereas with any of the 2-stroke cycle, single-acting arrangements, e.g. Nos. 18, 19, and 20 in the table, the 6th order torque reaction forces and couples are completely unbalanced. This is important in relation to frame vibration.

Nos. 34 and 35 are similar to No. 33 and have somewhat similar torsional vibration characteristics. An advantage of these two alternative arrangements is that the magnitude of the unbalanced primary couple is considerably reduced, No. 35 being the best arrangement in this respect. With No. 35 the unbalanced primary couple could be reduced to negligible proportions by quite small balance weights attached to the endmost crankwebs.

With both these arrangements the 6th order torque reaction forces on the engine frame are completely balanced, but the torque reaction couples are unbalanced. In general, however,

an unbalanced couple is less important from the point of view of frame vibration than an unbalanced force.

Seven-Cylinder.—Any of the 7-cylinder crank arrangements employed for 2-stroke cycle, single-acting engines can also be used for the double-acting type. No. 36 in the table is the arrangement usually employed in practice because it provides the best degree of engine balance. As already mentioned the use of an odd number of cylinders for a double-acting engine automatically avoids simultaneous firing of the top side of one piston with the bottom side of another piston. In the case of 7-cylinder engines there are fourteen impulses per revolution at equal intervals of 25.714° . The remarks already made in connection with the torsional vibration characteristics of 7-cylinder, 2-stroke cycle, single-acting engines are applicable to double-acting engines having the same crankshaft arrangements, bearing in mind, however, that the odd order harmonic components of the double-acting engine combined tangential effort diagram are relatively small.

Eight-Cylinder.—Any of the crank arrangements normally employed for 2-stroke cycle, single-acting engines can also be used for the double-acting type. With these arrangements the top side of one piston fires simultaneously with the bottom side of another piston, so that there are eight firing impulses per revolution equally spaced at intervals of 45° . For example, No. 38 in the table is the same crank arrangement as No. 23, and in the case of a double-acting engine the firing order is (1T, 6B)–(8T, 3B)–(2T, 4B)–(5T, 7B)–(6T, 1B)–(3T, 8B)–(4T, 2B)–(7T, 5B).

The torsional vibration characteristics of these crank arrangements are the same as already described for 8-cylinder, 2-stroke cycle, single-acting engines, bearing in mind, however, that the odd order harmonic components of the double-acting engine combined tangential effort diagram are relatively small.

No. 39 in the table is an arrangement in which the top sides of two pistons and the bottom sides of two other pistons fire simultaneously, so that there are four impulses per revolution evenly spaced at 90° intervals. The only interest of this arrangement is that there are no unbalanced harmonic orders

when the node is at the centre of the crankshaft. This arrangement therefore provides an engine which is free for all practical purposes from torsional vibrational disturbances, and which is in complete primary and secondary balance. These remarks are only true, of course, for the mode of vibration corresponding to a node at the centre of the crankshaft. If other modes exist these must be investigated separately.

Nine-Cylinder.—Any of the 9-cylinder crank arrangements employed for 2-stroke cycle, single-acting engines can also be used for the double-acting type. No. 40 in the table is the arrangement usually employed because it gives the best degree of engine balance. In common with all double-acting engines having an odd number of cylinders simultaneous firing of the top side of one piston with the bottom side of another piston is automatically avoided. In the case of 9-cylinder, double-acting engines there are eighteen impulses per revolution evenly spaced at equal intervals of 20° . The remarks already made in connection with the torsional vibration characteristics of 9-cylinder, 2-stroke cycle, single-acting engines are applicable to the double-acting type, bearing in mind, however, that the odd order harmonic components of the double-acting engine tangential effort diagram are relatively small.

Ten-Cylinder.—Any of the 10-cylinder arrangements normally employed for 2-stroke cycle, single-acting engines can also be used for the double-acting type. With these arrangements the top side of one piston fires simultaneously with the bottom side of another piston, so that there are ten impulses per revolution evenly spaced at intervals of 36° .

For example, the double-acting engine firing order for the crank arrangement shown at No. 28 in the table is (1T, 6B)–(10T, 5B)–(2T, 7B)–(8T, 3B)–(4T, 9B)–(6T, 1B)–(5T, 10B)–(7T, 2B)–(3T, 8B)–(9T, 4B).

The remarks already made in connection with the torsional vibration characteristics of 10-cylinder, 2-stroke cycle, single-acting engines are applicable to the double-acting type, bearing in mind, however, that the odd order harmonic components of the double-acting engine tangential effort diagram are relatively small.

Alternatively, any of the 10-cylinder arrangements normally used for 4-stroke cycle, single-acting engines can also be employed for the double-acting type. With these arrangements simultaneous firing of the top sides of two pistons alternates with simultaneous firing of the bottom sides of two other pistons, so that again there are ten firing impulses per revolution evenly spaced at intervals of 36° .

For example, No. 42 in the table is the same crank arrangement as No. 12.

With this arrangement, if the node is remote from the crankshaft, the only unbalanced orders are the 5, 10, 15, etc., and these are completely unbalanced.

If the node is near the end of the crankshaft, the 5, 10, 15, etc., orders are completely unbalanced, but the remaining order vector summations are small.

If the node is at the centre of the crankshaft there are no unbalanced orders. This arrangement therefore provides an engine which is free for all practical purposes from torsional vibrational disturbances when the node is at the centre of the crankshaft, and which is in complete primary and secondary balance. This is only true, of course, for that mode of vibration corresponding to a node at the centre of the crankshaft.

If other important modes exist these must be investigated separately.

The foregoing discussion is by no means exhaustive, although it does contain most of the crankshaft arrangements commonly employed in practice. It will be shown in the next chapter that the phase and vector diagrams can be used to provide a quick estimate of the relative magnitudes of torsional vibration at the various critical speeds, by which means the relative merits of different crankshaft arrangements for a given engine aggregate can be rapidly assessed.

The device of permitting simultaneous firing of cylinders, which are symmetrically disposed relative to the node, has been used very successfully in practice for multi-cylinder engines in cases where the necessary symmetrical arrangement of the masses and elasticities can be made.

It may be of interest to set down the firing orders which

correspond to no large resultant vector summations in the gaps between consecutive major criticals.

In 4-stroke cycle engines the major criticals are those whose order numbers are integral multiples of half the number of cylinders for all crank arrangements which provide even firing intervals over the two revolutions occupied by the working cycle. In 2-stroke cycle engines the major criticals are those whose order numbers are integral multiples of the number of cylinders for all crank arrangements which provide even firing intervals during each revolution of the crankshaft, i.e. for all crankshafts having the crankpins evenly spaced round the crank circle. The major orders for engines having different numbers of cylinders are given in column 6 of Table 64. The following arrangements therefore ensure a disposition of critical speeds in which the vector summations at the middle of the gaps between consecutive major criticals are small, thus providing the widest possible speed range free from large amplitude disturbances.

This quiet zone is naturally wider the greater the number of cylinders, due to the wider spacing between consecutive major criticals.

CRANKSHAFT ARRANGEMENTS WHICH HAVE NO LARGE VECTOR SUMMATIONS
IN THE GAPS BETWEEN CONSECUTIVE MAJOR CRITICALS.

Four-Stroke Cycle Engines.

No. of Cylrs.	Major Criticals.	Firing Order.	Crank Arrangement.
5	2.5, 5.0, 7.5, etc.	1-2-4-5-3	1-5-2-3-4
6	3, 6, 9, etc.	1-2-4-6-5-3	(1, 6)-(2, 5)-(3, 4)
7	3.5, 7.0, 10.5, etc.	1-2-4-6-7-5-3	1-7-2-5-4-3-6
8	4, 8, 12, etc.	1-2-4-6-8-7-5-3	(1, 8)-(2, 7)-(4, 5)-(3, 6)
9	4.5, 9.0, 13.5, etc.	1-2-4-6-8-9-7-5-3	1-9-2-7-4-5-6-3-8
10	5, 10, 15, etc.	1-2-4-6-8-10-9-7-5-3	(1, 10)-(2, 9)-(4, 7)-(6, 5)-(8, 3)
11	5.5, 11, 16.5, etc.	1-2-4-6-8-10-11-9-7-5-3	1-11-2-9-4-7-6-5-8-3-10
12	6, 12, 18, etc.	1-2-4-6-8-10-12-11-9-7-5-3	(1, 12)-(2, 11)-(4, 9)-(6, 7)-(5, 8)-(3, 10)

(Note.—In 4-stroke cycle engines the crank sequence differs from the firing order.)

Two-Stroke Cycle Engines.

No. of Cyls.	Major Criticals.	Firing Order and Crank Sequence.
5	5, 10, 15, etc.	1-2-4-5-3
6	6, 12, 18, etc.	1-2-4-6-5-3
7	7, 14, 21, etc.	1-2-4-6-7-5-3
8	8, 16, 24, etc.	1-2-4-6-8-7-5-3
9	9, 18, 27, etc.	1-2-4-6-8-9-7-5-3
10	10, 20, 30, etc.	1-2-4-6-8-10-9-7-5-3
11	11, 22, 33, etc.	1-2-4-6-8-10-11-9-7-5-3
12	12, 24, 36, etc.	1-2-4-6-8-10-12-11-9-7-5-3

(*Note.*—In 2-stroke cycle engines the crank sequence and firing order are identical.)

The 4-stroke cycle crankshafts tabulated are also excellent from the point of view of engine balance. In engines with an even number of cylinders there is complete balance of primary and secondary forces and couples, whilst in engines with an odd number of cylinders there are no unbalanced primary or secondary forces, and the unbalanced primary couple is minimised.

In 2-stroke cycle engines, however, the crank arrangements are not ideal from the point of view of engine balance. Primary and secondary forces are, of course, balanced, but there is a very large unbalanced primary couple in all cases. For this reason the crank arrangements given in Table 64 are usually adopted in practice for 2-stroke cycle engines.

Vee-Engines.—In this type of engine there are two pistons operating on each crankpin. As a rule one piston is connected to the common crankpin by a forked rod and the other by a plain rod, as already described. Alternatively, an arrangement employing two identical connecting rods, arranged side-by-side on the common crankpin, with the lines of stroke of the two pistons slightly offset, is popular in automobile practice. Articulated rods are not commonly employed in Vee-engines.

A multi-cylinder engine of this type consists therefore of two banks of cylinders, the lines of stroke of the two banks being inclined with an included angle δ which is called the Vee-angle. In the following discussion each pair of cylinders

whose lines of stroke occupy the same plane transversely to the longitudinal axis of the crankshaft will be referred to as a row of cylinders. Thus a Vee-engine always has two banks of cylinders but may have any number of rows.

The types usually found in practice have four, six, or eight rows of cylinders, i.e. four-, six-, or eight-throw crankshafts, and it is possible to choose the Vee-angle so that there are equal firing intervals between the cylinders, although this is not regarded as an absolutely essential requirement.

Since the working cycle of a 4-stroke engine occupies 720° the Vee-angle for a 4-stroke cycle Vee-engine, having equally spaced firing intervals, is obtained as follows :—

Let m = number of cylinders per bank, i.e. total number of cylinders = $2m$.

$$\begin{aligned} \text{Then } \delta &= \frac{720}{2m}, \text{ or } \left(\frac{720}{2m} + \frac{720}{m}\right), \text{ or } \left(\frac{720}{2m} + \frac{2 \times 720}{m}\right), \text{ etc.} \\ &= \frac{360}{m}, \text{ or } \frac{3 \times 360}{m} \text{ or } \frac{5 \times 360}{m}, \text{ etc.} \end{aligned}$$

Furthermore, for equal firing intervals between the cylinders in each bank, the angular spacing of the crankpins, ψ , is

$$\psi = 720/m, \text{ and this is also the firing interval between the cylinders in each bank.}$$

The firing interval between the two cylinders of one row is $\sigma = \delta$ or $(360 - \delta)$, and $(\delta + 360)$ or $(720 - \delta)$,

where δ is the Vee-angle.

Finally, the interval between consecutive firing impulses for the whole engine is $360/m$ degrees.

The corresponding expressions for 2-stroke cycle engines, where the working cycle occupies one revolution, are

$$\delta = \text{Vee-angle for even firing} = \frac{180}{m}, \text{ or } \frac{3 \times 180}{m}, \text{ or } \frac{5 \times 180}{m}, \text{ etc.,}$$

$$\psi = \frac{\text{crank angle and firing}}{\text{interval per bank}} = \frac{360}{m},$$

$$\sigma = \text{firing interval per row} = \delta,$$

and the interval between consecutive firing impulses for the whole engine is $180/m$ degrees.

Table 65 gives a summary of the possible arrangements of 4- and 2-stroke cycle Vee-type engines with equal firing intervals

TABLE 65.

MULTI-CYLINDER VEE-TYPE ENGINES. VEE AND CRANK ANGLES FOR EVEN FIRING.

Total No. of Cylinders	4-Stroke Cycle			2-Stroke Cycle			
	Firing Interval			Firing Interval			
2 ($m = 1$)	360°	$\delta = 360^\circ$ 		180°	$\delta = 180^\circ$ 		
4 ($m = 2$)	180°	$\delta = 180^\circ$ 		90°	$\delta = 90^\circ$ 		
6 ($m = 3$)	120°	$\delta = 120^\circ$ 	$\delta = 360^\circ$ 	60°	$\delta = 60^\circ$ 	$\delta = 180^\circ$ 	
8 ($m = 4$)	90°	$\delta = 90^\circ$ 		45°	$\delta = 45^\circ$ 	$\delta = 135^\circ$ 	$\delta = 90^\circ$
10 ($m = 5$)	72°	$\delta = 72^\circ$ 	$\delta = 360^\circ$ 	36°	$\delta = 36^\circ$ 	$\delta = 108^\circ$ 	$\delta = 180^\circ$
12 ($m = 6$)	60°	$\delta = 60^\circ$ 	$\delta = 180^\circ$ 	30°	$\delta = 30^\circ$ 	$\delta = 90^\circ$ 	$\delta = 150^\circ$
14 ($m = 7$)	$51\frac{3}{4}^\circ$	$\delta = 51\frac{3}{4}^\circ$ 	Even firing is also obtained when $\delta = 102\frac{3}{4}^\circ$, $154\frac{1}{4}^\circ$ or 360°	$25\frac{3}{4}^\circ$	$\delta = 25\frac{3}{4}^\circ$ 	Even firing is also obtained when $\delta = 77\frac{1}{4}^\circ$, $128\frac{1}{2}^\circ$ or 180° .	
16 ($m = 8$)	45°	$\delta = 45^\circ$ 	$\delta = 135^\circ$ 	$22\frac{1}{2}^\circ$	$\delta = 22\frac{1}{2}^\circ$ 	Even firing is also obtained when $\delta = 67\frac{1}{2}^\circ$, $112\frac{1}{2}^\circ$ or $157\frac{1}{2}^\circ$.	

for the engine as a whole, and also equal firing intervals between the cylinders in each bank.

This table shows that in multi-cylinder Vee-type engines there is considerable scope for choosing a Vee-angle which best

suits the torsional vibration characteristics of a specific installation. The cases where the Vee-angle is 360° (i.e. 0°) are of academic interest only since it is, of course, impossible to have superimposed cylinders. The cylinders could be placed side by side but this merely provides an ordinary in-line engine aggregate.

Equal firing intervals are obtained with zero Vee-angle for 4-stroke cycle engines when there is an odd number of cylinders in each bank, but equal firing intervals with zero Vee-angle cannot be obtained with 2-stroke cycle engines.

It must be borne in mind that the torsional vibration problem is not the only factor influencing the choice of Vee-angle. In aero-engine practice it is generally considered desirable to minimise the frontal aero of the engine with the object of reducing the drag of the power plant, and this consideration naturally directs attention towards the choice of a small Vee-angle. In the case of engines intended for installation in the wing of an aircraft a Vee-angle of 180° , i.e. a flat engine, has some attraction. Equal firing intervals with a Vee-angle of 180° are obtained in the case of 4-stroke cycle engines having an even number of cylinders in each bank, provided the number of crankpins divided by two is an odd number. In the case of 2-stroke cycle engines even firing intervals with a Vee-angle of 180° are obtained when there is an odd number of cylinders in each bank.

In the case of 8-cylinder, 2-stroke cycle engines even firing intervals for the engine as a whole are not obtained with Vee-angles of 90° and 180° when the crankshaft is of the type which provides even firing intervals between the cylinders in each bank. By employing crankshafts of the type shown at 29 and 30, in Table 64, however, even firing intervals for the engine as a whole are obtained with Vee-angles of 90° and 180° , although the firing intervals between the cylinders in each bank are uneven.

It is also possible to obtain even firing intervals for the engine as a whole in the case of 12-cylinder 2-stroke cycle arrangements with Vee-angles of 60° and 180° by employing crankshafts of the type shown at 33, 34, and 35 in Table 64.

In this case also the firing intervals between the cylinders in each bank are uneven.

In the case of automobile engines the choice of Vee-angle tends towards the wider angles, since this shape of engine fits more conveniently into the bonnet space. The flat 180° Vee-engine is also used in automobile practice.

The engine must be carefully examined for unbalanced forces and couples due to the inertia of the reciprocating and revolving parts, and in some cases the best compromise between the requirements for engine balance and freedom from severe torsional vibrational disturbances will require a departure from the ideal on which Table 65 is based, namely, even firing intervals.

For example, from the balancing standpoint a 2-cylinder Vee-engine with a Vee-angle of 90° is very favourable, because primary forces can be eliminated by a balance weight attached to the crankweb opposite the crankpin, and there is only a partially unbalanced secondary force in the horizontal plane.

Similarly, an 8-cylinder Vee-engine can be arranged to have complete balance of primary and secondary forces and couples by employing a Vee-angle of 90° in conjunction with a crankshaft of the type shown at 16 in Table 64.

If the left-hand bank of cylinders is designated by the letter A and the right-hand bank by the letter B, then one firing order for a 4-stroke cycle engine of this type is 1A-1B-4A-4B-2B-3A-3B-2A. There are four firing impulses per revolution for the engine as a whole, and these are evenly spaced at 90° intervals. The firing intervals in each bank of cylinders are, however, uneven, and the firing order in bank A is different from the firing order in bank B. There are altogether 8 different firing orders corresponding to this arrangement when used for a 4-stroke cycle engine, namely:—

- (a) 1A-1B-3B-4B-2B-3A-4A-2A
- (b) 1A-1B-3B-2A-2B-3A-4A-4B
- (c) 1A-1B-4A-4B-2B-3A-3B-2A
- (d) 1A-1B-4A-2A-2B-3A-3B-4B
- (e) 1A-3A-3B-4B-2B-1B-4A-2A
- (f) 1A-3A-3B-2A-2B-1B-4A-4B
- (g) 1A-3A-4A-4B-2B-1B-3B-2A
- (h) 1A-3A-4A-2A-2B-1B-3B-4B

It should be noticed that with firing orders (a), (e), (g), and (h) there is only one crankpin which receives its two impulses at 90° apart.

With firing orders (b), (c), (d), and (f), however, there are three crankpins each receiving two impulses at 90° apart, so that from the point of view of bearing loading these four firing orders are inferior. On the other hand, with firing orders (a), (e), (g), and (h), the four cylinders of one bank fire one after the other at 90° intervals, followed by the four cylinders in the other bank, and this would not be good from the point of view of mixture distribution in petrol engines. The firing order usually employed in practice is (c).

With this crankshaft and cylinder arrangement primary forces and couples can be eliminated by balance weights attached to the crankwebs opposite the crankpins, whilst secondary forces and couples are completely balanced for each bank of cylinders individually. Due to the better degree of engine balance this arrangement is often preferred to the alternative 90° Vee, 8-cylinder, 4-stroke cycle engine arrangement which employs a crankshaft of the type shown at 1 in Table 64.

In 8-cylinder, 2-stroke cycle, 90° Vee-engines the above completely balanced arrangement is not normally employed because it necessitates simultaneous firing of two cylinders, one in each bank.

Inertia Balance of Vee-Engines.—Fig. 92 shows the influence of the Vee-angle on engine balance. The following discussion refers to one row of a multi-cylinder Vee-engine, i.e. to the two pistons operating on a common crankpin with their lines of stroke inclined at an angle δ .

Let W = weight of unbalanced rotating parts of one crankpin in lbs., i.e. the unbalanced weight of the crank element plus the revolving weight of two connecting rods,

W' = weight of reciprocating parts of one cylinder, in lbs.,

R = crank radius, in inches,

N = revolutions, per minute,

q = ratio : length of connecting rod/crank radius.

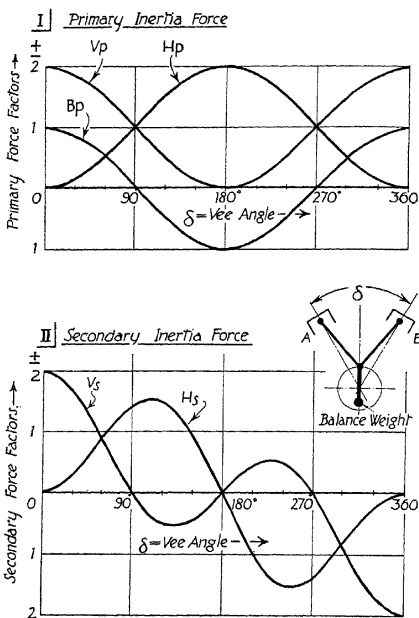


FIG. 92.—Balancing factors for Vee-engines.

Then, *Unbalanced primary force due to rotating parts*

$$= 0.0000284W \cdot R \cdot N^2 \text{ lbs.}$$

This is a constant radial force acting along the crank arm.

Unbalanced Primary Force due to Inertia of Reciprocating Parts.

Maximum vertical primary force

$$= F_{pv} = 0.0000284W' \cdot R \cdot N^2 \cdot V_p \text{ lbs.}, \quad (269)$$

Maximum horizontal primary force

$$= F_{ph} = 0.0000284W' \cdot R \cdot N^2 \cdot H_p \text{ lbs.}, \quad (270)$$

where V_p and H_p are shown in Fig. 92 and can be calculated for different Vee-angles from the following expressions:—

$$V_p = (1 + \cos \delta) \quad (271)$$

$$H_p = (1 - \cos \delta) \quad (272)$$

Unbalanced Secondary Force due to Inertia of Reciprocating Parts.

Maximum vertical secondary force

$$= F_{sv} = 0.0000284W' \cdot R \cdot N^2 \cdot V_s/q \text{ lbs.}, \quad (273)$$

Maximum horizontal secondary force

$$= F_{sh} = 0.0000284W' \cdot R \cdot N^2 \cdot H_s/q \text{ lbs.}, \quad (274)$$

where

$$V_s = \left(\cos \frac{\delta}{2} + \cos \frac{3\delta}{2} \right), \quad (275)$$

$$H_s = \left(\cos \frac{\delta}{2} - \cos \frac{3\delta}{2} \right). \quad (276)$$

The resultant unbalanced primary force due to the reciprocating parts is therefore equivalent to

- (i) a weight W' at crank radius revolving with the crankpin,
- (ii) a weight $(W' \cos \delta)$ at crank radius revolving in the opposite direction to the crankpin at the same speed as the crankshaft.

It is therefore evident that a considerable proportion of the unbalanced primary force due to the reciprocating parts can be neutralised by attaching a balance weight to the crankwebs opposite the crankpin. The optimum size of the balance weights should be such that their combined effect is equivalent to a weight $(W + W')$ at crankpin radius opposite the crankpin, where W is the weight of the unbalanced rotating parts of the

crank element, including the revolving weight of *two* connecting rods, and W' is the weight of the reciprocating parts of one cylinder.

When the crankshaft is counterbalanced in this way the unbalanced primary force becomes

$$F_p = 0.0000284 W' \cdot R \cdot N^2 \cdot B_p \text{ lbs.}, \quad (277)$$

where $B_p = \cos \delta.$ (278)

This is a constant radial force acting along the crank arm so that the maximum unbalanced primary force in the vertical plane is the same as the maximum unbalanced primary force in the horizontal plane.

This residual unbalanced primary force can only be eliminated by employing a balance weight equivalent to $(W' \cos \delta)$ at crank radius and arranging means for driving it in the opposite direction to the crankshaft at crankshaft speed.

The resultant unbalanced secondary force is equivalent to

(i) A weight $\left(\frac{W'}{q} \cos \frac{\delta}{2}\right)$ at crank radius revolving in the same direction as the crankpin at twice the speed of the crankshaft.

(ii) A weight $\left(\frac{W'}{q} \cos \frac{3\delta}{2}\right)$ at crank radius revolving in the opposite direction to the crankpin at twice the speed of the crankshaft.

The secondary force cannot be counterbalanced by simple balancing masses attached to the crankwebs.

In multi-row Vee-type engines the unbalance produced by the rotating masses can be investigated in precisely the same way as for an ordinary in-line engine, and the effect of fitting counterbalancing masses is the same in both cases.

The unbalance produced by the reciprocating parts can be investigated by combining the unbalance of each row with the unbalance of each bank.

For example, if the crankshaft arrangement is such that there are no unbalanced primary forces or couples for each bank, then there will be no primary unbalance of the engine as a whole irrespective of the Vee-angle.

Similarly, if the Vee-angle is such that there is no unbalanced primary force for a row (e.g. when the Vee-angle is 90° or 270° there is no unbalanced primary force provided balance weights are fitted opposite the crankpins as already explained), then there will be no primary unbalance for the engine as a whole irrespective of the type of crankshaft employed.

Again, if the crankshaft arrangement is such that there are no unbalanced secondary forces or couples for each bank and the Vee-angle is such that there are no primary forces for each row, then the engine as a whole will be in complete primary and secondary balance.

Where there is a residual primary or secondary force or couple for the engine as a whole, the following expressions can be used:—

$$F_{pv} = 0.0000284 \cdot W' \cdot R \cdot N^2 \cdot K_p \cdot V_p$$

= maximum vertical primary force, (279)

$$F_{ph} = 0.0000284 \cdot W' \cdot R \cdot N^2 \cdot K_p \cdot H_p$$

= maximum horizontal primary force, (280)

$$C_{pv} = 0.0000284 \cdot W' \cdot R \cdot N^2 \cdot L \cdot K_p' \cdot V_s$$

= maximum vertical primary couple, (281)

$$C_{ph} = 0.0000284 \cdot W' \cdot R \cdot N^2 \cdot L \cdot K_p' \cdot H_p$$

= maximum horizontal primary couple, (282)

$$F_{sv} = 0.0000284 \cdot W' \cdot R \cdot N^2 \cdot K_s \cdot V_s$$

= maximum vertical secondary force, (283)

$$F_{sh} = 0.0000284 \cdot W' \cdot R \cdot N^2 \cdot K_s \cdot H_s$$

= maximum horizontal secondary force, (284)

$$C_{sv} = 0.0000284 \cdot W' \cdot R \cdot N^2 \cdot L \cdot K_s' \cdot V_s$$

= maximum vertical secondary couple, (285)

$$C_{sh} = 0.0000284 \cdot W' \cdot R \cdot N^2 \cdot L \cdot K_s' \cdot H_s$$

= maximum horizontal secondary couple, (286)

where W' = weight of reciprocating parts for one cylinder, in lbs.,

R = crank radius, in inches,

N = revolutions, per minute,

L = cylinder pitch, in inches,

K_p, K_p', K_s, K_s' = force and couple factors for cylinder banks, from Table 64,

V_p, H_p, V_s, H_s = force factors for cylinder rows, from Fig. 92, or Equations (271) to (276).

(Note.—In equations (279) to (286) forces are in lbs. and couples in lbs.-ins.)

If the reciprocating parts of one cylinder are counter-balanced by crankweb balance weights placed opposite the crankpins as already explained, the factors V_p and H_p in Equations (279) to (282) should be replaced by the factor ($B_p = \cos \delta$), i.e. the vertical unbalance then becomes the same as the horizontal unbalance.

The products ($K_p \cdot V_p$), ($K_p \cdot H_p$), etc., from Equations (279) to (286), can be used as a very quick means for comparing the merits of different combinations of crankshaft and Vee-angle from the point of view of engine balance.

As an example, consider the effect on engine balance of altering the Vee-angle of an 8-cylinder, 4-stroke cycle Vee-engine having a crankshaft of type 1 in Table 64.

The force and couple factors corresponding to this crankshaft arrangement, see Table 64, show that the only unbalance in each bank of four cylinders is a secondary force and that the factor for calculating the magnitude of this force is $K_s = 4/g$. Since primary forces and couples and secondary couples are balanced for each bank they are also balanced for the engine as a whole irrespective of the Vee-angle, so that alterations in Vee-angle will only affect the magnitude of the residual secondary force. The comparative effect of such alterations can therefore be obtained by comparing the values of the row factors V_s and H_s for different Vee-angles. These values can either be read from Fig. 92 or be calculated from Equations (275) and (276), as follows:—

Vee-Angle.	Relative Magnitude of Secondary Force.	
	Vertical.	Horizontal.
90°	0	1·414
75°	0·411	1·176
60°	0·866	0·866
45°	1·307	0·541

The above comparison shows that an 8-cylinder, 90° Vee-engine with this type of crankshaft has a large unbalanced secondary force in the horizontal plane. Experience has shown that this horizontal unbalance can cause unpleasant and even destructive vibration. Since secondary unbalance cannot be reduced by simple balance weights, engines with this type of crankshaft have been used in automobile and aeroplane practice with the Vee-angle reduced to 60° , thus reducing the unbalanced horizontal secondary force by about 40 per cent. at the expense of introducing an equal degree of unbalance in the vertical plane, and also uneven firing impulses. Although this expedient reduces the unbalanced vertical secondary force to 0.866 of the unbalanced force in the case of a 4-cylinder, in-line, 4-stroke cycle engine, the presence of a correspondingly large horizontal secondary force is still a considerable disadvantage. The alternative 8-cylinder, 90° Vee, 4-stroke cycle engine with a crankshaft of type 3 in Table 64 is therefore preferred in automobile practice, because with suitable balance weights there is complete primary and secondary balance. In aeroplane practice the large amount of weight which must be added for balancing purposes renders this type of engine unsuitable, and since the alternative just discussed is unsatisfactory from the point of view of engine balance, the 8-cylinder, Vee, 4-stroke cycle engine is not a popular type of aeroplane engine.

The influence of engine balance on the choice of Vee-angle becomes less important as the number of cylinders increases, because for engines having twelve or more cylinders the balance of each bank of cylinders is inherently good.

There is therefore more latitude for choosing a Vee-angle to suit torsional vibration characteristics alone in engines having a large number of cylinders.

For example, 12-cylinder, 4-stroke cycle engines with the conventional 6-throw crankshaft shown at 5 in Table 64, possess complete primary and secondary balance for each bank independently, and therefore the engine as a whole is also in complete primary and secondary balance irrespective of the Vee-angle. In practice engines of this type have been built

with Vee-angles of 45° , 50° , 55° , and 60° , the 60° angle being the correct one for equal firing intervals in each bank and for the engine as a whole, whilst the 45° angle was used on the well-known "Liberty" aero-engine.

When it is realised that in a multi-cylinder Vee-engine both the Vee-angle and the firing order can be chosen in a great many different combinations, the complexity of the problem makes the selection of the best angle and firing order a rather difficult matter. It is recommended, however, that the Vee-angle be chosen in the first instance to give even firing intervals in each bank and for the engine as a whole, in accordance with the data given in Table 65, and where there is a choice of angles the one which best fits into the space available for installation should be taken.

In 4-stroke cycle engines the crankshaft arrangement should be chosen in the first instance from considerations of engine balance, using the data given in Table 64. Since there are usually several alternative firing orders in the case of 4-stroke cycle engines having six and any greater even number of cylinders, the opportunity of selecting a firing order to give the best disposition of critical speeds to suit the particular installation still remains. In this way it will usually be possible to obtain an engine aggregate which is economical in shape, possesses good balance, and has a speed range free from serious torsional vibrational disturbances.

Firing Order in Vee-Engines.

(a) Four-Stroke Cycle, Single-Acting Vee-Engines with an Even Number of Cylinders in each Bank.

In the case of 4-stroke cycle, in-line engines having an even number of cylinders the crankpins are arranged in pairs at equal angular intervals round the crank circle, and one half of the crankshaft is the mirror image of the other half, as shown at 1, 5, 8, 12, and 13 in Table 64. This arrangement provides complete primary and secondary force and couple balance, as well as equal firing intervals, in engines having six and more cylinders.

In the case of Vee-type engines, if there is no residual primary or secondary unbalance for each bank, there will be none for the engine as a whole. Hence when there is an even number of cylinders in each bank and the crankshaft is of the type just described, the engine will be in complete primary and secondary balance.

It has already been shown that in 6-cylinder in-line engines there is one such balanced crankshaft arrangement and that there are four different firing orders corresponding to this arrangement; in 8-cylinder engines there are three balanced crankshaft arrangements each having eight different firing orders; in 10-cylinder engines there are twelve balanced crankshaft arrangements each having sixteen different firing orders; and in 12-cylinder engines there are sixty balanced crankshaft arrangements each having thirty-two different firing orders. Thus there are altogether 4, 24, 192, and 1920 different firing orders for 6-, 8-, 10-, and 12-cylinder in-line engines of the balanced type. These numbers also apply to each bank of a Vee-type engine having 6, 8, 10, and 12 cylinders in each bank, or 12, 16, 20, and 24 cylinders for the engine as a whole. Furthermore, in a Vee-engine one of the possible firing orders can be chosen for one bank and another for the other bank, whilst the two cylinders comprising each row can either fire consecutively or after a lag of $(360 + \delta)$, where δ is the Vee-angle.

The following table shows the number of possible balanced crank arrangements and firing orders for Vee-engines having various numbers of cylinders:—

Total No. of Cylrs.	No. of Balanced Crank Arrangements.	No. of Firing Orders per Crankshaft Arrangement.	Total Number of Firing Orders.
12	1	32	32
16	3	128	384
20	12	512	6,144
24	60	2,048	122,880

The thirty-two alternative firing orders for the 12-cylinder Vee-engine are shown in the following table :—

<i>Bank A :</i>			
1-2-3-6-5-4	1-2-4-6-5-3	1-5-3-6-2-4	1-5-4-6-2-3
<i>Bank B :</i>			
1-2-3-6-5-4	1-2-3-6-5-4	1-2-3-6-5-4	1-2-3-6-5-4
<i>Alternative Firing Orders for Bank B :</i>			
1-2-4-6-5-3	1-2-4-6-5-3	1-2-4-6-5-3	1-2-4-6-5-3
1-5-3-6-2-4	1-5-3-6-2-4	1-5-3-6-2-4	1-5-3-6-2-4
1-5-4-6-2-3	1-5-4-6-2-3	1-5-4-6-2-3	1-5-4-6-2-3
6-5-4-1-2-3	6-5-4-1-2-3	6-5-4-1-2-3	6-5-4-1-2-3
6-5-3-1-2-4	6-5-3-1-2-4	6-5-3-1-2-4	6-5-3-1-2-4
6-2-4-1-5-3	6-2-4-1-5-3	6-2-4-1-5-3	6-2-4-1-5-3
6-2-3-1-5-4	6-2-3-1-5-4	6-2-3-1-5-4	6-2-3-1-5-4

In practice, it is customary to use the same firing order for each bank of cylinders and to choose the firing interval ($\delta + 360^\circ$) between corresponding cylinders in the two banks. When the firing order is the same in both banks of cylinders mixture distribution, ignition and valve timing, etc., are simplified, whilst the choice of the longer interval between the firing impulses of corresponding cylinders in the two banks avoids having two consecutive impulses on each crankpin, and is the only possible arrangement in cases where the valves of corresponding cylinders in each bank are operated by a common centrally situated cam. For example, in a 12-cylinder, 60° Vee-engine each cylinder in bank B must fire 60° or 420° of crankshaft rotation after the corresponding cylinder in bank A. The corresponding camshaft motion is 30° or 210° , and it would be impossible to use a common cam for operating the valves of both A and B bank cylinders with the smaller angle because the two cam followers would interfere.

The above considerations reduce the number of alternative firing orders to four in the case of 12-cylinder engines; 24 in the case of 16-cylinder engines; 192 in the case of 20-cylinder engines; and 1920 in the case of 24-cylinder engines. The choice is still large for engines having more than twelve cylinders.

The four alternative arrangements for the 12-cylinder engine are as follows :—

- (i) 1A-6B-2A-5B-3A-4B-6A-1B-5A-2B-4A-3B,
i.e. firing order in each bank = 1-2-3-6-5-4.
- (ii) 1A-6B-2A-5B-4A-3B-6A-1B-5A-2B-3A-4B,
i.e. firing order in each bank = 1-2-4-6-5-3.
- (iii) 1A-6B-5A-2B-3A-4B-6A-1B-2A-5B-4A-3B,
i.e. firing order in each bank = 1-5-3-6-2-4.
- (iv) 1A-6B-5A-2B-4A-3B-6A-1B-2A-5B-3A-4B,
i.e. firing order in each bank = 1-5-4-6-2-3.

No. (iii) is the firing order usually adopted in practice, because it gives good longitudinal spacing of firing impulses in each bank and simplifies the mixture distribution problem in the case of petrol engines.

It should be noticed that by reversing the firing order in each bank, four apparently different firing orders are obtained for the engine as a whole.

These are not, however, really different arrangements, because the characteristics of the engine with regard to balance, torsional vibration, mixture distribution, etc., are not altered when the firing order is reversed in both banks. The reversed firing order for the arrangement usually employed in practice, viz. No. (iii), is

$$1A-6B-4A-3B-2A-5B-6A-1B-3A-4B-5A-2B,$$

i.e. firing order in each bank = 1-4-2-6-3-5.

In an 8-cylinder, 90° Vee-engine with the crankshaft arrangement shown at 1 in Table 64, the firing interval between bank B and bank A is 90° or 450°, the latter being usually adopted for the reasons stated above.

The firing order in each bank is 1-3-4-2, or the reverse order 1-2-4-3 (see Table 64). The firing order for the whole engine is therefore

$$1A-4B-3A-2B-4A-1B-2A-3B, \text{ or } 1A-4B-2A-3B-4A-1B-3A-2B.$$

(b) *Four-Stroke Cycle, Single-Acting Vee-Engines with an Odd Number of Cylinders in Each Bank.*

When there is an odd number of cylinders in each bank there is only one practical firing order for each bank, since it is desirable to have even firing in each bank over the complete working cycle of two revolutions. The firing orders usually employed in practice for in-line engines having an odd number of cylinders are given in Table 64, and these can be used to determine the firing order of the corresponding Vee-type engine.

For example, the firing order normally employed for a 5-cylinder, in-line, 4-stroke cycle engine is 1-2-4-5-3, the crank arrangement being shown at 4 in Table 64. If this crankshaft is used for a 10-cylinder Vee-engine the firing order for the complete engine is therefore

$$1A-1B-2A-2B-4A-4B-5A-5B-3A-3B,$$

i.e. firing order per bank = 1-2-4-5-3.

Alternatively, the engine will have the same characteristics if the firing order in each bank is reversed, giving the following firing order for the whole engine:—

$$1A-1B-3A-3B-5A-5B-4A-4B-2A-2B,$$

i.e. firing order per bank = 1-3-5-4-2.

It should be noted that the two pistons operating on each common crankpin fire consecutively, and for this reason and also because the engine is not in complete primary and secondary balance, 4-stroke cycle Vee-engines with an odd number of cylinders in each bank are not normally employed.

(c) *Two-Stroke Cycle, Single-Acting Vee-Engines.*

In 2-stroke cycle Vee-engines the firing order in each bank is necessarily the same as the crank sequence, and the two cylinders in each row must fire consecutively, the firing interval between corresponding cylinders in each bank being the same as the Vee-angle.

The crank sequences and firing orders for 2-stroke cycle,

in-line engines are given in Table 64, and these can also be used for the corresponding Vee-type engines.

For example, the firing order normally employed for a 5-cylinder, 2-stroke cycle engine is 1-5-2-3-4, as shown at 17 in Table 64. If this crankshaft arrangement is used for a 10-cylinder Vee-engine the firing order for the whole engine is

$$1A-1B-5A-5B-2A-2B-3A-3B-4A-4B,$$

i.e. firing order per bank = 1-5-2-3-4

Alternatively, the engine will have the same characteristics if the reversed firing order is used in each bank, giving the following firing order for the whole engine :—

$$1A-1B-4A-4B-3A-3B-2A-2B-5A-5B,$$

i.e. firing order per bank = 1-4-3-2-5.

Torsional Vibration Characteristics of Vee-Engines.

—Since the firing order is necessarily the same for each bank of a 2-stroke cycle Vee-engine, and is usually made the same for each bank of a 4-stroke cycle engine, it follows that the resultant vector summations for any given harmonic order are identical for both banks of cylinders.

Also, since the firing interval between each pair of cylinders which constitute a row is necessarily the same for all the rows in a 2-stroke cycle engine, and is usually made the same in the case of 4-stroke cycle engines, it follows that the resultant vector summations for any given harmonic order are identical for all rows.

These two summations will be referred to as the bank and row summations respectively, the resultant vector summation for the engine as a whole being the product of the bank and row summations.

This method of obtaining the resultant vector summations for the engine as a whole is very convenient when investigating the effect of altering the bank firing order whilst retaining the Vee-angle unaltered. It is also a very quick method for investigating the effect of changes of Vee-angle when the bank firing order remains unaltered.

Row Summation.—Referring to Fig. 93, the resultant vector summations for each row of cylinders is obtained as follows:—

- Let δ = the Vee-angle,
 σ = firing interval between banks, i.e. between the two cylinders which constitute a row
 = δ or $(\delta + 360^\circ)$ for 4-stroke cycle engines having an even number of cylinders in each bank.
 In practice this angle is invariably $(\delta + 360^\circ)$
 = δ for 4-stroke cycle engines having an odd number of cylinders in each bank, and for all 2-stroke cycle engines,
 Σb = n th order vector summation for one row of cylinders, assuming unit amplitude at the point on the normal elastic curve where the row is situated,
 n = the harmonic order number, i.e. the number of complete oscillations per revolution.

Since the amplitude on the normal elastic curve is the same for both the cylinders in any one row, it follows, from the phase and vector diagrams in Fig. 93, that

$$\Sigma b = 2 \cdot \cos^{n \cdot \sigma} \quad . \quad . \quad . \quad (287)$$

The values of Σb for various firing intervals between banks, i.e. for various values of σ , are shown graphically in Fig. 93 for orders 0.5 to 6.

This diagram can be used for both 2-stroke and 4-stroke cycle engines, bearing in mind that in the case of 2-stroke cycle engines there are no half orders.

Bank Summation.—The bank summation Σa is carried out in precisely the same manner as already described for in-line engines. That is to say, each bank of cylinders is regarded as an ordinary in-line engine and the resultant vectors sums are determined in the usual manner.

Resultant Vector Summation for the Whole Engine.—Since unit amplitude was assumed for the cylinders in each row when determining the row summation, and since the bank summation

is based on unit amplitude at the free end of the crankshaft and takes into account the variation of amplitude at the several cylinders in each bank, the resultant vector summation for the whole engine is simply the product of the row and bank summations,

$$\text{i.e. } \Sigma A = \Sigma a \cdot \Sigma b, \quad . \quad . \quad . \quad (288)$$

where ΣA = the resultant vector sum for the engine as a whole, assuming unit amplitude for each of the two cylinders in the row which is situated at the free end of the crankshaft,

Σa = the vector summation for each bank, assuming unit amplitude at the free end of the crankshaft,

Σb = the vector summation for each row, assuming unit amplitude for each of the two cylinders which constitute a row.

Also, if T_n = the maximum value of the n th order harmonic component of the tangential effort curve for *one cylinder*, in lbs. per sq. in.,

R = the crank radius, in inches,

A = the area of the cylinder, in sq. ins.,

then the work done by the n th order component per unit deflection at the free end of the crankshaft for the whole engine is

$$W_n = \pi \cdot T_n \cdot A \cdot R \cdot \Sigma A, \text{ ins.-lbs. per cycle [see also Equation (307)].}$$

Equation (288) shows that ΣA is zero when either Σa or Σb is zero, hence by finding the condition for which Σb is zero it is possible to determine the Vee-angle which will eliminate any given harmonic order.

$$\text{Now} \quad \Sigma b = 2 \cos \frac{n \cdot \sigma}{2}, \quad . \quad . \quad . \quad (287)$$

and this is zero when $\cos \frac{n \cdot \sigma}{2} = 0$,

$$\text{i.e. when} \quad \frac{n \cdot \sigma}{2} = (i + 0.5) 180 \text{ degrees,}$$

or
$$\sigma = \frac{360}{n}(i + 0.5),$$

where $i =$ any integer $= 0, 1, 2, 3,$ etc.,

$n =$ the harmonic order number,

$\sigma =$ firing interval between banks, i.e. between the two cylinders which constitute a row,

but $\sigma = \delta$ for all 2-stroke cycle engines and for 4-stroke cycle engines with an odd number of cylinders in each bank,

$\sigma = (\delta + 360)$ for 4-stroke cycle engines with an even number of cylinders in each bank.

Hence,
$$\delta = \frac{360}{n}(i + 0.5) \text{ degrees} \quad . \quad . \quad . \quad (289)$$

where $\delta =$ the Vee-angle.

The above expression applies to either 2-stroke or 4-stroke engines, bearing in mind that there are no half orders in the case of 2-stroke cycle engines. It should also be noted that since the shape of the normal elastic curve does not enter into the expression for the row summation, the elimination of a specified harmonic order by a suitable choice of Vee-angle holds good for all modes of vibration, and for engines having any number of cylinders in each bank.

EXAMPLE.—Determine the Vee-angles which will eliminate the 3rd, 4.5th, and 6th order criticals.

3rd Order :

$$\begin{aligned} n = 3, \text{ hence, } \delta &= \frac{360}{3}(i + 0.5) \text{ degrees} \\ &= 60, 180, 300, \text{ etc., degrees.} \end{aligned}$$

4.5th Order :

$$\begin{aligned} n = 4.5, \text{ hence, } \delta &= \frac{360}{4.5}(i + 0.5) \\ &= 40, 120, 200, \text{ etc., degrees.} \end{aligned}$$

Finally, it is of interest to determine the Vee-angles which make the resultant vector summation for the whole engine, i.e. ΣA , the same as the vector summation for each bank, i.e. Σa .

This condition is fulfilled when $\Sigma b = 1$,

$$\text{i.e. when} \quad \cos \frac{n \cdot \sigma}{2} = 1/2 \quad [\text{from Equation (287)}]$$

$$\text{or} \quad \frac{n \cdot \sigma}{2} = (3 \cdot i \pm 1) 60 \text{ degrees,}$$

$$\text{whence,} \quad \delta = \frac{120}{n} (3 \cdot i \pm 1). \quad . \quad . \quad (291)$$

EXAMPLE.—Determine the Vee-angles which make the vector summations for the whole engine the same as the vector summations for each bank, in the case of the 3rd, 4.5th, and 6th order criticals.

3rd Order :

$$n = 3, \text{ hence, } \delta = \frac{120}{3} (3 \cdot i \pm 1) = 40, 80, 160, 200, \text{ etc.,} \\ \text{degrees.}$$

4.5th Order :

$$n = 4.5, \text{ hence, } \delta = \frac{120}{4.5} (3 \cdot i \pm 1) = 26.67, 53.33, 106.66, \\ 133.33, \text{ etc., degrees.}$$

6th Order :

$$n = 6, \text{ hence, } \delta = \frac{120}{6} (3 \cdot i \pm 1) = 20, 40, 80, 100, \text{ etc.,} \\ \text{degrees.}$$

Note.—It must be carefully borne in mind that the foregoing analysis is only applicable in cases where both banks of cylinders have the same firing order. This condition is automatically fulfilled in the case of 2-stroke cycle engines.

The following example illustrates the application of the foregoing methods to a 12-cylinder, 60° Vee, 4-stroke cycle, single-acting engine. The firing order in each bank is

1-5-3-6-2-4; the firing interval between the pairs of cylinders constituting each row is $(\delta + 360) = 420^\circ$; and the normal elastic curve and vector summations for each bank are shown in Fig. 94. The firing order for the whole engine is therefore 1A-6B-5A-2B-3A-4B-6A-1B-2A-5B-4A-3B.

Case a: Node near end of Crankshaft.—The normal elastic curve is shown at (a) in Fig. 94, and is representative of the type of curve obtained for the one-node mode of vibration of aero-engine/air-screw combinations. From Fig. 94 the vector summations for each bank are

Orders (n).	Bank Vector Summations (2a).
0.5, 3.5, 6.5, etc. } 2.5, 5.5, 8.5, etc. } 1, 4, 7, etc. } 2, 5, 8, etc. } 1.5, 4.5, 7.5, etc. 3, 6, 9, etc.	0.485 0.214 1.298 4.280

The row summations, from Fig. 93, or from Equation (287), where $\sigma = 420^\circ$, are

Orders (n).	Row Vector Summations (2b).
0.5, 6.5, 12.5, etc. } 5.5, 11.5, 17.5, etc. } 1, 7, 13, etc. } 5, 11, 17, etc. } 1.5, 7.5, 13.5, etc. } 4.5, 10.5, 16.5, etc. } 2, 8, 14, etc. } 4, 10, 16, etc. } 2.5, 8.5, 14.5, etc. } 3.5, 9.5, 15.5, etc. } 3, 9, 15, etc. 6, 12, 18, etc.	0.518 1.732 1.414 1.000 1.932 0 2.000

The resultant vector summations for the whole engine are therefore as follows:—

Order Numbers (n).	Resultant Vector Summations ($\Sigma A = \Sigma A_x + \Sigma A_y$).	
	F.O. 1-5-3-6-2-4. $\delta = 60^\circ$.	F.O. 1-2-4-6-5-3. $\delta = 60^\circ$.
0.5, 6.5, 12.5, etc. } 5.5, 11.5, 17.5, etc. }	$(0.485 \times 0.518) = 0.252$	0.537
1, 7, 13, etc. } 5, 11, 17, etc. }	$(0.214 \times 1.732) = 0.371$	0.371
1.5, 7.5, 13.5, etc. } 4.5, 10.5, 16.5, etc. }	$(1.298 \times 1.414) = 1.835$	0.167
2, 8, 14, etc. } 4, 10, 16, etc. }	$(0.214 \times 1.000) = 0.214$	0.214
2.5, 8.5, 14.5, etc. } 3.5, 9.5, 15.5, etc. }	$(0.485 \times 1.932) = 0.938$	2.000
3, 9, 15, etc. }	$(4.280 \times 0) = 0$	0
6, 12, 18, etc. }	$(4.280 \times 2.000) = 8.560$	8.560

The above analysis shows that with a Vee-angle of 60° the 3, 9, 15, etc., orders are zero, but the 6, 12, 18, etc., orders are completely unbalanced. The 1.5, 4.5, 7.5, etc., orders are also of appreciable amplitude.

The frequency values usually found in practice are such that both the 4.5 and the 6th order criticals are liable to occur in or near the operating speed range, and in such cases it is desirable to make some alteration in the system which will reduce the amplitude at these critical speeds.

It has already been shown in connection with in-line engines that in a 6-cylinder, 4-stroke cycle engine altering the firing order from 1-5-3-6-2-4 to 1-2-4-6-5-3 brings about a considerable reduction of the 1.5, 4.5, 7.5, etc., amplitudes but leaves the 3, 6, 9, 12, etc., amplitudes unaltered. In the present example, if the bank firing order is altered to 1-2-4-6-5-3, the resultant vector summations are as shown in the 3rd column of the above table. The effect of this alteration is to reduce the 4.5 order considerably, at the expense of a considerable increase in the 3.5 order, leaving the 6th order unaltered. This alteration would only be effective, therefore, where the 3.5

order is well above and the 6th order well below the running speed range.

A 60° Vee-angle is the correct angle for even firing impulses in a 12-cylinder, 4-stroke cycle engine. If even firing is sacrificed in the interests of the torsional vibration problem it is possible to alter the relative amplitudes at the various critical speeds by altering the Vee-angle. The following table shows the effect of altering the angle to 30° with firing order 1-5-3-6-2-4, and also with firing order 1-2-4-6-5-3. For a 4-stroke cycle engine the firing interval between the pairs of cylinders constituting a row is $(30 + 360) = 390^\circ$ when the Vee-angle is 30°.

Order Numbers (n).	Resultant Vector Summations ($\Sigma A = \Sigma z \cdot \Sigma b$).	
	F.O. 1-5-3-6-2-4. $\delta = 30^\circ$.	F.O. 1-2-4-6-5-3. $\delta = 30^\circ$.
0.5, 12.5, 24.5, etc. }	0.127	0.270
11.5, 23.5, 35.5, etc. }		
1, 13, 35, etc. }	0.413	0.413
11, 23, 35, etc. }		
1.5, 13.5, 25.5, etc. }	0.995	0.090
10.5, 22.5, 34.5, etc. }		
2, 14, 26, etc. }	0.371	0.371
10, 22, 34, etc. }		
2.5, 14.5, 26.5, etc. }	0.590	1.260
9.5, 21.5, 33.5, etc. }		
3, 9, 15, etc.	6.060	6.060
3.5, 15.5, 27.5, etc. }	0.770	1.640
8.5, 20.5, 32.5, etc. }		
4, 16, 28, etc. }	0.214	0.214
8, 20, 32, etc. }		
4.5, 16.5, 28.5, etc. }	2.400	0.218
7.5, 19.5, 31.5, etc. }		
5, 17, 29, etc. }	0.111	0.111
7, 19, 31, etc. }		
5.5, 17.5, 29.5, etc. }	0.962	2.050
6.5, 18.5, 30.5, etc. }		
6, 18, 30, etc.	0	0
12, 24, 36, etc.	8.560	8.560

The above table shows that when the Vee-angle is altered to 30° the 6th order is eliminated irrespective of firing order,

but the 3rd order becomes completely unbalanced. The 4.5 order is large for firing order 1-5-3-6-2-4, but is very considerably reduced by changing the firing order to 1-2-4-6-5-3 at the expense of an increase in the magnitude of the $3\frac{1}{2}$, $5\frac{1}{2}$ and $6\frac{1}{2}$ orders.

The 12th order is also completely unbalanced for both firing orders, but since the 12th order harmonic component is small this should not be important.

The foregoing discussion may therefore be summarised as follows :—

With Vee-angle 60° , which gives even firing impulses, and firing order 1-5-3-6-2-4 in each bank, the 3rd order critical is eliminated, but the 4.5 and 6th order criticals are not negligible. Unless suitable damping means are provided, therefore, this arrangement should only be used where the running speed range lies between the 2.5 (which is not negligible because of the large magnitude of the 2.5 order tangential effort component) and the 4.5 order criticals, or between the 4.5 order and the 6th order criticals, or below the 6th order critical. For example, if the natural frequency of the system is 7500 vibs./min., and allowing a margin of 10 to 20 per cent. clear of the critical speeds, the above considerations imply that the operating speed range should lie between about 1900 and 2600 r.p.m.; be confined to about 1400 r.p.m., or lie below about 1100 r.p.m.

With Vee-angle 60° and firing order 1-2-4-6-5-3, the 3rd order critical is still eliminated; the 6th order critical remains unaltered, but the 4.5 order is very considerably reduced at the expense of a considerable increase in the 3.5 order critical. This arrangement is therefore suitable where the running speed range lies between the 3.5 and 6th order criticals, or lies below the 6th order critical. If the natural frequency is 7500 vibs./min., therefore, the running speed range should lie between about 1400 and 1900 r.p.m., or be below 1100 r.p.m.

With Vee-angle 30° , which gives uneven firing, and firing order 1-5-3-6-2-4, the 6th order critical is eliminated, but the 3rd and 4.5 order criticals are not negligible. This arrangement is therefore suitable where the running speed range lies between the 3rd and 4.5 order criticals, or below the 4.5

order critical (assuming that the 7.5 order stress is not found to be serious).

Assuming a frequency of 7500 vibs./min., the above considerations imply that the running speed range should lie between 2000 and 1900 r.p.m., or below about 1500 r.p.m. The narrow range between the 3rd and 4.5 orders is due to the necessity for providing a margin of at least 20 per cent. clear of the powerful 3rd order critical.

With Vee-angle 30° and firing order 1-2-4-6-5-3, the 6th order critical is still eliminated, the 3rd order remains unaltered, but the 4.5 order is considerably reduced at the expense of an increase in the 3.5, 5.5 and 6.5 orders. If the stress calculations show that the 3.5, 5.5 and 6.5 orders are not negligible, the running speed range should lie between the 3.5 and 5.5 order criticals, or below the 6.5 order critical. Thus for a frequency of 7500 vibs./min., the permissible speed ranges are 1500 to 1900 r.p.m., or below about 1100 r.p.m.

In general, the effect of altering the Vee-angle on the magnitude of any given critical speed can be quickly obtained from Fig. 93. For example, in the case just discussed Fig. 93 shows that the 3rd order critical is zero when the Vee-angle is 60° , and gradually increases in amplitude as the Vee-angle is reduced, until it is completely unbalanced when the Vee-angle is 0° . The 6th order critical, on the other hand, is completely unbalanced when the Vee-angle is 60° , and gradually diminishes as the Vee-angle is reduced, until it becomes zero when the Vee-angle is 30° .

Case b: Node at Centre of Crankshaft.—The normal elastic curve is shown at (b) in Fig. 94. This diagram shows that the only unbalanced orders for each bank are the half orders.

The row summations are the same as already given for the Case *a*, i.e. the shape of the normal elastic curve does not affect the row summations.

Since the resultant vector summations for the whole engine are the products of the bank and row summations, it follows that only the half orders need be considered when the node is at the centre of the crankshaft. The following table shows

the relative magnitudes of the half-order resultant torque summations when the Vee-angle is 60° :—

RESULTANT VECTOR SUMMATIONS: 12-CYLINDER 60° VEE-ENGINE.

Order Numbers.	Firing Order per Bank. 1-5-3-6-2-4.	Firing Order per Bank. 1-2-4-6-5-3.
0.5, 6.5, 12.5, etc. } 5.5, 11.5, 17.5, etc. }	0.665	1.610
1.5, 7.5, 13.5, etc. } 4.5, 10.5, 16.5, etc. }	5.650	0.003
2.5, 8.5, 14.5, etc. } 3.5, 9.5, 15.5, etc. }	2.490	6.000
All other orders are eliminated.		

The above table shows that with firing order 1-5-3-6-2-4 and the node at the centre of the crankshaft the only really severe critical speeds are the 1.5, 4.5, 7.5, etc., orders, although it should be borne in mind that the 2.5 and 3.5 orders will also require consideration, because the 2.5 and 3.5 order components of the tangential effort curve are large. This arrangement is therefore suitable in cases where the running speed lies between the 3.5 and 4.5 order criticals, or below the 4.5 order critical. In the latter case the 7.5 order should be considered as a possible source of vibration if the 7.5 order torque component is sufficiently large.

If the firing order is altered to 1-2-4-6-5-3, the 1.5, 4.5, 7.5, etc., orders are very nearly zero, but the 2.5 and 3.5 orders are increased. Due to the elimination of the 4.5, 7.5, etc., orders this arrangement provides an engine which is for all practical purposes free from any serious torsional vibration when the running speed is kept below the 3.5 order critical speed.

The foregoing analysis is a quick and easy method of assessing the torsional vibration characteristics of Vee-type engines with various combinations of Vee-angle, crankshaft arrangement, and bank firing order.

It can be applied to other types of engines with equal facility, for example, fan-type engines in which there are three banks of cylinders, with three cylinders in each row, and X-type engines in which there are four banks of cylinders with four cylinders in each row. In all cases, provided the firing order is identical for each bank, it is only necessary to determine the row and bank summations separately and then obtain their products to give the resultant vector summations for the engine as a whole.

The device of permitting two cylinders to fire simultaneously with the object of providing a favourable disposition of critical speeds has been used successfully for engines having several banks of cylinders. For example, Fig. 95 shows a 12-cylinder, 2-stroke cycle engine with two banks of diametrically opposed cylinders arranged for simultaneous firing. In this case the Vee-angle is 180° , and a crankshaft of the type shown at 5 in Table 64 is employed. The engine therefore possesses complete primary and secondary balance. The firing order is (1A, 6A)-(3B, 4B)-(2A, 5A)-(1B, 6B)-(3A, 4A)-(2B, 5B), and there are six double-firing impulses per revolution equally spaced at intervals of 60° .

The phase diagrams in Fig. 95 show that when the node is at the centre of the crankshaft the bank vector summations for all orders are zero, hence for all practical purposes the complete engine is free from torsional vibrational disturbances. Furthermore, since the firing interval between the two cylinders in each row is 180° , the odd order row summations are zero (see Fig. 93). The odd orders are therefore completely cancelled for all modes of vibration. The even orders, however, are only cancelled for the mode of vibration corresponding to a node at the centre of the crankshaft. If other important modes of vibration exist these must be investigated separately with respect to the even order critical speeds.

In the case of 2-stroke cycle engines there are, of course, no half orders.

Resultant Vector Summation for Vee-type Engines when the Firing Order is not the same in Both Banks of Cylinders.—In 4-stroke cycle Vee-engines having an even number of cylinders

in each bank and employing crankshafts with mirror symmetry, for example, Nos. 1, 5, 8, 12, and 13 in Table 64, there are several possible alternative firing orders for each bank, and it is possible to employ any one of these alternative firing orders for one bank whilst at the same time employing one of the remaining alternatives for the other bank. It is normal practice, however, to employ the same firing order in both banks, but if for one reason or another it is necessary to investigate the effect of departing from this general rule the following method can be used.

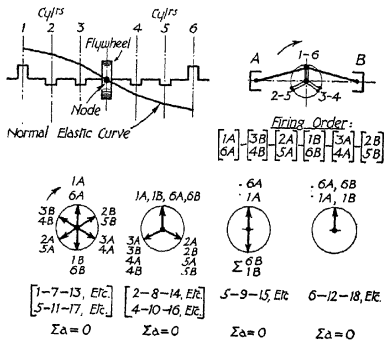


FIG. 95.—12-cylinder 180° Vee 2-stroke engine. Bank summations.

Fig. 96 shows a 12-cylinder, 4-stroke cycle, 60° Vee-engine with firing order 1-5-3-6-2-4 in bank A and firing order 1-2-4-6-5-3 in bank B, the firing order for the whole engine being 1A-6B-5A-5B-3A-3B-6A-1B-2A-2B-4A-4B, the firing interval between 1A and 1B, and 6A and 6B being 420°, whilst the pairs of cylinders in the remaining rows it is 60°.

The resultant vectors summations for the whole engine are obtained in precisely the same way as for an ordinary in-line engine, by setting down the phase diagrams,

with the half-order diagram in the case of a 4-stroke cycle engine and the 1st order diagram in the case of a 2-stroke cycle engine.

In the case of 4-stroke cycle engines the cylinders come into action in the half-order phase diagram at intervals equal to half the firing interval apart and in the same order as the firing order. In the case of 2-stroke cycle engines the cylinders come into action in the 1st order phase diagram at intervals equal to the firing interval apart and in the same order as the firing order. The remaining phase diagrams are obtained from these basic phase diagrams by multiplying the basic phase angles by 2, 3, 4, etc., exactly as already described in connection with in-line engines. The vector summations are then obtained from the phase diagrams, bearing in mind that the specific amplitude is the same for the two cylinders in any one row. For example, if the amplitude on the normal elastic curve for cylinder 2A is 0.947, then it is also 0.947 for cylinder 2B, and so on.

Since Fig. 96 applies to a 4-stroke cycle engine and the Vee-angle is 60° , there are six firing impulses per revolution evenly spaced at 60° intervals. Hence the cylinders come into action in the half-order phase diagram at intervals of 30° , and in the same order as the firing order for the whole engine, namely, 1A-6B-5A-5B-3A-3B-6A-1B-2A-2B-4A-4B. The remaining phase diagrams, derived from this basic phase diagram, are shown in Fig. 96.

The vector summations are then obtained by drawing the vector diagrams in the usual way, and in this case these summations are the resultants for the whole engine. The normal elastic curve in Fig. 96 is the same as that shown at (a) in Fig. 94, so that the only difference between these two cases is the change in the firing order of one bank of cylinders. If the resultant vector summations for the whole engine in Fig. 96 are compared with the resultants for diagram (a) of Fig. 94, the Vee-angle being 60° in both cases, it is seen that the change in the firing order of one bank only affects the magnitudes of the half-order summations. This is the same result as was obtained when the firing order of both banks was altered. Hence, in

general, when the Vee-angle remains unaltered, the order numbers corresponding to the bank summations which remain unaltered when the bank firing order is changed, are also the order numbers of the resultant vector summations for the whole engine which remain unaltered irrespective of whether one or both bank firing orders are changed.

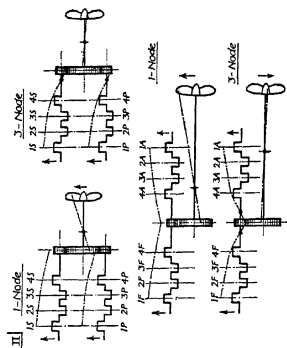
The foregoing method can also be applied to engines having more than two banks of cylinders. Once the firing order for the whole engine has been settled the basic phase diagram can be set down and from this all the remaining phase diagrams can be quickly obtained.

Geared Engines.—Fig. 97 shows some examples of geared oil engine installations in which two identical prime movers are geared to a common driving shaft.

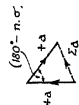
It was shown in Chapter 5 that in addition to the normal modes of vibration in which the whole system executes torsional oscillations, the duplicated parts of the system, i.e. the prime movers, can execute torsional oscillations independently of the remainder of the system. The latter modes of vibration will be called the "node-at-gears" case, since there is always at least one node at the gear faces.

Diagram I of Fig. 97 shows the node-at-gears case in which the fundamental mode occurs when one of the duplicated engine systems swings against the other with a node or nodes at the gear faces. The upper diagrams illustrate the case when the engines are on the same side of the gear assembly, whilst in the lower diagrams the engines are on opposite sides of the gear assembly. Higher modes of vibration are possible, but in all cases there is at least one node at the gear face, the remainder occurring within the engine crankshafts.

Since one of the duplicated systems swings in opposite phase to the other it follows that the n th order component harmonic of the engine torques will cancel if the crank arrangement and firing order is the same for each duplicated engine, and if the firing interval between corresponding cranks of each engine is such that the n th order harmonic torques for these cranks are in phase.



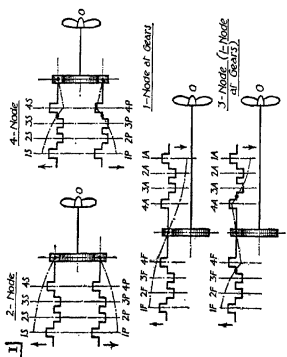
Vector diagrams for one pair of corresponding cranks for example, cranks 1S and 1P, or 1F and 1A.



Vector Diagram



Phase Diagram



Vector diagrams for one pair of corresponding cranks for example, cranks 1S and 1P or 1F and 1A.



Phase Diagram



Vector Diagram

FIG. 97.—Firing angles of geared oil engines.

The necessary firing angle between corresponding cranks of each engine to fulfil this condition is determined as follows :—

Referring to the phase and vector diagrams at the bottom of Diagram I of Fig. 97—

Let σ = firing angle between corresponding cranks of each engine,

n = harmonic order number,

+ a = amplitude at any selected crank of one engine.

Then - a = amplitude at the corresponding crank of the other engine,

$n \cdot \sigma$ = phase angle of n th order torque components,

and, from the vector diagram,

$$\Sigma a = 2 \cdot a \cdot \sin n \cdot \sigma/2.$$

Hence, Σa is zero, i.e. these modes of vibration are not excitable when

$$\sin (n \cdot \sigma/2) = 0,$$

i.e. when $n \cdot \sigma = 0, 360^\circ, 720^\circ, 1080^\circ, 1440^\circ, \text{etc.}$

The following table gives the firing angles, σ , which render the node-at-gears modes non-excitable in the case of the first six harmonic orders :—

FIRING ANGLES BETWEEN CORRESPONDING CRANKS OF DUPLICATED GEARED ENGINES WHICH MAKE THE NODE-AT-GEARS MODES OF TORSIONAL VIBRATION NON-EXCITABLE

Harmonic Order n .	Firing Angle between Corresponding Cranks σ , Degrees.												
0.5	0°	720°											
1.0	0	360	720°										
1.5	0	240	480	720°									
2.0	0	180	360	540	720°								
2.5	0	144	288	432	576	720°							
3.0	0	120	240	360	480	600	720°						
3.5	0	102 $\frac{2}{7}$	205 $\frac{4}{7}$	308 $\frac{6}{7}$	411 $\frac{8}{7}$	514 $\frac{10}{7}$	617 $\frac{12}{7}$	720°					
4.0	0	90	180	270	360	450	540	630	720°				
4.5	0	80	160	240	320	400	480	560	640	720°			
5.0	0	72	144	216	288	360	432	514	576	648	720°		
5.5	0	65 $\frac{5}{11}$	131 $\frac{10}{11}$	196 $\frac{15}{11}$	261 $\frac{20}{11}$	327 $\frac{25}{11}$	392 $\frac{30}{11}$	458 $\frac{35}{11}$	523 $\frac{40}{11}$	589 $\frac{45}{11}$	654 $\frac{50}{11}$	720°	
6.0	0	60	120	180	240	300	360	420	480	540	600	660	720°

The above table applies to both 2-stroke cycle and 4-stroke cycle engines. In 2-stroke cycle engines, however, there are no half-order harmonics and the firing angles repeat after 360° .

The table shows that all harmonic orders of the node-at-gears modes of vibration, i.e. the modes shown in Diagram I of Fig. 97, are non-excitabile when the firing angle between corresponding cranks of the duplicated engines is zero. This condition is fulfilled when corresponding cranks of each engine reach top-dead-centres and fire together and is therefore referred to as "Simultaneous Firing." It does not provide so smooth an output torque as when the two crankshafts are phased so that the firing impulses for the two engines are evenly spaced, but in many cases the advantages gained by the complete elimination of a whole series of troublesome critical zones more than compensates for the somewhat greater normal torque variation.

It should also be noted that when the firing angle between corresponding cranks is 180° all even orders cancel, whilst if the angle is 360° both odd and even orders cancel. The latter condition implies that in a 4-stroke cycle engine only half orders remain, whilst in a 2-stroke cycle engine where there are no half orders all node-at-gears vibration is suppressed. The foregoing considerations may in certain cases enable all serious vibration of the node-at-gears type to be suppressed, whilst at the same time yielding a smoother normal torque curve than would be obtained by adopting simultaneous firing. This possibility can be investigated easily in any specific example with the help of the above table.

It should be kept in mind in applying the above results that the same firing interval must be adopted for each pair of corresponding cranks, as shown in Fig. 97.

Diagram II of Fig. 97 shows the conditions which apply for the normal modes of vibration of the system, i.e. when the system vibrates as a whole.

In this case the duplicated parts of the system swing in phase, so that the n th order component harmonic of the engine torques will now cancel if the crank arrangement and firing order is the same for each duplicated engine, and if the firing

interval between corresponding cranks of each engine is such that the n th order harmonic torques for these cranks are out-of-phase.

Referring to the phase and vector diagrams at the bottom of Diagram II of Fig. 97, and using the same symbols as before,

$$\Sigma a = 2 \cdot a \cdot \sin(90^\circ - n \cdot \sigma/2) = 2 \cdot a \cdot \cos(n \cdot \sigma/2).$$

Hence, in this case Σa is zero, i.e. these modes of vibration are not excitable when

$$\cos(n \cdot \sigma/2) = 0,$$

i.e. when $n \cdot \sigma = 180^\circ, 540^\circ, 900^\circ, 1260^\circ, 1620^\circ$, etc.

The following table gives the firing angles, σ , which render these modes of vibration non-excitable in the case of the first six harmonics:—

FIRING ANGLES BETWEEN CORRESPONDING CRANKS OF DUPLICATED GEARED ENGINES WHICH MAKE THE NORMAL MODES OF TORSIONAL VIBRATION NON-EXCITABLE.

Harmonic Order n .	Firing Angle between Corresponding Cranks σ , Degrees.										
0.5	360°										
1.0	180 540°										
1.5	120 360 600°										
2.0	90 270 450 630°										
2.5	72 216 360 504 648°										
3.0	60 180 300 420 540 660°										
3.5	51 $\frac{2}{3}$ 154 $\frac{2}{3}$ 257 $\frac{2}{3}$ 360 462 $\frac{2}{3}$ 565 $\frac{2}{3}$ 668 $\frac{2}{3}$ °										
4.0	45 135 225 315 405 495 585 675°										
4.5	40 120 200 280 360 440 520 600 680°										
5.0	36 108 180 252 324 396 468 540 612 684°										
5.5	32 $\frac{2}{11}$ 98 $\frac{2}{11}$ 163 $\frac{2}{11}$ 229 $\frac{2}{11}$ 294 $\frac{2}{11}$ 360 425 $\frac{2}{11}$ 490 $\frac{2}{11}$ 556 $\frac{2}{11}$ 621 $\frac{2}{11}$ 687 $\frac{2}{11}$ °										
6.0	30 90 150 210 270 330 390 450 510 570 630 690°										

The above table applies to both 4-stroke cycle and 2-stroke cycle engines. In 2-stroke cycle engines, however, there are no half orders, and the firing angles repeat after 360°.

The table shows that for the normal modes of vibration all odd orders cancel when the firing angle between corresponding cranks of the duplicated engines is 180°, and that all half orders cancel when the angle is 360°.

This is, as it should be, the same as for one row of a Vee-engine, see Fig. 93.

The above table and also Fig. 93 show that when the firing angle is 90° , orders 2, 6, 10, etc., cancel.

The foregoing tables will be found useful for determining which orders of both the node-at-gears modes and the normal modes cancel for any given firing order, or, conversely, will enable the possibility of choosing a firing angle which will cancel any prescribed order or orders to be explored quickly.

Propeller Torque Variation—Marine Installations.—

In marine turbine installations the principal exciting force is that due to torque variation at the propeller. From published information, and from the author's own observations, it appears reasonable to assume that the principal harmonic of the propeller torque variation has an amplitude of 10 to 12 per cent. of the mean torque under normal operating conditions, assuming constant immersion. This harmonic torque variation reaches a maximum four times per revolution for a 4-bladed propeller and three times a revolution for a 3-bladed propeller.

Torque variation originated at the propeller may also be of some importance in marine installations employing reciprocating steam or oil engines. In the case of a 6-cylinder, 4-S.C., S.A. marine oil engine, for example, it will be shown later that for the one-node mode of vibration, the only harmonic component of the engine torque curve of practical importance is the 3rd major order. All minor orders practically cancel.

If this engine drives a four-bladed propeller, however, the possibility of appreciable disturbances being originated by the 4th order propeller torque variation should be investigated.

Fig. 98 shows curves of the approximate torque variation to be expected from 3- and 4-bladed marine propellers. If the propeller moved in a perfectly uniform stream of water and was remote from other bodies no vibratory forces would be produced. In practice, however, the wake in the vicinity of the propeller is by no means uniform, and the propeller works in more or less close proximity to the hull of the ship. In the case of 3-bladed propellers of twin-screw ships the variable portion of the propeller torque consists of three impulses per revolution, the

resistance being a maximum when a blade tip is nearest to the hull, as shown at X in diagram (a) of Fig. 98, and a minimum when a blade tip is furthest from the hull, as shown at Y. In the case of 3-bladed propellers of single-screw ships the variable portion of the propeller torque consists of two superimposed periodic torques, one having a three per revolution impulse frequency and the other a six per revolution impulse frequency. The maximum value of the three per revolution impulse occurs when a blade tip passes the bottom of the propeller aperture, as shown at X in diagram (a) of Fig. 98, and the minimum value occurs when a blade tip passes the top of the propeller aperture, as shown at Z. The maximum value of the six per revolution impulse occurs when a blade tip is about 30° from the propeller aperture, as shown at Y.

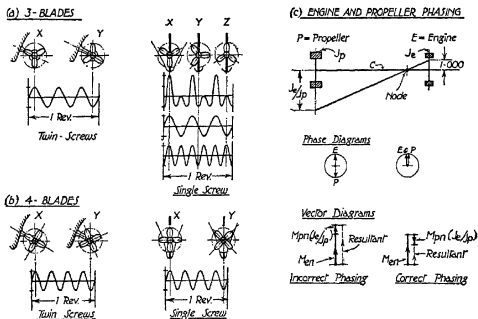


FIG. 98.—Marine propeller torque variation.

as shown at X in diagram (a) of Fig. 98, and the minimum value occurs when a blade tip passes the top of the propeller aperture, as shown at Z. The maximum value of the six per revolution impulse occurs when a blade tip passes either the top or the bottom of the propeller aperture, as shown at X and Z, and the minimum value occurs when a blade tip is about 30° from the propeller aperture, as shown at Y.

In the case of 4-bladed propellers of twin-screw ships the variable portion of the propeller torque consists of four impulses per revolution, the resistance being a maximum when a blade

tip is nearest to the hull, as shown at X in diagram (b) of Fig. 98, and a minimum when a blade tip is at its greatest distance from the hull, as shown at Y.

In the case of 4-bladed propellers of single-screw ships the variable portion of the propeller torque is mainly composed of four impulses per revolution, the resistance being a maximum when the blades are passing through the propeller aperture, as shown at X, and a minimum when the blades are at an angle of about 45° from the aperture, as shown at Y. In addition, however, the variable torque of a 4-bladed propeller in a single-screw ship has components having impulse frequencies of two and eight impulses per revolution. These are, however, of smaller magnitude than the four per revolution impulse.

The magnitude of the variable portion of the propeller torque depends on many factors, such as the characteristics of the hull in the vicinity of the propeller, the location of the propeller in relation to the hull, the depth of immersion of the propeller, the prevailing weather conditions, and so on.

It is therefore impossible to reduce the matter to a cut and dried mathematical formula, and reliance must be placed on experimental data. In this connection Professor Lewis gives a tabulation method for determining the tangential forces from wake variation in his paper, "Propeller Vibration," *Trans. Soc. Naval Architects and Marine Engineers*, New York, 1935. This method was applied to the evaluation of the 3rd order propeller torque variation in a twin-screw vessel and gave a value ± 3.2 per cent. of the mean torque, and subsequent torsigraph tests on the ship showed a 3rd order variation of ± 3.3 per cent.

The vessel was a 630-ft. electrically driven twin-screw passenger boat with three-bladed propellers, the mean torque being 355,000 lbs.-ft.

Some information relating to propeller torque variation is contained in a paper by Messrs. Thorne and Calderwood entitled "Notes on Torsional Oscillations, with Special Reference to Marine Reduction Gearing," *Trans. N.E. Coast Instn. of Engineers and Shipbuilders*, Vol. XXXIX, Part 2, 1922. This information was derived from torsigraph measurements on

single- and twin-screw turbine driven ships, and in all cases the torsiongraph readings were divided by the appropriate dynamic magnifiers to obtain the equivalent "static" torque variation.

For a 3-bladed propeller in a twin-screw vessel a three impulses per revolution torque variation was obtained having a maximum amplitude of ± 4.5 per cent. of the mean torque. There was also a slight indication of a six impulses per revolution torque variation.

For a 3-bladed propeller in a single-screw vessel a three impulses per revolution variation of maximum amplitude ± 4.75 per cent. superimposed on a six impulses per revolution variation of maximum amplitude ± 5.5 per cent. of the mean torque was obtained.

For a 4-bladed propeller in a twin-screw vessel a four impulses per revolution torque variation was obtained having a maximum amplitude of ± 4 to ± 6 per cent. of the mean torque.

For a 4-bladed propeller in a single-screw vessel the torque variation was found to contain several components, as follows :

With propeller tips immersed 7 ft. :

- 1 per revolution amplitude = ± 6.8 per cent. of mean torque.
- 2 per revolution amplitude = ± 1.8 per cent. of mean torque.
- 4 per revolution amplitude = ± 5.3 per cent. of mean torque.
- 8 per revolution amplitude = trace (not measurable).

With propeller immersed only 90 per cent. :

- 1 per revolution amplitude = ± 4.8 per cent. of mean torque.
- 2 per revolution amplitude = ± 1.6 per cent. of mean torque.
- 4 per revolution amplitude = ± 3.6 per cent. of mean torque.
- 8 per revolution amplitude = ± 0.3 per cent. of mean torque.

The large one per revolution torque variation was considered to be due to the propeller, because an abnormal tooth error in the low speed wheel would have been necessary to account for such a large variation.

With perfect propellers no vibration of once a revolution frequency would be experienced unless the propellers were

damaged in service, and although absolute perfection is not attainable ordinary care in manufacture should suffice to render it difficult to detect any once a revolution disturbance.

As a result of the experiments described in this paper the authors concluded that the torque variation of a marine propeller was not likely to exceed about ± 10 per cent. of the mean torque under any conditions of immersion of the propeller or at any speed of the ship.

It can also be safely assumed that the principal impulse frequency in the case of 4-bladed propellers, whether fitted in single- or in twin-screw vessels, is four impulses per revolution. In the case of 3-bladed propellers, however, the impulse frequency can be taken as three per revolution for twin-screw vessels, but for single-screw installations a six per revolution impulse frequency as well as a three per revolution disturbance must be considered.

In an article entitled "Torsional Vibration Amplitudes in Marine Diesel Installations," *Engineering*, 29th May, 1931, p. 694, Dr. Lockwood Taylor quotes a harmonic torque variation of ± 12 per cent. for a propeller in a single-screw ship with rather extreme wake distribution. He considers that this probably represents the extreme limit of torque variation under normal conditions, and that a twin-screw vessel should show less variation than a single-screw vessel, whilst a 3-bladed propeller should give less variation on a single-screw ship, but possibly more on a twin-screw ship, than a propeller with four blades.

The two per revolution disturbance mentioned above in connection with the 4-bladed propeller in a single-screw ship is probably due to interference between the four blades of the propeller and the stern post and rudder, the latter being virtually equivalent to two stationary blades.

The expression given in the next section for the number of torque variations per revolution when a rotating member with n blades passes a stationary member with n_1 blades can be applied,

i.e.
$$N = \frac{n \cdot n_1}{\text{H.C.F. of } n \text{ and } n_1}.$$

For a 4-bladed propeller passing a rudder (equivalent to two stationary blades),

$$N = \frac{4 \times 2}{2} = 4 \text{ impulses per revolution.}$$

The above expression is of interest where guide vanes or contra propellers are used. For example, if four guide vanes are used in conjunction with a 4-bladed propeller, the principal impulse frequency is obtained as follows:—

$$n = \text{number of propeller blades} = 4,$$

$$n_1 = \text{number of fixed blades} = 6 \text{ (i.e. 4 guide vanes and 2 virtual vanes due to the rudder),}$$

$$\text{H.C.F.} = \text{highest common factor of } n \text{ and } n_1 = 2.$$

Then, assuming that the six vanes are evenly spaced at 60° ,

$$N = \frac{4 \times 6}{2} = 12 \text{ impulses per revolution.}$$

It is also of interest to note that if n and n_1 have no common factor, then, in addition to the above periodic torque, there will be an unbalanced periodic lateral force in any fixed direction through the centre of the propeller hub of frequency $F = n \times (\text{revs. per min.})$.

If, however, there is a common factor this lateral force disappears.

The above considerations indicate that the fitting of guide vanes might result in an appreciable reduction of propeller vibration, provided the number of vanes is such that high impulse frequencies are obtained.

Phasing of Engine and Propeller Torque Variations.—Diagrams (c) and (d) of Fig. 18 show that in marine engine installations the specific vibration amplitude at the propeller is large for the one-node mode of vibration and very small for the two-node mode of vibration.

It is evident, therefore, that a periodic torque at the propeller will be effective in producing vibration corresponding to the one-node mode of vibration, but will have a negligible effect in the case of two-node vibrations.

These diagrams also show that for the one-node mode of vibration all the engine cylinders vibrate with the same amplitude, so that, as already explained, the only unbalanced harmonic torque orders for the engine are the major orders which are all in phase. If the transmission shaft between the engine and the propeller is very flexible compared with the engine crankshaft the oscillating system can be reduced to the simple two-mass system shown at (c) in Fig. 98, which consists of the engine masses at one end of the transmission shaft and the propeller mass at the other end.

- Let J_e = polar moment of inertia of the engine masses,
 J_p = polar moment of inertia of the propeller,
 C = torsional rigidity of the transmission shaft,
 ω_c = phase velocity of the one-node mode of vibration,
 M_{en} = max. value of the n th order harmonic torque of the engine,
 M_{pn} = max. value of the n th order harmonic torque of the propeller.

Then, assuming unit amplitude at the engine, the amplitude at the propeller is $-(J_e/J_p)$.

The equilibrium amplitude at the engine is given by equation (246), viz.,

$$\theta_{oe} = \frac{T_n \cdot A \cdot R \cdot \Sigma a}{\omega_c^2 \Sigma (J \cdot a^2)} \text{radian.} \quad (246)$$

In this case,

$$T_n \cdot A \cdot R \cdot \Sigma a = M_{en} \pm M_{pn}(J_e/J_p) = (M_{en} \cdot J_p \pm M_{pn} \cdot J_e)/J_p,$$

$$\omega_c^2 = \frac{C(J_e + J_p)}{J_e \cdot J_p} \quad [\text{from Equation (16)}]$$

$$\Sigma (J \cdot a^2) = J_e + J_p(J_e/J_p)^2 = J_e(J_e + J_p)/J_p.$$

Hence,
$$\theta_{oe} = \frac{(M_{en} \cdot J_p \pm M_{pn} \cdot J_e)}{C(J_e + J_p)} \times \frac{J_p}{(J_e + J_p)}.$$

This is the equilibrium amplitude at the engine. The equilibrium amplitude of twist between the engine and the propeller, i.e. the total twist in the transmission shaft, is

$$|\theta_o| = (\theta_{oe} - \theta_{op}), \text{ where } \theta_{op} = -\theta_{oe}(J_e/J_p).$$

$$\text{Hence, } |\theta_o| = \theta_{oe} \left(\frac{J_e + J_p}{J_p} \right),$$

$$\text{i.e. } |\theta_o| = \frac{(M_{en} \cdot J_p \pm M_{pn} \cdot J_e)}{C(J_e + J_p)} \text{ radian.} \quad (292)$$

Also f_{so} = equilibrium stress in transmission shaft

$$= \frac{C \cdot |\theta_o|}{Z}, \text{ where } Z = \text{polar moment of resistance of shaft} = \pi \cdot d^3/16 \text{ for a solid shaft of diameter } d,$$

and f_s = maximum vibratory stress in transmission shaft
 $= f_{so} \times (\text{dynamic magnifier}).$

Equation (292) shows that the magnitude of the vibratory stress in the transmission shaft depends on the phase relationship between the engine and propeller torque variations. These relationships are shown in Fig. 98.

For the fundamental or one-node mode of vibration the propeller swings in opposite phase to the engine. Hence for minimum input energy and therefore minimum vibratory stress in the propeller shaft the engine and the propeller harmonic torques must be in phase as shown in the phase and vector diagrams in Fig. 98.

The torque variation curves shown at (a) and (b) in Fig. 98 are the harmonic torques exerted by the propeller on the shaft, i.e. they represent the propeller resistance torques. Since driving and resisting torques act in opposite senses it follows that the engine driving torque is in phase with the propeller resisting torque when the greatest positive value of the engine torque variation occurs at the same instant as the greatest negative value of the propeller resistance torque variation.

The position of, say, No. 1 engine crank when the n th order harmonic component of the engine torque curve has its greatest positive value can be determined from an harmonic analysis of the engine torque curve, as already explained. If this crank is assumed to be placed in this position the corresponding position of the propeller for correct phasing is as follows:—

For the 3rd order component of 3-bladed propellers in twin-screw ships, position Y in Fig. 98.

For the 3rd order component of 3-bladed propellers in single-screw ships, position Z in Fig. 98.

For the 6th order component of 3-bladed propellers in single-screw ships, position Y in Fig. 98.

For the 4th order component of 4-bladed propellers in twin-screw ships, position Y in Fig. 98.

For the 4th order component of 4-bladed propellers in single-screw ships, position Y in Fig. 98.

With correct phasing the equilibrium amplitude of twist in the transmission shaft becomes

$$|\theta_0| = \frac{(M_{sn} \cdot J_p - M_{pn} \cdot J_e)}{C(J_s + J_p)} \quad (293)$$

Since, for the single-node mode of vibration the only unbalanced harmonics of the engine torque curve are the major orders, the engine types to which Equation (293) applies are those having a major order number equal to the number of propeller blades. Thus for 3-bladed propellers this method of reducing the vibration stress in the transmission shaft could be employed with 6-cylinder, 4-stroke cycle engines, or 3-cylinder, 2-stroke cycle engines. In both types the fundamental unbalanced engine harmonic is the 3rd order.

In the case of 4-bladed propellers the method applies to 8-cylinder, 4-stroke cycle engines and 4-cylinder, 2-stroke cycle engines, since both these types have the 4th order harmonic unbalanced.

In steam reciprocating engines the torque curve must be analysed to see if there is a sufficiently large unbalanced harmonic of blade impulse frequency.

It should be noted that for the oil engines,

$$M_{sn} = T_n \cdot A \cdot R \cdot \Sigma a,$$

where T_n = the resultant n th order harmonic component of the tangential effort curve for one cylinder,

A = area of cylinder,

R = crank radius,

Σa = vector sum of ordinates at each cylinder from normal elastic curve, assuming unit amplitude

at free end of crankshaft (if the transmission shaft is very flexible compared with the crankshaft, $\Sigma a =$ the number of cylinders, very nearly).

The foregoing method of determining the position of the propeller blades relative to the engine cranks should be regarded as approximate only because in specific examples peculiarities of wake distribution and of the combustion characteristics of the engine cylinders might cause serious departures from this theoretical method of phasing for minimum vibrational energy. In all cases, therefore, it is desirable to check the phasing by torsigraph tests.

Furthermore, due to the variation of the individual phasing of the engine torque harmonics with engine speed and mean indicated pressure, and the variation of the individual phasing of the propeller harmonics with the speed and trim of the ship, and with the prevailing weather conditions, it follows that the phase relationship between the propeller blades and the engine cranks which is correct for one set of operating conditions is not necessarily the optimum setting for other operating conditions.

For these reasons it is not easy in practice to apply the principle of phasing the propeller and cranks for minimum vibrational energy, except perhaps in the case of strongly marked impulses such as are obtained when the three per revolution impulse from a 3-bladed propeller interferes with the three per revolution torque impulse from a 6-cylinder, 4-stroke cycle engine.

There is therefore a tendency to avoid using a propeller which excites the same fundamental impulse frequency as the engine. When this is done it is, of course, not possible to utilise the propeller impulses as a means for partially cancelling the engine impulses. On the other hand, the possibility of the propeller impulses augmenting the engine impulses is avoided irrespective of the prevailing operating conditions.

Thus, for example, according to this last arrangement, a 3-bladed propeller would not be used with a 6-cylinder, 4-stroke cycle engine or with a 3-cylinder 2-stroke cycle engine.

Similarly, a 4-bladed propeller would not be used with an 8-cylinder, 4-stroke cycle engine, or a 4-cylinder, 2-stroke cycle engine. In steam engine installations a 3-bladed propeller would not be used with an engine having a strong three per revolution component of the torque curve, and a 4-bladed propeller would not be used with an engine having a strong 4th order torque component.

The principles underlying the phasing of the blades of a propeller relative to the engine cranks, so that the vibrational energy is minimised, can also be applied where the driven unit is of a type which has a strongly marked torque harmonic of the same impulse frequency as the corresponding harmonic of the engine torque, e.g. an oil engine driven air-compressor plant. In such cases it is necessary to make an harmonic analysis of the torque curve of the driven unit to determine the amplitude and phase of the relevant harmonic component. The idea already described of arranging a multi-cylinder in-line engine so that the node occurs at the centre of the cylinder group with the cylinders arranged in symmetrical pairs relative to the node and then firing these symmetrically disposed pairs of cylinders simultaneously is, in effect, an application of the phasing principle just discussed.

In geared engine installations or of engines driving through clutches, it is, of course, impossible to fix any phase relationship between the driving and the driven units.

Aero-Engine/Air-Screw Combinations.—Just as in the case of marine propellers the air forces on an air-screw are liable to cause torsional vibration in the shaft system when the airflow is not uniform over the air-screw disc. Such effects would be experienced, for example, with two air-screw discs operating close together, or when the air-screw blades pass close to other bodies such as fuselage, wings, radiators, etc., or when the air-screw shaft is inclined to the direction of flight.

Although these disturbing factors can be expected to produce noticeable effects in severe cases, they are not likely to be dangerous, because the node is usually situated very close to the air-screw, so that the vibrational energy imparted to the shaft by air-screw disturbances is small, and is insignificant

compared with the energy imparted by the engine torque components.

It is of interest in this connection to note that if an air-screw having n blades is mounted directly in front of another air-screw having n_1 blades and the two air-screws rotate in opposite directions at the same speed, the fundamental frequency of the impulses imparted to the shaft is

$$N = \frac{2 \cdot n \cdot n_1}{\text{H.C.F. of } n \text{ and } n_1} \text{ impulses per revolution.}$$

For example, if both air-screws have three blades,

i.e. $n = n_1 = 3$,

then $N = 2 \times 3 \times 3/3 = 6$ impulses per revolution.

If, however, $n = 2$ and $n_1 = 3$,

then $N = 2 \times 2 \times 3/1 = 12$ impulses per revolution.

It should also be noted that in the latter example, since n and n_1 have no common factor (excluding 1), there is a periodic lateral force of the same fundamental frequency as the periodic torque. This lateral force is an additional source of vibration which is not present in the first example.

With regard to the phasing of air-screw blades relative to engine cranks, it is customary in the case of small ungeared in-line engines fitted with 2-bladed air-screws, where the engine is invariably started by hand, to phase the air-screw so that a good leverage can be obtained by pulling on a blade when the engine passes over compression centres. In larger installations where the engine is started mechanically this requirement need not be fulfilled, and in such cases it is desirable to phase the air-screw so that the blades are favourably located relative to the engine cranks for withstanding the explosion shocks originated in the engine cylinders. This is especially so in the case of metal air-screws. The blades are responsive to the explosion shocks originated adjacent to the air-screw, the shocks from the cylinders being cushioned to some extent by structure. If, for example, a blade is located to the adjacent crankthrow the explosion pin tend to produce lateral acceleration rise and descend.

plane of rotation and at right angles to the length of the blade, which may cause very high blade stresses. The stiffness of the crankcase prevents the whole of the explosion force from being applied to the air-screw, and the effect is further reduced if the blade is phased so that its length lies parallel to the adjacent crank-arm.

The problem of the phasing of air-screw blades does not arise, of course, in the case of geared installations.

Engine Direct-Coupled to a Hydraulic Dynamometer.

—Examples of torsional vibration of the shaft systems of engines undergoing bench tests due to periodic impulses originated by rotation of the rotor of a hydraulic dynamometer within its casing are not unknown.

If n = number of cells in each side of the rotor, and n_1 = number of cells in each side of the casing, then

$$N = \frac{n \times n_1}{\text{H.C.F. of } n \text{ and } n_1},$$

where N = number of torque variations per revolution of the rotor,

H.C.F. = highest common factor.

The frequency of the applied impulses is, therefore,

$$F = N \times \text{revs. per min. of rotor.}$$

If n and n_1 have no common factor, then in addition to the above periodic torque there will be an unbalanced periodic lateral force in any fixed direction through the centre of the rotor of fundamental frequency

$$F_1 = (n \times \text{revs. per min.}).$$

It should be noted that if n and n_1 are both even there is no net lateral force.

When both members rotate the frequency of the air-screw shaft can be expressed by the following expression:—

Although the number of impulses per minute when the two members rotate in the same direction is $n + n_1$, the number of impulses per minute when the two members rotate in opposite directions is $n - n_1$.

Thus, if the natural frequency of torsional vibration of this installation is 600 vibs./min., corresponding to a 4th order critical speed at 150 r.p.m., a 6th order critical at 100 r.p.m. and a 12th order critical at 50 r.p.m., the values of the 4th, 6th and 12th order harmonic components corresponding to mean indicated pressures of 82, 48 and 27 lbs. per sq. in. respectively, should be used for calculating the equilibrium amplitudes and stresses when these are intended for the subsequent evaluation of the amplitudes and stresses at resonance.

Another important aspect of the variation of mean indicated pressure with speed is the effect on the magnitudes of the forced vibration amplitudes and stresses at non-resonant speeds. Since any reduction of mean indicated pressure usually causes a corresponding reduction of the magnitudes of the harmonic components, the equilibrium amplitudes are likewise reduced. This in turn implies a reduction of the forced vibration amplitudes and stresses.

Thus a true representation of the resonance curve, corresponding to any given harmonic order, can only be obtained by evaluating the forced vibration amplitudes at each non-resonant speed from the equilibrium amplitude corresponding to the mean indicated pressure at that speed. As a general rule, this method of obtaining the resonance curves is regarded as a refinement, and these curves are usually plotted by multiplying the equilibrium amplitude corresponding to the mean indicated pressure at the resonant speed by the dynamic magnifiers appropriate to each speed. The more accurate method of plotting the resonance curve must, however, be used when it is required to compare the theoretical diagram with torsiongraph measurements at non-resonant speeds.

Aero engines.—Since a similar relationship exists between the torque and speed of a fixed pitch air-screw as between the torque and speed of a marine propeller, it might be thought, at first sight, that the foregoing method of evaluating the vibration amplitudes at reduced speeds could also be used for aero-engine/air-screw combinations. It must be remembered, however, that an aeroplane possesses an additional principal degree of freedom, namely, the ability to rise and descend.

This implies that theoretically any mean indicated pressure from no load to full load can be maintained at all r.p.m. In a marine propeller drive, for example, if full load mean indicated pressure is applied at low r.p.m. there is an immediate increase of r.p.m. until a speed is attained at which the power developed by the engine balances the power absorbed by the propeller, all in accordance with the propeller law. The same result would be obtained in the case of an aero engine coupled to a fixed pitch air-screw and operating under steady conditions in level flight. In both cases the difference between the power absorbed by the propeller or air-screw at low speed and the power which could be developed by the engine at maximum permissible mean indicated pressure is an indication that energy is available for accelerating the power plant to full speed.

In the case of the aero engine, however, even when coupled to a fixed pitch air-screw, it is possible to put the machine into an appropriate climbing attitude which will absorb the power corresponding to maximum permissible mean indicated pressure at any r.p.m. within the operating range of the engine. If the engine is coupled to a variable pitch propeller, and assuming that there is sufficient pitch range, it is possible to maintain the maximum permissible mean indicated pressure in level flight at any r.p.m. within the operating range by an appropriate adjustment of blade pitch. Conversely, by putting a machine with a fixed pitch air-screw into a glide it is possible to reduce the mean indicated pressure below that corresponding to the propeller law, and the same result can be achieved with a variable pitch air-screw in level flight by fining the blade pitch.

A fundamental difference between aircraft and marine engines therefore is that whereas the mean indicated pressure of marine engines operating at low r.p.m. is fixed within fairly narrow limits by the propeller law, the mean indicated pressure of aero engines can be varied over a wide range at each operating speed by alterations in the attitude of the aircraft or by altering the setting of a variable pitch air-screw.

In common with other types of prime mover, however, the mean indicated pressure of an aero engine is limited by the necessity for avoiding overloads. Thus to avoid detonation

the use of full throttle at low r.p.m. is not permissible, whilst the mean indicated pressure of a supercharged engine at rated altitude must not be exceeded at lower altitudes because of mechanical and heat dissipation problems. In general, therefore, the calculation of torsional vibration amplitudes and stresses in aero-engine installations should be based on the following mean indicated pressures.

For a normally aspirated engine, the maximum permissible mean indicated pressure at sea-level should be assumed at all speeds from minimum to maximum cruising r.p.m., and at take-off. Below minimum cruising r.p.m., i.e. at idling and warming-up speeds, the mean indicated pressure determined from the normal air-screw load curve may be used. If a variable pitch air-screw is employed the high pitch load curve should be used.

In supercharged engines the maximum permissible mean indicated pressure at rated altitude should be assumed at all speeds from minimum to maximum cruising r.p.m., whilst at idling and warming-up speeds the mean indicated pressure corresponding to the normal air-screw load curve may be used. It should be borne in mind, however, that in supercharged engines a somewhat higher mean indicated pressure is permitted for short periods during take-off than would be permitted for continuous operation at sea-level, and this higher pressure should be used for determining the torsional vibration amplitudes and stresses at take-off r.p.m.

In the absence of specific data full throttle operation down to 1000 r.p.m. should be assumed.

An important factor which must be taken into account when evaluating the torsional vibration stresses originated by the harmonic components of the torque curves of high-speed engines is the effect of the inertia correction.

Table 54 shows that the 2nd, 3rd and 4th order inertia components have negative values. These are all sine terms, and since the 2nd, 3rd, and 4th order gas pressure sine components all have positive values, it follows that at high rotational speeds the magnitudes of the 2nd, 3rd and 4th order resultant harmonic components for each cylinder may increase when the

mean indicated pressure is reduced, and thus attain their maximum values when the gas pressure is zero.

For this reason it is necessary to investigate the effect of reducing the mean indicated pressure in certain cases. For example, the major 3rd order component of a high-speed 6-cylinder, in-line, 4-stroke cycle engine has a large inertia term. It is therefore possible that when the rotational speed exceeds a certain value the numerical value of the inertia term is greater than that of the gas pressure sine term corresponding to the maximum permissible mean indicated pressure. When this occurs the magnitude of the resultant 3rd order harmonic component increases when the mean indicated pressure is reduced and reaches its maximum value when the inertia term alone is acting. Under these circumstances, therefore, the torsional vibration stresses in an aero-engine installation would be more severe when the air-screw was wind-milling than when it was being driven by the engine.

The same conditions may occur in all types of power plant where it is possible to idle the engine at high rotational speeds and where, under full load, the numerical value of the inertia term at these high rotational speeds is greater than that of the gas pressure sine term. In all such cases it is advisable to calculate the torsional vibration stresses at the relevant speeds, on the assumption that there is no gas pressure in the engine cylinders.

It should also be noted that even when the numerical value of the inertia term is smaller than that of the gas pressure sine term, the magnitude of the resultant harmonic component may still attain its maximum value when the gas pressure in the cylinder is zero. It is only when the numerical value of the inertia term is less than one-half that of the gas pressure sine term that the maximum value of the resultant harmonic component is attained at full load mean indicated pressure.

In a paper entitled "Permissible Amplitudes of Torsional Vibration in Aircraft Engines" (*S.A.E. Preprint*, March, 1939), F. Masi states that the modern high performance aircraft engine requires complete freedom from excessive torsional vibration throughout its normal operating range, extending

from 50 per cent. to 110 per cent. of rated speed, whilst military engines intended for extensive diving manoeuvres should be safe up to possibly 130 per cent. of rated speed.

The most severe engine operating conditions from the point of view of torsional vibration, according to the above statement, are shown in Fig. 99, where rated power and speed refers to take-off conditions.

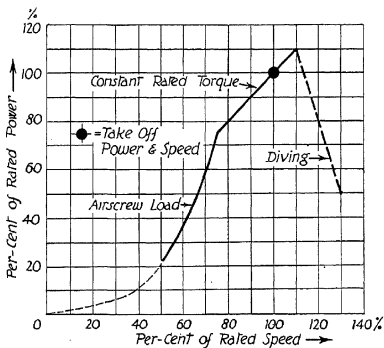


FIG. 99.—Recommended limiting operating conditions for torsional vibration calculations. (Masl.)

Operation beyond the limits shown in this diagram is either prohibited or is impossible with a fixed pitch air-screw.

Automobile Engines.—The undulations of the road and the presence of a gearbox render it possible for an automobile engine to develop a wide range of mean indicated pressure at each operating speed. It is advisable, therefore, to assume full load mean indicated pressure over the whole of the speed range, although in general the engine will never be called upon to run for any length of time at very low r.p.m. with wide open throttle.

*Typical Values of the Full Load Mean Indicated Pressure.**(a) High-Speed, Four-Stroke Cycle, Spark Ignition (Petrol) Engines.*

Automobile engines :	100 to 130 lbs. per sq. in.
Aero engines :	From 140 lbs. per sq. in. for a normally aspirated engine using low octane fuel to 240 lbs. per sq. in. for a fully supercharged engine using high octane fuel.

(b) High-Speed Compression Ignition Oil Engines.

100 to 130 lbs. per sq. in.

(c) Large, Slow-Speed Marine Oil Engines.

4-Stroke cycle, single-acting engines, normally aspirated	90 to 95 lbs. per sq. in.
4-Stroke cycle, single-acting engines, supercharged	120 to 130 lbs. per sq. in.
2-Stroke cycle, opposed-piston engines	85 to 90 lbs. per sq. in.
2-Stroke cycle, single-acting and double-acting engines	80 to 85 lbs. per sq. in.

Examples of Calculations for Equilibrium Amplitudes and Torsional Vibration Stresses at Non-Resonant Speeds.

EXAMPLE 46.—Calculate the equilibrium amplitudes and vibration stresses at non-resonant speeds for the one-node mode of vibration of a 4-stroke cycle, single-acting engine direct coupled to a 275 kw. electrical generator, 6-cylinders, 13½-inch bore × 18-inch stroke, operating at 310 r.p.m. ; firing order, 1-3-5-6-4-2.

The equivalent oscillating system is shown in Fig. 13 ; the one-node frequency calculation in Table 1 ; and the phase and vector diagrams in Fig. 86.

(a) *Equilibrium Amplitudes.*—These are calculated from Equation (248), viz.,

$$\theta_0 = \frac{4100 \cdot D^2 \cdot R \cdot T_n \cdot \Sigma a}{F^2 \cdot \Sigma(J \cdot a^2)} \text{ degrees,} \quad (248)$$

where D = diameter of cylinder in inches = 13.5 ins.,
 R = crank radius in inches = 9 ins.,
 T_n = n th order resultant harmonic component of tangential effort curve for one cylinder in lbs. per sq. in. of piston area, from Table 60,*
 Σa = vector sum for one-node vibrations, from Fig. 86,
 F = one-node frequency of torsional vibration, 2520 vibs./min., from Table 1,
 $\Sigma(J \cdot a^2)$ = effective moment of inertia of whole system referred to free end of crankshaft in lbs.-ins. sec.².

The value of $\Sigma(J \cdot a^2)$ is obtained from columns D and \bar{F} of the frequency tabulation, Table 1 (see next page).

Hence,

$$\theta_0 = \frac{4100 \times 13.5^2 \times 9 \times T_n \cdot \Sigma a}{2520 \times 2520 \times 570} \frac{T_n \cdot \Sigma a}{538} \text{ degrees.}$$

Table 66 gives the values of the equilibrium amplitudes and equilibrium stresses for orders $5\frac{1}{2}$ to 12. The values for orders less than $5\frac{1}{2}$ have not been included, because these critical speeds are well above the normal operating speed.

The equilibrium stresses are obtained from the equilibrium amplitudes by multiplying the latter by the maximum stress

* Strictly speaking, the values of T_n corresponding to the mean indicated pressure at each speed as determined from the generator load characteristics should be used instead of the values given in Table 60, which are for a constant mean pressure corresponding to full load conditions. The mean pressure at reduced speeds and therefore the values of T_n are smaller than the full load values. Hence the low speed amplitudes and stresses in Table 66 are over-estimated. Since an electrical generator is essentially a constant speed machine, however, the more refined method need only be employed if there is an unduly severe critical in the lower speed range which has to be negotiated when starting or stopping the engine.

for one degree deflection at the free end of the crankshaft given in column K of Table 1, viz. ± 7600 lbs. per sq. in. per degree.

The stresses so calculated are the maximum stresses, and they occur at the nodal point, where the slope of the normal elastic curve is a maximum. If required, the stress at any other point in the shaft system can be obtained by multiplying the equilibrium amplitudes by the stress for one degree deflection given in column K of Table 1 corresponding to the point in question, e.g. the stresses at No. 3 cylinder are obtained by multiplying the equilibrium amplitudes by 5040.

EFFECTIVE MOMENT OF INERTIA.

One-Node Frequency.

Mass.	J , Col. D of Table 1.	a , Col. F of Table 1.	a^2 .	$(J \cdot a^2)$.
No. 1 cyl. .	165	1.0000	1.0000	165.0
No. 2 cyl. .	165	0.9430	0.8900	147.0
No. 3 cyl. .	165	0.8325	0.6930	114.5
No. 4 cyl. .	165	0.6745	0.4540	75.0
No. 5 cyl. .	165	0.4780	0.2285	37.7
No. 6 cyl. .	165	0.2540	0.0645	10.6
Generator .	23,500	-0.0293	0.0009	20.2
$\Sigma(J \cdot a^2) = 570.0$				
				<i>lbs.-ins. sec.².</i>

It should be noted that the specific stresses in column K of Table 1 are based on a shaft diameter of $8\frac{1}{4}$ ins., which is the actual diameter of the shaft at the nodal point in this installation. If the stress at any other point is being investigated, care should be taken to allow for any difference in shaft diameter, as follows:—

$$f_s = f_{s1} \cdot \left(\frac{d_1}{d}\right)^3,$$

where

$$f_s = \text{actual stress for diameter } d,$$

$$f_{s1} = \text{stress based on diameter } d_1.$$

The vibration stress at any non-resonant speed N is obtained from the values of the equilibrium stresses by multiplying the latter by the dynamic magnifier given in Equation (234),

$$\text{i.e. Vibration stress at } N \text{ r.p.m.} = f_{s0} \times \frac{1}{1 - \frac{N^2}{N_c^2}}$$

TABLE 66.

EQUILIBRIUM AMPLITUDES AND EQUILIBRIUM STRESSES.

One-Node Frequency, $F = 2520 \text{ Vibs./Min.}$

Harmonic Order. n	Critical Speed. N_c R.P.M.	Res. Harm. Compt. per Cyl. T_n Lbs./Sq. In.	Vector Sum. Σa	Res. Harm. Compt. all Cyls. $T_n \cdot \Sigma a$	Equilibrium Amplitude. θ_0 Degrees.	Equilibrium Stress. f_{s0} Lbs./Sq. In.
5½	459	± 6.0	1.090	± 6.540	± 0.01215	± 92.50
6	420	4.5	4.182	18.800	0.03500	266.00
6½	388	3.5	1.090	3.820	0.00710	54.00
7	360	3.0	0.223	0.669	0.00124	9.40
7½	336	2.5	0.123	0.307	0.00057	4.33
8	315	2.0	0.223	0.446	0.00083	6.30
8½	297	1.5	1.090	1.635	0.00303	23.00
9	280	1.0	4.182	4.182	0.00777	59.10
9½	265	0.8	1.090	0.872	0.00162	12.30
10	252	0.7	0.223	0.156	0.00029	2.20
10½	240	0.6	0.123	0.074	0.00014	1.06
11	229	0.5	0.223	0.112	0.00021	1.60
11½	219	0.4	1.090	0.436	0.00081	6.15
12	210	0.3	4.182	1.255	0.00233	17.70
	$\frac{F}{n}$	Table 60	Fig. 86		$\frac{T_n \cdot \Sigma a}{538}$	7600 . θ

Values of the dynamic magnifier, $\frac{1}{1 - \frac{N^2}{N_c^2}}$, corresponding to

different values of the frequency ratio N/N_c are given in Table 51, from which the vibration stress at any non-resonant speed may be determined.

For example, the vibration stresses at various speeds for the 9th order are as follows :—

$$f_{90} = \pm 59.1 \text{ lbs./sq. in. for 9th order (Table 66),}$$

$$N_c = 280 \text{ r.p.m. for 9th order critical.}$$

R.P.M. N.	N/N _c .	Dynamic Magnifier. (Table 51.)	Vibration Stress. f_s Dyn. Mag. $\times f_{90}$.
140	0.5	1.34	± 79.1 lbs./sq. in.
168	0.6	1.56	92.1
196	0.7	1.96	116.0
224	0.8	2.78	164.0
252	0.9	5.26	310.0
308	1.1	4.76	281.0
336	1.2	2.27	134.0
364	1.3	1.45	85.6
392	1.4	1.04	61.6
420	1.5	0.80	47.3

The values given in the last column of the foregoing table may be plotted to give the flanks of a resonance curve similar to that shown in Fig. 75, and similar curves may be obtained for other orders from the corresponding values of N_c and f_{90} .

EXAMPLE 47.—Marine Installation.—Calculate the equilibrium amplitudes and vibration stresses at non-resonant speeds for the one- and two-node frequencies of a 4-stroke cycle, single-acting marine oil engine. Six cylinders, 620 mm. bore \times 1300 mm. stroke, developing 2750 B.H.P. at 138 r.p.m. Firing order 1-4-2-6-3-5.

The equivalent oscillating system is shown in Fig. 15; the one-node and the two-node frequency calculations in Tables 3 and 4 respectively; and the phase and vector diagrams in Fig. 87.

A. One-Node Frequency Calculations.—Since in this example there is a long length of intermediate shafting between the engine and the propeller, the two-mass method of calculating the equilibrium stresses can be employed without much error.

For steel shafts the equilibrium stresses are given by Equations (240) or (241) in cases where the system is subjected to a single harmonically varying torque. When there are several cylinders, each having a series of harmonically varying components of the torque curve, these equations are modified as follows:—

$$f_{so} = \frac{4 \cdot D^2 \cdot R \cdot T_n \cdot \Sigma a}{d^3} \left(\frac{J_p}{J_e + J_p} \right) \quad (294)$$

when R and d are in inches,

$$f_{so} = \frac{D^2 \cdot R \cdot T_n \cdot \Sigma a}{36} \left(\frac{J_p}{J_e + J_p} \right) \quad (295)$$

when R and d are in feet.

In these expressions

f_{so} = equilibrium stress in lbs. per sq. in.,

D = diameter of cylinder in inches,

R = crank radius, unit as specified above,

T_n = n th order harmonic component of tangential effort curve in lbs. per sq. in. of cylinder area,

Σa = vector sum for n th order,

d = diameter of shaft at node, unit as specified above,

J_e = moment of inertia of engine masses, including fly-wheel if fitted,

J_p = moment of inertia of propeller. (Including allowance for entrained water as explained in Chapter 3.)

In the present example it is convenient to have R and d in feet, i.e. to employ Equation (295).

Hence, $D = 620 \text{ mm.} = 24.4 \text{ ins.},$

$R = 650 \text{ mm.} = 2.13 \text{ ft.},$

$T_n =$ values from Table 60,

$\Sigma a =$ values from Fig. 87 for one-node vibs.,

$d = 1 \text{ ft.},$

$J_e = 8.175 \text{ tons-ft. sec.}^2$ (from Table 3),

$J_p = 1.97 \text{ tons-ft. sec.}^2$ (from Table 3),

$$\begin{aligned} \text{i.e. } f_{so} &= \frac{24.4^2 \times 2.13 \times T_n \times \Sigma a}{36 \times 1^3} \left(\frac{1.97}{10.145} \right) \\ &= 6.85 \cdot T_n \Sigma a \text{ lbs. per sq. in.} \end{aligned}$$

Table 67 gives the values of the equilibrium stresses and amplitudes for orders $\frac{1}{2}$ to 6, the equilibrium amplitudes being obtained from the equilibrium stresses by dividing the latter by the maximum stress for one degree deflection at the free end of the crankshaft given in column K of Table 3, i.e. 3260 lbs. per sq. in.

TABLE 67.

EQUILIBRIUM AMPLITUDES AND EQUILIBRIUM STRESSES.

One-Node Frequency, $F = 165.5$ Vibs./Min.

Harmonic Order.	Critical Speed.	Res. Harm. Compt. per Cyl.	Vector Sum.	Res. Harm. Compt. all Cyls.	Equilibrium Amplitude.	Equilibrium Stress.
"	N_c R.P.M.	T_n Lbs./Sq. In.	Σa	$T_n \cdot \Sigma a$	θ_0 Degrees.	f_{θ_0} Lbs./Sq. In.
$\frac{1}{2}$	331	40	0.048	1.920	± 0.00404	± 13.15
1	166	40	0.024	0.960	0.00202	6.57
$1\frac{1}{2}$	110	40	0.179	7.160	0.01500	49.00
2	83	35	0.024	0.840	0.00176	5.75
$2\frac{1}{2}$	66	30	0.048	1.440	0.00303	9.87
3	55	25	5.781	144.500	0.30400	990.00
$3\frac{1}{2}$	47	20	0.048	0.960	0.00202	6.57
4	41	15	0.024	0.360	0.00076	2.47
$4\frac{1}{2}$	37	10	0.179	1.790	0.00375	12.25
5	33	8	0.024	0.192	0.00040	1.31
$5\frac{1}{2}$	30	6	0.048	0.288	0.00060	1.97
6	28	4.5	5.781	26.000	0.05450	178.00
	F/n	Table 60	Fig. 87		$f_{\theta_0}/3260$	$6.85 \cdot T_n \cdot \Sigma a$

The equilibrium stresses are the maximum stresses occurring at the node, and the equilibrium amplitudes are the amplitudes at the free end of the crankshaft.

The equilibrium amplitudes and stresses may also be obtained from Equation (247) or (248).

In the present example it is convenient to express R in feet and J in tons-ft. sec.², so that Equation (247) applies—

$$\theta_0 = \frac{1.83 \cdot D^2 \cdot R \cdot T_n \cdot \Sigma a}{F^2 \cdot \Sigma(J \cdot a^2)} \text{ degrees,} \quad (247)$$

- where D = diameter of cylinder in inches = 24.4 ins.,
 R = crank radius in feet = 2.13 ft.,
 T_n = n th order harmonic component of tangential effort curve for one cylinder, lbs./sq. in.,
 Σa = n th order vector sum,
 F = one-node frequency = 165.5 vibs./min., from Table 3,
 $\Sigma(J \cdot a^2)$ = effective moment of inertia of system referred to free end of crankshaft, in tons-ft. sec.².

TABLE 68.
EFFECTIVE MOMENT OF INERTIA—MARINE INSTALLATION.

Mass.	One-Node Vibs.				Two-Node.		
	J, Col. D. (Table 3.)	a, Col. F. (Table 3.)	a ² .	(J . a ²).	a, Col. F. (Table 4.)	a ² .	(J . a ²).
No. 1 cyl.	1.6350	1.0000	1.0000	1.6350	1.0000	1.0000	1.6350
No. 2 cyl.	0.8175	0.9943	0.9860	0.8075	0.7748	0.5990	0.4900
No. 3 cyl.	1.6350	0.9858	0.9710	1.5900	0.4626	0.2140	0.3500
No. 4 cyl.	1.6350	0.9541	0.9100	1.4900	-0.4764	0.2260	0.3695
No. 5 cyl.	0.8175	0.9346	0.8720	0.7125	-0.7854	0.6175	0.5050
No. 6 cyl.	1.6350	0.9124	0.8325	1.3600	-1.0064	1.0120	1.6500
Propr. .	1.9700	-4.0076	16.0600	31.6500	0.0210	0.0004	0.0008
			$\Sigma(J \cdot a^2) = 39.2450$ tons-ft. sec. ²			$\Sigma(J \cdot a^2) = 5.0003$ tons-ft. sec. ²	

$\Sigma(J \cdot a^2)$ is obtained from columns D and F of Table 3, as shown in Table 68 above.

$$\text{Hence, } \theta_0 = \frac{1.83 \times 24.4^2 \times 2.13 \times T_n \cdot \Sigma a}{165.5 \times 165.5 \times 39.2450}$$

$$- \frac{T_n \Sigma a}{464} \text{ degrees at free end of crankshaft.}$$

The equilibrium stress is obtained by multiplying the equilibrium amplitude by the maximum stress per degree in column K of Table 3,

$$\text{i.e. } f_{so} = \frac{T_n \Sigma a}{464} \times 3260 = 7.03 \cdot T_n \cdot \Sigma a \text{ lbs./sq. in.}$$

This value is only 3 per cent. greater than the value obtained by applying Equation (295), viz. $f_{s0} = 6.85 \cdot T_n \Sigma a$, so that the values tabulated in Table 67 are confirmed by applying Equation (247).

In the case of marine installations with the machinery at the after end of the vessel, i.e. with a short stiff shaft between the engine and the propeller, the agreement may not be so good as in the present example, and in such cases Equation (247) or (248) should be used in preference to Equation (294) or (295).

Propeller Torque Variation.—In the present example the engine drives a 4-bladed propeller, so that there is a fourth order torque variation due to the passage of the propeller blades through the varying wake.

The equilibrium stress may be obtained by modifying Equation (240) as follows:—

$$f_{s0} = \pm \frac{5 \cdot 1 \cdot T_p}{d^3} \cdot \left(\frac{J_e}{J_e + J_p} \right) \text{ lbs./sq. in.,}$$

where T_p = maximum value of propeller torque variation in lbs.-ins.,

d = diameter of shaft at node in inches,

J_e and J_p = moments of inertia of engine masses and of propeller, in lbs.-in. sec.², or tons-ft. sec.².

The engine develops 2750 B.H.P. at 138 r.p.m., and the 4th order critical speed is at 41 r.p.m.

Hence, B.H.P. at 41 r.p.m. = $2750 \left(\frac{41}{138} \right)^3 = 72$ B.H.P.

$$\begin{aligned} \text{Mean torque} &= \frac{\text{B.H.P.} \times 33000}{2 \cdot \pi \cdot N} \\ &= \frac{72 \times 33000}{2 \cdot \pi \cdot 41} = 9250 \text{ lbs.-ft.} \end{aligned}$$

The propeller torque variation may be taken to be 10 per cent. of the mean torque,

$$\begin{aligned} \text{i.e. 4th order propeller torque} &= \pm 925 \text{ lbs.-ft.,} \\ \text{variation} &= \pm 11100 \text{ lbs.-ins.} \end{aligned}$$

Also, $d = 12$ ins.; $J_e = 8.175$ tons-ft. sec.²; and $J_p = 1.97$ tons-ft. sec.² (from Table 3).

$$\begin{aligned} \text{Hence, } f_{so} &= \pm \frac{5.1 \times 11100}{12^3} \left(\frac{8.175}{8.175 + 1.97} \right) \\ &= \pm 26.4 \text{ lbs./sq. in.} \end{aligned}$$

(Note.—The equilibrium stress for the 4th order engine torque variation is only ± 2.47 lbs. per sq. in. from Table 67. Hence, the principal cause of 4th order one-node vibrations is the propeller torque variation.)

B. *Two-Node Frequency Calculations.*—The equilibrium amplitudes and stresses for the two-node mode of vibration are obtained from Equation (247) or (248). In the present example it is convenient to express R in feet, and J in tons-ft. sec.², so that Equation (247) applies, viz.,

$$\theta_0 = \frac{1.83 \cdot D^2 \cdot R \cdot T_n \cdot \Sigma a}{F^2 \cdot \Sigma(J \cdot a^2)} \text{ degrees, . . . (247)}$$

where D = diameter of cylinder in inches = 24.4 ins.,

R = crank radius in feet = 2.13 ft.,

T_n = n th order harmonic component of tangential effort curve for one cylinder in lbs./sq. in. (Table 60),

Σa = n th order vector sum (Fig. 87),

F = two-node frequency = 1041 vibs./min. (Table 4),

$\Sigma(J \cdot a^2)$ = effective moment of inertia referred to free end of crankshaft

= 5.0003 tons-ft. sec.² (Table 68).

$$\begin{aligned} \text{Hence, } & \frac{1.83 \times 24.4^2 \times 2.13 \times T_n \cdot \Sigma a}{1041 \times 1041 \times 5} \\ &= \frac{T_n \cdot \Sigma a}{2330} \text{ degrees.} \end{aligned}$$

The equilibrium stress is obtained by multiplying the equilibrium amplitude by the maximum stress per degree from column K of Table 4, viz. $\pm 18,270$ lbs. per sq. in.,

$$\text{i.e. } f_{so} = \frac{T_n \cdot \Sigma a}{2330} \times 18270$$

$$= 7.83 \cdot T_n \cdot \Sigma a \text{ lbs. per sq. in.}$$

Values of θ_0 and f_{so} for orders 6 to 12 are given in Table 69.

The vibration stresses at any non-resonant speed for any given order may be obtained by multiplying the equilibrium stress for that order by the appropriate dynamic magnifier from Table 51.

TABLE 69.

EQUILIBRIUM AMPLITUDES AND EQUILIBRIUM STRESSES.

Two-Node Frequency, $F = 1041$ Vibs./Min.

Harmonic Order. n	Critical Speed. N_c R.P.M.	Res. Harm. Compt. per Cyl. T_n Lbs./Sq. In.	Vector Sum. Σa	Res. Harm. Compt. all Cyls. $T_n \Sigma a$	Equilibrium Amplitude. θ_0 Degrees.	Equilibrium Stress. f_{80} Lbs./Sq. In.
6	174	4.5	0.031	0.1395	± 0.000060	± 1.096
6½	160	3.5	0.029	3.2510	0.001395	25.455
7	149	3.0	0.007	0.0210	0.000009	0.164
7½	139	2.5	4.506	11.3000	0.004850	88.500
8	130	2.0	0.007	0.0140	0.000006	0.110
8½	123	1.5	0.929	1.3950	0.000600	10.960
9	116	1.0	0.031	0.0310	0.000013	0.243
9½	110	0.8	0.929	0.7430	0.000319	5.830
10	104	0.7	0.007	0.0049	0.000002	0.038
10½	99	0.6	4.506	2.7100	0.001160	21.200
11	95	0.5	0.007	0.0035	0.000001	0.027
11½	91	0.4	0.929	0.3720	0.000160	2.930
12	87	0.3	0.031	0.0093	0.000004	0.073
	F/n	Table 60	Fig. 87		$f_{80}/18270$	$7.83 \cdot T_n \cdot \Sigma a$

For example, the vibration stresses at non-resonant speeds for $7\frac{1}{2}$ order two-node vibrations are

$$f_{80} = \pm 88.5 \text{ lbs. per sq. in., from Table 69,}$$

$$N_c = 139 \text{ r.p.m. for } 7\frac{1}{2} \text{ order critical.}$$

The values given in the last column of the following table may be plotted to give the flanks of a resonance curve similar to that shown in Fig. 75, and similar curves may be obtained for other orders from corresponding values of N_c and f_{80} .

R.P.M.	N/N _c	Dyn. Magn. (Table 51.)	Vibration Stress, $f_s = \text{Dyn. Magn.} \times f_{80}$.
69	0.5	1.34	± 119
83	0.6	1.56	138
97	0.7	1.96	174
111	0.8	2.78	246
125	0.9	5.26	466
153	1.1	4.76	421
167	1.2	2.27	201
181	1.3	1.45	128
195	1.4	1.04	92
208	1.5	0.80	71

The vibration stresses in the foregoing table are calculated on the assumption that the mean indicated pressure remains constant and equal to the full load value over the whole of the speed range, whereas, to be strictly accurate, the mean indicated pressure corresponding to the propeller law should have been used.

If this refinement is introduced the table is modified as follows:—

The full load M.I.P. and M.B.P. are 130 and 110 lbs. per sq. in. respectively, these values corresponding to 2750 B.H.P. at 138 r.p.m.

The mean friction pressure is therefore 20 lbs. per sq. in. The mean indicated pressures at speeds differing from 138 r.p.m. can therefore be calculated in the manner already explained and the revised vibration stresses are then obtained as shown in the following table:—

R.P.M.	M.B.P.	M.F.P.	M.I.P.	T _n .	T _n Σa.	f ₈₀ .	f _s .
138	110	20	130	—	—	—	—
69	27	20	47	2.4	10.8	± 84.5	± 113
83	39	20	59	2.4	10.8	84.5	132
97	54	20	74	2.3	10.4	81.5	160
110	69	20	89	2.2	9.9	77.5	216
124	88	20	108	2.1	9.5	74.3	392
152	132	20	152	1.8	8.1	63.3	302

Note.— $\Sigma a = 4.506$ for 7.5 order, from Table 69.

T_n is obtained from Fig. 83A.

$f_{s0} = 7.83 T_n \Sigma a$, as before.

$f_s = \text{dyn. mag.} \times f_{s0}$; the dynamic magnifier being obtained from Table 51.

Above 138 r.p.m. the mean indicated pressure reaches unattainable values.

EXAMPLE 48.—Calculate the equilibrium amplitudes and stresses for the system shown in Fig. 100, i.e. a triple expansion steam engine direct coupled to a marine propeller.

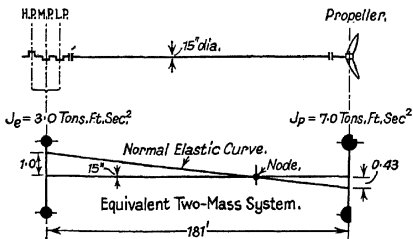


FIG. 100.—Marine steam engine installation.

The engine dimensions are: H.P. cylinder, 26-inch diameter; M.P. cylinder, 45-inch diameter; L.P. cylinder, 77-inch diameter; 54-inch stroke, developing 3000 I.H.P. at 70 r.p.m.

In this example there is a long length of shafting between the engine and the propeller, so that the system may be reduced to the equivalent two-mass system shown in Fig. 100 without much error.

For one-node vibrations the engine masses vibrate with practically equal amplitudes. Hence, only the major orders need to be considered, i.e. the 3rd, 6th, etc., orders. All other orders very nearly cancel.

Natural Frequency of System.—This is obtained from Equation (229)—

$$F = 9.55 \sqrt{\frac{C(J_e + J_p)}{J_e \cdot J_p}},$$

where C = torsional rigidity of shaft = $G \cdot I_p$

$$I_p = \frac{\pi \cdot d^4}{32} = \frac{\pi \times 1.25^4}{32} = 0.239 \text{ ft.}^4 \text{ units,}$$

i.e. $C = \frac{772000 \times 0.239}{181} = 1020 \text{ tons-ft. per radian.}$

Hence, $F = 9.55 \sqrt{\frac{1020(3 + 7)}{3 \times 7}} = 210 \text{ vibs./min.}$

and $N_3 = 210/3 = 70 \text{ r.p.m. for 3rd order}$
 $= 210/6 = 35 \text{ r.p.m. for 6th order.}$

Resultant Harmonic Torque.—Since the harmonic components of the engine torque curve for each cylinder are in phase for the major orders, and since in this example all cylinders vibrate with very nearly equal amplitudes, the resultant harmonic torque for the whole group of cylinders is the sum of the torques due to each cylinder.

The 3rd and 6th order harmonic torques are therefore obtained from the factors given in Table 60 as follows:—

Cylinder.	Area of Cylinder. Sq. In.	3rd Order.		6th Order.	
		Factor from Table 60. Lbs./Sq. In.	Harmonic Tangential Effort. Lbs.	Factor from Table 60. Lbs./Sq. In.	Harmonic Tangential Effort. Lbs.
H.P.	532	± 12.0	± 6384	± 3.0	± 1596
M.P.	1590	4.0	6360	1.0	1590
L.P.	4660	1.3	6058	0.3	1398
Total tan. effort for all Cylinders = ± 18,802 lbs.					± 4584 lbs.

Equilibrium Amplitudes.—These are obtained from Equation (232),

$$\text{i.e. } *|\theta_0| = \frac{|T_n| \cdot R}{C} \cdot \left(\frac{J_p}{J_e + J_p} \right) \text{ radians,}$$

where $|T_n|$ = tangential effort for all cylinders in tons

= 8.4 tons for 3rd order

= 2.05 tons for 6th order,

R = crank radius in feet = 2.25 ft.,

C = torsional rigidity of shaft in tons-ft. per radian

= 1020,

J_e and J_p = moments of inertia of masses

= 3 and 7 tons-ft. sec.² respectively (see Fig. 100).

Hence,

$$|\theta_0| = \pm \frac{8.4 \times 2.25 \times 7}{1020 \times 10} = \pm 0.013 \text{ radian for 3rd order.}$$

Similarly, $|\theta_0| = \pm 0.00317$ radian for 6th order.

Equilibrium Stresses.—These are obtained from Equation (241),

$$\text{i.e. } f_{s0} = \frac{79.3 \cdot |T_n| \cdot R}{d^3} \left(\frac{J_p}{J_e + J_p} \right) \text{ lbs. per sq. in.,}$$

where d = diameter of shaft at node in feet = 1.25 ft.

$$\text{Hence, } f_{s0} = \pm \frac{79.3 \times 8.4 \times 2.25 \times 7}{1.25^3 \times 10}$$

$$= \pm 538 \text{ lbs. per sq. in. for 3rd order.}$$

Similarly, $f_{s0} = \pm 131$ lbs. per sq. in. for 6th order.

The vibration stresses at any non-resonant speed may be obtained from the equilibrium stresses by multiplying the latter by the dynamic magnifiers given in Table 51.

The foregoing calculations are based on the assumption that, although for any given order the magnitudes of the harmonic components differ for the various cylinders, the position of the respective crankpins relative to top dead centre, when the harmonic components attain their maximum ampli-

* $|\theta_0|$ is the equilibrium amplitude of twist, i.e. the angular deflection between the engine masses and the propeller.

tudes, is the same for all cylinders. It has already been explained that, in general, this condition is not fulfilled in the case of reciprocating steam engines. The differences in phase are, however, usually small, so that the assumption of identical phasing is permissible for a preliminary analysis. The phase relationships should be taken into account in the manner previously described if the preliminary investigation shows that a more detailed analysis is desirable.

The calculations also assume that full load mean indicated pressure is maintained over the whole of the speed range. Since, in this example, the 3rd order critical speed happens to coincide with the full load operating speed this procedure is correct for calculating the equilibrium amplitude and stress at the 3rd order critical speed. It is not accurate for speeds above and below the 3rd order critical speed where, strictly speaking, the magnitudes of the harmonic components corresponding to mean indicated pressures determined according to the propeller law should be used. For example, the equilibrium amplitude and stress at the 6th order critical speed, i.e. at 35 r.p.m., is over-estimated in the foregoing calculations to the following extent:—

$$\text{Since } (M.I.P.) = (M.B.P.) + (M.F.P.),$$

and assuming a mechanical efficiency at full load, i.e. at 70 r.p.m., of 90 per cent., hence, at full load,

$$M.B.P. = 0.9 (M.I.P.), \text{ and } M.F.P. = 0.1 (M.I.P.).$$

At the sixth order critical speed, i.e. at 35 r.p.m., therefore,

$$(M.B.P.)' = 0.9 (M.I.P.) (35/70)^2 = 0.225 (M.I.P.),$$

$$\text{i.e. } (M.I.P.)' = 0.225 (M.I.P.) + 0.1 (M.I.P.) = 0.325 (M.I.P.).$$

The magnitude of the harmonic component is approximately proportional to the M.I.P.

Hence, if $|T_n|$ = 6th order tangential effort at 70 r.p.m.
(i.e. the value assumed in the foregoing calculations),

$$|T_n'| = 6\text{th order tangential effort at 35 r.p.m.} \\ \text{(i.e. at the 6th order critical speed),}$$

$$\text{then } |T_n'|/|T_n| = (M.I.P.)'/(M.I.P.) = 0.325.$$

The equilibrium amplitude and stress is directly proportional to the magnitude of the harmonic component.

Hence, at the 6th order critical speed, i.e. at 35 r.p.m.,

$$|\theta_0| = 0.325 \times 0.00317 = \pm 0.00103 \text{ for 6th order,}$$

$$f_{s0} = 0.325 \times 131 = \pm 42.5 \text{ lbs. per sq. in.}$$

An excellent analysis of the tangential effort diagrams for reciprocating steam engines is given in a paper by F. P. Porter, *Trans. American Soc. of Mech. Engs.*, APM-51-22.

EXAMPLE 49.—Assuming that the system shown in Fig. 100 employs a 3-bladed propeller giving a propeller torque variation of ± 10 per cent. of the mean torque, calculate the equilibrium amplitude and stress at the 3rd order critical speed, i.e. at 70 r.p.m. (a) when the propeller is correctly phased relative to the engine cranks; and (b) when the propeller is incorrectly phased relative to the engine cranks.

Propeller Torque Variation.—The engine shown in Fig. 100 develops 3000 I.H.P. at 70 r.p.m.

Assuming a mechanical efficiency of 90 per cent. and a propeller torque variation of ± 10 per cent., the maximum amplitude of the propeller torque variation is

$$M_{pn} = \pm \frac{0.1(\text{B.H.P.} \times 33000)}{2 \cdot \pi \cdot N} = \pm \frac{0.1 \times 0.9 \times 3000 \times 33000}{2 \times 3.1416 \times 70}$$

$$= \pm 20,250 \text{ lbs.-ft.}$$

$$= \pm 9.04 \text{ tons-ft.}$$

The 3rd order harmonic torque due to the engine is

$$M_{en} = \pm |T_n| \cdot R, \quad \text{where } |T_n| = \pm 18,802 \text{ lbs. and}$$

$$R = 2.25 \text{ ft., from Example 48,}$$

i.e. $M_{en} = \pm 18,802 \times 2.25 = \pm 42,300 \text{ lbs.-ft.}$

$$= \pm 18.9 \text{ tons-ft.}$$

Equilibrium Amplitude.

From Equation (292)

$$|\theta_0| = \frac{(M_{en} \cdot J_p \pm M_{pn} \cdot J_e)}{C(J_e + J_p)},$$

where, in this example,

$$\left. \begin{aligned} J_p &= 7.0 \text{ tons-ft. sec.}^2 \\ J_e &= 3.0 \text{ tons-ft. sec.}^2 \\ C &= 1020 \text{ tons-ft./radian} \end{aligned} \right\} \text{from Example 48.}$$

$$\begin{aligned} \text{Hence, } |\theta_o| &= \frac{18.9 \times 7 \pm 9.04 \times 3}{1020(3 + 7)} = (132.3 \pm 27.12)/10200 \\ &= 0.0156 \text{ or } 0.0103 \text{ radian.} \end{aligned}$$

The equilibrium amplitude is therefore ± 0.0103 radian with correct phasing and ± 0.0156 radian with incorrect phasing.

$$\text{Equilibrium Stress.}—f_{so} = C \cdot |\theta_o|/Z.$$

The stress will be expressed in lbs. per sq. in. if C is expressed in lbs.-in. per radian, and Z in ins.³,

$$\text{i.e. } C = 1020 \text{ tons-ft./radian} = 27,400,000 \text{ lbs.-ins./radian.}$$

The shaft diameter is 15 ins. at the node.

$$\text{Hence } Z = \pi \cdot d^3/16 = 663 \text{ ins.}^3,$$

$$\begin{aligned} \text{i.e. } f_{so} &= \pm 27,400,000 \times |\theta_o|/663 = \pm 41,300 |\theta_o| \\ &= \pm 41,300 \times 0.0103 = \pm 426 \text{ lbs. per sq. in. with} \\ &\quad \text{correct phasing} \\ &= \pm 41,300 \times 0.0156 = \pm 645 \text{ lbs. per sq. in. with} \\ &\quad \text{incorrect phasing.} \end{aligned}$$

These values compare with the value of ± 538 lbs. per sq. in. for the 3rd order engine torque variation acting alone, and show that the forced vibration stresses with the propeller correctly phased are over 30 per cent. less than those which occur when the propeller is incorrectly phased.

Forced Vibration Amplitudes.—The amplitudes of forced vibration at any point in a complex system at speeds above or below a critical speed, where damping can be neglected, may be obtained by the tabulation method described in Chapter 2, for it can be shown that the system as a whole vibrates with the same frequency as the forcing torque, and that as for free or natural vibration each mass is at one of its extreme positions of displacement at the same instant as the remaining masses.

The method is best described with the aid of one or two simple examples.

Two-Mass Systems.—A simple two-mass system is shown at (I) in Fig. 101. In this system the two masses have the

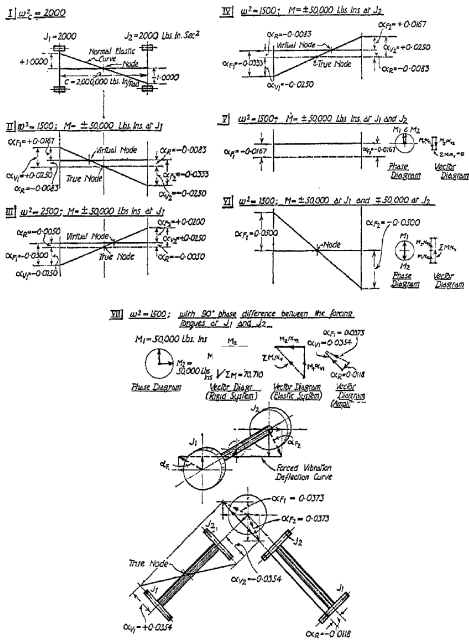


FIG. 101.—Forced Vibration Amplitudes. Two-mass system.

same polar moments of inertia, so that there is only one principal mode of free vibration, the node being situated

midway between the masses. Assuming that a periodic torque of magnitude $\pm 50,000$ lbs.-ins. is applied to the left-hand mass J_1 , at a frequency of 370 cycles per minute, determine the forced vibration amplitudes.

Natural Frequency.—The natural frequency of the system is given by Equation 17, viz.,

$$F_e = 9.55\sqrt{2 \cdot C/J} = 9.55\sqrt{2 \times 2,000,000/2000} \\ = 427 \text{ vibs./min.},$$

or $\omega_e^2 = 2000$.

Tabulation Method.—The forced vibration tabulation is given at (i) in Table 70 (pp. 628-9), which is built-up as follows:—

Column A.—Corresponds to column A of Table 1, and contains a description of the various masses in the oscillating system.

Column B.—Corresponds to column D of Table 1, and contains the polar moments of inertia of the masses.

Column C.—Corresponds to column E of Table 1, and contains the maximum acceleration torques due to vibration of the masses with unit amplitude, at the frequency of the forcing impulses.

The frequency of the forcing impulses in this example is 370 per minute.

Hence, $\omega^2 = (2 \cdot \pi \cdot F/60)^2 = 1500$,

and the torque per radian deflection is $M = J \cdot \omega^2$,

i.e. for mass J_1 , $M = 2000 \times 1500 = 3,000,000$ lbs.-ins.

Column D.—Corresponds to column F of Table 1. Since, however, there is an external torque acting on the system the amplitude at the first mass cannot be assumed to be unity as in a natural frequency tabulation. Instead, the symbol x is inserted to denote the unknown forced vibration amplitude at the first mass J_1 . The remaining amplitudes are then obtained in terms of x as the tabulation proceeds.

Column E.—Corresponds to column G of Table 1, and contains the torques due to acceleration of the various masses, i.e. the products of columns C and D.

TABLE 70.
FORCED VIBRATION AMPLITUDES—TWO-MASS SYSTEM.

$F = 370 \text{ Vibs./Min.}$; $\omega^2 = 1500$.

(i) With a Single Forcing Torque at Mass J_1 .

A	B	C	D	E		F	G	H	I
				Torque in Plane of Mass.					
Mass.	Moment of Inertia, J , Lbs.-Ins. ² / Ins.-Sec. ²	Acceleration Torque per unit Amplitude, $J \cdot \omega^2$, Lbs.-Ins./ Radian.	Deflection in Plane of Mass, α , Radians.	Acceleration Torque, $J \cdot \omega^2 \cdot \alpha$, Lbs.-Ins.	External Torque, M , Lbs.-Ins.	Total Torque, $\Sigma(J \cdot \omega^2 \cdot \alpha + M)$, Lbs.-Ins.	Shaft Stiffness, C , Lbs.-Ins./ Radian.	Change of Deflection.	
J_1	2000	3,000,000	\ast	3,000,000 \ast	50,000	3,000,000 $\ast + 50,000$	2,000,000	Col. G/Col. H.	
J_2	2000	3,000,000	$-0.5\ast - 0.025$	$-1,500,000\ast - 75,000$	0	$1,500,000\ast - 25,000$	—	$1.5\ast + 0.025$	
$\ast = 25,000/1,500,000 = 0.0167$.									
J_1	2000	3,000,000	0.0167	50,000	50,000	100,000	2,000,000	0.05	
J_2	2000	3,000,000	-0.0333	$-100,000$	0	0	—	—	

TABLE 70 (continued).

(ii) With a Single Forcing Torque at Mass J_2 .										
$x = -0.0333$.										
J_1	2000	3,000,000	-0.0333	-100,000	0	-100,000	2,000,000	-0.0500		
J_2	2000	3,000,000	0.0167	50,000	50,000	0	—	—		
(iii) With Forcing Torques of Equal Magnitude and of the same Phase at Masses J_1 and J_2 .										
$x = -0.0167$.										
J_1	2000	3,000,000	-0.0167	-50,000	50,000	0	2,000,000	0		
J_2	2000	3,000,000	-0.0167	-50,000	50,000	0	—	—		
(iv) With Forcing Torques of Equal Magnitude but Opposite Phase at Masses J_1 and J_2 .										
$x = 0.0500$.										
J_1	2000	3,000,000	0.0500	150,000	50,000	200,000	2,000,000	0.1000		
J_2	2000	3,000,000	-0.0500	-150,000	-50,000	0	—	—		

Column F.—This column does not occur in Table 1. It contains the values of the externally applied forcing torques at the various masses. In the present example there is only one external forcing torque and this is applied at mass J_1 . It is therefore entered in column F opposite mass J_1 .

Column G.—Corresponds to column H of Table 1, and contains the total torque, including the externally applied torque.

Column H.—Corresponds to column I of Table 1, and contains the torsional rigidities of the respective sections of the shaft system. In the present example there is only one shaft section.

Column I.—Corresponds to column J of Table 1, and contains the change in deflection up to the next following mass, i.e. column G divided by column H.

In general the tabulation proceeds in the same manner as for the natural frequency tabulations described in Chapter 2, except for the introduction of the externally applied forcing torque and the insertion of the symbol x to denote the unknown forced vibration amplitude at the first mass.

The value of x is obtained by equating the last torque summation in column G to zero, since the torque beyond the last mass is zero.

In this example

$$x = 25,000/1,500,000 = 0.0167 \text{ radian.}$$

Finally, the forced vibration tabulation is completed by inserting this value of x in the table, as shown by the lower part of Table 70 (i).

It is of the utmost importance to observe all changes of sign carefully.

Diagram (II) in Fig. 101 shows the forced vibration amplitudes for this system when a forcing torque of $\pm 50,000$ lbs.-ins. is applied to mass J_1 at a frequency of 370 per minute. The apparent shift of the node towards mass J_1 should be noted.

Alternative Method.—The forced vibration amplitudes may also be determined by the following analytical method.

Referring to Diagrams (I) and (II) of Fig. 101,

- let α_{F_1} = amplitude of forced vibration at mass J_1 ,
 α_{F_2} = amplitude of forced vibration at mass J_2 ,
 α_R = amplitude of oscillation assuming rigid shafting,
 α_{V_1} = amplitude at mass J_1 due to twisting of the shaft,
 α_{V_2} = amplitude at mass J_2 due to twisting of the shaft.

α_R will be referred to as the *rolling* amplitude, since it is calculated on the assumption of rigid shafting, under which condition the whole system would simply be rolled back and forth by the action of an externally applied periodic torque. It should be noted that this amplitude corresponds to the speed fluctuation obtained from calculations which neglect the elasticity of the shafting. α_R is constant throughout the system, and this gives the misleading impression that the speed fluctuation is also constant throughout the system, a subject which will be discussed later. Since α_R is constant throughout the system, it does not induce any stress in the shafting.

α_V is the amplitude of the twist in the shaft and therefore the magnitude of the stress induced in the shaft is proportional to α_V .

α_R may be calculated by equating the maximum value of the externally applied torque to the maximum value of the acceleration torque when the masses are oscillating at the impulse frequency, assuming rigid shafting,

$$\text{i.e. (max. amp. of applied torque) = (max. ang. accn. of masses)} \\ \times (\text{total moment of inertia of masses}),$$

$$\text{or} \quad M = -\omega^2 \cdot \alpha_R (\Sigma J).$$

$$\text{In this example, when } \omega^2 = 1500, \quad M = -1500 \times 4000 \times \alpha_R \\ = -6,000,000 \cdot \alpha_R,$$

$$\text{and, since } M = 50,000, \quad \alpha_R = -50,000/6,000,000 \\ = -0.0083 \text{ radian.}$$

α_{V_1} may be obtained by multiplying the equilibrium amplitude corresponding to the mode of free vibration under consideration by the appropriate dynamic magnifier.

The equilibrium amplitude is given by Equation (246), namely,

$$\theta_0 = \frac{T_n \cdot A \cdot R \cdot \Sigma a}{\omega_c^2 \cdot \Sigma(J \cdot a^2)}.$$

In this example the forcing torque of $\pm 50,000$ lbs.-ins. is applied at mass J_1 , where, as shown at Diagram (I) in Fig. 101, the amplitude on the normal elastic curve is unity.

Hence, $T_n \cdot A \cdot R \cdot \Sigma a = \Sigma(M \cdot \alpha_V) = 50,000$,

also $\omega_c^2 = 2000$,

and $\Sigma(J \cdot a^2) = (2000 + 2000) = 4000$ lbs.-ins. sec.²,
since the amplitude on the normal elastic curve is unity at both masses,

$$\text{i.e.} \quad \theta = \frac{50,000}{2000 \times 4000} = 0.00625 \text{ radian.}$$

The dynamic magnifier is given by Equation (234), namely,

$$\text{Dynamic magnifier} = \frac{1}{1 - \omega^2}$$

In this example $\omega^2 = 1500$; and $\omega_c^2 = 2000$.

Hence, Dynamic magnifier $= \frac{1}{1 - 1500/2000} = 4$,

and $\alpha_{V_1} = \theta_0 \times \text{dynamic magnifier} = 0.00625 \times 4$
 $= 0.0250$ radian.

This is the twist amplitude at mass J_1 . The twist amplitude α_{V_2} at mass J_2 is determined from that at J_1 by the respective ordinates on the normal elastic curve,

$$\text{i.e.} \quad \alpha_{V_2} = -\alpha_{V_1} = -0.0250 \text{ radian.}$$

The forced vibration amplitudes can now be evaluated by simple algebraical summation of the rolling and twist amplitudes,

$$\text{i.e.} \quad \alpha_F = (\alpha_R + \alpha_V).$$

In this example, therefore,

$$\begin{aligned} \alpha_{F_1} &= -0.0083 + 0.0250 = +0.0167 \text{ radian,} \\ \text{and } \alpha_{F_2} &= -0.0083 - 0.0250 = -0.0333 \text{ radian.} \end{aligned}$$

These values agree with the values obtained by the tabulation method, see Table 70.

The dotted line in Diagram (II) of Fig. 101 represents the rolling amplitude α_R , which is constant throughout the system. It is of interest to note that the rolling amplitude line cuts the vibration amplitude line at the true nodal point. Thus the total motion of the shaft can be regarded as compounded of a periodic twisting motion superimposed on a periodic rolling motion of the same frequency, and phased as shown in Fig. 101.

It should also be observed that the virtual node divides the shaft into two lengths, such that the torsional rigidity of the portion between the virtual node and the right-hand mass is 3,000,000 lbs.-ins. per radian. The frequency of the right-hand mass J_2 about the virtual node is therefore 370 vibs./min., which is the frequency of the forcing torque applied to mass J_1 .

Coefficient of Speed Fluctuation.—This is obtained from Equation (421), viz.,

$$C = 2 \cdot \alpha_F \cdot n,$$

where n = order number of oscillations, i.e. the number of complete oscillations per revolution.

Assuming 1 oscillation per rev. in this example, then,

$$\text{At mass } J_1 : C = 2 \times 0.0167 \times 1 = 0.0334 = 1/30.$$

$$\text{At mass } J_2 : C = 2 \times 0.0333 \times 1 = 0.0666 = 1/15.$$

Thus the cyclic irregularity at mass J_1 is only half that at mass J_2 .

If rigid shafting is assumed the cyclic irregularity at both J_1 and J_2 is

$$C = 2 \cdot \alpha_R \cdot n = 2 \times 0.0083 \times 1 = 0.0167 = 1/60.$$

It is therefore apparent that large errors can be introduced if the elasticity of the shafting is neglected when calculating cyclic speed fluctuation.

Diagram (III) in Fig. 101 shows the forced vibration amplitude curve when the forced vibration frequency is greater than the natural frequency of the system. In this diagram $\omega^2 = 2500$, and the forced vibration amplitudes are calculated as follows :—

Rolling Amplitude.

$$M = -2500 \times 4000 \times \alpha_R,$$

i.e. $\alpha_R = -50,000/10,000,000 = -0.0050$ radian.

Twist Amplitude.

$\theta_o = 0.00625$ radian, as before (this assumes that there is no change in the magnitude of the forcing torque due to the change of speed).

$$\text{Dynamic magnifier} = \frac{1}{1 - 2500/2000} = -4.$$

The negative sign should be carefully observed. It is important in these calculations, although it is usually neglected when plotting resonance curves (see Fig. 75),

i.e. $\alpha_{v_1} = -4 \times 0.00625 = -0.0250$ radian,

and, from the normal elastic curve,

$$\alpha_{v_2} = -\alpha_{v_1} = 0.0250 \text{ radian.}$$

Hence, finally,

$$\alpha_{F_1} = -0.0050 - 0.0250 = -0.0300 \text{ radian,}$$

$$\alpha_{F_2} = -0.0050 + 0.0250 = 0.0200 \text{ radian.}$$

These values would also be obtained by applying the tabulation method.

Forced Vibration Amplitudes with Forcing Torques Applied to both Masses.—If the forcing torque at J_2 is exactly in phase with the forcing torque at J_1 the forced vibration amplitudes can be determined by the tabulation method already described. The final tabulation is given at (iii) in Table 70 and the forced vibration amplitudes are shown graphically at (V) in Fig. 101.

It should be noticed that since the forcing torques are in phase they have the same sign in the forced vibration tabulation.

The forced vibration amplitudes may also be determined from the rolling and twisting amplitudes as follows :—

Rolling Amplitude.—Since the forcing torques are equal in magnitude and phase the total torque acting when the system is assumed to be rigid is the sum of the two forcing torques.

$$\begin{aligned} \text{Hence,} \quad (M_1 + M_2) &= -\omega^2 \cdot \alpha_R \cdot (\Sigma J), \\ \text{i.e.} \quad (50,000 + 50,000) &= -1500 \times 4000 \times \alpha_R, \\ \text{or} \quad \alpha_R &= -100,000/6,000,000 = -0.0167 \text{ radian.} \end{aligned}$$

Twist Amplitude.—The phase and vector diagrams are shown at (V) in Fig. 101, from which the value of $T_n \cdot A \cdot R \cdot \Sigma a$ in the expression for the equilibrium amplitude is found to be zero. Hence the equilibrium amplitude and therefore the twist amplitude is zero at all points in the system. This result can also be deduced from the fact that the forcing torques are of equal magnitude and of the same phase, whereas the specific deflections on the normal elastic curve, Diagram I of Fig. 101, are of equal amplitude but opposite phase. Thus the energy imparted to the system by the forcing torque at mass J_1 is neutralised by the energy imparted to the system by the forcing torque at mass J_2 .

In this case, therefore, the forced vibration amplitude has a constant value -0.0167 radian throughout the system, i.e. both masses vibrate in phase through an amplitude ± 0.0167 radian at a frequency of 370 vibrations per minute, and there is no twist and therefore no stress in the connecting shaft due to this vibratory motion. The speed fluctuation, assuming that there is one complete oscillation per revolution, is

$$C = 2 \cdot \alpha_R \cdot n = 2 \times 0.0167 \times 1 = 0.0333 = 1/30.$$

These results agree with the tabulation method.

An alternative method of obtaining the forced vibration amplitudes, where there are several masses and several forcing torques applied at different points in the system, is to prepare separate tabulations for each forcing torque and then combine the results of the various tabulations vectorally. This method must be employed when the various forcing torques are not in phase.

In the present example, Table 70 (i) is the tabulation for the forcing torque at mass J_1 , whilst Table 70 (ii) is the tabulation for the forcing torque at mass J_2 . Since the forcing torques are in phase the resultant motions when the two forcing torques act together are obtained by adding, algebraically, the motions given by the separate tables,

$$\begin{aligned} \text{i.e. } \alpha_{F_1} &= 0.0167 - 0.0333 = -0.0167 \text{ radian at mass } J_1, \\ \alpha_{F_2} &= -0.0333 + 0.0167 = -0.0167 \text{ radian at mass } J_2. \end{aligned}$$

This result agrees with the previous results.

The special case when the forcing torques are in exact anti-phase can also be solved by a single forced vibration tabulation. The final result in the present example is given at Table 70 (iv). In this case the forcing torque at mass J_2 must be entered in its appropriate position in the forced vibration table with a negative sign, indicating that it is of opposite phase to the forcing torque at mass J_1 .

The forced vibration amplitudes in this case are shown at (VI) in Fig. 101.

The forced vibration amplitudes can also be determined from the rolling and twisting amplitudes, as follows:—

Rolling Amplitude.—Since the forcing torques are equal in magnitude but opposite in phase, the total torque acting when the system is assumed to be rigid is zero. Hence there is no rolling amplitude in this case.

Twist Amplitude.—The phase and vector diagrams are shown at (VI) in Fig. 101, from which it is seen that the value of $T_n \cdot A \cdot R \cdot \Sigma a$ in the expression for the equilibrium amplitude is $\Sigma M \cdot \alpha_V = 100,000 \text{ lbs.-ins.}$

$$\text{Hence, } \theta_o = \frac{T_n \cdot A \cdot R \cdot \Sigma a}{\omega_e^2 \cdot \Sigma(J \cdot a^2)} = \frac{100000}{2000 \times 4000} = 0.0125 \text{ radian.}$$

The dynamic magnifier is

$$\frac{1}{1 - \frac{1500}{2000}} = 4.$$

$$\begin{aligned} \text{i.e. } \alpha_{V_1} &= 4 \times 0.0125 = 0.0500 \text{ radian,} \\ \text{and } \alpha_{V_2} &= -\alpha_{V_1} = -0.0500 \text{ radian.} \end{aligned}$$

This agrees with the values obtained by tabulation.

Alternatively, the forced vibration amplitudes may be obtained by combining the separate tabulations at (i) and (ii) in Table 70. Since the forcing torque at mass J_2 is in anti-phase to the forcing torque at J_1 , the values in Table 70 (ii) must be subtracted, algebraically, from the values in Table 70 (i),

$$\begin{aligned} \text{i.e.} \quad \alpha_{F_1} &= 0.0167 + 0.0333 = 0.0500 \text{ radian,} \\ \alpha_{F_2} &= -0.0333 - 0.0167 = -0.0500 \text{ radian.} \end{aligned}$$

This result also agrees with the previous results, and shows that when the forcing torques are of equal magnitude and opposite phase the shaft connecting the masses is subjected to a pure twist and there is no rolling motion.

The cases discussed so far are all fairly simple and easy to interpret. It should be noted that although the examples are based on a symmetrical system with two equal masses and forcing torques of equal magnitude, the same methods can be applied in cases where the system is not symmetrical and where the forcing torques are not of equal magnitude.

The case where the forcing torques are not in phase (excluding the simple special arrangement where the forcing torques are in anti-phase) will now be discussed.

Diagram VII in Fig. 101 refers to the case when the forcing torque at mass J_2 is 90° out of phase with the forcing torque at mass J_1 . As already mentioned the resultant forced vibration amplitudes can be obtained by combining amplitudes produced by applying each torque separately. The separate tabulations are given at (i) and (ii) in Table 70, and since the forcing torques are phased at 90° the separate amplitudes must also be combined vectorally with this phase difference. The phase diagram is shown at the top of Fig. 101 (VII), and from this the following resultant forced vibration amplitudes are obtained:—

$$\begin{aligned} \alpha_{F_1} &= \sqrt{0.0167^2 + 0.0333^2} = 0.0373 \text{ radian.} \\ \alpha_{F_2} &= \sqrt{0.0333^2 + 0.0167^2} = 0.0373 \text{ radian.} \end{aligned}$$

There is a phase relationship between α_{F_1} and α_{F_2} which is determined by the signs of the displacements in the separate tabulations.

The resultant forced vibration amplitudes can also be calculated from the rolling and twist amplitudes, as follows:—

Rolling Amplitude.—The vector diagram when the system is assumed to be rigid is shown at the top of Fig. 101 (VII), the resultant forcing torque being 70,710 lbs.-ins.

Hence, the rolling amplitude when $\omega^2 = 1500$ is

$$\alpha_R = -70,710/6,000,000 = -0.0118 \text{ radian.}$$

Twist Amplitude.—The vector diagram for obtaining the resultant specific input energy is shown at the top of Fig. 101 (VII). In this case the vector for M_2 must be drawn in the opposite direction to the corresponding crank in the phase diagram, because the normal elastic curve at (I) in Fig. 101 shows that the specific amplitude at mass J_2 is -1 .

Hence, in the expression for the equilibrium amplitude, $T_n \cdot A \cdot R \cdot \Sigma a = 70,710$ lbs.-ins. per radian deflection at mass J_1 ,

$$\text{i.e. } \theta_0 = \frac{T_n \cdot A \cdot R \cdot \Sigma a}{\omega_c^2 \cdot \Sigma(J \cdot a^2)} = \frac{70710}{8000000} = 0.0088 \text{ radian.}$$

$$\text{The dynamic magnifier is } \frac{1}{1 - \frac{1500}{2000}} = 4,$$

$$\text{so that } \alpha_{v_1} = 4 \times 0.0088 = 0.0354 \text{ radian,}$$

$$\text{and } \alpha_{v_2} = -\alpha_{v_1} = -0.0354 \text{ radian.}$$

It is now necessary to bear in mind that the rolling amplitude is in anti-phase to the resultant forcing torque, whereas the twist amplitude is in phase with the torque when the applied frequency is less than the natural frequency, and is in anti-phase to the torque when the applied frequency is greater than the natural frequency, assuming, of course, that damping is negligible at non-resonant speeds.

In the present case the applied frequency is less than the natural frequency, so that the twist amplitude is in phase with the torque.

Thus there is a 90° phase relationship between the rolling and twist amplitudes, so that the resultant motion must be

obtained by means of the vector diagram shown at the top of Fig. 101 (VII),

i.e. $\alpha_{F_1} = 0.0373$ radian,
 similarly, $\alpha_{F_2} = 0.0373$ radian,

and there is a phase relationship between α_{F_1} and α_{F_2} which can be determined by means of vector diagrams.

These results agree with those previously obtained.

The motion cannot be portrayed in a simple co-planar diagram because of the 90° phase relationship between the rolling and twist diagrams, but the three-dimensional sketch in the middle of Fig. 101 (VII) may help to enable the motion to be visualised.

The lower diagram in Fig. 101 (VII) gives an end view of the various motions at each end of the shaft from which the rolling and twisting motions have been projected.

As in the simple cases previously described, the resultant motion is composed of rolling and twisting, the former causing merely a cyclic variation of speed, and the latter stressing the connecting shaft. As before, the node for the twisting motion is at the same position in the shaft as the node formed by the normal elastic curve for natural vibration.

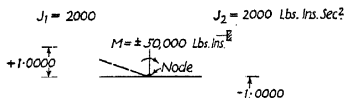
Two-Mass System with Forcing Torque Applied at Node.—

This interesting special case is illustrated in Fig. 102, the system being the same as before. Since this system is symmetrical the node is located at the middle of the shaft and the stiffness of the sections of shafting between each mass and the node is therefore $C = 4,000,000$ lbs.-ins. per radian, as shown at (I) in Fig. 102.

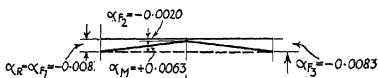
The forced vibration amplitudes can be determined by the tabulation method already described, a third line being introduced between the lines for J_1 and J_2 in which the forcing torque is entered in column F. Since there is no mass at the point of application of the forcing torque the value of J in column B is zero, as shown in Table 71. The tabulation is carried out precisely as before, and the forced vibration amplitudes for the case where $\omega^2 = 1500$ are shown graphically at (II) in Fig. 71.

These amplitudes can also be determined by calculation, as follows :—

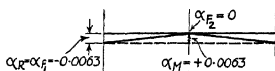
$$\text{I] } \omega^2 = 2000$$



$$\text{II] } \omega^2 = 1500 \quad C_1 = 4000,000 \quad C_2 = 4000,000 \text{ Lbs. Ins./Radian}$$



$$\text{III] } \omega^2 = 2000$$



$$\text{IV] } \omega^2 = 2500$$

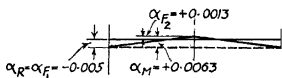


FIG. 102.—Forced vibration amplitudes. Two-mass system.

Rolling Amplitude.—Since the forcing torque and the mass system are the same as at (II) in Fig. 101, the rolling amplitude is also the same, namely, -0.0083 radian.

TABLE 71.
FORCED VIBRATION AMPLITUDES—TWO-MASS SYSTEM.
(Forcing Torque at Node.)

F = 370 Vibs./Min.; $\omega^2 = 1500$.

A	B	C	D	E	F	G	H	I
J ₁	2000	3,000,000	*	3,000,000*	0	3,000,000*	4,000,000	0.75*
—	0	0	0.25*	0	50,000	3,000,000* + 50,000	4,000,000	0.75* + 0.0125
J ₂	2000	3,000,000	-0.5* - 0.0125	-1,500,000* - 37,500	0	1,500,000* + 12,500	—	—
* = - 12,500/1,500,000 = - 0.00833.								
J ₁	2000	3,000,000	- 0.0083	-25,000	0	-25,000	4,000,000	- 0.0063
—	—	—	- 0.0020	—	50,000	25,000	4,000,000	0.0063
J ₂	2000	3,000,000	- 0.0083	-25,000	0	0	—	—

Twist Amplitude.—Since the forcing torque is applied at the node where the specific amplitude is zero, the value of $T_n \cdot A \cdot R \cdot \Sigma a$ is also zero. Hence in this case there is no dynamic magnification of the applied torque, even at resonance.

There is, however, a definite amount of twist in the sections of shafting at either side of the point where the forcing torque is applied, due to the transmission of this torque to the masses.

Let C_1 and C_2 = the torsional rigidities of the sections of shafting between the node and masses J_1 and J_2 respectively,

m_1 and m_2 = the corresponding proportions of the forcing torque,

α_M = the twist amplitude at the node due to the transmission of m_1 and m_2 .

Then, if C = the torsional rigidity of the total length of shafting,

$C_1 = C \cdot (J_1 + J_2)/J_2$; and $C_2 = C \cdot (J_1 + J_2)/J_1$;

also $m_1 = M \cdot J_1/(J_1 + J_2)$; and $m_2 = M \cdot J_2/(J_1 + J_2)$,

where M = the total forcing torque,

but $m_1 = C_1 \cdot \alpha_M$; and $m_2 = C_2 \cdot \alpha_M$.

Hence, $\alpha_M = m_1/C_1 = m_2/C_2 = \frac{M \cdot J_1 \cdot J_2}{C(J_1 + J_2)^2}$

Now, the frequency equation for a two-mass system is

$$\omega_c^2 = \frac{C(J_1 + J_2)}{J_1 \cdot J_2}$$

so that, finally, $\alpha_M = \frac{M}{\omega_c^2(J_1 + J_2)}$.

In the present example $\omega_c^2 = 2000$; $C = 2,000,000$; $J_1 = J_2 = 2000$; and $M = 50,000$.

Hence, $\alpha_M = \frac{50000}{2000 \times 2 \times 2000} = 0.0063$ radian.

The forced vibration amplitudes are therefore as follows:—

At mass J_1 , $\alpha_{F_1} = -0.0083$.

At point of application of forcing torque,

$$\begin{aligned} \alpha_{F_2} &= -0.0083 + 0.0063 \\ &= -0.0020 \text{ radian.} \end{aligned}$$

At mass J_2 , $\alpha_{F_2} = -0.0083$ radian.

These values agree with the values obtained by tabulation, as shown at (II) in Fig. 102.

The forced vibration amplitudes at other frequencies of application of the forcing torque are determined in precisely the same way. Fig. 102 (III) shows the forced vibration amplitudes when the applied frequency is equal to the natural frequency, i.e. $\omega^2 = \omega_0^2 = 2000$. In this case the rolling amplitude is the same as the twist amplitude, so that the resultant forced vibration amplitude is -0.0063 at each mass and zero at the node. Fig. 102 (IV) shows the forced vibration amplitudes when the applied frequency is greater than the natural frequency. In this case the rolling amplitude is smaller than the twist amplitude, so that the resultant forced vibration amplitude is -0.0050 at each mass and $+0.0013$ at the node.

At very low applied frequencies the twist amplitude is very much smaller than the rolling amplitude, so that the resultant forced vibration is very nearly constant and equal in magnitude to the rolling amplitude throughout the system. At resonance the two masses simply swing through a sufficient amplitude to balance the applied torque and there is no dynamical magnification, the amplitude at the node being zero. At very high applied frequencies the rolling amplitude becomes very nearly zero, so that the amplitude at the masses also becomes very nearly zero, whilst the point of application of the forcing torque, i.e. the node, vibrates with the same amplitude that the masses would have to swing through to balance the applied torque without any dynamical magnification.

Three-Mass Systems.—A simple three-mass system is shown in Fig. 103. A symmetrical system has been chosen as an example purely for the purpose of simplifying the calculations. The methods are, of course, equally valid for unsymmetrical systems.

Natural Frequencies.—There are two principal modes of vibration in the case of a three-mass system, the natural frequencies for the symmetrical system shown in Fig. 103 being

$$F = 9.55\sqrt{C/J} \quad \text{or} \quad 9.55\sqrt{3 \cdot C/J} \quad (\text{see Chapter 1}).$$

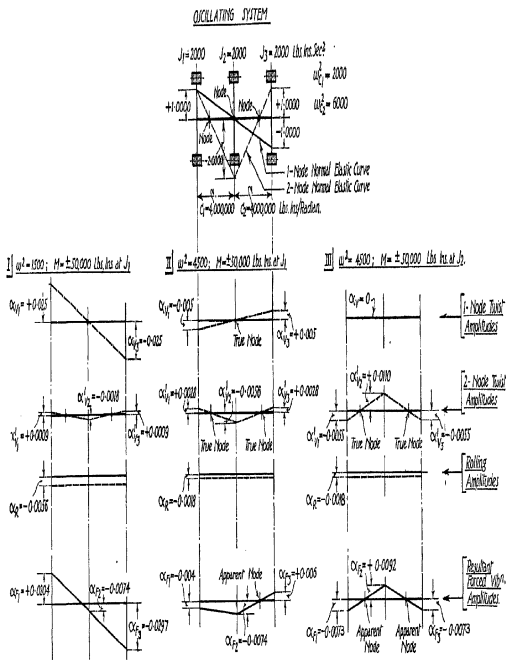


FIG. 103.—Forced vibration amplitudes. Three-mass system.

In the present example

$$C = 4,000,000 \quad \text{and} \quad J = 2000,$$

i.e. One-node frequency

$$= F_1 = 9.55 \sqrt{4,000,000/2000} = 427 \text{ vibs./min.},$$

and $\omega_{c,1}^2 = 2000$.

Two-node frequency

$$= F_2 = 9.55 \sqrt{3 \times 4,000,000/2000} = 740 \text{ vibs./min.},$$

and $\omega_{c,2}^2 = 6000$.

Tabulation Method.—The forced vibration tabulation when the applied frequency is 370 vibs./min. ($\omega^2 = 1500$) and an external torque of $\pm 50,000$ lbs.-ins. is applied at J_1 is given in Table 72. This table is built-up in precisely the same way as already described for two-mass systems, an additional line being inserted for the third mass.

The forced vibration amplitudes are shown graphically in the bottom diagram at (I) in Fig. 103.

The forced vibration amplitudes can also be determined from the rolling and twist amplitudes in the manner already described for two-mass systems, but modified to take account of the fact that with three masses there are two principal modes of natural vibration.

Rolling Amplitude.—As before, $M = -\omega^2 \cdot \alpha_R \cdot (\Sigma J)$.

In this example

$$\omega^2 = 1500; \quad M = 50,000; \quad \text{and} \quad (J) = (J_1 + J_2 + J_3) = 6000.$$

$$\text{Hence,} \quad \alpha_R = -\frac{50000}{1500 \times 6000} = -0.0056 \text{ radian.}$$

The rolling amplitude diagram is shown separately at (I) in Fig. 103.

Twist Amplitudes (1-Node Mode).

$$\text{As before; equilibrium amplitude, } \theta_o = \frac{T_n \cdot A \cdot R \cdot \Sigma a}{\omega_o^2 \cdot \Sigma (J \cdot a^2)}.$$

In this example the forcing torque is $\pm 50,000$ lbs.-ins. applied at mass J_1 , where the specific amplitude on the one-node normal elastic curve is $+1$ (see diagram of oscillating system in Fig. 103).

The value of $(T_n \cdot A \cdot R \cdot \Sigma a)$ is, therefore, 50,000.

TABLE 72.
FORCED VIBRATION AMPLITUDES—THREE-MASS SYSTEM.

$F = 370 \text{ Vibs./Min.}; \omega^2 = 1,500.$

A	B	C	D	E		F	G	H	I
				Torque in Plane of Mass.					
Mass.	Moment of Inertia.	Acceleration Torque per Unit Amplitude.	Deflection in Plane of Mass.	Acceleration Torque.	External Torque.	Total Torque.	Shaft Stiffness.	Change of Deflection.	
	$J, \text{ Lbs.-Ins./Sec.}^2.$	$J \cdot \omega^2, \text{ Lbs.-Ins./Radian.}$	$\alpha, \text{ Radians.}$	$J \cdot \omega^2 \cdot \alpha, \text{ Lbs.-Ins.}$	$M, \text{ Lbs.-Ins.}$	$\Sigma(J \cdot \omega^2 \cdot \alpha + M), \text{ Lbs.-Ins.}$	$C, \text{ Lbs.-Ins./Radian.}$	Col. G/Col. H.	
J_1	2000	3,000,000	$\%$	3,000,000 $\%$	50,000	3,000,000 $\%$ + 50,000	4,000,000	0.75% + 0.0125	
J_2	2000	3,000,000	0.25% - 0.0125	750,000 $\%$ - 37,500	0	3,750,000 $\%$ + 12,500	4,000,000	0.9375% + 0.0031	
J_3	2000	3,000,000	- 0.6875% - 0.0156	-2,062,500 $\%$ - 46,875	0	1,687,500 $\%$ - 34,375	—	—	
$\% = 34.375/1,687,500 = 0.02037.$									
J_1	2000	3,000,000	0.02037	61,111	50,000	111,111	4,000,000	0.02777	
J_2	2000	3,000,000	-0.00741	-22,222	0	88,888	4,000,000	0.02222	
J_3	2000	3,000,000	-0.02963	-88,888	0	0	—	—	

Also, $\omega_c^2 = 2000$, and $\Sigma(J \cdot a^2) = 4000$, since the specific amplitudes on the one-node normal elastic curve are $+1$ at mass J_1 , -1 at mass J_3 , and zero at mass J_2 .

$$\text{Hence, } \theta_0 = \frac{50000}{2000 \times 4000} = 0.0063 \text{ radian.}$$

The dynamic magnifier when

$$\omega^2 = 1500 \text{ is } \frac{1}{1 - \frac{1500}{2000}} = 4,$$

$$\begin{aligned} \text{i.e. } \alpha_{v_1} &= 4 \times 0.0063 = 0.0250 \text{ radian,} \\ \alpha_{v_2} &= -\alpha_{v_1} = -0.0250 \text{ radian,} \\ \alpha_{v_3} &= 0 \text{ (since } J_2 \text{ is at the node for this mode of vibration).} \end{aligned}$$

Twist Amplitudes (2-Node Mode).

For this mode of vibration $\omega_c^2 = 6000$.

The value of $(T_n \cdot A \cdot R \cdot \Sigma a)$ is the same as for the one-node mode, viz. 50,000, since the specific amplitude on the two-node normal elastic curve is also $+1$ at the point of application of the forcing torque, i.e. at mass J_1 . The value of $\Sigma(J \cdot a^2)$ for the two-node mode is

Mass. J.	Specific Amplitude. a.	J . a ² .
2000	1.0000	2000
2000	-2.0000	8000
2000	1.0000	2000
		Σ(J . a ²) = 12,000

$$\text{Hence, } \theta'_0 = \frac{50000}{6000 \times 12000} = 0.00069 \text{ radian.}$$

The dynamic magnifier is $\frac{1}{1 - \frac{1500}{6000}} = 1.3333$,

$$\begin{aligned} \text{i.e. } \alpha'_{v_1} &= 1.3333 \times 0.00069 = 0.0009 \text{ radian at mass } J_1, \\ \alpha'_{v_2} &= -2 \cdot \alpha'_{v_1} = -2 \times 0.0009 = -0.0018 \text{ radian at} \\ &\quad \text{mass } J_2, \\ \alpha'_{v_3} &= \alpha'_{v_1} = 0.0009 \text{ radian at mass } J_3. \end{aligned}$$

These amplitudes are shown separately at (I) in Fig. 103.

Forced Vibration Amplitudes.—The forced vibration amplitudes are now simply obtained by adding the rolling and twist amplitudes, algebraically, thus—

$$\begin{aligned}\alpha_{F_1} &= \text{forced vibration amplitude at mass } J_1 \\ &= (\alpha_R + \alpha_{V_1} + \alpha'_{V_1}) \\ &= (-0.0056 + 0.0250 + 0.0009) \\ &= +0.0203 \text{ radian, at } J_1, \\ \alpha_{F_2} &= (-0.0056 + 0 - 0.0018) = -0.0074 \text{ radian, at } J_2, \\ \alpha_{F_3} &= (-0.0056 - 0.0250 + 0.0009) \\ &= -0.0297 \text{ radian, at } J_3.\end{aligned}$$

These values agree with the values obtained by tabulation.

The curve of forced vibration amplitudes, given at the bottom of Fig. 103 (I), shows that when the impulse frequency is 370 vibs./min. the one-node twist amplitudes predominate. This is because the impulse frequency is much closer to the one-node than to the two-node natural frequency, so that the dynamical magnification of the one-node amplitudes is greater.

It is also of interest to note that the true coefficients of speed, assuming 1 oscillation per revolution in this example, are as follows:—

$$\begin{aligned}\text{At mass } J_1, \mathbf{C} &= 2 \cdot \alpha_{F_1} \cdot n = 2 \times 0.0203 \times 1 \\ &= 0.0406 = 1/25. \\ \text{At mass } J_2, \mathbf{C} &= 2 \cdot \alpha_{F_2} \cdot n = 2 \times 0.0074 \times 1 \\ &= 0.0148 = 1/68. \\ \text{At mass } J_3, \mathbf{C} &= 2 \cdot \alpha_{F_3} \cdot n = 2 \times 0.0297 \times 1 \\ &= 0.0594 = 1/17.\end{aligned}$$

If rigid shafting is assumed,

$$\mathbf{C} = 2 \cdot \alpha_R \cdot n = 2 \times 0.0056 \times 1 = 0.0112 = 1/89.$$

The importance of taking into account the elasticity of the shafting when calculating speed fluctuation is therefore apparent.

Fig. 103 (II) shows the rolling and twist amplitude diagrams and the resultant forced vibration amplitude diagram when the forcing torque is applied at mass J_1 with an impulse frequency of 640 vibs./min., i.e. $\omega^2 = 4500$.

These amplitudes are obtained exactly as in the previous case.

In the present case the impulse frequency is greater than the one-node natural frequency, so that the twist amplitude at mass J_1 for one-node vibration is in anti-phase to the applied torque. The impulse frequency is less than the two-node natural frequency, so that the twist amplitude at mass J_1 for two-node vibrations is in phase with the applied torque. Neither mode of vibration dominates the resultant forced vibration curve. These relationships are automatically obtained when the tabulation method is employed, whilst the analytical method enables the twist amplitudes due to one-node vibration to be determined independently of those due to two-mode vibration.

The analytical method is carried out precisely as before, thus—

Rolling Amplitude.—In this case $\omega^2 = 4500$ and, as before, $M = 50,000$ and $J = 6000$.

$$\text{Hence, } \alpha_R = -\frac{50000}{4500 \times 6000} = -0.0018 \text{ radian.}$$

Twist Amplitudes (One-Node Mode).

$$\theta_o = 0.0063 \text{ radian, as before.}$$

In this case, however, the dynamic magnifier is

$$\frac{1}{1 - \frac{4500}{2000}} = -0.8$$

$$\text{Hence, } \alpha_{v_1} = -0.8 \times 0.0063 = -0.0050,$$

$$\alpha_{v_2} = 0,$$

$$\alpha_{v_3} = -\alpha_{v_1} = 0.0050.$$

Twist Amplitudes (Two-Node Mode).

$$\theta'_o = 0.00069, \text{ as before.}$$

In this case, however, the dynamic magnifier is

$$\frac{1}{1 - \frac{4500}{6000}} = 4.$$

$$\begin{aligned} \text{Hence, } \alpha'_{v_1} &= 0.00069 \times 4 = 0.0028, \\ \alpha'_{v_2} &= -2 \times \alpha'_{v_1} = -0.0056, \\ \alpha'_{v_3} &= \alpha'_{v_1} = 0.0028 \end{aligned}$$

Forced Vibration Amplitudes.

$$\begin{aligned} \alpha_{F_1} &= (\alpha_R + \alpha_{v_1} + \alpha'_{v_1}) \\ &= (-0.0018 - 0.0050 + 0.0028) = -0.0040 \text{ radian.} \\ \alpha_{F_2} &= (-0.0018 + 0 - 0.0056) = -0.0074 \text{ radian.} \\ \alpha_{F_3} &= (-0.0018 + 0.0050 + 0.0028) = +0.0060 \text{ radian.} \end{aligned}$$

These results will be found to agree with the results obtained by the tabulation method.

Fig. 103 (III) shows the rolling and twist amplitude diagrams and the resultant forced vibration amplitude diagram when the forcing torque is applied at mass J_2 with an impulse frequency of 640 vibs./min., i.e. $\omega^2 = 4500$.

In this case, since the forcing torque is applied at the node of the one-node normal elastic curve, the one-node twist amplitudes are zero at all points in the system, i.e. the applied torque cannot excite one-node vibration.

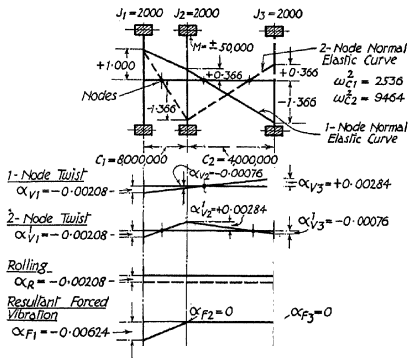
The resultant forced vibration amplitude curve is therefore composed of the two-node twist amplitude curve superimposed on the rolling amplitude curve. It should also be noted that the rolling amplitude line crosses the twist amplitude lines at the true nodal positions, as determined by the normal elastic curve for the two-node mode of natural vibration. As in the previous cases these relationships are automatically obtained by applying the tabulation method, whilst the rolling and twist amplitudes can be obtained independently by applying the analytical method.

Fig. 104 shows a three-mass system which is of interest because it serves to illustrate the principle of the dynamic vibration absorber.

If masses J_2 and J_3 are regarded as forming a separate two-mass system, the natural frequency of this separate system is given by

$$\omega_e^2 = C_2(J_2 + J_3)/(J_2 \cdot J_3) = 4000.$$

Assuming that the forcing torque acts at mass J_2 , if a third mass, J_3 , is attached to J_2 by a shaft of torsional rigidity C_1 , such that the natural frequency of this added mass on its shaft, regarded as fixed at mass J_2 , is equal to the natural frequency of the original system, then it will be found that



By Tabulation :- $\omega^2 = 4000$

A	B	C	D	E	F	G	H	I
J_1	2000	8000,000	-0.00625	-50,000	—	-50,000	8000,000	-0.00625
J_2	2000	8,000,000	0	0	50,000	0	4000,000	0
J_3	2000	8,000,000	0	0	0	0	—	—

FIG. 104.—Forced vibration amplitudes. Three-mass system.

when the system vibrates at the original natural frequency the forcing torque is completely absorbed by the added mass, so that the original system remains quiet. The mass J_1 on its shaft C_1 forms an undamped vibration absorber for the system composed of masses J_2 and J_3 on shaft C_2 , with the forcing torque M acting at mass J_2 .

This action can be investigated by the methods already discussed, as follows :—

The natural frequencies of the three-mass system shown in Fig. 104 can be obtained from Equation (19) and are as follows :—

For the one-node mode, $\omega_{e1}^2 = 2536$.

For the two-node mode, $\omega_{e2}^2 = 9464$.

The corresponding normal elastic curves, assuming unit amplitude at mass J_1 , are shown in the topmost diagram of Fig. 104.

Assuming that the forcing torque is applied to mass J_2 with a frequency corresponding to $\omega^2 = 4000$, the forced vibration amplitudes are obtained by the analytical method as follows :—

Rolling Amplitude : $M = -\omega^2 \cdot \alpha_R \cdot (\Sigma J)$,

$$\text{i.e.} \quad \alpha_R = -\frac{50000}{4000 \times 6000} = -0.00208 \text{ radian.}$$

One-Node Twist Amplitudes.

$$\text{Equilibrium amplitude} = \theta_o = \frac{T_n \cdot A \cdot R \cdot \Sigma a}{\omega_e^2 \cdot \Sigma(J \cdot a^2)}.$$

In this case, $T_n \cdot A \cdot R = 50,000$, whilst Σa is 0.366 at mass J_2 , where the forcing torque is applied. The one-node phase velocity is $\omega_{e1}^2 = 2536$, and the value of $\Sigma(J \cdot a^2)$ is 6000,

$$\text{i.e.} \quad \theta_o = \frac{50000 \times 0.366}{2536 \times 6000} = 0.0012 \text{ radian.}$$

The dynamic magnifier is $\frac{1}{1 - \frac{4000}{2536}} = -1.73$.

Hence the twist amplitudes are

$$\alpha_{v_1} = -1.73 \times 0.0012 = -0.00208 \text{ radian,}$$

$$\alpha_{v_2} = 0.366 \alpha_{v_1} = -0.00076 \text{ radian,}$$

$$\alpha_{v_3} = -1.366 \alpha_{v_1} = 0.00284 \text{ radian.}$$

Two-Node Twist Amplitudes.—For this mode,

$$\Sigma a = -1.366; \omega_e^2 = 9464; \text{ and } \Sigma(J \cdot a^2) = 6000,$$

which happens to be the same as for the one-node mode,

$$\text{i.e. } \theta_n = \frac{50000 \times 1.366}{9464 \times 6000} = -0.0012 \text{ radian.}$$

The dynamic magnifier is

$$1 - \frac{4000}{9464} = 1.73.$$

Hence the twist amplitudes are

$$\alpha'_{v_1} = -1.73 \times 0.0012 = -0.00208 \text{ radian,}$$

$$\alpha'_{v_2} = -1.366 \alpha'_{v_1} = 0.00284 \text{ radian,}$$

$$\alpha'_{v_3} = 0.366 \alpha'_{v_1} = -0.00076 \text{ radian.}$$

Forced Vibration Amplitudes.—By algebraical addition of the rolling and twist amplitudes the following values are obtained :—

$$\alpha_{E_1} = (-0.00208 - 0.00208 - 0.00208) \\ = -0.00624 \text{ radian at } J_1,$$

$$\alpha_{E_2} = (-0.00208 - 0.00076 + 0.00284) = 0 \text{ at } J_2,$$

$$\alpha_{E_3} = (-0.00208 + 0.00284 - 0.00076) = 0 \text{ at } J_3.$$

The curves of twist, rolling and forced vibration amplitude are shown in Fig. 104, together with the values of the forced vibration amplitude obtained by applying the tabulation method. It is seen that the two methods are in complete agreement.

Multi-Mass Systems.—The tabulation method can be used for obtaining the resultant forced vibration amplitudes for a given speed at all points in a multi-mass system. If there are several forcing torques applied at different points in the system and all these torques have the same phase and frequency, a single tabulation will suffice. In such cases it is only necessary to add the values of the forcing torques into the table at the correct points to complete the tabulation.

If some of the forcing torques are in anti-phase to others a single tabulation still suffices. In this case, however, it is

necessary to regard the forcing torques which are in anti-phase as negative when inserting their values in the table.

If there is a phase relationship between the forcing torques (other than the anti-phase relationship just mentioned) a single table will not suffice. In such cases it is necessary to prepare separate tables for each forcing torque as though it were acting on the system alone, the separate forcing torque being added at the appropriate point in each table. The resultant forced vibration amplitudes are then obtained by combining the results of the separate tables vectorally, i.e. in their correct phase relationships.

The detailed explanations already given in connection with the simple two- and three-mass systems indicate the methods which must be employed.

If each of the several forcing torques is composed of a number of component harmonics, then the resultant forced vibration amplitudes for each harmonic must be determined separately. This will yield a resultant forced vibration tabulation for each separate harmonic, and the maximum torques and stresses in the system due to each component harmonic can be determined from the total torque summations in column G of the tables.

These maximum values can then be plotted in the form of separate sinusoidal curves of the type shown at the right-hand side of Fig. 105, taking care to preserve the correct phase relationships between the several component curves. Finally, these component curves can be combined to give the total forced vibration torques and stresses. If the magnitudes of the total forced vibration torques and stresses are required at several different points in the oscillating system, the corresponding values for each separate component must be determined from the appropriate position in column G of the separate tables, and these values must then be combined by drawing the sinusoidal wave forms and adding their ordinates algebraically.

If the magnitudes of the total forced vibration torques and stresses are required at several different operating speeds the whole of the above work must be repeated for each speed.

It should also be observed that if one of the harmonic components comes into resonance at one of the selected speeds then

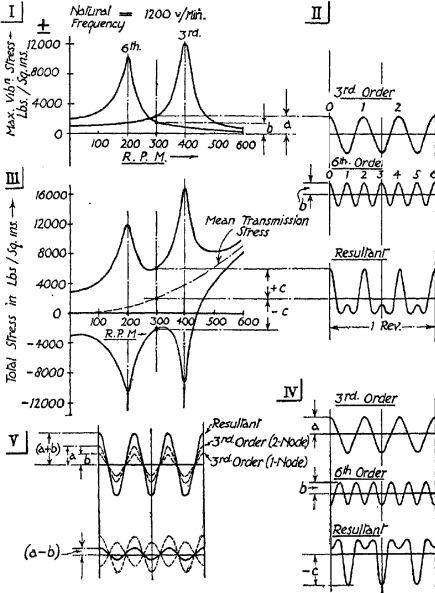


FIG. 105.—Summation of forced vibration stresses.

the forced vibration tabulations for this harmonic must be omitted, the summation being confined to the non-resonating harmonics. The amplitude of the resonating harmonic is

then estimated by the method to be described in the next chapter and added to the summation of the non-resonating harmonics, bearing in mind that at resonance the forcing torque leads the vibration torque by a quarter of a cycle.

A detailed investigation of this type is given by Carter and Muir in *R. and M.*, 1304, "Torsional Resonance Characteristics of a Twelve Vee Aero Engine," H.M. Stationery Office.

Table 73 shows the application of the tabulation method to the determination of the forced vibration amplitudes originated by the 6th order harmonic component of the engine torque for the system shown in Fig. 13, at the normal operating speed of 310 r.p.m. Since the engine is a 6-cylinder, 4-stroke cycle, single-acting engine the 6th order is a major order, so that the forcing torques at the six cylinders are all in phase. A single tabulation will therefore be sufficient in this example.

The forced vibration tabulation is given in Table 73, and since this is built up in exactly the same way as Table 70 there should be no difficulty in following the procedure.

The frequency of the forcing impulses for the 6th order torque variation at 310 r.p.m. is

$$F = 6 \times 310 = 1860 \text{ vibs./min.},$$

i.e. $\omega = 2 \cdot \pi \cdot F/60 = 194.5 \text{ radians/sec.},$
 or $\omega^2 = 37,900.$

Also, in the present example the 6th order forced vibration is being investigated, so that the values to be inserted in column F are the 6th order harmonic components of the engine torque for each cylinder,

$$\text{i.e. } M_n = T_n \cdot A \cdot R \cdot \text{lbs.-ins. per cylinder,}$$

where $T_n = 6\text{th order harmonic component of the tangential effort curve for one cylinder in lbs. per sq. in. of piston area,}$
 $A = \text{area of piston in sq. ins.},$
 $R = \text{crank radius in ins.}$

In this example the cylinders are 13.5-in. bore \times 18-in. stroke, 4-S.C., S.A. engine, and the mean indicated pressure at 310 r.p.m. is 100 lb. per sq. in.

DETERMINATION OF STRESSES

657

TABLE 73.—FORCED VIBRATION AMPLITUDES.
 $F = 1860 \text{ Vibs./Min.}; \omega = 194.5 \text{ Radians/Sec.}; \omega^2 = 37930 \text{ Radians}^2/\text{Sec.}^2$

A	B	C	D	E		F	G	H	I
				Torque in Plane of Mass.					
Mass.	Moment of Inertia.	Ascn. Torque per Unit Amplitude.	Deflection in Plane of Mass.	Acceleration Torque.	Residual Harmonic Torque.	Total Torque.	Total Torque.	Shaft Stiffness.	Change of Deflection.
	J , Lbs.-Ins. ² /Sec. ²	$J \cdot \omega^2$, Lbs.-Ins./Rad.	δ , Radians.	$J \cdot \omega^2 \cdot \theta$, Lbs.-Ins.	M_H , Lbs.-Ins.				
No. 1 Cyl.	165	6,259,000	\times	6,259,000x	5,795	6,259,000x + 5,795	6,259,000x + 5,795	20.2×10^7	$0.0310x + 0.0000287$
No. 2 Cyl.	165	6,259,000	$0.9690x - 0.0000287$	6,065,000x	179	12,324,000x + 11,411	12,324,000x + 11,411	20.2×10^7	$0.0610x + 0.0000564$
No. 3 Cyl.	165	6,259,000	$0.9808x - 0.0000851$	5,686,000x	533	18,004,000x + 16,673	18,004,000x + 16,673	20.2×10^7	$0.0891x + 0.0000825$
No. 4 Cyl.	165	6,259,000	$0.8189x - 0.0001676$	5,123,000x	1,050	23,129,000x + 21,418	23,129,000x + 21,418	20.2×10^7	$0.1145x + 0.0001061$
No. 5 Cyl.	165	6,259,000	$0.7944x - 0.0002737$	4,400,000x	1,710	27,529,000x + 25,593	27,529,000x + 25,593	20.2×10^7	$0.1363x + 0.0001261$
No. 6 Cyl.	165	6,259,000	$0.5681x - 0.0003998$	3,586,000x	2,500	31,089,000x + 28,798	31,089,000x + 28,798	17.0×10^7	$0.1830x + 0.0001691$
Generator	23,500	891,500,000	$0.3851x - 0.0005669$	343,500,000x - 507,500	0	374,589,000x - 478,702	374,589,000x - 478,702	—	—
$\times = 478,702/374,589,000 = 0.001276 \text{ radian.}$									
No. 1 Cyl.	165	6,259,000	0.001276	7,975	5,795	13,770	13,770	20.2×10^7	0.000068
No. 2 Cyl.	165	6,259,000	0.001268	7,555	5,795	27,120	27,120	20.2×10^7	0.000134
No. 3 Cyl.	165	6,259,000	0.001074	6,720	5,795	30,655	30,655	20.2×10^7	0.000196
No. 4 Cyl.	165	6,259,000	0.000878	5,490	5,795	50,820	50,820	20.2×10^7	0.000252
No. 5 Cyl.	165	6,259,000	0.000626	3,915	5,795	60,690	60,690	20.2×10^7	0.000300
No. 6 Cyl.	165	6,259,000	0.000326	2,040	5,795	68,405	68,405	17.0×10^7	0.0004027
Generator	23,500	891,500,000	-0.000977	-68,405	0	0	0	—	—

The value of T_n for the 6th order at 100 lbs. per sq. in. M.I.P. is 4.5 lbs. per sq. in., from Fig. 83A, and Table 54 shows that the 6th order inertia component is small and may be neglected.

Hence, $M_n = 4.5 \times 143 \times 9 = 5795$ lbs.-ins. per cylinder.

Assuming identical indicator diagrams, this value is the same for all cylinders, and since the 6th order is a major order all the forcing torques are in phase.

In multi-mass systems the alternative method of obtaining the forced vibration amplitudes by algebraical summation of the rolling and twist amplitudes at each point in the system is not always easy to apply. This is because the number of different modes of free vibration increases in proportion to the number of shafts. In the present example, since there are seven masses connected together by six shafts, there are six principal modes of free vibration. Theoretically, therefore, the twist amplitudes corresponding to all six modes of vibration must be determined before the forced vibration amplitude summation can be carried out. The method, however, is precisely the same as for the simple two- and three-mass systems already discussed.

In a great many practical cases there is not much error in neglecting the higher modes of vibration. For example, in the case of marine installations of the type shown at (c) and (d) in Fig. 18, the one- and two-node modes of free vibration are usually the only modes which need be considered when evaluating both forced and resonant vibration amplitudes. In the case of closely coupled installations of the type shown at (b) in Fig. 18, the one-node mode of free vibration is usually the only mode which need be considered when evaluating both forced and resonant vibration amplitudes. In the majority of normal practical cases it is rarely necessary to consider modes of free vibration with three or more nodes.

The example on which Table 73 is based is a closely coupled system (see Fig. 13). Hence it is of interest to determine the error in the forced vibration amplitudes when these are obtained by algebraical summation of the rolling and one-node twist amplitudes instead of by tabulation.

Rolling Amplitude.—The applied torque, assuming rigid shafting, is six times the 6th order harmonic torque for one-cylinder, since the engine under consideration is a six-cylinder unit,

i.e. applied torque = $\Sigma M_n = 5795 \times 6 = 34,770$ lbs.-ins.

The total polar moment of inertia of the oscillating masses is the sum of the quantities in column B of Table 73, namely, 24,490 lbs.-ins. sec.².

The phase velocity of the 6th order forced vibration at 310 r.p.m. is $\omega = 194.5$ radians per sec., i.e. $\omega^2 = 37,900$.

Now, for a rigid system,

$$\Sigma M_n = -\omega^2 \cdot \alpha_R \cdot (\Sigma J).$$

Hence,

$$\alpha_R = \text{rolling amplitude} = -\frac{34770}{37900 \times 24490} = -0.0000375 \text{ radian.}$$

Twist Amplitudes (One-Node Mode).—The value of the equilibrium amplitude, θ_0 , for the 6th order harmonic component of the engine torque is 0.035° , or 0.00061 radian (from Table 66, since the magnitude of the resultant 6th order harmonic component per cylinder is 4.5 lbs. per sq. in. in Table 66 and in this example).

The one-node natural frequency for this installation is 2520 vibs./min., i.e. $\omega_0^2 = 69,750$ (from Table 1), so that the dynamic magnifier at 310 r.p.m., where $\omega^2 = 37,900$ for the 6th order impulse, is

$$\text{Dynamic magnifier} = \frac{1}{1 - \frac{37900}{69750}} = 2.19.$$

Hence, $\alpha_{v_1} = 0.00061 \times 2.19 = 0.00134$ radian.

This is the twist amplitude at No. 1 cylinder, i.e. at the free end of the crankshaft, since the equilibrium amplitude applies to this point in the oscillating system.

The twist amplitudes at the other points in the system are directly proportional to the amplitudes given in column F of the natural frequency tabulation (Table 1).

Thus

$$\alpha_{v_2} = \text{twist amplitude at No. 2 cylinder} = \alpha_{v_1}(0.9430/1.0000) \\ = 0.00134 \times 0.943 = 0.00126 \text{ radian,}$$

and so on.

The following table shows the forced vibration amplitudes obtained by algebraical summation of the rolling and one-node twist amplitudes compared with the values obtained by tabulation, to the fifth decimal place:—

Mass.	α_R (Rolling).	α_T (Twist).	$(\alpha_R + \alpha_T)$.	α_p (From Col. D of Table 73).
No. 1 cyl.	-0.00004	0.00134	0.00130	0.00128
No. 2 cyl.	-0.00004	0.00126	0.00122	0.00121
No. 3 cyl.	-0.00004	0.00112	0.00108	0.00107
No. 4 cyl.	-0.00004	0.00090	0.00086	0.00088
No. 5 cyl.	-0.00004	0.00064	0.00060	0.00063
No. 6 cyl.	-0.00004	0.00034	0.00030	0.00033
Generator	-0.00004	-0.00004	-0.00008	-0.00008

The above table shows that the amplitudes obtained by algebraical summation of the rolling and one-node twist amplitudes are very nearly the same as the forced vibration amplitudes obtained by tabulation. The error would be even smaller if the twist amplitudes corresponding to the two-node mode of free vibration were also taken into account, but even without this refinement the error is not large. It should be observed that since the rolling amplitude is small the swinging form for the forced vibration is very nearly the same as the swinging form for one-node natural vibration.

Forced Vibration Torque and Stress.—The resultant forced vibration torque in any section of shafting due to a given harmonic of the forcing torque is given in column G of the forced vibration tabulation, and the corresponding stress in the shaft is easily determined from the relationship

$$f = T/Z \text{ lbs. per sq. in.,}$$

- where f = maximum value of the shear stress in the shaft at the section under consideration,
- T = resultant forced vibration torque in the section of shaft under consideration, from column G of the forced vibration tabulation, in lbs.-ins.,
- Z = torsional modulus of the shaft section under consideration in in.³ units
= $\pi \cdot d^3/16$ for a solid shaft of diameter d inches.

In multi-cylinder internal combustion engines, where there are several forcing torques, each containing a great many component harmonics, applied at different points in the oscillating system, the exact determination of the resultant forced vibration amplitudes, torques, and stresses is exceedingly complex, especially if the engine operates over a wide speed range with a load characteristic which changes with speed and if there is more than one mode of vibration to be considered.

Fortunately, in practice, only those harmonics of the forcing torques which excite strong resonant vibrations at the appropriate critical speeds within or near to either end of the operating speed range need, in general, be considered. In most cases, therefore, it suffices to determine the positions of the various critical speeds corresponding to those modes of vibration which experience has shown to be a likely cause of trouble, and then to estimate the relative magnitudes of the forcing torques at those speeds in accordance with the methods already discussed.

The equilibrium amplitudes for each mode and for each component harmonic can then be determined as already explained, and the flanks of the various resonance curves can be drawn at their appropriate positions in the speed range. Finally, the resonance curves can be completed by estimating the amplitude at resonance, using the methods to be described in the next chapter. These calculations yield diagrams of the type shown at the top of Figs. 122 and 123, each resonance curve being plotted separately and no attempt being made to obtain a combined diagram.

Cases do arise in practice, however, where it is desirable to obtain at least an approximation to the combined forced vibration diagram. For example, Diagram I in Fig. 105 shows the separate resonance curves for the 3rd and 6th order forced vibration stresses occurring at the most highly stressed section in the oscillating system. It is desired to determine the resultant stress when the engine is operating in the gap between these two criticals, say at 300 r.p.m.

The usual approximation made in practice is simply to add the separate stresses arithmetically, the resultant curve being shown at III in Fig. 105. The steady stress due to transmission of the mean torque is usually included in this summation, so that the resultant diagram gives an indication of the stress ranges at each speed.

Thus in Diagrams I and III of Fig. 105 the resultant stress at 300 r.p.m. is obtained as follows :—

$$\begin{aligned} \text{If } a &= \text{3rd order forced vibration stress at 300 r.p.m.} \\ &= \pm 2250 \text{ lbs. per sq. in.,} \\ b &= \text{6th order forced vibration stress at 300 r.p.m.} \\ &= \pm 1550 \text{ lbs. per sq. in.,} \\ \text{then } c &= \text{resultant forced vibration stress at 300 r.p.m.} \\ &= (a + b) = \pm (2250 + 1550) = \pm 3800 \text{ lbs. per sq. in.} \end{aligned}$$

The steady stress due to the transmission of the mean torque is 2000 lbs. per sq. in. at 300 r.p.m.

Hence, total stress at 300 r.p.m. = $2000 \pm 3800 = +5800$
and -1800 lbs. per sq. in.

The above approximate method is equivalent to assuming that the vibration stresses are in phase at some point in the cycle. Diagram II of Fig. 105 shows the summation of the 3rd and 6th order vibration stresses at 300 r.p.m., assuming that they are in phase at the commencement of the cycle.

This diagram shows that the resultant stress varies from $+3800$ to -1960 lbs. per sq. in., so that in this case the approximate method is correct so far as the positive value of the resultant vibration stress is concerned, but over-estimates the magnitude of the negative value.

Diagram IV of Fig. 105 shows the summation when the components are in anti-phase at the commencement of the cycle. In this case the negative value of the resultant vibration stress agrees with the approximate method, but the positive value is over-estimated. In general, the approximate method tends to over-estimate the magnitudes of the resultant vibration stresses, but this error is not usually very serious. Moreover, it provides a useful factor of safety against the possibility of phase changes occurring in operation, due to any small changes in operating conditions which are liable to occur from time to time.

For this reason it is doubtful whether a more elaborate method of calculating the resultant stresses would really provide a truer picture.

The foregoing method applies to cases where the component resonance curves are all for the same mode of vibration, so that the component harmonics have different frequencies at any selected speed. For example, in Diagram I of Fig. 105 the frequency of the 6th order component is 1800 cycles per minute at 300 r.p.m., whereas the frequency of the 3rd order component is only 900 cycles per minute at the same r.p.m. The natural frequency is, of course, the same for both harmonics since they both correspond to the same mode of vibration, i.e. 3rd order resonance occurs at 400 r.p.m. and 6th order resonance at 200 r.p.m., the natural frequency being 1200 cycles per minute in each case.

The method given in Fig. 105 cannot be used for obtaining the resultant force vibration stresses due to the combined action of several harmonics which have the same frequency at the selected speed. For example, if the curve which peaks at 200 r.p.m. in Diagram I of Fig. 105 is assumed to be the 3rd order one-node resonance curve and the curve which peaks at 400 r.p.m. the 3rd order two-node resonance curve, the error in adding these together without regard to phase might be very serious. Diagram V in Fig. 105 illustrates this point. It is evident that the resultant may have any value from the sum to the difference of the component values depending on the phasing.

In this example both curves are excited by the 3rd order component harmonic of the forcing torque, so that the forced vibration frequencies at any selected speed are the same; for example, at 300 r.p.m. the forced frequency is 900 cycles per minute in each case. The natural frequency for one curve, of course, differs from that for the other, i.e. 3rd order one-node resonance occurs at 200 r.p.m., the corresponding one-node natural frequency being 600 vibs./min., whilst the 3rd order two-node resonance occurs at 400 r.p.m., the corresponding natural frequency being 1200 vibs./min.

So far as the evaluation of forced vibration stresses is concerned it is not necessary to combine the stresses caused by different modes of vibration, because in all normal practical cases the point in the shaft system at which the most severe stress due to one mode of vibration occurs, does not coincide with the point at which the stress due to another mode of vibration is most severe. Thus in a marine propeller drive the most severe one-node stress is felt in the propeller shafting, whilst the one-node stress in the crankshaft section is negligible. Similarly, the most severe two-node stress occurs in the crankshaft section, whereas the two-node stress in the propeller shafting is negligible (see Diagram (c) of Fig. 18). In a great many other cases the two-node mode of vibration is so high that the two-node stresses which occur in the operating range are quite unimportant and can be completely neglected. It is rarely necessary to consider more than two modes of vibration.

In the extremely rare case where severe stresses due to two different modes of vibration do occur at a speed within the operating range and at the same point in the system, the resultant forced vibration stress can be determined by the tabulation method. In such cases it is highly probable that the severe condition will be confined to a single component harmonic of the forcing torque, so that the tabulation need only be carried out for this particular harmonic. Such cases are difficult to visualise, however, and in any case it is desirable to design the installation so that such conditions do not arise. An example of poor design in this connection is the system

shown at (a) in Fig. 18, where the nodes for two modes of vibration are all closely grouped round the flywheel mass.

In general, therefore, the calculation of forced vibration stresses can be reduced to the comparatively simple procedure given in the earlier part of this chapter, which can be summarised as follows:—

- (i) Determine the natural frequencies of the modes of vibration which experience has shown are a likely source of troublesome vibration. For example, the one- and two-node modes of marine propelling installations and the one-node modes of close-coupled installations such as aero-engine/air-screw systems, electrical generator systems, and so on.
- (ii) Determine the resultant magnitudes of the harmonic components of the forcing torques which occur within or near the operating speed range, including any severe components which occur in the lower speed range and which will be negotiated when starting, stopping, or idling.
- (iii) Determine the equilibrium amplitudes and the corresponding stresses at the most severely stressed section of the shaft system.
- (iv) The forced vibration stresses at different speeds may then be obtained for each component harmonic by multiplying the relevant equilibrium stresses by the appropriate dynamic magnifiers.
- (v) The combined stress diagram may be obtained by arithmetical addition of the several component resonance curves and the curve of mean transmission stress.

Forced vibration tabulations are required, however, when investigating the question of speed fluctuation at different points in the transmission system, and at a selected speed. The tabulation automatically shows the magnitudes of the forced vibration amplitudes at each mass, due to all modes of vibration, and including the rolling motion which does not appear in the equilibrium amplitude calculations. The cyclic

speed variation for any given harmonic can then be obtained from the tabulated amplitudes in the manner already described. As a general rule only the dominating harmonic need be considered when evaluating cyclic speed variation, for example, the 3rd order component in the case of a 6-cylinder in-line, 4-stroke cycle oil engine. If more than one harmonic needs to be considered, then separate tabulations will be required for each, and the motions will then require combining in correct phase relationship to give the overall motions at the different masses.

EXAMPLE 50.—Calculate the coefficient of speed fluctuation at the service speed of 138 r.p.m. due to the 3rd order harmonic component of the engine torque curve for the marine installation shown in Fig. 15.

The engine is a 6-cylinder, 4-stroke cycle, single-acting oil engine, with cylinders 620 mm. bore \times 1300 mm. stroke, developing 2750 B.H.P. or 3250 I.H.P. at 138 r.p.m. and 130 lbs. per sq. in. M.I.P.

Resultant 3rd Order Harmonic Component of Engine Torque Curve.

$$T_n = \sqrt{(A + B)^2 + C^2} \text{ lbs. per sq. in. of piston area tangential effort acting at crank radius,}$$

where $A =$ sine term of 3rd order harmonic component of tangential effort curve for gas pressure alone
 $= 23.5$ lbs. per sq. in. of piston area at 130 lbs. per sq. in. M.I.P. (from Table 6r),

$B =$ 3rd order harmonic component of inertia tangential effort curve (sine term only)
 $= 0.000284 W \cdot R \cdot N^2 \cdot H_n$ (see Table 54),

$W =$ weight of reciprocating parts per cylinder in lbs. per sq. in. of cylinder area
 $= 11.5$ lbs. per sq. in. in this example,

$R =$ crank radius in ins. $= 25.6$ ins.,

$N =$ r.p.m. $= 138$,

$H_n =$ 3rd order multiplier (from Table 57)

$= -0.192$ for a con. rod/crank ratio of 4,

- i.e. $B = -0.0000284 \times 11.5 \times 25.6 \times 138^2 \times 0.19217$
 $= -30.6$ lbs. per sq. in. of piston area,
 $C =$ cosine term of 3rd order harmonic component of tangential effort curve for gas pressure alone
 $= -9.5$ lbs. per sq. in. of piston area at 130 lbs. per sq. in. M.I.P. (from Table 61).

Hence, $T_n = \sqrt{(23.5 - 30.6)^2 - 9.5^2} = 11.85$ lbs. per sq. in. of piston area.

Equilibrium Amplitude.—This is obtained from Equation (247),

$$\theta_0 = \frac{1.83D^2 \cdot R \cdot T_n \cdot \Sigma a}{F^2 \cdot \Sigma(J \cdot a^2)} \text{ degrees,} \quad (247)$$

- where $D =$ diameter of cylinder in ins. $= 24.4$ ins.,
 $R =$ crank radius in feet $= 2.13$ ft.,
 $T_n =$ 3rd order resultant harmonic component of tangential effort curve for one cylinder
 $= 11.85$ lbs. per sq. in. of piston area,
 $\Sigma a =$ 3rd order vector sum $= 5.781$ (from Table 67),
 $F =$ one-node natural frequency $= 165.5$ vibs./min. (from Table 3),

$\Sigma(J \cdot a^2) =$ effective moment of inertia of system referred to free end of shaft
 $= 39.245$ tons-ft. sec.² (from Table 68).

Hence, $\theta_0 = \frac{1.83 \times 24.4^2 \times 2.13 \times 11.85 \times 5.781}{165.5^2 \times 39.245} = 0.148^\circ$
 $= 0.00258$ radian at No. 1 cylinder.

Vibration Amplitude at 138 r.p.m. at No. 1 Cylinder:

$$\alpha_v = \frac{a}{1 - \frac{(N)^2}{(N_0)^2}}, \quad (\text{from Equation (234)})$$

where $N =$ impulse frequency $= 138 \times 3 = 414$ impulses/min.,

$N_0 =$ natural frequency $= 165.5$ vibs./min.,

i.e. $\alpha_v = \frac{0.00258}{1 - \frac{(414.0)^2}{(165.5)^2}} = -0.000492$ radian at No. 1 cylinder.

Oscillation Amplitude, assuming Rigid Shafting :

$$\alpha_R = - \frac{M_n}{J \cdot \omega}$$

where M_n = total externally applied torque, assuming rigid shafting

$$= T_n \cdot A \cdot R = 11.85 \times 468 \times 2.13/2240 .$$

$$= 5.275 \text{ tons-ft. per cylinder}$$

$$= 31.65 \text{ tons-ft. for the six cylinders,}$$

J = total moment of inertia of oscillating parts, assuming rigid shafting

$$= 10.145 \text{ tons-ft. sec.}^2 \text{ (i.e. the sum of the values in column D of Table 3),}$$

$$\omega = \text{phase velocity of forced vibration} = 2 \cdot \pi \cdot F/60$$

$$= 43.3 \text{ radians/sec. for } F = 414 \text{ vibs./min.}$$

Hence, $\alpha_R = - \frac{31.65}{10.145 \times 1880} = - 0.00166$ radian at all points in the system.

Forced Vibration Amplitudes :

(i) At No. 1 cylinder :

$$\alpha_F = \alpha_V + \alpha_R = - 0.000492 - 0.00166$$

$$= - 0.002152 \text{ radian.}$$

(ii) At propeller :

this is obtained from column F of Table 3, viz.,

$$\alpha_V = - 0.000492 \times \frac{(- 4.0076)}{(1.0000)} = 0.00197 \text{ radian,}$$

i.e. $\alpha_F = \alpha_V + \alpha_R = 0.00197 - 0.00166 = 0.00031$ radian.

Coefficient of Speed Fluctuation :

this is obtained from Equation (421), viz.,

$$C = 2 \cdot \alpha_F \cdot n,$$

where n = order number of the oscillations, i.e. number of complete oscillations per revolution

$$= 3 \text{ in this example.}$$

Hence, $C = 2 \times 0.002152 \times 3 = 0.0129 = 1/77.5$ at No. 1 cylinder

$$= 2 \times 0.00031 \times 3 = 0.00186 = 1/538 \text{ at propeller.}$$

In a 6-cylinder, 4-stroke cycle, single-acting oil engine 3rd order forced vibrations predominate, and are the main cause of cyclic variation of speed. The values in column F of Table 3 show that there is not much variation of the specific vibration amplitudes between No. 1 and No. 6 cylinders, so that for practical purposes the coefficient of speed fluctuation in this example may be taken as $1/77.5$ at the engine end of the installation and $1/538$ at the propeller. These values show that the propeller has comparatively small regulating effect on the engine, which is typical of installations where the propeller is separated from the engine by a long length of intermediate shafting.

TORSIONAL VIBRATION ANALYSIS—EFFECTIVE INERTIA METHOD.

(With Special Reference to Aero-Engine/Air-Screw Systems.)

THE conception underlying the method discussed in the following pages has already been briefly described in Chapter 3, where it was shown that a mass elastically connected to an oscillating system can be replaced by an equivalent rigidly connected mass, the polar moment of inertia of which is not a constant quantity but varies with the frequency of the torsional oscillations [see Fig. 49, and Equation (92)].

It will now be shown that any system capable of executing torsional oscillation can be regarded as composed of two portions, one of which is regarded as an elastically connected portion which can be replaced by a single equivalent mass rigidly connected to the other portion at the point of division. This device will be found exceedingly useful in the case of complex systems, such as geared installations having several branches or installations containing distributed inertias, such as heavy shafts. Furthermore, the method leads to a comparatively simple experimental means for determining the natural frequencies and other torsional vibration characteristics of systems containing members which have complex or mathematically indeterminate mass/elastic characteristics, such as air-screws.

Simple Two-mass System.—Diagram (a) of Fig. I shows a simple two-mass system comprising masses of polar moments of inertia, J_1 and J_2 , on a shaft of torsional rigidity C .

If it is assumed that this system is divided at any arbitrary point Z into two portions, and if the right-hand portion, i.e. mass J_1 on shaft C_1 is regarded as the *basic system*, then the left-hand portion, i.e. mass J_2 on shaft C_2 , can be regarded as an *elastically connected portion* which can be replaced by a single equivalent mass J_s rigidly connected to the basic system at the point of division Z .

The equivalent mass J_s will be referred to as the *effective inertia* of that portion of the original system which is regarded as the elastically connected portion.

The natural frequency of the original system can be determined from the characteristics of the separated portions, as follows :—

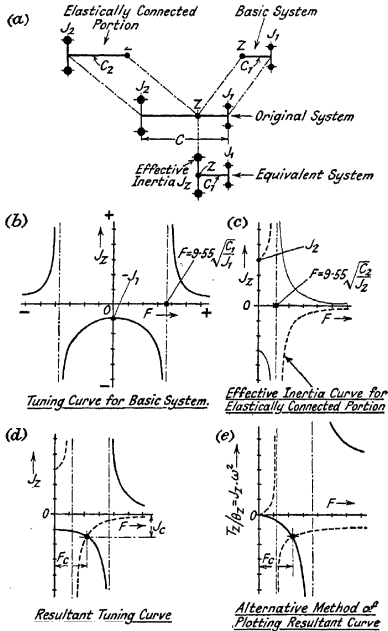


FIG. 1.—Tuning curves—two-mass system.

(i) *Tuning Curve for Basic System.*—The first step is to plot a curve showing the variation of the natural frequency of the basic system with variation of the effective inertia J_z .

This curve is shown at (b) in Fig. I, and is plotted from the familiar expression for the natural frequency of a two-mass system, Equation (16),

$$\text{i.e.} \quad F = 9.55 \sqrt{C_1(J_1 + J_2)/(J_1 \cdot J_2)}.$$

It should be noted that, as shown at (b) in Fig. I, the tuning curve must be plotted for *all* values of the effective inertia J_z , from minus to plus infinity.

The natural frequency of the basic system corresponding to any selected value of the effective inertia J_z can thus be read directly from the tuning curve.

The curve shown at (b) in Fig. I is the complete tuning curve for the basic system and therefore shows negative as well as positive roots of the frequency equation. Since, however, negative frequency values have no practical significance, the negative frequency branches of the tuning curve, i.e. the branches on the left-hand side of the axis of ordinates, can be disregarded, and will be omitted in all subsequent diagrams.

The plotting of the tuning curve is facilitated by noting the following special cases:—

Since the frequency equation can be written,

$$F = 9.55 \sqrt{C_1(1/J_z + 1/J_1)}.$$

Hence, when

$$J_z = -J_1, \quad F = 0;$$

$$J_z = \text{inf.}, \quad F = 9.55 \sqrt{C_1/J_1}, \quad \text{which is the natural frequency of mass } J_1 \text{ on shaft } C_1;$$

$$J_z = 0, \quad F = \text{inf.}$$

Thus the negative branch of the tuning curve commences at a value $J_z = -J_1$, and the asymptote is situated at a value

$$F = 9.55 \sqrt{C_1/J_1},$$

as shown in Diagram (b) of Fig. I.

(ii) *Effective Inertia Curve for the Elastically Connected System.*

Let J'_z = polar moment of inertia of the mass, assumed to be rigidly connected at point Z in the elastically connected portion, which is necessary to tune the elastically connected portion to any prescribed frequency F,

T'_z = torsional vibration torque applied by the basic system at point Z in the elastically connected portion,

θ'_z = torsional vibration amplitude at point Z in the elastically connected portion,

ω = phase velocity of the torsional vibration = $2 \cdot \pi \cdot F/60$,

F = frequency of torsional vibration in vibs./min.

Then, from the fundamental relationship,

$$\text{Torque} = (\text{polar moment of inertia}) \times (\text{angular acceleration}),$$

$$T'_z = J'_z \cdot \theta'_z \cdot \omega^2.$$

Now let J_z = the effective inertia of the elastically connected portion at point Z ,

T_z = torsional vibration torque applied by the elastically connected portion at point Z in the basic system,

θ_z = torsional vibration amplitude at point Z in the basic system.

Then, assuming that, as shown at (a) in Fig. I, there is no mass at Z in the original system,

$$T_z = -T'_z, \text{ and } \theta_z = \theta'_z,$$

i.e. $T_z = J_z \cdot \theta'_z \cdot \omega^2 = -J'_z \cdot \theta'_z \cdot \omega^2,$

or $J_z = -J'_z.$

This is an important result, since it implies that the effective inertia curve for any system is simply the mirror-image of the tuning curve about the $O-F$ axis. Thus in Diagram (c) of Fig. I the full lines show the tuning curve, whilst the dotted lines show the corresponding effective inertia curve.

In the example shown in Fig. I, the tuning curve for the elastically connected portion is plotted from the expression for the natural frequency of a two-mass system, namely,

$$F = 9.55 \sqrt{C_2(J_2 + J'_z)/(J_2 \cdot J'_z)},$$

or $J_z = \frac{J_2}{F^2 \cdot J_2 - 1} \cdot C_2$

but $J_z = -J'_z,$

i.e. $J_z = \frac{J_2}{1 - F^2 \cdot J_2} \cdot C_2$

This expression agrees with Equation (92).

Note that, when $F = 0, J_z = J_2;$
 $F = 9.55 \sqrt{C_2/J_2}, J_z = \text{inf.};$
 $F = \text{inf.}, J_z = 0.$

(iii) *Resultant Tuning Curve.*—Diagram (c) in Fig. I gives the values of the effective inertias of the elastically connected portion when this portion is assumed to be replaced by a mass rigidly connected to the basic system at point Z , whilst Diagram (b) gives the values of the polar moments of inertia of the mass which must be

rigidly connected to the basic system at point Z to tune it to any prescribed frequency F , and which will be referred to as the *tuning mass*.

It is therefore evident that if these two diagrams are superimposed their points of intersection will give the true natural frequencies of the combined portions, i.e. the natural frequencies of the original system.

The combined tuning curve is shown at (d) in Fig. I, where, at the point of intersection, F_c is the true natural frequency of the original system, whilst J_c is the polar moment of inertia of the mass which would have to be rigidly attached to the basic system at point Z to tune it to a frequency F_c if the elastically connected portion were removed.

Since in this example the original system has only one-degree of freedom there is only one natural frequency and therefore only one point of intersection in the combined tuning curve.

Diagram (e) in Fig. I shows an alternative method of plotting the tuning and effective inertia curves in which the quantity $T_z/\theta_z = J_z \cdot \omega^2$ is plotted against F . This gives diagrams which are somewhat easier to read, but since the type of diagram shown at (d), where $J_z = T_z/(\theta_z \cdot \omega^2)$ is plotted against F , is easier to interpret it will be used throughout the following discussion.

Once the fundamental principles are understood, however, it will be found more convenient in practice to work with diagrams of type (e), and the function T_z/θ_z can be plotted directly from experimental determinations of T_z and θ_z , as will be explained later.

Three-Mass System.—A typical three-mass system is shown in Fig. II, consisting of masses J_1 , J_2 , and J_3 on shafts C_1 and C_2 .

An arrangement of this type would normally be solved by means of the frequency equation for a three-mass system, i.e. Equation (19).

In applying the *Effective Inertia Method*, the same procedure is used as already described for a two-mass system, i.e. the original system is assumed to be divided into two portions, one of which is regarded as the *Basic System* and the other as the *Elastically Connected Portion*. The point of division can be chosen anywhere in the original system, although usually the computation details are simplified appreciably by choosing this point judiciously. For example, in the case of an internal combustion engine driving a flywheel with flexible spokes or an air-screw with flexible blades, there is considerable advantage in choosing the point of division at the flywheel or air-screw hub and regarding the engine portion as the basic system, mainly because this simplifies the evaluation of the vibrational energy input from the engine, as will be explained later.

For purposes of illustration two methods of dividing a three-mass system are shown in Fig. II, where the diagrams in column (a)

correspond to a point of division Z in the shaft between masses J_2 and J_3 , whilst in column (b) the point of division is at mass J_2 .

Dealing first with the diagrams in column (a).

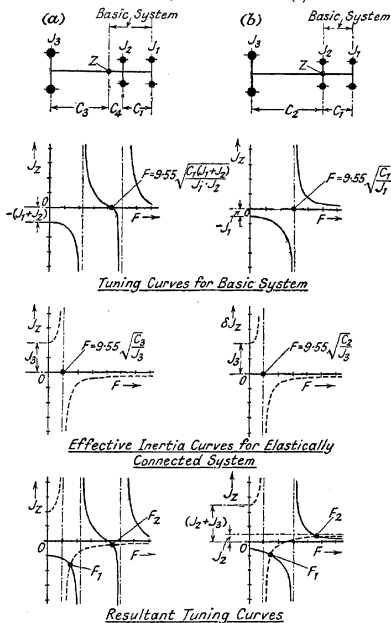


FIG. II.—Tuning curves—three-mass system.

(i) *Tuning Curve for Basic System.*—Assuming that the system to the right of point Z is the basic system, the quantities involved are masses J_1 , J_2 , and J_z on shafts C_1 and C_2 , where J_z is the effective inertia of the elastically connected portion.

The tuning curve for the basic system can therefore be plotted from the frequency equation for a normal three-mass system, i.e. Equation (19), by substituting values of J_z between minus and plus infinity and solving the equation for F .

The following special points should be noted:—

$$\text{When } J_z = -(J_1 + J_2), F = 0;$$

$$J_z = 0, F = \text{inf. or } 0.55 \sqrt{C_1(J_1 + J_2)/(J_1 \cdot J_2)}$$

(i.e. the system reduces to a two-mass system comprising masses J_1 and J_2 on shaft C_1 when J_z is zero).

$$\text{When } J_z = \text{inf.}, \text{ the frequency equation reduces to Equation (18),}$$

$$\text{i.e. } 1 - (J_1/C_1 + J_1/C_2 + J_2/C_2)\omega^2 + J_1 \cdot J_2 \cdot \omega^4/(C_1 \cdot C_2) = 0.$$

The roots of this equation give the values of F at the asymptotes of the tuning curve for the basic system.

The complete tuning curve shows that except between the values $J_z = 0$ to $-(J_1 + J_2)$ there are two positive roots of the frequency equation, i.e. the tuning curve has three branches.

(ii) *Effective Inertia Curve for the Elastically Connected Portion.*—Since the elastically connected portion simply consists of mass J_3 on shaft C_3 the effective inertia curve can be plotted from the frequency equation for a two-mass system, Equation (16);

$$\text{i.e. } F = 0.55 \sqrt{C_3(J_3 + J'_z)/(J_3 \cdot J'_z)},$$

whence $J_z = -J'_z$, as already explained,
where $J_z =$ the effective inertia of the elastically connected system.

$$\text{Note that when } J_z = J_3, F = 0;$$

$$\text{and when } J_z = \text{inf.}, F = 0.55 \sqrt{C_3/J_3}.$$

(iii) *Resultant Tuning Curve.*—This is obtained by superimposing the tuning curve for the basic system (full lines) on the effective inertia curve for the elastically connected portion (dotted lines).

The points of intersection of the two families of curves give the true natural frequencies F_1 and F_2 shown in Fig. II.

The alternative method of dividing the original system shown in column (b) of Fig. II will now be considered. In this alternative method the point of division Z is at mass J_3 . Mass J_2 can thus be regarded as part of the basic system; or as part of the elastically connected portion; or as an independent mass. The latter choice will be assumed, since in most cases this simplifies the computations.

(i) *Tuning Curve for Basic System.*—When J_2 is regarded as an independent mass the basic system comprises mass J_1 on shaft C_1 . Hence the tuning curve is plotted from the expression

$$F = 0.55 \sqrt{C_1(J_1 + J_z)/(J_1 \cdot J_z)},$$

where J_z is the effective inertia of the elastically connected system.

(ii) *Effective Inertia Curve for the Elastically Connected Portion.*—When J_2 is regarded as an independent mass the elastically connected portion comprises mass J_3 on shaft C_2 . Hence the effective inertia curve is obtained from the equation

$$F = 9.55 \sqrt{C_2(J_3 + J'_2)/(J_3 \cdot J'_2)},$$

and $\delta J_x = -J'_x =$ the effective inertia of the elastically connected portion.

(iii) *Resultant Tuning Curve.*—This is obtained by superimposing the tuning curve for the basic system (full lines) on the effective inertia for the elastically connected portion (dotted lines), taking care to make due allowance for the influence of the independent mass J_2 , i.e. J_2 must be added to all values of δJ_x when transferring the effective inertia curve for the elastically connected portion to the tuning curve for the basic system.

Thus $J_x = (\delta J_x + J_2)$, and this addition is readily carried out by displacing the $O - F$ axis of the effective inertia curve by an amount J_2 , as shown in Fig. II.

The intersections of the two families of curves, i.e. F_1 and F_2 , give the true natural frequencies of the original three-mass system.

If the resultant tuning curve in column (b) is compared with that in column (a) it will be seen that the natural frequencies, F_1 and F_2 are the same in both cases. The corresponding values of the effective inertias are different, however, due to the different locations of the point of division Z . It is evident that the method given in column (b) of Fig. II is simpler than that in column (a), mainly because the tuning curve for the basic system is plotted from the frequency equation for a two-mass system in column (b), whereas it is plotted from the frequency equation for a three-mass system in column (a).

Flywheel with Flexible Spokes.—Fig. III shows a system consisting of a single-crank engine driving a flywheel which has the rim connected to the hub by flexible spokes. The following treatment also applies where a flywheel rim is connected to its hub or centre-piece by bonded rubber, as described in Chapter 10.

This system can be represented diagrammatically by a three-mass arrangement comprising masses J_1 , J_2 , and J_3 on shafts C_1 and C_2 , where

- $J_1 =$ polar moment of inertia of engine masses,
- $J_2 =$ polar moment of inertia of flywheel hub,
- $J_3 =$ polar moment of inertia of flywheel rim,
- $C_1 =$ torsional rigidity of shaft between engine and flywheel hub,
- $C_2 =$ torsional rigidity of flywheel spokes (see Chapter 4).

If it is assumed that the original system consists of two portions with the point of division Z located at the flywheel hub, that the engine portion of the divided system is the basic system, and that the hub mass J_2 is an independent mass, then the resultant tuning curves shown at the bottom of Fig. III are readily obtained by the methods just described.

The resultant tuning curve at (a) is for a normal value of the polar moment of inertia of the flywheel hub, J_2 . There are two intersections, F_1 and F_2 , and these are the true natural frequencies of the original system.

The lower value F_1 corresponds to vibration with a node in the flexible spokes, whilst the upper value F_2 corresponds to vibration with two nodes, one in the shaft and one in the spokes.

If the flexibility of the spokes had been neglected, i.e. if the flywheel and its hub had been regarded as fixed rigidly to the engine shaft, then the system would have become a simple two-mass system with only one natural frequency, which is readily obtained from the resultant tuning curve by drawing a line parallel to the $O - F$ axis at a value $J_2 = (J_2 + J_3)$, the combined polar moment of inertia of the flywheel rim and hub. This is shown in Fig. III, where F_3 is the natural frequency of the system when the flexibility of the spokes is neglected. It is evident that large errors are introduced when the spoke flexibility is neglected.

The resultant tuning curve shown at (b) is for the case where the flywheel hub is so small relative to the rim that its polar moment of inertia can be neglected. In this case J_2 disappears and the original system reduces to a two-mass system with only one natural frequency, i.e. there is only one point of intersection F_1 in the tuning curve. The node is located, in this example, in the flexible spokes. It is evident that in this case also considerable error would be introduced by neglecting the flexibility of the spokes.

The resultant tuning curve shown at (c) is for the case where the polar moment of inertia of the flywheel hub is very large. In this case there are two natural frequencies, the values of which tend to approach the asymptotic values as the hub inertia approaches infinity. At the same time all the nodes tend to coincide at the hub or, in other words, the two natural frequencies are simply the natural frequencies of each of the end masses on their shafts regarded as fixed at the hub. Thus the upper frequency tends to become the same as the frequency for a rigidly connected flywheel, and the effect of spoke flexibility is to introduce an additional mode of vibration which is merely the vibration of the rim on its spokes regarded as fixed at the hub.

In practice it is improbable that a flywheel with a flexible connection between the rim and the hub would be treated as a rigidly connected mass so that the errors referred above are unlikely to

APPENDIX

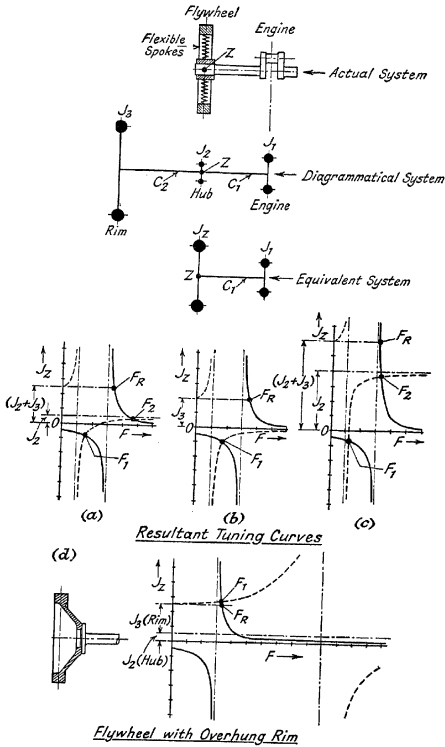


FIG. III.—Tuning curves for a system containing a flywheel with flexible spokes.

occur. The foregoing discussion is important, however, in relation to aero-engine/air-screw installations, since it indicates the possibility of important errors arising through using the commonly accepted practice of regarding the air-screw as a rigid body and neglecting the flexibility of its blades when investigating the torsional vibration characteristics of the system. This matter will be discussed later.

The resultant tuning curves shown at (a), (b), and (c) apply to cases where a flywheel rim is so flexibly connected to its hub that the natural frequency of the elastically connected portion of the original system is appreciably lower than the natural frequency of the basic system, i.e. the asymptote for the effective inertia curve (dotted lines) occurs at an appreciably lower frequency than the asymptote for the tuning curve (full lines).

Another case which occasionally occurs in practice is where the flywheel rim is overhung from the point of attachment to the shaft, as shown at (d) in Fig. III. In this case, since the disc connecting the rim to the shaft is usually very stiff torsionally the natural frequency of the elastically connected portion, i.e. the rim (dotted lines) is considerably higher than the natural frequency of the basic system (full lines). In most cases, therefore, the true natural frequency of the complete system F_1 is not greatly different from the value, F_r , obtained by assuming that the flywheel rim is rigidly connected to the shaft, as shown on the tuning curve at (d) in Fig. III. Thus the error in neglecting the overhang is negligible in the majority of practical cases.

Simple Systems with Several Branches.—Fig. IV shows a simple branched system with four branches each comprising a single mass elastically connected to a common point at which a fifth mass is situated. The torsional vibration frequencies of this system are readily determined by an extension of the methods just described.

The first step is to select one of the branches as the basic branch. In the case of a prime mover having a number of auxiliaries driven by branches geared to the main transmission shaft for example, the branch containing the prime mover should be selected as the basic system, and the common point at which the several branches join the main transmission shaft should be selected as the point of division Z between the basic and the elastically connected portions.

If the gear ratios of the branched drives differ from unity then all masses and elasticities should be reduced to their equivalent values referred to the speed of the basic branch, using the methods explained in Chapter 5.

In the system shown in Fig. IV, mass J_1 on shaft C_1 has been selected as the basic branch, with the point of division Z at the common point of intersection of the remaining branches. The

remaining branches therefore constitute the elastically connected portions, whilst mass J_6 at the point of division Z is regarded as an independent mass.

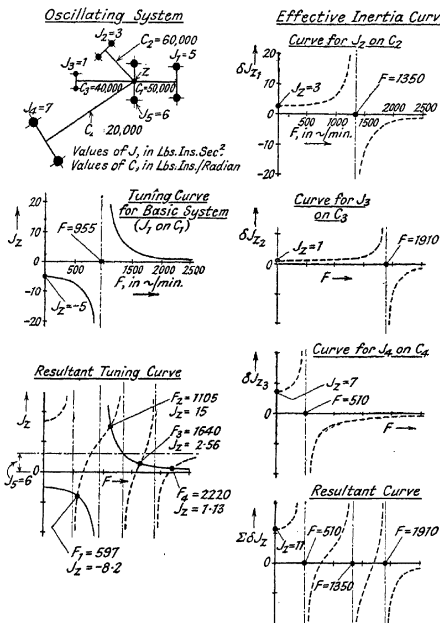


FIG. IV.—Tuning curves—simple branched system.

The tuning curve for the basic system is shown immediately below the diagrammatical arrangement of the system. This curve

is plotted from the frequency equation of a normal two-mass system, namely,

$$F = 9.55 \sqrt{C_1(J_1 + J_2)/(J_1 \cdot J_2)} = 9.55 \sqrt{C_1(1/J_1 + 1/J_2)},$$

or, substituting actual values, $F = 2135 \sqrt{1/5 + 1/J_2}$ vibs./min.

Note that, when $F = 0$, $J_2 = -J_1 = -5$,
 $F = 955$; $J_2 = \text{inf.}$

The effective inertia curves for the elastically connected portions are shown in the right-hand column of Fig. IV.

A separate curve must be plotted for each of the elastically connected portions, so that each of these curves represents a proportion of the total effective inertia and the values are therefore written, δJ_{s1} , δJ_{s2} , and δJ_{s3} .

The frequency equations for the respective two-mass systems are used for plotting the curves. Thus for the branch containing mass J_2 on shaft C_2 ,

$$F = 9.55 \sqrt{C_2(J_2 + \delta J'_{s1})/(J_2 \cdot \delta J'_{s1})} = 9.55 \sqrt{C_2(1/J_2 + 1/\delta J'_{s1})},$$

or, inserting actual values, $F = 2340 \sqrt{1/3 + 1/\delta J'_{s1}}$.

Whence $\delta J_{s1} = -\delta J'_{s1}$ can be evaluated for various values of F .
 Note that, when $F = 0$, $\delta J_{s1} = 3$;

when $F = 1350$ vibs./min., $\delta J_{s1} = \text{inf.}$

The tuning curves for the remaining elastically connected portions are obtained in precisely the same way, using the appropriate values of J and C .

The resultant effective inertia curve for the elastically connected portions shown at the bottom of the right-hand column in Fig. IV is obtained by adding together the component curves:

i.e. $\Sigma \delta J_s =$ resultant effective inertia for the elastically connected branches
 $= (\delta J_{s1} + \delta J_{s2} + \delta J_{s3})$.

Thus, when $F = 0$, $\Sigma \delta J_s = (3 + 1 + 7) = 11$.

Also, when $\Sigma \delta J_s$ is infinite the values of F , namely, 510, 1350, 1910 vibs./min., are the same as the values of F at the asymptotes in the component effective inertia curves, i.e. the resultant curve has as many asymptotes as there are elastically connected portions of the original system, and these asymptotes occur at frequencies corresponding to vibration of each branch about a node at the common point of intersection.

The resultant tuning curve for the whole system is shown at the bottom of the left-hand column in Fig. IV, and is obtained by superimposing the resultant effective inertia curve for the whole system (dotted lines) on the tuning curve for the basic system (full lines).

The resultant effective inertia curve for the whole system consists, in this example, of the resultant curve for the elastically connected portions plus the independent mass J_5 at the common point of division Z. The addition of J_5 is most easily accomplished by plotting the resultant effective inertia curve for the elastically connected portions on a base which is displaced a distance corresponding to $J_5 = 6$ from the $O-F$ axis, as shown in Fig. IV.

The resultant tuning curve for the whole system has four points of intersection, so that there are four possible modes of vibration of the complete system, and the corresponding natural frequencies are 597, 1105, 1640, and 2220 vibs./min. respectively.

Multi-Mass Systems.—In the preceding discussion simple oscillating systems, which would normally be handled by the methods described elsewhere in this book, have been used merely for the purpose of explaining fundamental principles. There is no difficulty, however, in extending the results to more complex systems.

(i) *Tuning Curve for Basic System.*—When there are several masses in the basic system the tuning curve is most conveniently plotted by carrying out a sufficient number of frequency tabulations in which the tuning inertia J_z is regarded as an adjustable variable. A separate tabulation is required for each assumed frequency F , and each table commences at the free end of the basic system. Each table is completed down to the last mass J_z , and the value of J_z which is necessary to make the last torque summation zero is the value of the tuning inertia corresponding to the chosen frequency.

The following table shows a typical calculation:—

FREQUENCY TABULATION FOR $F = 100$ VIBS./MIN., i.e. $\omega^2 = 110$.

J Lbs.-Ins. Sec. ² .	$J \cdot \omega^2$ Lbs.-Ins./ Rad.	θ Radian.	$J \cdot \omega^2 \cdot \theta$ Lbs.-Ins.	$\Sigma J \cdot \omega^2 \cdot \theta$ Lbs.-Ins.	C Lbs.-Ins./ Radian.	$\Sigma J \cdot \omega^2 \cdot \theta / C$ Radian.
165	18,150	1.00000	18,150	18,150	202,000,000	0.00009
165	18,150	0.99991	18,148	36,298	202,000,000	0.00018
165	18,150	0.99973	18,145	54,443	202,000,000	0.00027
165	18,150	0.99946	18,140	72,583	202,000,000	0.00036
165	18,150	0.99910	18,134	90,717	202,000,000	0.00045
165	18,150	0.99865	18,125	108,842	202,000,000	0.00054
J_z	$110 \cdot J_z$	0.99811	$109.8 \cdot J_z$	0	—	—

i.e. $109.8 \cdot J_z + 108,842 = 0$,
 or $J_z = -991$ lbs.-ins. sec.².

Fig. V shows some typical tuning curves for multi-mass systems. The first column shows the oscillating system, Z being the point at which the elastically connected portion is assumed to join the basic system, whilst J_z is the effective inertia of the elastically connected portion and is also the inertia necessary to tune the basic system to the prescribed frequency.

The second column shows the tuning curve, and the third column gives the frequency equation. The tuning curve can either be plotted from the frequency equation by inserting various values of ω and solving for J_z , or by carrying out a sufficient number of frequency tabulations, as just described. The latter method will be found less laborious when the number of masses exceeds three, and the labour will be very considerably reduced and the accuracy increased by employing an electrically operated calculating machine for handling the numerical computations. When a large number of routine calculations of this type have to be performed, the use of a mechanical calculating machine will be found to be an excellent investment, especially bearing in mind that these machines are able to save many hours of time in other directions, e.g. harmonic analysis.

The oscillating systems shown in Fig. V represent arrangements in which there are from one to six masses each of polar moment of inertia J_s connected by shafts each of torsional rigidity C_s . The right-hand mass in each case is connected to the tuning inertia J_z by a shaft of torsional rigidity C_z . The arrangements are thus representative of engine aggregates having from one to six equally-pitched cylinders.

The tuning curves are plotted for the case where $C_z = C_s$, i.e. where the point of division Z between the basic system and the elastically connected portion is so chosen that the torsional rigidity of the shaft connecting the adjacent mass to Z is the same as the torsional rigidity of each of the shafts connecting the basic masses.

If the location of Z cannot be chosen so that this condition is fulfilled the tuning curves should be used with caution.

The following special characteristics of these tuning curves should be noted :—

- (a) When $F = 0$, $J_z = -\Sigma J_s$,
i.e. the tuning inertia for zero frequency is negative and equal in magnitude to the sum of the polar moments of inertia of the masses composing the basic system. This is true irrespective of the number of masses or of the magnitudes and distribution of the torsional rigidities of the connecting shafts.
- (b) When the basic system consists of a number of concentrated masses the number of branches of the tuning curve is equal to $(n + 1)$, where n is the number of basic masses, whilst the number of asymptotes is equal to the number of basic masses.

Heavy Shaft.—Fig. V also shows the tuning curve for a heavy shaft, and in this case the following interesting characteristics are revealed:—

- (a) When $F = 0$, $J_z = -J_0$, where J_0 is the total polar moment of inertia of the heavy shaft,
 i.e. $J_z = -\pi \cdot d^4 \cdot L \cdot \rho / (32 \times 386)$, lbs.-ins. sec.².
- (b) When $J_z = 0$, $F = 9.55 \cdot U \cdot v / L$ vibs./min.,
 where $v =$ velocity of propagation of torsional impulses in
 ins./sec.
 $= \sqrt{386 \cdot G / \rho}$,
 $G =$ modulus of rigidity of shaft material in lbs./ins.²,
 $\rho =$ specific weight of material of shaft in lbs./ins.³,
 $L =$ length of shaft in inches,
 $U = \pi, 2\pi, \text{etc.}$, i.e. there is an infinite number of intersections of the tuning curve with the $O - F$ axis.

These values of F correspond to vibration of the shaft with both ends free. The odd multiples of π correspond to vibration with one, three, five, etc., nodes in the shaft with the free ends swinging against one another.

The even multiples of π correspond to vibration with two, four, six, etc., nodes in the shaft with the ends swinging in phase.

- (c) When $J_z = \text{infinity}$, $F = 9.55 \cdot U' \cdot v / L$ vibs./min.,
 where $U' = \pi/2, 3\pi/2, 5\pi/2, \text{etc.}$, i.e. the tuning curve contains an infinite number of asymptotes.

These values of F correspond to vibration of the shaft with one end free and the other end fixed, since there is a node at point Z when J_z is infinite.

The lowest, or fundamental, mode corresponds to vibration with a node at Z , whilst the remaining modes correspond to vibration with one node at Z and one, two, three, etc., nodes in the shaft.

The foregoing frequency equations can be written:

- $$F = U \cdot Q' / L \text{ vibs./min., when } J_z = 0,$$
- $$F = U' \cdot Q' / L \text{ vibs./min., when } J_z = \text{infinity},$$
- where $Q' =$ 9,400 for rubber (average value for structural rubber),
 = 470,000 for synthetic resin, fabric bonded materials (Micarta),
 = 840,000 for brass and bronze,
 = 970,000 for cast iron,
 = 1,020,000 for monel metal,
 = 1,160,000 for duralumin,

= 1,200,000 for magnesium alloy (elektron),

= 1,220,000 for steel.

Note: $Q' = 9.55 \cdot v = 188\sqrt{G/\rho}$.

It is of interest to note that the value of Q' is practically the same for steel as for light alloys, i.e. the frequencies of a uniform steel shaft are approximately the same as those of elektron and duralumin shafts of the same length. Also, inspection of the foregoing frequency equations shows that the frequency of a *uniform* shaft is independent of its cross-sectional dimensions, i.e. the frequencies for a shaft of given length are the same irrespective of the size or shape of its cross-section; round or square, solid or hollow, etc.

The number of nodes corresponding to any selected value of the frequency F can also be deduced from the tuning curves. Thus the frequency corresponding to any point on the branch which lies between the origin and the first asymptote corresponds to vibration with no node in the oscillating system; frequencies corresponding to points on the branch which lies between the first and second asymptotes corresponds to vibration with one node in the oscillating system, and so on, as shown in Fig. V.

(ii) *Effective Inertia Curve for the Elastically Connected Portion.*—The rule already given for plotting the effective inertia curves of simple systems also applies in cases where the elastically connected system contains several masses, namely, the effective inertia curve is simply the mirror-image about the $O-F$ axis of the tuning curve for the elastically connected portion. Thus the tuning curves in Fig. V are easily converted into the corresponding effective inertia curves by plotting their mirror-images about the $O-F$ axis, as shown by the dotted lines in the two-mass arrangement.

The truth of this rule when applied to a multi-mass system is illustrated by the arrangement shown in Fig. VI. The actual system is shown at (a) and the one-node frequency tabulation is given in the following table:—

$F = \text{ONE-NODE FREQUENCY} = 4000 \text{ VIBS./MIN.}, \text{ i.e. } \omega^2 = 175,500.$

J	$J \cdot \omega^2$	θ	$J \cdot \omega^2 \cdot \theta$	$\Sigma J \cdot \omega^2 \cdot \theta$	C	$\Sigma J \cdot \omega^2 \cdot \theta / C$
2	351,000	1.0000	351,000	351,000	3,000,000	0.1170
2	351,000	0.8830	310,000	661,000	3,000,000	0.2203
2	351,000	0.6627	232,500	893,500	3,000,000	0.2978
2	351,000	0.3649	128,000	1,021,500	3,000,000	0.3405
0	0	0.0244 (θ_2)	0	1,021,500 (T_2)	1,500,000	0.6810
8.86	1,555,000	-0.6566	-1,021,500	0	—	—

The above table is similar to a normal frequency tabulation except that an additional line is included at point Z where the original system is assumed to be separated into two partial systems. This is done so that the values of the torsional vibration torque and amplitude, T_z and θ_z , can be determined.

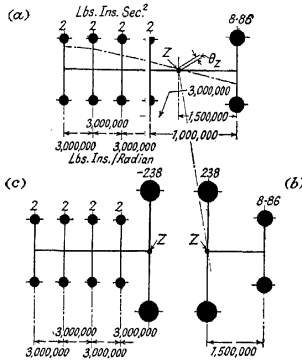


FIG. VI.—Effective and tuning inertias.

In this example, $T_z = 1,021,500$; and $\theta_z = 0.0244$.

Now, torque = (polar moment of inertia) \times (angular acceleration),

$$i.e. \quad T_z = J_z \cdot \omega^2 \cdot \theta_z,$$

$$or \quad J_z = T_z / (\omega^2 \cdot \theta_z) = 1,021,500 / (175,500 \times 0.0244) = 238 \text{ lbs. ins. sec.}^2.$$

Since T_z and θ_z are the values of the vibration torque and amplitude at point Z due to oscillation of the system with unit amplitude at the extreme left-hand mass when the frequency is 4000 vibs./min., the above value of J_z represents the polar moment of inertia of a mass which if rigidly connected at Z will be equivalent to the actual mass system on the left-hand side of Z , i.e. it will tune the system on the right-hand side of Z to a frequency of 4000 vibs./min. The equivalent system when this single mass is substituted is shown at

(b) in Fig. VI, the natural frequency being obtained from the frequency equation for a two-mass system, as follows:—

$$F = 9.55 \sqrt{1,500,000 (8.86 + 238) / (8.86 \times 238)} \\ = 4000 \text{ vibs./min., which is correct.}$$

Now, according to the rule previously determined, if 238 lbs.-ins. sec.² is the *effective inertia* of the partial system on the left-hand side of Z in Diagram (a) of Fig. VI, then - 238 lbs.-ins. sec.² should be the value of the *tuning inertia* required to tune this portion of the system to a frequency of 4000 vibs./min.

The following frequency table for the partial system on the left-hand side of Z shows that this condition is fulfilled:—

$$F = 4000 \text{ Vibs./Min. ; } \omega^2 = 175,500.$$

J	J. ω^2	θ	J. $\omega^2 . \theta$	$\Sigma J. \omega^2 . \theta$	C	$\Sigma J. \omega^2 . \theta / C$
2	351,000	1.0000	351,000	351,000	3,000,000	0.1170
2	351,000	0.8830	310,000	661,000	3,000,000	0.2203
2	351,000	0.6627	232,500	893,500	3,000,000	0.2978
2	351,000	0.3649	128,000	1,021,500	3,000,000	0.3405
-238	-41,770,000	0.0244	-1,021,500	0	—	—

The foregoing calculations confirm that for a frequency of 4000 vibs./min. the *effective inertia* of the partial system to the left of Z is 238 lbs.-ins. sec.², and that this is also the *tuning inertia* for the partial system on the right of point Z. Conversely the *effective inertia* for the partial system to the right of Z is - 238 lbs.-ins. sec.², and this is also the *tuning inertia* for the partial system to the left of point Z.

(iii) *Resultant Tuning Curve*.—This is obtained in the same way as for the simple systems previously discussed by superimposing the tuning curve for the basic system on the effective inertia curve for the elastically connected portion. The points of intersection of the two families of curves then give the true natural frequencies of the original system.

If the system contains several branches as shown in Fig. IV but with several masses on each branch, the procedure is the same as previously described, i.e. one branch, preferably the branch containing the excitation source, is selected as the basic branch and its family of tuning curves is determined. The remaining branches are then regarded as the elastically connected portions and the families of effective inertia curves are separately determined for each elastically connected portion. These are then added together and the resultant family of curves is superimposed on the tuning curve for

the basic system. The points of intersection of the two sets of curves give the true natural frequencies of the complete system.

Fig. V will be found useful for making a preliminary sketch of the tuning and effective inertia curves. Thus if the salient characteristics of the curves, i.e. the locations of the asymptotes and the points where the several branches of the curves cross the $O-F$ axis, are plotted with the help of Fig. V and the branches themselves are roughly sketched in, a useful approximate picture of the torsional vibration characteristics of the complete system is rapidly obtained. The more detailed calculations can then be confined to frequency values in the regions where the families of curves intersect.

EXAMPLE.—Fig. VII shows an example where the foregoing method can be usefully applied. The complete system consists of a four-cylinder engine coupled to a heavy shaft. The effective inertia method is applied by assuming that the system is divided at Z , the engine portion being regarded as the basic system and the heavy shaft as the elastically connected portion.

The full lines in the resultant tuning curve show the family of tuning curves for the engine portion, whilst the dotted lines show the effective inertia curves for the heavy shaft portion. The method of obtaining these curves is precisely the same as for the simpler systems previously discussed.

Fig. V shows that the tuning curve for a four-cylinder engine aggregate has five branches; and that the tuning curve and therefore the effective inertia curve for a heavy shaft has an infinite number of branches. There is thus an infinite number of intersections between the two families of curves for the system shown in Fig. VII and of these the first eight intersections are shown in the resultant tuning diagram. Each of these intersections represents a mode of vibration of the complete system.

The approximate locations of the nodes can also be deduced from Fig. VII. Thus the lowest intersection F_1 lies on the first branch of the engine tuning curve (full lines) and on the second branch of the effective inertia curve for the elastically connected portion (dotted lines). Hence F_1 corresponds to the one-node mode of vibration of the whole system, the node being located in the heavy shaft portion. Similarly, intersection F_2 corresponds to vibration with two nodes, one in the engine portion and one in the heavy shaft portion; intersection F_3 corresponds to vibration with three nodes, one in the engine portion and two in the heavy shaft portion, and so on.

In practice it is not necessary to plot these diagrams over a greater frequency range than that which previous experience indicates is likely to cover all critical zones of practical importance. Thus, if it is known that harmonic orders higher than the 10th order

can be neglected as too feeble to excite appreciable vibratory disturbances, and if the maximum running speed is, say, 2000 r.p.m., then the tuning curves need not extend beyond a frequency of

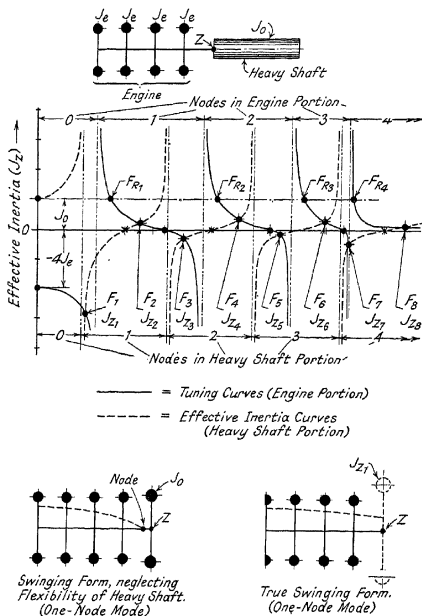


FIG. VII.—Heavy shaft system.

$(10 \times 2000) = 20,000$ vibs./min. plus a reasonable working margin of, say, 20 per cent., giving a maximum practical frequency range of about 24,000 vibs./min.

The natural frequencies of the complete system when the flexibility of the heavy shaft J_0 is assumed to be concentrated at point Z are easily obtained from the resultant tuning curve by drawing a line parallel to the $O-F$ axis at the value $J_z = J_0$, as shown in Fig. VII. The intersections of this line with the several branches of the engine tuning curve give the required frequencies F_{r1} , F_{r2} , etc. Fig. VII shows that in this example there are four such frequencies, and that most of these are appreciably different from the true values obtained when the flexibility of the heavy shaft is taken into account.

Input Energy Due to Harmonic Torque.—Fig. VII also illustrates another important consideration when dealing with systems containing members which are not rigid and cannot therefore be regarded as concentrated inertias.

The left-hand diagram at the bottom of Fig. VII shows the shape of the normal elastic curve for the engine portion of the system when the heavy shaft is assumed to be a torsionally rigid body of polar moment of inertia J_0 concentrated at the point of division Z , whilst the right-hand diagram shows the true shape of the normal elastic curve. This is obtained for any mode of vibration by replacing the heavy shaft by the true equivalent inertia given by the corresponding point of intersection on the resultant tuning curve. Thus for the one-node mode of vibration of the system shown in Fig. VII the heavy shaft is replaced by an inertia J_{z1} ; for the two-node mode by an inertia J_{z2} , and so on.

Once the value of the true equivalent inertia is known the shape of the normal elastic curve is readily determined by carrying out a normal frequency tabulation commencing at the free end of the engine system and terminating at the equivalent inertia. The frequency value to be used in this tabulation is, of course, the value given by the point of intersection in the resultant tuning diagram for the particular mode of vibration under consideration. Thus for the one-node mode it is F_1 , for the two-node mode F_2 , and so on.

Incidentally these frequency tabulations are an excellent check on the accuracy of the plotting of the tuning and effective inertia curves, since, if the values of J_z and F obtained from the resultant tuning diagram are correct, the last torque summation in the frequency table should be zero.

The two diagrams at the bottom of Fig. VII show that the shape of the normal elastic curve, when the flexibility of the heavy shaft is neglected, differs considerably from the true shape. This, in turn, implies that the vector summations, and therefore the magnitudes of the input energies due to the harmonic torques originated by the several cylinders of a multi-cylinder engine, will differ considerably from the true values. Thus the relative importance of the various component harmonics cannot be judged correctly if the flexibility of the heavy shaft is neglected.

Caution.—Systems of the type shown in the right-hand bottom diagram of Fig. VII, i.e. where the flexible component is replaced by its effective inertia given by the intersection on the resultant tuning curve, cannot be used for the purpose of determining equilibrium amplitudes. If it is required to determine amplitudes the actual specific vibratory amplitudes at all points in the system must be known.

Once the true natural frequency has been determined, however, the specific vibratory amplitudes throughout the system can generally be determined by carrying out a frequency tabulation which includes all parts of the original system.

In systems where the excitation is due to the component harmonics of the torque from an internal combustion engine, a useful indication of the *relative importance* of the several criticals is obtained from the vector summations. Thus there is a real advantage in choosing the engine portion of the system as the basic portion, since, as just explained, the true shape of the normal elastic curve for the engine portion is then readily obtained by carrying out a frequency tabulation with the appropriate effective inertia of the elastically connected portion added to the basic system at the point of division Z.

Aero-Engine/Air-screw Systems.—An aero-engine/air-screw installation is probably the most important application of the Effective Inertia Method of torsional vibration analysis. Enough has already been said to indicate that the custom of regarding the air-screw as a rigid body is liable to cause quite important errors in the determination of critical zones and the magnitudes of the vibratory amplitudes occurring in those zones. This is especially the case with modern highly efficient, high duty air-screws fitted with the lightest permissible metal blades, and experience has shown that the flexibility of these blades does have a marked influence on the torsional vibration characteristics of the power plant.

In applying the effective inertia method to an engine/air-screw installation the complete oscillating system comprising the engine and air-screw is regarded as separated at the air-screw hub, the engine portion being treated as the basic system and the air-screw complete with its hub as the elastically connected portion.

The tuning curve for the engine system is obtained by carrying out a sufficient number of frequency tabulations covering the frequency range likely to be of practical interest, as already explained. For example, if it is known that harmonic components of the engine torque curve higher than the 10th order are unlikely to cause appreciable vibratory disturbances, and if the maximum operating speed of the engine is 3000 r.p.m., then there is no real need to carry the frequency range of the tuning curve above about 35,000 vibs./min.

The diagrams and formulæ in Fig. V will be found useful for sketching down the general shape of the tuning curves for various engine aggregates.

If the engine is geared to the air-screw, since the assumed point of division of the original system is in the air-screw shaft at the air-screw hub, it is simpler *not* to convert the original system to an equivalent system reduced to crankshaft speed, i.e. the real values of all masses and elasticities should be used in the frequency tabulations as shown, for example, in Tables 24, 25, or 36.

In this way the influence of gear inertia is automatically and correctly taken into account. Furthermore, the effective inertia curve for the elastically connected portion, i.e. for the air-screw, then gives the real values of the effective inertias corresponding to different frequencies, which is an advantage when applying the experimental method to be described later.

The plotting of the tuning curve for the engine or basic system presents no serious difficulties, however many masses and shafts compose the engine system and whether the engine is geared or not. The real practical difficulty arises when attempting to plot the effective inertia curve for the air-screw, since the mass/elasticity characteristics of the air-screw blades cannot be correctly represented by a series of concentrated masses connected by massless shafts, and the problem is so complex that no complete mathematical analysis has yet been made.

Mathematical solutions for blades of simple form such as uniform laths of rectangular cross-section, and tapered laths of a particular form, have been worked out, however (see "Airscrew Blade Vibration," B. C. Carter, *Journal R.Ae.S.*, Sept., 1937), and these form a useful indication of the results to be expected from actual blades.

Fig. VIII shows a portion of the effective inertia curve for an air-screw with blades of uniform rectangular section, from which it is noticeable that the form of the curve is similar to that for a heavy shaft of uniform cross-section shown in Fig. V, bearing in mind that the curve in Fig. V is the tuning curve for the heavy shaft and that the corresponding effective inertia curve is its mirror-image about the $O-F$ axis.

Just as in all the previous examples, the effective inertia of the air-screw at zero frequency is equal to the polar moment of inertia of the air-screw regarded as a rigid body, i.e. $J_e = J_0$ when $F = 0$.

The frequency values in Fig. VIII at the asymptotes correspond to infinite effective inertia, the physical meaning of which is that there is a node at the air-screw hub or, in other words, that the blades vibrate as though fixed at the hub. These modes of vibration will be referred to as *fixed root modes*, the lowest mode corresponding

to vibration of the blades as simple cantilevers built-in at the hub as shown in the diagrams at the top of Fig. VIII.

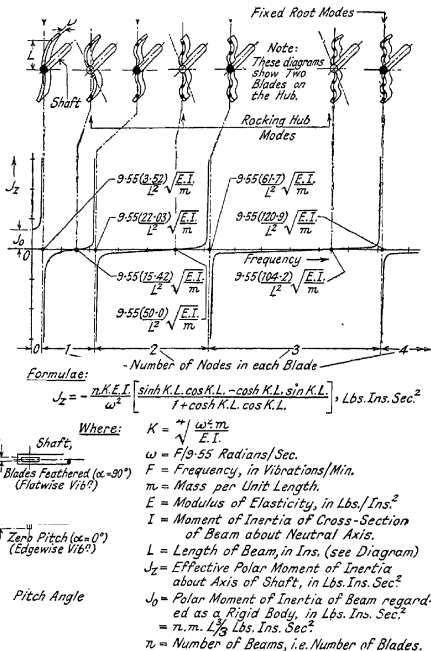


FIG. VIII.—Effective inertia curve for a uniform rectangular beam.

The frequency values where the several branches of the tuning curves cross the $O-F$ axis correspond to zero effective inertia at

the hub, the physical meaning of which is that there is no inertia restraint at the hub and the hub therefore simply rocks to-and-fro, as shown in the diagrams at the top of Fig. VIII.

The expression for the frequencies of the fixed root and rocking hub modes can be written

$$F = QUD/L^2 \text{ vibs./min.},$$

where

$$F = \text{frequency in vibs./min.},$$

$$D = \text{depth of beam in inches,}$$

$$L = \text{length of beam in inches,}$$

$$Q = \text{a constant which depends on the material of the beam,}$$

$$= 558,000 \text{ for steel,}$$

$$= 548,000 \text{ for duralumin,}$$

$$= 540,000 \text{ for magnesium alloy (elektron),}$$

$$= 473,000 \text{ for compressed and impregnated wood,}$$

$$= 380,000 \text{ to } 467,000 \text{ for wood (mahogany and walnut),}$$

$$= 373,000 \text{ for bronze,}$$

Note: $Q = 54 \cdot 3 \sqrt{E/\rho},$

U = a constant which depends on the mode of vibration, as follows:—

For the Fixed Root Modes, i.e. when $J_z = \text{inf.}$ (asymptotes),

$$U = 3 \cdot 52, 22 \cdot 03, 61 \cdot 7, 120 \cdot 9, 200, 299, 417, \text{ etc.},$$

or $(\pi/2)^2, (3 \cdot \pi/2)^2, (5 \cdot \pi/2)^2, (7 \cdot \pi/2)^2, \text{ etc.},$ approximately.

For the Rocking Hub Modes, i.e. when $J_z = 0,$

$$U = 15 \cdot 42, 50 \cdot 0, 104 \cdot 2, 178, 272, 386, \text{ etc.},$$

or $(5 \cdot \pi/4)^2, (9 \cdot \pi/4)^2, (13 \cdot \pi/4)^2, (17 \cdot \pi/4)^2, \text{ etc.},$ approximately.

It should be noted that these frequencies are independent of the width of the beam, but are directly proportional to the depth D. It should also be noted that the frequencies are inversely proportional to L if the ratio D/L remains constant.

In calculating the frequencies and equivalent inertias for a uniform rectangular beam care should be taken to use the correct value for the depth D, namely, that dimension of the rectangular cross-section which lies in the plane of rotation of the shaft, as shown in Fig. VIII. This implies that two distinct families of effective inertia curves exist according to whether the beam vibration is edgewise, i.e. with the longer side of the rectangle in the plane of rotation, or flatwise, i.e. with the shorter side of the rectangle in the plane of rotation. It is evident that both the fixed root and rocking hub modes of vibration occur at higher values for edgewise than for flatwise vibration.

As long as the beam is set with the longer side of the rectangle in the plane of rotation, corresponding to zero pitch in the case of an actual air-screw, only edgewise vibration can be excited by the

component harmonics of the engine torque. Conversely, if the beam is set with the shorter side in the plane of rotation, corresponding to the feathered condition in the case of an actual air-screw, only flatwise vibration can be excited.

The slightest deviation from either of these settings, however, implies that both edgewise and flatwise vibration must be taken into account, and this is the condition which must be dealt with in an actual air-screw.

A little reflection will reveal, therefore, that the resultant effective inertia curve for an actual air-screw must contain all the asymptotic values corresponding to the fixed root modes of vibration, both edgewise and flatwise, irrespective of the pitch setting of the blades. This is the only general conclusion which can be drawn since the shapes of the branches of the resultant effective inertia curve between the asymptotes and the points at which these branches cross the $O-F$ axis do depend on the pitch angle α .

Furthermore, the resultant effective inertia curve cannot, in this case, be obtained by direct summation of the effective inertia curves for edgewise and flatwise vibration. The resultant values must be determined by applying the following formula :—

$$J_z = [(J_f \cdot \sin^2 \alpha) + (J_e \cdot \cos^2 \alpha)],$$

where J_z = resultant effective inertia for air-screw with blades set at pitch angle α ,

$$J_e = \text{effective inertia when } \alpha = 0^\circ \text{ (edgewise vibration),}$$

$$J_f = \text{effective inertia when } \alpha = 90^\circ \text{ (flatwise vibration).}$$

It should be noted that since J_0 , the polar moment of inertia of the air-screw, when it is regarded as a rigid body, is the same for edgewise as for flatwise vibration, then at zero frequency,

$$J_z = J_0 (\sin^2 \alpha + \cos^2 \alpha) = J_0,$$

i.e. the value of J_z at zero frequency is J_0 for the resultant effective inertia curve as well as for the separate effective inertia curves for edgewise and flatwise vibration.

If the resultant effective inertia curve is plotted for a given value of α , it will be found that the flatwise zones are much more sharply tuned than the edgewise zones. It is therefore more difficult to initiate and sustain flatwise vibration, a fact which is usually found to agree with practical observations. It will also be found that pitch changes do not appreciably affect flatwise modes but do have a considerable influence on edgewise modes. Hence in cases where an edgewise vibration occurs, it should be borne in mind that pitch changes might have an appreciable influence on the resonant frequency.

So far only those modes of vibration which are excitable by the component harmonics of the shaft torque have been considered. In addition to these modes, however, an air-screw blade is capable of

vibration both flatwise and edgewise as a free-free beam. These modes of vibration are usually referred to as *symmetrical modes*, since, for example, in a two-bladed air-screw the hub oscillates along the shaft axis with the blade tips oscillating in the opposite direction. The natural frequencies of the various modes of symmetrical vibration are given by the same expression as for the torsional modes, namely,

$$F = QUD/L^2 \text{ vibs./min.},$$

where, in this case,

When the effective inertia of the air-screw is zero,

$$U = 5.54, 30.2, 74.5, \text{ etc.},$$

$$\text{or } (3 \cdot \pi/4)^2, (7 \cdot \pi/4)^2, (11 \cdot \pi/4)^2, \text{ etc., approximately};$$

When the effective inertia of the air-screw is infinite,

$$U = 3.52, 22.03, 61.7, \text{ etc.},$$

$$\text{or } \left(\frac{\pi}{2}\right)^2, \left(\frac{3 \cdot \pi}{2}\right)^2, \left(\frac{5 \cdot \pi}{2}\right)^2, \text{ etc., approximately.}$$

It should be noted that the values of U for the symmetrical modes when the effective inertia of the air-screw is infinite are the same as for the fixed root modes previously discussed.

Also, as before, Q = a constant which depends on the material of the blades, as previously given,

D = depth of blade in inches

= width of blade for edgewise vibration

= thickness of blade for flatwise vibration,

L = length of blade in inches, see Fig. VIII.

In normal cases the symmetrical modes occur independently of the torsionally excited modes, since there is no appreciable coupling whereby the component harmonics of the shaft torque are able to excite symmetrical blade vibration.

It should be mentioned, however, that under certain circumstances a strong coupling action can occur. For example, in the case of an engine directly coupled to an air-screw the torque impulses are capable of exciting axial vibration of the crankshaft. If, therefore, the thrust bearing between the air-screw and the crankshaft is slack these axial motions can be transmitted to the air-screw hub and so excite symmetrical blade vibration.

The foregoing discussion indicates that even in the case of a simple non-rotating blade of uniform rectangular cross-section the mathematical problem is difficult. In an actual air-screw this difficulty is greatly increased and no complete mathematical treatment has yet been achieved, even for the case of a non-rotating blade.

Furthermore, even if a mathematically correct solution could be obtained there would still remain some doubt as to the exact degree of blade root fixation, particularly in the case of variable pitch air-screws.

Fortunately, however, the effective inertia method of attacking the problem leads to a comparatively simple experimental arrangement for determining the resultant effective inertia curve for an air-screw.

Experimental Method of Determining the Resultant Effective Inertia.—Fig. IX shows the experimental apparatus. The upper diagram shows a non-rotating testing arrangement in which torsional impulses of known frequency are applied to the hub of a stationary air-screw. The impulses are generated by a suitable exciter, consisting, for example, of a series of unbalanced masses evenly disposed round a housing which is connected by a more or less flexible shaft to the air-screw hub, the housing being held from rotating by light springs.

The masses are driven by a central sun wheel which, in turn, is driven by a variable speed electrical motor. The unbalanced masses thus transmit a sinusoidal torque T_z , of known frequency F , through the connecting shaft to the air-screw.

For any given value of the applied frequency F , the torque T_z , at the air-screw hub, is measured by an electrical or mechanical torsional strain gauge, whilst simultaneously the hub amplitude θ_z is measured by a torsigraph of the inertia-flywheel type. Descriptions of suitable instruments are given in Chapter 8.

Now, torque = (polar moment of inertia) \times (angular acceleration),

$$\begin{aligned} \text{i.e.} \quad T_z &= J_z \cdot \theta_z \cdot \omega^2, \\ \text{or} \quad J_z &= T_z / (\theta_z \cdot \omega^2). \end{aligned}$$

Thus for any given value of ω the value of the effective inertia at the point of attachment of the hub can be determined from the above expression, since T_z and θ_z are known.

In carrying out a test the applied frequency is increased in small steps from zero, and values of $\omega = F/9.55$ and of T_z and θ_z are obtained for each step.

The plotting of the complete resultant effective inertia curve for the air-screw is then merely a question of obtaining a sufficient number of values of J_z .

The curve will be of the general form shown in Fig. VIII and by starting at zero frequency and gradually working up the frequency range the correct sign for J_z is automatically determined. As previously explained, there is some advantage in plotting the function T_z/θ_z against F instead of $J_z = T_z/(\theta_z \cdot \omega^2)$.

In the case of variable pitch air-screws, at any rate until further light is shed on this complex subject, it is desirable to carry out separate tests with a number of different pitch settings, including the zero pitch and feathered conditions. In most cases it will be found that there are comparatively small changes of J_x when the pitch is varied over the normal range encountered in practice, excluding, of

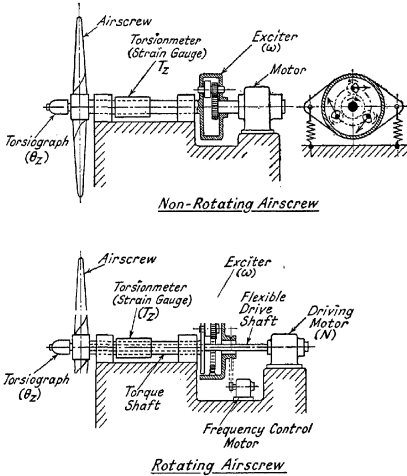


FIG. IX.—Air-screw vibration testing equipment.

course, the zero pitch condition when only edgewise modes are excited and the feathered condition when only flatwise modes are excited.

A fundamental defect of the static method just described is the necessity for applying correcting factors to take into account the influence of centrifugal force on a rotating air-screw. This influence is twofold, firstly there is a virtual stiffening action on the blades which tends to raise the frequencies, and secondly the degree of blade root fixation is liable to change.

This defect is overcome in the apparatus shown at the bottom of Fig. IX, where the pulsating torque is applied to the air-screw hub through a torque tube whilst the air-screw is rotating. The air-screw is driven through a very flexible shaft which serves to isolate the main driving motor, N, from the pulsating system. The torque impulses are generated by an exciter which consists of a series of unbalanced planetary masses driven by an annular wheel, which, in turn, is driven by a separate variable speed electrical motor.

The apparatus should be designed so that the applied frequency can be varied independently of the r.p.m. of the air-screw to enable the influence of rotation on blade frequency to be studied.

A description of some practical apparatus of the types shown diagrammatically in Fig. IX is contained in a paper entitled "Airscrew Blade Vibration," by Major B. C. Carter (*Journal R.Ae.S.*, 1937).

If the simpler arrangement shown at the top in Fig. IX is used, the resultant effective inertia curve must be corrected for the effect of rotation before applying the results to an actual example. The general effect of rotation is to stiffen the air-screw and so raise the natural frequencies.

A stationary air-screw blade vibrates by virtue of the elastic restraint due to the bending stiffness of the material, and in the absence of this property the frequency would be zero. Imagine, however, a rotating body without bending stiffness, e.g. a cord or chain, then the effect of centrifugal force on the particles composing the body is to cause the chain to rotate stiffly about the axis of rotation with its particles lying along a straight line originating at the centre of rotation. If the chain is disturbed during rotation the centrifugal force tends to restore all particles to the equilibrium position, thus initiating vibrations of a definite frequency.

Let δm = the mass of a particle,
 ω = angular velocity of rotation,
 r = radius at which particle is situated.

Then, centrifugal force = $\delta m \cdot \omega^2 \cdot r$.

Now assume that the particle is displaced through a small angle θ from the equilibrium position, then the circumferential displacement is $r \cdot \theta$ and there is a restoring force acting circumferentially and of magnitude $\delta m \cdot \omega^2 \cdot r \cdot \sin \theta$ tending to restore the particle to its equilibrium position. For small angles this restoring force is very nearly $\delta m \cdot \omega^2 \cdot r \cdot \theta$.

Hence, F = natural frequency of particle = $9.55 \sqrt{\frac{\text{restoring force}}{\text{dispt.} \times \text{mass}}}$

$$= 9.55 \sqrt{\delta m \cdot \omega^2 \cdot r \cdot \theta / (r \cdot \theta \cdot \delta m)}$$

$$= 9.55 \cdot \omega$$

= N , where N is the r.p.m. of the chain about its axis of rotation.

And, since this result holds for all particles of the chain, irrespective of the mass distribution along the chain, it follows that the natural frequency of a rotating chain, i.e. of a body without bending stiffness, is equal to the r.p.m. of the body about its axis of rotation.

In a rotating air-screw blade the restraint due to the action of centrifugal force is supplementary to the elastic restraint of the material.

Now when a mass M is controlled by two springs of inch rates K_1 and K_2 arranged in parallel, then the total elastic restraint is $(K_1 + K_2)$ and the natural frequency of the system is

$$F = 9.55 \sqrt{(K_1 + K_2)/M}, \text{ i.e., } F^2 = 91.2 (K_1/M + K_2/M).$$

Now $9.55 \sqrt{K_1/M}$ is the natural frequency of the mass with spring K_1 acting alone, whilst $9.55 \sqrt{K_2/M}$ is the natural frequency of the mass with spring K_2 acting alone.

$$\text{Hence, } F^2 = F_1^2 + F_2^2.$$

Thus, in the case of an air-screw blade, if F_s is the natural frequency of the non-rotating blade and F_r is the frequency when the bending stiffness of the rotating blade is neglected, then, remembering that $F_2 = N$,

$$F^2 = F_s^2 + N^2.$$

This expression, however, is only an approximation to the true value of the natural frequency of the blade, since the configuration of a rotating and vibrating blade differs from that of a non-rotating vibrating blade, and also from that of a rotating and vibrating chain.

It is customary, therefore, to employ the following semi-empirical expression:—

$$F^2 = F_s^2 + S \cdot N^2,$$

where S is a factor to be determined by experiment.

Unfortunately there is considerable inconsistency between the values of S determined by different investigators even for the same mode of vibration.

This is probably due to certain fundamental differences between the conditions under which the individual experiments were carried out. For example, it seems reasonable to assume that the form of the air-screw blade itself will have an appreciable influence on the value of S , since the effect of centrifugal loading is likely to be different for, say, a circular root section than for a rectangular or aerofoil root section.

It is not surprising, therefore, to find published values of S varying from 1.4 to 1.7 for the fundamental fixed root mode; from 4.0 to 6.0 for the second fixed root mode; 12.0 to 12.3 for the third fixed root mode; and 21 to 24 for the fourth fixed root mode. In

the absence of specific data the average of these values should be used but the results obtained should be regarded with caution.

These values apply to the fixed root modes, the values for the rocking hub modes being obtained as follows:—

$$S' = S(F'_s/F_s),$$

where S' = factor for rocking hub mode,
 F'_s = rocking hub frequency for non-rotating air-screw,
 S = factor for fixed root mode,
 F_s = fixed root frequency for non-rotating air-screw.

There is one more complication to be considered before the centrifugal correction can be applied to the resultant effective inertia curve for the non-rotating air-screw. This is due to the fact that the correcting factor is a function of the rotational speed of the air-screw.

Let N_e = r.p.m. of engine crankshaft,
 n = order number of the component harmonic of the engine torque which is exciting the blade vibration under consideration,
 ϕ = gear ratio = (air-screw r.p.m.)/(engine r.p.m.),
 F'_s = fixed root frequency for non-rotating air-screw^r, in vibs./min.,
 F = fixed root frequency for rotating air-screw, in vibs./min.
 Then, N = r.p.m. of air-screw = $N_e \cdot \phi$,
 also $N_e = F/n$,

i.e. $N = F \cdot \phi/n$.

Hence, $F^2 = F_s^2 + S(F \cdot \phi/n)^2$,

or $F^2 = \frac{F_s^2}{1 - S \cdot \phi^2/n^2}$.

This expression enables the corrected values of the fixed root frequencies to be determined and also, by replacing S by S' and F_s by F'_s , the corrected values of the rocking hub frequencies.

These corrected values enable the corrected positions of the asymptotes and of the points at which the branches of the resultant effective inertia curve cross the $O-F$ axis to be plotted. The branches themselves can then be sketched in by assuming that each point on a branch shifts an amount proportional to the shift of the corresponding asymptote and zero point. It should be clearly understood that this procedure is merely an approximation, and that the true shape of the corrected branches can only be obtained from actual tests.

An important characteristic of the foregoing expression for the

blade frequencies of a rotating air-screw is that for real values of F the denominator must be positive,

i.e. for real values of F , $S \cdot \phi^2/n^2 < 1$,

also, if $S \cdot \phi^2/n^2 = 1$, or $n = \phi \sqrt{S}$, the value of F is infinite, or, in other words, *blade vibration of the mode for which S is the centrifugal correcting factor cannot be excited by harmonic components of order number equal to or less than $\phi \sqrt{S}$.*

Thus for the fixed root modes the following order numbers cannot excite blade vibration:—

1st mode :	$S = 1.5$,	$n = 1.22 \cdot \phi$ or less.
2nd mode :	$S = 5.0$,	$n = 2.23 \cdot \phi$,,
3rd mode :	$S = 12.15$,	$n = 3.48 \cdot \phi$,,
4th mode :	$S = 22.5$,	$n = 4.74 \cdot \phi$,,

Similarly, the non-effective order numbers for the rocking hub modes can be obtained by substituting S' for S in the above expression.

In the case of directly coupled installations, where $\phi = 1$, assuming that the engine is of the four-stroke cycle type, orders 0.5 and 1 are non-effective for the 1st fixed root mode; orders 0.5 to 2.0 for the 2nd fixed root mode, and so on. For these non-effective orders the air-screw is assumed to be a rigid body for the purpose of evaluating the natural frequencies of the installation, i.e. the resultant effective inertia curve consists of a line drawn parallel to the $O-F$ axis from the value $J_s = J_0$, since all blade frequencies have moved to infinity. It is evident that geared engines have fewer non-effective orders than directly coupled engines.

Strictly speaking, a separate resultant effective inertia curve should be plotted for all order numbers likely to cause trouble in the operating speed range, and in most cases this implies plotting curves for each order up to the 10th or 12th, excluding, of course, the non-effective orders. In the case of the higher order numbers, however, and especially where the engine is geared to the air-screw, the corresponding air-screw r.p.m. are so low that the centrifugal correction is negligible. In any case much labour can be saved by determining the approximate values of the frequencies and effective inertias by using the effective inertia curve for the non-rotating air-screw. This will enable the approximate relative magnitudes of the torque input energies for different harmonic orders to be determined, as previously explained, and from these values it will be possible to decide which of them should be investigated more completely.

EXAMPLE.—Calculate the natural frequencies of the first fixed root and rocking hub modes of vibration when the non-rotating frequencies are 3000 and 5000 vibs./min. respectively, assuming

that the 4th order excitation is being investigated and that the gear ratio between the engine and the air-screw is 0.5. State also the non-effective orders, assuming that the engine is of the four-stroke cycle type.

- (i) *Fixed Root Mode.* $F_s = 3000$ vibs./min.; $\phi = 0.5$; $n = 4$,
 $S = 1.5$ for the 1st fixed root mode.

$$\text{Hence, } F = \frac{3000}{\sqrt{1 - 1.5 \times 0.25/16}} = 3035 \text{ vibs./min.,}$$

and $F = \text{infinity}$ when $n = \phi \sqrt{S} = 0.5 \sqrt{1.5} = 0.61$,
 i.e. the 0.5th order is non-effective in this case.

- (ii) *Rocking Hub Mode.* $F'_s = 5000$; $\phi = 0.5$; $n = 4$,
 $S' = S(F'_s/F_s) = 1.5 \times 5000/3000 = 2.5$.

$$\text{Hence, } F = \frac{5000}{\sqrt{1 - 2.5 \times 0.25/16}} = 5100 \text{ vibs./min.}$$

and $F = \text{infinity}$ when $n = 0.5\sqrt{2.5} = 0.79$,

i.e. in this case also the only non-effective order is the 0.5th order.

Resultant Tuning Curve.—This is obtained by superimposing the tuning curve for the basic system, i.e. the engine system, on the resultant effective inertia curve for the air-screw, the points of intersection of the two families of curves giving the natural frequencies of the complete installation and also the values of the resultant effective inertias of the air-screw. This procedure is similar to that previously described for simpler systems, except that the following points need special consideration due to the influence of rotation on the vibrational characteristics of the air-screw blades.

- (a) For certain order numbers air-screw blade vibration is non-excitable. In these cases the air-screw is treated as a rigid body, and there is no need to employ the effective inertia method for evaluating frequencies and amplitudes.
- (b) A separate resultant effective inertia curve must be plotted for the air-screw for all orders where rotation has an appreciable effect on the vibrational characteristics of the air-screw blades.
- (c) The resultant effective inertia curve for the non-rotating air-screw can be used for all orders where the influence of rotation is negligible. In this connection it is always worth while carrying out a trial investigation based on the effective inertia curve for the non-rotating air-screw. This will enable the relative magnitudes of the harmonic torque input energies at different order numbers to be evaluated approximately, and thus enable the more detailed calculations to be confined to those orders likely to be troublesome.

Input Energy Due to Harmonic Torque.—Once the true natural frequencies of the complete system are known, the resultant harmonic torque input energy for unit amplitude at the free end of the crankshaft and for any order number is easily obtained by carrying out a frequency tabulation commencing at the free end of the shaft and using the phase velocity corresponding to the natural frequency given by the appropriate intersection on the resultant tuning curve. The relative magnitudes of the harmonic torque input energies for different order numbers are then obtained from phase and vector diagrams in the usual way.

Caution.—Although it will be found that the value of the effective inertia given by the intersection on the resultant tuning curve is the value required to complete the frequency table correctly, this value cannot be used for calculating the equilibrium amplitude of the system, and so enable torsional vibration amplitudes to be determined.

If it is required to determine these amplitudes, then the specific amplitude at all points in the oscillating system must be known.

In the case of an air-screw the mass/elastic characteristics of the blades are so complex that the only reliable method of determining the actual vibratory amplitudes and stresses is by actual measurement under operating conditions.

The vibratory stresses in the engine and air-screw shafts are most conveniently determined from torsiongraph records taken at the free end of the engine crankshaft, since this is always an anti-node in the oscillating system, and is therefore a suitable point for favourable recording with inertia flywheel type instruments (see Chapter 8). Analysis of the records will reveal the amplitude and frequency in the important critical zones, and from these values the vibratory stress in any part of the shaft system is readily determined by carrying out a frequency tabulation, using the phase velocity corresponding to the recorded frequency and commencing the table with the amplitude recorded at the free end of the crankshaft.

Measurements of shaft vibration can also be made at the air-screw end of the shaft system, but these are not so reliable as those taken at the free end of the crankshaft. For example, if a torsiongraph is used, no measurable vibration will be recorded in those critical zones where the air-screw hub happens to be a node. Conversely, if a torsionmeter is used no measurable vibration will be recorded in those critical zones where the air-screw hub happens to be an anti-node.

The air-screw blade stresses can be measured by means of strain sensitive electrical pick-up units secured to the blades at intervals along their lengths. A description of these methods is outside the

scope of the present work, although some information is given in Chapter 8. The equipment used by the de Havilland Aircraft Co. is described in an article in *The Aeroplane*, 30 Aug., 1939, p. 281, entitled "Measuring the Stresses in Vibrating Air-screws by Electricity."

Tuning Curves for Engines fitted with Rotating Pendulum Absorbers.—The rotating pendulum absorber is described in detail in Chapter 11, where it is shown that the effect of fitting this device to a crank element is to change the polar moment of inertia of the element to a value which can lie anywhere between positive and negative infinity, depending on the tuning of the absorber. Moreover, the value of this equivalent inertia is different for different harmonic orders, as explained in Chapter 11. It is therefore evident that when applying the effective inertia method of torsional vibration analysis to a system containing an engine fitted with rotating pendulum absorbers a separate engine tuning curve is required for all harmonic orders where the effect of the rotating pendulum is to change the polar moment of inertia of the crank masses appreciably.

Thus an installation comprising an engine fitted with rotating pendulum absorbers driving an air-screw probably represents one of the most complex systems encountered in practice, since the correct disposition of the resonant zones can only be determined by the effective inertia method, and in applying this method it is necessary to plot separate resultant effective inertia curves for the air-screw as well as separate engine tuning curves, for each important harmonic order.

The importance of knowing the shapes of the effective inertia curves for actual air-screws is only now becoming generally appreciated, so that information on this subject is unfortunately very meagre. The following values give a very approximate indication of the frequency bands in which various modes of blade vibration are likely to fall in practice :—

1-node in blade,	F = 2000 to 7000 vibs./min.
2-nodes ,,	F = 5000 to 12000 ,,
3-nodes ,,	F = 7000 to 18000 ,,
4-nodes ,,	F = 9000 to 24000 ,,

It has been estimated that if all vibratory excitation could be eliminated the specific weight of modern high-duty variable pitch air-screws could be reduced from its present value of about 0.33 lb. per horse-power to approximately 0.20 lb. per horse-power. The possibility of achieving even a proportion of this saving explains the very great attention which is being given to vibration problems associated with engine/air-screw installations both here and abroad. Most of the progress which has been made up to date is due to the

development of suitable vibration measuring technique during the last few years, notably by Hamilton Standard Propellers in the United States of America, by de Havilland Airscrews in this country, and by government establishments for aeronautical research in Great Britain, the United States, and Germany (see Bibliography).

One of the difficulties in analysing the results obtained by different investigators is lack of uniformity of notation. The effective inertia method of analysis just described is perhaps the simplest possible treatment, since it leads to a simple and straightforward experimental procedure and at the same time gives an excellent physical interpretation of the exceedingly complex mathematical problem associated with vibration of rotating air-screws.

Despite the great complexity of the problem, however, and despite the very large number of air-screws in service the number of failures of variable pitch air-screws in the air is quite negligible, which is a tribute to the wisdom of the makers in giving vibration study a prominent place in design and test procedure, as well as an excellent measure of the success of the methods adopted.

Up to the present time experience has indicated the importance of carrying out a thorough series of vibration tests on each new engine/air-screw combination with the object of revealing any undesirable vibratory conditions and of obtaining information which will enable these conditions to be overcome.

In this connection it is interesting to note that in a paper entitled "Vibration Characteristics of Aircraft Engine-Propeller Systems," S.A.E. Preprint, May, 1939, Charles M. Kearns of Hamilton Standard Propellers states, as the result of extensive investigation, that air-screw blade design changes are inadequate as a general method for solving vibration problems, and that changes in the stiffness of the air-screw shaft of relatively small amount have been more effective in certain cases than any amount of blade design variation. Fundamental data of this kind is of the utmost value, and there is no doubt that the next few years will see the aero-engine/air-screw vibration problem placed on a sure foundation of observed facts. In some quarters it is considered that the ultimate solution will be to isolate the air-screw from the engine completely, and attempts in this direction, using long flexible air-screw shafts, are already being tried. Very effective isolation could be obtained by using hydraulic or electro-dynamic couplings between the engine and the air-screw, but it is doubtful whether these devices could be designed within the weight and space limitations imposed by aircraft.

BIBLIOGRAPHY.

(a) VIBRATION (GENERAL).

- BROWN. "Vibration Problems from the Marine Engineering Point of View." *Trans. N.E. Coast Instn. of E. & S.*, February, 1939.
- BROWNE. "Dynamic Suspension—a Method of Aircraft Engine Mounting." *S.A.E. Journal*, May, 1939.
- CARTER. "Airscrew Blade Vibration." *Journal R.Ae.S.*, September, 1937.
- "Vibration in Aircraft." *Engineering*, 26th August and 2nd September, 1938. (Paper read before Section G of the British Association, 23rd August, 1938.)
- "Whirling of Radial Engines in their Mountings." R. & M. 1783, H.M. Stationery Office.
- COLE. "Vibrations for Engineers." Crosby Lockwood, London.
- D'AUBARÈDE. "Etude sur les Vibrations des Automobiles." (Automobile Vibrations), *Conférence faite devant la Société des Ingenieurs de l'Automobile*, 12th May, 1936.
- DEN HARTOG. "Mechanical Vibrations." McGraw-Hill Book Co., London.
- DOREY. "Strength of Marine Engine Shafting." *Trans. N.E. Coast Instn. of E. & S.*, March, 1939.
- GREY. "The Elimination of Vibration." *Trans. Diesel Engine Users' Assn.*, 1931.
- HULL. "The Use of Rubber in Vibration Isolation." *Journal of Applied Mechanics*, September, 1937.
- LIFFE. "The Theory of Flexible Mountings for Internal Combustion Engines." *Journal Instn. of Aut. Eng.*, Vol. VIII, No. 3, December, 1939.
- JACKSON. "The Vibrations of Oil Engines." *Trans. Diesel Engine Users' Assn.*, 1933.
- JULIEN. "La Suspension Elastique des Moteurs d'Aviation." (Elastic Suspension of Aero Engines), *Conférence*

- faite devant la Société des Ingenieurs de l'Automobile, 9th June, 1936.*
- KEARNS. "Vibration Characteristics of Aircraft Engine-Propeller Systems," *S.A.E. Journal*, December, 1939.
- KERR, SHANNON and ARNOLD. "The Problems of the Singing Propeller," *Proc. I. Mech. E.*, 1940.
- KLOPSTOCK. "The Design of Elastically-Supported Foundations for Reciprocating Engines." *Trans. Diesel Engine Users' Assn.*, 1937.
- LAUGHARNE THORNTON. "Mechanics Applied to Vibrations and Balancing." Chapman & Hall, London.
- LEMAIRE. "Les Etouffeurs Dynamiques de Vibrations." (Dynamic Vibration Absorbers), *Conférence faite devant la Société des Ingenieurs de l'Automobile, 9th June, 1936.*
- LEWIS. "Propeller Vibration." *Trans. Soc. N.A. & Mar. E.*, New York, 1935.
- LUGT and VISSER. "Whirl in Diesel Engine Crankshafts." *Int. Con. of N.A. & Mar. E.*, 1938.
- LÜRENBAUM. "Vibration of Crankshaft-Propeller Systems." *S.A.E. Journal*, December, 1936.
- LÜRENBAUM and BEHRMANN. "Schwingungstechnische Gesichtspunkte der federnden Aufhängung von Flugmotoren." (Flexible Mounting of Aero Engines), *D.V.L. Yearbook*, 1937.
- MORRIS. "The Whirling of a Crankshaft." *Aeronautics*, 10th July, 1919, p. 45.
"The Whirling of a Coplanar Crankshaft." *Aeronautics*, 11th September, 1919, p. 258.
- OESER. "Schwingungen am Kraftfahrzeug und deren Isolierung gegen die Umgebung." (Rubber Suspensions), *Automobiltechn. Z.*, Vol. 10, 1934.
- ROBERTSON. "Vector Methods of Studying Mechanical Vibrations." *The Engineer*, 27th February, 6th, 13th and 20th March, 1931.
- ROOT. "Dynamics of Engine and Shaft." Chapman & Hall, London.
- SCHLIPPE. "Zur Frage der elastischen Motorlagerung" (Flexible Engine Mountings). *D.V.L. Yearbook*, 1937.
- STIIZ. "Vibration Isolating Radial Engine Mounts," Air Corps Technical Report, No. 4215.
- TAYLOR and BROWN. "Vibration Isolation of Aircraft Power Plants." *Journal of the Aeronautical Sciences*, Vol. 6, No. 2, December, 1938.

- THEODORSEN. "Propeller Vibrations and the Effect of Centrifugal Force." *N.A.C.A. Tech. Note*, No. 516.
- TIMOSHENKO. "Vibration Problems in Engineering." Constable, London.

(b) TORSIONAL VIBRATION.

- BAUER. "Untersuchungen über die periodischen Schwankungen in der Umdrehungsgeschwindigkeit der Wellen von Schiffsmaschinen." (Research on Cyclic Speed Variation in the Shafting of Ships), *Jahrbuch der Schiffbautechn.* Ges. 1900.
- BIOT. "Vibration of Crankshaft-Propeller Systems—New Method of Calculation." *Journal of the Aeronautical Sciences*, Vol. 7, No. 3, January, 1940. (Assumes a rigid propeller.)
- BRITISH ELEC. AND ALLIED MAN. ASSOCN. (BEAMA). "Standardisation Rules for Torsional Oscillation in Shaft between Engine and Generator."
- CARTER. "Torsional Vibration in Engines." R. & M. 1053, H.M. Stationery Office.
- CARTER and MUIR. "Torsional Vibration Resonance Characteristics of a Twelve Cylinder Vee Aero Engine." R. & M. 1304, H.M. Stationery Office, 1933.
- FITCHETT. "The Design and Construction of Alternators for Coupling to Diesel Engines." *Trans. Diesel Engine Users' Assn.*, 1939.
- FRAHM. "Neuere Untersuchungen über die dynamischen Vorgänge in den Wellenleitungen von Schiffsmaschinen mit besonderer Berücksichtigung der Resonanzschwingungen." (New Research on the Dynamics of the Shafting of Ships with Special Reference to Resonant Vibration), *Z.D.V.I.*, 1902.
- FRITH and LAMB. "The Breaking of Shafts in Direct-Coupled Units, due to Oscillations set up at Critical Speeds." *Journal Instn. of Elect. Engs.*, Vol. 31, p. 646, 1901.
- GEIGER. "Die Untersuchung von Schwingungsvorgängen an Arbeitsmaschinen." (Investigation of Vibration Characteristics of Prime Movers), *Die Werkzeugmaschine*, Part 15, 1929.
- GREGORY. "Progress in the Development of In-Line Air Cooled Engines." *S.A.E.* Preprint, October, 1939 (Camshaft Vibrations).

- GÜMBEL. "Ueber Torsionschwingungen von Wellen." (Torsional Vibration of Shafts), *Schiffbau*, 1901-1902.
- HOLZER. "Die Berechnung der Drehschwingungen." (Calculation of Torsional Vibrations), Julius Springer, Berlin, 1921.
- KELLER. "Torsional Oscillations in Marine Shafting." *Trans. Liverpool Eng. Soc.*, Vol. LV, 1934.
- KER WILSON. "Torsional Vibration Characteristics of Six-Cylinder Four-Stroke Cycle Single-Acting Oil Engines." *Gas and Oil Power*, 4th August and 6th October, 1932.
- "Torsional Vibration in Automobile Engine Crankshafts." *Journal Inst. of Aut. Engs.*, No. 1, Vol. IV, 1935.
- KJAER. "Torsional Vibration in Diesel Crankshafts." *The Motorship*, August, 1930.
- LEWIS. "Torsional Vibration in the Diesel Engine." *Trans. Soc. N.A. & Mar. E.*, New York, 1925.
- LOCKWOOD "Torsional Vibration Frequencies of Marine Diesel Installations." *Engineering*, 20th February, 1931.
- TAYLOR. "Torsional Vibration Amplitudes of Marine Diesel Installations." *Engineering*, 29th May, 1931.
- LÜRENBAUM. "Practical Investigation of Torsional Oscillation in Aero Engines." *D.V.L. Year Book*, 1932.
- MANCY. "Theorie des Oscillations de Torsion des Lignes D'Arbres de Moteurs a Combustion Interne." (Torsional Oscillations in Internal Combustion Engine Shafts), *Bulletin Technique du Bureau Veritas*, August, 1931.
- "Oscillations de Torsion des Arbres." (Torsional Oscillations of Shafts), *Mécanique*, No. 273, July/August, 1937.
- MASI. "Permissible Amplitudes of Torsional Vibration in Aircraft Engines." *S.A.E.* Preprint, March, 1939.
- MEYER. "Die Kopplung der Luftschrauben-Biegeschwingungen mit den Kurbelwellen-Drehschwingungen." (The Coupling of Airscrew Flexural Vibrations with the Torsional Vibrations of Crankshafts), *D.V.L. Yearbook*, 1938, Vol. II, p. 141.
- MUIR and "A Harmonic Analysis of the Torque Curves of a Single-Cylinder Electric Ignition Engine." R. & M. 1305, H.M. Stationery Office, 1930.
- TERRY.

- PORTER. "The Range and Severity of Torsional Vibration in Diesel Engines." *Trans. Amer. Soc., Mech.E.*, 1929 (APM-50-8).
- "Practical Determination of Torsional Vibration in an Engine Installation which may be simplified to a Two-Mass System." *Trans. Amer. Soc. Mech.E.*, 1927 (APM-51-22).
- SCHAEFKE. "Der Einfluss des V-winkels auf die Kurbelwellen Drehschwingungen von V-motoren." (The Influence of Vee-angle on the Torsional Vibration Characteristics of Vee-engines), *Z.D.V.I.*, No. 41, 10th October, 1936.
- SCHUEERMAYER. "Einfluss der Zündfolge auf die Drehschwingungen von Reihenmotoren." (The Influence of Firing Order on the Torsional Vibration Characteristics of In-line Engines), *Werft Reederei Hafen*, 1st March, 1933.
- SHANNON. "The Interpretation of Some Torsiograph Records." *Journal Roy. Tech. Coll.*, Glasgow, Vol. 3, Part 3, January, 1935.
- SHRÖN. "Die Zündfolge der Vielzylindrigen Verbrennungsmaschinen, insbesondere der Fahr- und Flugmotoren." (Firing Orders of Multi-Cylinder-Internal Combustion Engines with Particular Reference to Transport and Aero-Engines), *Oldenbourg*, Munich, 1939.
- STEIGLITZ. "Torsional Oscillations in Engines with Cylinders in Line." *Luftfahrtforschung*, No. 5, 24th July, 1929.
- SULZER. "Torsional Stresses in Tunnel and Propeller Shafting." *Sulzer Technical Review*, 1929.
- TAYLOR and MORRIS. "Harmonic Analysis of Engine Torque due to Gas Pressure." *Journal of the Aeronautical Sciences*, Vol. 3, February, 1936.
- TUPLIN. "Torsional Vibration," Chapman & Hall.
- WYDLER. "Drehschwingungen in Kolbenmaschinenanlagen und das Gesetz ihres Ausgleichs." (Torsional Vibration in Reciprocating Engines and its Damping), Julius Springer, Berlin, 1922.
- I.MECH.E. "Sixth Report of Marine Oil Engine Trials Committee." *Proc. I. Mech. E.*, Vol. 121, p. 268, 1931.

(c) TORSIONAL VIBRATION (GEARED SYSTEMS).

- BRADBURY. "The Geared Marine Oil Engine." *Proc. I. Mech. E.*, Vol. 125, 1933.

- DEN HARTOG "The Torsional Critical Speeds of Geared Airplane
and Engines," *Journal of the Aeronautical Sciences*,
BUTTERFIELD Vol. 4, No. 12, October, 1937.
- HAGEN and "Torsional Vibration in In-Line Aircraft Engines."
MONTIETH. *S.A.E. Journal*, August, 1938.
- MCLEOD. "Mechanical Gearing." *Trans. Liverpool Eng. Soc.*,
Vol. LIII, 1932.
- SMITH. "Nodal Arrangements of Geared Drives." *Trans.*
Inst. N.A., 1922.
- THORNE and "Notes on Torsional Oscillations with Special
CALDERWOOD Reference to Marine Reduction Gearing."
Trans. N.E. Coast Instn. of E. & S., Vol. 39,
Part 2, December, 1922.
- TUPLIN. "Torsional Flexibility of Geared Drives."
Engineering, 9th January, 1931.
"Torsional Vibration with Angular Backlash."
The Engineer, 23rd August, 1935, p. 199.

(d) MISCELLANEOUS.

- ALEXANDER. "Hydraulic Analysis of Vulcan Couplings." *The*
Mar. Eng. & Motorship Builder, November,
1930.
- ANGLE. "Engine Dynamics and Crankshaft Design."
Simmons-Boardman, New York.
- BIERMANN. "Effect of Spark Timing on Knock Limitation of
Engine Performance." *N.A.C.A. Tech. Note*,
No. 651.
- CAUNT. "An Introduction to the Infinitesimal Calculus."
Oxford Univ. Press.
- CORMAC. "The Design of Dynamically Balanced Crank-
shafts for Two-Stroke Cycle Engines." *Engineer-
ing*, 11th October, 1929, p. 458.
"A Treatise on Engine Balance using Exponen-
tials." Chapman & Hall, London.
- DOREY. "Some Factors Influencing the Sizes of Crankshafts
for Double-Acting Diesel Engines." *Trans.*
N.E. Coast Instn. of E. & S., 1931.
- EAGLE. "A Practical Treatise on Fourier's Theorem and
Harmonic Analysis for Physicists and Engineers."
Longmans, London.
- HEIN. "Parallel Operation of A.C. Diesel-Generator Sets."
A.E.G. Progress, May/June, 1928, p. 129.
- KERR. "The Balance of Internal Combustion Engines."
Inst. of E. & S. in Scotland, 1928.
- KER WILSON. "Balancing of Oil Engines." Griffin, London.

- LLOYD'S
REGISTER of
SHIPPING. "Rules and Regulations."
- PITMAN. "Handbook of Aeronautics." Vols. I and II.
Pitman, London.
- POMEROY. "Fluid Flywheel Transmission." *Trans Inst. of
Aut. Eng.*, December, 1931.
- SHARP. "Balancing of Engines." Longmans, London.
- TOFT and
KERSEY. "Theory of Machines." Pitman, London.
- WORTHINGTON. "Dynamics of Rotation." Longmans, London.

Note.—*Z.V.D.I.* = Zeitschrift des Vereines deutscher Ingenieure.

For additional Bibliography see Vol. II.

NAME INDEX.

(Text references to Authors and Firms.)

AUTHORS.

- Biermann, A. E. (*N.A.C.A. Tech. Note 651*), 406.
 Butterfield, J. P., 359, 386.
- Calderwood, J., 590.
 Caldwell, F. W., 358.
 Carter, B. C., 187, 188, 192, 358, 656, 693, 700.
 Cormac, P., 513.
- Den Hartog, J. P., 359, 386.
 Dorey, S. F., 231.
- Fullagar, H. F., 196.
- Geiger, J., 126, 205.
 Gregory, A. T., 405.
 Griffith, A. A., 168, 169.
 Gumbel, L., 52.
- Hankins, G. A., 232.
- Kearns, C. M., 707.
 Keller, K. O., 204.
 Kjaer, V. J., 125.
- Lewis, F. M., 590.
 Lürenbaum, K., 352, 424.
- Mancy, M., 125.
 Masi, F., 606, 607.
 Morris, E. W., 456.
 Muir, N. S., 656.
- Pearson, K., 168.
 Prandtl, 168.
- Root, R. E., 465.
- Saint-Venant, 168, 169, 173.
 Scheuermeyer, M., 125.
 Seely, F. B., 168.
 Sharp, A., 119.
 Smith, J. H., 302.
- Taylor, E. S., 456.
 Taylor, G. I., 168, 169.
 Thorne, A. T., 590.
 Todhunter, 168.
 Tuplin, W. A., 351.
- Wahl, A. M., 245.
- Zimmerli, F. P., 248.

FIRMS.

- | | |
|--|---|
| Armstrong Siddeley Motors, 281, 282. | M.A.N. (<i>Maschinenfabrik Augsburg Nürnberg</i>), 252. |
| Barnes-Gibson-Raymond, 248. | Marine Oil Engine Trials Committee (I.Mech.E.), 188. |
| Blohm and Voss, 401. | Metalastic, 281. |
| Daimler, 408. | M.I.T. (<i>Massachusetts Institute of Technology</i>), 454. |
| De Havilland Airscrews, 707. | Pendulastic, 281, 282. |
| Doxford, 200. | R.A.E. (<i>Royal Aircraft Establishment</i>), 452, 453, 454, 455. |
| D.V.L. (<i>Deutsche Versuchsanstalt Für Luftfahrt</i>), 424. | Stationery Office, H.M., 454, 656. |
| Dynaflex (<i>Manganese Bronze and Brass Co.</i>), 282, 286. | Wellman Bibby, 262, 269. |
| General Electric Research Laboratories, 153. | Workman Clark, 302. |
| Hamilton Standard Propellers, 707. | |
| Junkers, 200, 350, 399. | |

SUBJECT INDEX.

- A**BSORBERS, vibration; See "Dampers."
- Acceleration, simple harmonic motion: angular 10, linear 8.
- Accessory drives; See "Auxiliary drives."
- Aero-engine/Air-screw systems 692; Counter-rotating air-screws 599; Direct-drive 95; Effective inertia method of analysis 670, 692; Geared 328, 340, 342, 386; See "Aero-engines" and "Air-screws."
- AERO-ENGINES:** Articulated connecting rod systems 457, 486, 548, influence on engine torque 462, 470, 486, influence on inertia torque 464, influence on piston displacement 460, 466; Auxiliary drives 350, 402, camshaft 402, 404, effective inertia of 680, supercharger 350; Balance weights 191, 494, 503, 514, 526, 534, 543, 552, 555, influence on frequency 347, 505; Crankshaft stiffness 184, 187, 189, influence on torsional vibration 97, 98, 105, 341, 347, 349, 494; Flexible shafts and couplings 105, 281, 350; Forced vibration, tabulation method 653; Frequency values 107, 342, 347, influence of balance weights 347, 505; Friction damper, geared engines 350; Harmonic components of tangential effort, compression ignition 453, 454, petrol 452, 455, with articulated connecting rods 462, 464, influence of air-screw load 603, supercharged engines 605; Mean indicated pressure, typical values 608; Moment of inertia of running gear 130; Test-bed couplings 283; Test-bed vibration 353; Torque curve 603; Types of aero-engine 95; Vibration amplitudes and stresses at non-resonant speeds 410, 625, 660.
- IN-LINE ENGINES:** Balancing 504; Crank arrangements and firing orders 493, 500, 584; Normal elastic curves 100, 103, 126, 343, 355; Phase and vector diagrams 471, 474, 500, 501.
- Direct-drive:* Equivalent systems 99; Frequency calculations 102; Frequency tabulations 107; Methods of tuning 104; Vibration characteristics 99, 493.
- Geared:* Equivalent systems 342, with flexible mountings 361; Frequency calculations 345, with flexible mountings 362; Frequency tabulations 346, with flexible mountings 363; Methods of tuning 347, 348, with flexible mountings 388, 392, 394; Vibration characteristics 346, with flexible mountings 367, 392, 507; Wing mounted 399.
- RADIAL ENGINES:** Balancing 488, 490; Crank arrangements and firing orders 484; Double-row radials 488, location of master cylinders 489; Normal elastic curves 97, 355; Phase and vector diagrams 485, 487; Resultant harmonic components for 7- and 9-cylinder engines 470; Two-stroke engines 485.
- Direct-drive:* Equivalent systems 25, 96; Frequency calculations 25, 96, 97; Methods of tuning 98; Vibration characteristics 96, 486.
- Geared:* Equivalent systems 333, with flexible mountings 361; Frequency calculations 338, 341, with flexible mountings 372, 380; Frequency tabulations 339, with flexible mountings 374, 377, 381, 384; Methods of tuning 341, 342, with flexible mountings 388, 392, 394; Vibration characteristics

- 341, with flexible mountings 367, 392, 507.
- VEE-ENGINES:** Balancing 514, 532, 552, 553, influence of vee-angle 558; Connecting rod systems 457; Crank arrangements and firing orders 548, 550, 561; Effect of altering vee-angle 574, 575; Normal elastic curves 573, 580, 581; Phase and vector diagrams 573, 580, 581, influence of vee-angle 567; Vibration characteristics 548, 565, with different firing orders in each bank 579; See "In-line engines."
- Aeroplane fuselage,** moment of inertia of 364.
- Air-screw, Counter-rotating** 599; Effective inertia of 693; Experimental determination of effective inertia 698; Influence on torsional vibration, radial engines 98, in-line engines 104; Moment of inertia of 131, 136, 139, 142; Phasing of 599; Torque variation 598; Weight of 141, 706.
- Air-screw blade:** Flexibility of, influence on vibration 96, 142, 352, 355, 670, 692; Materials 153; Stresses, measurement of 705; Vibration of, edgewise and flatwise modes 696, fixed root modes 693; frequency values 706, influence of design changes 707, influence of pitch setting 695, influence of root fixation 698, influence of rotation 700, non-effective orders 703, rocking hub modes 695, symmetrical modes 697.
- Air-screw drives:** Armstrong Siddeley spring hub 281; Flexible shaft or coupling 105; Quill shaft 349, 707.
- Air-screw shaft:** Influence on frequency 98, 105, 341, 348, 349; Quill drive 349, 707; Torsional rigidity 163.
- AMPLITUDE:** Camshaft 405; Definition 7; Engine, due to unbalanced parts 505; Equivalent, geared systems 288; Oscillation, with rigid shafting 631, 668; Permissible, accessory drives 402, camshaft drives 405; Relationship between linear and angular 10; Simple harmonic motion, angular 10, linear 7; Specific 58, 60, 67, 107.
- AMPLITUDE: EQUILIBRIUM:** Complex systems 692; Marine engine/propeller system 594, influence of propeller phasing 596; Marine oil engine, one-node 612, 614, two-node 617; Marine steam engine 620, 622; Multi-mass systems 429, 431, 432, 433; Oil Engine/Generator set 608; Two-mass systems 414, 427, 432.
- Forced Vibration:** 410, 625; Two-mass systems, torque at one mass 414, 626, torque at two masses 634, torque at node 639; Three-mass systems 643; Multi-mass systems 429, 433, 653; Tabulation method, two-mass systems 627, three-mass systems 645, multi-mass systems 657.
- Relative:** Geared systems, two-shaft 295, multi-shaft 310; Three-mass systems 37; Multi-mass, systems, approximate 42, 47, tabulation method 58, 60, 67.
- Vibration:** Definition 7; Marine steam engine 483; At non-resonant speeds; See "Forced vibration Amplitude."
- Analysis, harmonic;** See "Harmonic analysis."
- Angular motion,** relationship to linear motion 10.
- Apparent damping,** 126.
- Armstrong Siddeley flexible hub for air-screws** 281, 282.
- Articulated connecting rods** 457; Influence on engine torque 462, 470, 486; Influence on inertia torque 464; Influence on piston displacement 460, 466; Radial engines 461, 486; Vee-engines 548.
- AUTOMOBILE ENGINES:** Articulated connecting rods 457; Auxiliary drives 402; Balance weights 157, 194; Balancing 504, 510; Crank arrangements and firing orders 493, 500; Crankshaft stiffness 193; Equivalent systems 88; Flexible mountings 409; Frequency calculations 91; Frequency values 95; Harmonic components of tangential effort, compression ignition 453, 454, petrol 436, 452, 455, influence of engine load 607; Mean indicated pressure, typical values 608; Methods of tuning 94, 408; Moment of inertia of running gear 130; Nor-

- mal elastic curves 89, 126; Torque variation 407; Transmission systems 88, 90, 299, 407; Vee-engines 548, influence of V-angle 552; Vibration characteristics 88, 299, with flexible mountings 409; See "Aero-engines."
- Auxiliaries: Chain or belt driven 403; Effective inertia of 680; Engine driven 128, 402; Influence on vibration characteristics of main system 402; Lever driven 129; Moment of inertia of 128; Permissible amplitudes 402, 405; Quill drive 350.
- B**ACKLASH: Camshaft drives 405; Gears 351, 399; Splined and serrated shafts 163.
- Balance weights: Aero-engine 191, 347, 494, 503, 505, 526; Automobile engine 157, 194; In-line engines 495, 514, 534, 543; Influence on frequency 79, 347; Influence on moment of inertia 130; Marine oil engines 83, 87, 88; Moment of inertia of 117, 157; Oil engine/generator set 78, 79; Vee-engines 514, 532, 552, 555.
- Balancing: Automobile engines 510; In-line engines 504, comparative calculations 507, influence of higher order forces and couples 513; Method of comparing engine balance 505; Primary balancers 528; Radial engines 488, 490; Relative importance of forces and couples 511, 513; Relative importance of primary and secondary unbalance 506; Secondary balancers 514; Vee-engines 514, 532, 552, influence of vee-angle 558.
- Bearing, influence of clearance and restraint, 186, 193, 205.
- Bearing loads 495, 523.
- Belt drives, engine accessories 403.
- Bibby flexible coupling 262; Design of 268; Proportions 263, 267; Resilience 265; Strength of 268.
- Bibliography 708.
- Blohm and Voss, torsionally rigid coupling 401.
- Branched systems; See "Geared systems."
- C**ALCULATING machine, mechanical, use of 684.
- Camshaft drives 402; Amplitudes 405; Torque variation 405; Tuning 404.
- Carburettor: See "Induction system."
- Carter, empirical formula for crankshaft stiffness 187.
- Chain drives 403.
- Coefficient of speed fluctuation; See "Cyclic irregularity."
- Coefficients for kinetic energy and moment of inertia of reciprocating masses 120, 121.
- Comparison of frequency calculations, multi-mass systems 43, 49.
- Compression ignition; See "Oil engines."
- Concentration, Stress; See "Stress concentration."
- Concentric gears; See "Gears."
- Connecting rod: Big-end load, method of reducing 495; Effect of obliquity 119; Equivalent dynamic system 117, 446; Moment of inertia 117; See "Articulated connecting rods."
- Connecting rod couple, influence on tangential effort 445.
- Correction factors for multi-mass system frequency calculations 50, 76.
- Correction for mass of shaft: One-mass system 14, 16; Two-mass system 25; Multi-mass system 148.
- Counterweights; See "Balance weights."
- Couple, vibration caused by 511.
- Coupled frequencies: Air-screw blades 352, 692; Engine mountings 358, 386.
- Couplings: Flexible; Electro-dynamic 707; Hydraulic 408, 707; Keyed 163; Shaft, torsional rigidity of 162; Torsionally rigid type 400; Turbine claw type 401; See "Flexible couplings."
- Crank masses, moment of inertia, 129.
- Crank sequence and firing order; See "Firing order."
- Crankcase, vibration of 127, 523; Distortion of 400, 495; See "Engine frame."

- Crankpin: Moment of inertia 0 113; Torsional rigidity of 185 with eccentric bore 203.
- Crankshaft: Arrangements, in-line engines 493, 500, geared 584, vee engines 548, 550, 561; D.V.L. fatigue testing machine 424. Forgings 495, 530; Moment of inertia of; See "Moment of inertia."
- Crankshaft stiffness 184; Aero-engines 189; Automobile engine 193; Carter formula 187; Empirical formula 192; Experimental determination of 204; Influence of bearing clearance 186, 193, 205; Influence of web form 200, 347; Method of altering 77. Strain energy method 193; Various engines 189.
- Influence on torsional vibration* 50; Aero-engine, in-line 97, 98, 105, 494, geared in-line 347, 349, radial 341; Automobile engine 94, 408; Marine oil engine 81, 86, 87; Oil engine/generator set 77.
- Crankweb: Influence of web form on stiffness 200, 347; Moment of inertia of 114, 156, with integral balance weights 157; Torsional rigidity of 185, 200.
- Critical speeds: Definition 410. Major 433.
- Cyclic irregularity: Calculation 633; Influence on governing characteristics 406; Marine oil engine 666, 669; Two-mass system 633, 635, 639; Three-mass system 648. Multi-mass system 665.
- Cyclic variation of natural frequency, 126.
- Cylinders, influence of number of 77.
- D**AIMLER fluid flywheel 408.
- Damper, automobile system 408; Geared system 350; Rotating pendulum absorber 706.
- Damping: Apparent, due variation of moment of inertia 126; In accessory drives 404; Influence on frequency 14; Proportional to velocity 14.
- Damping forces 14.
- Deflection of rubber-in-shear couplings 283, 285.
- Deflection of shaft, torsional 3.
- Degree numbers, definition 52, 71, 437.
- Detonation, limitation on M.E.P. of aero engines 604.
- Detuning effect of reciprocating masses 125.
- Diesel engine; See "Engine."
- Diesel-generator; See "Oil engine/generator."
- Direct-coupled generator sets 71; See "Oil engine/generator."
- Displacement, simple harmonic motion angular 10, linear 7; Relationship between linear and angular 10.
- Dynaflex rubber-in-shear couplings 282.
- Dynamic magnifier: Undamped 415, definition 415; Table of values, constant excitation 417, inertia excitation 418; Two-mass systems 415.
- Dynamic vibration absorber 650.
- Dynamometer, hydraulic, vibration originated by, 600.
- E**FFECTIVE inertia curve: Air-screw blades 694, correction for rotation 700; Experimental method of determining 698; Flywheel with flexible spokes or overhung rim 679; Heavy shaft system 690; Simple branched system 681; Two-mass system 672; Three-mass system 675; Multi-mass system 685; Uniform rectangular beam 694.
- Effective inertia method of torsional vibration analysis 670; Aero-engine/air-screw systems 692, geared 693; Engines with rotating pendulum vibration absorbers 706; Flywheel with flexible spokes 677; Heavy shaft system 685; Two-mass system 670; Three-mass system 674; Multi-mass system 683; Simple branched systems 680.
- Effective moment of inertia, referred to free end of shaft, multi-mass systems 432; Marine oil engine 615; Oil engine/generator set 670.
- Elastic deformation of shafts, laws governing 1.
- Elastic hysteresis; See "Hysteresis."
- Elastic limit, definition 1.
- Elastic moduli, table of values 164, 233.
- Elastic vibrations 2; See "Vibrations."

- Elastically connected mass, equivalent inertia of 209, 235, 670.
- Elasticity, definition 1; Equivalent 159; See "Torsional rigidity."
- Electrical generating sets; See "Oil-engine/generator."
- Electrical strain gauge 705.
- Electro-dynamic couplings 707.
- ENERGY; KINETIC, definition 4, due to recip. masses 121; *Potential*, definition 2; *Strain*, definition 2, calculation of 18; *Torque*, multi-cylinder engines 470; *Vibration*, definition 4.
- Energy input, due to harmonic torque, heavy shaft systems 691, aero-engine/air-screw systems 705.
- ENGINES: Accessories, influence on torsional vibration 402; Balancing 504, 553; Dimensions, influence on frequency 78; Frame vibration 127, 358, 513, 541, 543; Location of, to minimise structural vibration 512; Method of comparing balance 505, 512; Moment of inertia of, on flexible mountings 389; Similar, properties of, 78; Torque reaction 541, 543.
Influence of Crank Sequence and Firing order on Vibration and Balance: Four-stroke cycle, single-acting, in-line engines 513; Two-stroke cycle, single-acting, in-line engines 528; Two-stroke cycle, double-acting, in-line engines 538; Vee-engines 548, choice of vee-angle 549; Tables 500, 501, 502, 550; See "Aero-engine," "Automobile engine," "Oil engine," "Marine engine," and "Vee-engine."
- Engine mounts, flexible 358; Automobile engine 409; Design of 367, 389, 507; Force transmitted 508, 510; Influence on torsional vibration, direct-drive engines 359, geared engines 359, simple gears 360, concentric gears 369, epicyclic gears 378.
- Epicyclic gears; See "Gears."
- Equilibrium amplitude; See "Amplitude."
- Equilibrium stress; See "Stress."
- Equivalent amplitude, geared systems, 288.
- Equivalent disc, method of determining moment of inertia 132.
- Equivalent elasticities 159.
- Equivalent inertia, geared systems 288, 333; Elastically connected mass 209.
- EQUIVALENT LENGTH: 59, 159; Automobile crankshafts 193; Cast-iron and bronze shafts 164; Complex shaft 165; Shaft couplings 162; Shaft fillets 162; Shafts of non-circular cross-section 167, 170, 173; Shafts of varying diameter 162; Solid and hollow shafts 159; Tapered shafts 161; Various types of crankshafts 186.
- Equivalent masses 111; Geared system 287.
- EQUIVALENT OSCILLATING SYSTEMS 109; Aero-engine/air-screw systems, direct drive 95, 96, 99, geared in-line 342, geared radial 333, with flexible mountings 361; Air-screws 355; Automobile transmission systems 88, 90; Flywheel with flexible spokes 679; Geared systems 287, two-shaft 289, three-shaft 297, multi-shaft 303; Marine installations 38, 44, 50, oil engine 64, 109, exhaust steam turbine, geared 299, geared turbine and reciprocating engines 315; Oil engine/generating sets 45, 50, 57, 109; Two-mass system 38; Three-mass system 38.
- Equivalent torque, geared systems 288.
- Equivalent torsional rigidity, geared systems 288, 333, 340; Influence of gear flexibility 350.
- Exciting forces; See "Forces."
- Exhaust steam turbine systems 299, 315.
- Experimental demonstration of torsional vibration 5.
- Experimental determination of crankshaft stiffness 204; Opposed-piston engine 204.
- Experimental determination of moment of inertia 145; Example 147.
- Experimental determination of resultant effective inertia in complex systems 698.
- Experimental determination of vibration amplitudes in aero-engine/air-screw systems 705.

- ΓAN** drive, breakdown of, 483.
- Fatigue stress; See "Stress."
- Fatigue testing machine, D.V.L., 424
- Fillet, shaft, influence on torsional rigidity 162.
- Firing angle, for cancellation of a particular harmonic order; Between banks of vee-engines 568; Between cranks of geared engines 585 587; Between master cylinders of double-row radial engines 491.
- Firing order, influence on torsional vibration 476, in-line engines 493, radial engines 484, vee-engines 548. Influence on frame vibration 541, 543; Influence on induction 517, 563; Opposed-piston engines 528, 530, 532.
- Firing, simultaneous, of two cylinders of an in-line engine: Four-stroke engines 519, 526, 527; Two-stroke single-acting engines 533, 536, 538; Two-stroke, double-acting engines 542, 544, 545, 546; Geared engines 586; Vee-engines 579.
- Flexible connection, reduction gear 388.
- FLEXIBLE COUPLINGS:** Aero-engine 105, spring hub 281; Bibby see "Bibby"; M.A.N. sleeve type 252, design of 255; Non-linear type, in geared systems 308; Resilience of 220; Rubber-in-shear type 270, design of 279; Spring plate type 258, design of 261; With flexible spokes 213; design of 226; With helical springs 243, design of 246, torsional rigidity of 245.
- Flexible mountings; See "Engine mounts."
- Flexible shafts, in aero-engine/air-screw systems 105; In geared marine installations 396.
- Flexible spokes 213; Fixed at both ends 214; Flywheel 213, 235, 677, 680; Insecurely fixed 215; Resilience of 220; Stresses in 221; Torsional rigidity of 221; Uniformly stressed 217.
- Flexibly connected mass 209.
- Flexural resilience 223.
- Fluctuating stress, 232.
- FLYWHEEL:** Automobile engines 92, 93, 94; Camshaft drives 405; Daimler fluid 408; Dimensions, A.C. and D.C. generators 45, 75, marine engines 84, 87; Disposition of, for cancellation of certain harmonic orders 87, 503, 515; Effective inertia method of analysis 677, with bonded rubber between rim and hub 677, with flexible spokes 677, with overhung rim 680; Flywheels with flexible spokes 213, 677, example 235; Moment of inertia 143, experimental determination of 145.
- Influence on Torsional Vibration:* Automobile engines 92, 93, 94; In-line engines 503; Marine installations 81, 83, 84, 87; Oil-engine/generator sets 74, 78; One-mass systems 22; Two-mass systems 24.
- Flywheel effect, definition 11.
- Forced vibration amplitudes, torques and stresses; See "Amplitude," "Stress," "Torque," and "Vibration."
- Forced vibrations 411; Two-mass system 411.
- Forces, damping, proportional to velocity 14; Transmitted to foundation from unbalanced engines 508, 510.
- Four-stroke, double-acting engines, rules for determining harmonic torque components 448.
- Frame, vibration of 127, 358, 513, 541, 543; Influence of firing order 541, 543.
- Free torsional vibration 9; See also "Vibration."
- Frequency: Cyclic variation of 126; Definition 6; Errors between observed and calculated values 188; Influence of air-screw blade flexibility 96, 142, 352, 355, 670, 692; Influence of air-screw inertia 142; Influence of damping 14; Influence of engine mount flexibility 359; Influence of gearing flexibility 350, 399; Methods of modifying, see "Tuning"; Simple harmonic motion, angular 13, linear 9; Variation due to reciprocating masses 125.
- Frequency ratio, definition 416, 419; Influence on forced vibration amplitudes 420.
- REQUENCY CALCULATIONS** 52; Aero-engine 95, in-line, direct-

- coupled 102, geared 345, with flexible mountings 362, radial, direct-coupled 25, 96, 97, geared 338, 341, with flexible mountings 372, 380; Air-screw blade flexibility, influence of 357, 692; Effective inertia method, see "Effective inertia"; Engines with auxiliary drives 402, effective inertia method 680; Geared systems 287, two-shafts 292, three-shafts 302, multi-shafts 307, effective inertia method 680; Geared engines with flexible mounts 358; Geared marine steam turbine and reciprocating engine 315; Heavy shaft system 685, 689; One - mass system 15, 21, shaft fixed at both ends 21, with shafts of non-circular cross-section 183; Two-mass systems 26, shaft fixed at one end 27, shaft fixed at both ends 29; Three-mass systems 35; Rotating chain 700; Uniform rectangular beam 693.
- Approximate*: Aero - engine/air-screw systems 356, in-line, direct-coupled 102, 103, geared 345, radial, direct-coupled 97, geared 341; Automobile transmission systems 91; Engines with flexible mountings 395; Marine installations 40, 85; Multi-mass systems 40, 45, correcting factors 50, 76; Oil engine/generator sets 45.
- FREQUENCY EQUATIONS**: Automobile transmission systems 91; Geared systems, two-shaft 290, three-shaft 298, multi-shaft 304, with power taken off at two points 399; Heavy shaft systems 685; One-mass system 9, 12, 13, shaft fixed at both ends 19, mass controlled by helical springs 20; Two-mass systems 24, shaft fixed at one end 28, shaft fixed at both ends 30; Three-mass systems 33; Rotating chain 700; Uniform rectangular beam (air-screw blade) 695, 697, influence of rotation 701.
- Approximate*: Aero - engine/air-screw systems 356; Aero-engines, in-line 101, 102, geared in-line 344, radial 25, 96, geared radial 340; Automobile transmission systems 90; Engines on flexible mountings 386; Marine oil engine 38, 80; Multi-mass systems 38; Oil-engine/generator sets 70.
- FREQUENCY TABULATIONS** 52: Aero-engine, in-line type, direct-drive 107, geared 346, with flexible mounts, simple spur gear 363, 370, radial type, geared 339, with flexible mounts, concentric spur gear 374, 377, epicyclic 381, 384; Geared systems 294, two-shafts 295, 296, multi-shaft 310; General remarks 52, 69; Marine geared turbine and reciprocating engine 315; Marine installation 64, 67; Oil-engine/generator set 57, 58.
- FREQUENCY VALUES**: Aero-engines, direct-coupled 107, geared in-line 347, geared radial 342; Air-screw blades 706; Automobile transmission systems 95; Influence of balance weights 79, 347; Marine installations 83, 87; Oil-engine/generator sets 75.
- Frictional resistance 3, 5, 9, 14.
- GEAR** amplitudes, 360.
- Gear backlash, influence of 351, 399.
- Gear flexibility, influence of 350, 399.
- Gear ratios: Aero-engines 328; Concentric spur gear 329, 371; Epicyclic gear 331, 332, 333, 378; Equivalent systems 333; Simple spur gear 360.
- Gear tooth impact excitation 326, 328, 591.
- GEARED SYSTEMS** 287: Equivalent systems 287, two-shafts 290, three-shafts 297, multi-shafts 303; Frequencies, see "Frequency"; Nodal drive 302; Node at gears modes with identical prime movers 299, 301, 583; Tabulation method, two-shafts 294; Torque reaction 328, 359; Two-shaft systems 289; Three-shaft systems 297; Multi-shaft systems 303, effective inertia method 680.
- Geared drives: Marine installations 397; Power taken from two points simultaneously 398; Special types of 397; Wing mounted aero-engines 399; With two identical prime movers 299, 301, 583.
- Geared turbine installations 299, 315, 326.

- Geared Aero-engine/air-screw systems 328, approximate methods 340, with flexible mountings 358, approximate methods with flexible mountings 386, effective inertia method 693, equivalent systems 333.
- Gearing, types of 328; Gearing with flexible connection in reaction member 388; Ratios obtainable with concentric spur gears 329; Ratios obtainable with epicyclic gears 331, 332, 333; Tooth impulse frequency 404; Torque relationships, simple spur gear 360, concentric spur gear 372, epicyclic gear 379.
- Governor drives, characteristics of 406.
- Guide vanes, marine propeller, influence on impulse frequency 593.
- H**ARMONIC analysis, tangential effort curve 437, with articulated connecting rods 457.
- Harmonic components, propeller torque 588, with variable load and speed 601; See "Tangential effort."
- Harmonic motion, simple 5; Acceleration 8; Amplitude 7; Relationship between linear and angular 10; Velocity 7.
- Harmonic torque energy, resultant 470; In complex systems 691; Influence of air-screw blade flexibility 705.
- Heavy alloy; See "Tungsten alloy."
- Heavy shaft systems 670, 685.
- Helical springs, design of 246, end connections 243, in flexible couplings 243, in torsional systems 19, 243, safe stress ranges 248, strength of 245, Wahl factor 245.
- Hydraulic couplings 408, in aero-engine/air-screw systems 707, in automobile transmission systems 408.
- Hydraulic dynamometers 600.
- Hysteresis 2, in crankshaft torsion tests 209.
- I**MPULSE frequency, engine 367; Counter-rotating air-screws 599; Hydraulic dynamometer 600; Marine propeller 592, with guide vanes 593.
- Indicated pressure; See "Mean indicated pressure."
- Induction systems, in-line petrol engines 517, vee-engines 563.
- Inertia coupling, reciprocating masses, 359, 386.
- Inertia damper; See "Damper."
- Inertia, moment of; See "Moment of inertia."
- Inertia of reciprocating masses, influence on tangential effort 442, 447, with articulated connecting rods 464, 468.
- In-line engines; See "Aero-engines," "Automobile engines," etc.
- Input energy; See "Energy input."
- Interference diagram, engine/air-screw system 353, 354.
- Internal combustion engines; See "Aero-engine," "Automobile engine," etc.
- Internal friction, molecular 2; See "Hysteresis."
- K**EYED couplings, torsional rigidity of 163.
- Keyways, influence on resilience 181, influence on torsional strength 169, 171, 181, stress concentration at 169.
- Kinetic energy, definition 4, of reciprocating parts of engine 121.
- L**ENGTH, equivalent; See "Equivalent length."
- Lever-driven auxiliaries, moment of inertia of 129.
- Limit of proportionality; See "Elastic limit."
- Linear motion, relationship to angular motion 10.
- Load, influence on harmonic components of tangential effort 601.
- M**AGNIFIER, dynamic; See "Dynamic magnifier."
- Major criticals; See "Critical speeds."
- M.A.N. sleeve spring coupling 252, design of 255.
- Marine installations; Characteristics of 38, 44, 50, 80, 187, 514, 588, 612, geared systems 299, 315, with two identical prime movers 301, 583; Forced vibration in 411.

- MARINE OIL ENGINE:** Auxiliary drives 128; Balance weights 83, 87, 88; Balancing 504, opposed-piston type 528, 530, 532, 533; Coefficient of speed fluctuation 666; Crank arrangements and firing orders 493, 500, geared 584; Crankshaft stiffness 184, 190, 194, 196, 204; Equivalent systems 38, 44, 50, 64, 109; Frequency calculations 40, 82, 85; Frequency tabulations 64, 67; Frequency values 83, 87; Geared systems 299, with two identical prime movers 301; Harmonic components of tangential effort 434, 450, 456, influence of mean indicated pressure 619; Mean indicated pressure, influence of propeller load 602, typical values 608; Methods of tuning 81, 86, 396, 503; Moment of inertia of running gear 130; Normal elastic curves 65, 68, 72, 80; Phase and vector diagrams 473, 589; Vibration amplitudes and stresses at non-resonant speeds 612; Vibration characteristics 80, 588, influence of propeller phasing and torque variation 593, 616.
- Marine steam engine:** Breakdown due to torsional vibration 483; Harmonic components of tangential effort curve 450, 481, 621; Stress calculations at non-resonant speeds 620, influence of propeller phasing 624; With exhaust steam turbine 299, 315.
- Mass, effect of altering size and distribution of one-mass systems 13, two-mass systems 25, multi-mass systems 80, 82, 85; Elastically connected 209, 670.**
- Mass of shaft, corrections for one-mass systems 14, 16, two-mass systems 25, 148; See "Heavy shaft."**
- Materials:** crankcase 400; Elastic moduli 164, 233; Fatigue strength, torsion and bending 233; Specific resilience 234; Tungsten alloy (Heavy metal) 153, 164; Weight of 153.
- Mean indicated pressure:** Aero-engines 603; Influence of engine load 601; Influence on harmonic components of tangential effort 601, 619, 623; Relationship to mean tangential effort 435; Typical values, various engines 608.
- Mean torque, influence of 232, 411.**
- Metalastik rubber-in-shear coupling 281.**
- Mixture distribution; See "Induction system."**
- Mixture strength, influence on excitation torque 455.**
- Mode, fundamental, definition 33.**
- Modes of free vibration:** Aero-engine/air-screw systems 105, geared 340, 346, geared with flexible mountings 366, 376, 384; Air-screw blades 357, fixed root 693, 695, rocking hub 695, symmetrical 697; Automobile transmission systems 93; Geared systems, two-shaft 290, 294, with two identical prime movers 584, three-shaft 298, multi-shaft 305, 680; Heavy shaft system 685; Marine geared turbine and recip. engine 322, 326; Two-mass systems 28, 30; Three-mass systems 33; Multi-mass systems, 44, 52.
- Moduli of elasticity and rigidity Tables 164, 233.**
- MOMENT OF INERTIA 11:** Aircraft fuselage 364; Air-screws 131, 142; Camshaft system 405; Conic frustum 154; Crank masses, typical values 129, 130, 131; Crankpins, solid and hollow 113; Crankshaft and running gear 111, resultant 129, typical values 129, 131; Crankshaft balance weights 117, 157; Crankshaft journals, solid and hollow 111, 112; Eccentrics 113, 117; Effective, at free end of multi-mass system 432, 610, 615; Engine accessories 128, 402, lever driven 129; Engine on flexible mountings 389; Equivalent, elastically connected mass 209, geared systems 288; Experimental determination of 145; Flywheel 112, 143; Gearing assemblies 334, 336, 373; Marine propellers 131, 140, allowance for entrained water 135, small propellers 143; Reciprocating masses 118, 128; Rules for calculating 149; Running gear of engines, recip. parts 118, 128, revlg. parts 117, multi-bank engines 342, radial engines

- 131, vee-engines 131; Shaft couplings 112; Shafting, correction for mass of, see "Mass of shafting"; Typical solids 150; Variation of, due to recipg. masses 118, 125. (*Note: For Effective Inertia Method of Analysis see "Effectivis inertia."*)
- Motor car; See "Automobile."
- Mounts, engine; See "Engine mounts."
- Multi-cylinder engines, forced vibration amplitudes 433; See "Aero-engines," "Automobile engines etc.
- Multi-mass systems 38; Equilibrium amplitude 429; Equivalent two-mass systems 40, 49; Equivalent three-mass systems 40, 46; Influence of shaft stiffness 50, 80, 82.
- Multi-shaft systems; See "Geared systems."
- N**ATURAL frequency; See "Frequency."
- Natural torsional vibration 9 See "Vibration."
- Nodal drive, geared systems 302.
- Node, definition 23; One - mass system 3; Two-mass system 23, 24; Symmetrical disposition of, multi-cylinder in-line engines 88, 503, 515; Virtual, forced vibration 633.
- Node - at - gears mode of vibration, geared systems 299, 301, 583.
- Nodes: Aero-engine/air-screw systems, 693; Automobile transmission systems 91; Geared systems 297, two-shafts 291; Marine installations 72, 81; Multi-mass systems 41, 42, 43, 48, 52; Oil engine/generator sets 72; Ship's hull 512; Special two - mass systems 28; Three-mass systems 33, 34, 37; See "Normal elastic curves."
- Non-excitable harmonic orders: Air-screw blades 703; In-line engines 87, 500, 501, 502, 503, 515; Radial aero-engines 491; Vee-engines 568.
- Non-excitable modes of vibration, geared systems with duplicated prime movers 583, 587.
- Non-linear elasticity, shaft serrations and splines 163.
- Normal elastic curves: Aero-engine/air-screw system 126, 355, in-line engines 100, 103, 343, 355, radial 97, 355; Automobile transmission systems 89, 126; Characteristics of 71, 77, 83; Complex systems 690; Definition 52, 71; Geared systems 297, 300, with duplicated prime movers 584; Heavy shaft systems 691; Marine installations 65, 68, 72, 80, geared turbine and reciprocating engine 322; One mass systems 3, 19; Two-mass systems 22, 28; Three - mass systems 31; Seven-mass systems 39; Eight-mass systems 44; Multi - mass systems 52; Oil engine/generator sets 59, 63, 72, 77, 126; Typical 53, 72; Vee-engines 573, 580, 581.
- Normal modes of vibration; See "Modes."
- O**IL engines: Harmonic components of tangential effort curve, various engines 450, four-stroke, high-speed 453, 454, four-stroke, slow and medium speed 451, 456; four-stroke petrol 449, 452, 455, double-acting engines 448, 449, two-stroke engines 449; Geared engines, characteristics of 301, 583; Two or more pistons operating on each crankpin 484; Mean indicated pressures, typical values 608; See "Aero-engines," "Automobile engines," etc.
- Oil engine/generator sets: Balance weights 83, 87, 88; Balancing 504, 506, 514, 528; Crank arrangements and firing orders 493, 500, geared 584; Crankshaft stiffness 184, 190, 204; Equivalent systems 45, 50, 57, 109; Frequency calculations 45, 80; Frequency tabulations 57, 58; Frequency values 75; Geared systems 583; Harmonic components of tangential effort curve 434, 450, influence of mean indicated pressure 609; Mean indicated pressure, typical values 608, influence of generator load 609; Methods of tuning 73, 77, 78; Moment of

- inertia of running gear 129; Normal elastic curves 59, 63, 72, 77, 126; Phase and vector diagrams 472; Vibration amplitudes and stresses at non-resonant speeds 608, forced vibration tabulation 657; Vibration characteristics 45, 51, 71, 77, 514.
- One-mass systems 3, 9; Correction for mass of shaft 14; Frequency equation 13; Mass controlled by helical springs 19; Shaft fixed at both ends 18; With various types of non-circular shafts 183.
- Opposed-piston oil engines: Balancing 528, 530, 532, 533; Crankshaft stiffness 190, 195, 196, 200, experimental determination of 204; Crank arrangements and firing orders 528, 530, 532, 533; Harmonic components of tangential effort curve 449, 450; Mean indicated pressure, relationship to mean tangential effort 435; Moment of inertia of running gear 130; Phase and vector diagrams 476.
- Order numbers: Definition 435; In geared systems 293; Non-effective harmonic orders, air-screw blades 703, in-line engines 84, 87, 500, 501, 502, 503, 515, radial aero-engines 491, vee-engines 568.
- Oscillating systems, equivalent; See "Equivalent oscillating systems."
- P**ENDULASTIC rubber-in-shear couplings 281.
- Pendulum, compound 146; Simple torsional; See "One-mass system."
- Periodic time, definition 9; Simple harmonic motion 8.
- Periodic torque; See "Tangential effort."
- Petrol engine: Harmonic analysis of tangential effort curve 441, inertia correction 448; See "Aero-engine," "Automobile engine," and "Oil engine."
- Phase, definition 9.
- Phase angle; Definition 9; In harmonic analysis of tangential effort curve 437; In radial engines 491, 492; In vee-engines 549, 550.
- Phase diagrams 471; Use of 546; Geared engines 584; In-line engines, double-acting 476, 502, four-stroke 471, 500, two-stroke 474, 501, opposed-piston 476; Marine engine and propeller 589; Marine oil engine 473; Oil-engine/generator set 472, 480; Radial engines 485, 487; Vee-engines 573, 580, 581, influence of vee-angle 567.
- Phase velocity, definition, angular π , linear 6, 9.
- Phasing of aero-engines and air-screws 599; Geared engines 301, 583; Marine engines and propellers 593, 595, example 624.
- Piston displacement, with articulated connecting rods 460, 466.
- Poisson's ratio 165.
- Polyphemus*, T.S.M.V., comparison between observed and calculated frequencies 188.
- Potential energy, definition 2.
- Pressure, mean indicated; Oil engines, typical values 608; Relationship to mean tangential effort 435; Steam engines 451.
- Propeller: *Aeroplanes*, see "Air-screw"; *Marine*; Choice of number of blades 597; Impulse frequency 592, with guide vanes 593; Influence on cyclic irregularity 669; Moment of inertia of 131, 140, allowance for entrained water 135, small propellers 143; Torque variation 588, 616; Vibration of 588; Weight of 139.
- Propeller law, marine engines 602.
- Proportionality, limit of, definition 1.
- R**ADIAL aero-engines; See "Aero-engines."
- Radius of gyration, marine propeller 133, 139; See "Moment of inertia."
- Reciprocating masses: Correction for deadweight of 443, 447; Influence of inertia of on tangential effort 442, 447, example 666; Influence of variation of moment of inertia of 118, 125; Moment of inertia of 118, 128.
- Relative amplitudes; See "Amplitude."
- Resilience: Comparative values of, torsion bars of various cross-sections 181, various types of spring elements 230; Definition 2; Flexible couplings 220, with flexible spokes

- 223, 230; Flexural resilience 223; Non-circular shafts in torsion 181; Specific resilience, various materials and spring elements, table of 234; Torsional resilience 179, 222, influence of discontinuities 181.
- Resistance, frictional, 3, 5, 9, 14.
- Resultant harmonic components; See "Tangential effort."
- Resultant harmonic torque energy 470; Aero-engine/air-screw systems 705; Heavy shaft systems 691; Marine steam engine 621.
- Resultant tuning curves · Aero-engine/air-screw systems 704; Flywheel with flexible spokes 677; Heavy shaft systems 688; Simple branched systems 682; Two-mass system 673; Three-mass systems 677; Multi-mass systems 683.
- Revolving masses: Correction for deadweight of 443.
- Rigidity, moduli of, 164, 233; See "Torsional rigidity."
- Rubber: Ageing of 272; Bonding strength 277; Bulk modulus 272; Damping properties 276; Effect of oil 272; Effect of temperature 273; Elastic moduli 164, 233; Hardness of 274; Life of 273; Oil protection 272; Properties of, table 279; Resilience of 234; Weight of 153; Working stress 277; See "Flexible couplings," and "Engine mounts."
- Rubber belt drives 403.
- Rubber-in-shear engine mountings: Automobile engine 409; Design of 367, 389, 507; Force transmitted by 508, 510; Influence on torsional vibration, direct-drive engines 359, geared engines 359.
- Rubber-in-shear flexible couplings 270; Deflection of 283; Design of 279; Test of 283.
- Rubber, flywheel mounting 677.
- Running gear, moment of inertia of, 117, 118, 128, 129, multi-bank engines 342, radial engines 131, vee-engines 131.
- Fillet allowance 162; Influence of collars on torsional rigidity 163; Influence of sleeves and liners on torsional rigidity 163; Influence of splines and serrations on torsional rigidity 163; Quill shafts 229, in geared drives 315, 349, 350, 397.
- Shafts: Cast iron or bronze, torsional rigidity of 164; Heavy shaft systems 670, 685; Non-circular, torsional rigidity of 167, 173; Tapered, hollow and solid, torsional rigidity of 161; Torsional resilience of, comparative calculations 181.
- Shafting: Correction for mass of, one-mass systems 14, 16, two-mass system 25, multi-mass system 148; Elasticity of 159; Equivalent length of, solid and hollow 160; Marine, influence on torsional vibration 50, 81, 88.
- Ship's hull, vibration of 511, 513.
- Shrink fits, influence on torsional rigidity of shafts 163.
- Similar engines 78.
- Simple harmonic motion 5; See "Harmonic motion."
- Simultaneous firing, multi-cylinder engines, influence on torsional vibration, four-stroke 519, 526, 527, 528, two-stroke 533, 536, 538, two-stroke, double-acting 542, 544, 545, 546, vee-type 579, geared 586.
- Slit tube: torsional rigidity and strength of 170, 172.
- Soap film method of determining stress in non-circular shafts 168.
- Spark advance, influence on excitation torque 455.
- Spark ignition engines; See "Petrol engines."
- Spark timing, irregular, due to torsional vibration 406.
- Speed variation; See "Cyclic irregularity."
- Splines and serrations: Resilience 181; Stress concentration 169, 171; Influence on torsional rigidity 163.
- Spokes, flexible, 213; Fixed at both ends 214; Flywheel 213, 235, 677, 680; Insecurely fixed 215; Resilience of 220, 230; Stresses in 221; Torsional rigidity of 221; Uniformly stressed 217.

SHAFT: Complex, torsional rigidity of 165; Couplings, see "Couplings"; Expression for torsional deflection and stress 1;

Spring drive 243; See "Flexible couplings," and "Flexible shafts."
 Spring plate flexible couplings 258, design of 261.
 Springs, helical; See "Helical springs."
 Springs, steel, safe stress ranges 248.
 Steam engines, reciprocating: Example of breakdown due to torsional vibration 483; Harmonic components of tangential effort curve 450, 621; Vibration stress calculations at non-resonant speeds 620, influence of propeller phasing 624.
 Steam turbine, exhaust, in marine installations 299, 315.
 Stiffness of shafting; See "Torsional rigidity."
 Strain, definition 1.
 Strain energy: Calculation of 18; Definition of 2; Method of determining crankshaft stiffness 193.
 Strain gauge, electrical 705.
STRESS: Concentration of 106, in flexible spokes 228, helical springs 245, at key-ways 169, in non-circular shafts 169, at splines and serrations 169; Definition 1; D.V.L. torsional fatigue testing machine 424; Fatigue, repeated flexural loading 232, repeated torsional loading 231; Fluctuating, influence of mean stress 232; Maximum, in non-circular shafts 169, comparative calculations 175, in flexible spokes 217, 221, 229, in slit tubes 170, in one-mass systems 17; Maximum permissible shear stress for various stress ranges 232; Maximum permissible working stress, torsion and bending fatigue, table of values 233; Specific, in multi-mass systems 58, 62, 67, 68.
Equilibrium: Definition 429; Marine oil engine, one-node 613, two-node 617, due to propeller torque variation only 616; Multi-mass systems 429, 433; Oil-engine/generator sets 608; Two-mass systems 414, 428.
Forced Vibration 660; Resultant, due to several component harmonics acting simultaneously 663, 665; Resultant due to several different modes of vibration 664.
Vibration at non-resonant speeds 410, 660; Aero-engine/air-screw systems, experimental determina-

tion of 705; Marine oil engine 595, 612, 618; Marine steam engine 620, 622, 624; Oil-engine/generator sets 608, 612; Two-mass systems 414, 428.
 Stroke, influence of 79.
 Summation, harmonic torque energy 470; See "Phase diagrams," and "Vector diagrams."
 Summation, vibration torque and stress 660, for several harmonic components of the same mode 663, for the same harmonic component of several modes 663, practical method 665.
 Supercharged engines 605.
 Supercharger drive, aero-engine 350.
 Superposition, linear, principle of 433.
 Swinging form, see "Normal elastic curves."

TABULATION: FORCED VIBRATION AMPLITUDES: Two-mass systems 628, forcing torque at node 641; Three-mass systems 646, 651; Multi-mass systems 657.
Natural Frequencies 52; Aero-engine, in-line type, direct drive 107, geared 346, with flexible mounts, simple spur gear 363, 370, radial type, geared 339, with flexible mounts, concentric spur gear 374, 377, epicyclic 381, 384; Geared systems 294, two-shafts 295, 296, multi-shaft 310; Marine geared turbine and reciprocating engine 315; General remarks 52, 69; Marine installations 64, 67; Oil-engine/generator sets 57, 58.
TANGENTIAL EFFORT: HARMONIC COMPONENTS OF 412, 434; Correction for connecting rod couple 445, 447, 448; Correction for deadweight of reciprocating and revolving masses 443, 447, 448, radial and vee-engines 444; Correction for inertia of reciprocating parts 442, 447, 448; Influence of articulated connecting rods 459, 463; Influence of variable load and speed 601; Oil engines, four-stroke, compression ignition, high-speed 453, 454, slow and medium speed 456, double-acting 448, petrol engine 436, 441, 449, 452, 455, two-stroke 449, double-

- acting 449, opposed-piston 449
 Reciprocating steam engine 451
 621; Relationship to mean tangential effort 455; Resultant for 7 and 9 cylinder radial aero-engines 470; Table of values, various engines 450.
- Mean*: relationship to mean indicated pressure 435.
- Tapered shafting, solid and hollow, torsional rigidity of 161.
- Test report on rubber-in-shear coupling 283.
- Test-stand, aero-engine 353, with rubber-in-shear couplings 283.
- Three-mass systems 30; Effective inertia method 674.
- Throttle setting, influence on excitation torque 455.
- Timing, engine, influence on torsional vibration 406.
- TORQUE**: Equilibrium 417; Equivalent, in geared systems 288; Fluctuation, in geared systems 287; Forced vibration 660; In simple harmonic motion 12; Maximum, in one-mass systems 17; Specific in multi-mass systems 58, 61, 67.
- Torque energy, resultant, multi-cylinder engines 470, 691, 705.
- Torque reaction, on engine frame 541, 543, in geared systems 328, 359.
- Torque variation, accessory drives 404; Air-screw 598; Automobile transmission systems 407; Marine propellers 588, 616, phasing of 593, 624; Two-mass systems 23, 411.
- Torsiograph records, Aero-engine/air-screw systems 705; Camshaft drives 405; Geared systems 293; Use for determination of effective inertia of complex systems 698.
- Torsion of shafts, formula 1.
- Torsional deflection of crankshafts: Aero-engine 208; Opposed-piston oil engine 205.
- Torsional pendulum, simple; See "One-mass system."
- Torsional resilience 179; Table of values 181; Non-circular shafts 181.
- TORSIONAL RIGIDITY**: Definition 13; Equivalent, in geared systems 288; Flywheel with flexible spokes 213, 241; In three-mass systems 33; In multi-mass systems 61, 66.
- Crankshafts* 184; Carter formula 187, crankpins 185, crankwebs 185, empirical formula 192, experimental determination of 204, influence of web form 200, 347, journals 184, strain energy method 193; See "Crankshaft."
- Shafts* 159, air-screw 163, cast-iron or bronze 164, comparative calculations 175, complex shaft 165, influence of fillets 162, influence of shrink fits 163, non-circular shafts 167, 173, shafts in series 160, shafts of varying diameter 162, shafts with sleeves or liners 163, splined and serrated shafts 163, slit tubes 170, 172, tapered shafts, solid and hollow 161.
- Shaft Couplings*: flexible 213, flexible, in series 160, forged integral 162, keyed 163; See "Flexible couplings."
- Torsional vibration 1; See "Vibration."
- Torsionmeter, use for determination of effective inertia of complex systems 698.
- Transmitted force, engine on flexible mountings, 508, 510.
- Tungsten alloy (Heavy metal), 153, 164.
- TUNING CURVES**: Aero-engine/air-screw systems 692; Engine with rotating pendulum vibration absorbers 706; Flywheel with flexible spokes 679; Heavy shaft systems 685; Multi-mass systems 684; Simple branched systems 681; Two-mass systems 671, Three-mass systems 675.
- TUNING THE OSCILLATING SYSTEM**, methods of: Accessory drives 404; Aero-engine/air-screw systems, in-line, direct-coupled 104, geared 347, 348, with flexible mountings 388, 392, 394, radial, direct-coupled 98, geared 341, 342, with flexible mountings 388, 392, 394; Automobile transmission systems 94, 408; Camshaft drives 404; Marine geared turbine systems 322, 326; Marine oil engines 81, 86, 396, 503; Oil-engine/generator sets 73, 77, 78; One-mass system 13, 22; Two-mass system 25.

- Turbine, marine geared 299, 315, 326, nodal drive 302.
- Turning moment; See "Tangential effort."
- TWO-MASS SYSTEMS: 22; correction for mass of shaft 25, effective inertia method 670, equivalent one-mass system 26, frequency equation 24, position of node 23, 24, shaft fixed at one end 27, shaft fixed at both ends 29, summary of formulæ for natural and forced vibration 426.
- Two-stroke cycle, single- and double-acting engines, harmonic components of torque curve 449.
- V**ALVE gear, steam engines, moment of inertia of 128.
- Vector diagrams 476, use of 546; Geared engines 584; Marine engine and propeller 589; Marine oil engine 473; Oil-engine/generator set 472, 480; Radial engines 487; Vee-engines 567, 573, 580, 581; See "Phase diagrams."
- Vee-engines: Balancing 514, 532, 552, 553, influence of vee-angle 558; Connecting rod systems 457; Crank arrangements and firing orders 548, 550, 561; Effect of altering vee angle 574, 575; Normal elastic curves 573, 580, 581; Phase and vector diagrams 573, 580, 581, influence of vee-angle 567; Vibration characteristics 548, 565, with different firing orders in each bank 579; See "In-line engines."
- Velocity; Phase, definition 6, 9, 11; Simple harmonic motion, angular 10, linear 7.
- VIBRATION: Amplitude, definition 7, 10, see "Amplitude"; Elastic 2; Energy of 4; Engine frame 127, relative importance of unbalanced forces and couples 511, 513, relative importance of primary and secondary unbalance 506; Frequency, simple harmonic motion 9, 13, effective inertia method, see "Effective inertia"; Hydraulic dynamometer 600; Phase, definition 9; Stress, see "Stress."
- Characteristics:* Aero-engine/air-screw systems 95, 598; Aero engines, in-line, direct-coupled 493, geared 346, with flexible mountings 367, 392, radial, direct-coupled 96, 486, geared 341, with flexible mountings 367, 392, 507; Automobile transmission systems 88, 299, 407, with flexible mountings 409; Geared installations 301, 583; Engine accessories 402; Influence of crank sequence and firing orders, in-line engines 493, vee-engines 548; Marine installations 38, 44, 50, 80, 187, 514, 588, 612; Marine oil engines 80, 588, influence of propeller phasing and torque variation 593, 616; Marine steam engines 483, 620, influence of propeller phasing 624, with exhaust steam turbine 299, 315, 322; Oil-engine/generator sets 45, 51, 71, 77, 514; Similar engines 78.
- Forced* 625; Amplitudes, tabulation method, two-mass system 628, with forcing torque at node 641, three-mass system 646, 651, multi-mass systems 657; At non-resonant speeds 410; Damped 14; Undamped 411.
- Torsional*, free or natural 1; Aero-engine/air-screw systems 95; Automobile transmission systems 88; Definition 9; Displacement, velocity and acceleration 10; Experimental demonstration of 5; Geared systems 287, two-shafts 289, three-shafts 297, multi-shafts 303; Modes of, see "Modes"
- One-mass systems 9, 18; Two-mass systems 22, 27; Three-mass systems 30; Multi-mass systems 38.
- Vibration absorber, dynamic 650, employing helical springs 243, rotating pendulum type 706.
- W**AHL factor, for stress in helical springs 245.
- Water, allowance for entrained in propeller 135.
- Weight, air-screws 141, 706, marine propellers 139, specific, various materials 153.
- Wing mounted aero-engines, arrangement of gearing 399.
- Workman Clark, nodal drive, geared turbine systems 302.